

*for review*

# Volume 4

Principal Investigators' Reports  
July–September 1976

U. S. DEPARTMENT OF COMMERCE  
National Oceanic and Atmospheric Administration



- VOLUME 1. MARINE MAMMALS, MARINE BIRDS
- VOLUME 2. FISH, PLANKTON, BENTHOS, LITTORAL
- VOLUME 3. EFFECTS, CHEMISTRY AND MICROBIOLOGY, PHYSICAL OCEANOGRAPHY
- VOLUME 4. GEOLOGY, ICE, DATA MANAGEMENT

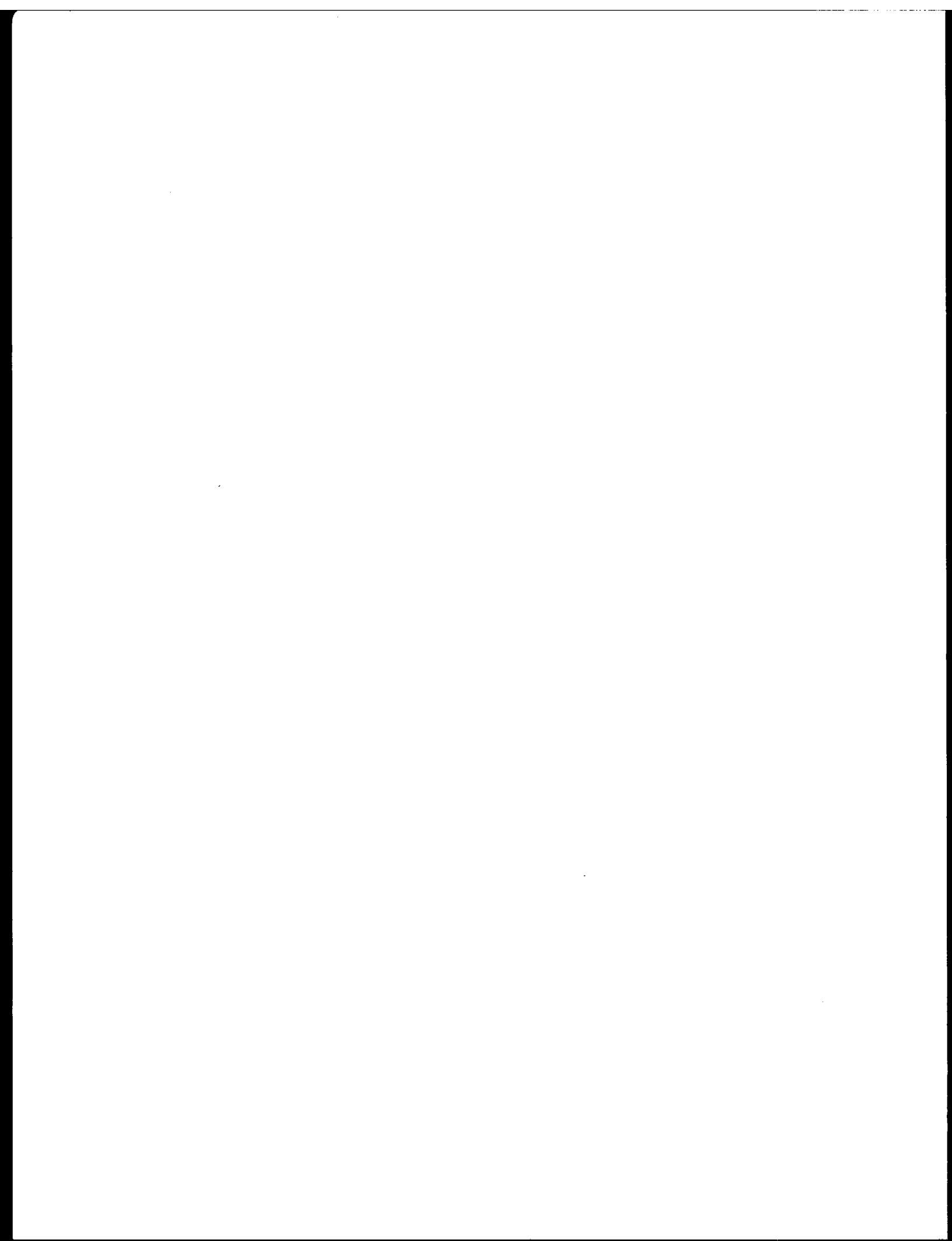
# Environmental Assessment of the Alaskan Continental Shelf

*July - Sept 1976 quarterly reports from Principal Investigators participating in a multi-year program of environmental assessment related to petroleum development on the Alaskan Continental Shelf. The program is directed by the National Oceanic and Atmospheric Administration under the sponsorship of the Bureau of Land Management.*

**ENVIRONMENTAL RESEARCH LABORATORIES**

Boulder, Colorado

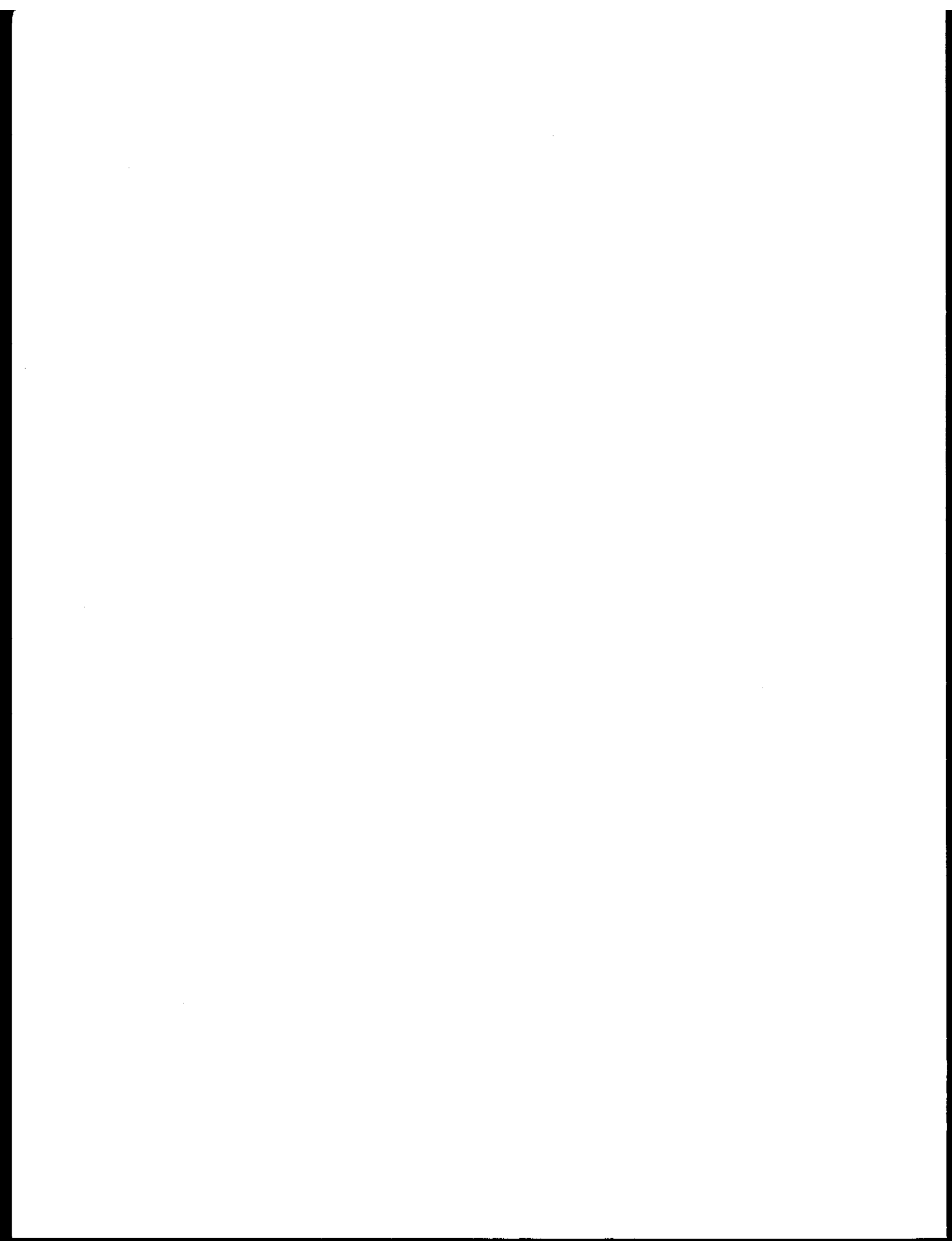
November 1976



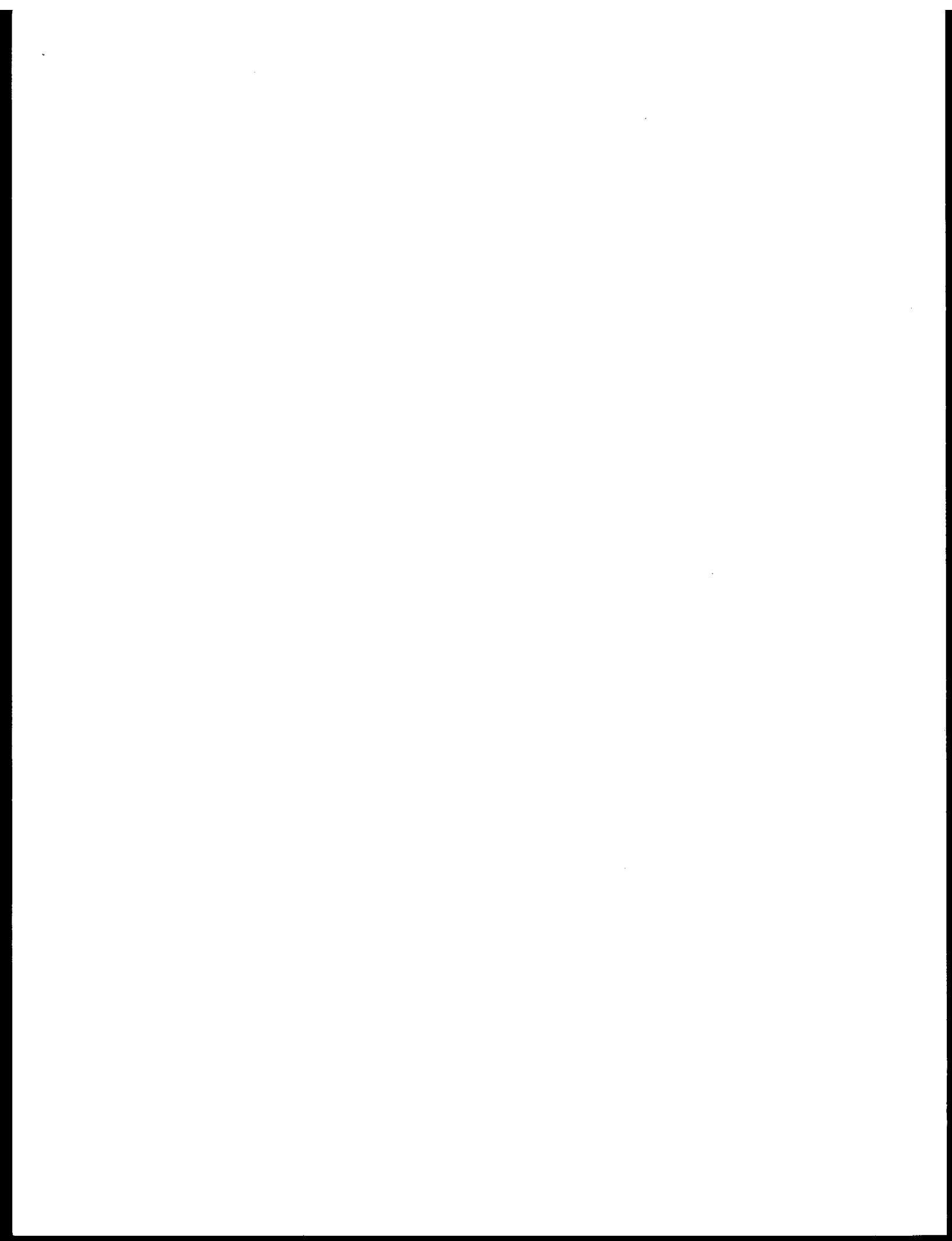
VOLUME 4

CONTENTS

GEOLOGY	1
ICE	225
DATA MANAGEMENT	609



## GEOLOGY



## GEOLOGY

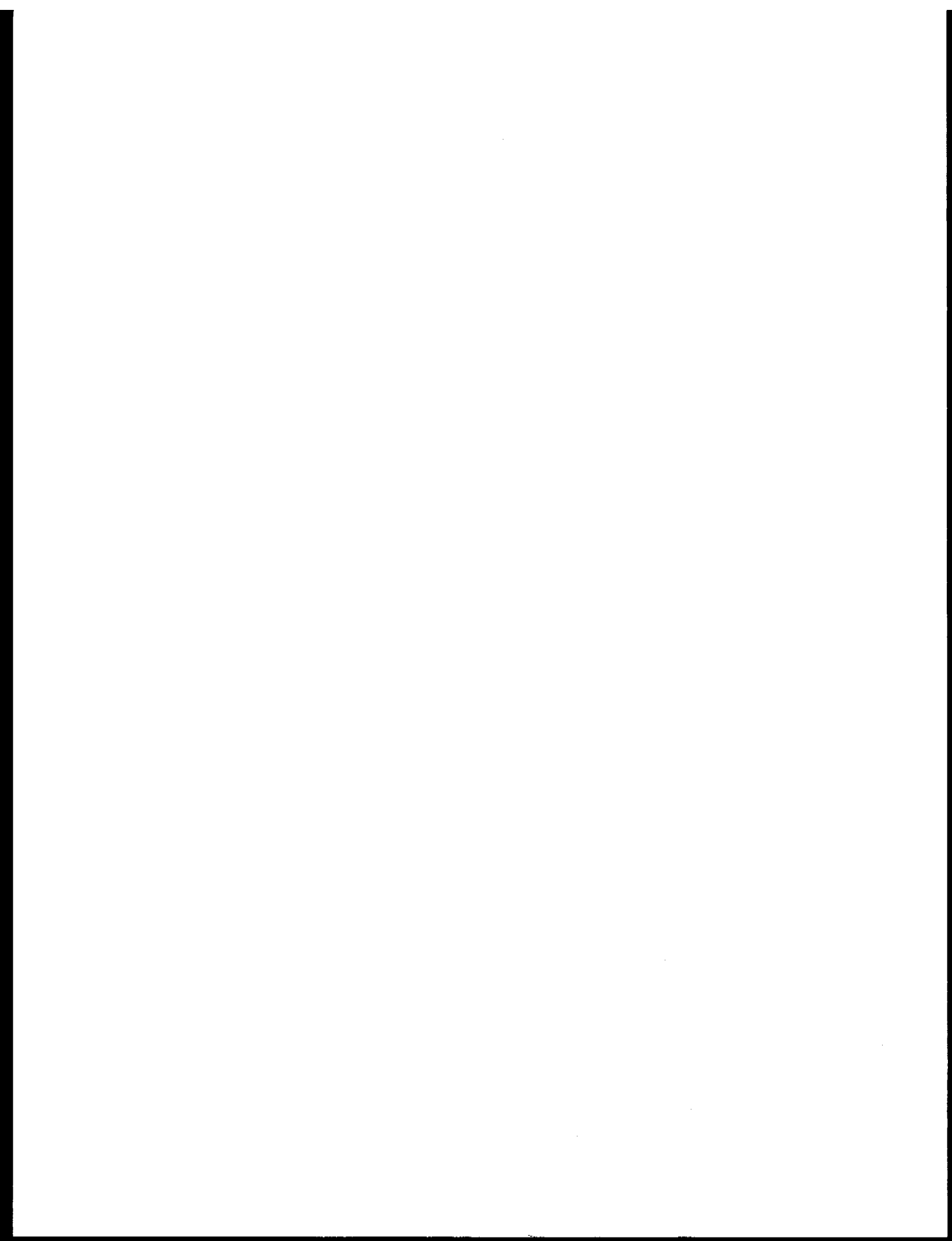
<u>Research Unit</u>	<u>Proposer</u>	<u>Title</u>	<u>Page</u>
16	John Davies Lamont-Doherty Geolo. Obs. Columbia U.	Seismotectonic Analysis of the Seismic and Volcanic Hazards in Pribilof Islands - Eastern Aleutian Islands Region of the Bering Sea	5
59	Jon C. Boothroyd Dept. of Geology U. of Rhode Island Mark S. Cable Raymond A. Levey Dept. of Geology U. of S. Carolina	Coastal Morphology and Sedimentation, Gulf Coast of Alaska	7
99	P. Jan Cannon Dept. of Geology U. of Alaska	The Environmental Geology and Geomorphology of the Gulf of Alaska Coastal Plain	48
105	P. Sellmann CRREL	Delineation and Engineering Characteristics of Permafrost Beneath the Beaufort Sea	53
152/ 154	Richard A. Feely Joel D. Cline PMEL/NOAA	Distribution, Composition and Transport of Suspended Particulate Matter in the Gulf of Alaska and Southeastern Bering Shelf	61
204	D. M. Hopkins USGS	Offshore Permafrost Studies, Beaufort Sea	83
205	Peter Barnes Erk Reimnitz David Drake USGS	Marine Environmental Problems in the Ice Covered Beaufort Sea Shelf and Coastal Regions	101
206	T. Vallier J. Gardner USGS	Faulting and Slope Instability in the St. George Basin Area and immediately Adjacent Continental Shelf and Upper Continental Slope of the Southern Bering Sea	106
208	William R. Dupre U. of Houston David M. Hopkins USGS	Yukon Delta Coastal Processes Study	109

## GEOLOGY

<u>Research Unit</u>	<u>Proposer</u>	<u>Title</u>	<u>Page</u>
209	David M. Hopkins M. L. Silverman USGS	Fault History of Pribilof Islands and its Relevance to Bottom Stability in the St. George Basin	122
210	Robert A. Page John C. Lahr USGS	Earthquake Activity and Ground Shaking in and along the Eastern Gulf of Alaska	145
212/ 216	Bruce F. Molnia Paul R. Carlson USGS	Faulting and Instability and Ero- sion and Deposition of Shelf Sediments, Eastern Gulf of Alaska	145
251	Hans Pulpan Jurgen Kienle Geophys. Inst. U. of Alaska	Seismic and Volcanic Risk Studies Western Gulf of Alaska	145
253/ 255/ 256	T. E. Osterkamp William D. Harrison Geophys. Inst. U. of Alaska	Offshore Permafrost-Drilling, Boundary Conditions, Properties, Processes and Models	147
271	James C. Rogers Geophys. Inst. U. of Alaska	Beaufort Seacoast Permafrost Studies	152
290/ 291/ 292	Charles M. Hoskin IMS/U. of Alaska	Benthos-Sedimentary Substrate Interactions	157
327	Monty Hampton Arnold H. Bouma USGS	Faulting and Instability of Shelf Sediments, Western Gulf of Alaska	160
352	Herbert Meyers EDS/NOAA	Seismicity of the Beaufort Sea, Bering Sea and Gulf of Alaska	198
407	R. Lewellen Arctic Research	A Study of Beaufort Sea Coastal Erosion, Northern Alaska	203
431	Ashbury H. Sallenger USGS	Coastal Processes and Morphology of the Eastern Bering Sea	205
423	Arthur Grantz et al USGS	Seismic and Tectonic Hazards in the Hope Basin and Beaufort Shelf	209

## GEOLOGY

<u>Research Unit</u>	<u>Proposer</u>	<u>Title</u>	<u>Page</u>
473	David Hopkins USGS	Shoreline History of Chukchi Sea as an Aid to Predicting Offshore Permafrost Conditions	213
483	N.N. Biswas L. Gedney Geophy. Inst. U. of Alaska	Evaluation of Earthquake Activity Around Norton and Kotzebue Sounds	219



RU# 16

NO REPORT AVAILABLE AT THIS TIME



6TH QUARTERLY PROGRESS REPORT  
1 October 1976  
Research Unit - 59

"Coastal Morphology and Sedimentation"

Miles O. Hayes, Principal Investigator  
Coastal Research Division  
Dept. of Geology  
University of South Carolina  
Columbia, S. C. 29208

TASK D-Y: Evaluate present rates of change in coastal morphology with particular emphasis on rates and patterns of man-induced changes; locate areas where coastal morphology is likely to be changed by man's activities; and evaluate the effect of the changes, if any. The relative susceptibility of different coastal areas will be evaluated.

Project 1. Shoreline of northern Gulf of Alaska (Dry Bay to Cape Yakataga).

Project 2. Shoreline of Kotzebue Sound.

Project 1. Shoreline of Northern Gulf of Alaska  
(Dry Bay to Cape Yakataga)

Field and Laboratory Activities

No field work has carried out on this project during the summer of 1976. Final laboratory analysis was completed on sediment samples, and computer analysis of the results is in progress. Main emphasis was on report writing and data synthesis.

Results

Two papers have been written and are enclosed as part of this report:

1. Hayes, Miles O., 1976, Part D. A Modern Depositional System - Southern Alaskan Coast: in Hayes, M. O., and Kana, T. W., eds., Terrigenous clastic depositional environments, some modern examples: Tech. Rept. No. 11-CRD, Dept. Geol., Univ. South Carolina, p. I-112 - I-120.
2. Hayes, M. O., Ruby, C. H., Stephen, M. F., and Wilson, S. J., 1976 Geomorphology of Southern Alaska: preprint, Proceedings 12th Coastal Engineering Conference.

The first paper treats the study area as a depositional system, and the second paper discusses the engineering problems related to the development of shore facilities in the study area. In addition to these two papers, a preliminary manuscript, which will be submitted during the next quarter, has been completed:

Ruby, C. H., and Hayes, M. O., 1976, Morphology and sedimentation of the shoreline of the Northern Gulf of Alaska: Tech. Rept. No. 12-CRD, Dept. Geol., Univ. South Carolina, 150 p. (approx.).

Estimate of Funds Expended

<u>Category</u>	<u>Amount</u>
Salaries	\$630
Supplies	600
Travel	100
Other	<u>6,000</u>
Total	\$7,330

Project 2. Shoreline of Kotzebue Sound

Introduction

During this past summer field season, a research team from the Coastal Research Division (composed of Miles O. Hayes, Ph.D., Principal Investigator; Christopher H. Ruby, M.S., research scientist; and Larry G. Ward, M.S., research scientist) completed a preliminary survey of the coastal geomorphology of Kotzebue Sound. The study area composes approximately 1,000 km of open coastline between Cape Prince of Wales to Cape Lisbourne. In addition, there is a well-developed delta and lagoonal system to the east of the Baldwin Peninsula (Kobuk, Noatak, and Selawik river deltas; Fig. 1).

## Methods of Study

To accomplish the study of such a large and remote area, special methods of data collection were employed. The first two field days were spent flying the entire 1000 km study area from Cape Prince of Wales to Cape Lisbourne. During these rather lengthy flights, data were collected at a number of levels:

1. Detailed oblique aerial photos were taken using both color and infrared film. Approximately 800 photographs were taken.
2. General sediment transport trends were interpreted using geomorphic indicators such as spits, barrier island recurves, deflected sediment plumes, tidal delta orientation and morphology, offset inlets, and other criteria. These trends were then summarized and plotted on topographic maps. They were later verified with ground surveys and will also be verified using SSMO data.
3. Changes in coastal geomorphology, which had taken place since the original topographic mapping, were added to our base maps.
4. A detailed description of the general geomorphology was made using a small tape recorder.
5. The potential for beach landing at each of the different coastal type areas was checked. This was necessary in order to plan the logistics for the ground surveys.
6. Each settlement (small eskimo villages, communication installations, etc.) in the study area was canvassed for possible logistic support, emergency landing potential, and acquisition of data such as weather and ice information.

These data were then used to plan the ground field program.

To assess regional trends in beach morphology, beach profiles and study sites were established at 10 km intervals throughout the study area. This spacing interval was necessary in order to precisely define the transitional phases from one coastal type to another. Further, this spacing permitted a very detailed sediment sampling scheme to be utilized. In all, 89 profile and study sites were established. Of them, 70 were surveyed and sampled in detail on the ground. The remaining 19 stations were impossible to land at due to:

1. High rock cliffs with no beach - 7 sites.
2. Lower tundra cliffs often strewn with large angular erratics - 5 sites.
3. Unconsolidated clay and silts unable to support the weight of the aircraft - 7 sites.

At each of these 19 stations, detailed oblique aerial photos were made from various elevations, and a complete description of the area was made on tape from the air.

At each of the 70 ground stations, the following studies were carried out:

1. A line transit of the active beach zone to delineate beach morphology. These profiles are then plotted by computer. Re-surveying of these profiles on repetitive visits results in precise documentation of erosional and depositional patterns.
2. Sediment samples were taken using a 15 cm coring tube following the method indicated in Figure 2. A total of 220 samples were collected. These samples are now being analyzed in our sedimentological laboratory, and the data will later be synthesized by computer.
3. A field sketch of each site was made to show surrounding geomorphology and geology as well as an aid to the field observer's perception.
4. Ground photos of the profile site and sediments were taken.
5. A tape-recorded description of the site and its surrounding geology and geomorphology, sediments and marine processes was made.
6. Wave height, angle of approach, direction and velocity of long-shore currents, general weather, tidal stage and range, and any other pertinent data were recorded at each site.
7. Metal posts were emplaced at each site to be revisited (47 in all) on return trips, should that be possible.

Two 8-hour aerial photo flights were made toward the end of the summer from 5000-6000 ft. This allowed complete aerial coverage of the area from a uniform height and under ideal photographic conditions. The photos are extremely useful when analyzing depositional land forms and for analysis of erosional-depositional trends.

Finally, vertical high altitude aerial photos are being used for comparison with this summer's photographs. This will permit more accurate interpretation of these erosional-depositional trends.

An attempt is being made to use LANDSAT photos for ice interpretation. The methods and results to be expected are as yet unclear. Continued cooperation with the University of Alaska Geology Department should aid greatly with respect to this ice interpretation.

## Results

Introduction. - On the basis of these preliminary studies, the coastline has been subdivided into six separate coastal types:

1. Microtidal barrier island complex.
2. Active delta system.
3. Retreating tundra cliffs.
4. Discontinuous narrow barriers and spits enclosing lagoons.
5. Bedrock headlands.
6. Cuspate foreland.

Figure 1 shows the distribution of these geomorphic types, as well as the location of our study sites. Each of the different coastal types is described briefly below.

Microtidal barrier island complex. - Stretching 250 km from the Cape Prince of Wales (a high intrusive bedrock headland) to Cape Espenberg, this system of barrier islands represents the largest single unbroken coastal type. At the southwestern terminus, the barriers are attached to the bedrock of Cape Prince of Wales. From that point, they sweep to the north and gradually to the northeast in a broad arc. This section is characterized by relatively thick barrier islands composed of multiple prograded ridge-and swale topography. Long linear lakes and lagoons often fill the swales. Sediments are primarily sand with some scattered gravels.

The barrier system then trends to the northeast as a relatively straight line to Cape Espenberg. The barrier islands are generally quite narrow, often backed by well-developed storm overwash fans extending into the lagoons behind the barriers (Fig. 2). Erosion dominates the geomorphology of these barriers. The only major section which is not highly erosional is at Cape Espenberg. Sediments are transported along the barriers to the northeast under the influence of waves approaching from the Bering Sea to the west. The sediments show a distinct fining trend toward the northeast. They ultimately are deposited at the spit at Cape Espenberg. This spit, which is similar to the barrier near Wales, is a set of prograded beach ridges with lakes and lagoons in the swales.

Active delta system. - The sheltered shorelines to the east of the Baldwin Peninsula in Hotham Inlet and Selawik Lake are dominated by three river deltas. The Noatak, Kobuk and Selawik rivers all flow into this area. Each has a prograding active delta at its terminus (Fig. 3). Migrations of the main distributary channels cause certain parts of the deltas to prograde when the distributaries are active, or to erode when the nearby distributaries are abandoned. For the most part, the coast in this area is extremely low and composed of silts, clays, and sands. It is pockmarked with innumerable lakes and is very unstable due to a changing rate of sediment supply. Its position behind the Baldwin Peninsula shelters it from any direct marine processes; therefore, there are no well-developed beaches.

Retreating tundra cliffs. - Much of the Kotzebue Sound study area is underlain by frozen Pleistocene gravels, sands, and muds. These sediments are marine coastal plain deposits, both alluvium and glacially derived. They form the large flat expanses of tundra, which usually has a characteristic polygonal topography (Fig. 4). Often, the tundra abuts directly on the coast. In these areas, there is generally a low eroding cliff with a poorly-developed beach. The sediments on the beach are very poorly sorted, ranging from silts and clays to large angular erratics. These sediments are supplied directly by the eroding cliffs. Beaches are narrow and unstable, especially in the more sheltered areas. Large waves developed during storms break over the beaches and directly onto the scarps behind. Precise estimates of the rates of retreat of the tundra scarps will be computed using vertical aerial photography.

Discontinuous narrow barriers and spits enclosing lagoons. - Most of the coastline on the northern section of the study area is erosional. Rock headlands and tundra scarps are retreating over much of that area. Sediments introduced by

this erosion move down the coast to the southeast under the influence of waves from the west. These sediments, mostly sands with some gravels, form narrow barriers and spits across the numerous low lagoonal areas (Fig. 5). These barriers and spits are generally either poorly vegetated or unvegetated. Storm waves overtop them completely, forming washover fans behind them and causing them to retreat landward. These barriers are extremely unstable due to their attachment to erosional headlands and scarps and to their own landward migration.

Bedrock headlands. - There are numerous short stretches of coast that have high bedrock cliffs (Fig. 6). These cliffs range from a few meters to well over 100 m in height. Rock types range from Tertiary and Quaternary basaltic and andesitic lava flows, to Paleozoic limestones and highly metamorphosed rocks. The coast here is characterized by sea stacks, sea caves, and large talus slopes. Beaches are virtually non-existent. These cliffs are of extreme importance due to the large number of nesting sea birds which use them as rookeries.

Cuspate foreland. - The northwestern end of the study area is a large cuspate foreland named Point Hope (Fig. 7). The foreland, which is composed of sand and well-sorted gravels, is located at a convergence zone of two longshore current directions. Sediment is moved along the coast from Cape Lisbourne toward Point Hope to the south. At Point Hope, waves approaching from the west move sediment to the southeast. As a result of this pattern and the extreme exposure of the area to the high waves generated in the fall, the northern limb of the foreland is eroding and migrating to the east; while the southeast limb just past the point is prograding slowly.

Summary. - In general, the study area is undergoing erosion over most of its length. Progradation is occurring only at the downdrift ends of some of the spits and on active deltas. Retreat is manifest as erosional rock and tundra scarps and as landward migration of barrier islands and spits.

## Discussion

At this time, we are well underway with the analysis of the field data collected during the summer 1976 field season. This includes sedimentological analysis and computer synthesis, geomorphic base map construction, interpretation of sediment transport trends, and detailed erosional-depositional histories for a number of sub-environments within the study area. Preliminary assessment of the possible effects of oil spills is also being investigated; however, a full understanding of this problem will not be possible without certain detailed hydrographic data. Possibly, these data could be collected during summer 1977 if funds were available.

Another important problem is ice effects. A systematic study should be undertaken to monitor the processes of freeze-up and break-up and their effects on the coastal morphology and sediments. Presumably, ice processes could have a major impact on problems related to coastal construction and oil spills.

## Problems

The only major problems that were encountered during the summer of 1976 were logistical. It was necessary to change our normal working aircraft from a Cessna 180 to a Piper Super Cub. This was necessary due to the extremely un-

consolidated nature of the sands and gravels of the beaches and their inability to support the C-180 (weight 1,800 lbs.). Any plans for projects calling for beach landings on the northern shores of the Kotzebue study area should keep this experience in mind.

Estimate of Funds Expended

<u>Category</u>	<u>Amount</u>
Salaries	\$3,000
Supplies	2,021
Travel	14,000
Other	<u>20,000</u>
Total	\$39,021

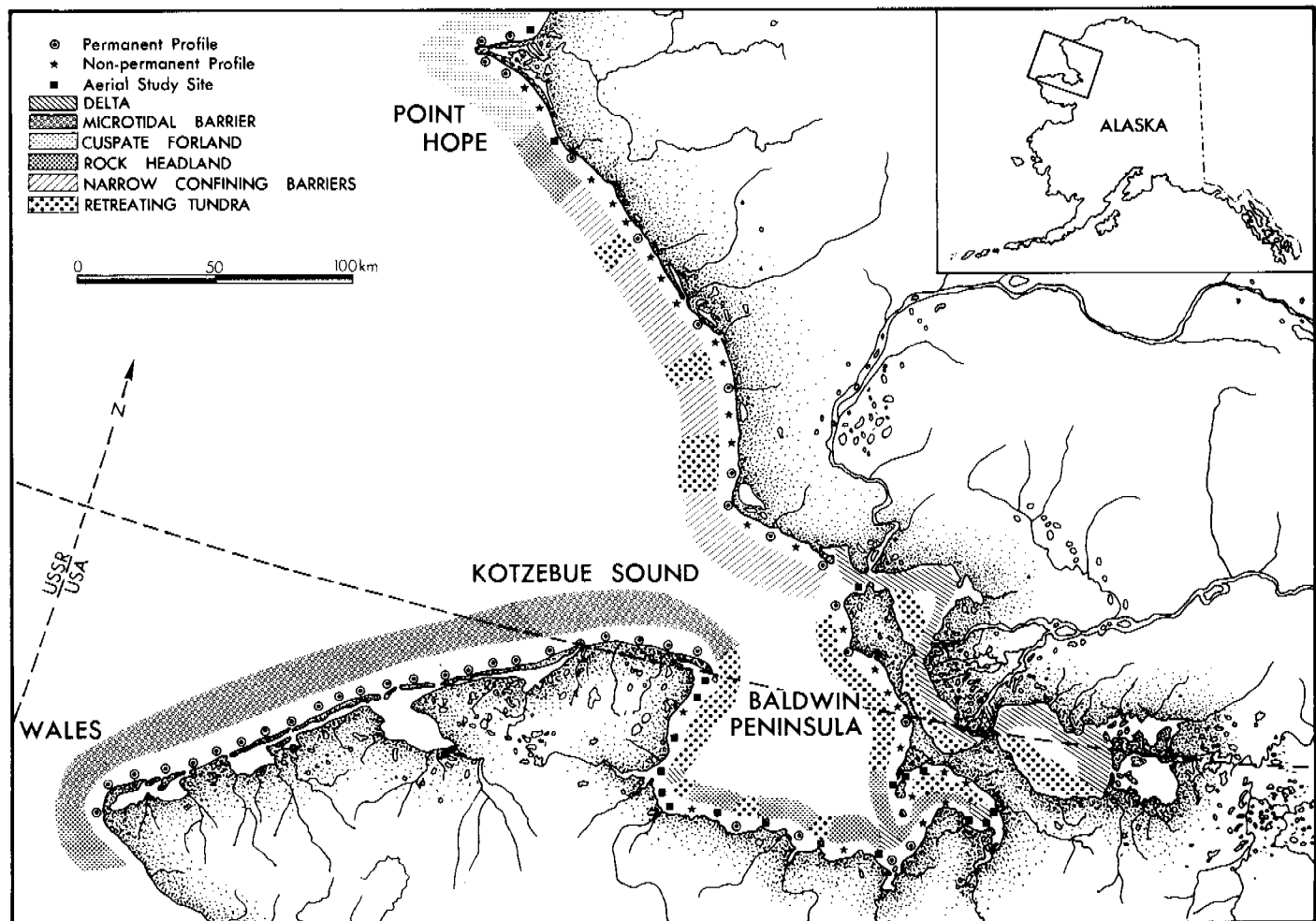


Figure 1. Preliminary classification of coastal types for the study area based on analysis of 89 separate 10 km wide coastal sections.



Figure 2. A. View looking southwest along the microtidal barrier island complex located 40 km to the S.W. of Cape Espenberg. Arrow indicates large washover fan shown below in B. B. Large washover fan (photo taken from 5500 ft.). C. Complex pattern of wash-through channels and concentric ridge-and-swale topography developed between the washthroughs. Note the development of numerous offshore bars.

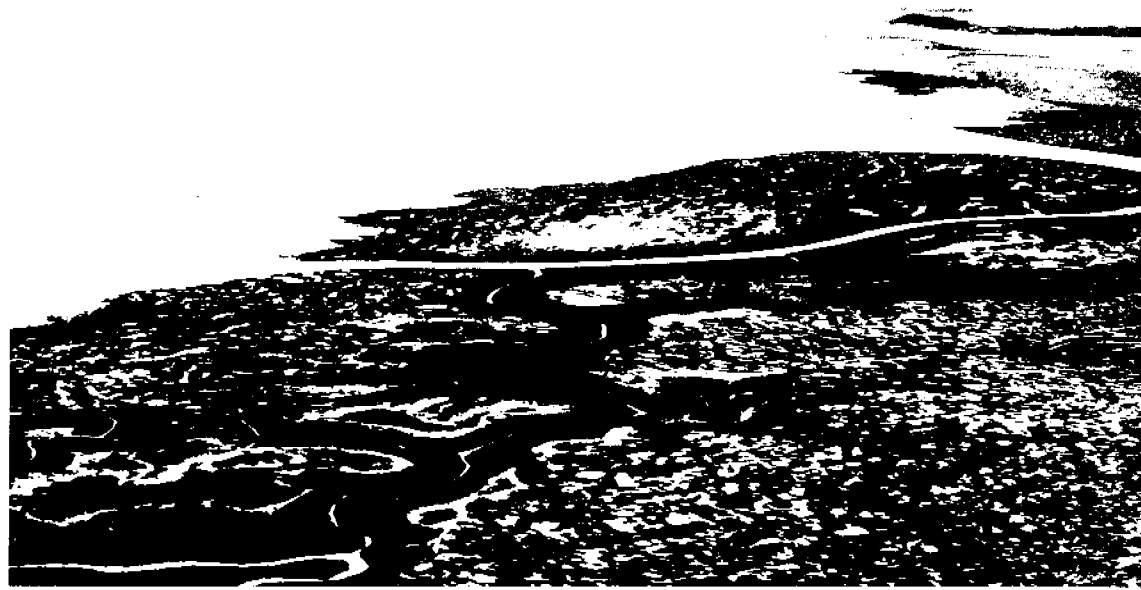


Figure 3. A. Delta developed by the confluence of the Noatak, Kobuk, and Selawik Rivers to the east of the Baldwin Peninsula. B. Arrow indicates old distributary channel on the Kobuk delta. The channel has been abandoned and infilled.

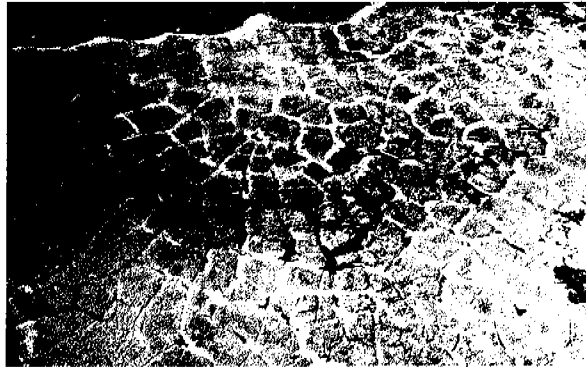
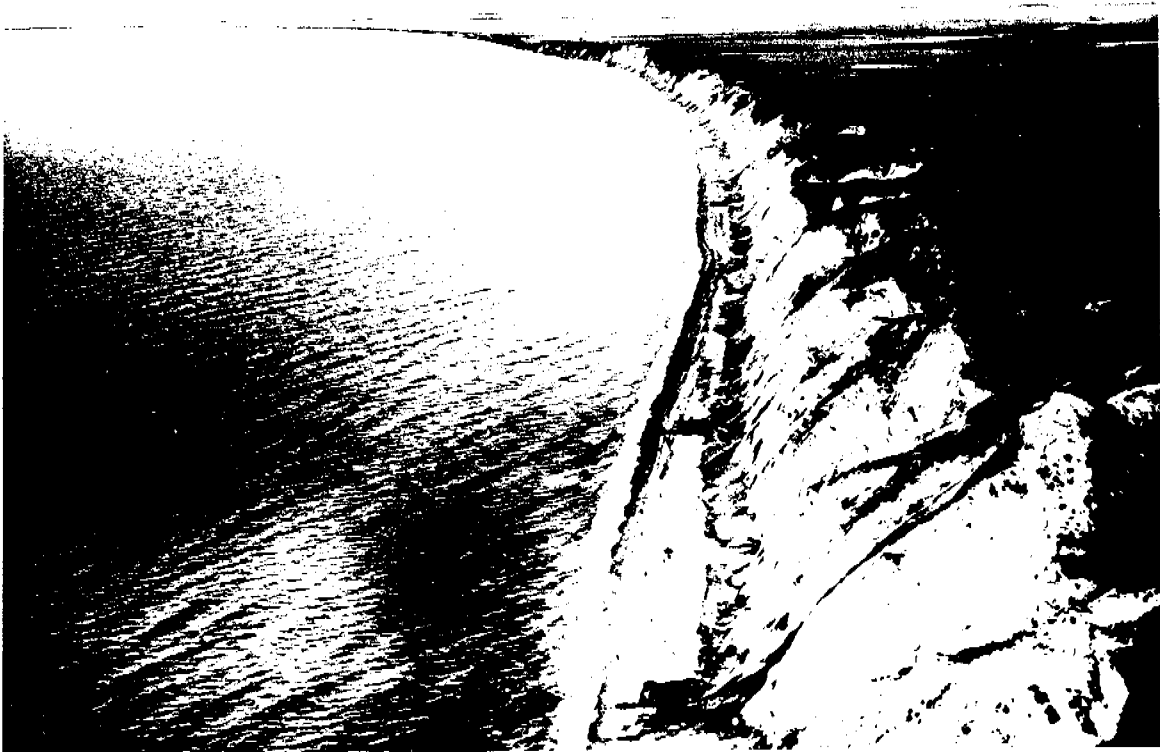


Figure 4. A. Typical eroding tundra scarps, which are common throughout the study area. B. Extremely narrow beaches at the base of the tundra scarps. Note the vegetated blocks that have slumped from the scarp face. C. Polygonal topography on the tundra surface. In this case, the concentric nature of the polygons is the result of a pingo.

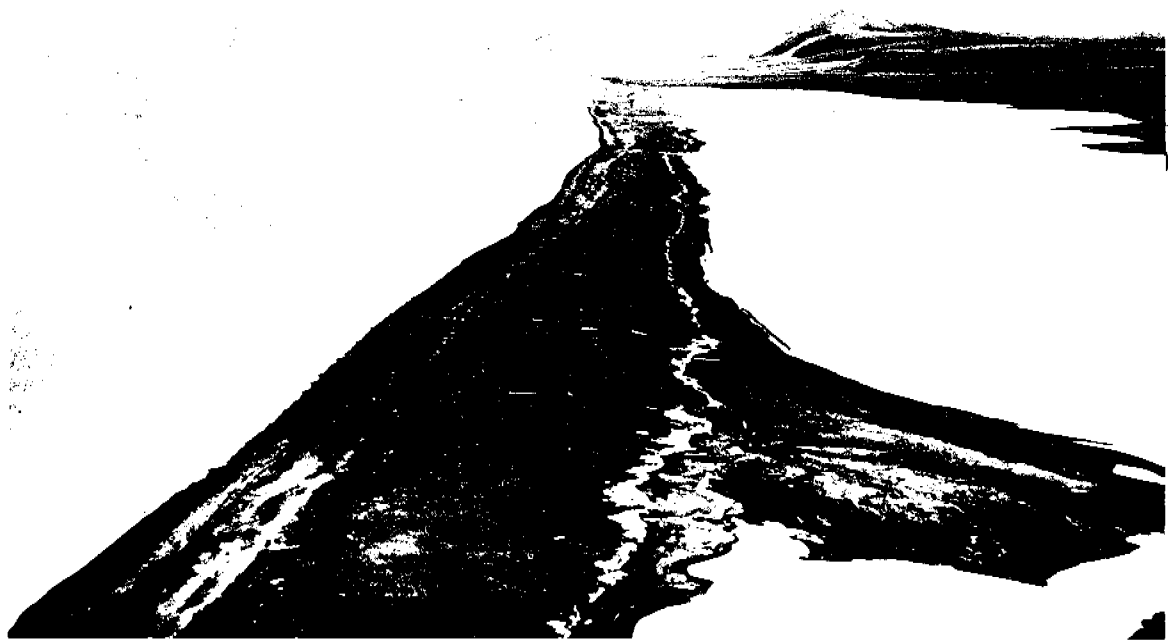


Figure 5. A. Narrow barrier chains confining lagoons on the north shore of the study area. B. Extremely narrow barrier developed down-drift of a headland in the area shown in A. These barriers are often completely unvegetated due to storm overwash.

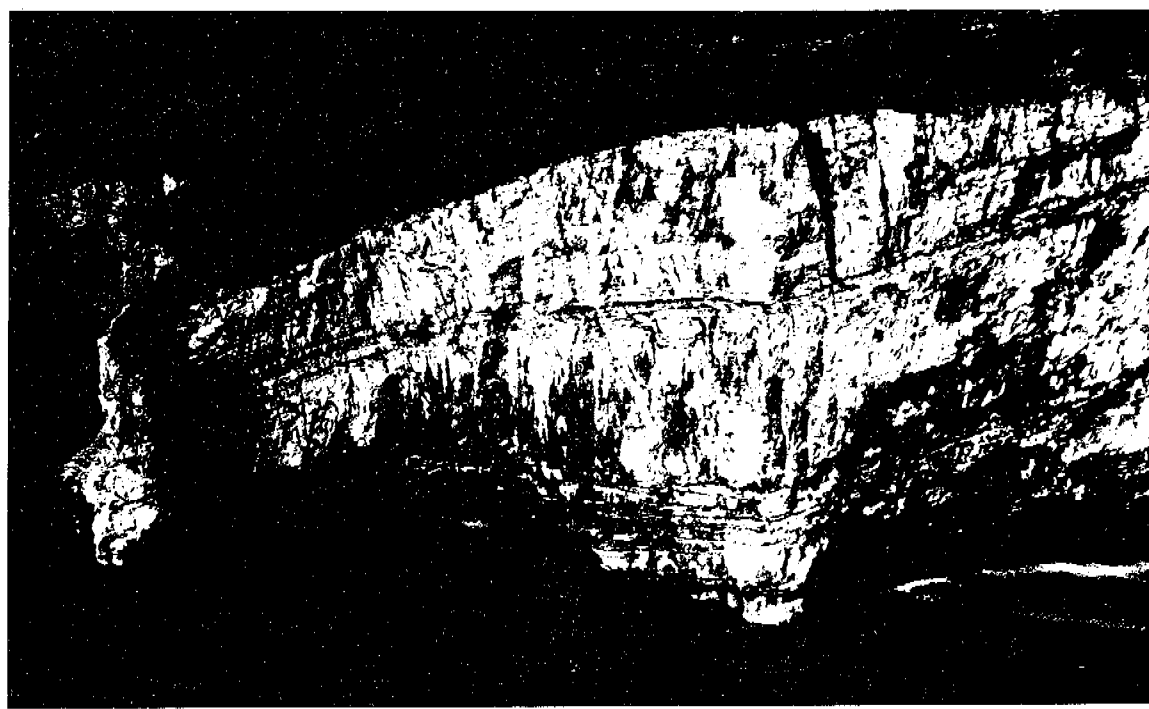
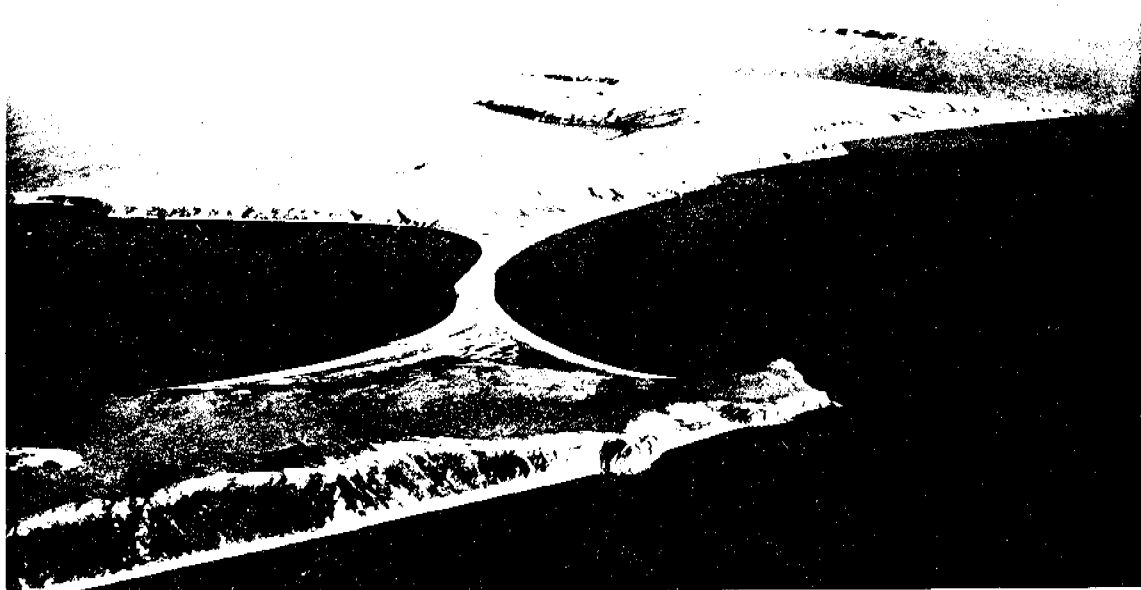


Figure 6. A. Rock headlands and tombolo system at the southern end of the Baldwin Peninsula. B. High bedrock cliffs with narrow gravel beaches form some of the most dramatic coastlines in the area. Sea caves are visible in the lower left of the photo.

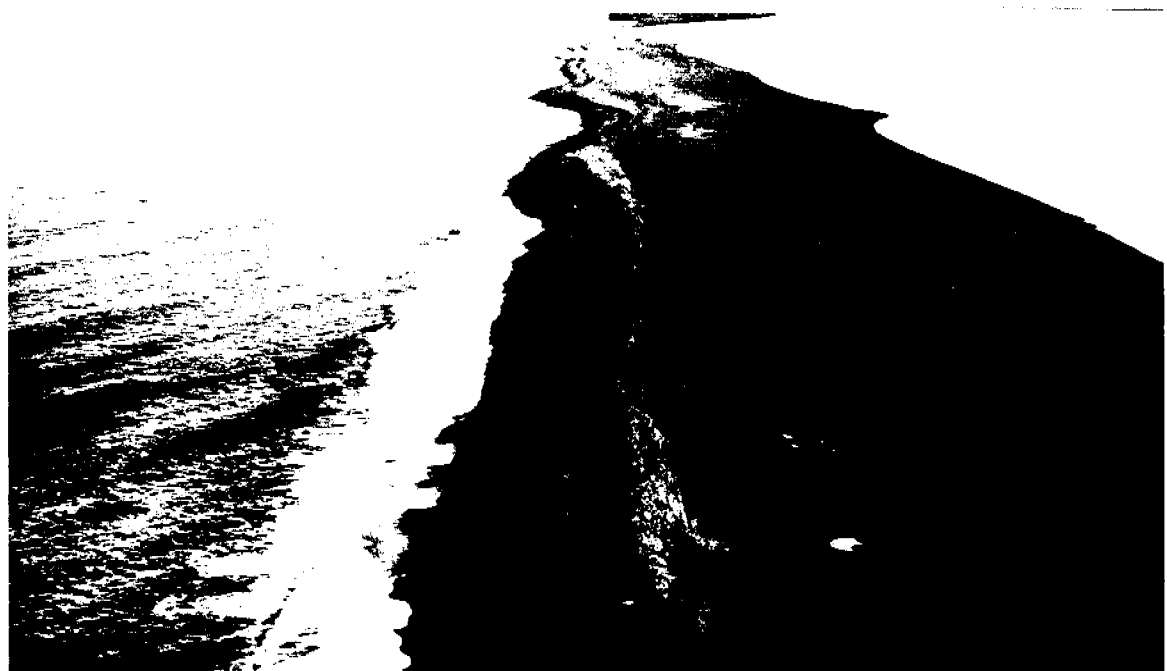
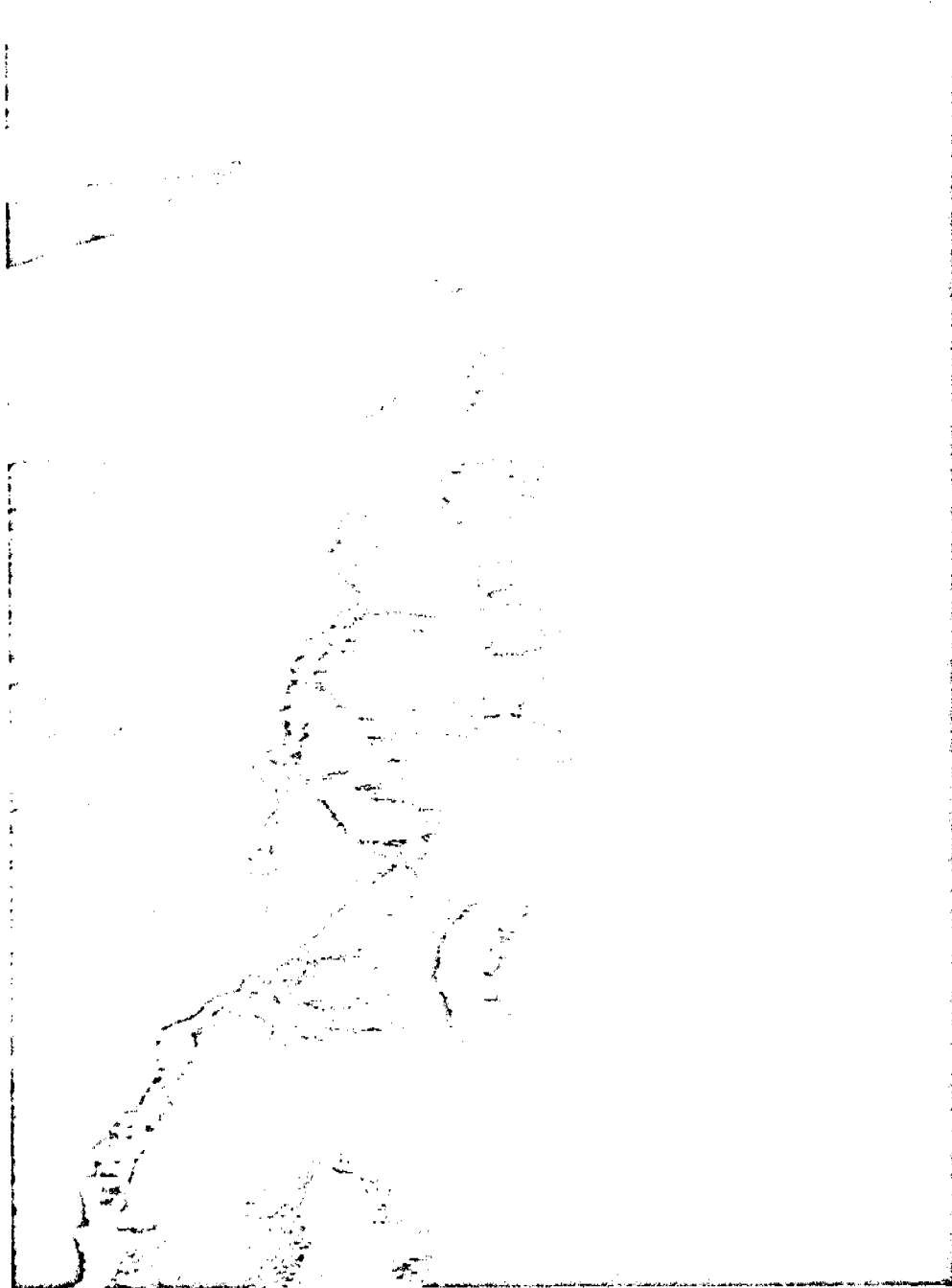


Figure 7. Unvegetated sand and gravel barrier which forms the western side of the Point Hope cuspatate foreland. This section is subject to very high waves that frequently overtop the barrier.

D. A MODERN DEPOSITIONAL SYSTEM -  
SOUTHEAST ALASKAN COAST



Rhythmic topography on the beach of the Bering Foreland, Alaska.

Photograph taken in June, 1975 (by M.O. Hayes).

From: Hayes, Miles O., and Kana, T. W., 1976, Terrigenous clastic depositional environments; some modern examples: Tech. Rept. No. 11-CRD, Dept. Geology, Univ. of South Carolina

## INTRODUCTION

This section gives a brief summary of data collected by our research group on the coastal environments of southeast Alaska, a mesotidal collision shoreline with narrow coastal and deltaic plains. It is unusual to find a depositional shoreline of this magnitude (Fig. 127) on a collision coast. It owes its origin to the huge sediment output of glaciers that drain the largest ice field in North America, and to the sediments of the Copper River, which has a mean annual load of  $100 \pm x 10^6$  metric tons (Reimnitz, 1966). This information is provided for comparison with the South Carolina area, an Amero-trailing edge shoreline.

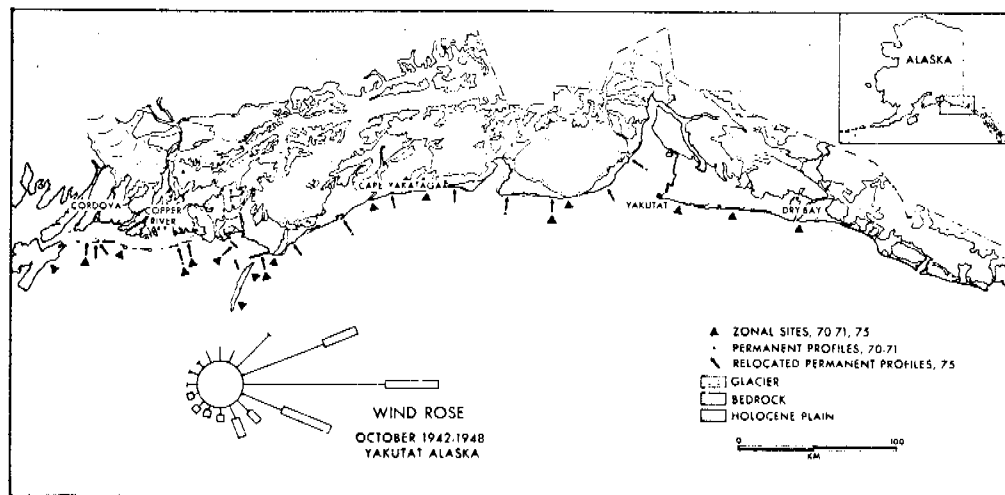
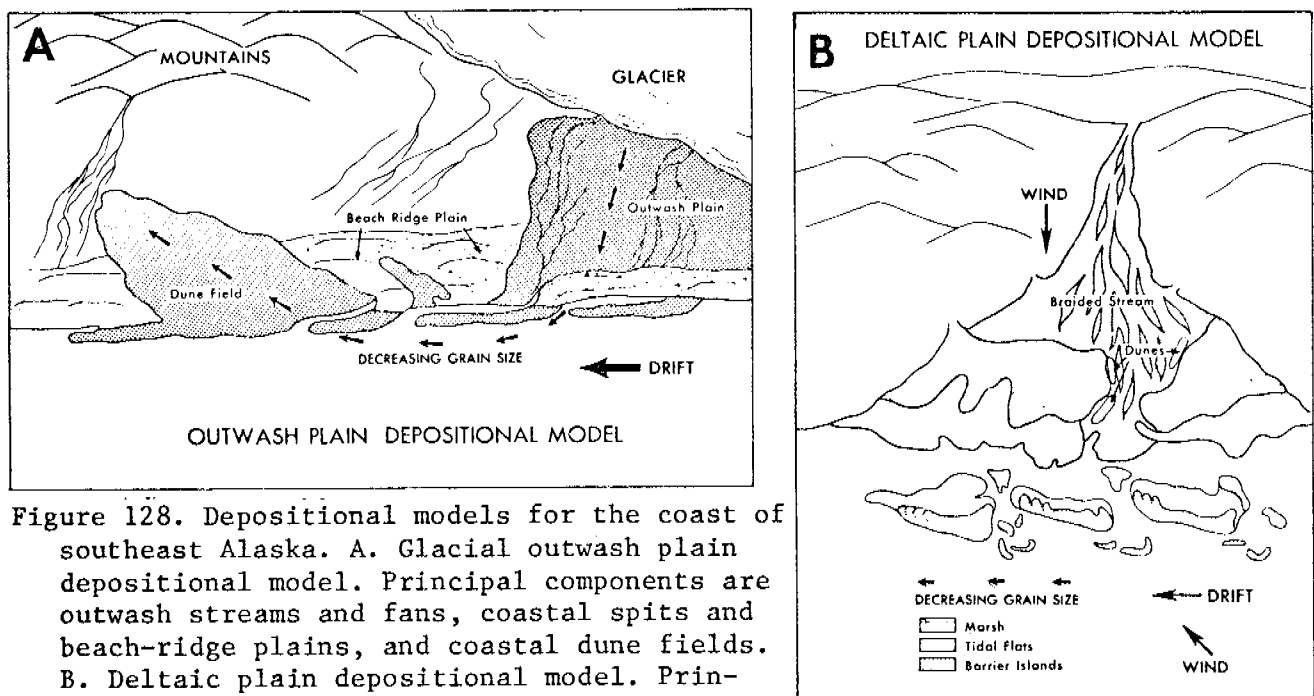


Figure 127. Study area in southeast Alaska. Note distribution of the Holocene coastal plain (max. width = 35 km).

## DEPOSITIONAL SYSTEMS

The morphology and sediments of the entire glacial outwash plain shoreline of the northeast Gulf of Alaska (Cordova to Icy Point) were studied on a reconnaissance basis in 1969-1971. Fifteen permanent beach profiles were established, eighteen detailed site studies (zonal studies) were carried out, and sediment samples were collected at ninety stations, using a 4 km spacing. The area was revisited in the summer of 1975, during which time the permanent profiles were remeasured and ninety beach profiling stations were occupied in the central portion of the study area (vicinity of Malaspina Glacier). The following general conclusions are derived from this study:

- (1) Coastal morphology of the area consists of:
  - (a) outwash plain shoreline, which is a complex of outwash streams with downdrift beach-ridge plains;
  - (b) the delta of the Copper River, which has a seaward margin made up of mesotidal barrier islands. Depositional models have been defined for these two morphological types (Fig. 128).



**Figure 128.** Depositional models for the coast of southeast Alaska. A. Glacial outwash plain depositional model. Principal components are outwash streams and fans, coastal spits and beach-ridge plains, and coastal dune fields. B. Deltaic plain depositional model. Principal components are braided stream, salt marsh, tidal flats, subtidal estuarine, and mesotidal barrier islands.

- (2) Southeasterly storms dominate the coastal processes, generating strong littoral drift from east to west (as indicated by beach morphology, grain size trends, and limited field measurements).
- (3) Recent earthquake activity has left a major imprint on the shoreline morphology, especially in bedrock areas, where uplifted wave-cut benches are well preserved.
- (4) Beach morphology:
  - (a) The large diurnal inequality of the tides has a striking effect on beach morphology, inasmuch as wave energy is focused at four different levels on the beach during a single tidal cycle. The diurnal tidal range is 3 m.
  - (b) Beach face slopes show great differences which correlate with grain size differences, the coarsest beaches having the steepest slopes.
  - (c) The erosional-depositional cycle on the beach closely follows the one described for the East Coast of the U.S. The cycle is initiated by a storm which leaves a flat, erosional profile. The recovery profile consists of landward-migrating ridge-and-runnel systems, and the mature profile consists of a wide, constructional berm. Storms are more numerous in Alaska, so the frequency of completion of the cycle is less than on the East Coast.

#### Outwash Plain Shoreline

Sediments. - Figure 129 compares the beach sediments of the outwash plain depositional system with the beach sediments of the barrier islands of the Copper River delta. The outwash plain beaches are both texturally and mineralogically immature. All of the samples have very low percentages of quartz, being classified as litharenites (using scheme of Folk, 1974) (Fig. 129A). The samples show a wide range of values of sorting and mean grain size (Fig. 129B).

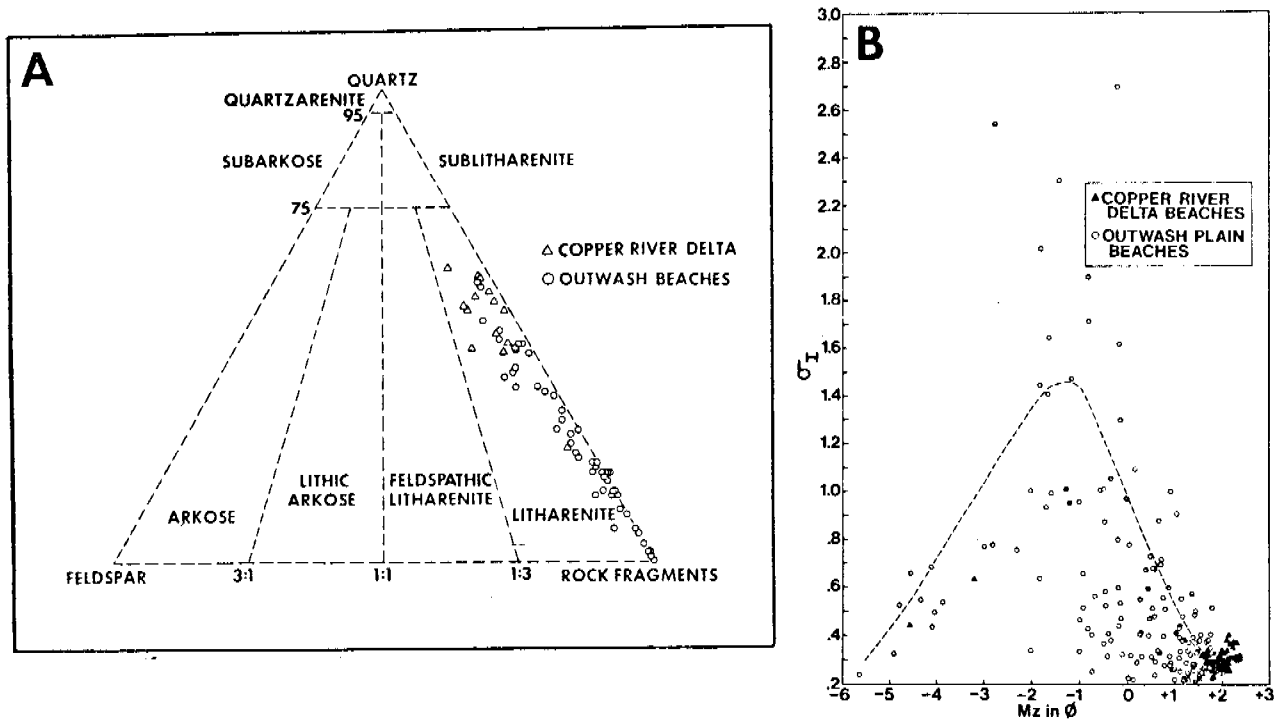


Figure 129. A. Composition of outwash plain and Copper River delta barrier island beach sediments. All samples are litharenites, with the barrier island sands being more quartz rich. B. Mean grain size ( $M_z$ ; Folk, 1968) vs. sorting ( $\sigma_I$ ). Copper River delta beaches are moderately sorted medium to fine sand, whereas the outwash plain sediments show a wide range in size and sorting.

Depositional facies. - The outwash stream and outwash fan facies were described in some detail by Boothroyd (this volume, p. I-17 - I-26) and will not be repeated here. The beach-ridge plain shoreline is illustrated in Figure 130, and a typical stratigraphic section through a preserved beach ridge is shown in Figure 131. The sequence most often found in the older beach ridges is essentially the landward half of the spits, which are primarily washover terraces. A typical sequence includes (from top to bottom) (see Fig. 132):

- (1) Large scale eolian crossbedding in medium to fine sand, usually bimodal with modes dipping at  $90^\circ$  to dominant wind direction (SE). Formed in longitudinal, vegetated dunes.
- (2) Small-scale eolian crossbedding in coarse to medium sand, usually bimodal with modes dipping at  $45^\circ$  to the SE wind. Formed in wind-shadow dunes.
- (3) Water-laid flat beds composed of mixed sand, granule, and gravel (sand and granule dominant). Gravel shows isolate imbrication and beds dip at small angle ( $\pm 5^\circ$ ) landward. Formed by spit-top overwash during storms.
- (4) Water-laid gravel deposits that dip landward at small angle ( $\pm 5^\circ$ ). Gravel highly imbricated. Formed by berm-top overwash during earlier periods of spit development.

Hypothetical paleocurrent rose diagrams constructed for the outwash plain sand bodies are shown in Figure 133.



Figure 130. Beach-ridge plain near Yakataga, Alaska. Arrow locates approximate position of stratigraphic section shown in Figure 131.

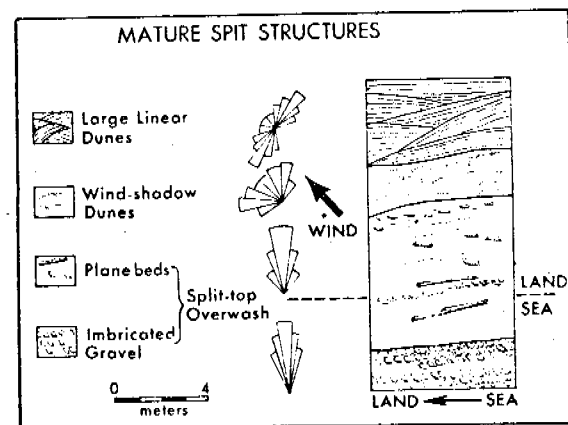
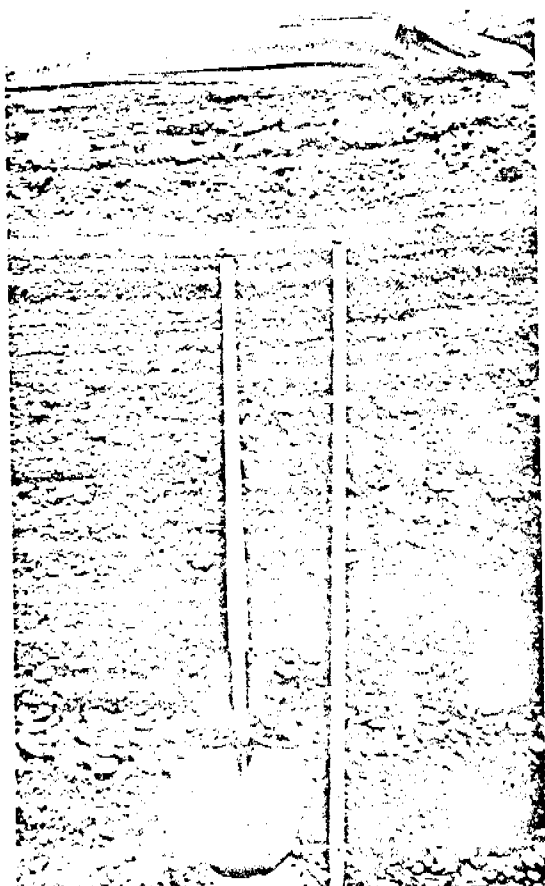


Figure 132. Typical stratigraphic sequence in mature spit complexes on the beach-ridge plains of southeast Alaska.

Figure 131. Vertical section of eroded beach ridge (located by arrow on Fig. 130), showing dominance of flat-bedded, spit-top overwash deposition. Face of cut is parallel with beach. View looks landward. Sand at top of section is aeolian (wind-shadow dune) deposit.

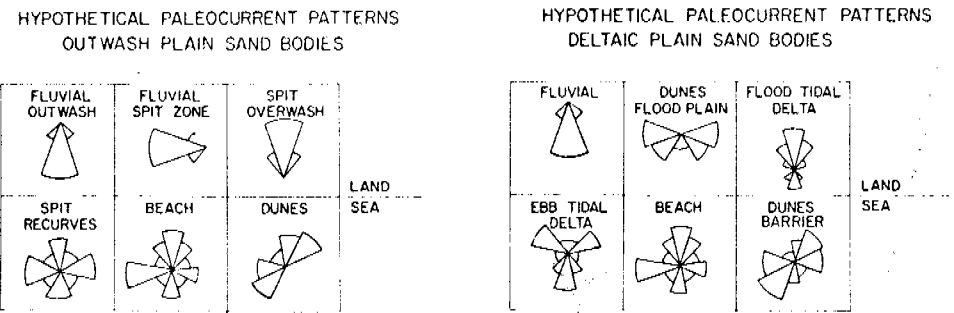


Figure 133. Hypothetical paleocurrent rose diagrams for the individual components of the outwash plain and deltaic plain depositional systems of southeast Alaska.

#### Barrier Island Shoreline

Sediments. - The sands of the barrier islands are mineralogically immature, averaging about 50% quartz and 50% metamorphic rock fragments (Fig. 129A). They are moderately sorted, medium and fine-grained sands.

Geomorphology. - These mesotidal barrier islands conform well to the drumstick model discussed earlier. The geomorphology of the islands is illustrated in Figure 134. Four systematic east to west changes in the barrier island system are apparent:

- (1) The downdrift offset increases in an east to west direction, except at the westernmost spit, which is anchored to bedrock;
- (2) The size of the ebb-tidal delta increases from east to west.
- (3) Inlet width increases from east to west.
- (4) The drumstick shape of the barriers becomes more pronounced in a westerly direction.

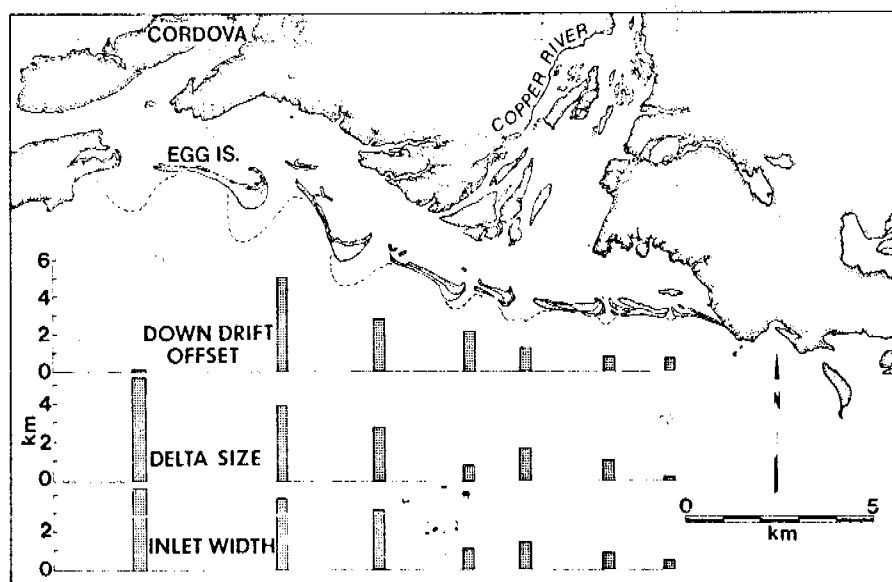


Figure 134. Barrier islands of the Copper River delta.

These changes are thought to be brought about by two interrelated factors. The river is rapidly filling in the eastern portion of the estuarine system, hence smaller tidal prisms and smaller ebb-tidal deltas are developed on the east side of the delta. A 20-km long island, Kayak Island (see Fig. 127), is located to the east of the delta, which partially protects the eastern end of the delta from the dominant southeasterly waves. Therefore, it is the western part of the delta that is more strongly affected by the oblique wave approach of the dominant waves. Therefore, the effect of wave refraction around the ebb-tidal deltas is greater on the west side of the delta. The drumstick shape of the barriers becomes more accentuated as the wave refraction increases.

These barrier islands have undergone some remarkable changes in the past twelve years. They were uplifted 3 m by the March 1964 earthquake. Since that time, they have largely prograded. Data for Egg Island (Figs. 135 and 136) illustrate these changes. A wave-cut scarp on a permanent profile at the east end of the island (EG-1; Fig. 135) eroded 40 m between February, 1970 and May, 1975. On the other hand, station EG-4, which is located at the widest point of the updrift bulge of the island, prograded 300 m during that same time. This process of overall aggradation of the barrier downdrift of the inlet accentuated the drumstick shape of the barrier. The process of downdrift accretion is illustrated by the photographs in Figure 136.

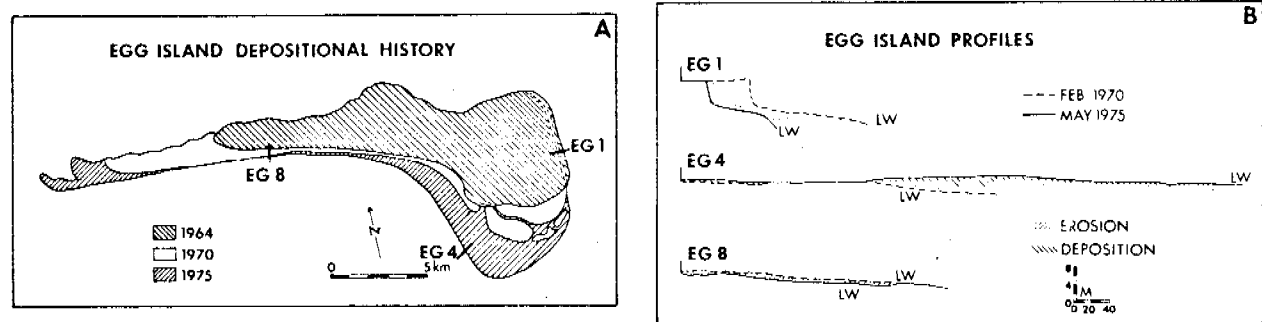


Figure 135. Changes of Egg Island, Copper River delta, Alaska, after the March, 1964 earthquake, which raised the delta 3 m. Note continual accentuation of the drumstick shape of the island through time.

Depositional facies. - The depositional facies of the barrier islands of the Copper River delta are very similar to those described for the mesotidal barriers along the east coast. There are differences in the details, because of differences in climate and sediment supply, but the general patterns are similar. Hypothetical paleocurrent rose diagrams for the delta system are given in Figure 133. Six units are described:

- (1) Fluvial-braided stream flowing perpendicular to the depositional strike. High gradient, mixed sand and gravel.
- (2) Dunes (flood plain) - adiabatic winds blow down the river canyon in winter (winds 50-100 mph common) forming huge longitudinal dunes on the flood plain. Large-scale bimodal crossbedding formed.
- (3) Flood-tidal delta - same as other mesotidal areas. Not well-developed in some inlets.
- (4) Ebb-tidal delta - same as other mesotidal areas.

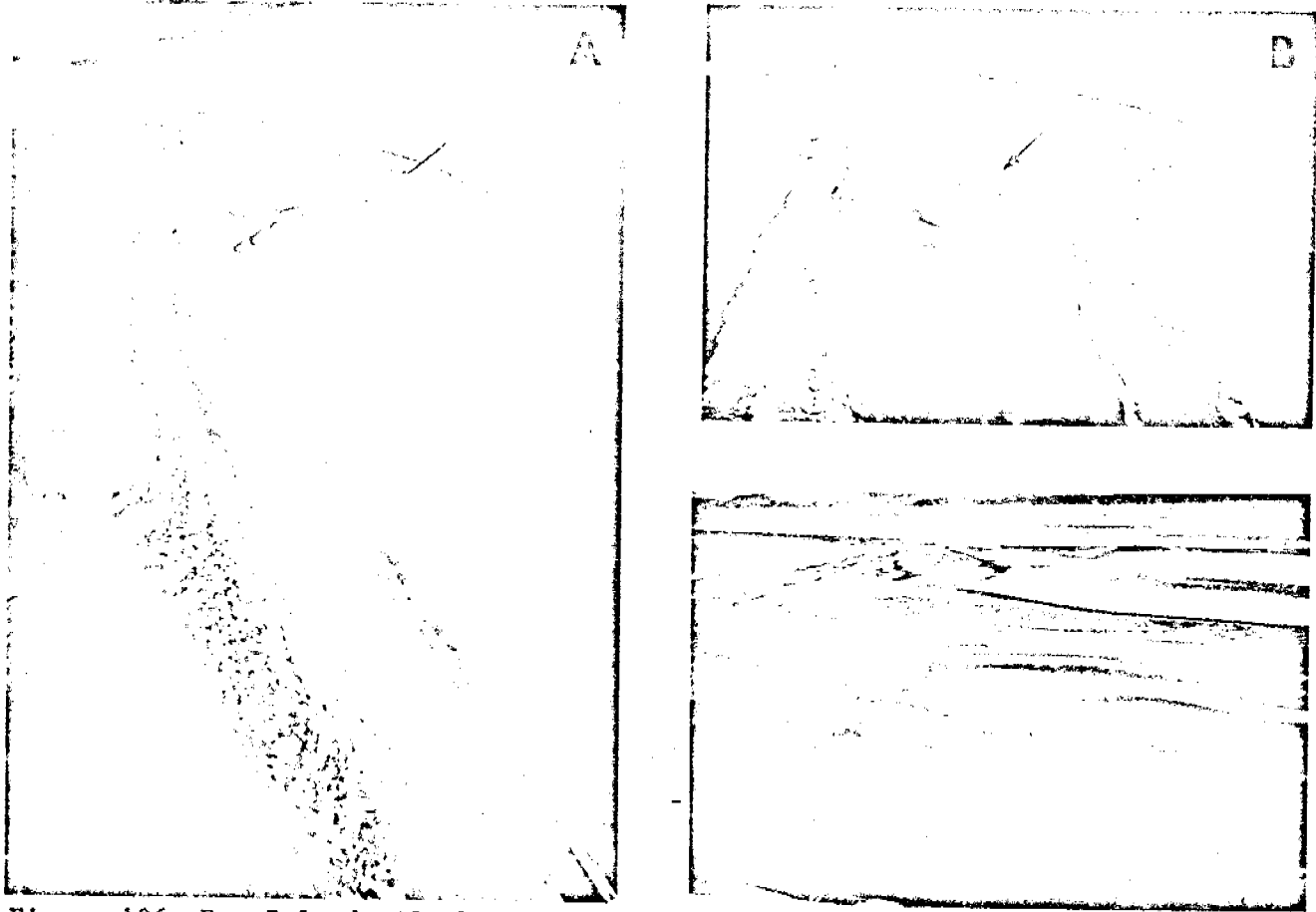


Figure 136. Egg Island, Alaska. A. Low-tide view taken in June, 1971. B. Low-tide view of east end of Egg Island taken in May, 1975. Arrow points to same sand bar as the one indicated by the arrow in A. This beach accreted 300 m between February, 1970 and May, 1975. C. Multiple intertidal ridges welding to the beach at station EG-4 (located in Fig. 135; near position of arrow in B). Low-tide photograph taken in summer of 1969 (by Stewart C. Farrell).

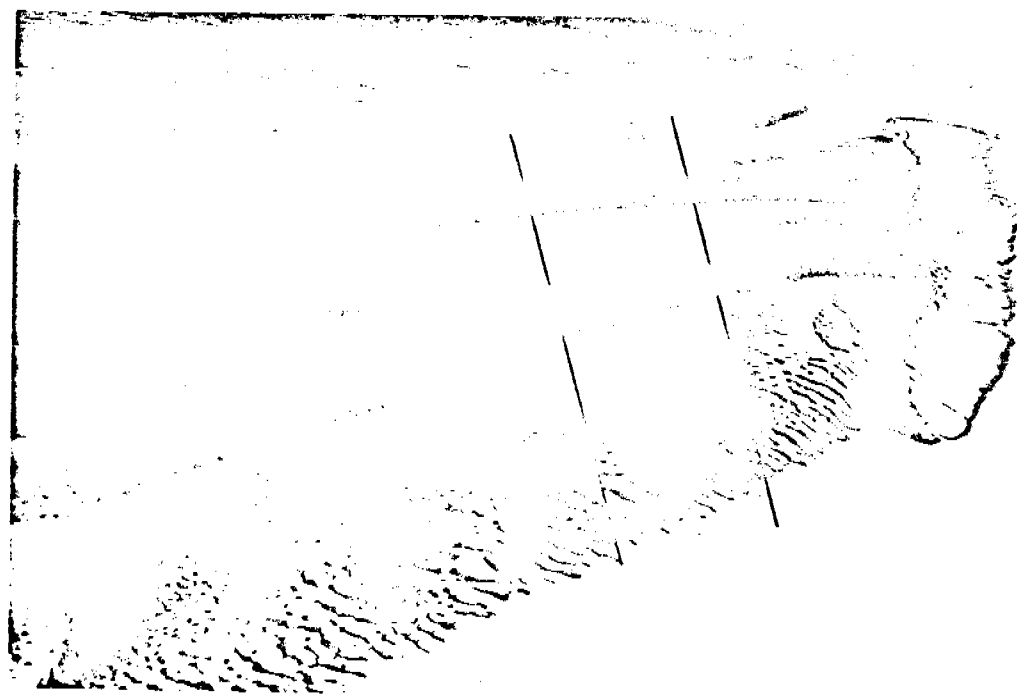


Figure 137. Low-spring tide view of beach near inlet of Softuk Bar, Copper River delta, Alaska. Lines indicate area mapped in Figure 138.

- (5) Beach - very similar to other mesotidal areas. Figures 137 and 138 illustrate bedforms at a beach station located near an inlet.
- (6) Barrier dunes - Mostly wind-shadow dunes. Bimodal crossbedding.

### CONCLUSIONS

This depositional complex, formed along a glaciated, collision coast, shows some surprising similarities to trailing edge shorelines. The barrier island complex is quite similar to other mesotidal barrier islands (e.g., New England and South Carolina). The major differences occur in the outwash plain areas, which are coarse-grained (gravel and sand) and dominated by flat-bed deposition.

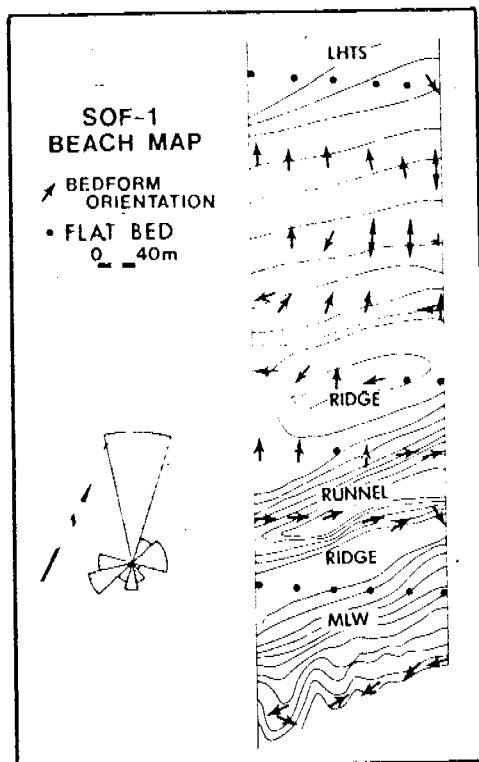


Figure 138. Map of 150m-wide section of the intertidal zone of beach at Softuk bar (located in Figure 137). Topography shows two ridge-and-runnel systems (compare with photograph, Fig. 137; LHTS = last high tide swash; MLW = mean low water). Orientation of bedforms indicated. Trimodal pattern is a result of alongshore flow (mostly megaripples) in runnels and wave uprush flow (mostly asymmetrical, linear ripples) on the upper half of the beach.

## E. SELECTED BIBLIOGRAPHY ON TERRIGENOUS CLASTIC DEPOSITIONAL ENVIRONMENTS

### General References

- \*Allen, J. R. L., 1963, Henry Clifton Sorby and the sedimentary structures of sands and sandstones in relation to flow conditions: *Geol. en. Mijnb.*, V. 42, p. 223-228.
- , 1966, On bedforms and paleocurrents: *Sedimentology*, V. 6, p. 163-190.
- , 1967, Depth indicators of clastic sequences, in: Hallam, E. A., *Depth indicators in marine sedimentary environments: Marine Geology*, Sp. Issue, V. 5, No. 5/6, p. 429-46.
- , 1968, Current ripples - their relation to patterns of water and sediment motion: North-Holland Publ. Comp., Amsterdam, Holland, 433 p.
- , 1970, *Physical processes of sedimentation - an introduction*: G. Allen and Unwin, London, England, 248 p.
- Barrell, J., 1906, Relative geologic importance of continental, littoral, and marine sedimentation: *Jour. Geol.*, V. 14, p. 316-362, 430-457, 524-568.
- Bernard, H. A., et al., 1970, Recent sediments of southeast Texas--a field guide to the Brazos alluvial and deltaic plains and the Galveston Island complex: Bur. Econ. Geology Guidebook 11, Univ. Texas, Austin, Texas, 67 p.
- \*Blatt, H., Middleton, G. V., and Murray, R. C., 1972, *Origin of sedimentary rocks*: Prentice Hall, Englewood Cliffs, N. J., 634 p.
- Chien, H. Y., 1967, *Hydraulics of rivers and deltas*: Ph.D. Dissertation, Colorado State Univ., Fort Collins, Colorado, 176 p.
- Conybeare, C.E.B., Crook, K.A.W., 1962, Manual of sedimentary structures: Bureau of Mineral Resources, Geology and Geophysics, Canberra A.C.T. Bull. no. 102, 327 p.
- Cornish, V., 1914, *Waves of sand and snow*: T. F. Unwin, London, England, 383 p.
- Crosby, E. J., 1972, Classification of sedimentary environments: in Ridgway, J.K., Hamblin, W.K., eds., *Recognition of ancient sedimentary environments*, SEPM Special Pub. No. 16, p. 4-11.
- Fisher, W.L., and Brown, L. F., 1972, Clastic depositional systems--a genetic approach to facies analysis: Bur. of Econ. Geol., Univ. of Texas at Austin, 211 p.
- , and McGowen, J. H., 1969, Depositional systems in Wilcox Group (Eocene) of Texas and their relation to occurrence of oil and gas: Am Assoc. of Petroleum Geologists Bull., V. 53, p. 30-54.
- Folk, R. L., 1966, A review of grain-size parameters: *Sedimentology*, V. 6, p. 73-93.
- \*Folk, R. L., 1968, *Petrology of sedimentary rocks*: Hemphill's, Austin, Texas.
- Frey, R. W., 1971, Ichnology--the study of fossil and recent lebensspuren: in Perkins, B. F., ed., *Trace fossils*. A field guide to selected localities in Pennsylvanian, Permian, Cretaceous and Tertiary of Texas and related papers: Louisiana State University School of Geosciences Misc. Pub., No. 71-1, Baton Rouge, La., p. 91-125.
- \*Friedman, G. M., 1961, Distinction between dune, beach and river sands from their textural characteristics: *Jour. Sed. Petrology*, V. 31, p. 514-529.
- Gilbert, G. K., 1899, Ripple marks and cross-bedding: *Geol. Soc. Am. Bull.*, V. 10, p. 135-140.
- , 1914, The transportation of debris by running water: U.S. Geol. Surv. Profess. Papers, V. 86, 263 p.
- \*Glenne, K. W., 1970, *Desert sedimentary environments*: Devel. in *Sedimentology*, No. 14, Elsevier, Amsterdam, 222 p.
- Gwynn, V. E., 1964, Deduction of flow regime from bedding characteristics in conglomerates and sandstones: *Jour. Sed. Petrology*, V. 34, p. 656-658.
- Harms, J. C., 1969, Hydraulic significance of some sand ripples: *Geol. Soc. Am. Bull.*, V. 80, p. 363-96.
- , 1974, *Depositional environments as interpreted from primary sedimentary structures and stratification sequences*: Lecture Notes, SEPM Short Course No. 7, Dallas, Texas, 161 p.
- \*Imbrie, J., and Buchanan, H., 1965, *Sedimentary structures in modern carbonate sands of the Bahamas*: in Middleton, G. V., ed., SEPM Special Pub. No. 12, Primary Sedimentary Structures and their Hydrodynamic Interpretation, p. 149-172.
- Inman, D. L., 1952, Measures for describing the size distribution of sediments: *J. Sed. Petrology*, V. 22, p. 125-145.
- Jopling, A. V., 1965, Hydraulic factors and the shape of laminae: *J. Sed. Petrology*, V. 35, p. 777-791.
- , Richardson, E. V., 1966, Backset bedding developed in shooting flow in laboratory experiments: *J. Sed. Petrology*, V. 36, p. 821-825.
- Klein, G. de V., 1967, Paleocurrent analysis in relation to modern sediment dispersal patterns: *Bull. Am. Assoc. Petrol. Geologists*, V. 51, p. 366-382.
- , 1975, Sandstone depositional models for explanation for fossil fuels: Cont. Education Pub. Co., Champaign, Ill., 108 p.
- Kukel, Z., 1970, *Geology of recent sediments*: Academia, Prague, 490 p.
- \*Leblanc, R. J., 1972, *Geometry of sandstone reservoir bodies*: in Cook, T. D., ed., *Underground waste management and environmental implications*: Amer. Assoc. Petroleum Geologists Mem., 18, p. 133-190.
- McKee, E. D., Weir, G. W., 1953, Terminology for stratification and cross stratification in sedimentary rocks: *Geol. Soc. Am. Bull.*, V. 64, p. 381-390.
- , 1957, Primary structures in some recent sediments: Amer. Assoc. Petrol. Geol. Bull., V. 41, p. 1704-1747.
- \*Matthews, R. K., 1974, *Dynamic stratigraphy*: Prentice Hall, N. J., 367 p.
- \*Middleton, G. V., 1965, ed., *Primary sedimentary structures and their hydrodynamic interpretation*: Soc. Econ. Paleontologists Mineralogists Spec. Publ. 12, 265 p.
- , 1965, Antidune cross-bedding in a large flume: *J. Sed. Petrology*, V. 35, p. 922-927.
- \*Moore, D. G., and Scruton, P. G., 1957, Minor internal structures of some recent unconsolidated sediments: *Bull. Amer. Assoc. Petrol. Geol.*, V. 41, p. 2723-2751.
- Peterson, J. A., and Osmond, J. C., 1961, eds., *Geometry of sandstone bodies*: Amer. Assoc. Petrol. Geologists, Tulsa, 240 p.
- Pettijohn, F. J., Potter, P. E., 1964, *Atlas and glossary of primary sedimentary structures*: Springer-Verlag, New York, 618 p.
- \*Potter, P. E., 1967, Sand bodies and sedimentary environments: a review: *Bull. Amer. Assoc. Petrol. Geol.*, V. 51, p. 337-365.
- , and Pettijohn, F. J., 1963, *Paleocurrents and basin analysis*: Academic Press, New York, 296 p.
- , Steyer, R., 1972, *Sand and sandstone*: Springer-Verlag, New York, 618 p.
- \*Reineck, H. E., and Singh, I. B., 1973, *Depositional sedimentary environments*: Springer-Verlag, New York, 439 p.
- , Wunderlich, R., 1968, Classification and origin of flaser and lenticular bedding: *Sedimentology*, V. 11, p. 99-104.
- Rigby, J. K., and Hamblin, W. K., 1972, Recognition of ancient sedimentary environments: Soc. of Econ. Paleon. and Mineral., Special Pub. No. 16, 340 p.
- Russell, R. J., 1967, *River and delta morphology*: Technical report No. 52, Coastal Studies Institute, Louisiana State University, Baton Rouge, La., p. 1-55.
- , 1968, *Glossary of terms used in fluvial, deltaic, and coastal morphology and processes*: Tech. Report No. 63, Coastal Studies Institute, Louisiana State Univ., Baton Rouge, La., 97 p.
- \*Saxena, R. S., 1976, ed., *Sedimentary environments and hydrocarbons*: Short course sponsored by AAPG and NOGS May, 1976, 217 p.
- , and Klein, G. de V., 1974, eds., *Sandstone depositional models for exploration*: Geol. Soc. Continuing Education Seminar, New Orleans.
- Selley, R. C., 1970, *Ancient sedimentary environments*: Chapman & Hall, London, Eng., 237 p.
- \*Sorby, H. C., 1859, On the structure produced by the currents present during the deposition of stratified rocks: *The Geologist*, V. 2, p. 137-147.
- , 1908, On the application of quantitative methods to the study of the structure and history of rocks: *Geol. Soc. London, Quart. Jour.*, V. 64, p. 171-233.
- Spearling, D. R., 1975, *Summary sheets of sedimentary deposits*: Geol. Soc. America Pub. MC-8.
- Stanley, D. J., and Swift, D.J.P., 1974, eds., *The new concepts of continental margin sedimentation, II: sediment transport and its application to environmental management*: Lecture notes, AGI Short Course, 15-17 Nov., 1974, Key Biscayne, Fla., Part 1 and 2, 1155 p.
- Tricart, J., 1970, *Geomorphology of cold environments*: Macmillan, Edinburgh, 320 p.
- Twenhofel, W. H., 1950, *Principles of sedimentation*: McGraw-Hill, New York, 6/3 p.
- Visher, G. S., 1969, Grain size distributions and depositional processes: *Jour. Sed. Petrology*, V. 39, p. 1074-1106.
- Walther, J., 1924, *Das Gesetz der Wüstenbildung in Gegenwart und Vorzeit*: Quelle & Meyer, 4th ed., Leipzig, 421 p.

### Fluvial Depositional Environments

#### General References

- Allen, J. R. L., 1964, Studies of fluviatile sedimentation: six cyclothsems from the Lower Old Red Sandstone, Anglo-Welsh basin: *Sedimentology*, V. 3, p. 163-198.
- , 1965, A review of the origin and characteristics of Recent alluvial sediments: *Sedimentology*, V. 5, p. 38-191.
- Arnborg, L., 1958, The lower part of the River Angermanalven: I. *Publ. Geogr. Inst. Univ. Uppsala* 1, p. 181-247.
- Bersier, A., 1958, Sequences détritiques et divagations fluviales: *Ecol. Geol. Helv.*, V. 51, p. 854-893.
- Boersma, J. R., 1967, Remarkable types of mega cross-stratification in the fluviatile sequence of a subrecent distributary of the Rhine: *Ameroneden: Geol. Mijnbouw*, The Netherlands, V. 46, p. 217-235.
- \*Brown, L. F., Cleaves, A. W., and Irkxleben, A. W., 1973, Pennsylvanian depositional systems in north-central Texas: *Geol. Soc. Amer. Guidebook* No. 14, Annual Meeting, 1973, 122 p.
- Brush, L. M., 1965, Sediment sorting in alluvial channels: in Middleton, G. V., ed., *Primary sedimentary structures and their hydrodynamic interpretation*: Spec. Publ. 12, Soc. Econ. Paleontol. Mineral., Tulsa, Okla., p. 25-33.
- Engelund, F., Hansen, E., 1966, Investigations of flow in alluvial streams: *Acta Polytechnica Scand. Civil. Eng. Bldg. Construct. Ser.*, V. 35, p. 1-100.
- Folk, R. L., Wurd, W., 1957, Brazos River bar: A study in the significance of grain size parameters: *J. Sed. Petrology*, V. 27, 3-26.
- Glenn, J. L., Dahl, A. R., 1959, Characteristics and distribution of some Missouri River deposits: *Proc. Iowa Acad. Sci.*, V. 66, p. 302-311.
- Guy, H. P., et al., 1966, Summary of alluvial channel data from flume experiments, 1956-61: U. S. Geol. Survey Prof. Paper 462-I, p. II-196.
- Harms, J. C., Fahnestock, R. K., 1965, Stratification, bed forms and flow phenomena (with an example from the Rio Grande): *Soc. Econ. Paleontologists Mineralogists Spec. Publ.*, V. 12, p. 84-115.
- Hjulstrom, F., 1935, Studies of the morphological activity of rivers as illustrated by the River Fyrish: *Geol. Inst. Uppsala Bull.*, V. 25, p. 25, 221-527.
- Jopling, A. V., 1967, Origin of laminae deposited by the movement of ripples along a streambed: A laboratory study: *J. Geol.*, V. 75, p. 297-307.
- Karcz, J., 1972, Sedimentary structures formed by flash floods in southern Israel: *Sediment. Geol.*, V. 7, p. 161-187.
- Kennedy, J. F., 1961, Stationary waves and antidunes in alluvial channels: W. M. Keck Lab. Hydraulics Water Resources Rep. KH-R-2, Cal. Inst. Techn., Pasadena, 146 p.
- \*Kennedy, J. F., 1968, The formation of sediment ripples, dunes, and antidunes: *Ann. Rev. Fluid Mech.*, V. 1, p. 147-168.
- Lattman, L. H., 1960, Cross-section of a flood plain in a moist region of moderate relief: *J. Sed. Petrology*, V. 30, p. 275-282.
- Leliavsky, S., 1965, An introduction to fluvial hydraulics: Constable, London, 257 p.
- Leopold, L. B., and Maddock, T., Jr., 1953, The hydraulic geometry of stream channels and some physiographic implications: U. S. Geol. Survey Prof. Paper 252, 57 p.
- , and Wolman, M. G., 1957, River channel patterns: braided, meandering, and straight: U. S. Geol. Survey Prof. Paper 287-B, p. 39-85.
- , and Miller, J. P., Jr., 1964, Fluvial processes in geomorphology: W. H. Freeman & Co., San Francisco, 522 p.
- McKee, E. D., 1938, Original structures in Colorado River flood plain deposits of the Grand Canyon: *J. Sed. Petrology*, V. 8, p. 77-83.
- , Crosby, E. J., Berryhill, H. L., 1967, Flood deposits, Bijou Creek, Colorado, June 1965: *J. Sed. Petrology*, V. 37, p. 829-851.
- Melton, M. A., 1965, The geomorphic and Paleoceanic significance of alluvial deposits in southern Arizona: *J. Geol.*, V. 73, p. 1-38.
- Morisawa, M., 1968, Streams, their dynamics and morphology: McGraw-Hill, N. Y., 175 p.
- , 1973, ed., *Fluvial geomorphology*: Proceedings Volume of the Fourth Annual Geomorphology Symposia Series, Binghamton, N. Y., Sept. 27-28, 1973, 314 p.
- Picard, M. D., and High, L. R., Jr., 1973, Sedimentary structures of ephemeral streams: Elsevier Scientific Publ. Co., Amsterdam, 223 p.
- Russell, R. J., 1954, Alluvial morphology of Anatolian rivers: *Ann. Assoc. Am. Geogr.*, V. 44, p. 363-391.
- , 1957, Aspects of alluvial morphology: in The earth, its crust and its atmosphere--Geomorphological and geophysical studies presented to Professor J. B. L. Hol: E. J. Brill, Leiden, Netherlands, p. 163-174.
- Sarkar, R. J., Basumatirik, S., 1964, Morphology, structure, and evolution of a channel island in the Barakar River, Barakar, West Bengal: *J. Sed. Petrology*, V. 38, p. 747-754.

\*References cited in lecture notes.

# GEOMORPHOLOGY OF THE SOUTHERN COAST OF ALASKA

Miles O. Hayes  
Christopher H. Ruby  
Michael F. Stephen  
Stephen J. Wilson

Coastal Research Division  
Department of Geology  
University of South Carolina  
Columbia, S. C. 29208

## ABSTRACT

The shoreline of southern Alaska is a narrow coastal plain dominated by large glaciers, periodic earthquake activity, and strong extratropical cyclones. Studies on the coastal geomorphology and sediments carried out in 1969-71 and in the summer of 1975 were directed at defining geological hazards with respect to developing shore facilities for OCS oil exploration activities. Most of the shoreline was found to undergo rapid changes and experience a variety of serious environmental hazards. The safest potential port areas are located inside Icy Bay and Yakutat Bay. The coastal areas in the vicinity of the Malaspina Glacier and the Copper River delta are examples of the two principal shoreline types (glacial outwash plain and deltaic).

The coastal area surrounding the Malaspina Glacier, the largest piedmont glacier in the world, was classified into 5 categories on the basis of its geomorphology, sediments, and local glacial history:

1. Regional retreating coast: This area, which is located at the mouth of Icy Bay, is eroding rapidly (approximately 1.5 km since 1900) as a result of retreat of a glacier (up the bay) a distance of over 40 km since 1900. Consequently, it should not be developed.
2. Prograding spits: Sandy spits that have built into either side of Icy Bay since the retreat of the glacier are also unstable because of the general recession of the shoreline as a result of erosion at the mouth of the bay.
3. Abandoned glacial coasts: These areas, located on the inner eastern shores of Icy Bay and Yakutat Bay, are coastlines of relatively low wave energy composed of abandoned glacial tills, kame terraces, and outwash sediments. These are the most stable and least hazardous areas on the southern Alaska coast.
4. Actively eroding glacial margins: This area, located at Sitkagi Bluffs on the southernmost terminus of the Malaspina Glacier, is an eroding scarp of glacial till jutting into the Gulf of Alaska.
5. Glacial outwash coasts: These shorelines are highly variable and are usually dominated by prograding spits composed of sand and gravel.

The shoreline of the Copper River delta is made up of a complex of six fine-grained mesotidal barrier islands separated by tidal inlets that increase in size in a westerly direction. The islands have undergone major readjustments since the Good Friday earthquake of 1964, which raised the area 3 m. For example,

Egg Island has increased significantly in size; shoreline accretion of 400 m between February 1970 and May 1975 was measured at a site on the updrift end of the island. The patterns of erosion and deposition on the islands conform to those of the barrier island drumstick model developed during studies of the South Carolina coast.

## INTRODUCTION

The southern coast of Alaska (Fig. 1) is an exceptionally dynamic area. Intense tectonic activity, large waves, strong tidal currents, highly variable winds, and active glaciation interact to produce one of the most rugged and variable coastlines in the world. The Chugach and St. Elias mountains, an extension of the Cordilleran Mountain system, control the gross orientation of the coastline. Fronting these mountains is a narrow coastal plain consisting of glacial and fluvial deposits undergoing active modification by tectonic, aeolian, and marine processes. Rapid advance and retreat of the numerous glaciers that border the coastal plain has caused sudden and dramatic shifts in loci of erosion and deposition along the beaches.

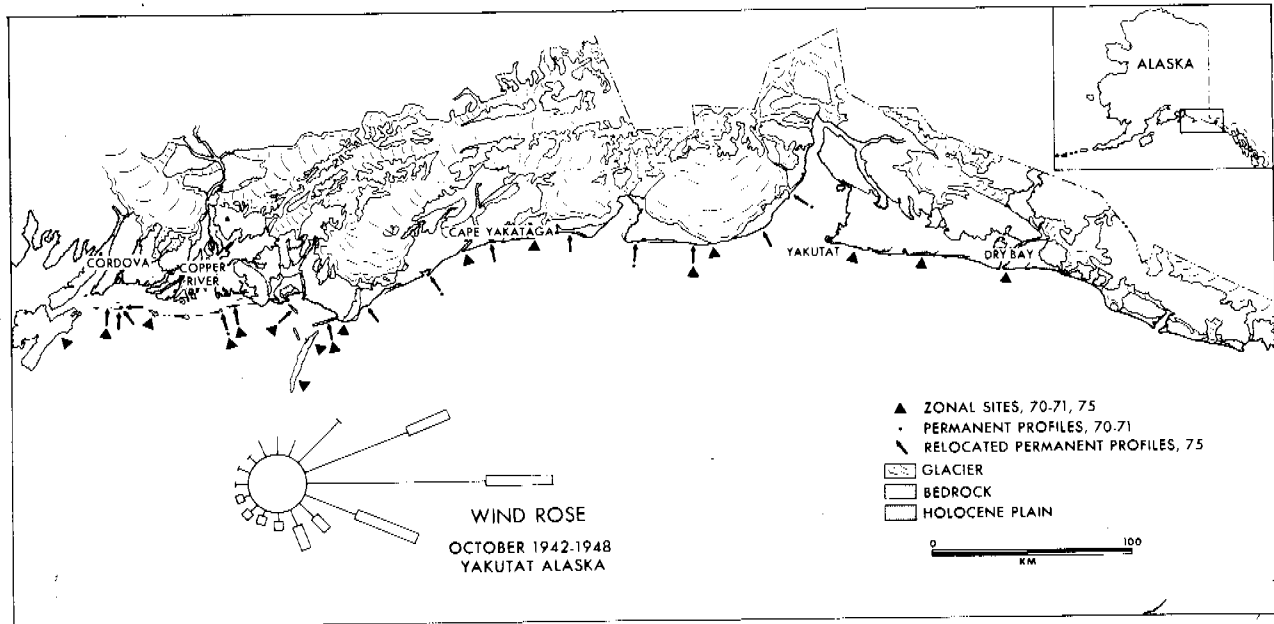


Figure 1. Study area. Note distribution of Holocene coastal plain (max. width = 35 km). Wind rose for Yakutat shows a dominance of easterly winds.

The coastal mountains, formed in response to subduction of the Pacific plate along this collision-type coast, are undergoing rapid uplift. Frequent earthquakes result in large ground displacements. During a single earthquake in 1899, the head of Yakutat Bay was uplifted 15 m. The entire coastal zone of southern Alaska has been subject to modifications resulting from this rapid tectonic activity.

The morphology and sediments of the coastal plain shoreline of southern Alaska were studied on a reconnaissance basis in 1969-71. Fifteen permanent beach profiles were established, 18 detailed specific site studies (zonal studies) were carried out (Fig. 1), and sediment samples were collected at 90 stations,

using a 4 km spacing. The area was revisited in the summer of 1975, during which time the permanent profiles were remeasured, and 99 beach profiling stations were occupied in the central portion of the study area (in the vicinity of the Malaspina Glacier). Using a 15 cm coring tube, sediment samples were taken at 3 stations at each of the 99 profile locations. The samples were then analyzed for grain size with a settling tube. Approximately 10,000 ground and aerial photos were taken. They have been analyzed and compared to photos taken during the 1969-71 studies and also compared with vertical aerial photos from various sources.

Extratropical cyclones that generate southeasterly winds dominate the coastal processes. Wind frequency diagrams for the entire Gulf of Alaska area are shown in Figure 2 (from Nummedal and Stephen, 1976). These winds create wave energy flux patterns that trend from east to west in the study area (Fig. 3), and, consequently, generate a dominant east to west littoral sediment transport pattern (Fig. 4).

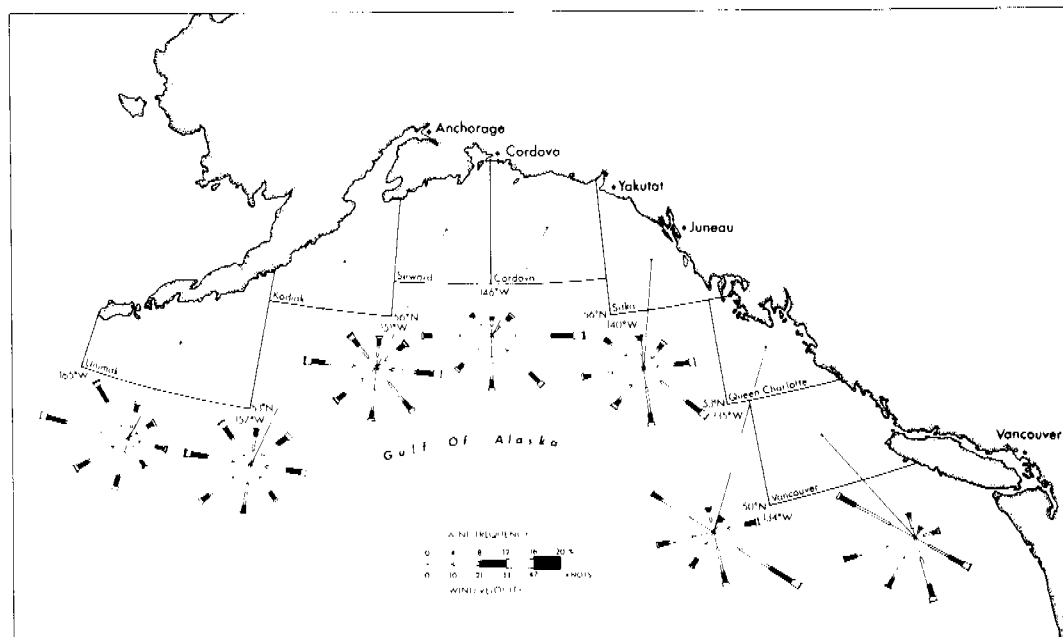


Figure 2. Wind frequency distributions for coastal data squares in the Gulf of Alaska. The diagrams are based on wind observations presented in Summary of Synoptic Meteorological Observations (U.S. Naval Weather Service Command, 1970). The dominant and prevailing winds are generally aligned parallel to the shoreline because of the temperature-induced pressure gradient along the coastal mountains. On the northeast coast of the Gulf, the dominant winds blow toward the northwest; on the northwest coast, they blow toward the east and northeast. (From Nummedal and Stephen, 1976; Fig. 13)

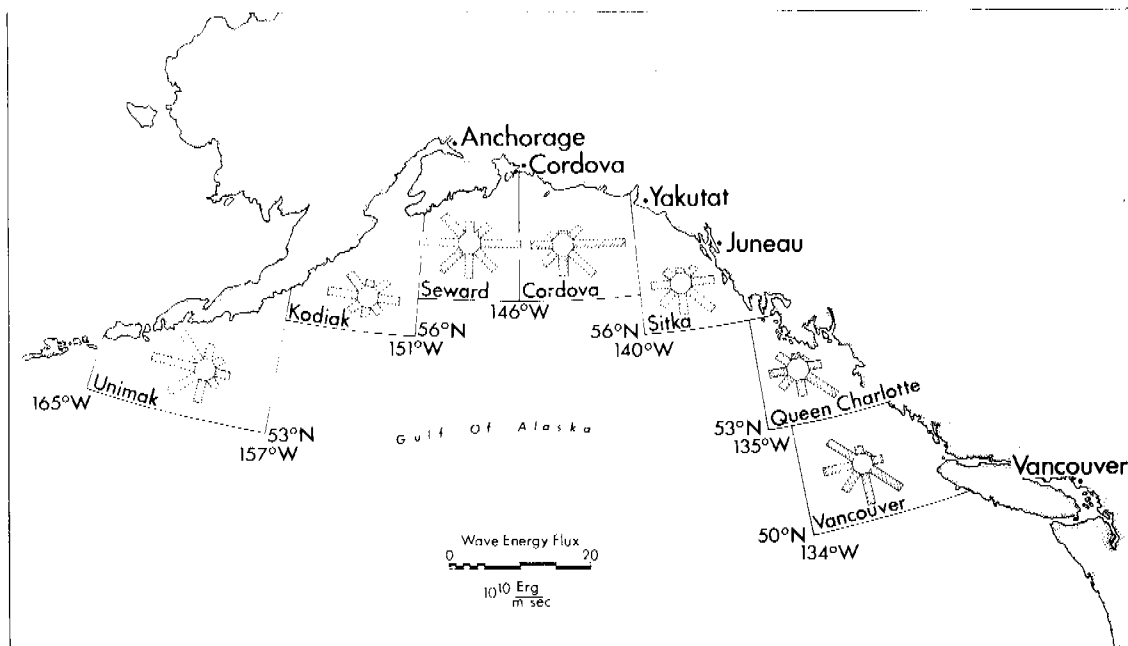


Figure 3. Wave energy flux distributions for the coastal areas of the Gulf of Alaska. The computations are based on deep water wave observations presented in Summary of Synoptic Meteorological Observations (U. S. Naval Weather Service Command, 1970). The wave energy flux is highest out of the southeast for the Vancouver, Queen Charlotte, and Sitka data squares, out of the east at Cordova, and out of the west at Seward, Kodiak, and Unimak. This pattern corresponds closely to that of the winds (Fig. 2). (From Nummedal and Stephen, 1976; Fig. 18)

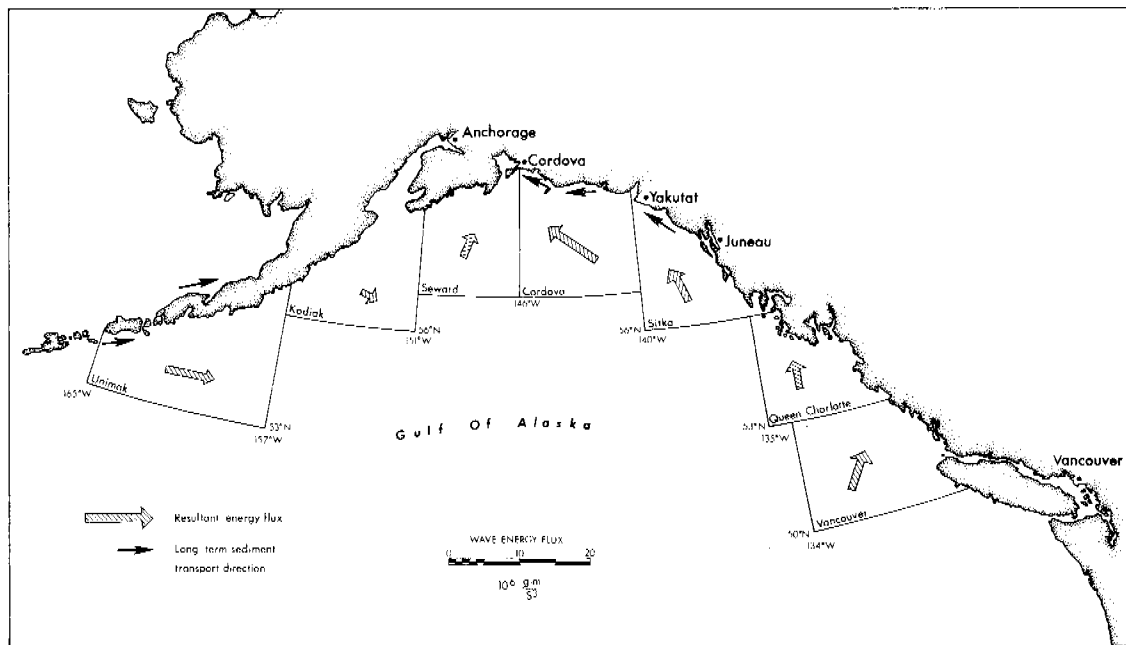


Figure 4. Direction of longshore sediment transportation based on large scale coastal geomorphic features and resultant wave energy flux distribution for the coastal areas of the Gulf of Alaska. Large scale coastal features used in establishing long-term transport directions include spits, inlet offsets, and crescentic embayments. The resultant wave energy flux is determined by vectorial addition of the distributions presented in Figure 3. Note the convergence of wave energy flux toward Prince William Sound. (From Nummedal and Stephen, 1976; Fig. 19)

The coastal morphology consists of (1) an outwash plain shoreline, which is a complex of outwash streams with downdrift beach-ridge plains, and (2) the delta of the Copper River, which has a seaward margin made up of mesotidal barrier islands. It is unusual to find a depositional shoreline of this magnitude (Fig. 1) on a collision coast. It owes its origin to the huge sediment output of glaciers that drain the largest ice field in North America, and to the sediments of the Copper River, which has a mean annual load of  $100 \pm 10^6$  metric tons (Reimnitz, 1966; see Table 1).

TABLE 1. Annual Sediment Load of the Copper River (Reimnitz, 1966)

WOOD CANYON	Suspended Load:	$66.0 \times 10^6$ metric tons
	Bed Load:	<u><math>9.9 \times 10^6</math> metric tons</u>
	Total:	$75.9 \times 10^6$ metric tons
DELTA	Total Load:	$100 \pm 10^6$ metric tons
<u>Comparisons:</u>		
COPPER RIVER (at delta)		$100 \pm 10^6$ metric tons
MISSISSIPPI RIVER		$450 \times 10^6$ metric tons
AMAZON RIVER		$347 \times 10^6$ metric tons

Figure 5 compares the beach sediments of the outwash plain depositional system with the beach sediments of the barrier islands of the Copper River delta. The outwash plain beaches are both texturally and mineralogically immature. All of the samples have very low percentages of quartz, being classified as litharenites (using scheme of Folk, 1974). The samples show a wide range of values of sorting and mean grain size (Fig. 5).

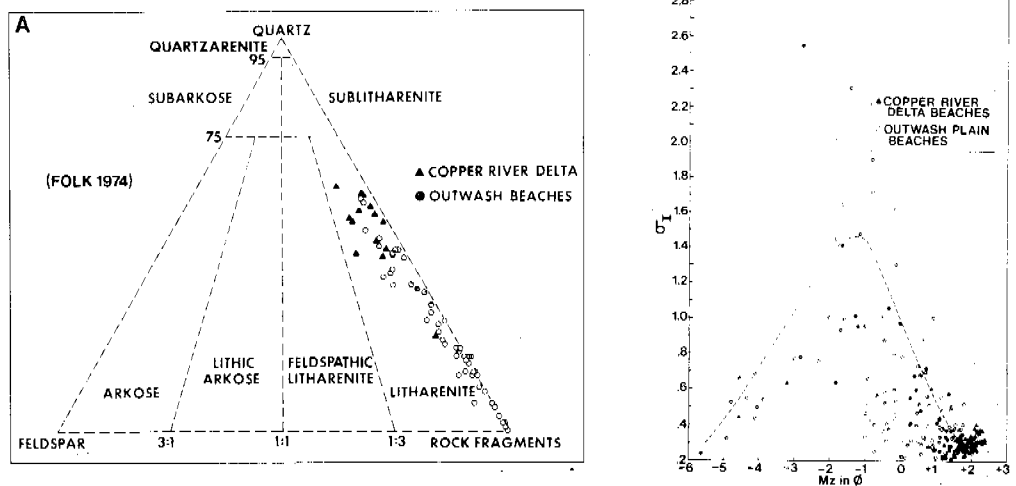


Figure 5. A. Composition of outwash plain and Copper River delta barrier island sediments. All samples are litharenites, with the barrier island sands being more quartz rich. B. Mean grain size ( $M_z$ ; Folk, 1974) vs. sorting ( $\sigma_I$ ). Copper River delta beaches are moderately sorted medium to fine sand; whereas the outwash plain sediments show a wide range in size and sorting.

## MALASPINA AREA

### Introduction

Study during the summer of 1975 was focused in the vicinity of the Malaspina Glacier (Fig. 6). The project was designed to provide process information and to continue our study of the coastal morphology and sedimentation. Beach profiles were measured at 3 km intervals over the entire study area (Fig. 6) in order to assess regional trends in beach morphology. The results of these studies allow the subdivision of the coast into five principal geomorphic type areas which are closely related to the local glacial history.

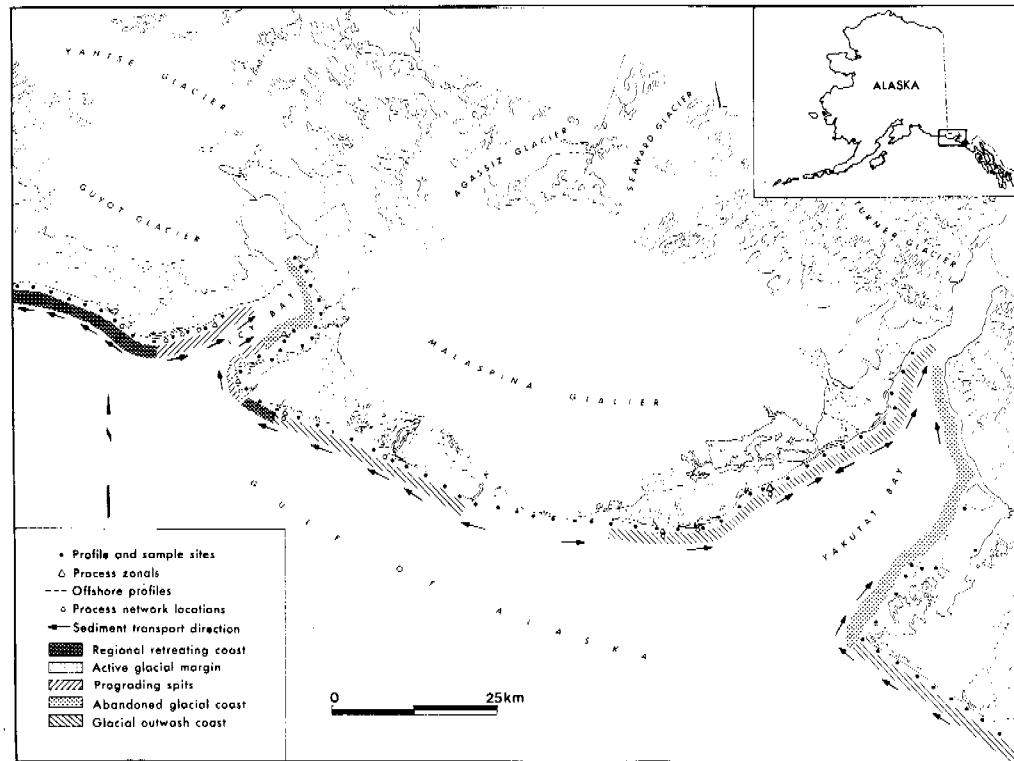


Figure 6. Location of area studied in summer of 1975. Arrows indicate dominant longshore sediment transport direction on the basis of combined morphological and process data. The different classes of shoreline types and location of study sites are also indicated.

### Regional retreating coast

This area is located at the mouth of and downdrift of Icy Bay (Fig. 6). The recent retreat of the Guyot Glacier up into Icy Bay resulted in a loss of sediment to this coastal section, causing widespread erosion (approximately 1.5 km since 1900). Beach profiles are generally flat with concave-upward upper beach faces backed by eroding scarps at the spring high-tide swash line (Fig. 7). Sediments are mixed sand and gravel. Heavily forested beach ridges, glacial outwash plains, and till areas on either side of Icy Bay are being cut back severely. Broad overwash terraces are advancing over low-lying areas. This area should be omitted from all considerations for shoreline development.

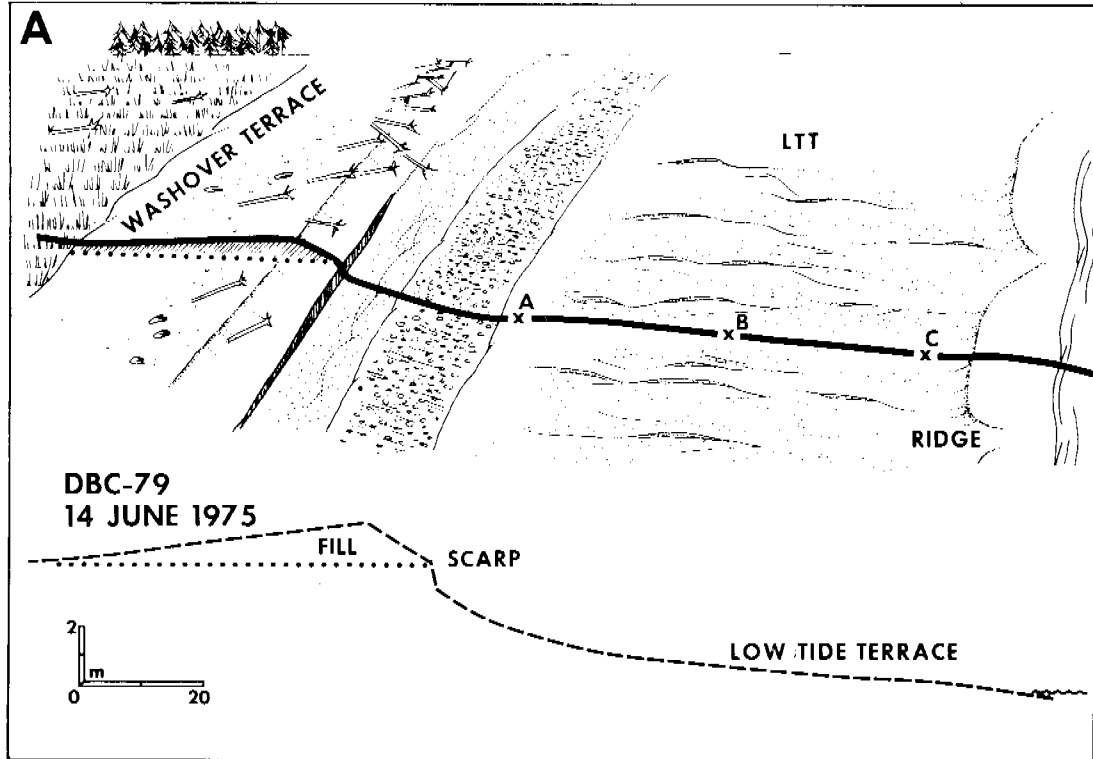


Figure 7. Regional retreating coast. A. Beach profile and sketch for station DBC-79, which is located approximately 5 km west of the entrance to Icy Bay (Fig. 6). Note the concave upward shape of the profile, the erosional scarp, and the developing washover terrace. LTT = low-tide terrace; A, B, C = sediment sampling localities. B. Station DBC-79 on 14 June 1975.



Figure 8. A. Riou Spit, a prograding sand spit at the eastern entrance to Icy Bay. Photo taken on 4 August 1975. B. Example of abandoned glacial shoreline, eastern margin of Yakutat Bay (Knight Island). Photo taken on 21 August 1975.

### Prograding spits

On either side of Icy Bay, sandy spits are prograding into deeper water as the shoreline around the mouth of the bay erodes. The largest, Riou Spit, is located on the east, or updrift, side of the Bay (Fig. 8A). Riou Spit is migrating both alongshore and landward because of recession of the shoreline adjacent to the bay. The beach profiles on the spits are relatively flat with broad berm-top overwash areas. These spit areas are considered to be quite unstable for development purposes because of their rapid rates of change and their exposure to open ocean waves.

### Abandoned glacial coasts

These areas, located on the inner eastern shores of Icy Bay and Yakutat Bay, are characterized by deposits of unconsolidated tills, kame terraces, and outwash sediments which supply abundant gravel to the beaches. An example is shown in Figure 8B. Profiles are very steep, short, and often have well-developed multiple cuspatate berms. High vegetated storm berms indicate infrequent but violent storms. Sediments are predominantly well-sorted and rounded gravel. Sand and gravel spits occur downdrift of till islands in Yakutat Bay. Because of their protected nature and slow rates of erosion and deposition, these are the most favorable areas available for the development of shore facilities.

### Actively eroding glacial margins

This area, located at Sitkagi Bluffs, on the southernmost terminus of the Malaspina Glacier, is an eroding scarp of glacial till on the shoreline of the Gulf of Alaska. Beach profiles in front of the Bluffs are extremely short and steep, backed by eroding till scarps (Fig. 9A). Beach material ranges from sand and angular gravels to large erratics left behind as the scarps retreat (Fig. 9B). These retreating scarps, and their adjacent boulder beaches, are virtually inaccessible for any kind of human activity at high tide.

### Glacial outwash coasts

These beaches are generally prograding, with abundant mixed sand and gravel spits trailing toward the west, except inside Yakutat Bay, where a major transport reversal occurs. Beach-ridge plains often develop downdrift of the major river mouths. Beach profiles are relatively flat with abundant ridge-and-runnel systems, resulting in a shoreline with a characteristic rhythmic topography. Typical examples of glacial outwash coasts are illustrated in Figure 10. When glacial sources are distant, sediments tend to have a high sand to gravel content. The beaches in these areas are relatively stable and are considered to be the second most desirable areas for shoreline development in southern Alaska.

### Process data

Process observations were obtained at two levels during July-August, 1975:

A) Process Network (Fig. 6). Regional process variability was determined by multiple observations during stable meteorological conditions.

MAL - 5

FIELD NOTES  
26 JULY 1970



Figure 9. Actively eroding glacial margins. A. Field sketch of profile Mal-5, located in front of the Malaspina glacier. B. Station Mal-5 (sketched in A) on 26 July 1970.

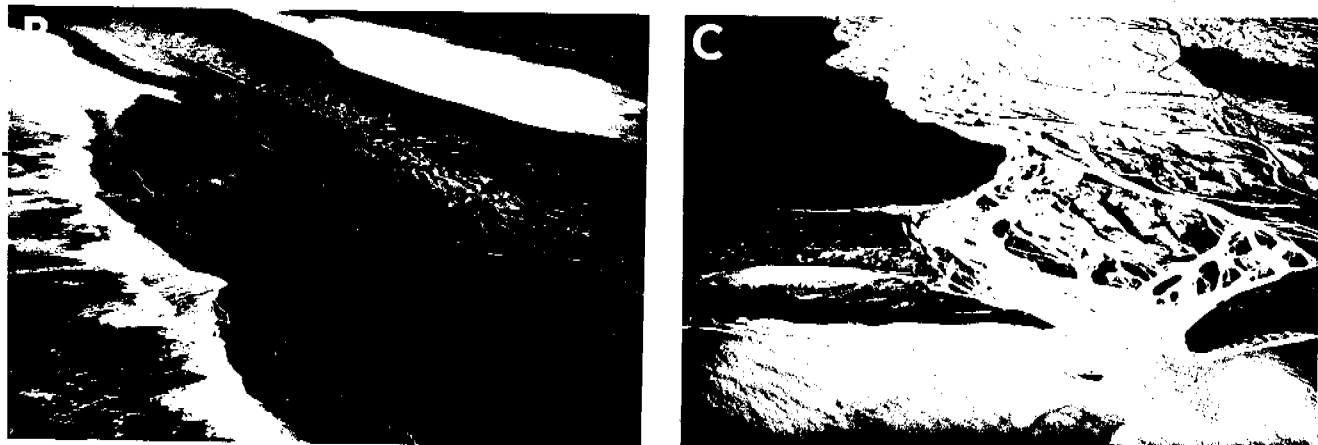
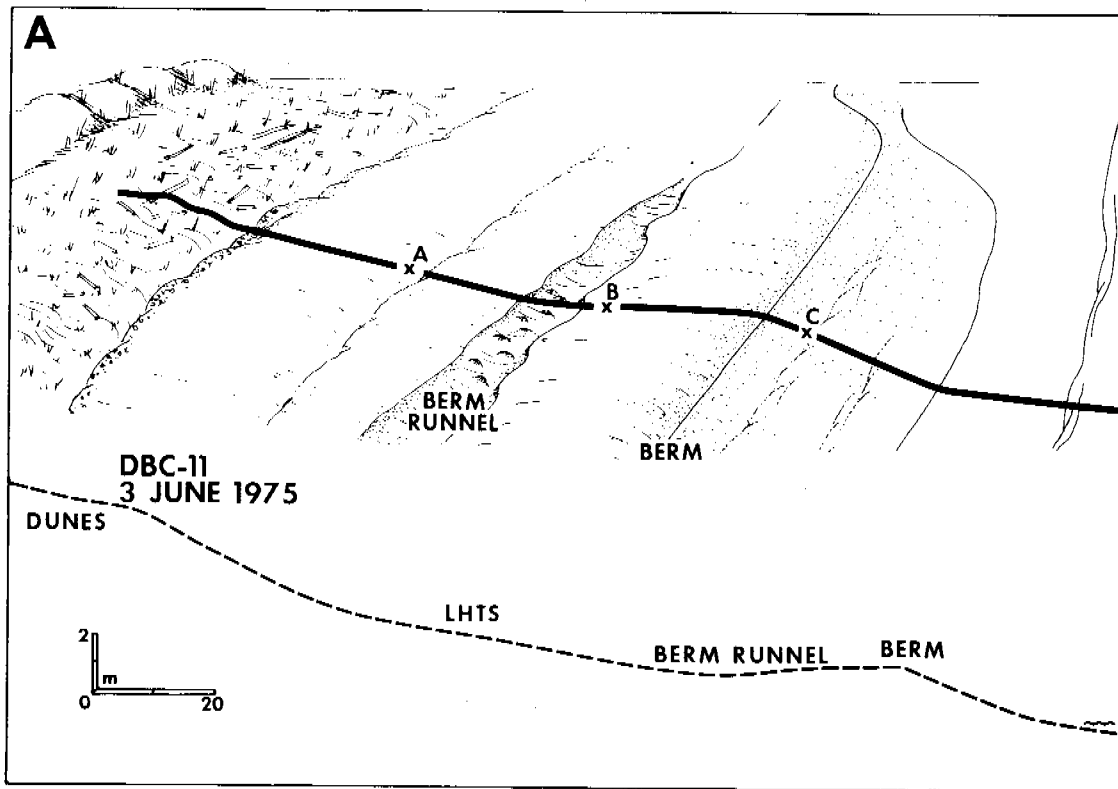


Figure 10. Glacial outwash coasts. A. Field sketch of station DBC-11, a fine-grained (sand dominant) spit on the outwash plain of the Yakutat foreland. B. Station DBC-11 on 3 June 1975. Note welded berm. C. Coarse-grained (gravel dominant) outwash plain near Malaspina Glacier. Photo taken in summer of 1970.

B) Six Process Zonals (Fig. 6). Continuous 48-hour monitoring of meteorological, wave, littoral, and morphological variability was maintained at single sites selected as representative of shoreline segments.

Regional process parameters document littoral transport in directions that correlate with regional morphology. Dominant south and southeast waves yielded sediment transport toward the west away from eroding till cliffs and from the mouths of outwash streams.

Process zonal measurements allowed documentation of the passage of a complete storm cycle. Commonly, two distinct wave trains were monitored. Under such conditions, drift directions and velocities were erratic and strong rip currents were prevalent. Dominant wave approach was a function of the path of low pressure systems moving through the Gulf of Alaska. Southerly waves were characteristic of calm conditions, and southeasterly waves were characteristic of storm conditions.

Breaker heights averaged 1.5 to 2.0 m, with a maximum measured height of 4 m recorded during a storm. Suspended sediment concentrations taken from the bore of plunging waves were as high as 150 gms/liter. Measured beach profiles revealed up to 15 cm of accretion to the beach face during one tidal cycle.

## COPPER RIVER DELTA AREA

### Introduction

The barrier island shoreline of the Copper River delta was uplifted 3 m by the Good Friday earthquake of March 1964 (Fig. 11). This has brought about many adjustments of the morphology of the islands in response to changes in the level of wave erosion and deposition. The sands of the barrier islands are mineralogically immature, averaging about 50% quartz and 50% metamorphic rock fragments (Fig. 5). They are moderately sorted, medium- and fine-grained sands.

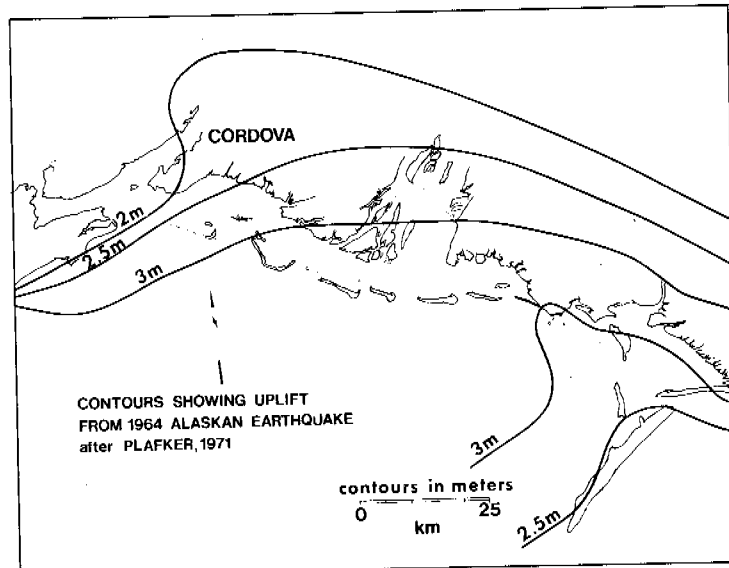


Figure 11. Uplift (in meters) of the Copper River delta area during the Good Friday earthquake of 1964.

## Mesotidal barrier islands

A tidal range of 3-4 m places the Copper River delta in the mesotidal class of Davies (1964). As has been pointed out elsewhere (Hayes et al., 1973; Hayes and Kana, 1976), mesotidal barrier islands have two distinctive morphological characteristics:

1. In coastal areas with dominant waves that approach the shoreline at an oblique angle, the tidal inlets commonly show downdrift offsets; that is, the barrier beach downdrift of the inlet protrudes further seaward than the one on the updrift side (Hayes et al., 1970). The tidal inlets of New Jersey, the Delmarva Peninsula, and South Carolina are good examples. The present downdrift offset at Price Inlet, S. C., which has changed from downdrift offset to updrift offset and back to downdrift offset again since 1941, is discussed in detail by FitzGerald (1976).
2. Many mesotidal barrier islands have a drumstick shape, with the bulbous part of the drumstick being located on the updrift side of the barrier (Fig. 12A). Drumstick-shaped mesotidal barrier islands from Alaska, the Netherlands, South Carolina, and Georgia are outlined in Figure 12B.

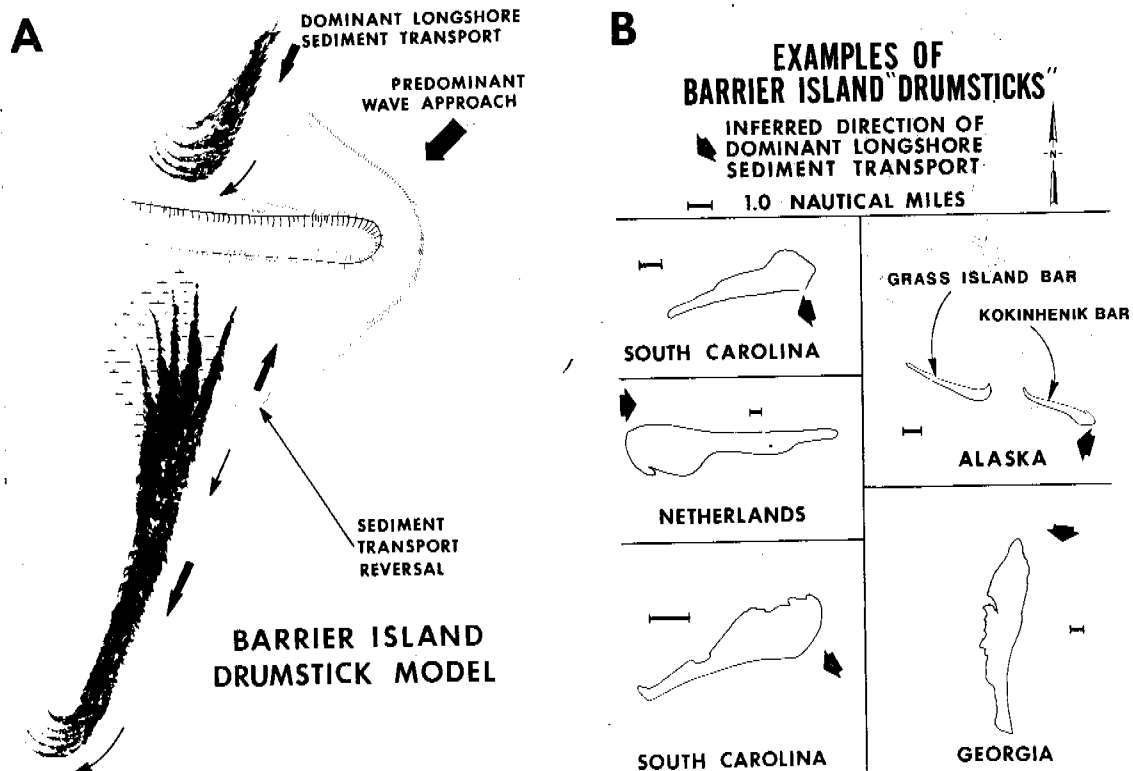


Figure 12. A. Barrier island drumstick model. B. Examples of barrier island "drumsticks" from South Carolina, Georgia, the Netherlands, and Alaska.

## Barrier islands of the Copper River delta

The mesotidal barrier islands of the Copper River delta conform well to the drumstick model discussed above. Four systematic east to west changes in the barrier island system are apparent (Fig. 13):

- (1) The downdrift offset increases in an east to west direction, except at the westernmost spit, which is anchored to bedrock;
- (2) The size of the ebb-tidal delta increases from east to west;
- (3) Inlet width increases from east to west; and
- (4) The drumstick shape of the barriers becomes more pronounced in a westerly direction.

These changes are thought to be brought about by two interrelated factors. The river is rapidly filling in the eastern portion of the estuarine system; hence, smaller tidal prisms and smaller ebb-tidal deltas are developed on the east side of the delta. A 20 km long island, Kayak Island (see Fig. 1), is located to the east of the delta, which partially protects the eastern end of the delta from the dominant southeasterly waves. It is, thus, the western part of the delta that is more strongly affected by the oblique wave approach of the dominant waves. Therefore, the effect of wave refraction around the ebb-tidal deltas is greater on the west side of the delta. The drumstick shape of the barriers becomes more accentuated as the wave refraction increases.

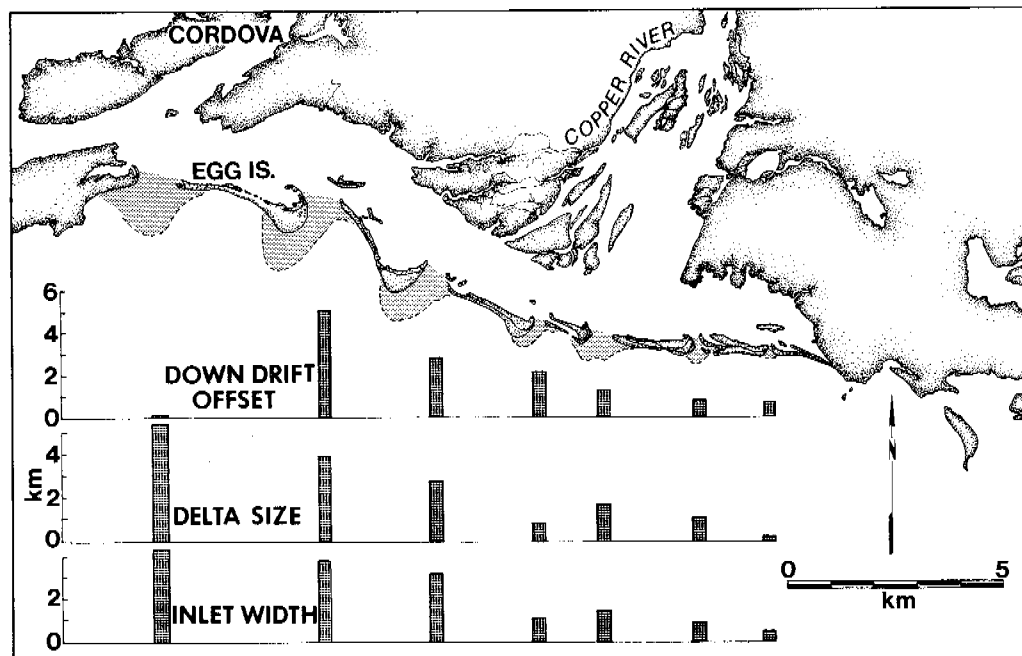


Figure 13. Barrier islands of the Copper River delta.

These barrier islands have undergone some remarkable changes in the past twelve years. They have largely prograded since they were uplifted by the March 1964 earthquake. Data for Egg Island (Figs. 14 and 15) illustrate these changes. A wave-cut scarp on a permanent profile at the east end of the island (EG-1; Fig. 14) eroded 56 m between February 1970 and May 1975. On the other hand, station EG-4, which is located at the widest point of the updrift bulge of the island, prograded 400 m during that same time. This process of overall aggradation of the barrier just downdrift of the inlet accentuated the drumstick shape of the barrier. This process of downdrift accretion is illustrated by the photographs in Figure 15.

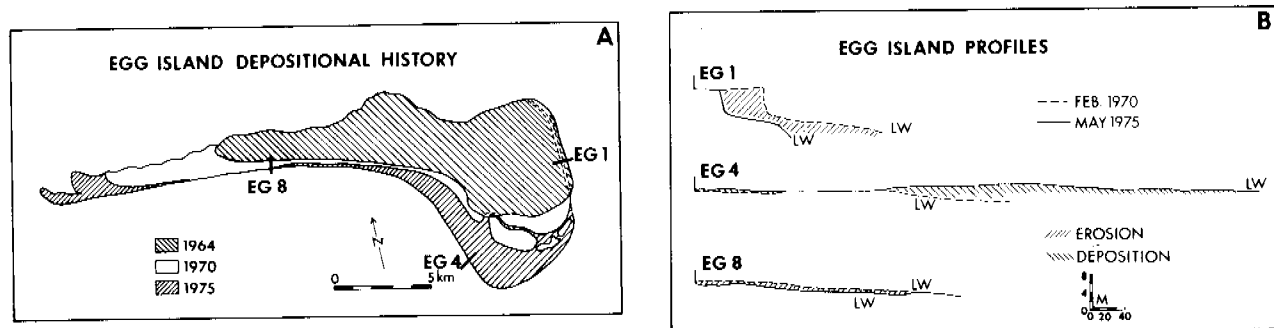


Figure 14. Changes of Egg Island, Copper River delta, Alaska, after the March 1964 earthquake, which raised the delta 3 m. Note continual accentuation of the drumstick shape of the island through time.

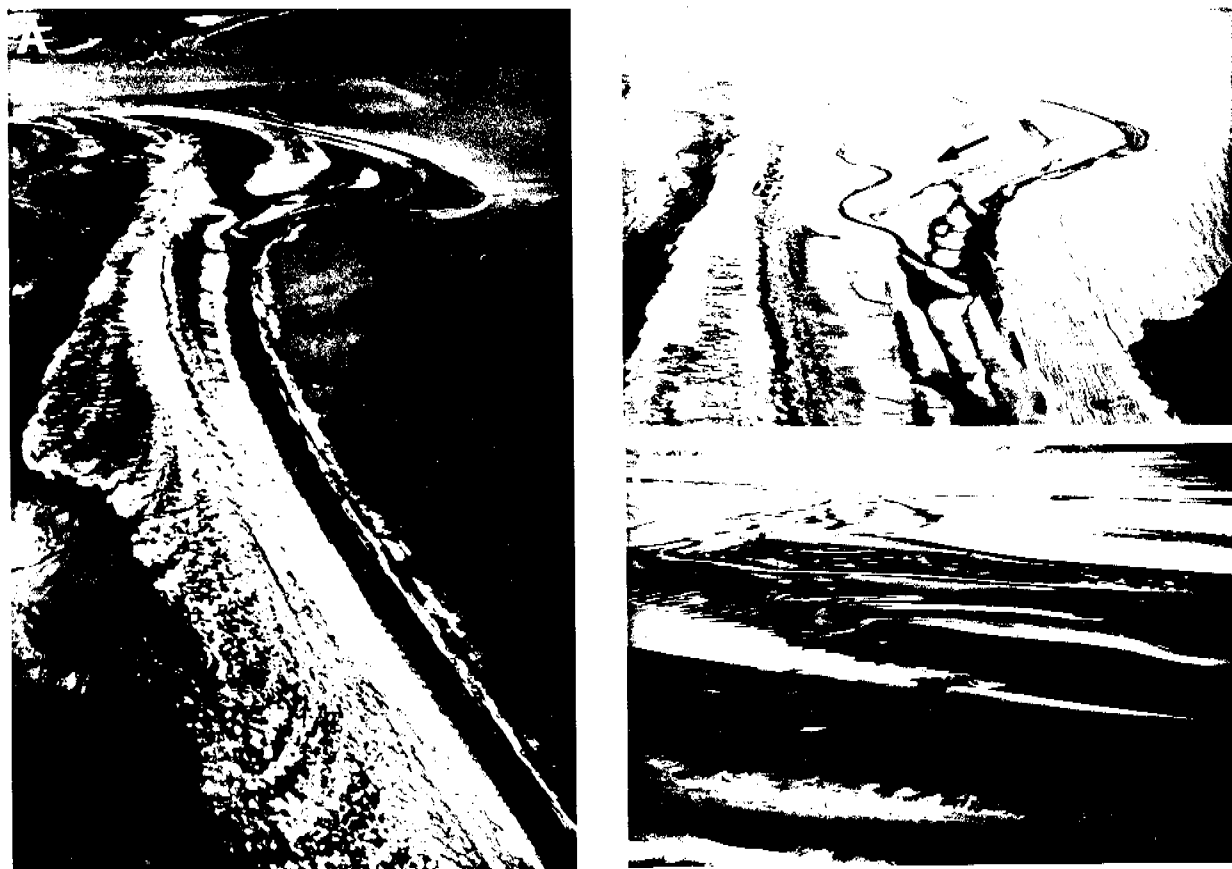


Figure 15. Egg Island, Alaska. A. Low-tide view taken in June, 1971. B. Low-tide view of east end of Egg Island taken in May 1975. Arrow points to same sand bar as the one indicated by the arrow in A. This beach accreted 400 m between February 1970 and May 1975 (see Fig. 14; profile EG-4). C. Multiple intertidal ridges welding on the beach at station EG-4. Photograph taken in the summer of 1969.

These remarkable changes, plus the occurrence of severe storms that overwash the islands, make the barrier islands of the Copper River delta an undesirable place to develop. On the other hand, Cordova, which has a sheltered harbor on Price William Sound, shows considerable promise.

## CONCLUSIONS

1. In the Malaspina Glacier area, the most desirable shorelines for coastal development are the stable, sheltered abandoned glacial coasts inside Icy Bay and Yakutat Bay. The least desirable area is the regional retreating coast at the mouth of Icy Bay, which is eroding rapidly.
2. Southeasterly storms (extratropical cyclones) play a primary role in shaping the morphology of the coastal zone.
3. Combination of wave hindcast data, field process measurements, and studies of coastal geomorphology indicate a dominant littoral sediment transport from east to west.
4. The mesotidal barrier islands of the Copper River delta area show characteristics typical of other mesotidal shorelines (downdrift offsets and drumstick shapes).
5. Major changes in the barrier islands have occurred since the area was uplifted during an earthquake in 1964. Changes continue to accentuate the drumstick shape of the islands.

## ACKNOWLEDGEMENTS

The earlier phases of this project (1969-71) were supported by the Geography Programs of the Office of Naval Research (Contract No. N00014-67-A-0230-0001, Miles O. Hayes, principal investigator), and the later phases were supported under contract with the National Oceanic and Atmospheric Administration (Contract No. 03-5-022-82; Miles O. Hayes, principal investigator).

## REFERENCES CITED

- DAVIES, J.L., 1964, A morphogenic approach to world shorelines: *Zeit. für Geomorph.*, Bd. 8, 27-42.
- FOLK, R.L., 1974, Petrology of sedimentary rocks: Hemphills, Austin, Texas, 117 p.
- FITZGERALD, D.M., 1976, Ebb-tidal delta of Price Inlet, South Carolina; Geomorphology, physical processes, and associated shoreline changes: in HAYES, M. O. and KANA, T. W., eds., *Terrigenous Clastic Depositional Environments*, Tech. Rept. 11 - CRD, Dept. Geol., Univ. South Carolina, II-143 - II-157.
- HAYES, M. O., GOLDSMITH, V., AND HOBBS, C. H. III, 1970, Offset coastal inlets: Am. Soc. Civil Engrs. Proc., 12th Coastal Engr. Conf., 1187-1200.

HAYES, M. O., OWENS, E. H., HUBBARD, D. K., and ABELE, R. W., 1973, The investigation of form and processes in the coastal zone: in COATES, D.R., ed., Coastal Geomorphology, Publications in Geomorphology, Binghamton, N. Y., 11 - 41.

HAYES, M. O., and KANA, T. W., 1976, Terrigenous clastic depositional environments: some modern examples: Tech. Rept. No. 11 - CRD, Dept. Geol., Univ. South Carolina, 308 p.

NUMMEDAL, D., and STEPHEN, M. F., 1976, Coastal dynamics and sediment transportation, northeast Gulf of Alaska: Tech. Rept. No. 9 - CRD, Geol. Dept., Univ. South Carolina, 148 p.

REIMNITZ, E., 1966, Late Quaternary history and sedimentation of the Copper River delta and vicinity, Alaska: Ph.D. diss., Univ. Calif., San Diego, 160 p.

Quarterly Report

Contract #03-5-022-56  
Research Unit #99  
Reporting Period 7/1 - 9/30/76  
Number of Pages 3

THE ENVIRONMENTAL GEOLOGY AND GEOMORPHOLOGY OF THE GULF OF ALASKA  
COASTAL PLAIN AND THE COASTAL ZONE OF KOTZEBUE SOUND

Dr. P. Jan Cannon  
Assistant Professor of Geology  
Institute of Marine Science  
University of Alaska  
Fairbanks, Alaska 99701

October 1, 1976

## Quarterly Report

### I. Task Objectives of Gulf of Alaska Project

- A. To produce three maps of the coastal plain section of the Gulf of Alaska.
- B. To produce a report on the application of radar imagery to the environmental geologic mapping of coastal zones.
- C. To construct an annotated mosaic of the area from radar imagery.
- D. To indicate the effects (beneficial and adverse) that oil and gas development might have in relation to the geologic setting.

### Task Objectives of Kotzebue Sound Project

- A. To produce three maps, with explanations, which will display certain baseline data necessary for an environmental assessment of the regions. The maps will be constructed from various types of remote sensing data.
- B. To produce a report on the unique geologic setting of Kobuk Delta indicating the possible effects (beneficial and adverse) of petroleum related development in the area.
- C. Direct the acquisition of remote sensing data of the area for Cannon, Hayes and other investigators.
- D. Construct a mosaic of the area of sequential LANDSAT data for Cannon, Hayes and other investigators.
- E. Construct an annotated mosaic of the area from SLAR imagery.

### II. Activities

Made final field check of basic map units of Gulf of Alaska coastal plain. Made aerial reconnaissance of beach during a storm to determine intensity of storm-generated beach processes.

Made preliminary aerial reconnaissance of Kotzebue Sound area from Cape Lisburne to Cape Prince of Wales. Acquired radar imagery of Kotzebue Sound Coastal Zone. Contacted Hayes, and field party, and discussed preliminary geomorphic assessment of coastal zone.

### III. Results

Final Report for Gulf of Alaska Coastal Plain is in the stages of final preparation. Winds along beach at 100 feet MSL were measured at 47 knots during storm.

In the Kotzebue Sound Coastal Zone analysis was made of various geomorphic features which indicate that the area is undergoing uplift. The radar imagery obtained of the coastal zone is of the highest quality.

#### IV. Preliminary Interpretation of Results

A tremendous amount of energy is expended upon the beaches of coastal plain of the Gulf of Alaska during storms. The wave action, generated during storms, constructs a steep beach face regardless of the grain size of beach material. Most of the beaches are stripped of sand sized material during a storm. The basic map data indicates one good site for a LNG plant in Yakutat Bay. That site is Broken Oar Cove.

Geomorphic analysis of radar and LANDSAT imagery of Kotzebue Sound indicates that the Baldwin Peninsula is a moraine that was constructed underwater. Recently raised, wave-cut benches line Kotzebue Sound, indicating that the area is undergoing uplift. This uplifting is that which is creating the numerous natural seal rookeries of the area.

#### V. Problems Encountered/Recommended Changes

Bathymetric data will be needed by investigator of Kotzebue Sound. A search is underway for existing data. Investigator plans to do field work in Kotzebue coastal zone during winter in order to study ice effects on beach.

OCS COORDINATION OFFICE

University of Alaska

ENVIRONMENTAL DATA SUBMISSION SCHEDULE

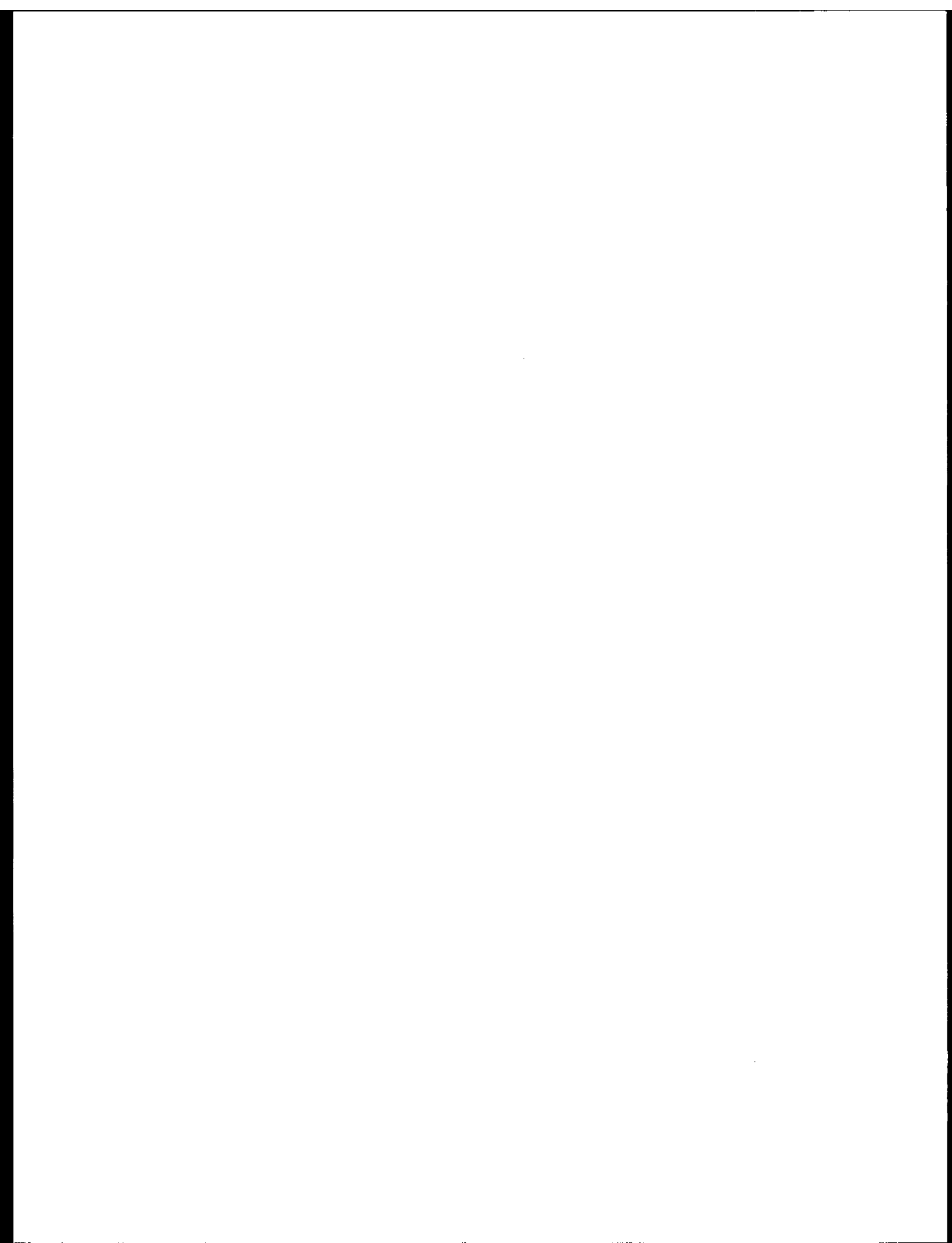
DATE: September 30, 1976

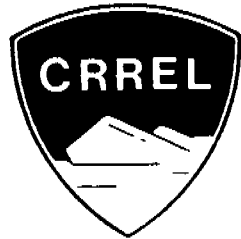
CONTRACT NUMBER: 03-5-022-56      T/O NUMBER: 6      R.U. NUMBER: 99

PRINCIPAL INVESTIGATOR: Dr. P. Jan Cannon

No environmental data are to be taken by this task order as indicated in the Data Management Plan. A schedule of submission is therefore not applicable<sup>1</sup>.

NOTE: <sup>1</sup> Data management plan was submitted to NOAA in draft form on October 9, 1975 and University of Alaska approval given on November 20, 1975. We await formal approval from NOAA.





Contract no. - 01-50-22-2313  
Research Unit no. - 105  
Reporting period - July - Sept 1976  
Number of pages - 7

Quarterly Report  
to

U.S. Department of Commerce  
National Oceanic and Atmospheric Administration  
Arctic Projects Office  
Fairbanks, Alaska

DELINEATION AND ENGINEERING CHARACTERISTICS OF  
PERMAFROST BENEATH THE BEAUFORT SEA

Principal Investigator:  
P.V. Sellmann

Associate Investigators:  
R. Berg  
J. Brown  
S. Blouin  
E. Chamberlain  
A. Iskandar  
H. Ueda

CORPS OF ENGINEERS, U.S. ARMY  
**COLD REGIONS RESEARCH AND ENGINEERING LABORATORY**  
HANOVER, NEW HAMPSHIRE

## I. TASK OBJECTIVES

The emphasis of the program is on quantifying the engineering characteristics of permafrost beneath the Beaufort Sea, and determining their relation to temperature, sediment type, ice content and chemical composition. These data will be used in conjunction with those from the marine and subsea permafrost projects listed below to develop a map portraying the occurrence and depth of permafrost under the Beaufort Sea. The drilling program will provide subsurface samples and control for the other programs. It is also designed to test drilling, sampling, and in situ measurement techniques in this offshore environmental setting where material types and ice conditions make acquisition of undisturbed samples extremely difficult.

Our activities are currently coordinated with the following OCS Beaufort Sea projects and David Hopkins, USGS:

Research Unit #204: Offshore permafrost studies, Beaufort Sea - Peter Barnes and Erk Reimnitz, U.S. Geological Survey.

Research Unit #205: Marine environmental problems in the ice-covered Beaufort Sea Shelf and coastal regions - Peter Barnes, Erk Reimnitz and David Drake, U.S. Geological Survey.

Research Units #253, 255, 256: Offshore permafrost drilling, boundary conditions, properties, processes and models - T.E. Osterkamp and William D. Harrison, University of Alaska.

Research Unit #271: Beaufort seacoast permafrost studies - James C. Rogers, University of Alaska.

Research Unit #407: A study of Beaufort Sea coastal erosion, northern Alaska - Robert Lewellen, Littleton, Colorado.

## II. FIELD OR LABORATORY ACTIVITIES

- A. Ship or field trip schedule: No field activity during reporting period.
- B. Scientific party: See A.
- C. Methods: See previous progress reports.
- D. Sample localities: See Figure 1.
- E. Data collected or analyzed: See previous reports and section III.

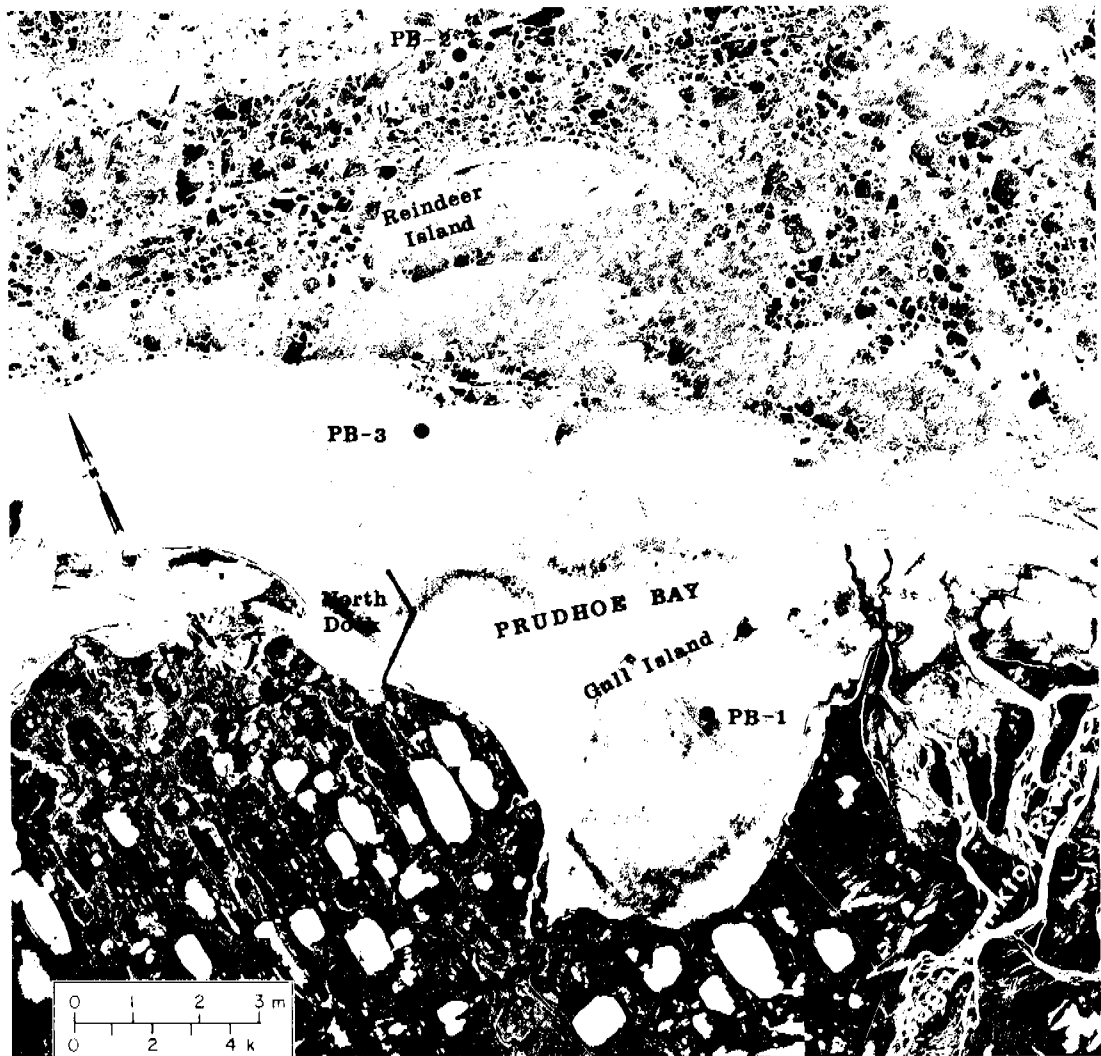


Figure 1. CRREL-USGS subsea drilling locations, Prudhoe Bay region.  
(Photograph from NASA, Flight no. 74-101, 27 June 1974.)

### III. RESULTS AND DISCUSSION

#### A. Drilling

A post-season operational report was prepared and is currently being reviewed by USGS prior to publication and distribution by CRREL as a Special Report. The report contains details of the drilling mobilization, equipment used, logs of cores, problems encountered, and cost information. The report will be distributed to OCS geology projects. Requests for additional distribution should be made to USACRREL or directly to Paul Sellmann.

## B. Engineering properties

The laboratory phase of the strength property study was completed as were most of the index property determinations.

Strength tests. Sixteen samples were selected and prepared for the strength tests. These included a selection of samples from each drill site. The range of samples available for testing was controlled by grain size since the coarse-grained material (sand to sandy gravel) commonly lacked sufficient integrity for testing. The best data were therefore primarily acquired on samples in the silt to sandy silt range, which generally included samples from the upper, fine-grained part of the sections common to all the sites.

These tests were performed on 5.1-cm (2-in.) diameter samples using triaxial testing procedures. During testing, in situ confining pressures and temperature (approximately -1.0°C) were maintained. In addition the tests were continued after initial failure using several additional and progressively higher confining pressures. In this report only the results obtained at the initial in situ confining pressures are presented.

The range of confined strengths observed was 50 to 530 kPa (7 to 77 psi). These values are for confining pressures in the range of 2.5 to 19 kPa (0.4 to 2.75 psi). In most cases increasing confining pressure to as high as 345 kPa (50 psi) did not significantly increase the strength. It appears that strength values are primarily controlled by grain size and density, with density not necessarily increasing with depth in the fine-grained sections.

The cone penetration tests conducted adjacent to each drill site indicate that in general the strength of the coarse-grained material found below the finer-grained sections is significantly greater. As mentioned, the lack of cohesion and large grain size of the materials common to the lower part of all the sections prevented confined strength tests. The initial comparison of strength data with penetration resistance information from the prototype engineering cone penetrometer at site PB-3 shows a strong correlation in the fine-grained material (Fig. 2). Extrapolating these results to the coarse-grained material found below the fine-grained sediment (approximately 11 m (35 ft) below the ice surface) indicates strengths may be an order of magnitude greater in the gravel. Total drill hole depth at this location was 50 m below the ice surface, with predominantly gravel and sand from 11 to 50 m.

Index property determinations. The index property determinations were run on the samples tested for strength as well as an additional 16 samples to aid in characterizing variations in the stratigraphic section. The properties determined were density, grain size distribution, specific gravity, Atterberg limits, and organic and water content. No thaw consolidation tests were conducted since bonded permafrost was not encountered. The presentation and interpretation of all these data will be covered in a future formal report.

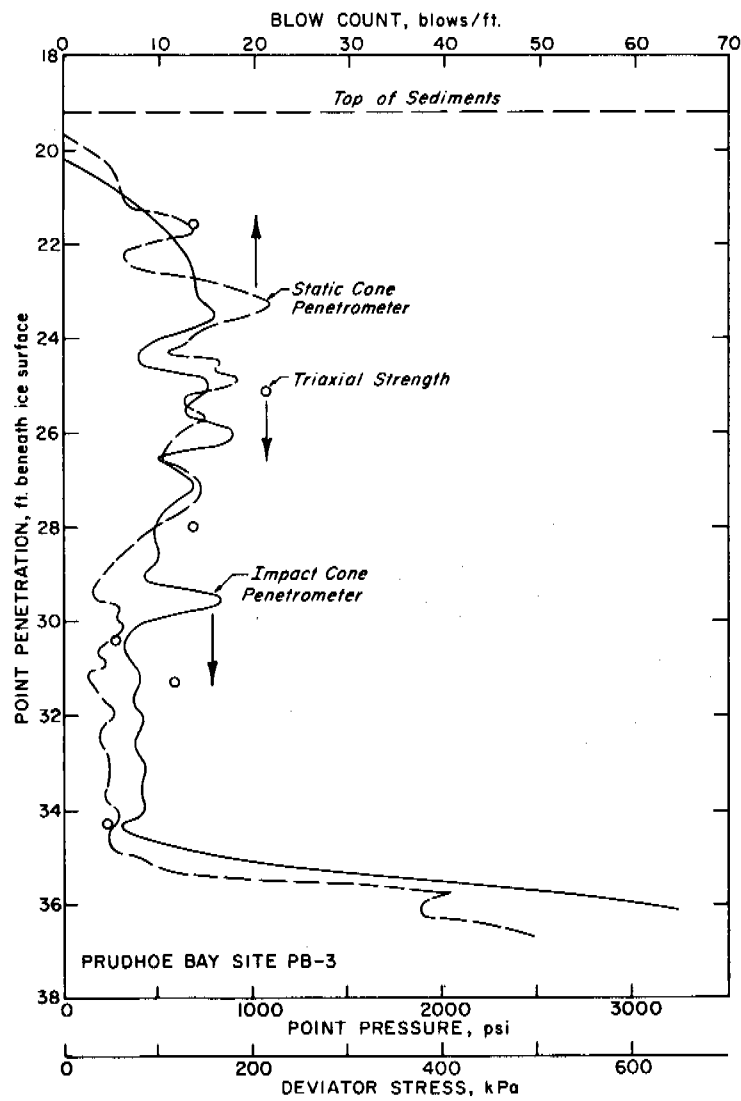


*Figure 2. Comparison of triaxial strength laboratory tests (open circles) and static and impact cone penetrometer results for the upper section of Prudhoe Bay sediments (CRREL site PB-3).*

Supporting data The USGS investigators provided CRREL with preliminary thermal and descriptive logs of the holes. This information will be covered in more detail in future formal reports.

#### C. Chemical analysis of interstitial water

The interstitial water was extracted from the core samples by centrifuging using special filtering centrifuge tubes commercially available from Millipore Corp. The filtering tubes were made of plastic and Teflon

to assure samples free of metal contamination. They also allowed processing of coarse-grained sediments not easily handled by some other techniques. The validity of filter centrifuging as a method of extracting interstitial water for chemical analysis is well established (Edmunds and Bath 1976).\*

The interstitial water was analyzed for total soluble salts (expressed as specific conductance), Na, K, Ca, Mg, Cl,  $\text{SO}_4$ ,  $\text{CO}_3$ , and  $\text{HCO}_3$  according to methods described in previous reports.

The total number of samples analyzed was 47. This included 40 interstitial water samples and 7 from the water columns above the borehole locations. Sixteen samples were processed from cores obtained from drill sites PB-1 and PB-1A, 8 from PB-2, and 16 from PB-3. The deepest sample processed came from a depth of 47.5 m (155.9 ft) below the ice surface at PB-3. Details such as the depth, lithology, and water content of the samples will be covered in future reports. Water samples were collected from the top, middle, and bottom of the water column above holes PB-2 and PB-3, while only one was collected at PB-1 since water depth below the ice cover was so small.

The profiles of total soluble salts in the interstitial water expressed as mmhos/cm at  $25^{\circ}\text{C}$  are shown for PB-1 and PB-3 (Fig. 3). The data for PB-2 will be covered in future reports since the samples were recovered by dilution techniques because of low moisture contents. The plotted data show only a slight vertical variation with depth. PB-1 values were much higher than those obtained in PB-3. This may be due to the fact that PB-1 was drilled in a basin closed by sea ice formation and where little mixing of the sea water can take place as indicated by the high salt content of the water. The specific conductance of the sea water at this site was 93 mmhos/cm compared to 53 at PB-3.

The data obtained in the present study compared well with those obtained by Osterkamp and Harrison (1976).† A comparison of their holes 3,370 and 481 was made with the data from PB-3 and PB-1 since they were from similar environments (Fig. 3). This agreement occurred despite the differences in field sample collection and analytical procedures. The values reported in Figure 3 are within the common range of values obtained from studies in the Barrow area (Brown 1969).\*\*

---

\*Edmunds, W.M. and A.H. Bath (1976) Centrifuge extraction and chemical analysis of interstitial waters. *Environ. Science and Tech.*, vol. 10, p. 467-472.

†Osterkamp, T.E. and W.D. Harrison (1976) Subsea permafrost at Prudhoe Bay, Alaska. Report 245, University of Alaska, Geophysical Institute.

\*\*Brown, J. (1969) Ionic concentration gradients in permafrost, Barrow, Alaska. CRREL Research Report 171.

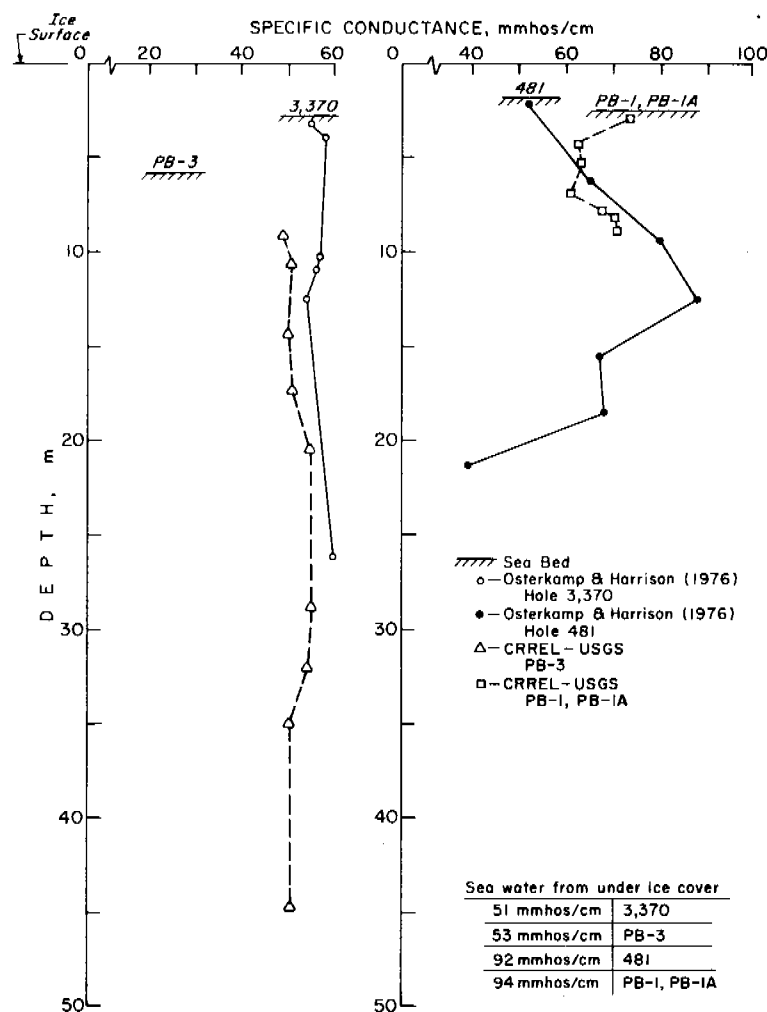


*Figure 3. Specific conductance of interstitial water from CRREL core samples (PB-1, -1A and -3) and the water column, and previous results of Osterkamp and Harrison (1976).*

Ranges in specific ion concentration from all holes were:

C1:	10-30	parts per thousand
Na:	15-33	ppt
K:	300-900	parts per million
Ca:	200-800	ppm
Mg:	1000-1900	ppm
SO <sub>4</sub> :	2000-6000	ppm
Mn:	0.5-3.0	ppm
Cu:	0.5-2.0	ppm
pH:	7.5-8.0	

D. Compilation of combined Soviet and non-Soviet bibliographies on subsea permafrost and related processes continued. Discussions related to current Soviet offshore activities were held at the International Geographical Congress in Leningrad and Moscow.

#### IV. PRELIMINARY INTERPRETATION OF RESULTS

Covered in Section III.

#### V. PROBLEMS ENCOUNTERED/RECOMMENDED CHANGES

No problems were encountered in the laboratory analyses. During the period a continuation proposal was prepared in conjunction with other OCS Beaufort subsea permafrost projects. The proposed 1977 project recommends the following field activities:

- a. Obtain data and samples for chemical, sediment and ice content analyses from one land-based control borehole at Prudhoe Bay.
- b. Obtain data and samples from several shallow additional offshore holes in the Prudhoe Bay area to establish the transgressive history of the area which is required for thermal analyses and modeling.
- c. Obtain data and samples from one deep hole in Prudhoe Bay to establish the upper boundary of bonded subsea permafrost, and related thermal, chemical, physical and engineering properties.
- d. Conduct shallow probing to obtain additional data on the boundary of the ice-bonded permafrost interface in support of Harrison and Osterkamp modeling.
- e. Obtain samples from one additional exploratory hole in the vicinity of or west of the Colville River as logistics and time permit.
- f. Conduct a shallow (10-15 meters deep) penetration test program in the Prudhoe Bay region for purposes of establishing the range in engineering properties.

#### VI. ESTIMATE OF FUNDS EXPENDED

At the end of this quarter, approximately \$267,000 of the total \$320,000 had been expended.

6TH QUARTER REPORT

Research Unit #152/154  
Reporting Period 7/1/75-10/1/76

Distribution, Composition, and Transport of Suspended  
Particulate Matter in the Gulf of Alaska and Southeastern  
Bering Shelf

Principal Investigators: Richard A. Feely, Oceanographer  
Joel D. Cline, Oceanographer

Pacific Marine Environmental Laboratory  
3711 15th Avenue N.E.  
Seattle, Washington 98105

## I. Task Objectives

The major objective of the particulate matter program in the Gulf of Alaska and southeastern Bering Shelf is to determine the seasonal variations in the distribution, composition, and transport of suspended particulate matter. Other objectives include: (1) determination of the high frequency variability in the distribution of suspended matter; and (2) an investigation of the processes controlling resuspension and redistribution of bottom sediments.

## II. Field or Laboratory Activities

### A. Field Activities

#### 1. Ship Schedule

- a. MOANA WAVE Cruise (RP-4-MW,76B-VIII, 24 June-9 July, 1976)
- b. River Sampling (Gulf of Alaska, 22-27 June 1976)
- c. DISCOVERER Cruise (RP-4-Di-76B-I, 19-31 July 1976)
- d. River Sampling (Bering Sea, 16-20 September 1976)

#### 2. Participants from PMEL

- a. Dr. Richard A. Feely, Oceanographer
- b. Mr. Gary Massoth, Oceanographer
- c. Ms. Jane Fisher, Oceanographer
- d. Ms. Joyce Quan, Physical Science Technician
- e. Mr. William Landing, Graduate Student
- f. Mr. Albert Chapdelaine, Student

#### 3. Methods

- a. Particulate Matter - Water samples were collected in 10-liter Top-drop Niskin bottles and filtered under vacuum through pre-weighed 0.4  $\mu\text{m}$  Nuclepore and Selas silver filters. The filters

were removed from the filtration apparatus, placed into individually marked petri dishes, dried in a desiccator for 24 hours and stored for shipment to the laboratory.

- b. Nephelometry - The vertical distribution of suspended matter was determined with a continuously recording integrating nephelometer. The instrument was interfaced into the Plessey CTD system using the sound velocity channel (14-16 KHz) such that real time measurements of forward light scattering were obtained at each station. In addition, a digital recording nephelometer was placed on a current meter array (station 62G) at approximately 1.5 m above the bottom (DISCOVERER Cruise RP-4-Di-76A-I). The nephelometer was deployed on 4 March 1976 and recovered on 16 May 1976.

#### 4. Sample Locations

Figures 1 and 2 show the locations of the suspended matter stations in the southeastern Bering Shelf (MOANA WAVE Cruise RP-4-MW-76B-VIII) and northeastern Gulf of Alaska (DISCOVERER Cruise RP-4-Di-76B-I). In figure 2 station 62/15 is the location of the bottom-mounted nephelometer. Figure 3 shows the locations of the stations from the river sampling expedition in the northeastern Gulf of Alaska.

#### 5. Data Collected

Particulate matter samples were collected from 54 stations in the southeastern Bering Shelf, 50 stations in the northeastern Gulf of Alaska and 35 river sampling stations. With the exception of the river samples, samples were taken from several preselected depths, depending on location. Nominally, these depths included: surface, 10m, 20m, 40m, 60m, 80m, 100m, and 5m above the bottom. For the river stations only surface samples were obtained.

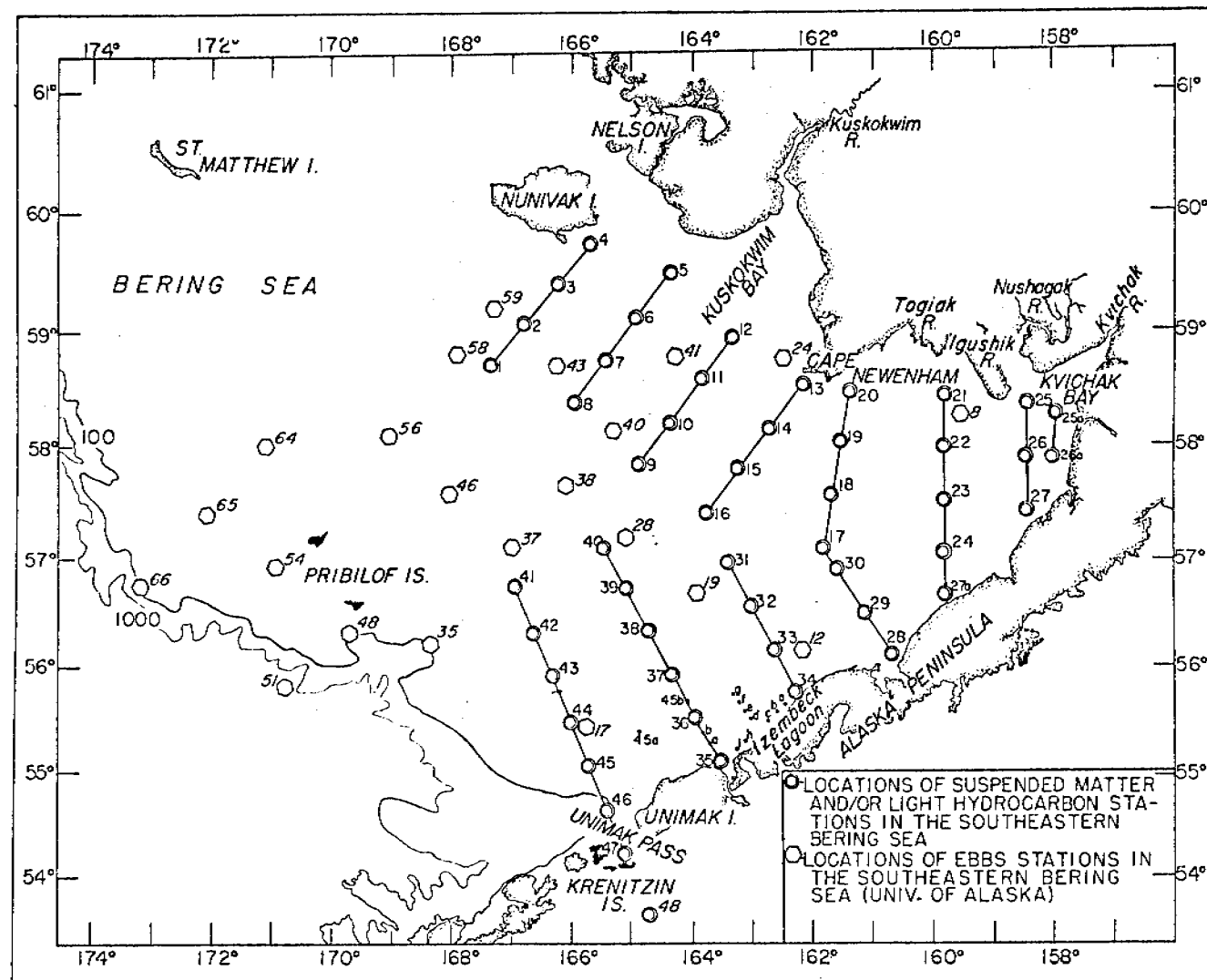


Figure 1. Locations of suspended matter stations in the southeastern Bering shelf (Cruise RP-4-MW-76B-VIII, 24 June-9 July, 1976)

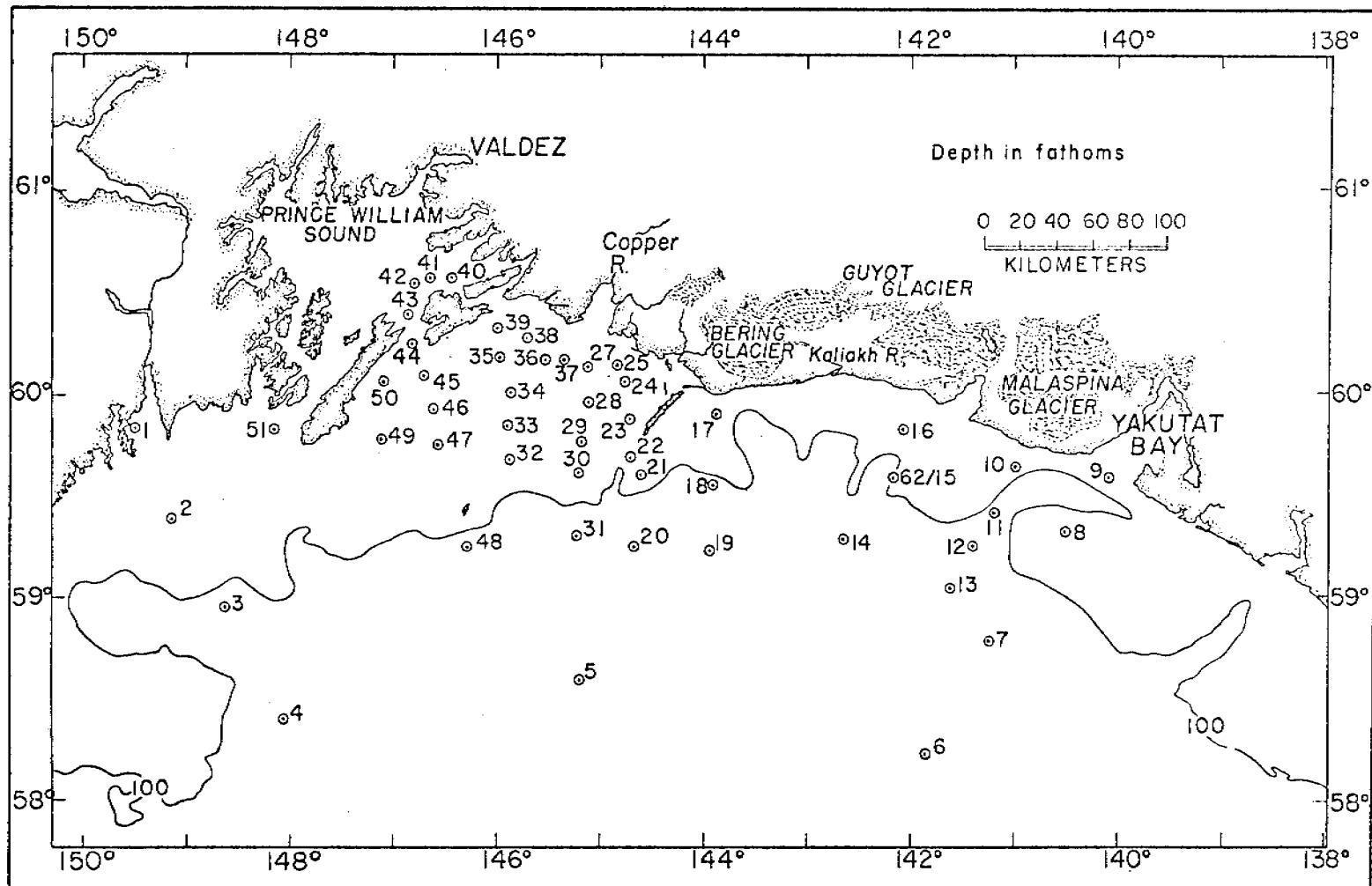


Figure 2. Locations of suspended matter stations in the northeastern Gulf of Alaska  
(Cruise RP-4-Di-76B-I, 19-31 July 1976)

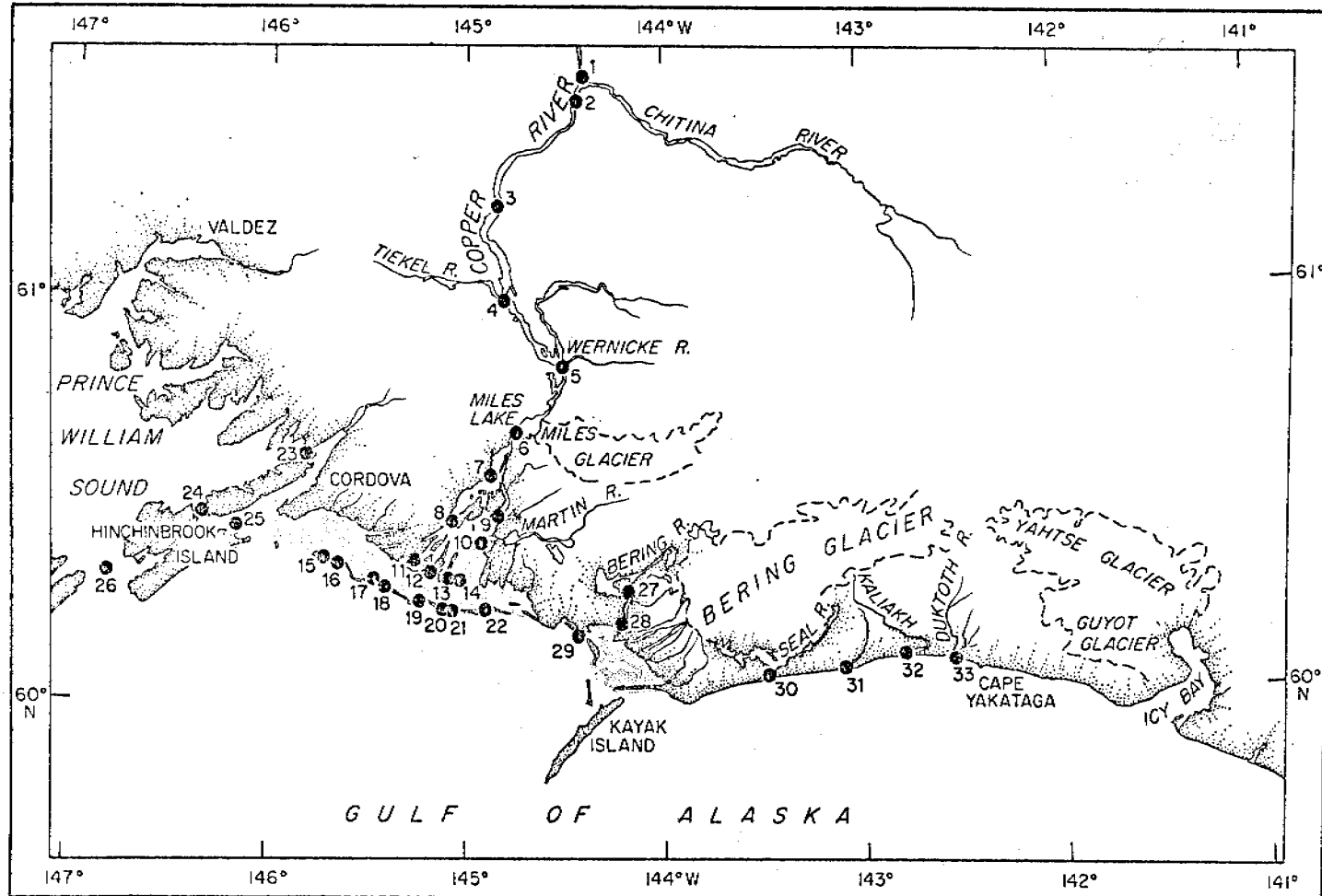


Figure 3. Locations of suspended matter stations in the major rivers  
draining into the northeastern Gulf of Alaska (22-27 June 1976)

## B. Laboratory Activities

### 1. Methods

The major (Mg, Al, Si, K, Ca, Ti, and Fe) and trace (Cr, Mn, Cu, Ni, Zn, and Pb) element chemistry of the particulate matter is being determined by secondary emission X-ray fluorescence spectrometry. This technique has been successfully used for the determination of the major element composition of particulate matter from coastal and deep water environments and the techniques are fairly well established (Baker and Piper, 1976). In our laboratory, we have developed techniques for the analysis of Cr, Mn, Cu, Ni, Zn, and Pb in addition to the major elements.

Radiation from a silver X-ray tube is used to obtain a monochromatic source of X-rays from a secondary target. We are using a combination of secondary targets (Se and Zr) to analyze the particulate matter for both major and trace elements. USGS standard rocks and NBS glass standards are used for calibration of the individual elements.

Particulate carbon and nitrogen are being analyzed by the Micro-Dumas combustion method, employing a Hewlett-Packard 185B C-H-N analyzer (Sharp, 1974). Particulate matter is removed from 1-liter volumes by vacuum filtration and the carbon and nitrogen combusted to CO<sub>2</sub> and N<sub>2</sub>. After separation by standard gas-solid chromatography (GC), the gases are quantitatively determined by thermal conductivity. Standardization is being effected with NBS acetanilide (Sharp, 1974).

### 2. Data Collected

To date, we have completed all five cruises in the Gulf of Alaska and southern Bering Shelf scheduled for the present fiscal

year. The first cruise RP-4-Di-75B-III of the NOAA ship DISCOVERER was conducted in the southeastern Bering Shelf during the fall of 1975 (12 September-5 October). The second cruise was conducted in the northeastern Gulf of Alaska during late fall of the same year (21 October-10 November). The third cruise, also in the northeastern Gulf, was conducted in early spring of 1976 (13-30 April). The fourth cruise was conducted in the southeastern Bering Shelf in early summer of 1976 (24 June-9 July). The last cruise was conducted in the northeastern Gulf of Alaska during the summer of 1976 (19-31 July). In addition to the five cruises, two field expeditions, designed to collect suspended matter samples from the major rivers discharging into the Gulf of Alaska and southeastern Bering Shelf, have been completed. At this point approximately 1500 samples have been collected and weighed for suspended loads. In addition, approximately 600 samples have been collected for elemental analysis of the particulate material.

### III. Results

#### A. Particulate Matter Distributions

The data on the distribution of suspended matter in the southeastern Bering Shelf and the northeastern Gulf of Alaska for the fall cruises (RP-4-Di-75B-III and RP-4-Di-75C-I) are complete and have been described in the First Annual Report, and therefore, will not be described here. We have completed the analyses of the samples from the spring cruise in the northeastern Gulf (RP-4-Di-76A-IV) and that data will be described below.

Figures 4 and 5 show the distribution of suspended matter at the surface and 5 m above the bottom during the spring cruise in the northeastern Gulf

of Alaska (RP-4-DI-76A-III, 13-30 April, 1976). The surface suspended matter distribution patterns are remarkably similar for the fall and spring cruises. East of Kayak Island the surface particulate matter distributions are dominated by the discharge of sedimentary material from the coastal streams which drain the Bering, Guyot, and Malaspina Glaciers. As this material is discharged into the Gulf, the westward flowing currents quickly deflect this material to the area along the coast until it reaches Kayak Island where it is deflected to the southwest around the southern tip of the Island. In a manner similar to the fall cruise, sharp suspended matter gradients exist near the coast. Along a line of stations perpendicular to the coastline from Yakutat Bay suspended matter concentrations drop from 3.28 mg/l to 0.25 mg/l within a distance of 40 km. Both the fall and spring cruises occurred during periods when the water discharge from the major rivers entering the Gulf was low and very nearly the same (for example, the monthly mean discharge rate of the Copper River near Chitina for the month of November is 256 m<sup>3</sup>/sec and 159 m<sup>3</sup>/sec for the month of April). Thus, it appears that since the discharge of terrestrial materials from the coastal rivers is relatively low and constant during the winter months, and because the prevailing surface currents have a net velocity to the northwest, most of the sedimentary materials that are discharged into the surface waters of the Gulf during the winter months remain within 40-60 km of the coastline.

Although the surface suspended matter distribution patterns are similar for the fall and spring cruises, the vertical distribution patterns are not. Figures 6 and 7 show vertical cross sections of the distribution of total suspended matter for stations 27 thru 31 for the fall and spring cruises, respectively. The vertical cross sections were determined from discrete samples (the locations of the samples are represented in the

figures as dots) and light scattering measurements. The figures reveal that the fall cruise is characterized by strong vertical suspended matter gradients, whereas, the spring cruise is characterized by weak vertical gradients. Drake (1971) demonstrated that in the Santa Barbara Channel vertical gradients in suspended matter distributions were strongly influenced by temperature-induced density gradients. Our data appear to support these findings. For example, at the time of the fall cruise the water column was thermally stratified. The temperature gradient at station 28 was approximately  $-0.05^{\circ}\text{C}/\text{m}$  from 50 to 100 meters. In contrast, the temperature gradient at the same station during the spring cruise was only about  $-0.003^{\circ}\text{C}/\text{m}$ . Thus, it is apparent that the stability of the water column, which on the continental shelf is primarily controlled by temperature-induced density gradients, strongly influences the vertical transport and subsequent residence times of particles in suspension.

#### B. Temporal Variability of Suspended Matter Near the Seabed

In order to obtain some information about the processes that control re-suspension and redistribution of bottom sediments along the shelf, a digital recording nephelometer was placed onto a current meter array at approximately 1.5m above the bottom (station 62G,  $59^{\circ}34' \text{N}$  and  $142^{\circ}10' \text{W}$ , which is located southeast of Icy Bay and has been used as the site for extensive measurements of bottom currents by the physical oceanographers at PMEL. It is situated near the shelf break at a depth of 184 meters). The nephelometer was deployed on March 4, 1976 and recovered on May 16, 1976. Figure 8 shows the record of the light scattering measurements for the period from March 6 thru March 31, 1976 for which useful data were recovered. Figure 8 also shows the 2.8-hour filtered (resolved with respect to the net drift axis and represented by dots) and the 35-hour low pass filtered (represented by vectors) current meter records from the current meter at 100m for the same time period. This current meter was chosen for this comparison as an alternative choice because the current meter that was deployed 1m above the nephelometer failed and no usable data

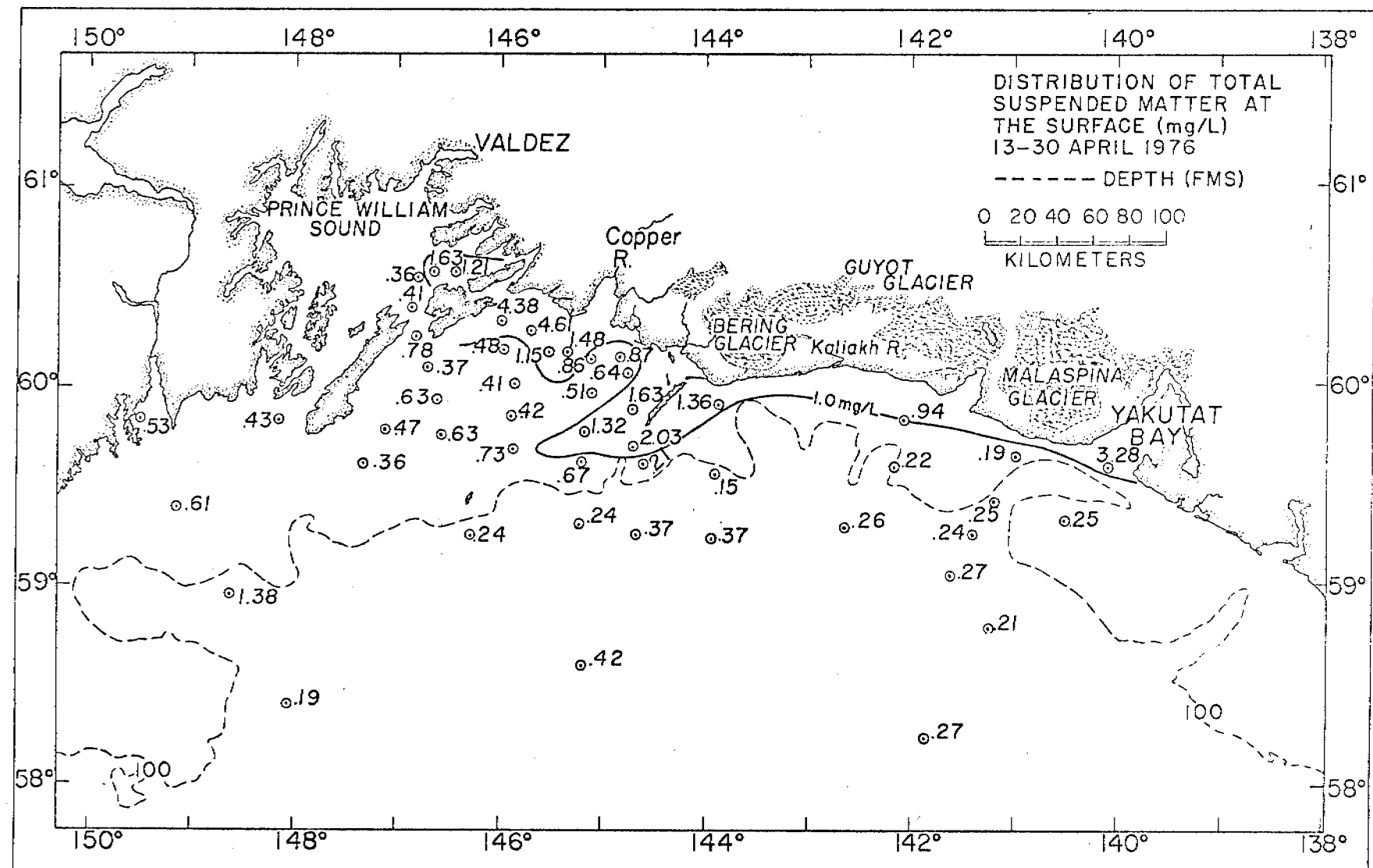


Figure 4. Distribution of total suspended matter at the surface in the northeastern Gulf of Alaska (Cruise RP-4-Di-76A-IV, 13-30 Apr., 1976)

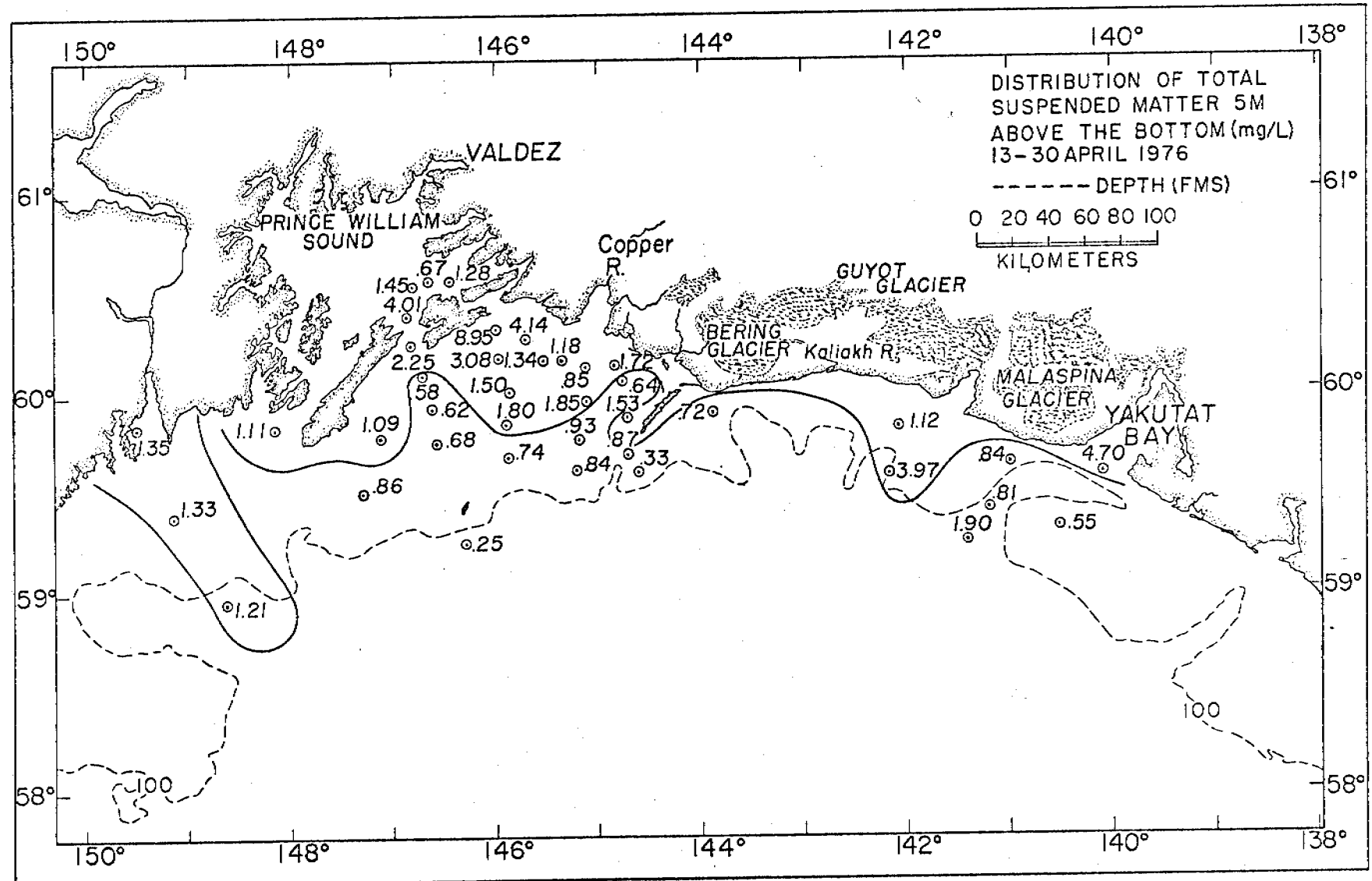


Figure 5. Distribution of total suspended matter at 5 meters above the bottom in the northeastern Gulf of Alaska (RP-4-Di-76A-IV, 13-30 Apr., 1976)

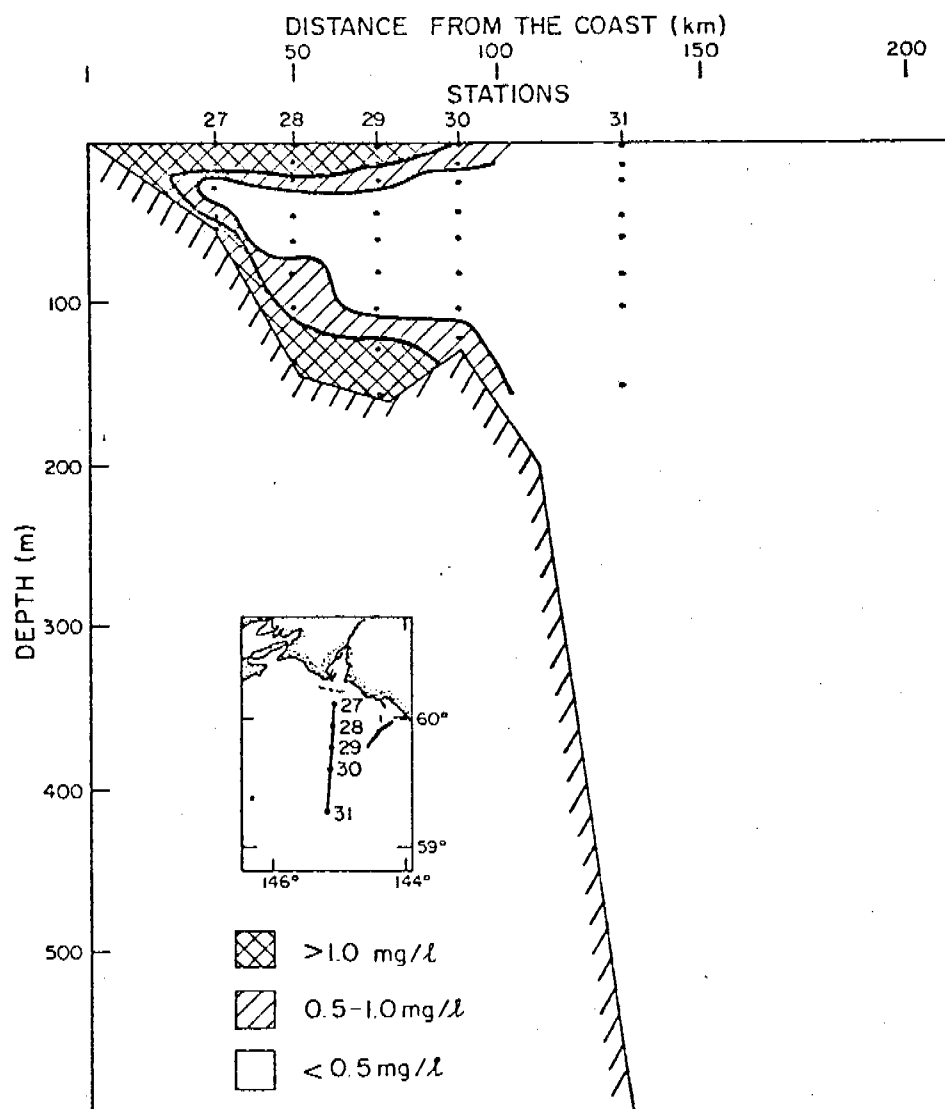


Figure 6. Vertical cross section of the distribution of total suspended matter for stations 27 thru 31 in the northeastern Gulf of Alaska (Cruise RP-4-Di-756-I, 21 Oct.-10 Nov., 1975).

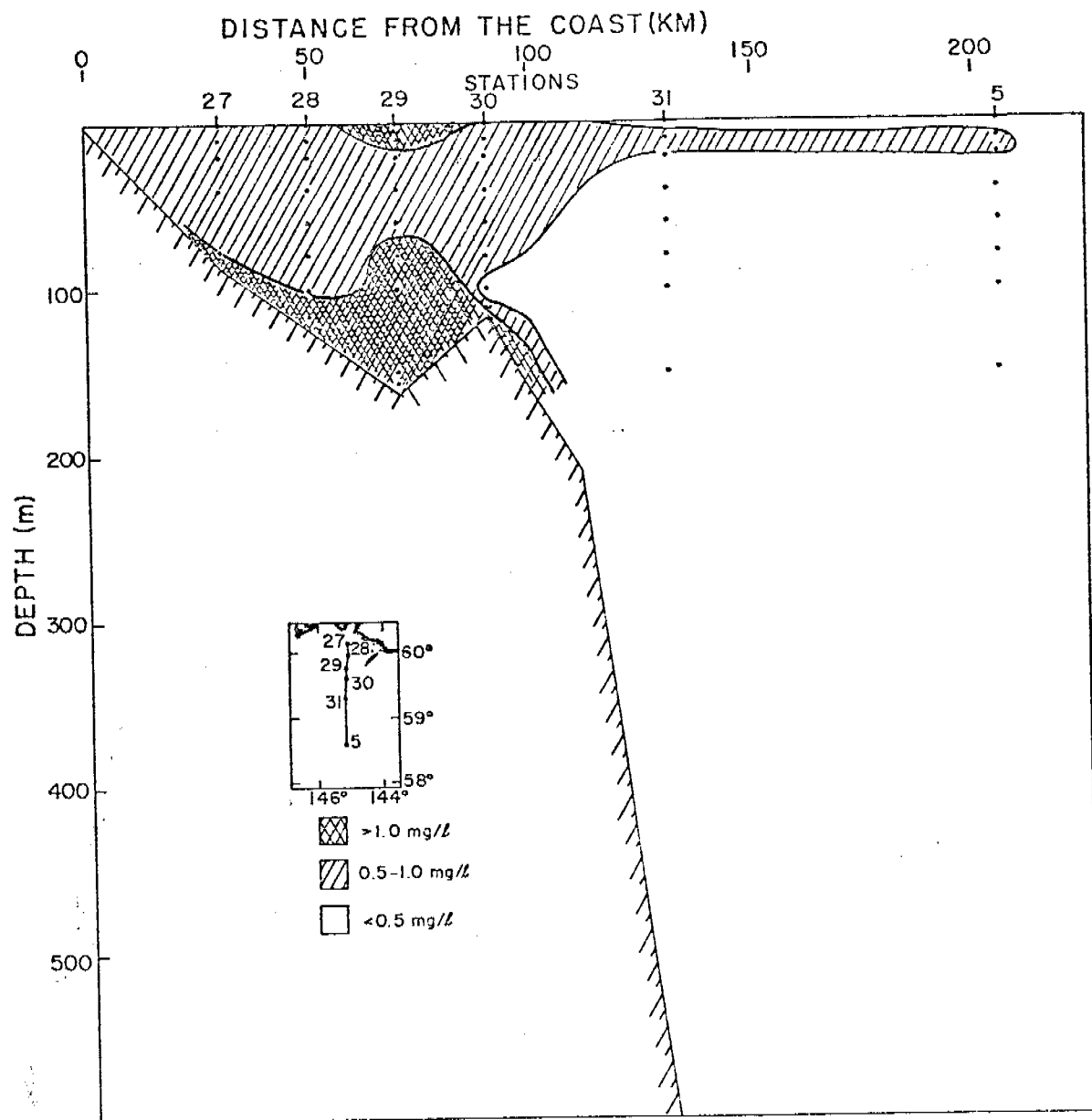


Figure 7. Vertical cross section of the distribution of total suspended matter for stations 27 thru 31 and station 5 in the northeastern Gulf of Alaska (Cruise RP-4-Di-76A-IV, 13-30 Apr., 1976)

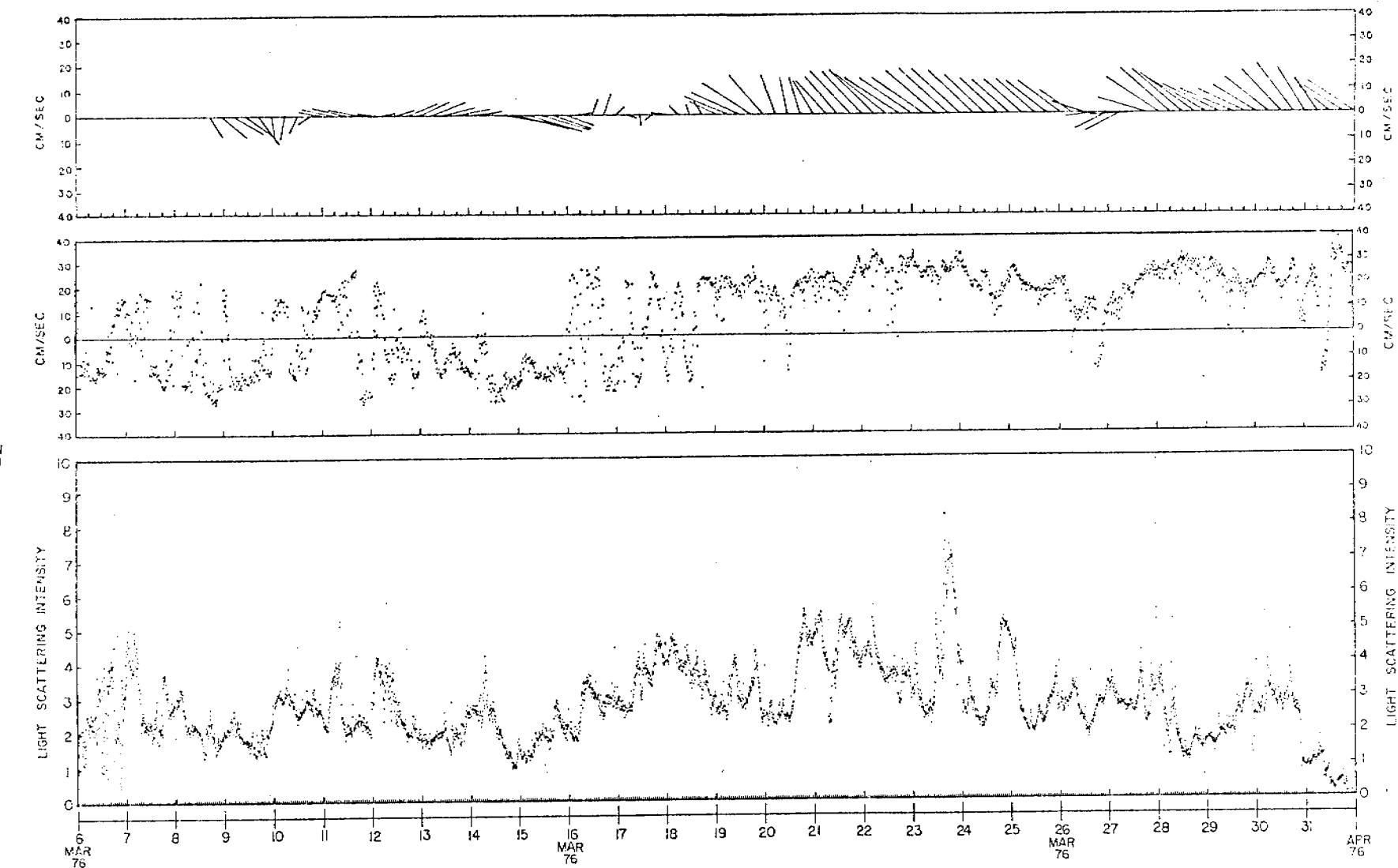


Figure 8. Comparison of the 26 day nephelometer record (bottom) from station 62G with the 2.8-hour filtered (middle) and the 35-hour filtered (upper) current meter record at 100m. The current meter data were supplied by R. L. Charnell and J. D. Schumacher.

were recovered. Considering the distance between the nephelometer and the current meter (= 80 meters), a comparison of this nature would seem to be marginal at best. However, we have examined current meter records from 1975 using linear regression and rotary coherence techniques and have found that a positive correlation ( $r=.62$ ) exists between the currents measured at 100m and the currents measured near the bottom for the winter months between September and March (J.D. Schumacher, personal communication, 1976).

The light scattering record has two salient features. First, associated with almost every maxima in the 2.8-hour filtered current meter record above a threshold velocity of approximately 17 cm/sec are corresponding peaks in the light scattering record. Spectral diagrams for both the current meter and nephelometer records, which are presented in Figures 9 and 10, respectively, show that the major peaks have frequencies of 0.3, 1.0, 1.7 and 1.9 cycles per day. These peaks are attributed to storm, diurnal, inertial and semidiurnal events (Charnell et al., 1976), respectively, and appear to have a significant effect on the concentration of suspended matter near the bottom. The diurnal and semi-diurnal events can be attributed to tidal activity which causes suspended matter fluctuations on the order of  $\pm 0.4 \text{ mg/l}$  (previous calibration of the nephelometer indicates that a light scattering intensity of 2.0 corresponds to a suspended matter concentration of approximately  $0.5 \text{ mg/l}$  and a light scattering intensity of 4.0 corresponds to a suspended matter concentration of  $2.0 \text{ mg/l}$ ). These findings suggest that tidal currents near the bottom are of sufficient velocity to resuspend bottom sediments at station 62G.

The second feature of the nephelometer record is the presence of a large gradual increase in light scattering which begins on March 16, 1976 and continues through March 26. There is a significant correlation between this feature and a similar event in the 35-hour filtered current meter record which shows the development of a strong onshore current having a net velocity of approximately 25 cm/sec at 310° TN. This event is characteristic of storm-induced bottom currents (Hayes and Schumacher, 1976) and represents a net water transport of approximately 230 km. The light scattering record indicates a corresponding increase in the near bottom suspended matter concentrations from about 0.5 mg/l to about 3.0 mg/l. Thus, the near bottom nephelometer and current meter records at station 62G clearly show that significant amounts of bottom sediments are being resuspended and transported by storm-induced bottom currents.

#### C. Elemental Chemistry of the Particulate Material

At this point, we have completed the analyses of the samples from the fall cruises in the Gulf of Alaska and southeastern Bering shelf. The results of the analyses were described in previous reports, and therefore, will not be reproduced here. Work is progressing on the samples from the spring and summer cruises. However, no data is available at this time.

#### IV. Preliminary Interpretation of the Results

The distribution patterns of particulate material at the surface represent a balance between the supply of sedimentary materials from the coastal rivers and the prevailing westward flowing currents which quickly divert the terrestrial material to the west along the coastline. Since the rate of supply of sedimentary materials from the rivers is relatively low and

constant during the winter season (November thru March), the surface distribution patterns are similar and somewhat predictable. Unfortunately, this is not the case for the subsurface layers. During the transition from fall to winter the thermal stratification of the water column decreases and the temperature-induced density gradients diminishes. This causes the vertical suspended matter gradients to break down and the distribution patterns become more uniform.

Near the bottom, tidal currents and storm-induced bottom currents are of sufficient velocity to resuspend bottom sediments which accounts for the near bottom nepheloid layer which covers most of the area along the shelf. Since the net drift of the bottom waters is in the shoreward direction ( $\approx 310^\circ$ TN), the resuspended sediments (and associated pollutants) are probably transported to depositional regions closer to shore.

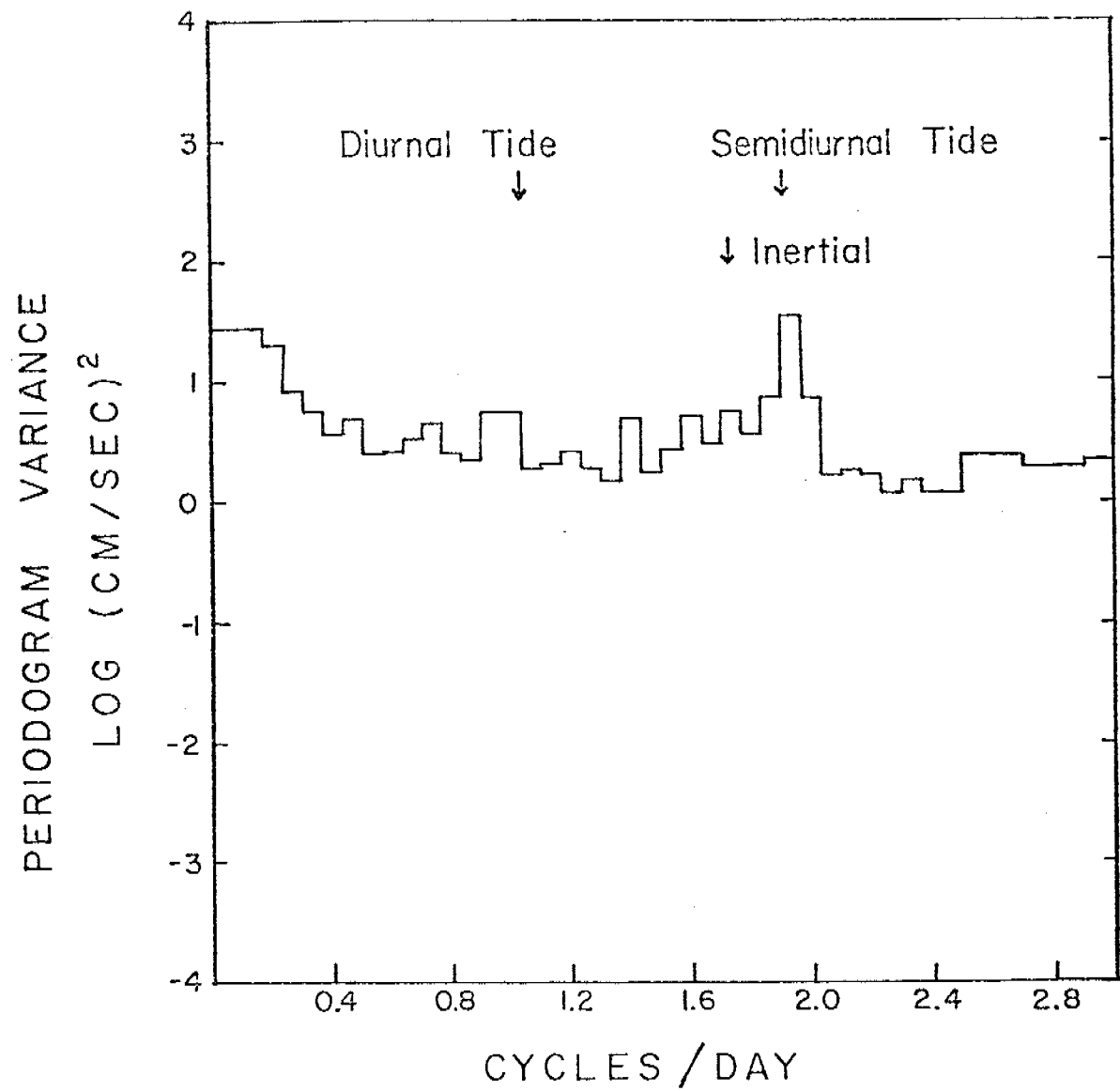


Figure 9. Energy spectra histogram of the 100m current meter at station G2G. Energy is given by logarithm of periodogram variance.

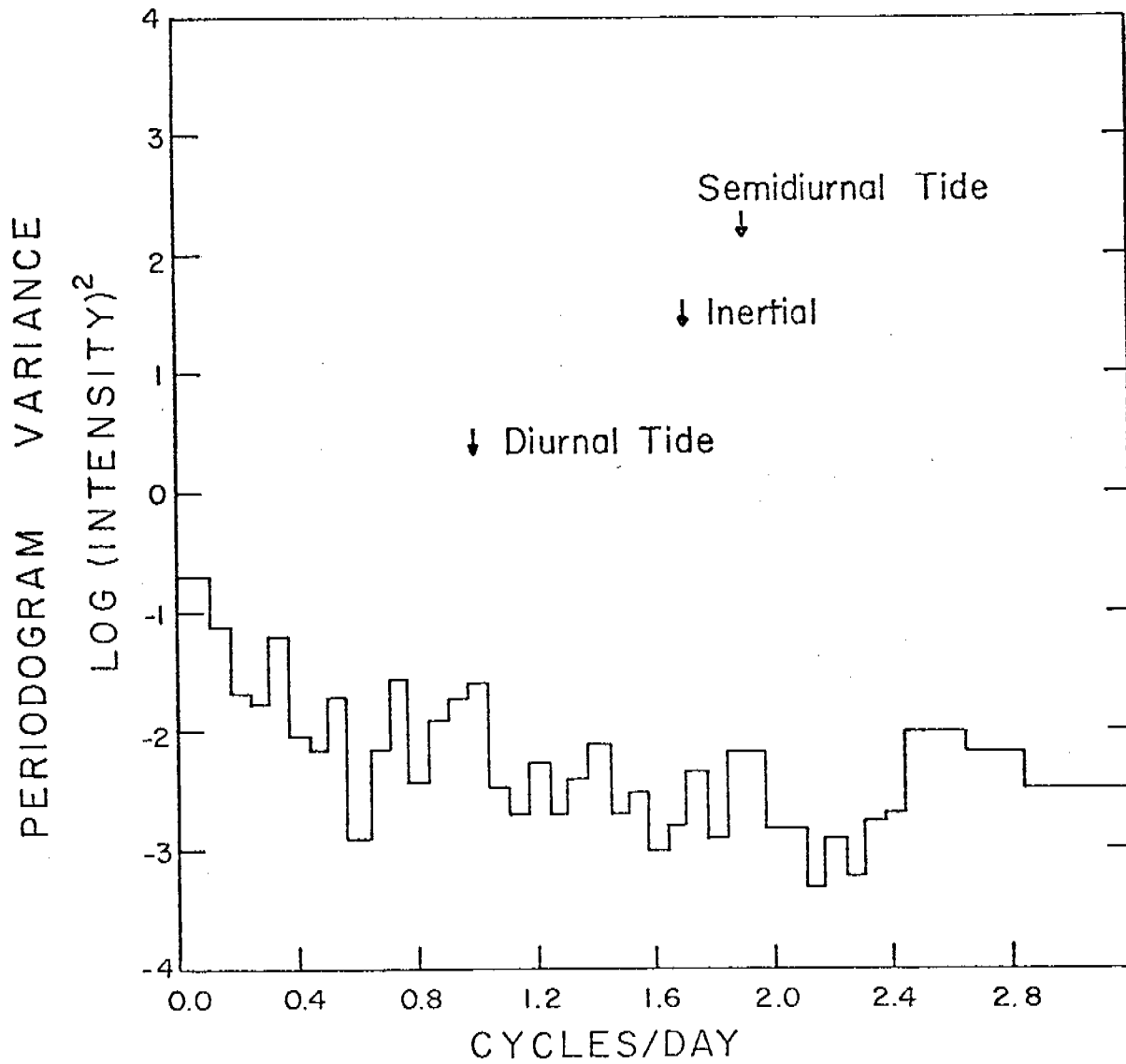


Figure 10. Energy spectra histogram of the nephelometer record at station G2G. Energy is given by logarithm of periodogram variance.

## V. Problems Encountered

We have no significant problems to report at this time.

## IV. Estimate of Funds Expended

	<u>Allocated</u>	<u>Expended</u>	<u>Balance</u>
Salaries and Overhead	125.6K	114.3K	11.3K
Travel and Shipping	20.0K	15.0K	5.0K
Current Meters	5.0K	5.0K	0.0K
Nephelometers	10.0K	28.3K	-18.3K
X-ray Fluorescence System	70.0K	80.0K	-10.0K
Publications	6.0K	4.0K	2.0K
Computer Time	9.8K	9.8K	0.0K
Miscellaneous	14.4K	14.4K	0.0K
Banked from FP 75	<u>10.0K</u>	<u>0.0K</u>	<u>10.0K</u>
	270.8K	270.8K	0.0K

## References

- Baker, E. T. and D. Z. Piper. 1976. Suspended Particulate Matter: Collection by pressure filtration and elemental analysis by thin film x-ray fluorescence, Deep Sea Research 23: 181 - 186.
- Charnell, R. L., J. D. Schumacher and C. A. Pearson. 1976. Extreme value analysis applied to current meter data, submitted for publication.
- Drake, D. E. 1971. Suspended sediment and thermal stratification in Santa Barbara Channel, California, Deep Sea Research 18: 763 - 769.
- Hayes, S. P. and J. D. Schumacher. 1976. Description of wind, current, and bottom pressure variations on the continental shelf in the N. E. Gulf of Alaska: February - May 1975, Jour. Geophy. Res., in press.
- Sharp, J. H., 1974. Improved analysis for "particulate" organic carbon and nitrogen from seawater, Limnology and Oceanography, 19 (6): 984 - 984.

Research Unit 204; Quarterly report, July-August-September, 1976

OFFSHORE PERMAFROST STUDIES, BEAUFORT SEA

1. Task Objective: D-9.

2. Field or Laboratory Activities:

A. R. E. Lewellen at Prudhoe Bay to prepare heavy equipment and to make preliminary rental arrangements for equipment needed for 1977 drilling program.

B. Scientific party active this quarter included:

D. M. Hopkins, geologist, U.S.G.S.

Peter Barnes, geologist, U.S.G.S.

Kristin McDougall, foraminiferal paleontologist, U.S.G.S.

Robert Lewellen, geologist, U.S.G.S.

C. Methods: R. E. Lewellen has been preparing a driller's log for the four holes drilled at Prudhoe Bay in 1976 to be included.

Peter Barnes and assistants have completed radiography of all core segments that were preserved intact from 1976 drilling.

A short description will be included in next quarterly report.

Kristin McDougall and assistants have sieved all marine sediments from 1976 drilling and picked forams, shells, and other organic remains and undertaken preliminary identification of the fossil foraminifera. Mollusks, seeds, and ostracodes have not yet been identified.

D. Sample localities: indicated on figure 1.

E. Data collected or analyzed:

Approximately 20 core radiographs.

Preliminary foram lists completed for 8 core samples.

28 core samples picked for forams, ostracodes, megafossils, and plant remains, but identifications not yet completed.

3. Results

Principal new data acquired during this quarter was some preliminary information on the faunal content of the borehole samples (see attached report by Kristin McDougall).

4. Preliminary Interpretations of Results

Figure 2 is an interpretive cross-section through the continental shelf in the Prudhoe Bay area, based upon our 1976 boreholes; the 1975 boreholes of Osterkamp and Harrison (1976), and 1969 borehole C-1 of Humble Oil Company (fig. 1).

Stratigraphy and environments of deposition.--Upon entering the sea bottom, most and probably all of the offshore boreholes in the Prudhoe Bay area enter marine mud (fine sand, silt, and clay) 5 to 10 m thick and then pass into beach sediments (well-rounded gravel, coarse sand, and some mud) 1 or 2 m thick. The surficial sediments commonly contain a few rounded pebbles, evidently material recently ice rafted from nearby beaches. The lower part of the marine mud sequence in PB-2, our outermost borehole, contains abundant small pebbles and granules. The pebbly mud is texturally similar to glaciomarine sediments, but the petrologic studies necessary to determine whether the pebbles are of glacial ice-berg origin or whether, instead, they were rafted from nearby beaches have not yet been completed.

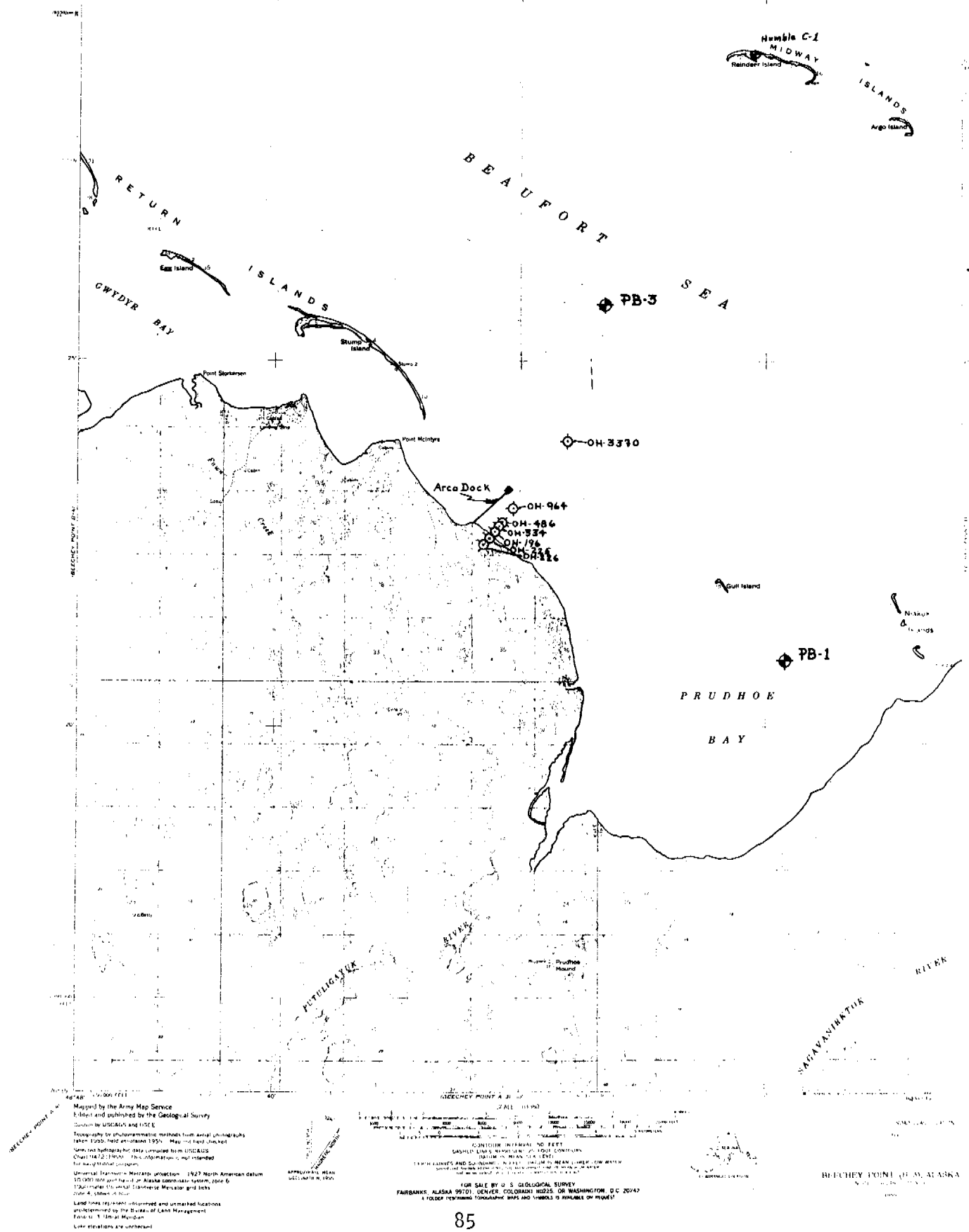
*Figure 1 Location of Permafrost Bore holes at Prudhoe Bay*

UNITED STATES  
DEPARTMENT OF THE INTERIOR  
GEOLOGICAL SURVEY

- PB: Holes drilled by CRREL-USGS, 1976
  - OH: Holes drilled by Univ. of Alaska, 1969
  - C: Hole drilled by Humble Oil Co., 1969

5

**BEECHY POINT (B-3) QUADRANGLE**  
ALASKA  
**1:63,360 SERIES (TOPOGRAPHIC)**



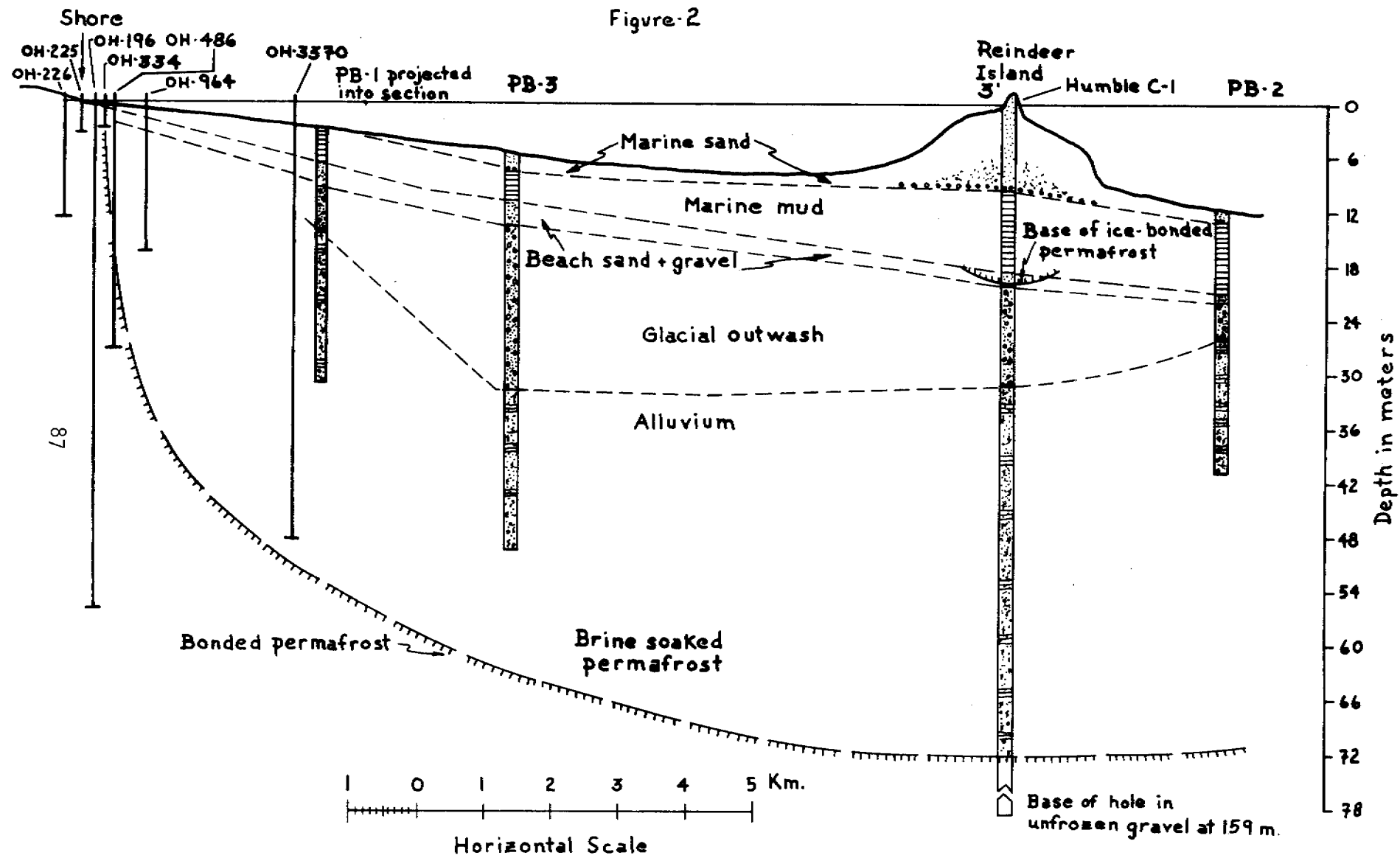
The Reindeer Island borehole passed through pebbly sand nearly 10 m thick and then into beach gravel before entering the marine mud sequence nearly 10 m below present sea level.

The marine sequence is underlain by poorly sorted angular gravel lacking any organic remains and probably representing glacial outwash. The outwash appears to be more than 15 m thick in boreholes PB-1 and PB-3 but less than 5 m thick in boreholes PB-1 and PB-2. Variations in the level of the base (fig. 2) suggest that the outwash gravel covers an erosional topography cut in the next older stratigraphic unit.

Our 1976 boreholes and some of the Osterkamp-Harrison 1975 boreholes terminate in an alluvial sequence of well-sorted sand, pebbly sand, and gravel containing lenses of detrital wood and plant fragments. We commonly lost circulation water while drilling through thick sand beds suggesting that the alluvium is much better sorted and more permeable than the glacial outwash.

Chronology and thermal history during deposition.--The continental shelf seaward at least to the position of Borehole PB-2 (fig. 1) was a subaerial river floodplain during the interval when the basal alluvial sediments were deposited. Osterkamp and Harrison (1976) report that wood fragments recovered from near the top of the alluvial sequence at -13.7 m in their borehole 3370 has a radiocarbon age of 22,300 ± 1,200 years (AU-115), an age determination that indicates deposition near the end of an interstadial (slight warming) interval within the last glaciation. In other parts of Alaska the climate at this time was similar to but slightly colder than the present climate. In a future report we will attempt to estimate mean annual temperatures at Prudhoe Bay at the time the alluvial sequence was accumulating.

Figure-2

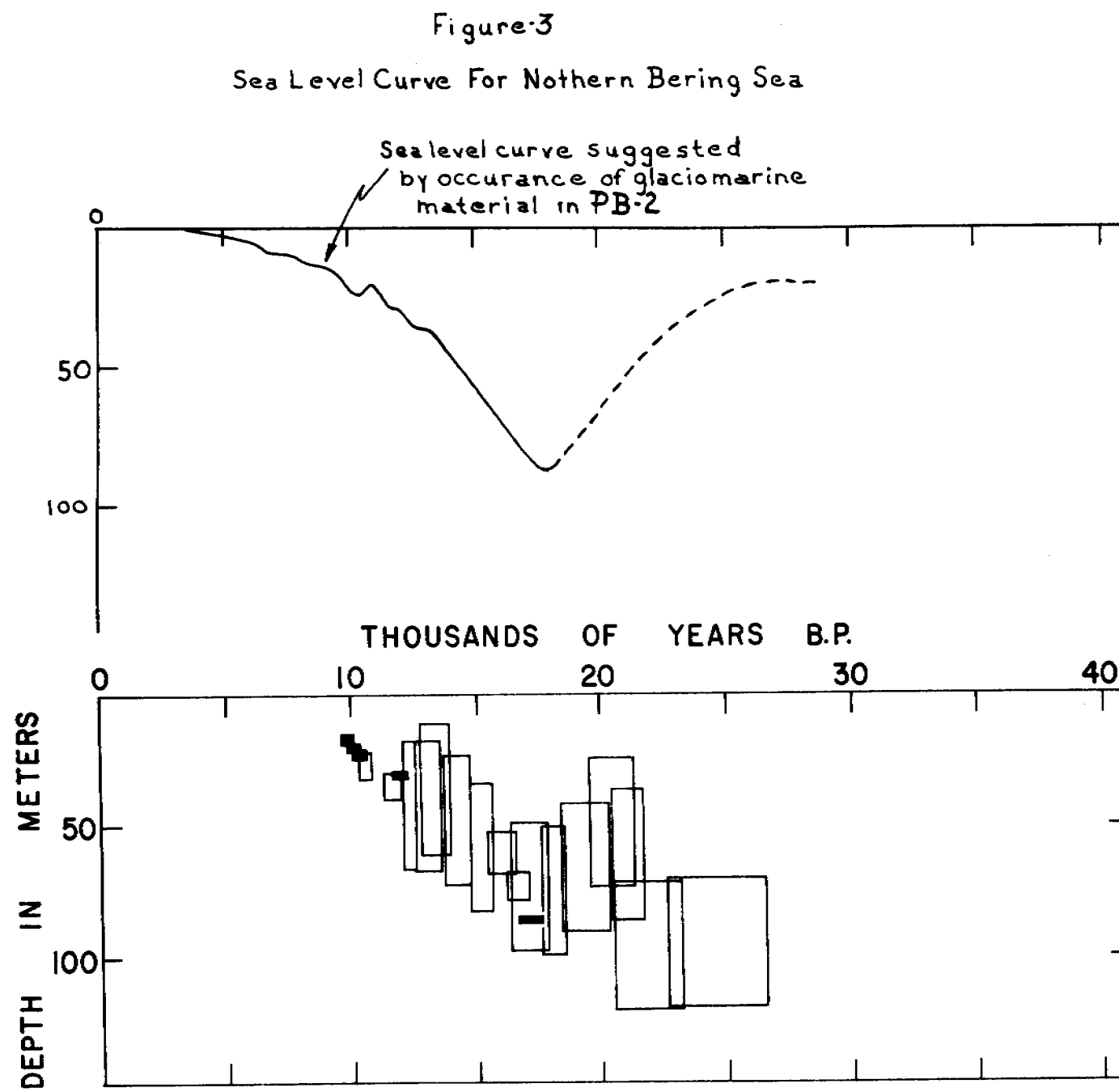


The outwash gravel is part of an outwash fan that extends from the Brooks Range down the Sagavanirktok River valley to the present coast and probably continues to the outer edge of the continental shelf. The shoreline probably lay at the margin of the shelf when the outwash was accumulating. The 22,300-year radiocarbon date on detrital wood in the underlying alluvium indicates that the outwash accumulated during the Itkillik (late Wisconsinan) Glaciation in the Brooks Range (Hamilton and Porter, 1975). In most parts of Alaska the climate was much drier and the snow cover thinner and less continuous during the last glaciation than at present (Hopkins, 1972). Nevertheless, snow line in the Brooks Range lay considerably lower (Porter, 1962), indicating that the mean annual temperature must have been reduced. In a future report, we will attempt to estimate mean annual temperatures at Prudhoe Bay during the period when the late Wisconsinan outwash was accumulating.

The surficial marine sequence will ultimately provide a direct record of the recent migration of the shoreline across the continental shelf to its present position and of the succession of marine environments that have existed during this Late Pleistocene and Holocene marine transgression. The radiocarbon-dating and amino-acid racemization programs are still in progress, and we do not yet have a locally derived chronology for the shoreline history. Some estimates can be made, however, based upon comparison with the better-known history of late Pleistocene and Holocene sea-level changes in the Bering Sea and upon inferences drawn from the possible glaciomarine sediments in borehole PB-2.

Knebel (1972) and Hopkins (1973) have prepared sea-level curves applicable to the Bering Sea and to southernmost Chukchi Sea (fig. 3).

68



In Bering Sea, sea level stood at -22 m, the level of the lowermost beach deposits in borehole PB-2 about 10,500  $\pm$  500 years ago; sea level reached a position of -13 m, the level of the deepest marine deposits in borehole PB-3 about 8,700  $\pm$  500 years ago; and sea level reached -9 m, the level of the deepest marine sediment in borehole PB-1 about 6,000  $\pm$  500 years ago. The first barrier bar on the site of Reindeer Island began to form a few centuries before the shoreline had reached the position of borehole PB-1.

Estimates of the position of the Beaufort Sea shoreline based upon the Bering Sea sea-level curve must be qualified, because the continental shelf of the Bering Sea is much wider and is also much more remote from areas of continental glaciation and consequently has undergone a different history of isostatic deformation during deglaciation and the last rise in sea level (Walcott, 1972). If we are correct in assigning a glaciomarine origin to the pebbly mud that forms the basal part of the marine sequence in borehole PB-2, we have another basis for inferring local sea-level and shoreline history.

Rodeick (1975) shows that glaciomarine sediments on the continental shelf of the Beaufort Sea are derived from icebergs that calved from the Laurentide ice sheet in the Amundsen Gulf and possibly in the Coronation Gulf north of the western Canadian mainland. During maximal phases of the late Wisconsin glaciation, the Laurentide ice sheet extended into gulfs and channels in the Canadian Arctic Archipelago, locally reading the continental shelf of the Beaufort Sea (Prest, 1969). When rising sea level began to flood the continental shelf, the ice was set afloat and began to calve rapidly. According to Prest (1969), the

Amundsen Gulf became cleared of ice about 10,500 years ago, and the more remote Coronation Gulf about 9,500 years ago. If the pebbly mud that extends from depths of 17 to 20 m in borehole PB-2 is of glaciomarine origin, it must be older than 9,500 years and it is probably more than 10,500 years old.

Until direct geochronological information is available, then, we can estimate the history of the shoreline in the Prudhoe Bay area only within rather broad limits. The shoreline migrated past borehole PB-2 no later than 9,000 and possibly as early as 11,000 years ago. It reached the position of borehole PB-3 between 8,200 and 10,000 years ago; and it reached the position of borehole PB-1 between 5,500 and 6,000 years ago.

Permafrost.--Temperature in all offshore boreholes that have been instrumented thus far in the Prudhoe Bay area have been below 0° C. It is clear that permafrost in the sense of ground at a temperature below 0° C extends at least 50 m below sea level and several tens of meters below the sea floor throughout the Prudhoe Bay area seaward to and beyond the 10-m isobath. Much of the permafrost encountered thus far, however, is brine-soaked, rather than ice-bonded.

Osterkamp and Harrison (1976) showed that ice-bonded permafrost lies just below the sea bottom in areas where water depths are shallower than 2 m and winter sea-ice contacts the bottom. Seaward from the 2 m isobath, the top of ice-bonded permafrost drops rapidly. Osterkamp and Harrison's borehole 3370 and our boreholes PB-1, PB-2, and PB-3 did not encounter ice-bonded permafrost, but extrapolation of temperature profiles indicates that ice-bonded permafrost is probably present below.

The Humble C-1 borehole on Reindeer Island encountered about 20 m of bonded permafrost extending downward from the emergent barrier bar, then passed through several tens of meters of ice-free sediment, and finally reentered permafrost between depths of approximately 70 and 125 m. This observation seems to confirm the inference based on our temperature profiles that ice-bonded permafrost is present a short distance below the bottoms of boreholes OH-3370, PB-1, PB-2, and PB-3.

5. Problems encountered and recommended changes: None.

6. Estimate of funds expended: \$35,000.

7. Bibliography:

Hamilton, T. D., and Porter, S. C., 1975, Itkillik Glaciation in the Brooks Range, northern Alaska: Quaternary Research, v. 5, p. 471-498.

Hopkins, D. M., 1972, The paleogeography and climatic history of Beringia during late Cenozoic time: Inter-Nord, no. 12, p. 121-150.

\_\_\_\_\_, 1973, Sea level history in Beringia during the past 250,000 years: Quaternary Research, v. 3, p. 520-540.

Knebel, H. J., 1972, Holocene sedimentary framework of the east-central Bering Sea continental shelf: Ph.D. thesis, Univ. Washington, 186 p.

Osterkamp, T. E., and Harrison, W. D., 1976, Subsea permafrost at Prudhoe Bay, Alaska; drilling report: Univ. Alaska Geophys. Inst., Sea Grant Rept. No. 76-5.

Porter, S. C., 1962, Geology of Anaktuvuk Pass, central Brooks Range, Alaska: Ph.D. thesis, Yale Univ., 276 p.

Prest, V. K., 1969, Retreat of Wisconsin and Recent ice in North America: Geol. Survey of Canada 1257-A.

Rodeick, C. A., 1975, The origin, distribution and depositional history of gravel deposits on the Beaufort Sea continental shelf, Alaska: M.S. thesis, San Jose State Univ., California, 98 p.

Walcott, R. I., 1972, Past sea levels, eustacy and deformation of the earth: Quaternary Research, v. 2, p. 1-14.

UNITED STATES GOVERNMENT

# Memorandum

TO : Dave Hopkins

DATE: 09/22/76

FROM : Kris McDougall

SUBJECT: Progress report on offshore boreholes PB-1, PB-2, and PB-3

All samples from the three boreholes have been processed for foraminiferal analysis. Samples from PB-1 are in being picked now. Samples from PB-2 and PB-3 are currently being identified. These faunas typically contain several species of *Elphidium*, *Buccella*, *Cassidulina*, *Quinqueloculina*, and Polymorphinids. This type of benthic assemblage indicates a neritic environment probably between 30-80 meters in depth. Fluctuations of the environment will become more apparent when counts of species are made and compared.

The following pages contain a list of samples indicating the presence of organisms and some preliminary identifications.

*Kristin McDougall*  
Kristin McDougall

Enclosures



5010-110

OFFSHORE BOREHOLE PB-2

R-1434 (PB-2 -- WS 43.8 - 48.8)

Benthonic Foraminifera:

*Cyclopygra involvens*  
*Elphidiella groenlandica*  
*Elphidium bartletti*  
*Elphidium clavatum*  
*Elphidium incertum*  
*Elphidium orbiculare*  
Polymorphinids  
*Quinqueloculina seminula*  
*Quinqueloculina vulgaris*

Ostracods

Megafossils

R-1435 (PB-2 -- WS 45.8 - 47)

Benthonic Foraminifera:

*Cassidulina* sp.  
*Elphidiella groenlandica*  
*Elphidium bartletti*  
*Elphidium clavatum?*  
*Elphidium orbiculare*  
Polymorphinids

Ostracods

Megafossils

R-1436 (PB-2 -- clay bit 68)

Benthonic Foraminifera:

*Buccella frigida*  
*Cassidulina norcrossi*  
*Dentalina* sp.  
*Elphidiella groenlandica*  
*Elphidium clavatum*  
*Elphidium incertum*  
*Elphidium orbiculare*  
*Lagena gracillima*

R-1436 (continued)

Benthonic Foraminifera (continued):  
Pseudopolymorphinids  
*Quinqueloculina* sp.

Ostracods

Megafossils

Plant fragments

R-1437 (PB-2 -- clay bit 49.7)

Benthonic Foraminifera:  
*Buccella frigida*  
*Dentalina* sp.  
*Elphidium clavatum*  
*Elphidium orbiculare*  
*Eponidella strombodes*  
Polymorphinids  
*Quinqueloculina seminula*  
*Quinqueloculina* cf. *Q. subrotunda*  
*Silicosigmolina groenlandica*

Ostracods

Megafossils

Plant fragments

R-1438 ( PB-2 -- GS3e)

Benthonic Foraminifera:  
*Buccella frigida*  
*Elphidium clavatum*  
*Elphidium incertum*  
*Elphidium orbiculare*  
Polymorphinids

Ostracods

Megafossils

R-1438 (continued)

Chara

Plant fragments

R-1439 (PB-2 -- GS04b)

Benthonic Foraminifera:

*Buccella frigida*  
*Cassidulina islandica*  
*Cassidulina norcrossi*  
*Dentalina* sp.  
*Elphidium clavatum*  
*Elphidium incertum*  
*Elphidium orbiculare*  
*Lagena gracillima*  
*Lagena* sp.  
Polymorphinids

Ostracods

R-1440 (PB-2 -- 4e)

Benthonic Foraminifera:

*Bulimina exilis*  
*Cassidulina islandica*  
*Cassidulina norcrossi*  
*Elphidium clavatum*  
*Elphidium orbiculare*  
*Fissurina* sp.  
Polymorphinids

Ostracods

Megafossils

Plant fragments

R-1441 (PB-2 -- GS05b)

Benthonic Foraminifera:

*Buccella frigida*

R-1441 (continued)

Benthonic Foraminifera (continued):

*Bulimina exilis*  
*Cassidulina islandica*  
*Cassidulina norcrossi*  
*Elphidium clavatum*  
*Elphidium orbiculare*  
*Fissurina sp.*  
*Lagena gracillima*  
Polymorphinids  
*Pyrulina sp.*

Ostracods

Megafossils

Plant fragments

	BENTHONIC FORAMINIFERA	OSTRACODS	MEGAFOSILS	PLANT FRAGMENTS
R-1442 (Pb-2, GS05e)	X	X	0	X
R-1443 (Pb-2, clay bit 58-60)	X	X	X	X
R-1444 (Pb-2, GS6x)	X	X	X	0
R-1445 (Pb-2, clay bit 65.8)	X	0	X	0
R-1446 (Pb-2, clay bit 70.75)	X	0	X	X
R-1447 (Pb-2, clay bit/core 72.9)	X	X	0	X
R-1448 (Pb-2, WS 73-81)	0	0	X	0
R-1449 (Pb-2, WS 88-92)	0	0	0	0
R-1450 (Pb-2, WS 92-101)	0	0	X	0
R-1451 (Pb-2, WS 101-111)	0	0	0	0
R-1452 (Pb-2, WS 111-112)	0	0	0	0
R-1453 (Pb-2, WS 123-126)	0	0	0	0
R-1454 (Pb-2, WS 127-129)	0	0	0	0
R-1455 (Pb-2, WS 129-131)	0	0	0	0
R-1456 (Pb-2, WS 131-133)	0	0	0	0
R-1457 (Pb-2, WS 133-135)	0	0	0	0
R-1458 (Pb-2, 08E)	X	X	X	X
R-1459 (Pb-2, GS 8-A)	X	X	X	X
R-1461 (Pb-2, 56-58.2 GS5C)	X	X	X	0
R-1462 (Pb-2, GS3)	X	X	X	X
R-1464 (Pb-3, GS-01b)	X	X	X	X
R-1465 (Pb-3, GS-02y)	X	X	X	0
R-1466 (Pb-3, GS03x)	X	X	X	X
R-1467 (Pb-3, GS04x)	X	X	X	X
R-1468 (Pb-3, GS05x)	X	X	X	X
R-1469 (Pb-3, GS06x)	X	X	X	X
R-1470 (Pb-3, WS 40-40.9)	X	X	X	0
R-1471 (Pb-3, WS 39.9-43.0)	0	0	X	0

	BENTHONIC FORAMINIFERA	OSTRACODS	MEGAFOSILS	PLANT FRAGMENTS
R-1472 (Pb-3, WS 43-44)	0	0	0	0
R-1473 (Pb-3, WS 44-46)	0	0	X	0
R-1474 (Pb-3, WS 46-52)	0	0	X	0
R-1475 (Pb-3, B2b)	X	X	0	X
R-1476 (Pb-3, 05 B 38-40.4)	X	X	X	X
R-1477 (Pb-3, 06 A 38-40.4)	X	X	X	X

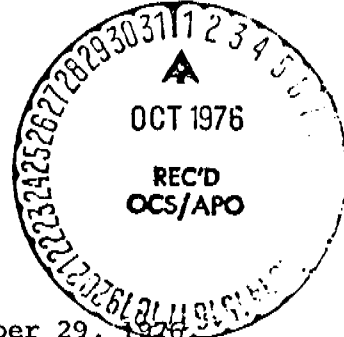


UNITED STATES  
DEPARTMENT OF THE INTERIOR

GEOLOGICAL SURVEY

Pacific-Arctic Branch of Marine Geology  
345 Middlefield Road  
Menlo Park, California 94025

RU 205



September 29, 1976

Dr. Gunter Weller  
Arctic Project Office  
Geophysical Institute  
University of Alaska  
Fairbanks, Alaska 99701

Dear Gunter:

I have unexpectedly had to return to Prudhoe to help finish work with the KARLUK. Our Quarterly Report due October 1 is not yet finished and I don't see any way of completing it before the due date. Also attachments A&B will be mailed when completed. However, we will have it to you by the 15th of the month.

To show that we are progressing, enclosed is a preliminary report of Field Activities during the first part of the Quarter which will be included in our Quarterly Report.

Regards,

Peter Barnes

Enclosure



REPORT OF FIELD ACTIVITIES: SUMMER 1976

The first part of the summer-open water-activities in the Beaufort Sea were completed from the R/V KARLUK, during July and August, under the direction of Peter Barnes and are reported on here. The first half of July was spent in Prudhoe Bay with the mundane job of preparing the KARLUK for the summer season. The hydraulic system was completely rebuilt, a new and stronger mast and boom were installed and the damage from last winters break-in and burglary was repaired. Two 50 foot towers for navigation beacons were installed; one on the eastern Cottle Island bench mark and the other at Tolaktovut Point on the Colville delta. We anticipate leaving these towers installed for the winter. They could be made available for other OCS projects.

On 24 July the ice in Prudhoe Bay had cleared sufficiently that a seismic refraction survey for sub-sea permafrost utilizing three 40 in<sup>3</sup> air guns and a 24-channel recording system was begun under the direction of James Rogers of the University of Alaska. Several lines were run inside Prudhoe Bay, including two transects over the permafrost drill hole in the northern part of the bay and two transects onto the beach (attachment A). Ice precluded operations outside Prudhoe Bay and the refraction equipment was offloaded on 29 July.

Subsequently, instrument moorings implanted in the fall of 1975 off Prudhoe Bay and in the channel between Egg Island and Long Island were recovered. The instrument package outside the entrance channel to

Prudhoe Bay had moved onshore in a southerly direction about 200 meters. Furthermore, it was badly damaged either by ice during the winter or from the barge unloading activities of late last fall. The instruments in the Egg Island channel were also recovered damaged, although not as severely. The 300 meter grappling line on the Egg Island implant was heavily covered with grasses and small twigs suggesting significant organic input from the nearby Kuparuk River during the early June flooding. Although damaged, both instruments had completely utilized their tapes which are presently being processed at NOAA/PMEL. Hopefully, they were damaged after their recording cycle. The least damaged meter was repaired and implanted with a nephelometer and tide gauge in 5 meters of water off of the Sagavanirktok River on July 31 (Attachment A).

Detailed bathymetry in the vicinity of the west dock and the entrance channel to Prudhoe Bay were taken to establish if changes have occurred since the U.S. Coast and Geodetic Survey of 1950 and to serve as a baseline for further changes. Precision range-range navigation system was used along with a fathometer which could be read to the nearest 0.1 meter. The preliminary interpretations from this survey are appended as Attachment B. Operations during the first week in August included about 200 km of sediment profiling coupled with bathymetry, surficial temperature salinity and transmissivity, spot current measurements and side scanning sonar data. Two track lines were run in Stefansson Sound essentially completing our coverage there. The remainder of the profiling was concentrated in western Harrison Bay where our

previous data had been sparse. It is apparent from this data that the near surficial geological conditions in western Harrison Bay differ from those to the east. Most significant is that subbottom records suggest that there is much less gravel in the sediments. In addition "tundra" capped ice was studied in the vicinity of a former island just east of Cape Halkett. The location of the former island was indicated by grounded ice concentrations and a 1 meter shoal.

The survey test lines established off Thetis and Spy Islands in 1973 and rerun in 1975 were reoccupied again this year. This years records indicated considerable ice gouge activity during the winter and spring. Ice observations during the spring and summer indicated that the stamukhi zone is poorly developed in the Olitok area during the winter of 1975-76. The absence of numerous large winter ice features coupled with evidence of ice gouging is puzzling.

On the 12th of August Erk Reimnitz and Larry Toimil joined the KARLUK for vibra coring work. The corer was assembled at the Prudhoe Bay camp and onloaded. After successful testing at the dock and in the central part of Prudhoe Bay a sampling transect was run from Stump Island offshore and across the Reindeer Island shoal (Attachment A). In addition the boulder patch south of Narwhal Island, the two meter bench off the Sagavanirktoq River were cored. Operations were then moved to Harrison Bay where a transect of cores was obtained from the one meter contour to 18 meters depth, 26 km seaward off the central delta. A short section across the western delta front platform obtained 3 more core samples.

Data from the rate of penetration of the hammer driven corer almost always indicated a sharp decrease at approximately one meter below the sea floor suggesting an increase in sediment strength. These data will be of significance when offshore structures are built. No ice or ice bonded sediments were recovered at any of our coring sites.

Studies during the second part of the summer activities from the KARLUK are being directed by Erk Reimnitz and Larry Toimil. Their efforts will include (a) the study of areas of outcrop by diving and TV observation; (b) creating an artificial ice gouge with a plow to be monitored in coming years; (c) studying changes in bathymetry and coastal configuration north of Pingok Island; and (d) to recover and reimplant current meters for the winter season off the Colville Delta.

QUARTERLY REPORT

Contract: #RK 6-6074

Research Unit: 206

Reporting period: Sixth Quarter

Number of pages: 3

FAULTING AND SLOPE INSTABILITY IN  
THE SAINT GEORGE BASIN AREA,  
SOUTHERN BERING SEA

T.L. Vallier and J.V. Gardner  
Pacific-Arctic Branch of Marine Geology  
U.S. Geological Survey  
Menlo Park, California 94025

October, 1976

QUARTERLY REPORT RU #206

I. Task Objectives

Research objectives are to outline and document problems related to seafloor instability of the St. George Basin and adjacent outer Beringian shelf, Southern Bering Sea.

II. Field and Laboratory Activities

We just completed 43 days of work at sea aboard the U.S.G.S. vessel R.V. SEA SCUNDER. Leg 1: Aug. 2 thru Aug. 20; Leg 2: Aug 22 thru Sept. 14. This cruise is designated S76-4.

The Scientific Party included:

T. Vallier, USGS Co-Chief Scientist  
J. Gardner, USGS Co-Chief Scientist  
A. Kaneps, Scripps Institution of Oceanography, Sedimentologist  
W. Dean, U.S.G.S./Denver, Inorganic geochemist  
B. Ruppel, USGS/Seattle, Geophysicist  
K. Kvenvolden, USGS, Organic Geochemist  
F. Cook, Univ. Calif. Santa Cruz, benthonic foraminifera  
E. Stanley, Univ. Calif. Davis, Radiolaria  
A. Budai, Calif. State Univ. Fresno, Sedimentologist  
S. Johnson, Univ. Washington, Physical Science Technician (PST)  
R. Garlow, USGS, Navigator  
R. Brady, USGS, PST  
D. Klise, USGS, PST  
S. Davenport, Univ. Calif. Santa Cruz, PST  
S. Lewis, Univ. Calif. Santa Cruz, PST  
K. Glikman, Calif. State Univ. San Francisco, PST  
G. Tanner, USGS, Electronics technician  
H. Hill, USGS, Electronics technician  
M. Underwood, USGS, PST  
G. Redden, USGS, PST  
J. Cudnohufsky, USGS, PST

The field methods used can be divided into two basic disciplines; geophysics and geology. Our geophysical methods include 3.5 KHz (3 kw source) 2.5 KHz (4-plate uniboom source), 60 to 125 HZ (60 KJ Sparker source), gravity, magnetics, and side-scan sonar. Geologic data was collected using gravity and piston coring, Van Veen sampling, dredging, and 35 mm bottom photography. Additional data were taken by expendable bathythermographs and thermosalinograph.

Our navigation was by integrated Loran C and satellite which gave accuracies typically better than  $\pm 200$  m.

Tracklines and sampling stations are shown on figures 1 & 2. The types and amounts of data collected on S76-4 are outlined in Table 1.

TABLE 1

DATA COLLECTED ON CRUISE S76-4

3.5 KHZ	4388 nautical miles (n.m.)
2.5 KHZ	3161 n.m.
60-125 Hz	3661 n.m.
Gravity	4388 n.m.
Magnetics	2509 n.m.
Side-scan sonar	82 n.m.
Gravity cores	96
Piston cores	8
Piston core trigger weights	3
Van Veen samples	27
Expendable bathythermographs	67
Bottom camera stations	3
Thermosalinograph	3500 n.m.
Number of Stations	85

III. Results

Our data is just arriving at the writing of this report; consequently, no analyses have yet been performed.

IV. Preliminary interpretation of results not applicable at this time.

V. We encountered no problems in the field.

VI. Estimate of funds expended : All funds expended.

**Quarterly Report**

**Research Unit # 208  
Reporting Period 7/1/76-9/30-76  
Number of pages: 13**

**Yukon Delta Coastal Processes Study**

**William R. Dupré  
Department of Geology  
University of Houston  
Houston, Texas 77004**

**David M. Hopkins  
Alaska Geology Branch  
U. S. Geological Survey  
345 Middlefield Road  
Menlo Park, Calif. 94025**

## QUARTERLY REPORT

### I. Task Objectives

The overall objective of this project is to provide data on geologic processes active within the Yukon-Kuskokwim delta in order to aid in the evaluation of the potential impact of scheduled oil and gas exploration and possible production. In particular, attention has been focused on the following:

- 1) Study the processes along the Yukon-Kuskokwim delta shoreline (e.g., tides, waves, sea-ice, river input) in order to develop a coastal classification including morphology, coastal stability, and dominant direction of longshore transport of sediments. (Task D-4, B-2).
- 2) Study the hydrology and sediment input of the Yukon and Kuskokwim Rivers as they largely determine the sediment budget of the northern Bering Sea. (Task B-11, B-2).
- 3) Determine the type and extent of Quaternary faulting and volcanism in the region. (Task D-6).
- 4) Reconstruct the late Quaternary chronology of the delta complex in order to determine:
  - a) frequency of major shifts in the course of the Yukon River.
  - b) effects of river diversion on coastal stability.
  - c) relative age of faulting and volcanism.
  - d) frequency of major coastal storms as recorded in chenier-like sequences along the coast.

### II. Field and Laboratory Activities

#### A. Field trip schedule

7/4/76 - 8/1/76: Summer field work in the Yukon delta.

B. Scientific Party:

- 1) William R. Dupré - Geologist - Project Chief  
Department of Geology  
University of Houston  
Houston, Texas 77004
- 2) Thomas Ager - Palynologist  
Mail Stop 971  
U.S. Geological Survey  
Reston, Virginia 22092
- 3) John McKinnon - Biologist - Field Assistant  
Box 155  
Auke Bay Fisheries Lab  
Auke Bay, Alaska 99821

C. Methods

- 1) Field studies included the following:
  - a) Interpretation of aerial photos and landsat imagery
  - b) Aerial reconnaissance in float plane
  - c) Selected field study sites: emphasizing sampling for radiocarbon dating, textural analysis, description of vegetation and thermal uplifting of soils.
  - d) Establishment of semi-permanent coastal stations, including beach profiles, offshore profiles using Zodiac and fathometer, sampling for textural analysis, study extent of permafrost in coastal areas.
  - e) Cored a volcanic lake using a Zodiac and modified Livingston piston corer, to obtain core for radiocarbon chronology of volcanic activity.
- 2) Lab Studies
  - a) Six samples collected during last summer's field season were sent to Steve Robinson at the U.S.G.S. at Menlo Park for radiocarbon dates. The dates have

been obtained giving some information as to the frequency of river shifting and delta formation.

D. Sample localities/aircraft tracklines

(See Figure 1).

E. Data collected or analyses

- 1) Number and types of samples/observations
  - a) Approximately 600 35mm slides were taken during aerial reconnaissance and selected site studies.
  - b) Approximately 50 samples collected for textural analysis (including 3 short cores).
  - c) Approximately 20 samples collected for radiocarbon dating.
  - d) Beach and offshore profiles measured for 12 coastal stations.
  - e) One 6½ meter core obtained from a volcanic lake in the delta region.
  - f) Thermal profiles of soils and description of vegetation for approximately 12 sites throughout the delta.
  - g) Surface pollen samples from 8 locations throughout the delta.
- 2) Number and types of analyses
  - a. Six radiocarbon dates obtained from samples collected last summer.

III. Results

Geologic and coastal stability maps remain in progress, although significant portions have been completed. Radiocarbon dates by Steve Robinson with U.S.G.S. at Menlo Park are give in Table 1.

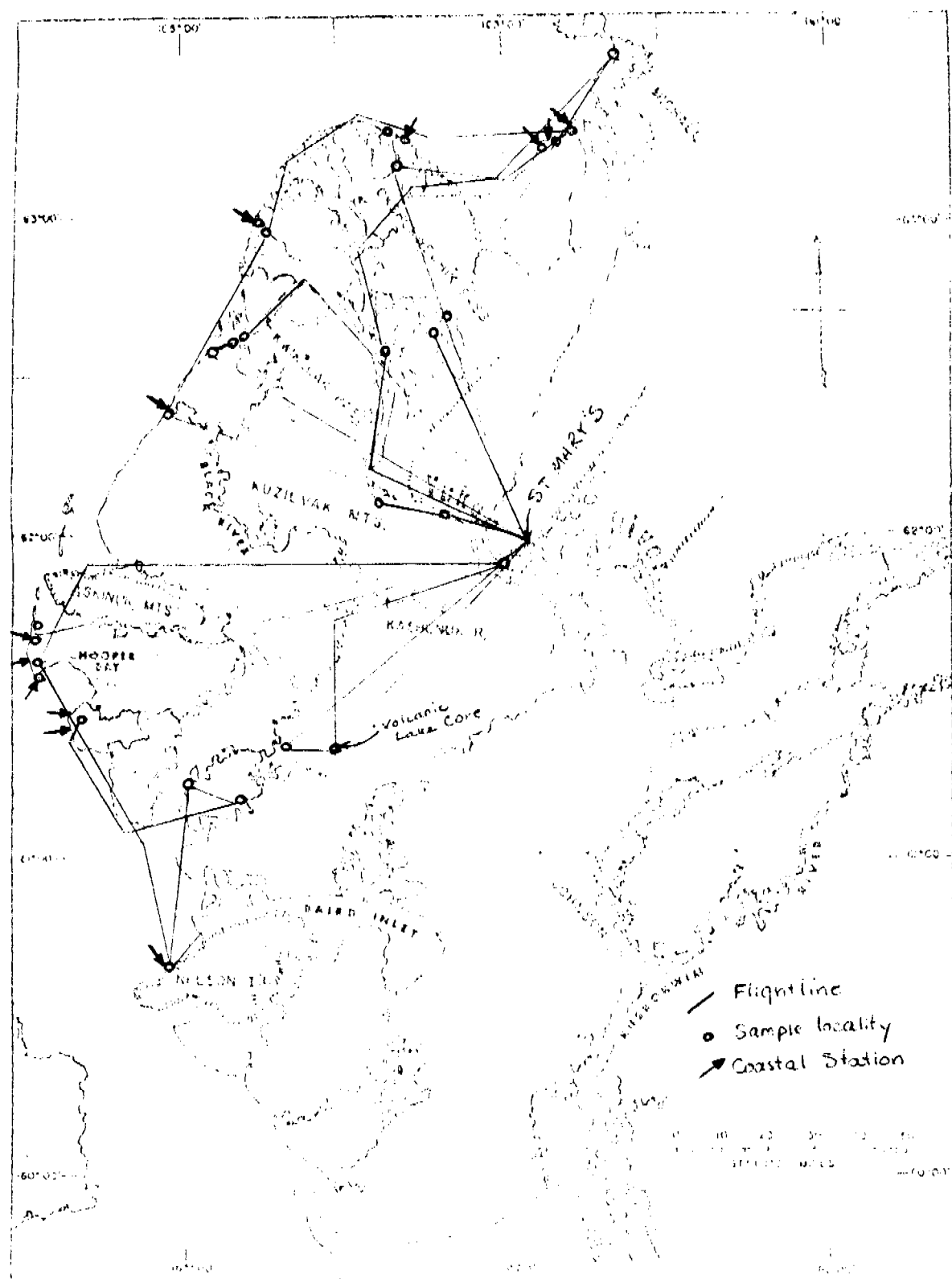


Figure 1.

Project No. - USGS No.		Lat.	Long.	Date
II-10	48	62° 55'-	164° 06'	820 <u>+90</u>
V-10	49	62° 09'	164° 59'	1350 <u>+80</u>
V-9	50	62° 02'	165° 14'	34,400 (poss. reworked?)
V-4	51	61° 32'	164° 46'	1200 <u>+60</u>
I-4	52	61° 36'	166° 10'	modern (contaminated sample)
II-10	53	62° 19'	165° 12'	1890 <u>+85</u>

Table I: Radiocarbon dates - Yukon delta

#### IV. Preliminary Interpretation of Results

##### A. Permafrost:

The presence of discontinuous permafrost is well evidenced by an abundance of geomorphic criteria, including thermokarst lakes, palsas, patterned ground, solifluction lobes, and string bogs. Its existence was further quantified by probing to frozen ground, examining rapidly eroding cut banks, and by the use of drillers reports of permafrost in the region.

Several types of ground ice were seen during the course of the field season. Pore ice and thin lenses of segregated (Taber) ice were seen, even in the Holocene deposits. The most impressive exposures were in older (late Wisconsinan?) deposits which cover much of the Yukon-Kuskokwin delta complex. In these areas, patterned ground was underlain by large ice wedges, up to a meter across at the top. These wedges appear to be truncated, and are probably inactive or only weakly active. Massive ice, similar to that described by MacKay in the northern part of Canada, is also present in these deposits. This massive ice is at least

two meters thick (its base was not exposed), continuous over the length of large outcrops, and is generally non-foliated.

Preliminary field work has demonstrated a strong correlation between topography, soils type, vegetation, and depth of the active zone. However the thickness of the permafrost could not be determined with present field methods. Nevertheless, interviews with engineers and water well logs give some evidence as to the distribution and thickness of permafrost in the region.

There is permafrost in much of the older parts of the modern Yukon delta, yet its thickness is probably on the order of 5-10 feet in most areas. Holocene fluvial deposits are underlain by over 35 feet of frozen ground near Bethel, however; the depth and distribution appears to be controlled by the path of the meandering river. The major rivers and some of the larger lakes are underlain by unfrozen ground; even where the ground is frozen, gravel layers may form unfrozen zones (taliks).

The older (Wisconsinan?)parts of the delta are underlain by great depths of permafrost, locally up to 600 ft. Depths up to 250 ft are present along the rapidly eroding coastal zone south of Cape Romanzof, thereby providing ideal conditions for the preservation of offshore permafrost, a possibility which needs closer attention in the future.

In summary, permafrost is present throughout the region, in varying contents and thickness, except in those few areas where rivers or deep lakes provide sufficient insulation to melt the underlying frozen zone, or where deposition has occurred so recently as to limit its formation. In many ways, its

distribution is similar to that of the Mackenzie delta in Canada, differing mainly in the thickness of the frozen zone.

B. Coastal Erosion:

Comparison of 1954 and 1975 aerial photos indicates that several hundreds of feet of erosion has occurred along much of the coast in the last 30 years. Most of that erosion occurs during late Summer/early Fall storms, particularly in response to strong winds and elevated storm surges. How much erosion might occur in a single storm isn't known, although photography is available before and after the 1973 storm surge, and will be examined. Similarly, the recurrence interval of such storms isn't known. Some estimate of frequency of storms should be provided which some of the storm-generated chenier ridges are dated.

Shorefast ice can be especially effective in eroding the shoreline, particularly if it formed early, lifted and drifted offshore to return on a storm tide. Lifting and shifting of ice in the tidal flats results in the formation of large-scale grooves. These grooves control the pattern of emergent vegetation, which in turn determines the rather complex drainage patterns which characterize emergent tidal flat deposits in the region.

C. River Shifting:

Careful examination of the Yukon-Kushokwim delta plain reveals a complex assemblage of uplifted mountain ranges and volcanoes, abandoned river courses, extensive dune fields, in addition to the modern-day fluvial and deltaic deposits (Figure 2). Of particular interest are the major shifts in the course of the

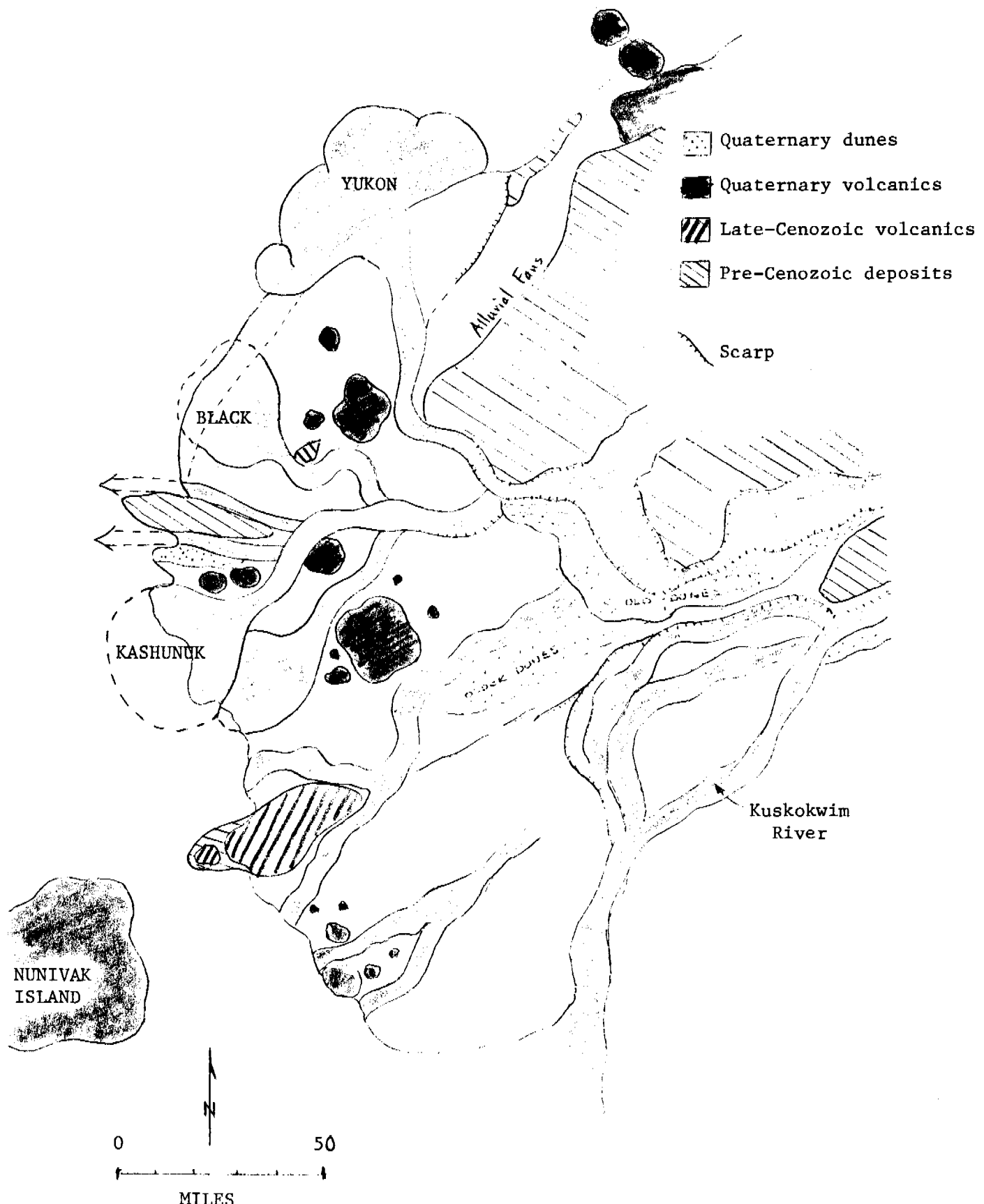


Figure 2

Yukon which have occurred several times during the late Pleistocene. The mechanism by which such shifts (river avulsion) occur is unclear. They may be related to the Quaternary faulting in the area; alternatively, they may have occurred in response to flooding associated with major ice jams. Whatever their cause, they have resulted in the diversion of the Yukon a hundred miles inland, causing a lateral shift of the Yukon of up to 150 miles along the coast.

Radiocarbon samples were collected along the Black and Kashunuk Rivers to date the most recent sediments carried when they were the main course(s) of the Yukon. Samples were collected in the modern delta to date the oldest part of that delta. These dates should bracket the time of river avulsion, and provide an estimate as to the age of the modern delta. The Black River was abandoned approximately 1300 years ago, the Kashunuk River about 1200 years ago. A sample from one of the oldest parts of the delta is approximately 820 years old. These dates suggest that the shift probably occurred about 1000-1200 years ago.

The question then arises as to the possibility of yet another shift, perhaps to reoccupy an older river course (e.g. the Kashunuk). Much water and sediment from the Yukon is diverted through the Kashunuk during Spring breakup. It certainly is possible for the Yukon to reoccupy the Kashunuk under natural conditions, much as the Mississippi would reoccupy the Atchafalaya Bayou and abandon its present course were it not for the Corp of Engineers. The implications of such a shift of the Yukon are staggering, affecting the physiography, economy, and circulation patterns throughout the region. For that reason special caution is urged, particularly if construction

is planned which might affect the hydrology of the river and increase the probability of river diversion.

D. Applications to Biological Habitat Studies:

An understanding of the geologic history of the delta region and the processes by which it continues to be shaped provides invaluable insights as to geologic hazards and engineering properties. Less obvious is the extent to which geologic processes and products combine to determine the topography, soils, and vegetation which are so important in defining biological habitats. Thus, it should be no surprise that the first report of pingo-like features (palsas) in the delta region was done to define their role as an important mink habitat. Similarly, the margins of abandoned distributary mouth bars mapped in the modern delta region have slopes and vegetation assemblages which, according to Bob Jones (U.S. Fish & Wildlife) are particularly important nesting areas.

Almost all of the delta is underlain by frozen ground. It is the selective melting of the permafrost which has resulted in the myriad of thermokarst lakes so important in making the area such a productive nesting area. This study is aimed at understanding the origins of these lakes, including the processes by which they drain and/or fill, thereby defining a continuum of lake types which might aid in regionalization of nesting habitats.

E. Volcanic Lake Core:

A 6½ meter core was obtained from a volcanic lake within the Ingakslagwat Hills ("much volcanoes") which will provide the most detailed record to date of vegetation and climatic change in this

region of Alaska. Two samples taken at two meters depth preserve a vegetation assemblage which records a late(?) glacial climate unlike any in Alaska today. Preliminary work suggests the core may contain up to 30,000 to 40,000 years of record. Of particular significance will be any ash beds, which if dated, should give the frequency of the most recent volcanism in the region.

V. Problems Encountered/Recommended Solutions

The most serious problem of the field season was the inaccessibility of most of the coast by wheeled or float plane. For that reason, an extremely inefficient system of plane shuttles, combined with the use of a Zodiac was used to establish coastal stations. Many areas still remain inaccessible, given the time constraints of this project. Thus it seems imperative that a helicopter be used in the future; the FY77 proposal includes such a request.

The timing of field work was chosen to take advantage of the good weather along the coast in July. Unfortunately, the active layer is still increasing at that time, and maximum depths to permafrost could not be determined. Next year's field season will continue into August. In addition, other field parties in the delta will be recording changing depth to frozen ground.

VI. Estimate of Funds Expended.

Salaries:

(1) GS-12 - 4 1/2 pay periods	\$ 4,500
(2) GS-12 - 3 pay periods	3,000

Field Expenses:

(1) Charters @ \$110/Hr	5,160
(2) Commercial air fare	1,290
(3) Air freight	1,270
(4) Equipment	
(a) Field gear (incl. medicine & tents)	527
(b) Coring gear	210
(c) Temperature probe	210
(d) Aerial photographs @ \$25/Frame	1,270
(5) Per Diem	
(50 days @ \$25/day)	1,750
(5 days @ \$50/day)	

Lab Expenses:

(1) Radiocarbon dates @ \$150/date (13 in progress)	3,150
Total this quarter	22,337
Previously spent	12,663
Total FY 76	35,000

Research Unit 209: Quarterly report, July-August-September, 1976

FAULT HISTORY OF THE PRIBILOF ISLANDS AND ITS RELEVANCE TO BOTTOM STABILITY IN THE ST. GEORGE BASIN

1. Task Objective: D-6

2. Field or Laboratory Activities:

A. No cruises or field work.

B. Scientific party: M. L. Silberman and D. M. Hopkins.

C. Methods: Efforts during the summer quarter were devoted to attempts to date lavas and sediments on the Pribilof Islands in order to refine existing knowledge of recurrence intervals of surface faulting and volcanic eruptions.

D. Sample localities were indicated in Annual Report.

E. Data collected and analyzed:

About 40 K/Ar determinations.

3. Results:

We have now completed at least partial age determinations on 39 samples of basement granitic and covering basaltic rocks from the Pribilof Islands, and have calculated the K-Ar ages of 27 of them (table 1). Of these determinations, 13 were completed at the Hawaii Institute of Geophysics. Work there was suspended due to a major equipment failure, which occurred when an HIG laboratory technician used an incorrect procedure while Silberman was temporarily away from HIG on another island.

4. Preliminary Interpretation of Results:

HIG equipment was specifically designed for dating extremely young volcanic rocks. However, upon arrival at Hawaii, it was discovered that problems with the equipment had been recurring frequently during the preceding few months, which resulted in anomalously low ages, even negative values for samples in the age range of the Pribilof basalts. Reproducibility was also a problem with some samples. We were not able to investigate reproducibility of data on the Pribilof samples at HIG due to the equipment failure. However, a test sample, that had been dated at Menlo Park yielded an age, lower than, but still within analytical uncertainty of that done at Menlo (table 1). The rock dated was similar in age and composition to the Pribilof basalts on St. Paul Island, and sample preparation techniques were identical.

After the equipment failure at HIG, and a projected several month period to repair the damage (which turned out to be an underestimate) we brought the samples back to Menlo Park and attempted to complete analyses here. Due to very heavy equipment usage, however, it was not possible to complete all the samples this quarter.

The table lists age determinations on rocks from St. Paul and St. George Islands done at the different laboratories, that have been completed to date. About 15 additional samples have been partially completed, and need mass analyses. These will be completed next quarter. The table shows a serious discrepancy in data from the two laboratories with the ages of the rocks dated at HIG being

significantly lower than the same rocks dated at Menlo Park. Many of the HIG values are negative ages. The first series of ages done at HIG from St. George Island were slightly younger than age determinations on the same lava sequences reported by Cox and others (1966) but are still consistent with the paleomagnetic stratigraphy with certain modifications, and we considered these ages as being reasonable. Our second group of HIG dates from St. Paul were extremely erratic ranging from anomalously old to negative.

The St. George HIG data appeared to be internally consistent stratigraphically, but we repeated the determinations at Menlo Park to check reproducibility. The Menlo St. George ages, however, are older by factors varying from 0.3 to 2 than the same rocks dated at HIG, and are much older than the ages of similar lava sequences reported by Cox and others (1966). They are also not consistent with the paleomagnetic stratigraphy (Cox and others, 1966) and hence we question their validity. These data, however, are consistent within their physical stratigraphy. The Menlo Park ages on St. Paul are again, older than we expected on the basis of two that were reported by Cox and others (1966) from this Island, but they are not in conflict with the paleomagnetic stratigraphy and we would not have questioned them were it not for the anomalously old values obtained on the St. George rocks.

During the same time the Pribilof samples were dated at Menlo Park, other samples from other areas, principally Nevada and New Mexico were dated using the same equipment and procedures; ages of these

specimens are apparently consistent with previous age determinations on specimens from those areas. The problem appears to be restricted to the rocks from the Pribilof Islands. The number of factors causing the problem in the procedure are large, and due to the total equipment failure at HIG we cannot repeat any of the determinations done there to check reproducibility or further diagnose the problem there. As far as analytical quality of the data, indicated by the relative proportions of radiogenic argon in the samples (table 1) which is the dominant factor controlling analytical precision, Silberman believes the Menlo Park data are superior. The negative ages obtained at HIG are suggestive of small leaks causing fractionation in the vacuum equipment used to extract argon from the samples. This would tend to produce abnormally high  $^{36}\text{Ar}$  contents and reduce the apparent ages. In the past, there have been problems at HIG with spuriously high amounts of argon-36 in the system, which we did not know about before arrival at HIG. We cannot confirm this diagnosis now because the equipment at HIG is being totally rebuilt.

The only way at present to resolve the conflict in the data is to obtain ages on selected samples from a completely independent source, and also to check ages on rocks dated at HIG before the present series of experiments were run. Both of these procedures are in progress. The Isotope Geology Laboratory of the USGS in Denver, which operates independently of that at Menlo Park, is checking the ages of several of the discrepant samples. We are checking here several samples run

at HIG in the months before the current samples were dated. We hope to complete all these experiments in the next quarter, and resolve the conflicting data.

One positive result has been obtained. The basement rocks on St. George Island have been dated as indicated in the preprint to be released on October 8, 1976, as a USGS open file report, and to be submitted for more formal publication in GEOLOGY. The results are consistent with other basement ages in the region.

5. Project funds transferred from NOAA were mostly exhausted during the April-May-June quarter. Silberman has devoted about 6 weeks and Hopkins about one week to R.U. #209 this quarter. \$3500 worth of salary was allocated to support Silberman's work during this period.

Table 1. Summary of Pribilof Islands age determinations, completed to date.

	MENLO PARK				H.I.G.				
	Sample #	Mineral	% Rad $^{40}\text{Ar}$	Age $\pm$		Sample #	Mineral	% Rad $^{40}\text{Ar}$	Age $\pm$
<b>St. George Island</b>									
(Samples in stratigraphic order)	G186AII	Whole rock	13.5	$2.34 \pm 0.23$		G186AI	Whole rock	7.0	$1.21 \pm 0.36$
	G206AII	"	Not completed	-		G206AI	"	21.1	$1.40 \pm 0.14$
	G14 II	"	18.9	$3.01 \pm 0.20$		G14I	"	11.9	$2.39 \pm 0.36$
	G201AII	"	Not completed	-		G201AI	"	13.7	$1.72 \pm 0.34$
	G115BII	"	16.5	$3.21 \pm 0.25$		G115BI	"	None	Negative age
	G188BII	"	33.1	$2.87 \pm 0.12$		G188BI	"	20.5	$1.99 \pm 0.20$
	G131 II	"	17.9	$3.94 \pm 0.28$		G131 I	"	14.2	$2.14 \pm 0.43$
	G142A II	"	4.7	$6.8 \pm 2.1$		G142AI	dirty sample, would not run.	-	
Basement	G199	Alkali Fspr Sericite	57 78	$55.0 \pm 2.2$ $49.5 \pm 2.0$					
	G200	K-feldspar Chlorite	49	$52.7 \pm 2.1$					
<b>St. Paul Island</b>									
(Samples in stratigraphic order)	75AHP39I	Whole rock	1.70	$0.423 \pm 0.250$					
	75AHP39III	"	5.62	$0.299 \pm 0.076$					
	75AHP40II	"	5.22	$0.305 \pm 0.084$		75AHP40I	Whole rock	None	Negative
	75AHP41III	"	5.55	$0.630 \pm 0.163$		75AHP41I	"	None	Negative
	75AHP41IV	"	0.67	$0.112 \pm 0.235$					
	75AHP26BI	"	0.10	$0.025 \pm 0.400$					
(Samples in stratigraphic order)	75AHP31II	"	Not completed	-		75AHP31I	"	8.62	$1.11 \pm 0.22$
	75AHP22II	"	Not completed	-		75AHP22I	"	None	Negative
	75AHP3III	"	6.37	$0.670 \pm 0.150$		75AHP3 I	"	0.40	$0.041 \pm 0.300$
Some flow unit	75AHP5 I	"	3.40	$1.09 \pm 0.47$		75AHP3II	"	0.30	$0.036 \pm 0.300$
	Test sample	Upsal AI	"	$3.61$	$0.291 \pm 0.175$	Upsal AII	"	2.10	$0.208 \pm 0.218$

1/ Same flow unit

POTASSIUM-ARGON AGES OF BASEMENT ROCKS FROM ST. GEORGE ISLAND, ALASKA

by

M. L. Silberman and D. M. Hopkins  
U.S. Geological Survey  
345 Middlefield Road  
Menlo Park, California

Introduction

St. George Island is one of the Pribilof Islands which lie between 56°35' and 57°11' N. lat. in the Bering Sea, 350 km north of the Aleutian chain. The islands are situated near the margin of the continental platform that underlies most of the northern half of the Bering Sea (fig. 1).

---

Figure 1 near here

---

The islands are made up mostly of olivine basalt and basanite flows, pillow breccias, pyroclastic deposits, sills and dikes, most of which are nepheline normative (Barth, 1956). The volcanic rocks are late Pliocene to Holocene in age (Cox and others, 1966; D. M. Hopkins and M. L. Silberman, unpub. data) and are interbedded with marine sand and gravel, glacially derived sediments, frost breccia, and windblown sand and silt.

Basement

Serpentinized peridotite crops out for a distance of 5 km along the southeast shore (fig. 2). In some places, the smoothly planed but

---

Figure 2 near here

---

tectonically deformed upper surface is covered by marine sediments and

then pillow breccia of Pliocene age (fig. 3), but between Garden Cove

---

Figure 3 near here

---

and Sea Lion Point, the serpentinized peridotite underlies a glaciated marine terrace of middle Pleistocene age (Hopkins and Einarsson, 1966).

North of Garden Cove, the peridotite is intruded by a 400 m-wide composite granitic body referred to as "aplite" by Barth (1956). Its margin is fine grained and about 3 m wide and contains alkali feldspar phenocrysts, some biotite, largely altered to sericite, and small amounts of garnet. The central portion of the body, which is more basic in composition, is a medium- to fine-grained granular rock, consisting largely of plagioclase, with interstitial quartz and K-feldspar. Amphibole is present, largely altered to chlorite. In both rocks the feldspars are heavily sericitized. Barth (1956) describes these rocks in greater detail. The granite is younger than the serpentinized peridotite, which it intrudes, and older than the alkaline olivine basalts, which unconformably overlie it. The peridotite and the granite are the only outcrops of pre-late Tertiary basement found in the Pribilof Islands.

K-Ar Ages

Due to alteration and lack of K-bearing minerals, the peridotite is not suitable for K-Ar age determination. We collected one sample each from the center and margin of the granitic body. Both samples are altered; the fine-grained margin is sericitized and mafic minerals in the coarser grained central portion are altered to chlorite. Feldspars in both samples are at least partially sericitized.

For sample G199, from the margin of the body, an alkali feldspar and a sericite concentrate were prepared, and for sample G200, from the coarser grained center, a K-feldspar and a chlorite mineral concentrate were prepared. Standard heavy liquid and magnetic techniques were used by J. A. Peterson to prepare the purified mineral concentrates. K-Ar ages and analytical data for the samples are listed in table 1.

---

TABLE 1 NEAR HERE

---

Discussion

The K-Ar ages of the samples are not concordant nor are they internally consistent. Table 2 lists the statistical probability levels of differences among the various minerals from the two samples of the granite. Probability levels for age differences exceed one standard deviation (68 percent) for all but two possible combinations of the numbers (table 2).

---

TABLE 2 NEAR HERE

---

As mentioned the rocks are altered to some extent and show evidence of recrystallization. We cannot specify at present whether this is a primary deuterio alteration or whether it is a thermal effect resulting from late Tertiary volcanic activity in the area or some earlier thermal event.

The ages, with one exception, vary inversely with potassium content. Similar inconsistencies in ages have been noted in areas where small to moderate amounts of extraneous argon (argon other than that generated by radioactive decay of potassium in place after crystallization) is present in minerals in a rock (MacDougall and others, 1969; Hayatsu and Carmichael,

Table 1

K-Ar ages of basement rocks from St. George Island, Alaska

Sample no.	Mineral	$K_2O^1$	$Ar^{*40}$ (moles/g) <sup>2</sup>	$Ar^{*40}/Ar_{\infty}^{40}$	Apparent age (m.y.)
G199	alkali feldspar	3.15	$2.532 \times 10^{-10}$	0.57	$55.0 \pm 2.2$
G199	sericite concentrate	3.35	$2.419 \times 10^{-10}$	0.78	$49.5 \pm 2.0$
G200	K-feldspar	7.21	$5.546 \times 10^{-10}$	0.49	$52.7 \pm 2.1$
G200	chlorite	0.407	$0.3404 \times 10^{-10}$	0.47	$57.2 \pm 2.3$

<sup>1</sup>Potassium was analyzed by flame photometry using a lithium metaborate fusion technique (Ingamells, 1970), the lithium serving as an internal standard. Mineral standards were used for calibration. Analysts: M. Cremer, J. H. Christie.

<sup>2</sup>Argon was analyzed by standard isotope dilution-mass spectrometry techniques described by Dalrymple and Lanphere (1969). Ar\* represents radiogenic argon. Analyst: M. L. Silberman.

Analytical uncertainty of apparent age estimated at one standard deviation is a combined estimate from uncertainties in the potassium and argon analytical techniques, and is approximately 4 percent.

Constants used in age calculation:

$$\lambda_e = 0.572 \times 10^{-10} \text{ yr}^{-1}$$

$$\lambda_{e'} = 8.78 \times 10^{-13} \text{ yr}^{-1}$$

$$\lambda_\beta = 4.963 \times 10^{-10} \text{ yr}^{-1}$$

$$K^{40}/K_{\text{total}} = 1.167 \times 10^{-4} \text{ mole/mole.}$$

Table 2

Statistical level of probability of age differences, from minerals  
from felsic dike, St. George Island

G200 KF	G200 Chl	G199 KF	G199 Ser
(1) 52.7	(2) 57.2	(3) 55.0	(4) 49.5
0	0	0	0
0.85	0.51	0.99	0.94
	0.55	0.73	P

P = level of probability of age difference; 68 percent = one standard deviation.

1970; Shafaqullah and Damon, 1974). The effect of extraneous argon is stronger on minerals with low K content because less radiogenic argon is generated over a given period of time. Thus, the age of the lowest K-bearing mineral in table 1, the chlorite from sample G200, yields the oldest age of the group, which would be expected if the model of excess argon is the correct explanation for the age discrepancies.

Using a technique developed by MacDougall and others (1969) and Hayatsu and Carmichael (1970), it is sometimes possible to obtain an initial or a reset K-Ar age (metamorphic age) from a suite of cogenetic samples that contain excess argon-40, or that have lost argon-40 (Shafaqullah and Damon, 1974). We have plotted the data for argon and potassium content from the minerals on an initial argon diagram (fig. 4). The slope in this diagram is proportional to age and the intercept yields the initial amount of argon present in each mineral in excess of the amount produced by radioactive decay of potassium. In practice, this method has yielded useful metamorphic ages in areas where thermal events have occurred, redistributing the argon among various minerals in a suite of rocks, and where the total system has remained either closed to argon gain or loss (Hayatsu and Carmichael, 1970) or where each sample has gained or lost a constant amount of argon (Shafaqullah and Damon, 1974).

Figure 3 shows the plot of points on this diagram. The equation of the best-fit line through the points is:  $\text{Ar}_{\text{e}}^{40} = \text{Ar}_{\text{e}}^{40} + \text{K}^{40} \frac{\lambda}{\lambda} (\text{e}^{\lambda T} + 1)$ ,

where:  $\text{Ar}^{40}$  = total argon-40 less atmospheric argon-40

$\text{Ar}_{\text{e}}^{40}$  = excess argon-40

$\lambda_{\text{e}}$  and  $\lambda$  are decay constants for  $\text{K}^{40}$

T = Age

the equation is of the form  $y = mx + b$ , where:

$y = Ar^{40}$  measured (corrected for atmospheric argon content)

$b$  = initial or excess argon

$x = K^{40}$

$m = \frac{\lambda}{\lambda} e^{-\lambda T} (e^{\lambda T} + 1)$  which can be solved for  $T$ .

From the data:

$Ar^{40} = 3.348 \times 10^{-12} + 3.045 \times 10^{-3} K^{40}$  (in moles).

The slope yields an isochron age of  $51.7 \pm 1.9$  m.y.

The isochron results suggest a small amount of excess radiogenic argon, on the order of  $3 \times 10^{-12}$  moles/g. In all probability, this age should be considered a metamorphic or minimum age, rather than the true age of crystallization of the rock. However, due to the small amount of excess argon, the resetting was probably not due to the late Tertiary or Holocene volcanic activity, but was rather due to an earlier thermal event.

#### Discussion and Conclusions

Marine geological and geophysical studies indicate that the Pribilof Islands lie near the southern margin of a belt of volcanic and plutonic rocks and minor interbedded continental sediments of Late Cretaceous and Paleocene age (the Okhotsk-Chukotsk volcanic belt of Russian authors) and near the northern margin of a belt of deep-water flysch deposits of Late Cretaceous age (the Koryak-Anadyr flysch belt of Russian authors) (Marlow and others, 1976; Patton and others, 1976). The two belts are separated in Northeast Siberia and southwestern Alaska by a belt 100-500 km wide consisting of shallow-water and nonmarine sedimentary rocks of Late

Cretaceous and Paleocene age (Patton and others, 1976), but if this belt is present near the Pribilof Islands, it must be very narrow.

On St. Matthew Island, 500 km north of St. George Island, the Okhotsk-Chukotsk volcanic belt is represented by calc-alkaline volcanic rocks of basaltic to rhyolitic composition which are intruded and locally metamorphosed by a small granodiorite pluton. The volcanic rocks have yielded K-Ar ages of 65 to 77 m.y. (Late Cretaceous) and hornblende from the granodiorite has yielded a K-Ar age of 61 m.y. (earliest Tertiary) (Patton and others, 1976). Flysch deposits from the Pribilof Canyon have yielded a Maestrichtian microfauna (Hopkins and others, 1969), indicating an approximate age of 65 to 68 m.y.

Scholl and others (1975) confirm earlier inferences that the edge of the continental shelf in the Bering Sea formed the boundary between the North American-Northeast Siberian continental plate and the Kula oceanic plate of Grow and Atwater (1970) during much of Mesozoic time. After reviewing the alternatives, they conclude that subduction probably shifted southward from the continental margin to the Aleutian arc-trench system during latest Cretaceous or earliest Tertiary time. We suggest that the serpentinized peridotite on St. George Island marks a subduction zone formed when the North American-Eurasian continental plate was overriding the Kula oceanic plate during Mesozoic time.

Our K-Ar age determinations indicate that the serpentinite on St. George Island was intruded by a small granitic body only slightly later than (and, since our determinations represent minimum ages, possibly contemporaneously with) intrusive and volcanic activity on St. Matthew Island.

Thus, we have the seemingly anomalous record of the superposition of a magmatic arc--the Okhotsk-Chukotsk volcanic belt--upon a subduction zone. We suggest that this superposition is the consequence of the shift in the position of the subduction zone from the continental margin in the Bering Sea to the Aleutian Trench in the North Pacific Ocean.

#### References

- Barth, T. F. W., 1956, Geology and petrology of the Pribilof Islands, Alaska: U.S. Geol. Survey Bull. 1028-F, p. 101-160.
- Cox, A. V., Hopkins, D. M., and Dalrymple, G. B., 1966, Geomagnetic polarity epochs; Pribilof Islands, Alaska: Geol. Soc. America Bull., v. 77, p. 883-910.
- Dalrymple, G. B., and Lanphere, M. A., 1969, Potassium-argon dating: San Francisco, California, W. H. Freeman and Co., 258 p.
- Grow, J. A., and Atwater, T., 1970, Mid-Tertiary tectonic transition in the Aleutian Arc: Geol. Soc. America Bull., v. 81, p. 3715-3722.
- Hayatsu, A., and Carmichael, C. M., 1970, K-Ar isochron method and initial argon ratios: Earth and Planetary Sci. Letters, v. 8, p. 71-76.
- Hopkins, D. M., and Einarsson, Th., 1966, Pleistocene glaciation on St. George, Pribilof Islands: Science, v. 152, p. 343-345.
- Hopkins, D. M., Scholl, D. W., Addicott, W. D., and others, 1969, Cretaceous, Tertiary, and early Pleistocene rocks from the continental margin in the Bering Sea: Geol. Soc. America Bull., v. 80, p. 1471-1480.
- Ingamells, C. O., 1970, Lithium metaborate flux in silicate analyses: Anal. Chim. Acta, v. 52, p. 323-334.
- MacDougall, Ian, Polach, H. A., and Stipp, J. J., 1969, Excess radiogenic argon in young sub-aerial basalts from the Auckland volcanic field, New Zealand: Geochim. et Cosmochim. Acta, v. 33, p. 1485-1520.

- Marlow, M. S., Scholl, D. W., Cooper, A. K., and Buffington, E. C.,  
1976, Structure and evolution of Bering Sea shelf south of St.  
Lawrence Island: Am. Assoc. Petroleum Geologists Bull., v. 60,  
no. 2, p. 161-183.
- Patton, W. W., Jr., Lanphere, M. A., Miller, T. P., and Scott, Richard,  
1976, Age and tectonic significance of volcanic rocks on St.  
Matthew Island, Bering Sea, Alaska: U.S. Geol. Survey Jour.  
Research, v. 4, p. 67-73.
- Scholl, D. W., Buffington, E. C., and Marlow, M. S., 1975, Plate  
tectonics and the structural evolution of the Aleutian-Bering  
Sea region, in Forbes, R. B., ed., The geophysics and geology  
of the Bering Sea region: Geol. Soc. America Spec. Paper 151,  
p. 1-32.
- Shafaqullah, M., and Damon, P. E., 1974, Evaluation of K-Ar isochron  
methods: Geochim. et Cosmochim. Acta, v. 38, p. 1341-1358.
- York, D., 1969, Least squares fitting of a straight line with  
correlated errors: Earth and Planetary Sci. Letters, v. 5,  
p. 320-324.

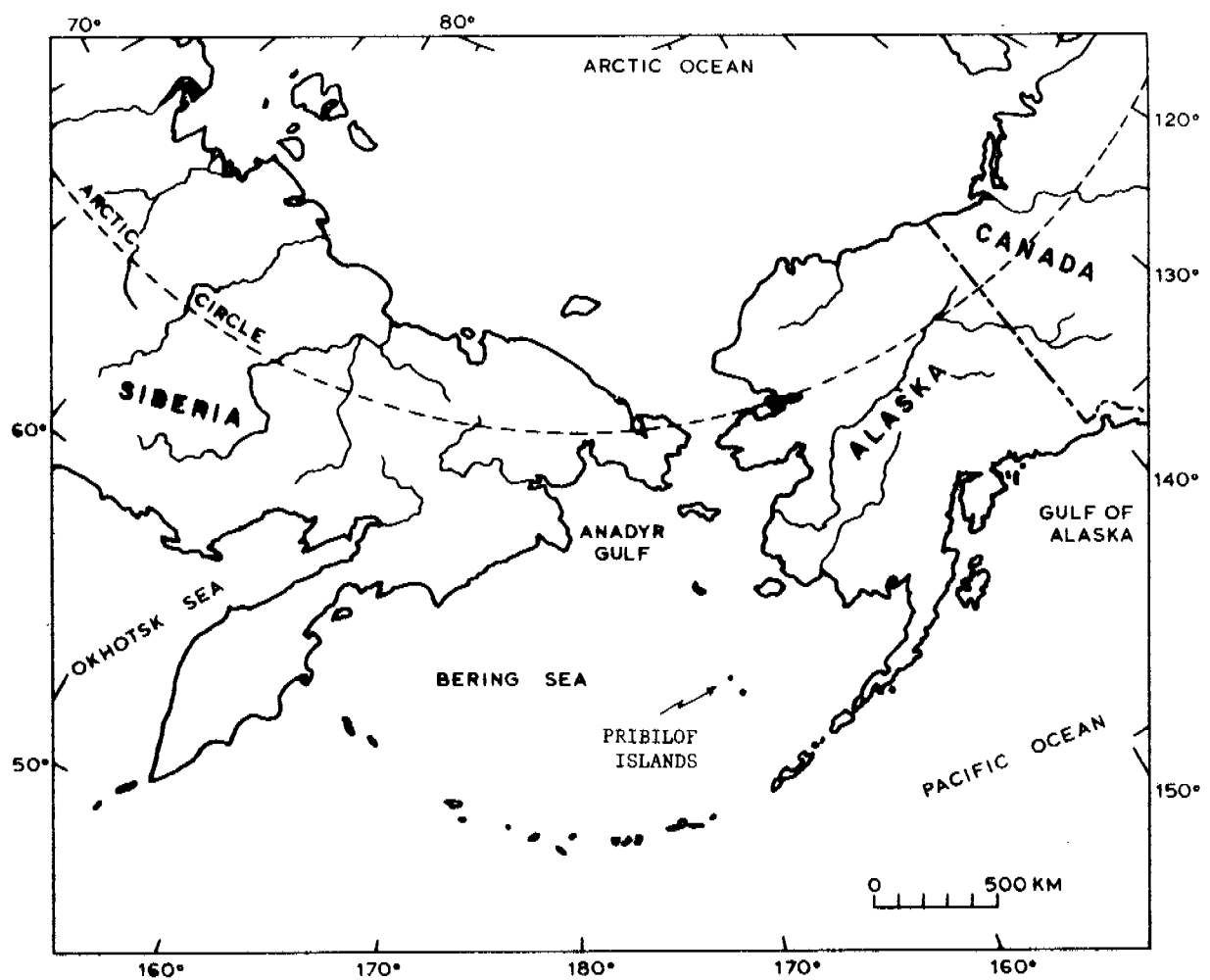


FIGURE 1.

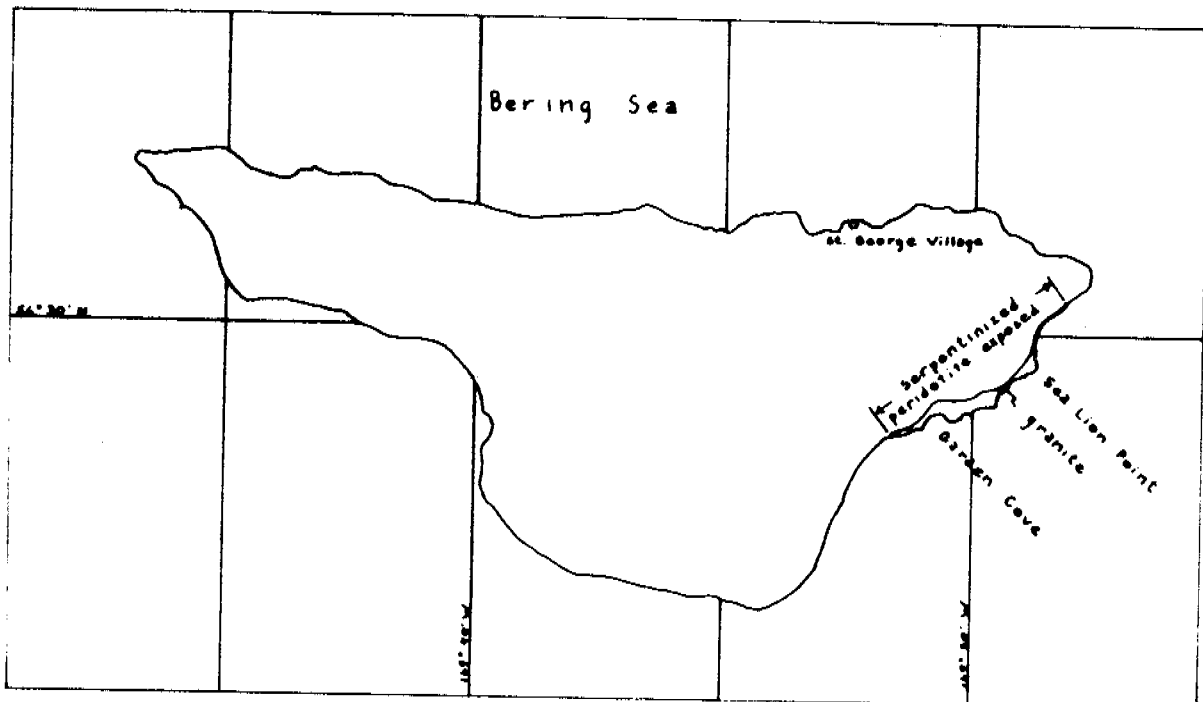
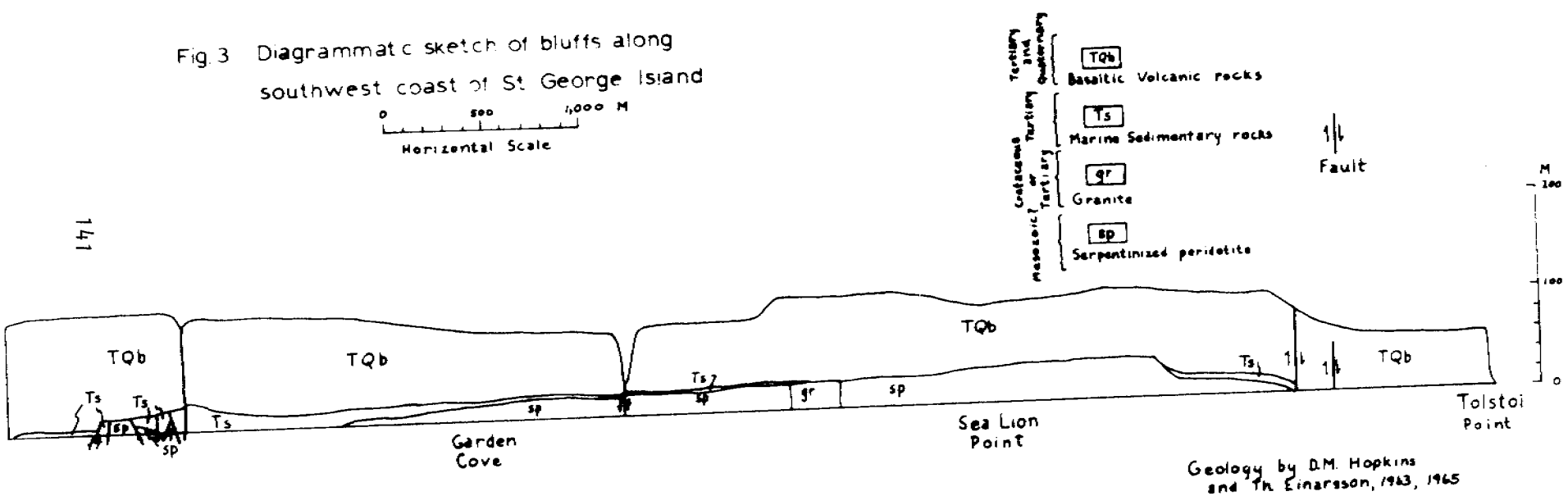


Fig. 2 Location of serpentinized peridotite  
and granite outcrops at base of cliffs  
on southeastern St. George Island

Fig. 3 Diagrammatic sketch of bluffs along southwest coast of St. George Island

0 500 1,000 M  
Horizontal Scale



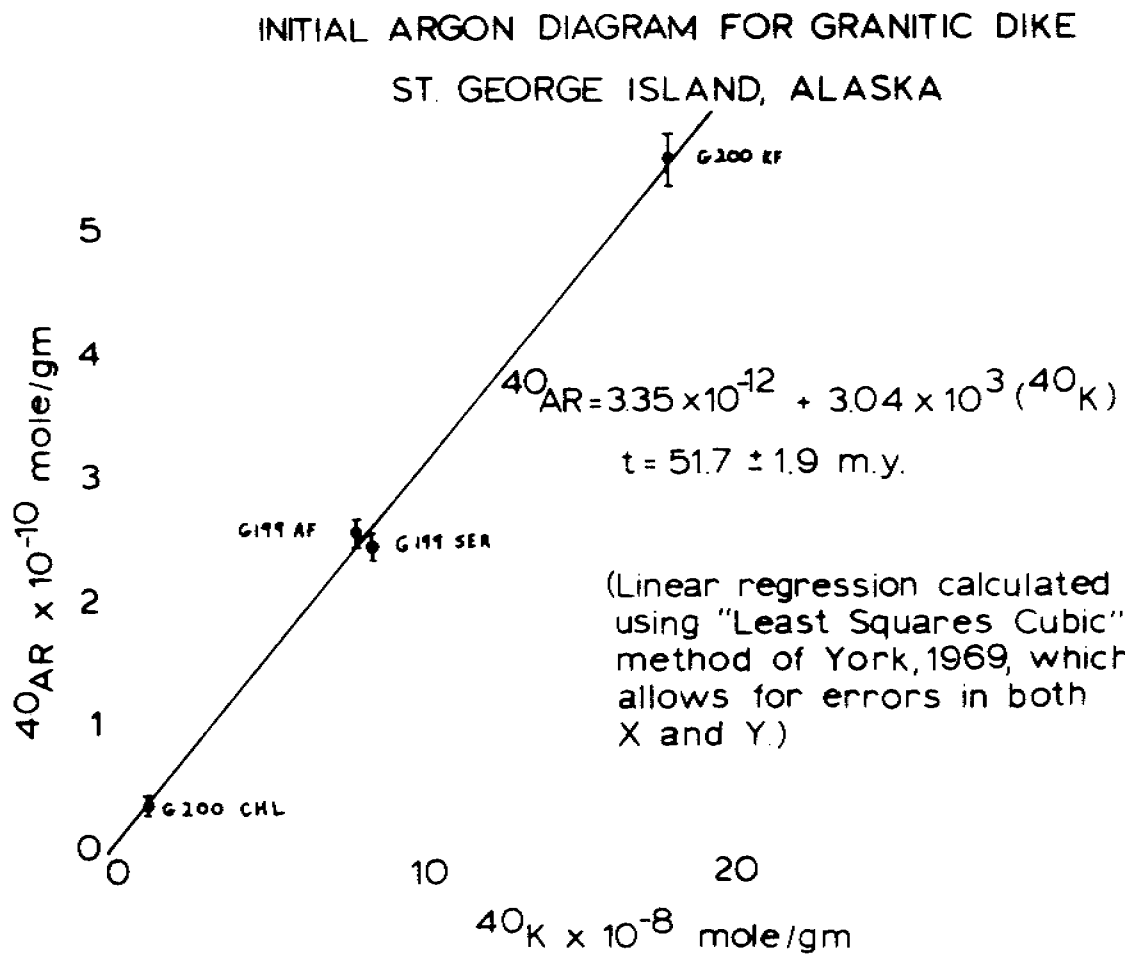


FIGURE 4.

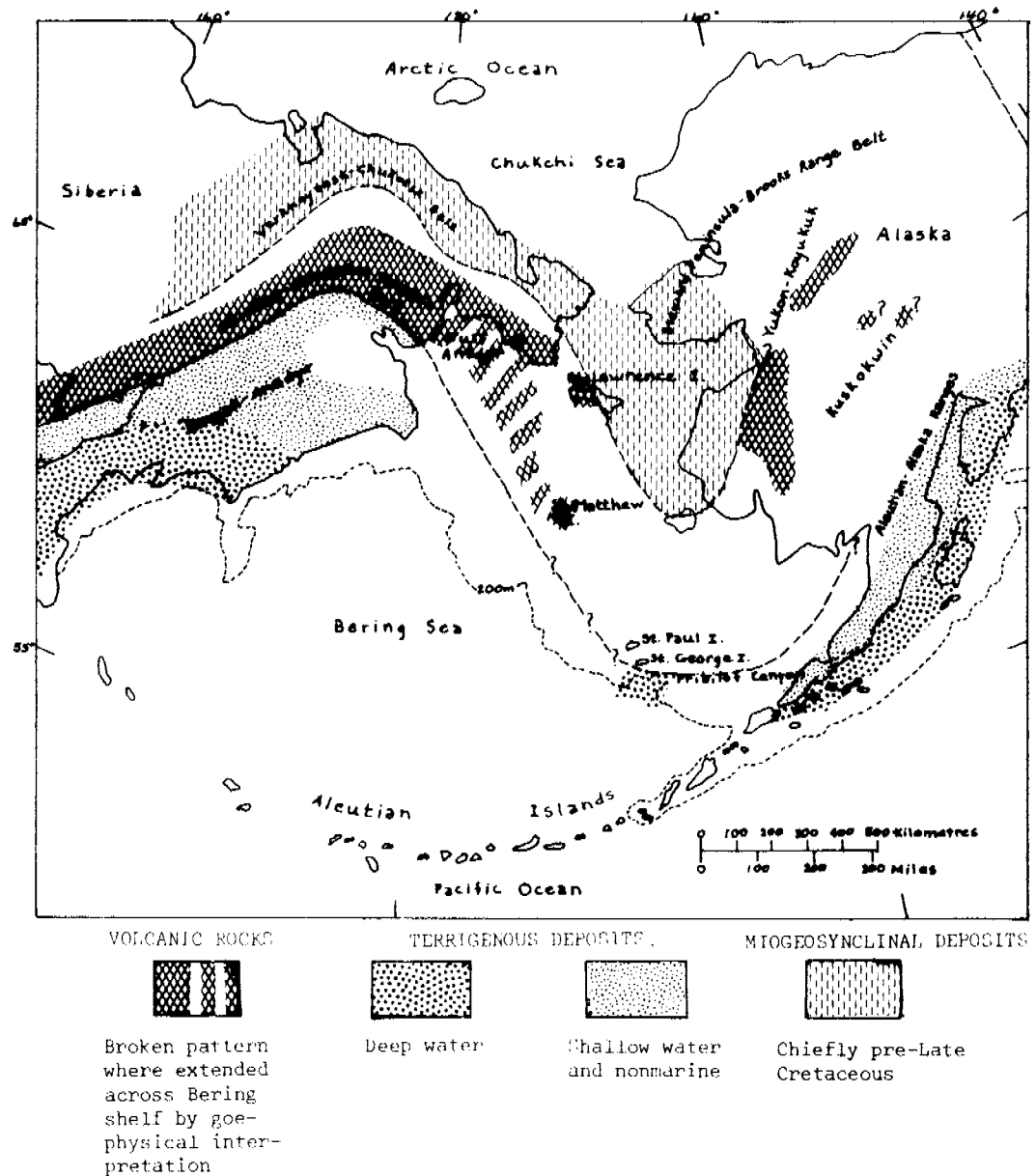
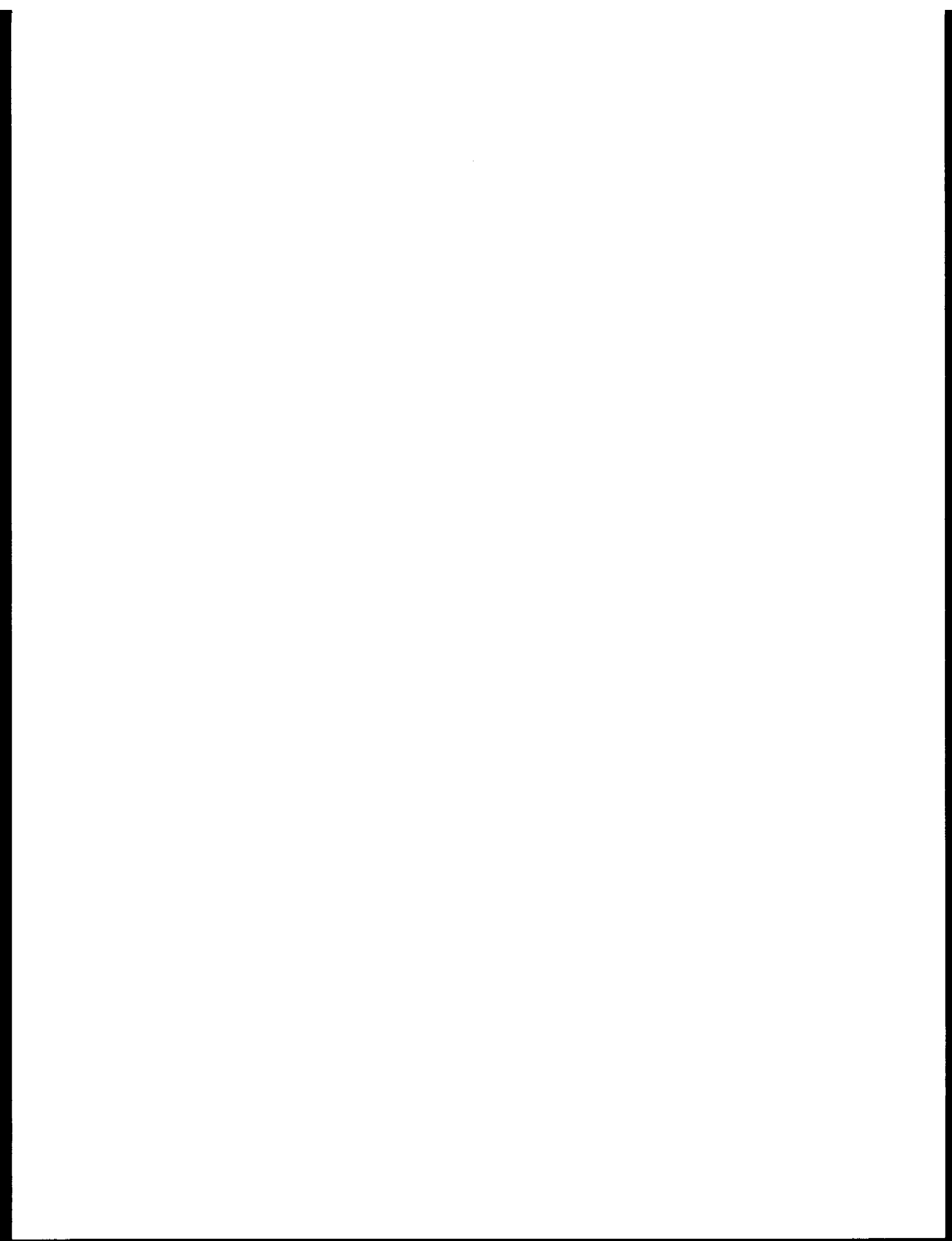


Fig. 5 Distribution of volcanism and terrigenous deposition in the Bering Sea region during Late Cretaceous and earliest Tertiary time ( $\approx 80$  to  $55$  m.y. ago). Outer margin of Bering Sea shelf at 200-m contour shown by dashed line.  
After Fenton and others, 1976; Marlowe and others, 1976.



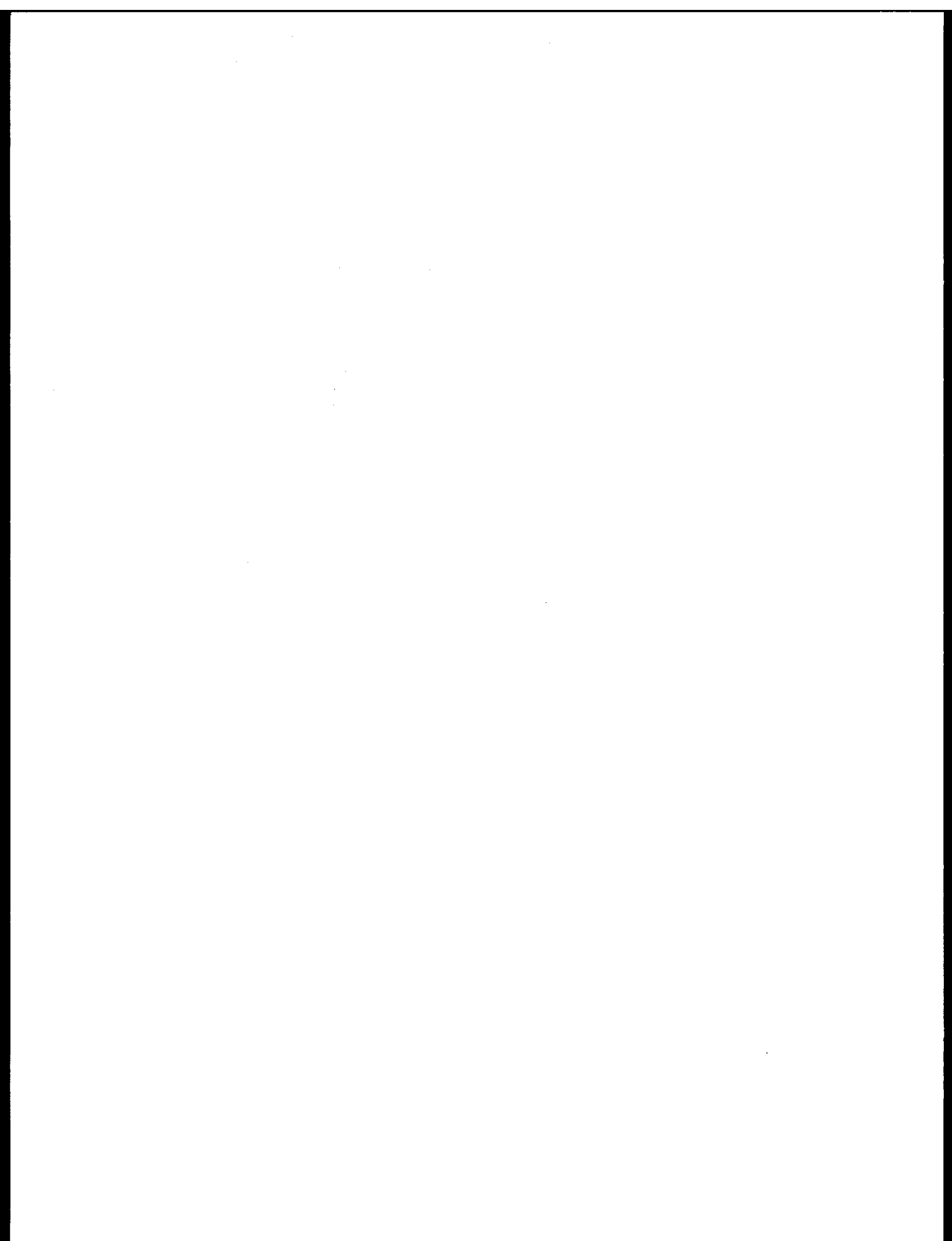
RU# 210

RU# 212

RU# 216

RU# 251

NO REPORTS AVAILABLE AT THIS TIME



Quarterly Report - July 1 to September 30, 1976

RU # 253

TITLE: Offshore Permafrost - Drilling, Boundary Conditions, Properties Processes and Models.

PERIOD: 1 April 1975 to 30 September 1976

PRINCIPAL INVESTIGATORS: T. E. Osterkamp and W. D. Harrison

Geophysical Institute, University of Alaska,  
Fairbanks, Alaska 99701

#### I. TASK OBJECTIVES

- (1) To carry out a nearshore drilling program during spring 1975 at Prudhoe Bay.
- (2) To determine the thermal and chemical boundary conditions of offshore permafrost in shallow water areas (< 5 m depth) and to determine the properties of sea bottom sediments in these areas.
- (3) To do preliminary laboratory and theoretical work necessary for an understanding of the offshore permafrost regime with an emphasis on the coupling of chemical and thermal processes.

#### II. FIELD AND LABORATORY WORK

- A. There was no field work done this quarter.
- B.
  - (1) Measurements of the thermal conductivity of selected subsea permafrost samples were begun. Results are not yet available.
  - (2) Reduction of the temperature data obtained during the 5 field trips this past 15 months has been completed.
  - (3) Probing data, obtained during May and November 1975, to give additional data on the position of the bonded-unbonded subsea permafrost boundary at the drilling site in NW Prudhoe Bay were reduced and partially analyzed.
  - (4) Temperature measurements made in our shallow onshore hole have been reduced and are now being analyzed.

#### III. RESULTS AND IV. INTERPRETATION

While almost all of our data has been reduced most of it has only been partially analyzed. The reduced data will be available next quarter.

The seabed temperatures, which represent the upper thermal boundary conditions for subsea permafrost, ranged from +2 to -15°C in very shallow water (< 1 m depth) during the annual cycle. In water several meters in depth, the range in seabed temperature is only a few degrees.

The position of the unbonded - bonded subsea permafrost boundary (determined by probing) is shown in Figure 1 for May and November 1975. The November data were obtained with a light hand-driven probe, and it is possible that the boundary is either slightly deeper than indicated or poorly defined. It appears that as much as 3 m of "thawing" occurs at the seabed in shallow water and that this refreezes during the winter. (Some liquid probably remains because of the salt.) This layer is therefore somewhat like an active layer in subaerial permafrost. We have not yet determined how much of this active layer is permafrost by the usual thermal definition (i.e., soil continuously at a temperature < 0° C). Our previous results show that the high salinity is due to transport processes other than molecular diffusion.

#### V. PROBLEMS, CHANGES

None

#### VI. FUNDS EXPENDED

About \$90,000

QUARTERLY REPORT - July 1 to September 30, 1976

RU #253

TITLE (Addition): Delineation of most probable areas for subsea permafrost  
in the Chukchi Sea from existing data.

PRINCIPAL INVESTIGATORS:

W. D. Harrison, S. S. #554-70-4301  
T. E. Osterkamp, S. S. #357-28-7107  
Geophysical Institute  
University of Alaska  
Fairbanks, Alaska 99701

GEOGRAPHICAL AREA AND INCLUSIVE DATES: (Addition)

Chukchi Sea  
April 1, 1976 - September 30, 1976

I. TASK OBJECTIVES

To delineate the most probable areas for subsea permafrost in  
the Chukchi Sea from existing data.

II. FIELD AND LABORATORY WORK

None.

III. RESULTS

Seabed temperatures between Bering Strait and latitude 72°N  
have been compiled together with ice cover and thickness, sea level  
history, and other information. Permafrost has formed under most of the  
Chukchi Sea shelf in the past, in response to periods of emergence.  
Simple calculations of the rate of growth and decay of this permafrost  
have been performed.

IV. PRELIMINARY INTERPRETATION OF RESULTS

Mean annual sea bottom temperature is an important permafrost boundary  
condition, but lack of data during months of partial ice cover makes a  
good estimate of it difficult. Despite this uncertainty, the calculations  
indicate that the possibility of the existence of ice under the southern  
Chukchi Sea, in the proposed Hope Basin lease sale area, is fairly  
small. Ice probably exists under near-shore areas, especially where  
coastal retreat is rapid. Much of the Chukchi Sea bed seems rocky, with  
little sediment cover. This alone suggests that ice rich permafrost  
should be rare. It also implies that probing and seismic study sites  
must be carefully chosen.

IV. PRELIMINARY INTERPRETATION OF RESULTS (Cont'd)

We hope to produce a preliminary report in the next week or so. This work is only part of the Chukchi Sea permafrost reconnaissance study; the relevant geological studies are being conducted by Hopkins (RU #473).

V. PROBLEMS

Only half of the funds was received and the project is badly overspent.

VI. FUNDS EXPENDED

About \$12,000.

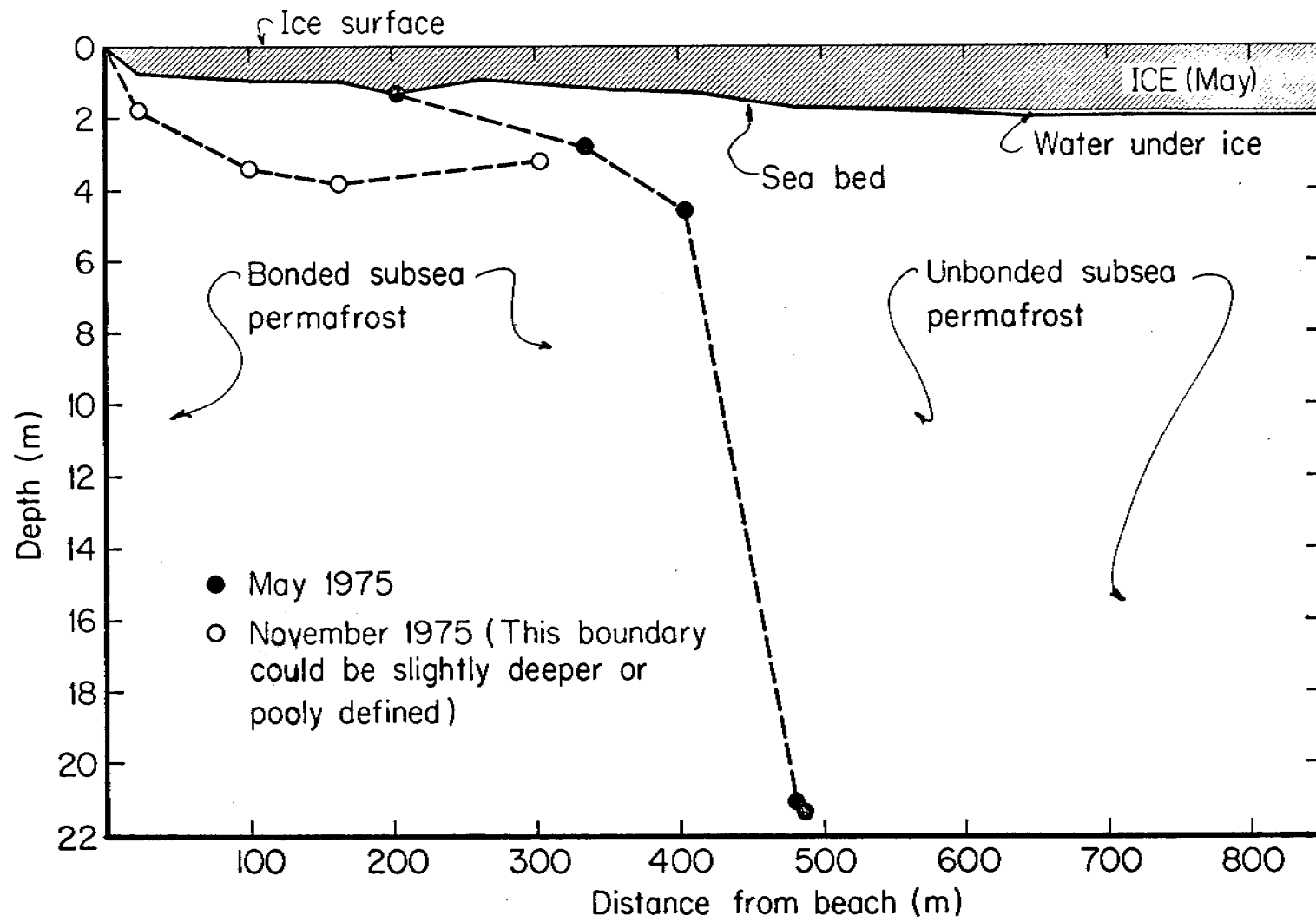


Figure 1.

QUARTERLY REPORT

CONTRACT #03-5-022-55

RESEARCH UNIT #271

REPORT PERIOD: 6th QUARTER ENDING SEPTEMBER 30

BEAUFORT SEACOAST PERMAFROST STUDIES

JAMES C. ROGERS

GEOPHYSICAL INSTITUTE

UNIVERSITY OF ALASKA 99501

907-272-5522 X225

- I. Task Objectives - See previous reports.
- II. A. Field work was conducted at Prudhoe Bay from July 17 through July 29. The major effort involved marine seismic refraction work from the USGS vessel "Karluk".
  - B. J. Rogers and J. Morack of the University of Alaska participated in data gathering during the field work and P. Barnes of the USGS aided in coordinating vessel activities.
  - C. Marine seismic refraction data were gathered. These data were recorded on an oscillograph and in analog form on magnetic tape. The data are also suitable for reflection analysis.
  - D. Figure 1 indicates the track of the Karluk in the South end of Prudhoe Bay. The northern end of the lines indicate the boundary of the ice in the bay during late July. The parameter on the lines is time of day in UT.
  - E. One hundred sixteen refraction records were obtained over approximately 25 kilometers of line as indicated in figure 1. Also included in the data is about one kilometer of refraction line data gathered on Cross Island and on Reindeer Island with a hammer seismograph.
- III. Preliminary results indicate high velocity refractors which are interpreted to be permafrost at the ends of line 15 and at the end of line 16, which is nearest the shore. The depth to the permafrost surface ranges from a few meters near shore to approximately 30 meters, at a distance of one to two kilometers from shore.

Figure 2 is a time-distance plot of the refraction data taken on line 16R of figure 1 at approximately 17:27 UT. Two layers are indicated by the time-distance plot, neither of which is frozen as the velocities are too low.

Figure 3, another refraction line from line 16R, taken at 16:26 UT, indicates permafrost approximately eight M. beneath the water surface. Additional data reduction is required in order to interpret the reflection events on the seismic records.
- IV. See III.
- V. Additional work is required in the area of Reindeer Island and along the Barrier Island. It is necessary that this work be scheduled in late August to ensure minimum interference from ice.
- VI. Funds spent to date in 18-month period - approximately \$80,000.

154

## PRUDHOE BAY



340  
1350  
1400  
1420  
1430  
1440  
1450

0 1 2 3  
kilometers

Figure 1. Vessel track of Karluk, 1976. Parameter on track lines is time in UT.

FIGURE 2: Refraction data from line 16 R  
taken at 17:29 UT

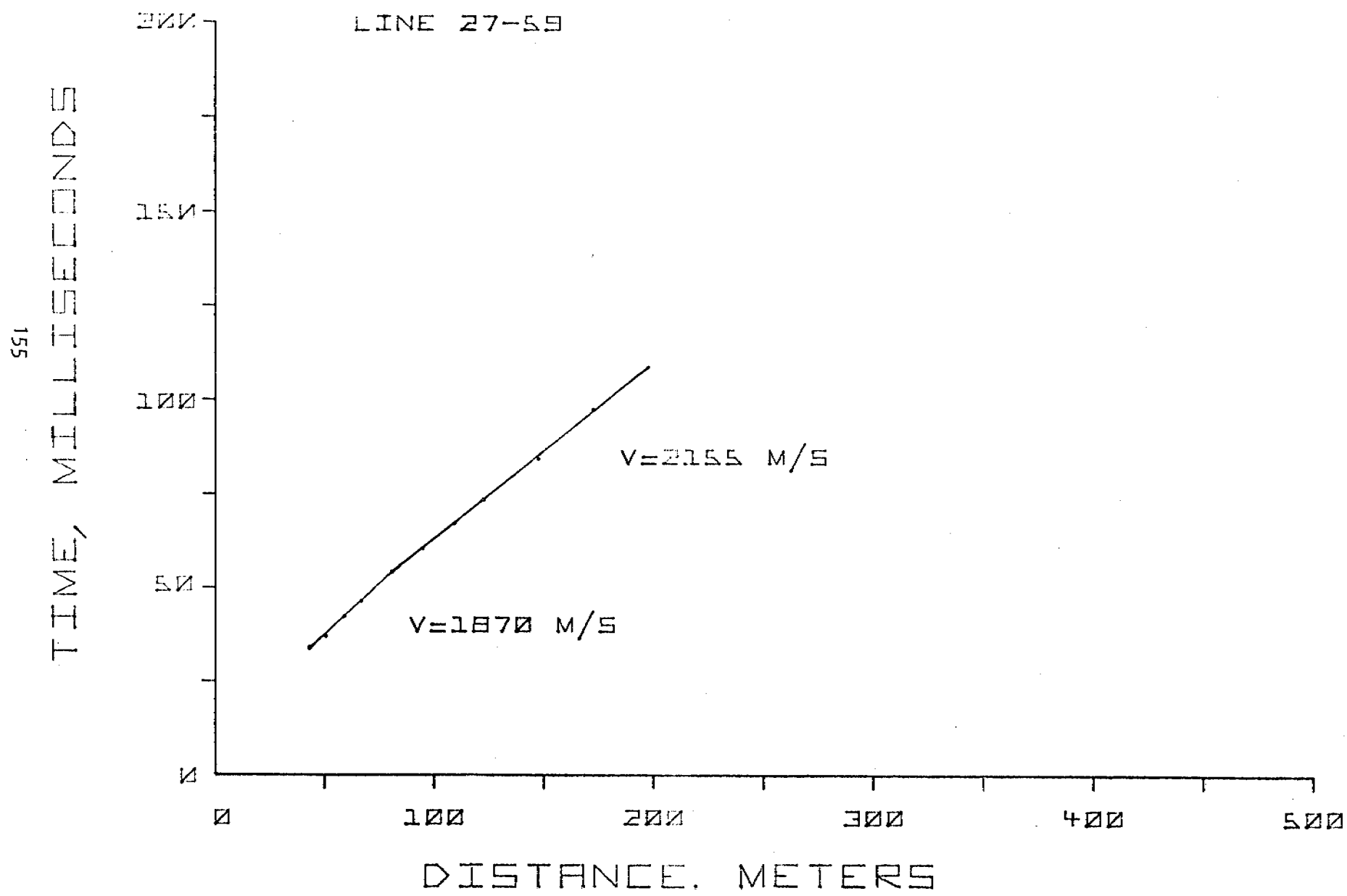
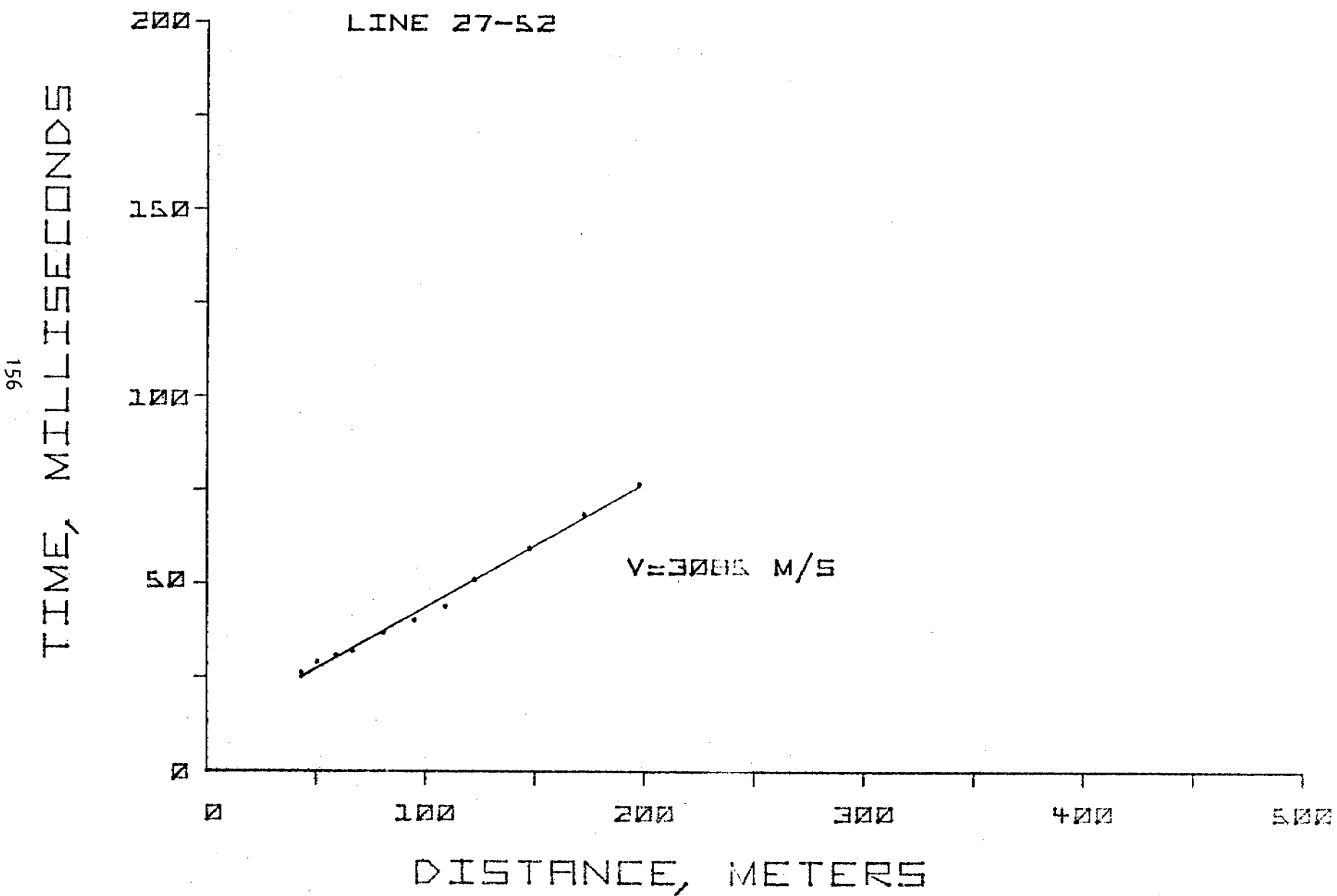


Figure 3: Refraction data from line 16R taken at 16:26 UT.



Quarterly Report

Contract #03-5-022-56  
Research Unit #291  
Reporting Period 7/1 - 9/30/76  
Number of Pages 2

BENTHOS-SEDIMENTARY SUBSTRATE INTERACTIONS

Dr. Charles M. Hoskin  
Associate Professor of Marine Science  
Institute of Marine Science  
University of Alaska  
Fairbanks, Alaska 99701

October 1, 1976

## Quarterly Report

### I. Task Objectives

Keypunching of grain size data is complete, and computer runs for determination of grain size descriptors is complete; however, see (IV). Determination of grain size modes is complete. Submission of all grain size data to Ray Hadley is expected to be done within the coming week. Correlation of grain size data with abundance and distribution of the maracobenthos has yet to be done because all data for the maracobenthos are not yet available; these correlations will be made as quickly as possible upon receipt of the requisite data.

### II. Field Activities

None.

### III. Results

None, see above.

### IV. Problems Encountered

Continued difficulties with the new computer greatly slowed our efforts in completing a print-out of the grain size data. Also, considerable difficulty was had in obtaining data for each sample from cruise reports, and much effort was expended in preparing an unequivocal listing of station and sample number, depth of water, date of sampling, and coordinates of latitude and longitude. It is suggested that to avoid confusion for later work, a list of these data be attached to the samples submitted to others for analysis.

## OCS COORDINATION OFFICE

University of Alaska

## ENVIRONMENTAL DATA SUBMISSION SCHEDULE

DATE: September 30, 1976

CONTRACT NUMBER: 03-5-022-56      T/O NUMBER: 3      R.U. NUMBER: 291

PRINCIPAL INVESTIGATOR: Dr. C. M. Hoskin

Submission dates are estimated only and will be updated, if necessary, each quarter. Data batches refer to data as identified in the data management plan.

<u>Cruise/Field Operation</u>	<u>Collection Dates</u>		<u>Estimated Submission Dates</u> <sup>1</sup>
	<u>From</u>	<u>To</u>	
Discoverer Leg I #808	5/15/75	5/30/75	*
Discoverer Leg II #808	6/2/75	6/19/75	*
Miller Freeman	8/16/75	10/20/75	*

Note: <sup>1</sup> Estimated submission dates are contingent upon final approval of data management plan submitted in draft form Oct. 9, 1975 and University of Alaska approved form Nov. 10, 1975, to NOAA.

\* Data will be available for transfer to magnetic tape by 30 July. Transfer and submission will be made approximately 30 days after data management plan approval.

6th Quarter Report  
OCSEAP RU #327

FAULTING AND INSTABILITY OF SHELF SEDIMENTS  
WESTERN GULF OF ALASKA

Monty A. Hampton

and

Arnold H. Bouma

U. S. Geological Survey  
Menlo Park, California

September 29, 1976

## SUMMARY

An environmental geologic study was performed during the summer of 1976 in lower Cook Inlet and on Kodiak Shelf, Alaska. Seismic information was collected over a total of 3524 nm (nautical miles) (6555 km) using single channel sparker, uniboom and 3.5 kHz (kilo Hertz) seismic profiling systems. Side-scan sonar records were obtained over 107 nm (198 km), and a bottom TV unit was utilized in lower Cook Inlet at three stations. Bottom sediments were collected at 154 stations by means of gravity and dart corers, Van Veen and a modified Van Veen grab sampler.

Lower Cook Inlet is characterized by a rather smooth bottom and strong tidal currents. The surficial sediments are sand to pebbly sand in the south becoming more pebbly to the north. The high-velocity currents during the last transgression and at the present time have formed a variety of bed-forms, including dunes that are up to one kilometer long and ten meters high.

Shallow structures, including numerous anticlines and synclines, are parallel to the major structural trends surrounding Cook Inlet. The Augustine-Seldovia Arch influences the fold style, which at the southern side of this arch is more complex and slightly different in orientation from the area to the north.

Kodiak Shelf consists of flat, relatively shallow banks that are cut by transverse troughs. Fold axes trend in a general northeast-southwest direction but are discontinuous and evidently have many deviations in orientation. Physiographic scarps, apparently representing surface faulting, occur over the shelf and are most abundant in three areas: 1) off the southeast coast of the Kodiak islands, 2) near the shelf break on Albatross Bank, and 3) on Portlock Bank. Significant slumps or sedimentary bedforms did not appear on our acoustic records on the shelf. However, several zones of slumping were found on the continental slope.

Unconsolidated sediments on Kodiak Shelf are distributed in relation to physiography. Sands bearing gravel and boulders, and commonly containing large amount of broken shell material, are characteristic of the banks. Fine sands to muds, commonly containing much volcanic ash, are characteristic of the deeper troughs. Hogback ridges, exposing siltstones and silty sandstones, occur at places on Albatross and Portlock Banks.

## INTRODUCTION

During the period June 18 through July 30, 1976 environmental geologic studies were conducted on board the R/V SEA SOUNDER in lower Cook Inlet and on Kodiak Shelf, Alaska (Fig. 1, Pls. 1, 2, Table 1). Regional information about the surface and shallow subsurface geology of both these areas was obtained primarily by seismic surveying and sediment sampling. The seismic surveying utilized a 90,000 joule sparker system, a hull-mounted uniboom system, a hull-mounted 3.5 kHz system and a magnetometer. Most sediment samples were obtained with a modified grab sampler, but several dart cores and gravity cores were also taken, as well as one dredge. Side scan sonar records were collected from selected areas, and in lower Cook Inlet four bottom television surveys were made.

All seismic records were directly studied on board ship and recognizable features were plotted on 1:500,000 scale charts. Subsamples were taken from all grab samples for smearslides and grainmounts, and grain sizes were estimated by microscopic observations. Gravity cores were split lengthwise, photographed, and radiographed. Also, routine geotechnical index properties were measured and subsamples taken.

This report contains information about the types of data collected (Table 1), locations of cruise tracks (Pls. 1 and 2), and locations of sampling stations (Pls. 6 and 9). Raw data maps from the sparker observations are given, as well as plots of the shipboard microscopic sediment analyses. In addition, separate maps showing only sand wave fields and surface faults in Cook Inlet and slumps and surface faults on the Kodiak shelf and slope, as deduced from preliminary inspection of our sparker records, are presented to clearly point out conditions of possible concern to resource development of these areas.

A shipboard regional interpretation of the sparker data from lower Cook Inlet is included in this report. However, a regional interpretation of sparker data from the Kodiak shelf has not yet been made. It will be done after the deep seismic, multichannel data, during 1975 and 1976 collected on board the research vessels CECIL GREEN and S.P. LEE, is processed and can be used as a base for the shallower, structural elements. This entire report should be considered as preliminary, and a more thorough analysis of data will be made during the winter season.

Only a limited number of references will be given in this report. For background information the reader is referred to two recent U.S. Geological Survey open-file reports (von Huene and others, 1976; Magoon and others, 1976) and the references listed in those.

Note: all seismic records, navigational and other pertinent data are on microfilm. These can be obtained from the National Geophysical and Solar Terrestrial Data Center EDS/NOAA, Boulder, Colorado 80302 or from Alaska Technical Data Unit, 345 Middlefield Road, Menlo Park, California 94025, telephone (415) 323-8111, ext. 2342.

## INSTRUMENTATION AND PROCEDURES

### Navigation

Two independent navigational systems were used by the scientific party. One unit consisted of a Magnavox integrated satellite-Loran C system, the other was a Motorola Mini-Ranger unit. The data from the integrated system were automatically recorded on magnetic tape, as well as typed out on a keyboard printer. The Mini-Ranger data were recorded on paper tape at 7-1/2 minute intervals.

Every 15 minutes the Mini-Ranger positions were plotted manually on a 1:500,000 scale chart, as were all acceptable satellite positions. For easy reference a shot-point number was given to each 15-minute position. In addition to the routine plots, the locations of major course changes were also plotted. Furthermore, dead-reckoning positions, based on satellite data, the ship's single-axis speed log and the gyro, were computed every two seconds by the integrated system and stored on magnetic tape.

The Mini-Ranger system received its return signals from shore-based transponders positioned at desirable locations by a land-based support group. A maximum line-of-sight range over 80 nautical miles was obtained for some transponder locations.

The Mini-Ranger was used as the primary navigational system because of the high frequency and accuracy of the data and because most tracklines were within range limits of the system. Also, many positions obtained by the integrated system were of low quality due to lack of adequate Loran C coverage in this region and because of a high percentage of satellite passes with elevations that precluded good position determinations.

In addition to the navigation by the scientific party, the ship's officers frequently succeeded in using radar and obtaining line-of-sight bearings. Correspondence between the ship's and scientific positions generally was very high.

#### Seismic Profiling and Visual Format Systems

Sparker: A total of 2419 nm of sparker data was recorded in Cook Inlet and on the Kodiak shelf, using a Teledyne system at a power of 30, 60, or 90 kilojoules. Seismic signals were received on a Teledyne 100-element, single-channel hydrophone, and the record was printed on a Raytheon model 1900 Precision Recorder. Usually, sweep and firing rates were at 2 seconds. Although several different settings were used, filters generally were adjusted to receive signals between 20 and 160 hertz. Records were annotated at 15-minute intervals with shot-point number, time (Greenwich Mean Time,GMT), and water depth.

Uniboom: Uniboom records were collected over a total of 2552 nm. The uniboom system used four EG&G model 234 power sources of 200 joules each driving hull-mounted plates. The hydrophone was an EG&G model 265. Data were recorded on an EPC 4100 recorder. Sweep and firing rates were typically at one-half second although some quarter-second rates were used. Filter settings typically were at about 600 to 1600 hertz.

Annotations were made in the same manner as those on the sparker system, but at 5-minute intervals.

High-resolution: A Raytheon TR-109 3.5 kilohertz seismic system, with a Raytheon 105 PTR transceiver and a CESP-II correlator, was used to gather 3524 nm of high-resolution - shallow-penetration seismic data, as well as bathymetry. The system operated with 12 hull-mounted transducers, and the data were recorded on an EPC 4100 recorder. Sweep and firing rates typically were at one-half second, but quarter-second rates also were used. Annotations were made in the same manner as those on the uniboom system.

Record quality: Three factors that significantly affected quality of the seismic records were the typically coarse-grained and hard nature of the unconsolidated surficial sediments, the shallow water depth throughout most of both areas, and acoustic vibrations from the vessel.

Coarse-grained and hard sediments had the most severe effect on the uniboom and 3.5 kHz records, causing much of the outgoing energy from these high-frequency systems to be reflected directly from the sea bottom with only a minor amount of energy penetrating through to subbottom reflectors. Some of the uniboom records show subtle, irregular traces of subbottom reflectors, which can be traced and correlated only with difficulty. Many of the 3.5 kHz records show no sign of subbottom reflectors and can be used only as indicators of water depth.

The shallow water depth caused multiples to appear at small distances below the initial sea-bottom reflection, partially or totally obscuring signals from deeper reflectors.

Vibrations from the ship's engines and gear boxes proved troublesome at certain RPM's, giving a noisy signal on the recorders. This problem was minimized by cruising at the optimum, least noisy speeds.

Although these three factors each has a deleterious effect on record quality it was found by varying ship speeds and filter settings that the nature of the bottom sediments was the main reason for the seismic systems to display "poor" subbottom acoustic reflections on the records. Depth of penetration and details in the record consequently varied with type of bottom and water depth. Except for certain parts, the records allow adequate subbottom interpretation of geology.

Magnetometer: A Varian proton magnetometer was used together with an X-Y plotter. The magnetometer fish was towed about 600 feet (200 m) behind the vessel. A sampling rate of 3 seconds was used. Due to the 2-second firing of the sparker, an overwhelming noise was introduced causing the magnetometer to give very poor records when both systems were operating at the same time.

Side scan sonar: The side scan sonar unit used was an EG&G model, normally operated at a 125 m scale and towed above the bottom at 10% of the scale employed. High quality records were obtained. Although all side scan sonar surveys were run at a ship speed of 4-41/2 knots, currents could be responsible for a higher speed over the bottom. A few times a survey was interrupted or had to be discontinued due to hitting an unexpected bottom high. Also, a few times the side scan sonar unit hit bottom due to a sudden drop in ship's speed caused by a sudden decrease in current velocities. A total of 107 nm (198 km) of side scan sonar records were obtained (Fig. 2 and 3).

Normally the uniboom and 3.5 kHz units were run simultaneously with side scan sonar for depth control and possible subbottom information.

Bottom television and bottom camera: A Hydro Products bottom television unit and an underwater mercury light were mounted on a small sled, about 30 cm

wide and 80 cm long. A four-point bridle was attached to the lowering wire. A multiconductor cable, leading to the camera and light, was taped at 5-m intervals to the winch cable.

The bottom television operation was conducted only in lower Cook Inlet (Fig. 2) and required four persons for smooth performance: One person operating the winch, one on the conducting cable, one on the TV monitor and tape recorder, and one on the 3.5 kHz (depth) and/or uniboom recorder. Continuous contact between the operators was maintained by means of walkie-talkie sets.

Since currents are always present in the lower Cook Inlet area it was impossible to fly the sled slowly and at a uniform distance over the bottom. Consequently a system of jumping had to be used, lowering the sled to the bottom and giving some slack wire. Due to ship's drift the cables became taut after a few seconds and the sled was then dragged over the bottom. The monitor operator then informed the winch operator to raise the unit, straighten the wire angle and lower it again.

Two fins, attached to the sled, oriented the sled in the current direction. A bar with divisions of 5 cm, and a compass attached to it, were mounted to the frame allowing direct and later measurements of bottom forms and local directions of current and/or sediment transport. Although a wide-angle lens was used, the area of observation was slightly more than 50% of the sled size, preventing observation of any bedform larger than about 50 cm.

The bottom camera was a 35 mm cassette EG&G unit mounted with its strobe in a large frame. Exposure was conducted via an electrical bottom contact, transporting the film as soon as a picture was obtained. Due to a longer focal length than the TV camera and the high amount of particulate matter, mainly organic, in the water column, few acceptable frames were obtained.

### Sampling Devices

Gravity corer: The gravity corer consisted of an 800-pound weight with valve to which a 6-foot, 3-inch ID sampling pipe can be attached. In the bottom of the pipe, a brass-fingered core catcher was inserted and kept in place by a core nose. A clean butyrate tube was used as liner.

As soon as the filled liner was removed from the pipe, excess water was drained off and the core capped on both ends. The caps were secured with tape and later glued to the butyrate.

In the ship's sediment laboratory the liner was cut lengthwise using a cutter similar to that used by Deep Sea Drilling Project on the D/V GLOMAR CHALLENGER. The core was cut either with an electro-osmotic knife or with a spatula (Bouma, 1969). One half was then selected for archive storage. This half was photographed (8 x 10 in. camera), radiographed, described and color coded. In addition smear slides and grain mounts were made during the descriptive phase.

The other half - the working half - was subjected to vane shear measurements (Torvane) and hand penetrometer tests. From the same depths, samples were collected for grain size analyses, faunal determinations (e.g., foraminifera), clay mineralogy, and geotechnical analyses (water content, bulk density, Atterberg limits).

After the shipboard processing, both core halves were placed in D-tubes and then stored in the scientific refrigerator.

Dart corer: Where seismic records indicated hogbacks of older sedimentary rocks cropping out on Albatross and Portlock Banks, a dart corer proved to be the only coring device capable of obtaining a sample. This device consisted of an 800-pound lead weight to which a 30 to 45-cm-long pipe was attached,

having an inside diameter of 1-3/4 inches. The procedure consisted of lowering the corer to about 40 m off the bottom, after which the winch was placed in neutral allowing the corer to obtain near-terminal velocities before striking the bottom. Pull-out varied due to depth of penetration and type of bottom material and reached values as high as 10,000 pounds, but typically was 3,000 to 5,000 pounds. The sediment was extruded on board ship using an hydraulic ram. However, about 40% of the cores could not be extruded. Subsamples were removed from the bottom of each dart core for faunal examinations.

Van Veen grab samplers: The normal Van Veen grab sampler proved to be too light for adequate sampling of the typically sandy-gravelly bottoms. Generally successful attempts were obtained with a heavy modified grab sampler constructed by Andy Soutar of Scripps Institution of Oceanography for Ian Kaplan at UCLA.

A four-legged frame housed two vertical rails along which the actual grab could move. The top covers of the sampler could be opened completely for full access. The addition of weight up to 400 pounds on top of the grab provided sufficient force for the half-round sides to dig into coarse material during the closing operation. When rock fragments got caught between both halves of the grab, incomplete closure resulted and part or all of the sample was lost. In general the results were good to adequate, and this instrument retrieved samples where other devices failed.

The Soutar grab sampler was teflon coated for geochemical work done by UCLA scientists. In addition to their subsamples, a core in plastic liner was taken from the least disturbed area of the grab sample for sedimentological work, and bulk samples were collected for petrographic studies.

Dredge: The rock dredge consisted of 1/2 inch by 2 inch flat-stock welded

into a rectangular frame. A chain net, made from metal rings makes the basket. To the front of the frame a yoke is mounted to which the winch cable was attached.

The dredge was used without an additional weight in front. Although only one lowering was made near the Barren Islands, the dredge worked very successfully.

Other sampling devices and subsamples: On board, subsamples were collected routinely for clay mineralogical investigations (J. Hein, U.S. Geological Survey), foraminiferal studies (R. Poore, U.S. Geological Survey) and heavy metal analyses (C. Holmes, U.S. Geological Survey). Cores and bulk samples will be used for petrological, mineralogical and granulometric studies. When algae and corals were present they were sampled for R. Rezak (Texas A&M Univ.).

## LOWER COOK INLET

The open waters of lower Cook Inlet are characterized by a fairly smooth bottom over which strong diurnal tidal currents move. As a consequence the surficial sediments are coarse grained, preventing significant penetration of high frequency seismic signals. It was found, however, that 30 kilojoules of the sparker system provided more than sufficient energy to obtain penetration to at least the first water-bottom multiple, and at the reduced power the strength of multiples was less. The uniboom records varied with ship's motion and coarseness of the bottom giving poor penetration in many areas. The 3.5 kHz system often failed to collect subbottom information and many records show no subbottom reflections.

The raw data map constructed from the sparker records reveals that many areas show subbottom reflectors that are more or less parallel to the bottom (Pl. 3). Although some lateral variation in intensity of such reflectors exists, no interpretation could be made due to absence of long cores and lack of public information on drill holes.

Many anticlines and synclines were encountered in the sparker profiles (Pl. 4). Density, shape and size varies between track lines making correlations occasionally questionable. Utilizing reports and personal assistance from L.B. Magoon (Magoon and others, 1976; Magoon and others, 1976 in press) an interpretation of the structural elements, as seen in the sparker records was attempted (Pl. 4). The general pattern of near surface folds is parallel to the surrounding tectonic pattern on shore. Distinctness of anticlines and synclines decreases from latitude  $60^{\circ}$  N south toward a line between Seldovia and the volcanic island Augustine. This line corresponds to the location of

the Augustine-Seldovia Arch (Magoon and others, 1976 in press).

South of this arch the folding is more intense and a change in direction toward the Mt. Douglas area becomes apparent. Correlation between tracklines in the same area, some of which were run in rougher seas than others, often becomes dubious. Part of the problem of correlation between tracklines is due to the presence of major unconformities that obscure deeper structural elements. In addition, the density and offset of surface and subsurface faults varies between tracklines (Pl. 5).

Adjacent to the Barren Islands specifically, and between the southwest part of Kenai Peninsula and Shuyak-Afognak Islands, is a strongly deformed zone containing small-scale faults, joints, horsts and grabens in basement outcrops, with little or no cover of unconsolidated sediments. The present density of the tracklines precludes any correlation.

Around Augustine Island the nature of the bottom sediments prevents good seismic penetration. This, together with rough seas while operating there, caused poor penetration and noisy records. Faults, likely of short length, form the major structural elements.

The raw data map (Pl. 3) also shows many dip symbols, some of them indicating smoothly dipping reflectors, others revealing a wavy character. The waviness varies and is considered to be local.

In the western part of lower Cook Inlet an escarpment was seen on many of the transverse crossings. Where the nature of this scarp is compatible between adjacent tracklines, correlations are shown (Pl. 4). To the north the scarp becomes less steep and dashed lines were used indicating possible connection. A short scarp was seen close to Augustine-Seldovia Arch. Its char-

escarpment was found in between.

In general, the shallow structural picture of Lower Cook Inlet does not seem to be complex, except in the zone between Kenai Peninsula and Shuyak Island and around Augustine Island. Long fault lines are not apparent and most faults may be of local importance. The influence of the Augustine-Seldovia Arch is visible, but the broad nature of this arch eliminates sudden changes in the near surface structural pattern. A few dashed correlation lines are presented on the interpretation map and their significance should be considered very tentative. Since correlation between tracklines south of the arch is more difficult is it thought that the deeper structures between the arch and the Mt. Douglas area are more complex than north of the arch.

The Lower Cook Inlet Draft Environmental Impact Statement (Bureau of Land Management, 1976) summarizes other information available on the hydrology and ice conditions in this area.

The pattern of textural characteristics of the surficial sediments is rather simple (Pl. 6). Except along coast lines, coarseness of the surficial sediment is directly related to the strength of the currents, which is proportional to the width of the water body. In general, the cross section of Lower Cook Inlet becomes narrower going north to the 60th parallel and an increase in coarseness of surficial sediments occurs. The granules and pebbles vary in size from 2 to 6 cm and are well-rounded. It could not be demonstrated that significant transport occurs at the present. It is likely, however, that all the surficial sediment is a lag deposit of transgressional nature, undergoing little net transport at the present time. A certain amount of transport is obvious as all sediment samples normally contain signi-

cant amounts of dispersed volcanic materials. Shells and shell fragments often form an important part of the upper sediments, but whether the fragmenting of shells is only the action of crabs or is also due to currents cannot be established at the present time. Shells, shell fragments and volcanic ash are not incorporated in the textural display given on the surficial sediment map (Pl. 6).

Although all of the samples from lower Cook Inlet proper are coarse grained, it is likely that the bays have considerably weaker currents that allow fine-grained sediment to settle there. For example, Tuxedni and Chinitna Bay have exposed mudflats at lower water level, and a gravity core (#2) collected behind the Homer Spit in Kachemak Bay consisted of a black muddy sediment with a high content of organic matter.

Uniboom and 3.5 kHz records showed many areas with wavy bedforms of varying sizes (Pl. 5). Insufficient time was available for detailed surveying but a number of side scan sonar records and bottom television lowerings were obtained between northern Kachemak Bay and the axis of lower Cook Inlet, and off Kenai Peninsula (Fig. 2). The side scan sonar records conform with earlier findings of the Alaska Fish and Game Department (P. Wennekens and J. Dygas, pers. comm., 1976) that elongated narrow patches, parallel to the main tidal current regime, occur with various other types of bedforms. Plate 5 shows where wavy bedforms were observed on uniboom and 3.5 kHz records and Figure 2 shows where side scan sonar and TV observations have been made from the R/V SEA SOUNDER.

Rippled bedforms differ in size and characteristics between these patches. In central Cook Inlet (Pl. 6, sta. 44) large asymmetric underwater dunes

were observed, some of them 1 km long and 10 meters high. Their asymmetry indicates a net transport to the south. However, during the television lowering over this area a northern sediment movement was observed, transporting sand via small current ripples.

In other areas northerly migrating asymmetric dunes were found, while more or less symmetric forms are not uncommon. Along some longitudinal tracklines dune fields appear and disappear without an observable change in water depth. Along such a stretch asymmetric ripples can change into symmetric ones, and even change direction of asymmetry.

Moving across Lower Cook Inlet with side scan sonar a rapid change in aspect of bottom morphology can be observed without a change of depth. One field may contain dunes with straight crests and some indication of superimposed megaripples. This may suddenly change into a megaripple field, with crest distances of about 20-25 m and with slightly sinuous or slightly rhomboid crests. Another common pattern consists of sinuous megaripples with a wavelength of about 7-10 m. Those fields can alternate with patches of boulders, flat-floored bottom or flat-floored with broad, shallow grooves with megaripples in each groove.

Coverage is insufficient to determine if the large dunes and/or megaripples are locally permanent features; if they move or if they are basically stable. No detailed and repetitive bathymetric surveys, covering a long span of time, are available for such analyses as was the case in the North Sea where similar features exist. It therefore is possible that the large features are relict forms from the last transgressive phase, or that they move only when extreme high water conditions and related currents occur, or are basically stable with minor modifications due to tidal flows.

Microscopic analyses of sand sized material on board ship reveal a basic bimodal distribution of the total sediment: pebbles and sand. The sand is mainly medium grained with mixed fine-grained sand. It depends on the location of a sample, especially in the ripple fields (crest or trough) if medium or fine sand predominates (Table 4). Petrologically, five major components were distinguished: quartz, total feldspar, heavy and mafic minerals, rock fragments and glass shards. The sand samples, when not inundated by shards, were about equally divided between quartz plus total feldspar on the one hand and heavy and mafic minerals plus rock fragments on the other hand. Considerable variations occur and rock fragments plus heavy minerals in some samples constitute 75% of the total sand fraction.

The heavy mineral assemblage is varied: epidote, garnet, magnetite, hornblende and biotite are most common. The rock fragments consist predominately of weakly foliated, fine-grained dark slate and phyllitic rock types, which are characteristic of the sediment. The source area for this type of material must have consisted of a high proportion of supracrustal metasedimentary rocks with only a minor amount of granite or hypabyssal rocks.

The textural aspects of the Lower Cook Inlet sediments may be characterized best by their good sorting and by the reworking of the lithic fragments. The sediments are very immature compositionally. The rounded nature of the pebbles either suggests transport at a lower stand of sea level, or slow movement continuing at the present. Transport from river mouths by ice and deposition as drop stones in Lower Cook Inlet may not be disregarded as presently little is known about the transporting role of sea ice in this area. However, the absence of angular rocks makes present ice transport doubtful.

## KODIAK SHELF

The seafloor of Kodiak Shelf consists of several flat, relatively shallow areas that are cut by transverse valleys (Fig. 4). This physiography reflects the erosive action of glaciers and waves as well as some bedrock structural control.

Sparker records show that the shallow bedrock structure of Kodiak Shelf consists of a series of folds that apparently trend in a general northeast-southwest direction (Pl. 7). However, they show enough deviation in trend and discontinuity that confident regional correlations of fold axes cannot be made at this time. Especially obvious, though, are major anticlinal crests that occur near the shelf break on Albatross Bank.

Several surficial scarps, underlain by offset reflectors, also are evident on the sparker records implying surface faulting. These features are most abundant in a zone just off the southeast coast of the Kodiak island group, near the shelf break on Albatross Bank, and on Portlock Bank (Pl. 8). Confident correlation of faults between track lines cannot yet be made.

Unconformities occur at several places on the shelf. Most commonly the sparker records show a relatively smooth unconformity surface separating folded and faulted bedrock below from flat-lying sediments above. The sparker records that extend beyond the shelf break, onto the continental slope, often show one or two unconformities separating sediments with successively decreasing dips above each unconformity surface.

The uniboom and 3.5 kHz records vary in quality according to the factors mentioned earlier. The uniboom records on Kodiak Shelf commonly show slightly undulating subbottom reflectors of irregular reflectivity. Zones of transparent, opaque, and inclined sediments also commonly occur.

Hogback ridges occur on Albatross and Portlock Banks. In these areas, inclined bedrock has been sculpted by differential erosion, and a significant cover of unconsolidated sediments is absent.

The sediments of Kodiak Shelf are distributed in relation to the physiography (Fig. 4, Pl. 9). The broad, flat elevated banks are covered by sands that commonly contain coarse material, up to boulder size, but rarely contain significant quantities of silt and clay. The sediments of the troughs, on the other hand, typically are finer grained than those of the adjacent banks, and a few are composed almost entirely of silt and clay. Gravel and coarser material does occur in the deep areas, however.

As in Cook Inlet, the composition of the sand fraction is quartz, feldspar, heavy minerals (hornblende, epidote, garnet, biotite, opaques, and others), and rock fragments (schist, phyllite, and less common volcanics). Heavy minerals and rock fragments are abnormally abundant in many samples, reaching up to a total of 75%.

In addition to epiclastic debris, the sand-size fraction also contains shell material and volcanic glass. The shell material is made up of various proportions of crushed megafaunal shells and of foraminiferal tests. Although not noted on the textural map, many of the bank sediments are predominately shell material (Table 4).

Fragments of volcanic glass are present in most unconsolidated sediments recovered from Kodiak Shelf, but are most abundant in the trough areas. Some essentially pure ash layers were encountered in the troughs, and some other trough sediments contain more than 75% volcanic glass.

The gravel to boulder-size material of Kodiak Shelf consists mostly of dark-colored slate and phyllite, with granitic types present in some instances.

Bedrock recovered from dart coring of the hogback ridges is mostly olive gray to gray siltstones and silty sandstones. Most of the core samples are barren of nannofossils, although a late Tertiary to Quaternary nannofossil age was determined at one site (Table 2). Attempts to date the bedrock by foraminifera and by pollen are currently underway.

The few sediment samples recovered on the continental slope off Kodiak are muds and sands containing some gravel, pebbles, and cobbles. A more extensive sampling program is necessary to characterize the slope sediments.

According to our records, the surface of Kodiak Shelf, both on the banks and in the troughs, generally is smooth and devoid of extensive bedforms or slumps. A side-scan sonar survey (Fig. 3), run for approximately 24 nm (43 km) in a northwesterly direction approaching Marmot Island, showed a surprisingly featureless bottom configuration, with only an occasional boulder. The survey was continued around the island and then in a southeasterly direction for about 16 nm (29 km) just to the northeast of Marmot Island, in an area of bedrock outcrop. An orthogonal joint pattern was clearly evident in these records.

Slumps occur abundantly in many zones on the Kodiak continental slope (Pl. 7 and 8). Within these zones, incipient slumping is often detectable on the upper slope, with block glides and internally deformed rotational slumps abundant on the lower portions. An important question, yet to be answered, is why the slumps occur in some areas of the slope but are absent in others.

## REFERENCES

Bouma, A.H., 1969. Methods in the Study of Sedimentary Structures: John Wiley and Sons, New York: 458p.

Bukrey, D., 1976. Nannofossil ages of Kodiak Shelf cruise SEA-3-76-WG: Memorandum to George W. Moore, Aug. 20, 1976: 2p.

Bureau of Land Management, 1976. Lower Cook Inlet, Draft Environmental Impact Statement: Alaska Outer Continental Shelf Office, Proposed Oil and Gas Lease Sale No. C 1, 3 volumes.

Magoon, L.B., Adkison, W.L., Chmelik, F.B., Dolton, G.L., Fisher, M.A., Hampton, M.A., Sable, E.G., and Smith, R.A., 1976. Hydrocarbon potential, geological hazards, and infrastructure for exploration and development of the lower Cook Inlet, Alaska: U.S. Geol. Survey open-file report 76-449: 124p.

Magoon, L.B., Adkinson, W.L., and Egbert, R.M., 1976. Map showing geology, wildcat wells, Tertiary plant-fossil localities, K-Ar age dates and petroleum operations, Cook Inlet area, Alaska: U.S. Geol. Survey Misc. Investigations Map I-1019, 3 sheets, color, 1: 250,000 (in press).

Von Huene, R., Bouma, A., Moore, G., Hampton, M., Smith, R., and Dolton, G., 1976. A summary of petroleum potential, environmental geology, and the technology, time frame, and infrastructure for exploration and development of the western Gulf of Alaska: U.S. Geol. Survey open-file report 76-325: 92p.

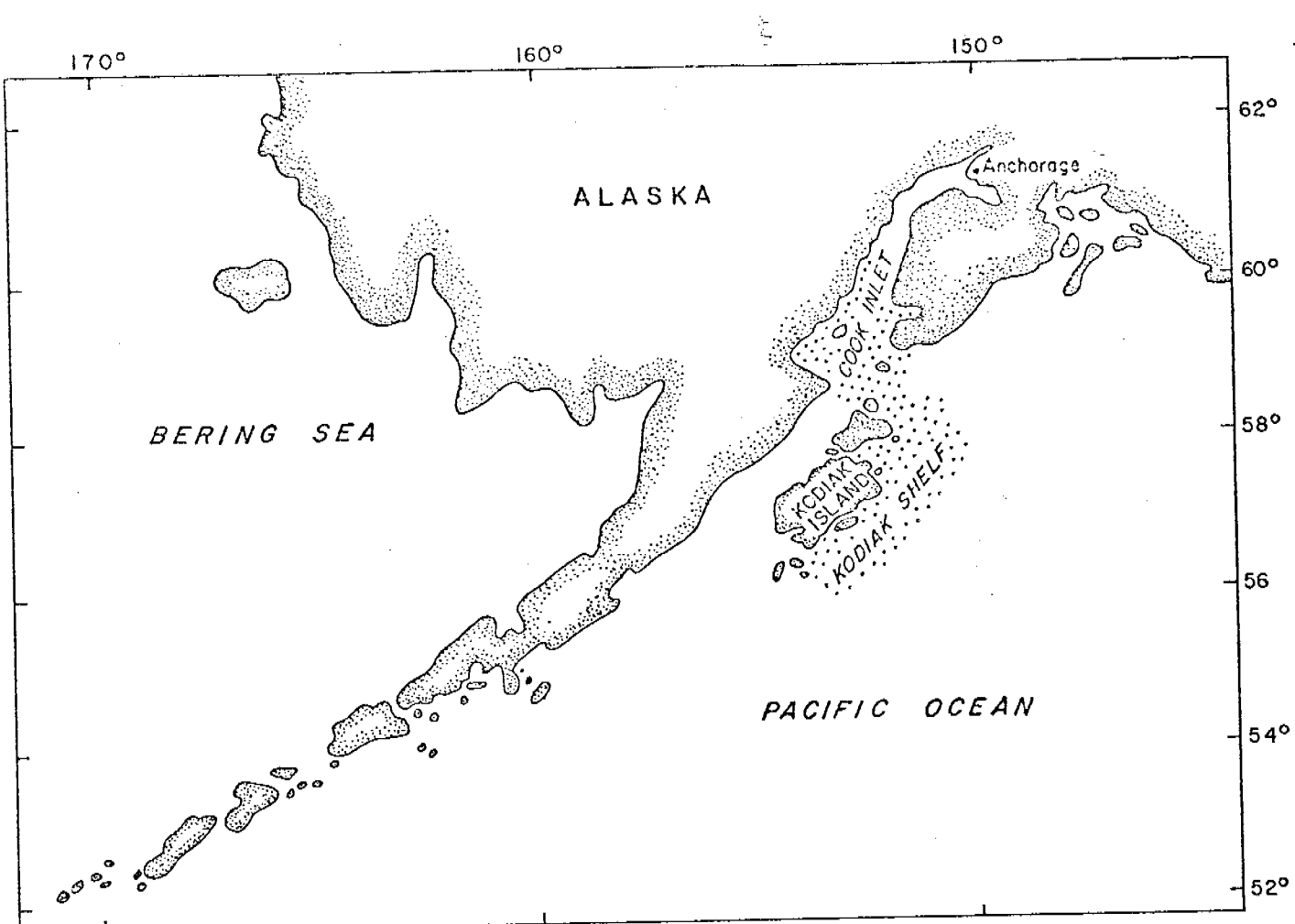


Figure 1.- Generalized location map of the study area

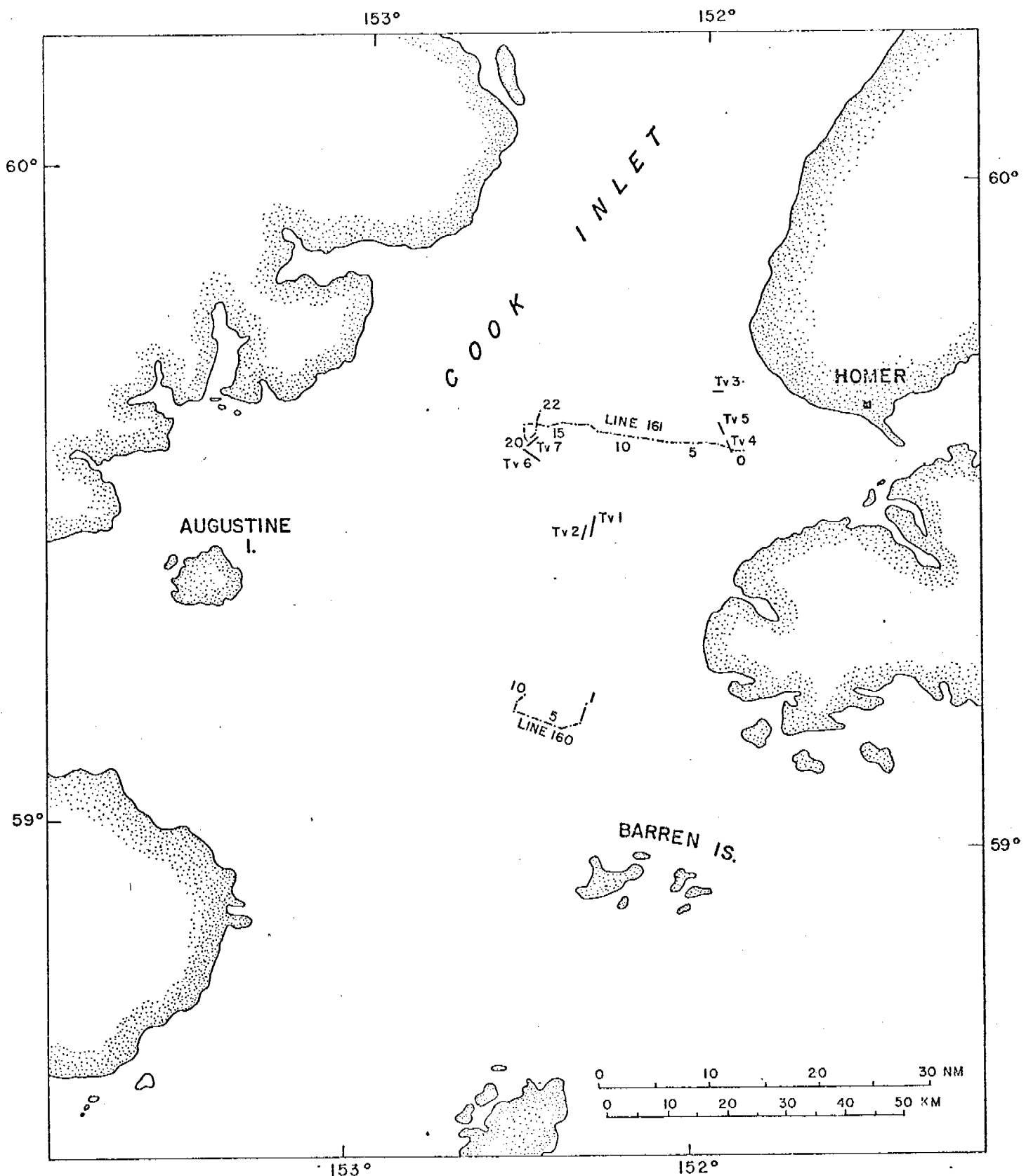


Figure 2.- Lower Cook Inlet, location of side-scan sonar lines  
and bottom television stations

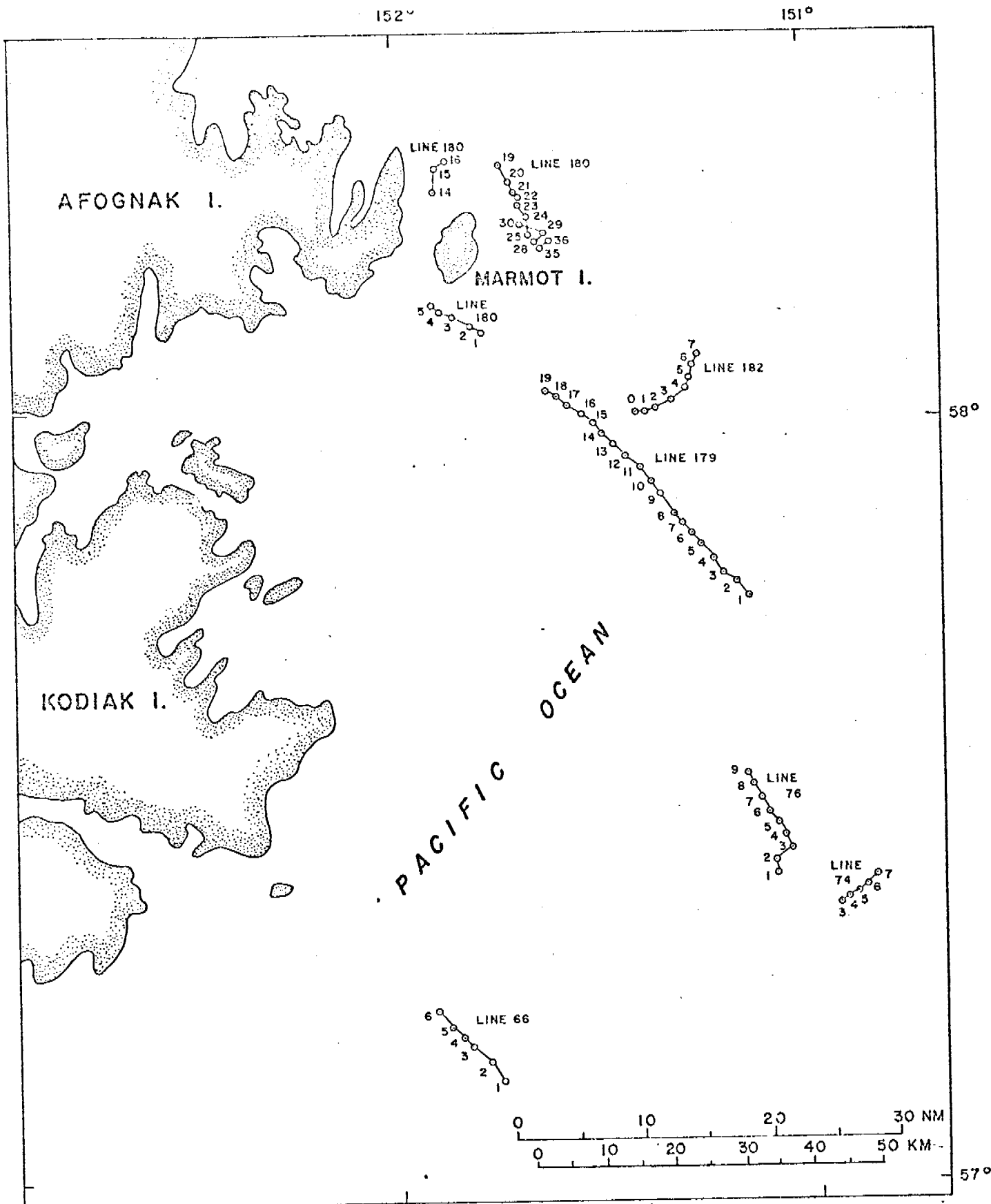


Figure 3.- Side-scan sonar lines on Kodiak Shelf

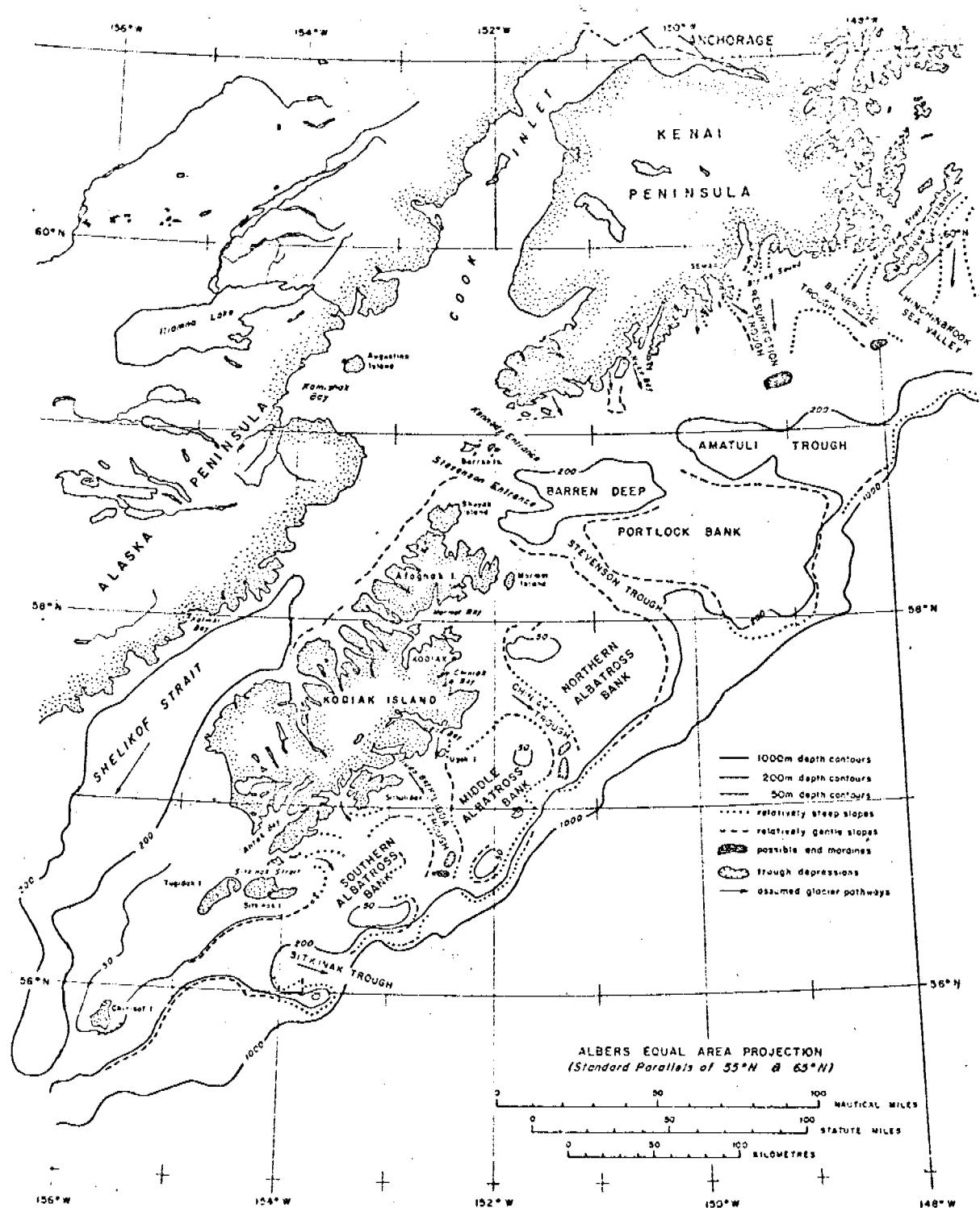


Figure 4 - Generalized physiographic map of Kodiak Shelf

Table 1. Cruise itinerary, and types and amounts of data collected on board the R/V SEA SOUNDER during 1976 in lower Cook Inlet and on Kodiak Shelf, Alaska. (Trackline distances computed using 5 nm/hr, as average ship speed)

<u>Port</u>	<u>Arrive</u>	<u>Leave</u>	<u>Leg</u>
Seward		June 18	I
Homer	June 22	June 22	I
Homer	July 1	July 3	
Homer	July 3	July 5	II
Kodiak	July 14	July 17	II
Kodiak	July 22	July 22	III
Kodiak	July 30		III

<u>Instrument</u>	<u>Trackline</u>	<u>Remarks</u>
Sparker	2419 nm =4499 km	12 rolls
Uniboom	2552 nm =4746 km	63 rolls
3.5 kHz	3524 nm =6555 km	73 rolls
Side Scan Sonar	107 nm =198 km	11 rolls
Magnetometer	1460 nm =2716 km	
Bottom Television		4 video tapes
Dredge		1 haul
Van Veen Grab		16 recoveries
Soutar Grab		114 recoveries
Gravity Core		9 recoveries
Dart Core		30 recoveries
Bottom Camera		1 station

~~ages or~~ ~~ages or~~ ~~Kuroshio~~ ~~bottom~~ sediments collected during the summer  
of 1976. Identifications by David Bukry, 1976.

<u>Sample and Interval</u>	<u>Age</u>	<u>Remarks or Zone</u>
83G 118-119 cm	Quaternary (C)	<u>Gephyrocapsa oceanica</u> or <u>Emiliania huxleyi</u>
84G 0-2 cm	Quaternary (C)	as above
84G 160-161 cm	Quaternary (C)	--
97G 0-2 cm	Quaternary (S)*	<u>Distephanus octangulatus</u>
98G 0-2 cm	Quaternary (S)*	as above
98G 93-94 cm	Quaternary (S)*	<u>Dictyocha aculeata</u>
110D 46-47 cm	Pliocene or Quaternary (D)*	contains the diatom <u>Denticula seminae</u>
110 47-48 cm	Quaternary (C)	--
116D 38-39 cm	Miocene to Quaternary (D)	--
117D 13-14 cm	Cenozoic (C)	rare <u>Coccolithus pelagicus</u>
133G 30-31 cm	Quaternary (C)	<u>Gephyrocapsa oceanica</u> or <u>Emiliania huxleyi</u>
133G 92-93 cm	Quaternary (C)	--
133G 104-105 cm	Quaternary (S)*	<u>Dictyocha aculeata</u>

notes: C= Coccoliths \* = Diatoms abundant

D= Diatoms G= gravity core

S= Silicoflagellates D= dart core

The following samples proved to be barren of coccoliths, diatoms, and silicoflagellates:

83G 0-2 cm  
99G 19-20 cm  
100D 16-17 cm  
101D 8-9 cm  
102D 15-16 cm  
103D 16-17 cm  
104D 15-16 cm  
106D only very small sample recovered  
107D 29-30 cm  
108D 24-25 cm  
112D 21-22 cm  
118D 19-20 cm  
120D 19-20 cm  
121D 9-10 cm  
123D 33-34 cm  
124D 19-20 cm  
125D 19-20 cm  
144D 22-23 cm  
145D 9-10 cm  
147D 11-12 cm  
148D 7-8 cm  
149D only very small sample recovered

Sample 116D is poorly preserved and could be upper Miocene to Quaternary.  
No recovery on dart core stations 109D, 122D, 126D, 142D and 143D.

Table 3. Scientific personnel on board the R/V SEA SOUNDER during the 1976 cruise in lower Cook Inlet and Kodiak Shelf, Alaska.  
 (Cruise leg numbers refer to the data given in Table 1.)

Arnold H. Bouma	co-chief scientist	I-III	U.S. Geol. Survey, Marine Geol.
Monty A. Hampton	co-chief scientist	I-III	id.
Leslie B. Magoon	I		U.S. Geol. Survey, Oil and Gas
George W. Moore	II		U.S. Geol. Survey, Marine Geol.
James R. Hein	I		id.
Sandra J. Owen	I		U.S.G.S., Cons. Div., Los Angeles
John W. Whitney	I		U.S.G.S., Cons. Div., Anchorage
Bruce W. Turner	II		id.
Andrew Stevenson	I		U.S. Geol. Survey, Marine Geol.
Gordon L. Tanner	I,II		id.
Harry Hill	III		id.
Thomas P. Frost	I-III		id.
Robert C. Orlando	I-III		id.
Roland H. Brady, III	II,III		id.
Christina E. Gutmacher	I		id.
Richard A. Garlow	I-III		id.
Dennis R. Kerr	I		id.
David T. McTigue	I,II		id.
James Evans	II,III		id.
Robert M. Egbert	I		U.S. Geol. Survey, Oil and Gas
Edward C. Ruth	I		UCLA
Mark Sandstrom	II		UCLA
Daniel Stuermer	III		UCLA
Ivan P. Colburn	II		Cal. State Univ., Los Angeles
Stuart O. Burbach	II,III		Texas A & M Univ.
Nelson M. Robinson, Jr.	II,III		id.
Michael E. Torresan	II,III		San Francisco State Univ.
Scott R. Morgan	II,III		id.
Joseph A. Dygas	I,II		Alaska Fish and Game Dept.
Ronald R. Murray	II,III		NAVOCEANO

#### Ships Officers

Alan McClenaghan	Captain
Don Phillips	Chief Engineer
Kelly Mitchell	First Mate

Table 4. Position, lithology, color and other shipboard characteristics of samples collected on board the R/V SEA SOUNDER in Lower Cook Inlet and Kodiak Shelf.

Sample No.	No. of attempts	Latitude	Longitude	Water Depth m /Core length, cm	Lithology, color and additional remarks
1 G	2	57°56.50'	150°13.55'	191	no recovery
1 V	1	57°56.54'	150°13.56'	192	Clean ms, dark with echinoid, and worm tubes
2 G	1	59°37.55'	151°18.87'	73	Slightly sl/c, dark, high amount of organic material sl/c=10-90
3 V	2	60°05.36'	152°34.13'	40	Slightly muddy sandy g with cobble sized material, grey.
4 V	1	60°05.45'	152°34.54'	40	Barnacles encrusted to rock fragments. g/s/sl/c=60-30-5-5
5 V	1	60°04.70'	152°33.83'	47	Sandy g with some rock fragments, greyish brown. Numerous small pelecypods and sea fans. g/s/sl/c=94-3-2-1
6 V	1	59°19.02'	153°41.45'	26	Slightly muddy pebbly s, grey. g/s/sl/c=40-55-3-2
7 V	1	59°16.22'	153°32.12'	32	Clayey sl/fs, dark grey. s/sl/c=45-40-15
7 S	1	59°16.24'	153°32.12'	32	Sl/s, dark grey, some pumice. s: 90% vf, 10% f. s/sl/c=80-15-5
8 S	1	59°10.69'	153°44.10'	36	Sl/fs, some pumice. Abundant gastropod shells, molluscs and worm tubes.
9 V	1	59°41.60'	152°36.10'	35	Slightly sandy pebbly clayey sl, dark grey. Abundant fauna: molluscs and barnacles. g/s/sl/c=30-6-58-6. Abundant shell fragments.
10 V	4	59°41.25'	152°34.90'	51	Pebbly s, dark, some sessile organisms. g/s/sl/c=30-67-2-1
11 V	2	59°34.50'	152°35.90'	75	Sandy g, dark grey. g/s/sl/c=95-4-tr-tr
12 V	2	59°34.60'	152°36.10'	67	Sandy g, dark grey. g/s/sl/c=54-44-1-tr
13 V	1	59°25.75'	152°50.09'	63	Ms, dark grey. 60% ms, 30% fs, 10% vfs
14 V	1	59°30.0'	152°46.01'	65	Ms, dark grey. 2% cs, 93% ms, 5% fs
14 S	1	59°30.06'	152°46.06'	61	Ms, dark grey. 5% cs, 95% ms, 5% fs
15 S	1	59°31.08'	152°54.0'	45	Ms, dark grey. Some shell debris, 4% cs, 93% ms, 3% fs

Sample No.:

G=gravity core

V=van Veen grab sample

S=Soutar modification of van Veen grab

CD=Chain dredge

D=Dart core

No. of attempts:

number of lowerings with that sampling device before an acceptable sample is obtained. If no recovery: see under remark.

Water Depth m/Core length cm:

waterdepth in meters at the time of the station without tidal correction/length of core in cm as recorded on board ship.

Lithology, color and additional remarks:

g/s/sl/c=gravel/sand/silt/clay ratio in percentages from smearslides.  
tr=trace, g=gravel, vcs=very coarse sand; cs=coarse sand; ms=medium sand; fs=fine sand; vfs= very fine sand; s=sand; sl=silt; c=clay

Table 4. cont.

Sample No.	No. of attempts	Latitude	Longitude	Water Depth m	Core length cm	Lithology, color and additional remarks
16 S	1	59°23.2'	153°06.6'	48		Pebbly s, grey. Small pebbles. g/s/sl/c=10-88-1-tr
17 S	1	59°20.7'	152°53.5'	74		Clean s, vf to c, grey. s=100%
18 S	3	59°12.15'	152°44.8'	122		Clean s, dark grey. s=98% pebbles and c 1%, ms 90%, fs 9%
19 S	1	58°56.25'	152°23.36'	75		Very slightly silty s with shell fragments (35%) s/sl/c=97-2-1. ms 90%, fs 10%
20 D	2	58°53.45'	152°25.50'	82		No recovery
21 CD	1	58°53.15' to 58°53.52'	152°22.28' to 152°19.15'	-		Chain dredge. Primarily rounded pebbles and boulders: sandstone, shale, basalt, plutonics. Varied biota: many sponges
22 S	3	58°51.20'	152°24.90'	154		Sandy g. 50% clastics and 50% shell fragments, forams, etc. g/s/sl/c=55-40-4-1
23 S	2	58°55.7'	152°34.3'	170		60-65% clastic, rest biogenic. S, grey. ms prim. g/s/sl/c=1-97-1-
24 S	1	58°58.49'	152°31.11'	147		Sl s, grey. 10% shell fragments. s/sl/c=97-2-1
24 G	1	58°58.90'	152°30.45'	147		Tr recovery
25 S	1	59°03.2'	152°31.2'	133		Pebbly s. g/s/sl/c=5-92-2-1
26 S	1	59°08.1'	152°22.1'	119		S. 100%. Range: c-f; ms=median. Some shell fragments
27 S	1	59°26.3'	152°20.7'	74		S, less than 1% g. Clean. Range vc-m; median=coarse
28 S	1	59°21.35'	152°25.9'	78		S 100%. Range: m-f; median=m. Some shells
29 S	2	59°14.98'	152°28.15'	89		S 100%. Range: m-f; median=m. Some shells. Large phlogopite flakes
30 S	2	59°16.65'	152°21.70'	91		Shelly s: 15% shell fragments, 85% s. Range: c-f; median=m.
31 S	2	59°20.25'	152°19.10'	90		Shelly s: 15% shell fragments, 85% s. Range: m-f; median=m.
32 S	1	59°19.45'	152°06.13'	69		Sandy g, grey. Shell fragments (25%), coral, molluscs. g/s/sl/c=67-32-tr-tr
33 S	2	59°26.35'	152°12.49'	50		Pebbly s, much fauna on surface. 35% shell fragments. g/s/sl/c=15-85-tr-tr
34 S	3	59°36.55'	151°52.00'	28		Fs with few animals. 20% shells, shell fragments, forams. 80% s: ms/fs/vfs=10-80-10
35 S	1	59°37.35'	152°14.30'	50		Sandy g with clams and brittle stars. g/s/sl/c=73-27-tr-tr.

Table 4. cont.

192

Sample No.	No. of attempts	Latitude	Longitude	Water Depth m/length cm	/Core	Lithology, color and additional remarks
36 S	2	59°41.50'	152°13.0'	46		Pebbly s with shells (25%). S range: vc-f; median: ms g/s/s1/c= 33-74-2-1
37 S	1	59°46.30'	151°13.0'	56		Sandy g with shells (20%). ms/fs=85-15 g/s/s1/c=69-31-0-0
38 S	2	59°44.65'	151°59.05'	18		G (100%). Rocks up to 15 cm, well rounded, one rounded cobble: 20 X 12 X 8 cm
39 S	1	59°40.75'	151°57.15'	35		G with abundant fauna: urchins, crabs, clams, etc. Very little fs
40						Pebbles and cobble well rounded. No sample station
41 S	1	59°36.25'	151°56.00'	30		Clean ms well sorted, sub-rounded to sub-angular 10% shells. ms/fs 85-15
42 S	2	59°36.20'	151°45.60'	30		Silty s, ms well sorted, sub-rounded to sub-angular, shells 5%, g/s 25-70
43 S	1	59°36.63'	151°22.07'	52		Silty s, well sorted, dark, some clams, s is vfs/fs/ms=75-20-5% s/s1/c=96.5-3-0.5
44 S	2	59°35.25'	152°22.90'	62		Clean s (98%) well sorted, some shell fragments, s is ms/fs/cs= 79-20-1 g/s/shells=1-98-1
45 S	1	59°34.80'	152°36.10'	-		Muddy s with pebbles abundant fauna.
46 S	2	59°44.40	152°32.05'	71		Sandy g, some shell fragments, g/s=75-24 1% shells, s is ms/fs/c= 85-14-1
47 S	2	59°55.49'	152°28.60'	25		Sandy g, shells (5%) s poorly sorted vcs/cs/ms/fs/vfs=2-25-50-18-5 g/s/shells=75-20-5
48 S	1	60°00.50'	151°22.46'	45		Sandy c, well sorted, sub-rounded to angular, 99% s fs/vfs/ms=90-7-1 s/s1=99-1
49 S	1	59°56.00'	152°03.90'	47		Shelly g, g well rounded, g/s/shells=80-15-5 s: cs/ms/fs=80-10-10
50 S	2	59°52.50'	151°54.50'	32		Sandy g, sub-angular to rounded, s: cs/ms/fs=30-55-15, g/s/shells= 70-15-10
51 S	1	58°12.54'	151°55.74'	60		Cobbles and boulders with fauna, washed sample, no s.
52 G	2	58°24.54'	151°14.35'	107		NO SUITABLE RECOVERY-small sample g/s/c=25-75-.1
52 S	1	58°24.42'	151°13.80'	86		Pebbly s with clams (no further analyses)
53 S	2	58°12.56'	150°39.79'	175		Sandy g, with shell fragments. s: cs/ms/fs/vfs=5-10-70-10, g/s/shells= 40-15-45
54 S	2	58°07.36'	150°30.26			Muddy s, also forams and shells=10%, glass shards, lithic fragments s, ms/fs/vfs=10-75-15, g/s/s1/c=.5-89-.5-.1%

Table 4. cont.

Sample No.	No. of attempts	Latitude	Longitude	Water Depth m	Core length cm	Lithology, color and additional remarks
55 S	2	58°01.86'	150°21.64'	184		Muddy s, ash-glass shards, s/sl=99.5-.5% s is 95% fs, well rounded
55 G	1	58°01.86'	150°21.64'	183		Pebbles, not much else.
56 S	1	57°55.22'	150°12.77'	194		S, overlain by small amount of clay and possible ash, s 100% well-sorted.
57 S	1	57°50.94'	150°03.74'	190		Muddy s, ash 97% s: cs/ms/fs/vfs=10-15-65-10%, lithics are rounded shell fragments and forams
58 S	1	57°46.99'	149°55.40'	232		Silty s w/pebbles. ash; s=cs/ms/fs/vfs=15-15-60-10; g/s/sl-c=5-94-?
59 S	1	57°46.60'	149°29.66'	495		Pebbly s, high amount of shards, s 90% fs to vfs. Lithics are well rounded; g/s/sl-c=3-97-tr
60 S	1	57°45.96'	149°37.41'	444		S 99%, glass shards, lithics are rounded, s=cs/ms/fs=1-9-90% g/s/sl-c=1-99-tr
61 S	1	57°35.61'	150°24.46'	112		Pebbly s w/g, forams, shells, ash. S very well sorted, g/s/shells=25-60-15
62 S	1	57°39.05'	150°32.48'	102		Pebbly s, abundant brittle stars and clams, pebbles well rounded, s well sorted g/s/sl-c/shells=20-55-1-24
63 S	1	57°43.96'	150°39.25'	90		Pebbly s, abundant fauna, lithics well rounded, s mod. sorted, g/s/sl-c/shells=25-40-1-34
64 S	1	57°47.50'	150°45.00'	83		Sandy g, shell fragments. Lithics well-rounded, mod. sorted s, sub-angular to sub-rounded; g/s/sl-c/shells=40-20-1-39%
65 S	2	57°51.50'	150°51.50'	77		Sandy g, with ash, s 85% fs-vfs, lithics well rounded; g/s/sl-c/she 35-20-1-44
66 S	1	57°55.10'	150°59.30'	-		Shelly s, much shell debris, glass shards, s 90% fs/vfs; g/s/sl-c/shells=5-15-1-79
67 S	3	57°59.70'	151°06.40'	82		Pebbly s, glass shards, s: cs/ms/fs/vfs=1-5-55-40, lithics rounded; g/s/sl-c/shells=10-30-1-59
68 S	2	57°28.10'	151°28.70'	154		S 97%- abundant glass shards, well sorted, s/sl/c=97-2-1
69 S	2	57°23.25'	151°10.95'	80		S 90%, about 95% ash, fs/vfs=75-25, lithics rounded; s/sl/c=90-9-1
70 S	1	57°24.08'	150°52.25'	96		Clean s, 99%, lithic fragments rounded, s:cs/ms/fs/vfs=<1%-12-80-8
71 S	1	57°20.01'	150°59.08'	95		Clean s, 99%, lithics round-subrounded, few shards, s-ms/fs/vfs=15-75-10. Clay-silt=1%
72 S	1	57°24.20'	151°05.10'	92		S 99%, lithics mostly sub-rounded, abundant shards, ms/fs/vfs=1-97-2, 1% clay-silt

Table 4. cont.

Sample No.	No. of attempts	Latitude	Longitude	Water Depth m	/Core length cm	Lithology, color and additional remarks
73 S	1	57°34.90'	151°12.15'	66		Shelly s, sample contained large basalt boulder at 86% of volume, ash, g/s/shells=.5-3-11
74 S	2	57°41.10'	151°00.40'	75		Shelly s, with cobbles and boulders, mode is rounded to sub-rounded b-c/g/s/sl-c/shell=80-4-2-tr-14
75 S	1	57°45.80'	151°08.05'	70		Shell fragments, with lithics, shards, s mod. sorted, g/s/sl-c/shells=1-16-tr-83
76 S	1	58°06.20'	151°46.10'	95		S, dark green, shell fragments, well sorted, shards, s 98% shells 2%
77 S	1	58°11.60'	151°37.00'	38		Shelly cobbles, some forams, shell hash, g/s/sl/shells=90-3-6-1
78 S	2	58°11.41'	151°37.15'	70		Totally brittle stars; some, very little, shell hash.
79 S	1	58°12.23'	151°38.07'	-		Brittle stars, shelly pebbles, lithic are rounded, few shards, g/s/sl-c/shells=36-6-tr-58
80 S	1	58°01.50'	151°21.90'	81		Pebbly shelly s, forams, shards, s vcs-cs/ms/fs/vfs=2-1-92-5 dark, rounded
81	1	58°05.21'	151°14.55'	143		Sandy mud, green, rich in ash, ms/fs/vfs=tr-56-45, s/sl/c/shells=88-10-tr-2
	3	58°05.21'	151°14.55'	145		No recovery
82 S	1	58°03.60'	151°15.90'	103		Sandy g, shards, lithics are sub-angular to rounded, g/s/sl/c/shells=50-29-1-tr-20
83 G	1	56°53.73'	151°29.84'	706/150		Coarse pebbly s with shells and mud.
84 G	1	56°55.06'	151°24.58'	859/175		Grey mud, some grit, strong H <sub>2</sub> S odor
85 S	1	57°45.00'	151°44.00'	55		Sandy shell hash, shards, forams; lithics are rounded to sub-rounded g/s/sl/c/shells=1-3-tr-96
86 S	1	57°41.48'	151°34.70'	61		Shelly s, shards and forams; vcs/cs/ms/fs/vfs=1-1-2-90-6; g/s/sl-c/shells=1-66-tr-33
87 S	1	57°36.50'	151°47.65'	132		Ash s 99%, very well sorted 98% fs. s/sl-c=99-1
87 G	2	57°36.50'	151°47.65'	137		No recovery
88 S	1	57°31.20'	151°38.00'	167		Ash s 76%, well sorted=fs-vfs=100%. s/sl/c/shells=76-23-tr-1
88 G	2	57°31.20'	151°38.00'	145		No recovery
89 S	1	57°28.50'	151°44.50'	70		Conglomerate, with shards, lithics sub-angular to sub-rounded, c-g/s/sl-c/shells=88-8-tr-4
90 S	1	57°25.10'	151°51.90'	67		Sandy, shell hash, ms=75% of s, lithics are rounded to sub-rounded, s/sl-c/shells=2-tr-98

Table 4. cont.

Sample No.	No. of attempts	Latitude	Longitude	Water Depth m/length cm	/Core	Lithology, color and additional remarks
91 S	1	57°19.29'	152°04.82'	73		S 99% with shell has, well sorted vfs; sub-rounded. s/shell=99-1
92 S	2	56°56.50'	152°33.00'	167		Silty c, olive-green color, H <sub>2</sub> S odor, vfs. s/sl/c=1-3-96
93 S	1	56°53.45'	152°40.90'	128		Silty s, vfs, shards present, olive-grey color. s/sl/c=90-8-2
94 S	1	56°48.15'	152°52.60'	63		Shelly s, shards, olive-grey color; well sorted fs. g/s/sl-c/shells= 49-36-tr-15
95 S	1	56°48.10'	153°21.35'	160		Conglomerate; shards; rounded to angular cobbles; g/s/sl-c/shells= 90-10-tr-tr
96 S	1	56°41.46'	153°05.90'	146		Sandy mud, well sorted; shards, s-vfs. s/sl/c=5-35-60
97 S	1	56°40.10'	153°10.02'	150		Sandy mud, well sorted round to sub-rounded. s/sl/c=4-26-70
97 G	1	56°39.90'	153°11.10'	138/100		Mud, greyish-olive, very little shell fragments
98 S	1	56°38.00'	153°16.00'	145		Silty, sandy mud, well sorted, well rounded, shards s/sc/c=3-20-77
98 G	1	56°37.80'	153°16.30'	144		Sandy mud, little recovery
99 D	2	56°24.50'	152°53.70'	55/20		Siltstone, olive grey
100 D	1	56°24.00'	152°53.50'	50/17		Siltstone, olive-grey
101 D	1	56°23.20'	152°54.10'	49/9		Sandstone, very fine grained, medium dark-grey color, silty.
102 D	1	56°23.10'	152°53.90'	45/16		Siltstone, olive-grey
103 D	1	56°22.70'	152°52.00'	50/17		Sandstone, very fine grained, silty, olive-grey
104 D	1	56°22.00'	152°50.90'	75/16		Sandstone, very fine grained, silty, olive-grey
105 S	1	56°19.04'	152°46.50'	178		No recovery
106 D	2	56°29.60'	152°43.70'	60/1		Silt, very small recovery olive-grey color
107 D	1	56°30.15'	152°44.10'	56/30		Siltstone, dark-grey
108 D	2	56°30.30'	152°44.90'	56/25		Siltstone, dark-grey
109 D	2	56°30.80'	152°46.20'	58		No recovery
110 D	1	56°31.40'	152°46.70'	64/47		Silt, medium dark-grey
111 D	1	56°31.70'	152°47.50'	65/48		Sandy silt, olive-grey
112 D	2	56°32.00'	152°48.20'	70/22		Shell hash, pale-olive color forams cs/ms/fs/vfs=2-11-85-2; s/sl/c/shells=18-1-1-80
113 S	1	56°33.50'	152°27.20'	197		Pebbly s, color 5Y 3/2; shards; p/g/s/sl/c/shells=5-3-89-2-tr-tr
114 S	1	56°37.60'	152°34.00'	160		Sandy g, g are sub-angular to sub-rounded, forams, p/s/sl/c=40-55-2-
115 S	2	56°57.02'	152°06.28'	80		S, 5Y 4/4, sub-angular to rounded; shards, lithics; s/sl/c/shells= 91-tr-tr-9

Table 4. cont.

Sample No.	No. of attempts	Latitude	Longitude	Water Depth m/length cm	/Core	Lithology, color and additional remarks
116 D	2	57°12.00'	151°51.10'	74/39		Sandy siltstone; medium dark grey, some pebbles
117 D	1	57°10.09'	151°50.70'	54/14		Sandy siltstone, dark-grey, with pebbles
118 D	1	57°11.00'	151°50.00'	54/20		Sandy siltstone, dark-grey
119 D	1	57°10.60'	151°49.10'	56/40		Coarse s, light olive-grey, shelly and pebbly
120 D	1	57°10.00'	151°48.40'	60/20		Sandy siltstone, dark-grey
121 D	2	57°09.25'	151°47.50'	70		Sandy siltstone, dark-grey
122 D	2	57°09.00'	151°46.90'	74		No recovery
123 D	2	57°08.75'	151°46.30'	76/34		Sandy siltstone, dark-grey
124 D	1	57°08.50'	151°45.60'	78/20		Fs, medium dark-grey
125 D	1	57°08.00'	151°45.00'	80/20		Fs ash, with dark sandy silt; well sorted s/sl/c=90-10-tr
126 D	2	57°07.40'	151°44.10'	80		No recovery
127 S	1	57°11.24'	151°29.59'	69		Pebbly s, shards, lithics-sub-angular to sub-rounded, vcs/cs/ms/fs/vfs=5-10-35-45-10 p/s/sl-c/shells=15-67-tr-28
128 S	1	58°31.47'	149°21.90'	121		Muddy s, with pebbles; shells and forams, shards, p/s/sl/c/shells=2-30-4-2-62
129 S	1	58°35.85'	149°14.91'	95		Pebbly s; shards, lithics sub-rounded to rounded. p/s/sl-c/shells=70-8-tr-22
130 S	1	58°42.23	149°03.38	145		S 98%, well sorted, sub-angular, few shards; cs/ms/fs/vfs=1-2-90-7, some c.
131 S	1	58°44.99'	148°58.18'	214		Silty s, sub-angular, lithics; shards; cs/ms/fs/vfs=1-4-85-10; p/s/sl/c/shells=3-76-15-5-1
132 S	1	58°49.24'	148°54.71'	236		Pebbly-silty s; shards sub-angular to sub-rounded; cs/ms/fs/vfs=5-25-65-5; p/s/sl/c/shells=10-80-44-2
133 G	1	58°54.41'	149°01.95	250/95		Sandy c, vfs; grey-green mud; s/sl/c=10-10-80
134 S	1	58°49.39'	149°14.22'	206		Pebbly s, boulders meta conglomerate and quartzite ss, mud green; p/s/sl/c/shells=11-73-6-8-2
135 S	1	58°40.39'	149°31.82'	136		S 93%; well sorted fs; sub-angular to sub-rounded; forams; s/sl/c/shells=93-2-4-1
136 S	1	58°34.90'	149°45.19'	125		S 97%, fs slightly green in color; coarser s towards bottom; sub-rounded; s/sl/c/shells=97-2-1-tr
137 S	1	58°29.46'	150°05.25'	93		Pebbly s; abundant forams; shards-bimodal sorting (due to washing?) sf; p/s/sl/c/shells=30-49-81-12

Table 4. cont.

Sample No.	No. of attempts	Latitude	Longitude	Water Depth m	/Core length cm	Lithology, color and additional remarks
138 S	1	58°22.07'	150°24.07'	60		Sandy g; shell hash on top; g/s/sl/c=70-29-1-tr; shell hash removed
139 S	2	58°15.96'	150°15.30'	54		Shell incrustment on foot of one large sponge-no sample analyzed
140 S	1	58°22.20'	149°54.26'	83		Sandy pebbles; rounded to sub-rounded; p/s/sl/c/shells=70-8-tr-tr-22
141 S	1	58°13.12'	149°11.85'	120		Pebbly s w/forams abundant; well rounded pebble; shards; p/s/sl/c shells=20-13-2-tr-65
142 D	2	58°08.70'	149°04.70'	114/0		Smear recovery; pipe well dented; only noted a foram bearing c
143 D	1	58°08.00'	149°03.80'	104/0		Smear recovery; sandy silt; only enough to make smear slide; olive grey
144 D	1	58°05.92'	149°01.44'	88/23		Conglomerate; Top-olive grey foram bearing silty cs; Base-dark grey sandy siltstone; p/s/sl/c/shells=44-37-2-7-10
145 D	1	58°06.59'	149°02.46'	90/10		Coarse s dark-grey to olive-grey; pebbly w/forams; g/s/sl/c/shells= 15-54-4-2-25
146 D	1	58°05.99'	149°01.25'	88		No recovery
147 D	2	58°05.60'	148°01.00'	88/12		Silty s; dark to olive grey; abundant pebbles; forams; fine sands; p/s/sl/c/shells=57-37-1-tr-5
148 D	1	58°04.96'	148°59.95	90/8		Sandy pebbles; dark to olive grey; siltstone; forams; shards; lithics; p/s/sl/c/shells=51-21-tr-tr-28
149 D	2	58°04.60'	148°59.50'	98/0		Sandy silt; enough for smear only. dark grey
150 S	1	59°04.55'	152°49.50'	147		Muddy s 98%; well sorted fs; sub-angular forams; s/sl/c/shells= 98-1-tr-1
151 S	1	59°11.90'	152°09.50'	112		No recovery
152 S	1	59°37.21	152°29.08'	70		S 99%; medium s well sorted; w/pebbles and shells=1% sub-angular; lithics rounded; vcs/cs/ms/fs/vf=tr-8-92-tr-tr
153 S	2	59°10.70'	152°31.55'	99		S 99% w/forams; well sorted fs; sub-angular to angular; s/sl-c/shells= 99-tr-tr-1
154 S	1	59°09.25'	153°05.63'	75		Muddy s 98%; fs, well sorted; sub-angular to sub-rounded; shards; s/sl/c/shells=98-tr-1

QUARTERLY REPORT

Contract:

Research Unit: No. 352

Reporting Period: July 1, 1976-Sept. 30, 1976

Number of pages: 1

SEISMICITY OF THE BEAUFORT SEA, BERING SEA AND GULF OF ALASKA

Herbert Meyers  
Solid Earth Data Services Division D62  
National Geophysical and Solar-Terrestrial  
Data Center  
EDS/NOAA  
Boulder, Colorado

September 30, 1976

- I. Task Objectives. To prepare a seismic history for Alaska in a manner which will permit independent assessment of risk for any specific region of interest.
- II. Field or Laboratory Activities.
  - A. Ship or Field trip schedule.  
None
  - B. Scientific Party.  
Work is being performed by various members of NGSDC under the direction of Herbert Meyers.
  - C. Methods.  
Data being used are those in the files of NGSDC, supplemented by appropriate data from other sources.
  - D. Sample localities/ship or aircraft tracklines.  
All available epicenter and felt information for Alaska and adjacent regions.
  - E. Data collected or analyzed.  
Approximately 10,000 epicenter determinations and 4,000 felt reports have been summarized.
- III. Results.  
Thus far, two publications in support of the OSCEAP Alaska project have been printed and distributed. The publications are:  
*A Historical Summary of Earthquake Epicenters In and Near Alaska*  
*Catalog of Tsunamis in Alaska*  
A third publication, *An Analysis of Earthquake Intensities and Recurrence Rates In and Near Alaska*, will be printed within a month. A copy of the table of contents is attached.
- IV. Preliminary interpretation of results.  
The data are presented in a fashion which will readily permit assessments of recurrence frequency of various types earthquakes and relative risks for areas of interest.
- V. Problems encountered/recommended changes.  
None
- VI. Estimate of funds expended.  
Approximately 100% of the \$32K available for this project has been spent.

## CONTENTS

	Page
INTRODUCTION . . . . .	
DESCRIPTION OF INTENSITY FILE . . . . .	
<i>Development of Earthquake Intensity Scales</i> . . . . .	
<i>Modified Mercalli Intensity Scale of 1931 (Abridged)</i> . . . . .	
<i>Collecting Intensity Data</i> . . . . .	
DATA SOURCES . . . . .	
<i>United States Earthquakes</i> . . . . .	
<i>Earthquake History of the United States</i> . . . . .	
<i>Other Sources</i> . . . . .	
EARTHQUAKES INTENSITIES IN ALASKA . . . . .	
FREQUENCY OF INTENSITY REPORTS FROM ALASKA LOCALITIES . . . . .	
INTENSITY VERSUS MAGNITUDE . . . . .	
MAXIMUM EARTHQUAKE INTENSITIES IN ALASKA USING A MAGNITUDE-	
MAXIMUM INTENSITY CONVERSION . . . . .	
MAGNITUDE-FREQUENCY RELATIONSHIPS . . . . .	
STRONG-MOTION STUDIES . . . . .	
DATA FORMATS . . . . .	
<i>Alaska Intensity File Tape Format</i> . . . . .	
ACKNOWLEDGMENTS . . . . .	
BIBLIOGRAPHY . . . . .	

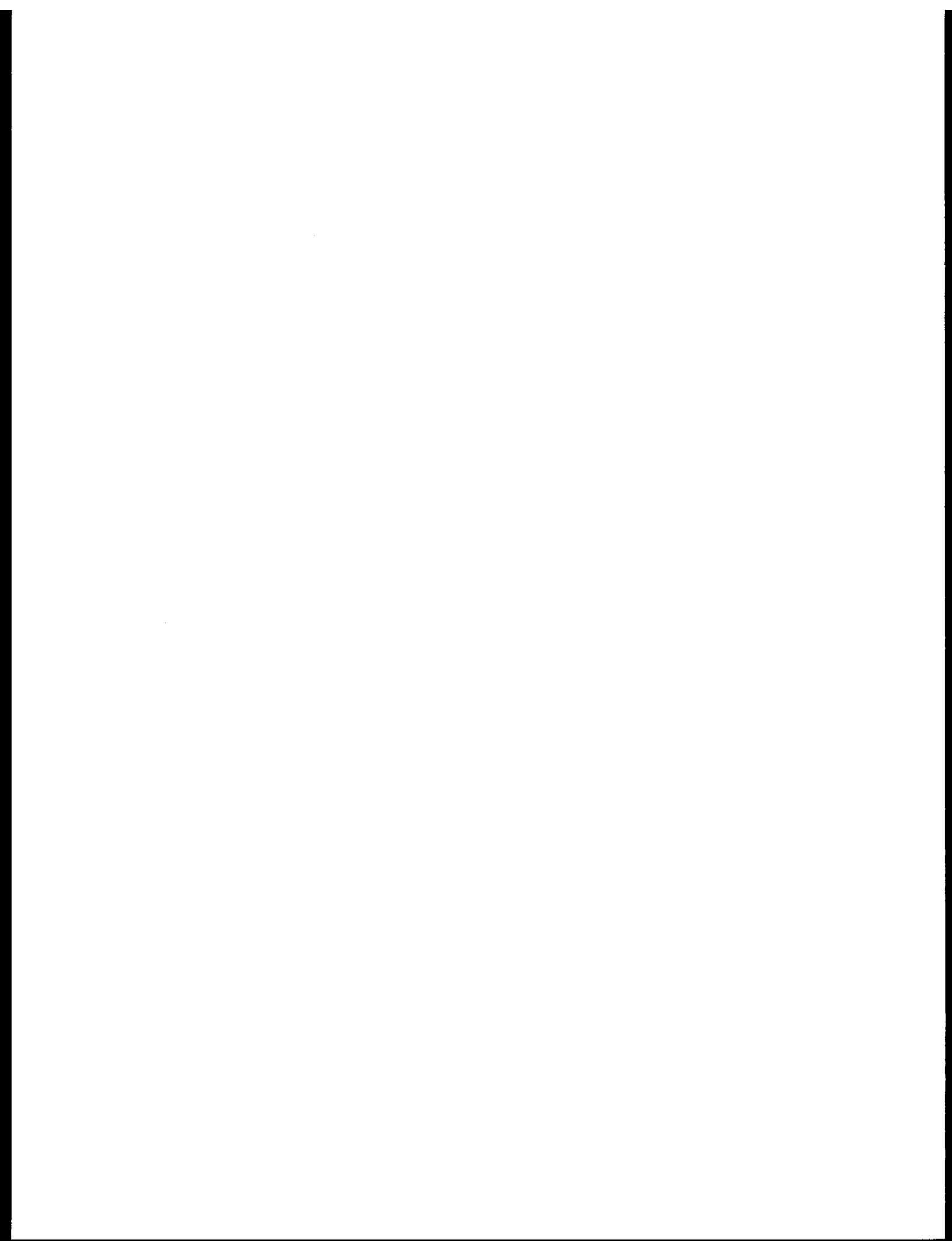
## TABLES

**Table**

1	Modified Mercalli intensities reported for earthquakes in Alaska, 1786-1974 . . . . .	
2	Frequency of reported earthquake intensities (Modified Mercalli Scale) for cities in Alaska, 1786-1974 (by latitude) . . . . .	
3	Magnitude-distance relationship for each intensity ( <i>I</i> ) for Alaska . . . . .	
4	Recurrence rate of earthquakes in Alaska by magnitude and geographic coordinates . . . . .	
5	Magnitude recurrence curve ( $\log N = \alpha - bM$ ) for localities listed in table 4. . . . .	
6	Summary of significant accelerograph records in Alaska, 1964-1975. . . . .	
	Alphabetical list of earthquake felt reports for Alaska (sorted by intensity and date within city) . . . . .	microfiche in pocket
	Chronological list of earthquake felt reports for Alaska (sorted by intensity and city within date) . . . . .	microfiche in pocket

## FIGURES

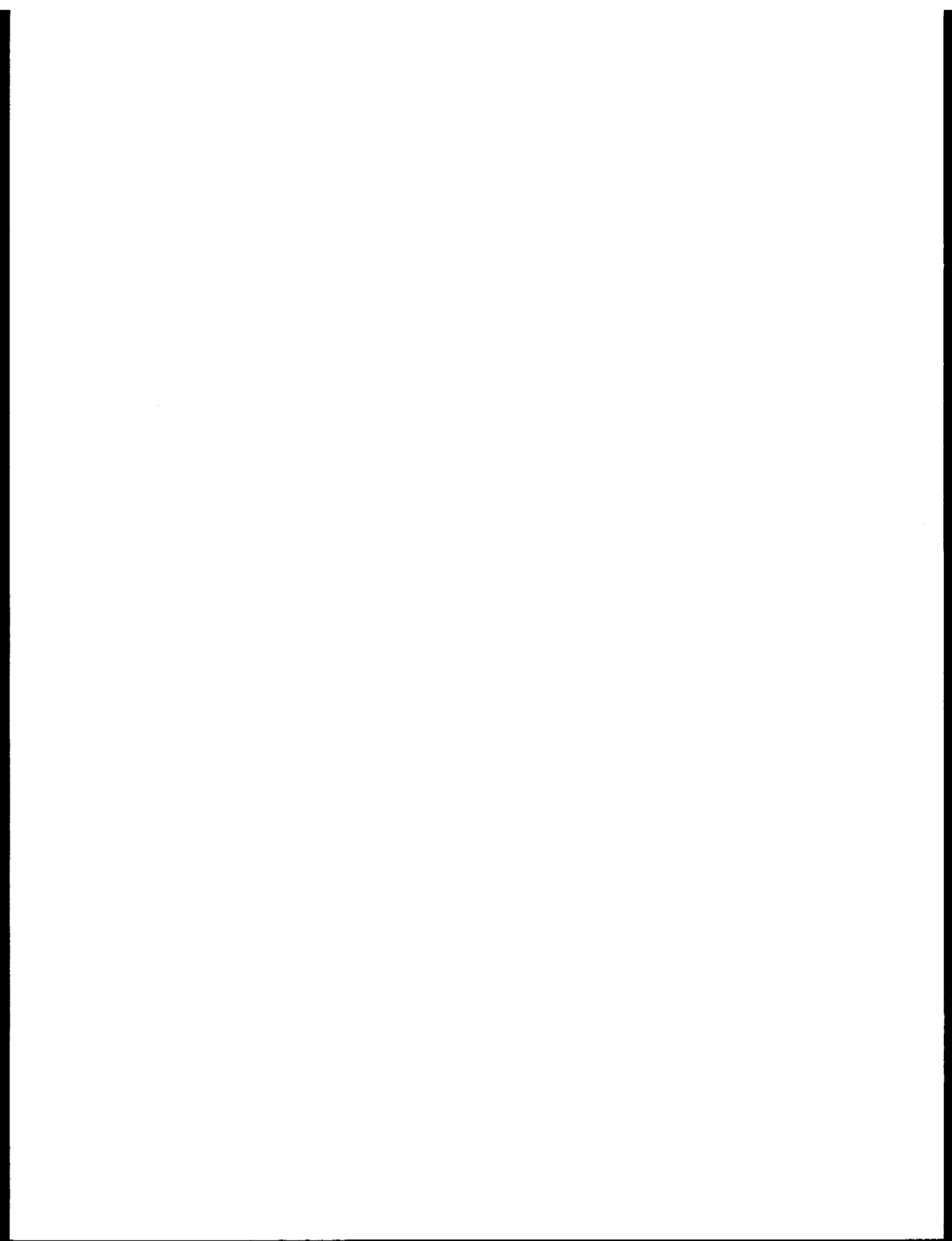
Figure		Page
1	Plot of maximum intensities reported in Alaska, 1786-1974 . . . . .	
2	Earthquake Report . . . . .	
3	Isoseismal map for Alaska earthquake of Mar. 27, 1964 . . . . .	
4	Isoseismal map for Alaska earthquake of June 21, 1967 . . . . .	
5	Isoseismal map for Alaska earthquake of Apr. 7, 1958 . . . . .	
6	Isoseismal map for Alaska earthquake of Oct. 29, 1968 . . . . .	
7a	Projected maximum intensities (Modified Mercalli Scale) of earthquakes in and near Alaska, 1786-1974 . . . . .	
7b	Projected maximum intensity contours in and near Alaska, 1786-1974, with actual reported intensities superposed . . . . .	
8	Graphical equivalence between magnitude and maximum intensity .	
9	Distance versus maximum intensity for Western United States . .	
10	Alaskan area included in table 4. . . . .	
11	Cumulative magnitude frequency relationships for 75-km radius of 54°N, 166°W. . . . .	
12	Cumulative magnitude frequency relationships for 75-km radius of 55°N, 160°W. . . . .	
13	Cumulative magnitude frequency relationships for 75-km radius of 57°N, 153°W. . . . .	
14	Cumulative magnitude frequency relationships for 75-km radius of 57°N, 158°W. . . . .	
15	Cumulative magnitude frequency relationships for 75-km radius of 60°N, 144°W. . . . .	
16	Cumulative magnitude frequency relationships for 75-km radius of 60°N, 150°W. . . . .	
17	Cumulative magnitude frequency relationships for 75-km radius of 61°N, 147°W. . . . .	
18	Cumulative magnitude frequency relationships for 75-km radius of 62°N, 150°W. . . . .	
19	Sample geographic search of Alaska Intensity File . . . . .	



RU# 407

NO REPORT WAS RECEIVED

A final report is expected next quarter



Quarterly Report

Contract #  
Research Unit # 43,  
April 1 - September 30, 1976  
Three Pages

Coastal Processes and Morphology of  
the Eastern Bering Sea

Asbury H. Sallenger, Jr.  
John R. Dingler  
Ralph E. Hunter

U.S. Geological Survey  
Menlo Park, CA 94025

September 30, 1976

## I. OBJECTIVES

- A. Categorization of coastal morphology and regional sediment characteristics of the northeast Bering Sea (Yukon River to Bering Strait).
- B. Categorization of coastal morphology and regional sediment characteristics of the northern coast of the Alaska Peninsula (Kvichak Bay to Unimak Island).
- C. Monitoring sediment-level variations on the beach and in the nearshore at selected locations in the northeast Bering Sea.
- D. Measurement of storm surge elevations of the November 11-12, 1974 storm utilizing indirect evidence around the coast of the northeast Bering Sea.

## II. FIELD ACTIVITIES

### A. Field Trip Schedule

- 1. June 21-28 (Bell 206B helicopter, chartered from Anchorage Helicopter Service, Anchorage, AK); coastal morphology, sediment characteristics and storm surge elevations of the northeast Bering Sea.
- 2. June 29-July 11; nearshore and beach surveying at selected sites in the northeast Bering Sea.
- 3. September 5-12 (Sikorsky 55T helicopter, chartered (NOAA) from ERA Helicopters, Anchorage, AK); coastal morphology and sediment characteristics of the northern coast of Alaska Peninsula.
- 4. September 13-25; resurvey of nearshore and beach profile locations in northeast Bering Sea.

### B. Scientific Party

- 1. Asbury H. Sallenger; U.S.G.S.; oceanographer.  
Ralph Hunter; U.S.G.S.; geologist.  
Harold Gibson; U.S.G.S.; physical science technician.
- 2. Asbury H. Sallenger; U.S.G.S.; oceanographer.  
Ralph Hunter; U.S.G.S.; geologist.  
Harold Gibson; U.S.G.S.; physical science technician.  
Herbert Pierce; U.S.G.S.; physical science technician.  
David M. Drucker; U.S.G.S.; physical science technician.
- 3. Asbury H. Sallenger; U.S.G.S.; oceanographer.  
Ralph Hunter; U.S.G.S.; geologist.  
John Dingler; U.S.G.S.; oceanographer.  
John McKinnan; N.O.A.A.; biologist.

4. Asbury H. Sallenger; U.S.G.S.; oceanographer.  
John Dingler, U.S.G.S.; oceanographer.  
Michael Field; U.S.G.S.; geologist.  
Harold Gibson; U.S.G.S.; physical science technician.  
Herbert Pierce, U.S.G.S.; physical science technician.  
David M. Drucker; U.S.G.S.; physical science technician.

C. Methods

1. Onshore profiles were measured with precision surveying equipment. Permanent profile markers were left at each profile location. At selected sites the profiles were extended into the nearshore utilizing a precision fathometer mounted in a 19 ft. inflatable boat powered by twin 40 h.p. engines. Offshore navigation was accomplished by measuring, with a sextant, angles on survey markers located on the beach.
2. Sediment samples of the beach were collected at each profile site to be analyzed for their size characteristics.
3. The elevations of debris lines representing storm surge heights were measured with precision surveying equipment.

D. Sample Localities and Data Collected

1. Forty-five onshore profiles were measured along the coast of the northeast Bering Sea. These averaged approximately 20 km apart beginning near Bering Strait and extending as far as Pastol Bay on the Yukon Delta. Sediment samples were obtained at each of these sites.
2. Fifteen of the profiles were extended into the nearshore during the July trip. Five of these profiles were located in the vicinity of Nome, four in the vicinity of Unalakleet and six near Port Clarence. Each of these profiles was remonitored in September and three additional profiles were added in the Nome area, one in the vicinity of Unalakleet and two in Port Clarence.
3. Forty-two onshore profiles were measured along the Bristol Bay coast of the Alaska Peninsula. These were spaced approximately 15 km apart from north of the Naknek River to Urillia Bay on Unimak Island. Sediment samples were obtained at each site.

Page Three.

III. RESULTS

We have gathered adequate field data and samples to meet our objectives as specified in the proposal. Results will be reported in detail after necessary laboratory and computational analyses are completed. These results will be included in the annual report.

IV. ESTIMATE OF FUNDS EXPENDED

\$65,000.

RU # 432  
Arthur Grantz - P.I.  
Quarterly Report  
October 1, 1976 - 6th Qtr.

Quarterly Report

Contract No. U4 32-76  
Research Unit: 432  
Reporting period: Fifth Quarter  
Number of pages: 4

Seismic and Tectonic Hazards in the  
Hope Basin and Beaufort Shelf

Arthur Grantz, Stephen Eittreim and Gary Boucher  
Pacific-Arctic Branch of Marine Geology  
U.S. Geological Survey, Menlo Park, CA 94025

October, 1976

## I. TASK OBJECTIVES

Data existing prior to 1976 suggest that certain areas in the southern Chukchi Shelf and the Beaufort Shelf may be subject to active faulting and earthquake hazards. To further investigate these possibilities, new data in the form of high resolution acoustic reflection profiles, seismicity using ocean bottom seismographs, and sediment and rock sampling will be taken in these areas and analysed to assess the presence or absence of such hazards.

## II. FIELD OR LABORATORY ACTIVITIES

### Shipboard work:

The U.S.G.S. Research Vessel S.P. LEE left Nome August 27, completed 4 days work in Hope Basin (southern Chukchi Sea) and returned to Nome on September 2. Three weeks work was originally planned, but due to failure of one of the main engines, an early return to Nome was necessitated.

The U.S. Coast Guard icebreaker GLACIER left Barrow on September 6 and returned October 2 after 23 days work along the central to northern Beaufort and Chukchi Shelves and 3 days work in the southern Chukchi Shelf (Hope Basin).

### Scientific Party:

#### S.P. LEE

A. Grantz, U.S.G.S., Chief Scientist  
G. Boucher, U.S.G.S., Marine Geophysicist  
S. Eittreim, U.S.G.S., Marine Geologist  
T. Whitney, U.S.G.S., General  
T. Kelley, U.S.G.S., Electronic Technician  
J. Edwards, U.S.G.S., Airgun Technician  
P. Twitchell, U.S.G.S., Airgun Technician  
A. Montez, Seismic Engineering Inc., Streamer Technician  
T. Thornton, U.S.G.S., Electronic Technician  
C. Carpenter, U.S.G.S., Data Curator  
B. Ruppel, U.S.G.S., Gravity and Navigation  
S. Davenport, U.C., Santa Cruz, General  
A. Long, U.S.G.S., Marine Seismologist  
D. Aldridge, U.S.G.S., Marine Seismologist  
K. Bachman, U. of Washington, General  
J. Krogstad, U. of Washington, General  
C. Carlson, U.C., Santa Cruz, General

#### GLACIER

A. Grantz, U.S.G.S., Chief Scientist  
G. Boucher, U.S.G.S., Marine Geophysicist  
S. Eittreim, U.S.G.S., Marine Geologist  
T. Whitney, U.S.G.S., Navigation  
S. Davenport, U.C., Santa Cruz, Navigation  
J. Nicholsen, U.S.G.S., Electronic Technician

M. Rappeport, U.S.G.S., Sedimentologist  
J. Rupert, U.S.G.S., Sedimentologist  
R. Arnal, U.S.G.S., Micropaleontologist  
W. Snydsman, U. of Washington, Heat Flow

Methods:

Acoustic reflection: Uniboom; 3.5 khz; 12 khz ; 12 KJ and 160 KJ single channel seismic reflection (sparker).  
4 Ocean bottom seismographs.

Sampling methods: dart and gravity cores and Van Veen surface sediment sampler; rectangular dredge.

Navigation on both ships was by satellite; on LEE, integrated with continuous doppler sonar.

Location of data:

Having just returned (October 5), charts of navigation are not yet available in a format suitable for copying. General locations of interest are indicated in "Results" section below.

Data collected:

1. 49 dart cores, 11 gravity cores, 25 dredge hauls, and 20 Van Veen samples were collected from GLACIER. 2 days of continuous recording with 3 ocean bottom seismographs were accomplished from LEE.

2. Approximately 800 miles of trackline were made on LEE with 3.5 khz sounding data, 500 miles with uniboom and 500 miles with single channel seismic reflection. Approximately 2500 miles of trackline were made on GLACIER with 12 khz precision depth recorder and 150 miles with single channel seismic reflection. All mileages are approximate pending finalized navigation. It should be pointed out that <sup>not</sup> all of these data were collected solely under the auspices of NOAA but rather were part of an ongoing U.S.G.S. program of geologic assessment of the Beaufort/Chukchi Shelves, partly funded by NOAA/OCSEAP. Roughly 25% of the work was aimed specifically at NOAA/OCSEAP objectives, although this segregation is somewhat artificial or arbitrary.

III. RESULTS

Since we have only recently returned from the field (October 5), only very preliminary results can be stated here, i.e., those arrived at from our on-board analysis of the data.

On the basis of the uniboom survey by LEE over the Kotzebue Ridge in Hope Basin, the myriad of faults that displace the pre-Holocene sediments over this ridge do not penetrate the approximately 10 m thick Holocene sediment cover. Thus these faults appear to be inactive at present. Neither were any seabed scarps encountered using the 12 khz records obtained in this area on GLACIER. The four OBS units were successfully deployed in Hope Basin on LEE with a minimum of difficulties, each deployment taking from 30 minutes to two hours to complete. Thus the operation

appears to be compatible with the maneuvering capabilities of a typical 200 ft. research vessel. Three out of the four units were recovered successfully. The fourth was lost due to failure of the hauling line. Based on spot-playbacks of the magnetic tapes, all three recovered OBS units appear to have operated satisfactorily.

South of Point Hope in the southern Chukchi Sea a buried base-ment escarpment was surveyed with single channel seismic reflection to better determine its trend and thus its tectonic significance. In the course of the surveying in the region, several scarps appearing to be active fault scarps were observed with the 12 khz precision depth recorder. Further analysis of these data and past year's data in this region is necessary before more definite conclusions can be reached about the tectonic significance of these scarps.

North of Barrow numerous crossings of the Barrow Sea Valley were made using the 12 khz precision depth recorder. These records will be used for a rather detailed morphologic description of this feature.

IV. Preliminary interpretation of results. Not applicable at this time.

V. Problems encountered:

1. One of the two main engines on LEE became inoperable and forced curtailment of the latter 80% of the planned cruise in the Chukchi and Beaufort Seas.
2. Ice conditions were bad in the early part of our GLACIER operations in the Beaufort Sea, a time during which we had anticipated the best conditions. Thus the eastern Beaufort Sea could not be reached for the planned ocean bottom seismograph deployments and studies planned for the shelf edge and slope in the Beaufort Sea were only partially carried out.
3. Sampling attempts from GLACIER were largely futile as we were unable, except perhaps in a few cases, to penetrate the thin Holocene sediment cover due partly to inadequate winch lowering speed and partly to reduced ship maneuverability because of the ice.

VI. Estimate of funds expended: all funds expended.

Research Unit 473: Quarterly report, July-August-September, 1976

SHORELINE HISTORY OF CHUKCHI SEA AS AN AID TO PREDICTING OFFSHORE PERMA-FROST CONDITIONS

I. Task objectives: D-9

II. Field and laboratory activities

A. Field trip schedule

North coast of Chukchi Sea (Point Lay to Point Barrow), July 1-30.

Kotzebue Sound and south coast of Chukchi Sea (Arctic Circle to  
Cape Thompson), July 31-Aug. 6.

Logistic support by NARL aircraft (July 1-30) and privately  
chartered aircraft (July 31-Aug. 6).

B. Scientific party:

D. M. Hopkins, geologist

Kristin McDougall, micropaleontologist

R. E. Nelson, palynologist

R. W. Hartz, field assistant

C. Methods:

Study morphology of offshore bars and mainland coast in order to determine frequency of storm wash-overs and rate and direction of shoreline change. Collect samples of Holocene tide-marsh peat in order to establish local rates of shoreline change or, conversely, local long-term stability. Survey barrier bars and mainland coast for coast-oriented archaeological sites as a means of recognizing areas of long-term coastal stability. Collect marine mollusks from beach drift and from lagoons in order to establish nature

of lagoon and open-water faunas as an aid to interpreting faunas from drill cores and in order to augment inadequate knowledge of present-day ranges of mollusks in Bering Sea.

Identify major sources of sediment and nature of sediment contributed in order to predict granulometry of sub-sea sediments.

Identify areas of ice-rich permafrost in coastal bluffs because these are areas where ice-rich permafrost is most likely to persist offshore.

D. Field sampling:

Field observations were made at approximately 200 localities, and samples were collected in most of these places. Samples collected include 56 samples of modern and fossil mollusks, 43 samples for marine microfossil analysis, 11 samples for pollen analysis, 18 archaeological collections, 39 samples for radiocarbon dating, and 7 pebble collections brought back to identify sources of sediment.

E. Data collected or analyzed:

Analysis of data is in initial stages and will be summarized on next Quarterly Report.

F. No change in Milestone chart.

III. Results

A. Data analysis is too incomplete for an extended discussion of results. The following are impressionistic statements that are subject to some revision as data analysis progresses:

(1) the morphology and archaeology of barrier-bar complexes

around Kotzebue Sound and northern Seward Peninsula provide a record of coastal progradation in many places, but the morphology and archaeology of barrier-bar complexes northward from Cape Krusenstern is suggestive of slow, steady, coastal retreat. Northward from Icy Cape, the mainland bluffs at the inland shores of the lagoons appear to be retreating at approximately the same pace as the barrier bars that confine them. Nevertheless, no part of the Chukchi Sea coast displays evidence of coastal retreat as rapid as that seen in many places along the coast of Beaufort Sea.

- (2) Major erosion of barrier bars and coastal bluffs along the coast of Chukchi Sea occurs chiefly during late summer and autumn storm surges. I have observed cliff retreat amounting to several meters along the coasts of Kotzebue Sound during the storm surges of 1961, 1969, 1975 and 1976. Driftwood lines and evidence of recent erosion indicates that a severe storm affected the coast between Icy Cape and Peard Bay in 1975. The 1975 storm surge was among the most intense surges in the past century; in many places, there is no driftwood line higher than that left by the 1975 storm surge.
- (3) A method was devised for measuring exceptional cliff-retreat in low bluffs in ice-rich sediments. The method is based upon recognition of active thermokarst collapses in the beach. Cliff retreat during the 1975 storm surge amounted to 5 to 10 meters in many places.

- (4) Despite the widespread evidence for slow, steady coastal retreat, a limit on the net retreat is set by coast-oriented archaeological sites, preserved near Kivalina (newly discovered), Point Hope, Icy Cape (newly discovered), Walakpa Bay, and the Navy Arctic Research Laboratory. In these places, total cliff retreat has amounted to no more than a few tens of meters in the last 2,000 years. The morphology of the intervening coast is such that total retreat can hardly have been more than a few hundred meters. Thus, rates of coastal retreat along the Chukchi Sea coast seem to be much lower than those observed along the Beaufort Sea coast.
- (5) Kotzebue Sound waters are warm, due to the influx of fresh water from several large rivers. Warm Bering Sea water in the Alaskan Current flows northward along the coast from Cape Krusenstern to Point Hope. Water temperatures are colder but still evidently above 0°C along the open coast from Point Hope north to Barrow. Sub-zero bottom temperatures probably occur in some lagoons north of Cape Lisburne, however.
- (6) Kotzebue Sound bottom sediments have been established by earlier research as consisting of fine muds introduced from the Noatak and Kobuk Rivers. Bottom sediments in the near-shore zone from Cape Krusenstern to Point Hope are fine sand and coarser sediments. From Icy Cape northward, the character of the sub-bottom sediments is mainly determined by the character of the coastal bluffs. Thick clays can be expected northward from Peard Bay and sandier sediments to the south.

(7) Several mollusk species range much further northward than was previously recognized. Macoma balthica, a small clam confined to brackish water and not previously reported north of Kotzebue Sound, lives in lagoons at least as far north as Peard Bay. Siliqua patula, the razor clam, previously thought to reach its northern limit at Bering Strait, is common at least as far north as Peard Bay. Pododesmus macroschisma, the rock oyster, is rare but present as far north as Point Franklin; the previous northern record (also mine) was in deep water along the north coast of St. Lawrence Island. Single individuals of Zyrphaea cristata, a boring clam previously unreported north of central Bering Sea, was collected on the beach at Point Franklin, and in several other places from Icy Cape northward.

#### IV. Preliminary interpretation of results:

Photo-interpretation has identified a few areas around Kotzebue Sound where ice-wedges are evidently thawing and collapsing beneath near-shore waters. This indicates that relict ice-rich permafrost is present but rapidly thawing in the few places where the coast is retreating rapidly. The warm bottom temperatures of Kotzebue Sound make it unlikely that offshore permafrost will be found at distances greater than one hundred meters from the beach.

Offshore permafrost is unlikely to be found along the low-lying, slowly retreating coast between Cape Krusenstern and Point Hope.

The coastal segment from Point Hope to the south end of Kasegeluk Lagoon has not yet been studied and cannot yet be discussed.

Offshore permafrost may be present in a nearshore zone a few hundred meters wide along the outer coast from Point Lay to Point Barrow.

Sub-bottom permafrost is likely to be found beneath parts of Kasegeluk Lagoon, Wainwright Inlet, and Peard Bay.

V. Problems encountered and recommended changes: None.

VI. Estimate of funds expended: \$20,000.

## FIRST QUARTERLY REPORT

PERIOD: July 1, 1976 - September 1, 1976

TITLE: Evaluation of earthquake activity around Norton and Kotzebue Sounds

PRINCIPAL INVESTIGATORS: N.N. Biswas and L. Gedney, Geophysical Institute, University of Alaska

I. TASK OBJECTIVE: To install a short-period seismic network to provide seismic coverage of the study area.

II. FIELD AND LABORATORY ACTIVITIES

A. STATION INSTALLATION: All the stations of the network excepting Savoonga on St. Lawrence Island have been installed. The distribution of the stations is shown in Figure 2 and the details are given in Table 1. The electronic package for stations KTX, TNC, ANV and NRI have been located in instrument racks in the White Alice microwave instrument buildings.

In order to minimize local cultural noise, seismometers at the sites have been located about 1/4 mile from the buildings and connected to the electronic packages by spiral-4 cable. For station REM (remote), the seismometer and the rest of the equipment could be placed close to each other as there is no human habitation within about 50 miles of the site.

B. INSTRUMENTATION: The stations have been equipped with matched instrumentation as shown in Table 2.

C. DATA TELEMETRY AND RECORDING: Data from the network are telemetered via the RCA-microwave communication system to the seismological laboratory of the Geophysical Institute at Fairbanks. In the case of station SVG on St. Lawrence Island, it is required that the data be telemetered to Fairbanks via the RCA satellite communication system. Since RCA could not provide this link during the time of installation at the other sites, the installation of SVG was postponed for a later date. We plan to install this station and to establish the needed telemetry link through RCA by the end of November, 1976.

The data received at the recording site are in mixed signal mode, that is, comprising several frequencies (one for each station). These signals are discriminated by a discriminator bank and then recorded in real time on 16 mm film on a GEOTECH Develocorder. The recording system has been made ready during the reporting period.

D. DATA REDUCTION: The computer program for the reduction of data has been debugged and compiled on the Honeywell-6000 computer disc for routine use. Some modifications of the subroutine to compute magnitude of the earthquakes are in progress.

III. RESULTS: none

IV. PRELIMINARY INTERPRETATION: none

V. PROBLEMS ENCOUNTERED: In addition to the unavoidable delay occurred in the installation of one station (Savoonga) of the network, a serious problem of high level radio-frequency noise pickup by the amplifier-VCO package was encountered in the field environment. We have resolved this problem now by incorporating necessary changes in the standard instrument packages; we anticipate routine flow of data by the end of October, 1976.

VI. ESTIMATES OF THE FUND EXPENDED: \$37,000

TABLE 1

<u>LOCATION</u>	<u>STATION CODE</u>	<u>LATITUDE(N)</u>	<u>LONGITUDE(W)</u>	<u>ELEVATION(m)</u>
Kotzebue	KTX	66°56'16"	162°36'21"	5+2m
Remote	REM	65°57'28"	164°37'46"	335+5m
Tin City	TNC	65°33'47"	167°56'24"	37+5m
Anvil Mountain	ANV(Nome)	64°33'48"	165°22'37"	326+6m
North River	NRI	63°57'34"	160°22'49"	750-900m
	(Unalakleet)			
Savoonga	SVG	63°41'54"	171°31'32"	15+5m
	(St. Lawrence Is.)			

TABLE 2

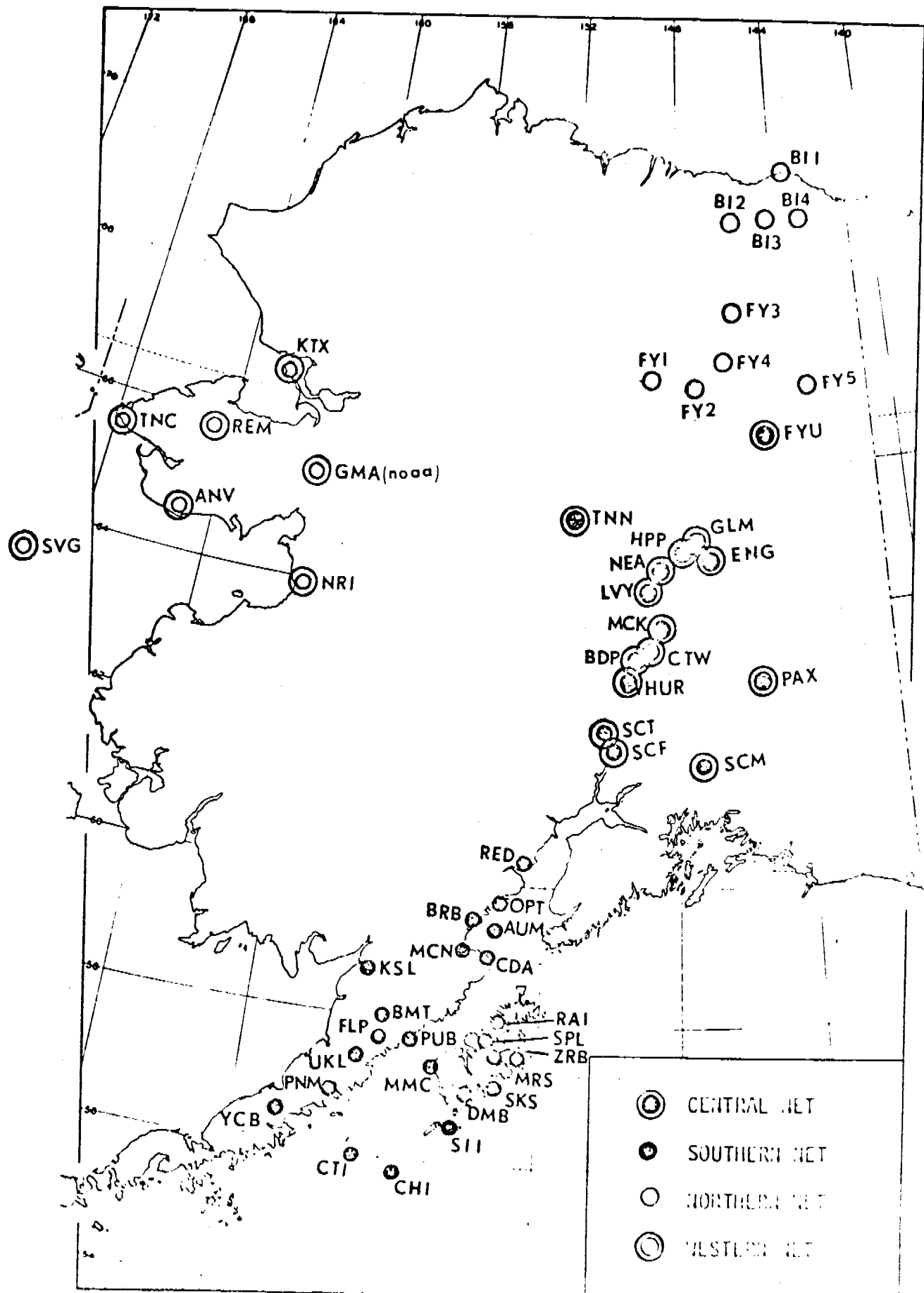
Seismometer: Geotech, Model No. 18300  
 Amplifier-VCO: Geotech, Model No. 42.21  
 Power Supply: Powermate, Model No. PT-99

Remote Site

Transmitter: Monitron, Model No. T15F20  
 Receiver: Monitron, Model No. R15F  
 Power Supply: 5 Carbonair Aircell ST-22  
 Antenna: Scala, Model No. C5A-150

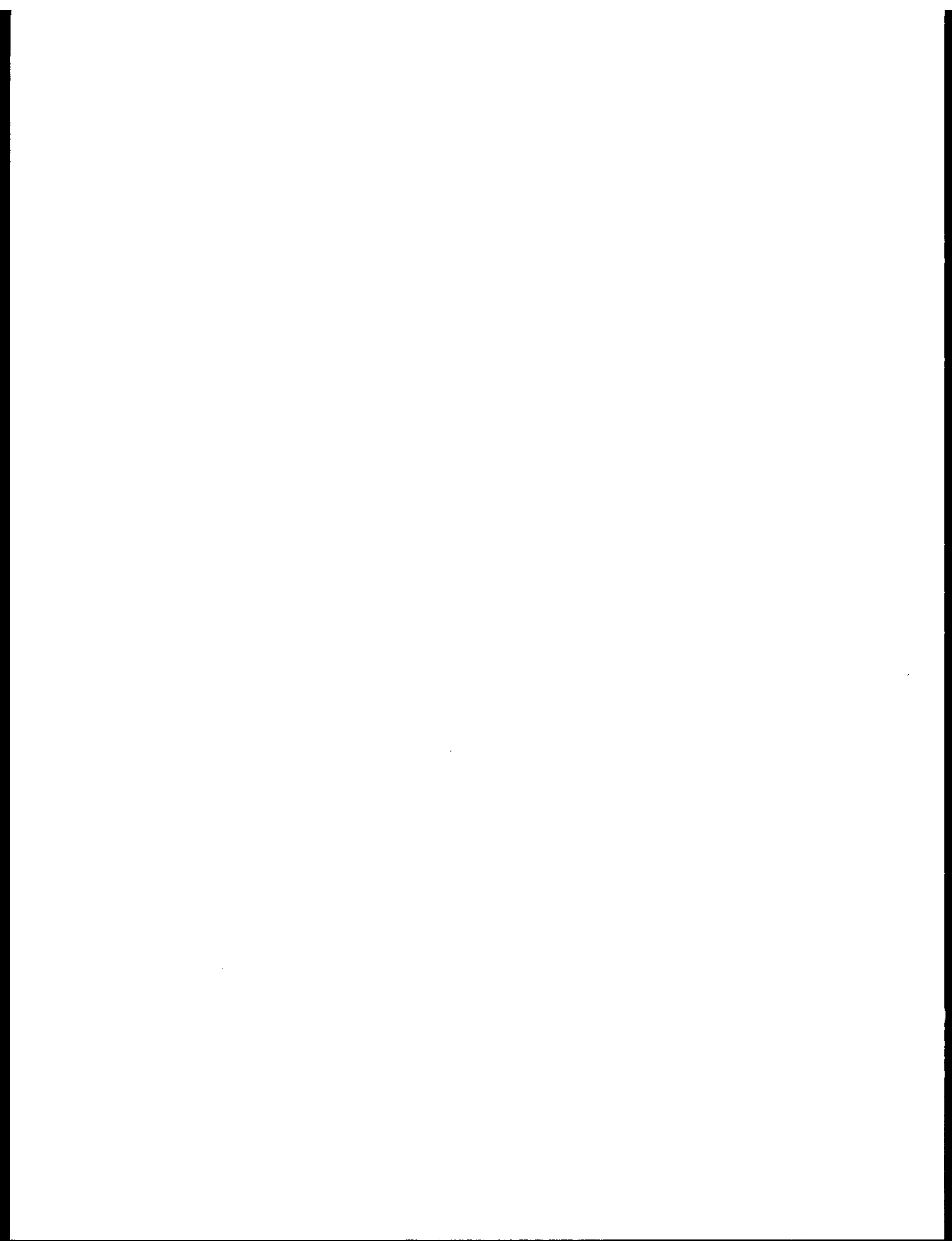
Recording Site

Discriminator Bank: Geotech, Model No. 46.11



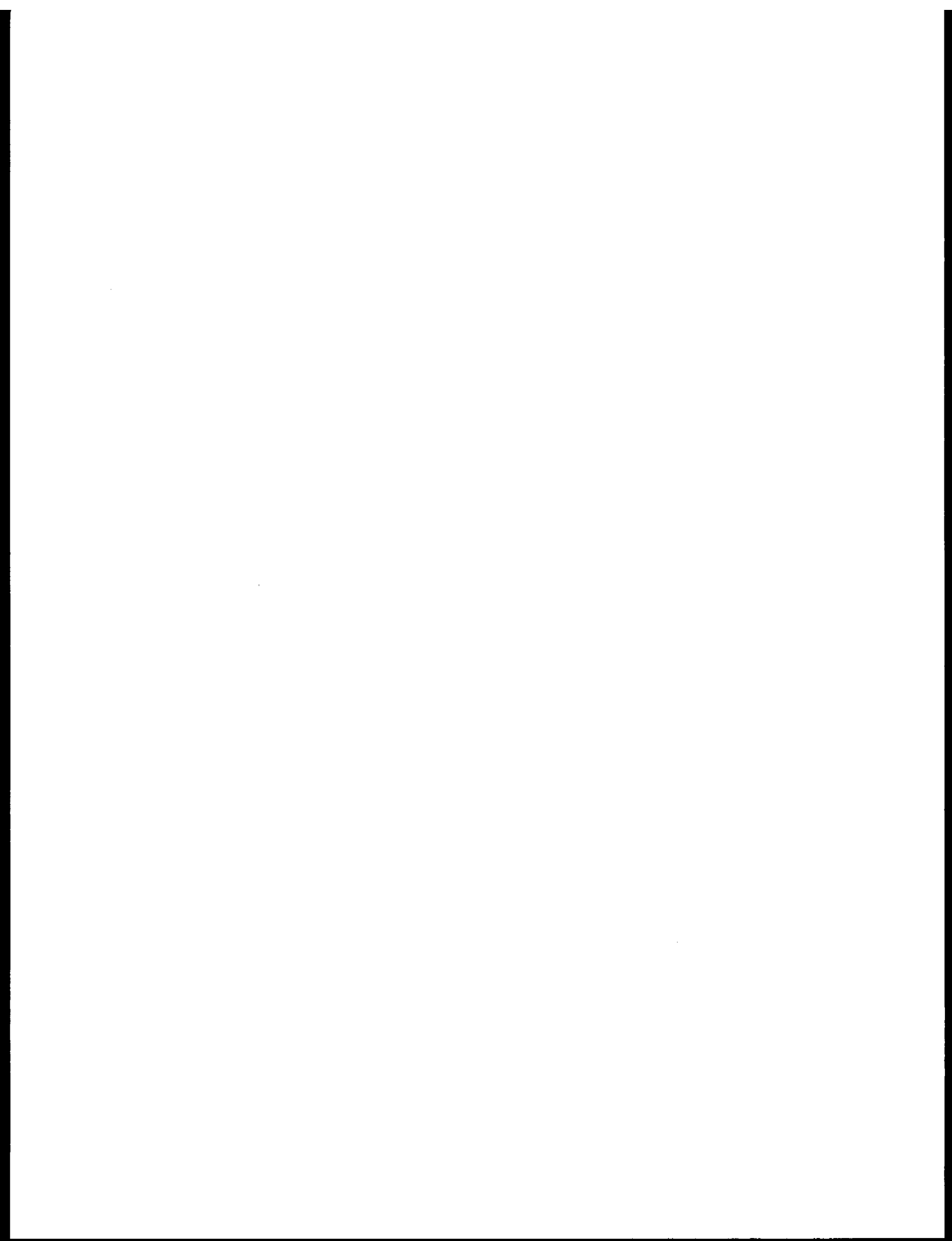
SEISMOGRAPHIC NETWORKS OPERATED BY  
THE UNIVERSITY OF ALASKA

ICE



## ICE

<u>Research Unit</u>	<u>Proposer</u>	<u>Title</u>	<u>Page</u>
87	Seelye Martin Dept. of Ocean. U. of Wash.	The Interaction of Oil with Sea Ice in the Arctic Ocean	227
88	William F. Weeks A. Kovacs CRREL	Dynamics of Near-Shore Ice	267
98	Norbert Untersteiner U. of Wash.	Dynamics of Near-Shore Ice (Data Buoys)	276
244	Roger G. Barry INSTAAR	I. Study of Climatic Effects on Fast Ice Extent and Its Seasonal Decay along the Beaufort Sea Coast	281
		II. Study of Climatic Effects on Fast Ice Extent and its Seasonal Decay in the Chukchi Sea Area	313
250	Lewis H. Shapiro William D. Harrison Geophys. Inst. U. of Alaska	Mechanics of Origin of Pressure Ridges, Shear Ridges and Hummock Fields in Landfast Ice	428
257	W. J. Stringer Geophys. Inst. U. of Alaska	Morphology of Beaufort Near-Shore Ice Conditions by Means of Satellite and Aerial Remote Sensing	429
258	W. J. Stringer Geophys. Inst. U. of Alaska	Morphology of Bering Near-Shore Ice Conditions by Means of Satellite and Aerial Remote Sensing	507
259	Richard D. Nelson William M. Sackinger Geophys. Inst. U. of Alaska	Experimental Measurements of Sea Ice Failure Stresses Near Grounded Structures	593
261/ 262	William R. Hunt Claus M. Naske Geophys. Inst. U. of Alaska	Beaufort Sea, Chukchi Sea, and Bering Strait Baseline Ice Study Proposal	595
265	Lewis H. Shapiro William M. Sackinger Richard D. Nelson Geophys. Inst. U. of Alaska	Development of Hardware and Procedures for <u>in situ</u> Measurement of Creep in Sea Ice	597
267	Albert E. Belon Geophys. Inst. U. of Alaska	Operation of an Alaskan Facility for Applications of Remote-Sensing Data to Outer Continental Shelf Studies	598



QUARTERLY REPORT

---

Contract # 03-5-22-67 TA6  
Research Unit #87  
Reporting Period: 1 July 1976 -  
30 September 1976  
Number of Pages: 37

THE INTERACTION OF OIL WITH SEA ICE IN THE BEAUFORT SEA

Seelye Martin  
Department of Oceanography, WB-10  
University of Washington  
Seattle, Washington 98195  
24 September 1976

I. Task Objectives: To understand the small scale interaction of petroleum and sea ice in the Beaufort, Bering, and Chukchi Seas. Our eventual aim is to predict how an oil spill or well blow-out will interact with the mobile pack ice of the Arctic Ocean.

II. Field or Laboratory Activities

II-1. Field Activities: we did not do field work during the last quarter.

II-2. Laboratory Activities: During the past quarter, we ran a series of experiments on the formation and growth of grease and pancake ice in a wavefield. We also looked at how petroleum spilled under this ice interacted with the grease and pancake ice. Because this research is applicable to the Bering and Chukchi Seas, we append a copy of our research results to this report.

III. Results: During the past quarter, we wrote up our field reports on the properties of the sea ice in the Beaufort Sea for our February 1976 field traverse and our May 1976 field traverse. Copies of these reports, which give the salinity, temperature and crystal structure of the observed ice cores, are available from the Juneau Project Office. We also wrote up the results of our laboratory experiments, a copy of which is appended to this report. Finally, we prepared a color movie film on our laboratory experiments which was shown at the OCS sessions of the Alaska Science Conference in August 1976.

IV. Preliminary Interpretation of Results: From our three field traverses for the project, we are beginning to understand the formation, growth, and decay of first year ice in the Beaufort Sea.

In summary, the ice grows as follows: during its initial growth, ice has a frazil crystal orientation for the top 10-30 mm, which then becomes columnar. Salt is rejected from the ice both downward through drainage channels, and upward to form the observed high salinity surface layer. As the season progresses and the air becomes colder, the ice grows in thickness with some downward brine drainage. Layers of snow are deposited on the ice surface, and during warm periods when the snow is warmer than the ice, the heat flux from the snow into the ice melts down the snow to form a layer snow ice with a thickness of the order of 10 mm on top of the sea ice.

The sea ice becomes active during the spring. The salinity layer which was trapped on top of the ice by the lack of brine drainage, is now released by the warming, and liquid brine moves down through the ice. This downward movement creates brine drainage tubes and also leaves void spaces with a diameter of 1-2 mm in the top 0.1-0.3 m of first year ice. The brine channels have a spacing of 0.1 to 0.2 m on a grid, and extend from top to bottom of the ice, giving the ice a water and air filled volume of 2-5%. Oil released under the ice at this time will both come to the ice surface, and be absorbed by the porous ice.

The ice cores from the area between the Barrier Islands and Prudhoe Bay resembled those from the Canadian Balaena Bay Test Site sufficiently so that we should understand the dynamics of small-scale oil entrainment in this region. We plan a more formal data report on this comparison during the coming contract year; however, the raw data for the Prudhoe Bay region plus some preliminary analysis is available in our report on our May 1976 field traverse.

V. Problems Encountered/Recommended Changes: none

VI. Estimate of Funds Expended: As of this date, we are about 99% expended.

A Laboratory Study of the Dispersion of Crude Oil within  
Sea Ice Grown in a Wave Field

A report from BLM/NOAA Contract No. 03-5-022-67, Task Order No. 6,  
Research Unit #87, Principal Investigator, Seelye Martin

by

Seelye Martin  
Department of Oceanography WB-10  
University of Washington  
Seattle, WA 98195

Peter Kauffman  
Department of Atmospheric Sciences AK-40  
University of Washington  
Seattle, WA 98195

and

Per Erik Welander\*  
Department of Oceanography WB-10  
University of Washington  
Seattle, WA 98195

Department of Oceanography Special Report Number 69  
23 September 1976

---

\* Present address: "Torbjörn Kluckaresgata 11, 11330 Stockholm, Sweden.

## ABSTRACT

In a laboratory experiment, we studied the formation and growth of sea ice in a wave field, and the interaction with the sea ice of oil released under it. The kinds of ice which grew in the wave field were grease and pancake ice. Our experiments show that the grease ice, which generally grew to a thickness of 100 mm, had a porosity of about 60% and a surface temperature which was only of the order of 0.1 degrees below the sea water temperature. The presence of grease ice did not inhibit oil released beneath it, rather the oil rose through the ice and spread out on the surface. The pancake ice formed when the grease ice thickness reached about 100 mm; our experiments showed that the length scale of the pancakes was about one-fifth of the driving wavelength. The rims around the pancakes were built up from grease ice which the oscillating wave field pumped onto the ice surface where it would freeze. Petroleum spilled under the pancakes rose to the surface in the cracks around the pancakes, where the oscillating motion pumped the oil both laterally through the cracks and onto the ice surface. Once on the ice surface, the pancake rims contained the oil so that it did not re-enter the water.

## 1. Introduction

The kinds of ice which grow on regions of open water in the polar oceans where cold, high velocity winds generate waves are called frazil, grease, and pancake ice. Our terminology follows the 'ice glossary' of both the World Meteorological Organization and the Scott Polar Research Institute, as discussed in Armstrong *et al.* (1966). They give the following definitions:

1. Frazil ice: "fine spicules or plates of ice in suspension in water (page 16)."
2. Grease ice: "A later stage of freezing than frazil ice, when the spicules and plates of ice have coagulated to form a thick soupy layer on the surface of the water. Grease ice reflects little light, giving the sea a matt appearance (page 18, see their Figure 4 for photograph)."
3. Pancake ice: "Pieces of new ice usually approximately circular, about 30 cm to 3 m across, and with raised rims due to the pieces striking against each other. Formed from the freezing together of grease ice, slush or shuga, or the breaking up of ice rind or nilas (page 31, see their Figure 3 for photograph)."

Of these three kinds of ice, grease and frazil ice occur in all ice-covered seas; we observed it frequently in the top 50-150 mm of the ice cores which we sampled for the OCSEAP program during the past year in the Beaufort Sea. In the Bering Sea, the results of the US/USSR Bering Sea Experiment (Kondratyev, K.Y. *et al.* 1975, hereafter called BESEX) show that frazil and grease ice occur all over the Bering Sea during their observational months of February and March. When grease ice is cooled, it solidifies to form sea ice with a random crystal structure; as opposed to 'columnar' ice, which is made up of vertically-oriented parallel platelets of ice. As an example, Figure 1 shows a photograph of the crystal structure of an ice core taken from the Beaufort Sea in May where the top 95 mm are frazil ice and the remainder of the core is columnar ice. From laboratory

and field studies of the Canadian Beaufort Sea Project (available from the Marine Sciences Directorate Pacific Region, 1230 Government Street, Victoria, B.C. V8W 1Y4, Canada), the oil absorption properties of columnar ice are well understood; the interaction of oil with grease ice in either its liquid or solid form is not.

Pancake ice is less frequently observed in the Beaufort Sea, but commonly occurs in the Bering Sea. The BESEX results (page 199) describe the ice growth as follows:

"The floes, no matter how large they become, have a very interesting growth history. The first generation of floes are pancakes which form during transition from grease to thin grey ice. The pancakes varies from 0.30 to 0.60 m in diameter. Several pancakes will then freeze together forming the first floe which may attain dimensions of the order of 1 to 3 m. These floes combine further to form bigger floes varying in size up to 900 m<sup>2</sup>. Finally, large fields of floes will form .... but still having the basic small floe as a characteristic."

W. J. Campbell (private communication, 1976) states from the results of overflights of the Chukchi Sea that the young ice forms in the same way as in the Bering, namely by the transition from grease to pancakes to floes. Because this growth process is very different from the simple growth of columnar ice, and because grease and pancake ice occur in the Bering and Chukchi Seas, an understanding of how grease and pancake ice form and grow is essential to the prediction of oil spill trajectories and to the understanding of both the weathering of crude oil spilled under this ice, and the interaction of spilled oil with marine mammals.

In the following, we first describe a laboratory study on the growth of grease and pancake ice from salt water, then discuss experiments on how spilled petroleum interacts with these kinds of ice.

## 2. The Experiment

The experiment took place in an insulated wave tank, made from Plexiglas, which was surrounded with 52 mm of polyurethane, and placed in a cold room. Figure 2 is a schematic drawing of the tank. The interior dimensions of the tank are 2.2 m in length, 0.93 m in width, and about 0.6 m in depth. The tank was filled with a 34 % NaCl solution to a depth of 0.41 m. At one end of the tank, a wedge-shaped paddle driven by a Scotch Yoke coupled to a stepping motor generated waves. In order to keep the paddle free of ice, we placed a heating tape in the water behind the paddle. In running the experiment, we initially set the cold room temperature slightly below -2°C until the water had cooled down to its freezing point of approximately -2.1°C. We then covered the tank with a plywood lid and set the room temperature to -20°C. When the room reached this temperature we removed the lid and started the paddle. Typically, the paddle had a peak-to-peak amplitude of 50 mm, with a driving frequency ranging from 0.60 s to 1.0 s, which yielded wavelengths of 0.6 m to 1.3 m.

We did a series of six experiments with the tank, namely a freshwater calibration experiment and five saltwater experiments. In one of the saltwater experiments we released diesel fuel into the tank; in another, we released Prudhoe Bay crude oil. Each experiment took about two weeks to set up, run, warm-up, and clean-up. The oil spill experiments took an additional week for oil clean-up.

We recorded the physical appearance of the ice photographically, and the temperature structure with thermistors. In the photography, we illuminated the tank with three 650 watt Sun Gun movie lamps with a color temperature of 3400°K, which equals that of Kodachrome Type A color movie and still film.

Because these lights radiate a great deal of heat which could liquify the ice surface, we did most of our photography in short, 10 minute periods, followed by 40-50 minute periods of darkness. We also set up fans to blow over the water-ice surface, which both generated capillary waves and advected away the heat.

We used the following cameras: a Nikon equipped with a Macro-Lens and loaded with Pan-X film; an additional Nikon with a wide angle lens and loaded with either Tri-X or Kodachrome Type A film; a Leica, which was the personal property of Peter Kauffman, equipped with a Macro-Lens and generally loaded with Pan-X film; and an Arroflex movie camera which was loaded with Kodachrome Type A movie film. We kept the cameras in an adjacent cold room at a temperature of  $0^{\circ}\text{C}$  and only brought them into the experimental room for short periods of time, to prevent both cold-soaking the cameras and condensation on the lenses. We photographed the ice both from above the tank and through a window in the side of the tank, measuring 0.3 m by 0.6 m. When we were not filming or observing, we covered this window with a polyurethane plug.

To observe the temperature structure of the ice, we used the thermistors which we developed for our field experiments; these are accurate to within  $0.01^{\circ}\text{C}$ . For grease ice, we built a thermistor array to record the vertical temperature profile; for pancake ice, we used a single probe to explore the temperature variations around the cakes.

In most of our experiments, we began with a standing wave with a period of 0.63 s, which yielded a wavelength of 0.68 m, or a mode 6 oscillation in our tank. We tuned this wave such that it was just at the breaking point; this generally yielded a peak-to-peak amplitude of about 200 mm. The first ice to form on this oscillating surface were small crystals of frazil ice; these quickly conglomerated into grease ice. After an additional 4-6 hours,

pancakes grew from the grease ice. In the following, we will discuss first the formation of grease ice, then the formation of pancake ice.

a. Grease Ice

The frazil ice crystals which initially formed in the tank were transported away from the paddle, even if the fans were blowing toward the paddle, by the phenomenon of wave herding. From Figures 3a and b, which show two views of the tank at an early stage of the experiment, we see that because of wave herding, the surface is partially open and partially covered with grease ice. The figure also shows that grease ice damps out the small-scale waves.

Qualitatively, following Phillips (1966, § 3.4), the wave herding shown in Figure 3 occurs for the following reasons. Because the ice alters the free surface boundary condition, either by imposing a no-slip condition or by forming a viscous slick, any ice formation tends to damp out the wave motion. For short capillary waves, the grease ice forms a no-slip surface boundary condition which rapidly damps out the waves. For longer gravity waves, the grease ice forms a viscous surface layer which imposes a stress condition on the waves and also causes wave attenuation. Therefore, for all scales of waves, the ice presence causes viscous decay, and thereby extracts energy from the waves. As the wave energy decreases, its momentum must also decrease. Because momentum must be conserved, the loss of wave momentum goes into a mean drift current which sweeps the ice crystals away from the paddle. For standing waves, which are made up of two  $180^\circ$  out-of-phase progressive waves propagating both toward and away from the paddle, the argument still applies, because when damping occurs, the wave propagating away from the paddle has more energy than the wave propagating toward the paddle.

Grease ice has a number of interesting properties. First, it tended to remain a fluid porous mass of ice up to a thickness of about 120 mm. Figures 4a and b show two sidewall photographs of the grease ice which were taken at times about one-half period apart on the standing wave cycle. Comparison of the two photographs show that the grease ice is compressed at the wave crest, and stretched at the trough. This observation agrees with the idea that the layer of grease ice behaves as a buoyant viscous fluid floating on the sea water. For all observed thicknesses, the ice within the slurry remained in the form of small platelets, with a characteristic diameter of 1-3 mm, and thickness of the order of 0.1 mm.

Second, we found from several measurements that the ratio of the volume of ice to the total volume of sea water and ice ranged from 35-40%, so that the grease ice shown in Figure 4 is about 60% sea water. We obtained this measurement by scooping up a sample of grease ice in a liter beaker, then quickly pouring off the sea water. We next allowed the remaining ice to melt, then measured the volume of both the sea water and the melted ice to obtain the porosity.

Third, the high porosity of the grease ice affected the heat transfer within the ice. Table 1 shows the distribution of temperature versus depth for grease ice of thickness 60 mm. To obtain this measurement, we placed our rake-like probe within the fluid, stopped the paddle, then recorded the temperatures. The table shows that the temperature within the grease ice equals the sea water temperature except at the very surface, where the temperature is depressed by only  $0.1^{\circ}$  below the deep temperature. The reason for this very weak temperature gradient within the ice is that the heat transfer very likely takes place by convection. Physically, convection occurs because for a

cooled salt water-ice mixture to remain in equilibrium, the solution salinity must increase by about 20 % per degree of temperature depression. Therefore, cooling the grease ice surface creates a salinity increase and thereby a density increase which generates heavy water at the grease ice surface. Because the grease ice is porous, this cold, heavy water sinks and is replaced by the sea water. This yields the observed convective temperature profile. The waves, which both stretch and compress the ice field and wash water through the ice, also add to the efficiency of the convection.

Table 1. Temperature versus depth in grease ice.

Height (mm)	Temperature (°C)	
+10	-18.8	(in air)
0	-2.33	(at grease ice surface, probe submerged)
-10	-2.23	
-20	-2.22	
-40	-2.22	
-90	-2.23	(in salt water below grease ice)

Because of this convection, on at least one occasion the grease ice thickness increased nearly linearly with time, rather than with time to the one-half power. Figure 5 is a plot of grease ice thickness versus time, which we made by stopping the paddle at different times during the experiment, then letting the grease ice spread out to an average thickness which we measured. The graph suggests that the thickness increased nearly linearly up to the point at which the pancakes formed, although because our surface heat flux

boundary condition was not carefully maintained, this result is only suggestive. A linear growth rate, however, is consistent with the convective heat transfer within the ice.

b. Pancake Ice

When the grease ice thickness reached 70-100 mm, the crystals at the surface began to join together into what we called 'proto'-pancakes. In Figure 6a, these proto-pancakes consist of clumps of crystals, measuring 50-100 mm in the cross tank direction, 50 mm wide, and 3-5 mm thick, which although they have a much lower porosity than the surrounding and underlying grease ice, are still so soft that we could not pick them up. The proto-pans apparently form when the heat flux from the deep water is no longer great enough to keep the surface liquid, and when the grease ice buoyancy slows the washing of sea water through the ice surface, so that the surface cools and solidifies.

These proto-pans quickly evolve into pancake ice. Figures 6b. and c are photographs of the ice field made one hour after 6a, where 6b and c are half a wave period out-of-phase. The two photographs show both the many small pans which make up the surface, and the presence of a large crack to the right of the thermometer which the waves periodically open and close. The photographs also show that, particularly to the right of the large crack, grease ice has been pumped onto the ice surface by the convergent-divergent motion of the wave field. This pumping of grease ice onto the surface leads to the formation of the raised rims on the pancake ice.

For the waves, the growth of pancakes from grease ice changes the surface boundary condition for waves with lengths of the order of the pancakes from that of a viscous stick to a solid, no-slip upper boundary condition. This greatly increases the wave damping for short waves. For longer waves, the surface boundary condition remains mixed, with the gaps between cakes allowing

some relative motion. The ice-induced decrease in wave amplitude permits the smaller pancakes to join together without being broken apart by the wave field, so that as the experiment progresses, small pans join up into larger cakes.

Figure 7a-7d is a photographic sequence showing the growth of pancakes from grease ice; the waves have a period of 0.81 s or a driving wavelength of 1 m. Near the paddle, the heat from the heating tape prevented the growth of pancakes; however, the photographs show that away from either end of the tank, the pancakes have an average width of 0.2 m or about one-fifth of the driving wavelength. Further, over the two hours covered by the sequence, the rims around the cakes grow from virtually nothing to a height of 20-40 mm. As with the proto-pans, the rims in Figure 7 appear to grow from grease ice which is pumped up onto the pancake surface. In Figure 8, the two close-up photographs, which were taken immediately preceding Figure 7b and half a wave period apart, show both the opening and closing of the gaps between the pancakes and that the rims appear to be formed from grease ice which has flowed down the edges of the rims toward the pancake center. Our movie films further show that the convergence of the rims pumps grease ice up between the rims to a height above the pancake surface. Because the pancakes oscillate together many times over their growth; for example the pancakes in the Figure 7 sequence oscillate together 9,000 times, the rims probably grow from the slow incremental pumping of grease ice up over the rims.

In the experiment, the pancakes floated in a much thicker layer of grease ice, which as Figure 5 shows, continued to increase in thickness even after the formation of pancakes. In addition to supplying material for the rims, the grease ice had several other effects. First the oscillating grease ice field

around the cakes caused the cakes to grow with a dish-shaped bottom profile. This occurred because heat was still transferred within the grease ice by convection to the air through the cracks around the pancakes, so that the grease ice remained warm at the surface. We observed with the thermistor probes that the surface temperature of the grease ice within the cracks was only 0.1 - 0.4 degrees colder than the sea water temperature.

At the same time, the temperature at the center of the pancake surface was 3-5 degrees colder. Because the sides of the pancake up to and above the water line are washed in warm grease ice, the temperature isotherms within the pancakes are curved as shown in Figure 9. This isotherm curvature means that the pancakes grow in thickness fastest at the center, which yields a dish-shaped cross-section.

As an example, Figure 10 shows the cross-section of a typical piece of pancake ice. To take this photograph, we cut a piece of pancake ice in half, rubbed the surface first with alcohol, then with an oil-soluble dye to bring out the crystal structure. The photograph shows both the dish-shaped profile and that most of the small crystals which make up the pancake lie parallel to the surface.

Second, the combination of the raised rims and the grease ice layer mean that the pancakes float so low in the water that the ice surface at the pancake center is slightly below the waterline. There are two reasons for this; first, the grease ice in which the pancakes float has a density less than sea water; second, the build-up of the rims on the pancakes adds weight above the waterline. To look at the effect of the grease ice, we assume that the grease ice consists of 40% freshwater ice with a density of  $920 \text{ kg m}^{-3}$  and 60% sea water with a density of  $1030 \text{ kg m}^{-3}$ , then the grease ice density is  $990 \text{ kg m}^{-3}$ . Therefore, if the pancakes, which have a salinity of about 20 ‰ or a density of  $930 \text{ kg m}^{-3}$ ,

float in grease ice, and if for the moment we neglect the weight of the rims, then pancakes with an average thickness of 20 mm will have a freeboard of 1.2 mm, as opposed to 2 mm if they were floating in pure sea water.

The additional weight of the rims is even more important. Figure 11 is a schematic diagram of a pancake based on the cakes in Figure 5. If we assume that the pancakes are two-dimensional bodies measuring 200 mm in width by 20 mm in depth and with rims measuring  $10 \times 20 \text{ mm}^2$ , then the effect of this additional mass above the water line is that the pancake now floats such that the mean water level is 0.7 mm above the ice surface at the pancake center.

As an example of the low freeboard, Figure 12 shows another cross-section of pancake ice taken in the following way. After running the experiment, we elevated the room temperature to  $-10^{\circ}\text{C}$ , and left the experiment overnight. On the following day, we cut a block of ice out of the tank which stretched across two pancakes from rim to rim, so that the center of the ice shown in Figure 12 is the boundary between two pancakes.

We cut this block into a section about 30 mm thick, rubbed the surface with alcohol and dye, then photographed the ice with a flash from behind the ice. Because the ice continued to grow after we turned off the paddle, the shape of the ice in Figure 12 is not that of a pancake; however, the small arrow on the photograph marks the bottom of a cavity between the two cakes, which is the water surface level at the time we turned off the paddle. Close examination of this photograph shows that the water level around the cake is higher than the ice surface height at the pancake center.

In all of our pancake experiments, we observed that the surface of the pancake was covered with a thin layer of liquid brine; one source of this brine is the water pumped over the rims and onto the ice. This lowered freeboard may

persist for even larger pancakes. W. J. Campbell (private communication, 1976) observed from low-level overflights of the Bering Sea during BESEX that pancake-like floes with diameters of the order of 2 m also had wetted surfaces. As we show later in this report, this lowered freeboard makes the pancakes more vulnerable to oil spilled under the ice being pumped onto the surface.

Third, because the pancakes grow from grease ice with its random collection of small crystal platelets, the pancakes also have a random crystal structure. Figures 13a and b, which are close-ups of the ice shown in Figure 12, clearly show the random orientation of the ice crystals within the pancakes. Our oil experiments suggest that this random orientation is less likely to capture oil flowing along the ice bottom than the parallel vertical crystals of columnar sea ice.

### 3. The Oil Spills

We did two oil spills during the course of our experiments. The first was a #2 diesel oil spill of 250 ml; the second, a Prudhoe Bay crude oil spill. The diesel oil spill was done just after the pancakes started to form; the Prudhoe spill was later in the growth of the pancakes.

#### a. The Diesel Spill

At the time of the spill, the grease ice thickness was about 100 mm, with the small ice pans of thickness 5-10 mm at the growth stage of those shown in Figure 6b. We discharged the oil through a small U-shaped tube which extended under the ice, so that the oil flowed out vertically in a turbulent jet at a depth of about 200 mm below the bottom of the grease ice. Because of the high porosity of the grease ice and the buoyancy of the diesel oil, the grease ice did not absorb the oil, rather the oil quickly appeared on the grease ice surface in the cracks surrounding the pancakes. The oscillatory motion of the pancakes then pumped the oil sidewise from its original discharge point.

Figure 14, a photograph of the spill following the discharge, shows that the

oil has been pumped laterally to cover an area measuring about  $0.4 \times 0.4 \text{ m}^2$ , so that the average thickness of the slick is about 1 mm. An unmeasured amount of oil was pumped up onto the ice, where it was contained by the raised rims. Once on the ice surface, the combination of the raised rims and the low freeboard prevented its return to the cracks.

b. The Prudhoe Bay Crude Oil Spill

For this experiment, we used 500 ml of Prudhoe Bay crude oil, which the Atlantic Richfield Company (ARCO) donated to our laboratory. This oil came from the following well: Atlantic Richfield-Humble, Sag River State No. 1, 2,637 feet from west line and 866 feet from north line, 4-10n-15e, UM, Alaska. The oil has a pour point of  $-9.5^\circ\text{C}$ , and a specific gravity of 0.893. We measured the following viscosities at different temperatures for this oil; at  $0^\circ\text{C}$ , 19 centipoise (cp); at  $-2^\circ\text{C}$ , 175 cp, and at  $-8^\circ\text{C}$ ,  $10^3$  cp. For comparison, fresh water at  $4^\circ\text{C}$  has a viscosity of 1.6 cp. For the experiment, the crude oil although very viscous remained fluid.

During the discharge, the total ice thickness was 120-130 mm, and the pancakes were 10-30 mm thick. Preceding the discharge by about one hour, we increased the period of the paddle from 0.63 s to 0.94 s, or to a wavelength of 1.3 m. This had the desired effect of increasing the amplitude of the convergent-divergent motion between the cakes from virtually nothing to 10-20 mm, but also allowed the smaller pancakes to join together into bigger cakes.

We discharged the oil through a fixed tube of 10 mm inner diameter that ran from one corner of the tank down along the bottom to terminate in a vertical tube pointing up under the ice. The top of this vertical tube was about 300 mm below the water surface. This tube was kept filled with air until just before the discharge, when we simultaneously released the air and poured the oil into a funnel attached to the tube. At the time of pouring the oil, its temperature

was +7.5°C; however, since it took about four minutes for the oil to flow completely through the tube into the tank, we suspect that it entered the water at a temperature very close to -2°C. Visually, the oil flowed out the discharge tube in viscous slugs resembling poured molasses, rather than in a turbulent jet such as occurred in the diesel spill. After the oil left the discharge tube, we observed the oil to disappear up into the grease ice, which showed no signs of either inhibiting or capturing the released oil.

Five minutes after we began to pour the oil into the funnel, the oil appeared on the grease ice surface in a crack between two pancakes. Figure 15a shows the ice appearance immediately preceding the spill, and 15b shows the first appearance of the oil at the surface. Figures 15b-15e were all taken within about 15 s of each other, so that the entire sequence lasts no more than two minutes. Within this time, the oil spread nearly all the way across the tank within the crack. The figure also shows that some of the oil was pumped onto the ice surface. Because of the low freeboard of the pancake ice, and the fact that the oil floats on top of the grease ice within the cracks, the oil was easily pumped onto the ice surface.

Figure 16a-16c, which are photographs of the ice surface 30 minutes after the discharge, show that a large amount of oil has been pumped up onto the ice by the combination of the oscillating motion of the pancakes and the confinement of the spilled oil by the tank walls. Figures 16b and c, which were taken about one-half wave period apart, show how the oscillating pancakes can pump oil either laterally or onto the ice. By scraping up the oil on the ice surface after the experiment, we determined that 290 ml of the 500 ml of oil spilled had been pumped onto the ice.

Figure 17 is a sketch of the location of the oil both under and on the ice which we made from our observations in cutting up the oiled ice on the day

following the experiment. Most of the oil appeared either to go to the ice surface or remain in the crack; however, there was a very light skim of oil on parts of the underside of the pancake. Because the flow of the oil within the crack was limited by the tank walls, the amount of oil on top of the ice is probably exaggerated in our experiment. As Figure 15 shows, however, the oscillations of the pancakes in a wavefield will drive the spilled oil both laterally and onto the ice surface.

#### 4. Other Properties of Pancake Ice: The Formation of Brine Drainage Channels

In spite of the random crystal structure of pancake ice, we still observed the formation of the brine drainage channels similar to those in columnar ice. The importance of these channels is that they provide an additional pathway of bringing oil from under the ice to the ice surface.

To study the formation of these channels, which are most prominent when cold sea ice is warmed up, following one experiment, we raised the room temperature up to  $-6^{\circ}\text{C}$  after growing pancake ice and let the room sit overnight. In the morning of the following day, we observed brine draining from the ice at several locations; and at two positions, we observed the formation of small ice stalactites with lengths of the order of 50 mm. We marked the location of one of these stalactites on the ice surface and removed the particular pancake from the tank. Upon removal, the stalactite disintegrated and a volume of water estimated at 250 ml poured out of the ice in a period of about 15 s. To examine the brine drainage system inside the ice, we marked the drainage channel, which from the bottom was a 3 mm diameter hole, with a small piece of wire, then set the pancake into a cold room at a temperature of  $-20^{\circ}\text{C}$ . After the ice had cooled down, we cut the block into a 30 mm thick section with one cut along the plane of the drainage tube.

Figure 18a and b shows two views of the pancake cross-section, which extends from rim to rim of the pancake. The first photograph, Figure 18a, is taken by transmitted light without any dye spread on the ice. The photograph clearly shows a cone-shaped dark region, funneling into the lower protuberance on the pancake bottom around which the stalactite grew. The lower photograph, 18b, shows the same piece of ice with dye rubbed on the surface to bring out the topography. This picture shows the large central drainage channel and pancake crystal structure. Comparison of this photograph to those from ice that was not warmed (Figure 13), shows that the warming of the ice modified the top 20 mm of the ice, and presumably caused both the downward movement of the surface brine and the formation of brine channels.

The significance of this observation is that brine drainage channels form as easily in ice with a frazil crystal orientation as in columnar ice. If an oil spill took place in the spring, these channels could serve as additional conduits of oil to the ice surface.

##### 5. Summary and Conclusions

Our experiments studied the growth of grease and pancake ice in a monochromatic, uni-directional wavefield. We found that the first ice to form was grease ice which had a high porosity and within which heat transfer took place by convection, so that the surface temperature was only a few tenths of a degree less than the deep water temperature. Because of the high porosity and warm surface temperature, oil spilled within grease ice will probably behave as if the grease ice were not present in the tank. Our experiments suggested that the oil rose through the grease ice and spread out on the surface, without any signs of oil absorption below the grease ice surface.

In our experiments, the grease ice grew in thickness until it reached a

depth of about 100 mm, at which time pancakes began to form on the surface. The pancakes grow from grease ice and initially float on a much thicker grease ice layer. The rims on the pancakes are built up from the many oscillations of the pancakes which force grease ice up onto the tops of the pancakes where it freezes. The combination of the additional mass of the rims above the waterline and the reduced density of the grease ice means that the pancakes float such that the pancake center is slightly below the waterline. The dimensions of the pancakes are a fraction of a wavelength; when we decreased the driving frequency, smaller cakes would join together to form larger cakes. Since grease and pancake ice serve as filters for water waves, with the shortest waves decaying fastest, this filtering may explain the gradual increase in floe size versus distance from the pack edge in the Bering Sea.

Crude oil spilled within the pancakes tended to move through the grease ice and appear on the grease ice surface in the spaces between the rims of the pancakes. The oil was then subjected to periodic oscillations, which both pumped the oil laterally and onto the ice surface. Once the oil reached the surface of the pancakes, it tended to remain there because of the raised rims around and the low freeboard of the cakes.

#### Acknowledgments

We thank Dr. C. P. Falls, Environmental Conservation Manager, Atlantic Richfield Company, North American Producing Division, Alaska, for supplying us with the crude oil used in these experiments. We also thank Mr. Terren Niedrauer for his help with the experiment; in particular, for taking the photographs in Figure 15. This work was primarily supported by BLM/NOAA Contract No. 03-5-022-67, Task Order No. 6, RU #87; Mr. Welander gratefully acknowledges the support of the Office of Naval Research under Task NR307-252 and Contract N00014-76-C-0234.

References

- Armstrong, T., Roberts, B., and Swithinbank, C., 1966: Illustrated Glossary of Snow and Ice, Scott Polar Research Institute, Cambridge, 60 pp.
- Kondratyev, K. Ya., Rabinovich, Yu. I., and Nordberg, W. (Ed.), 1975: USSR/USA Bering Sea Experiment, Gidrometeoizdat, Leningrad, 315 pp.
- Phillips, O. M., 1966: The Dynamics of the Upper Ocean, Cambridge University Press, 261 pp.

## FIGURE CAPTIONS

1. An ice core taken north of Deadhorse during May 1976 by two of the authors (S.M. and P.K.). The top of the core is to the left.
2. A schematic diagram of the apparatus.
3. Two photographs of open water with grease ice being herded to one end of the tank by the paddle. The wave period is 0.63 s, the wavelength is 0.68 m, and the paddle is on the left. Vertical lines on far wall are 100 mm apart.
4. Side view of grease ice in the tank at  $2\frac{1}{2}$  hours into the experiment. The wave period is 0.65 s, the wavelength is 0.68 m. The line of ice above the wave is frozen to the inner tank wall. (4a) is about one-half cycle out-of-phase with (4b).
5. Ice growth versus time for grease and pancake ice.
6. Formation of pancakes from grease ice; the wave period is 0.80 s, the wavelength is 1 m, the average ice thickness is 70 mm. (6a) 3 hours after the experiment began; (6b) and (6c) 4 hours after the experiment began; (6b) is about one-half cycle out-of-phase with (6c). The thermometer length is 145 mm.
7. Photographic sequence showing pancake growth with time; wave period is 0.81 s, wavelength is 1 m. (7a) 20 minutes after pancakes first start to form; (7b) 60 minutes after pancakes first start to form; (7c) 80 minutes; (7d) 140 minutes. See text for additional description.
8. Detail of pancake rims. (8a) and (8b) are about one-half cycle out-of-phase; see text for additional description.
9. Schematic diagram of the isotherms within a pancake.
10. Cross-section of a small piece of pancake ice.
11. Schematic diagram of a pancake cross-section.

12. Cross-section of two frozen-together pieces of pancake ice; the arrow marks the bottom of the gap between the two pieces. See text for additional description.
13. Two close-up photographs of the crystal structure of the ice in Figure 12.
14. Photograph of the diesel oil spill about 10 minutes after discharge.
15. The Prudhoe Bay crude oil discharge. (15a) immediately preceding the spill; the arrow marks the unfrozen crack. (15b-15f) the spreading of the oil on the surface with time; approximately 15 s separates each photograph.
16. The Prudhoe Bay crude oil discharge 20 minutes after the oil release. (16a and 16b) looking down on the spill; these two photographs are one-half cycle out-of-phase; (16c) the spill looking toward the paddle.
17. Schematic drawing of the pancake cross-section showing the location of the spilled oil.
18. Brine drainage from pancake ice. (18a) photograph of pancake ice cross-section by transmitted light only; (18b) photograph of same ice section with dye rubbed on the surface by transmitted light.

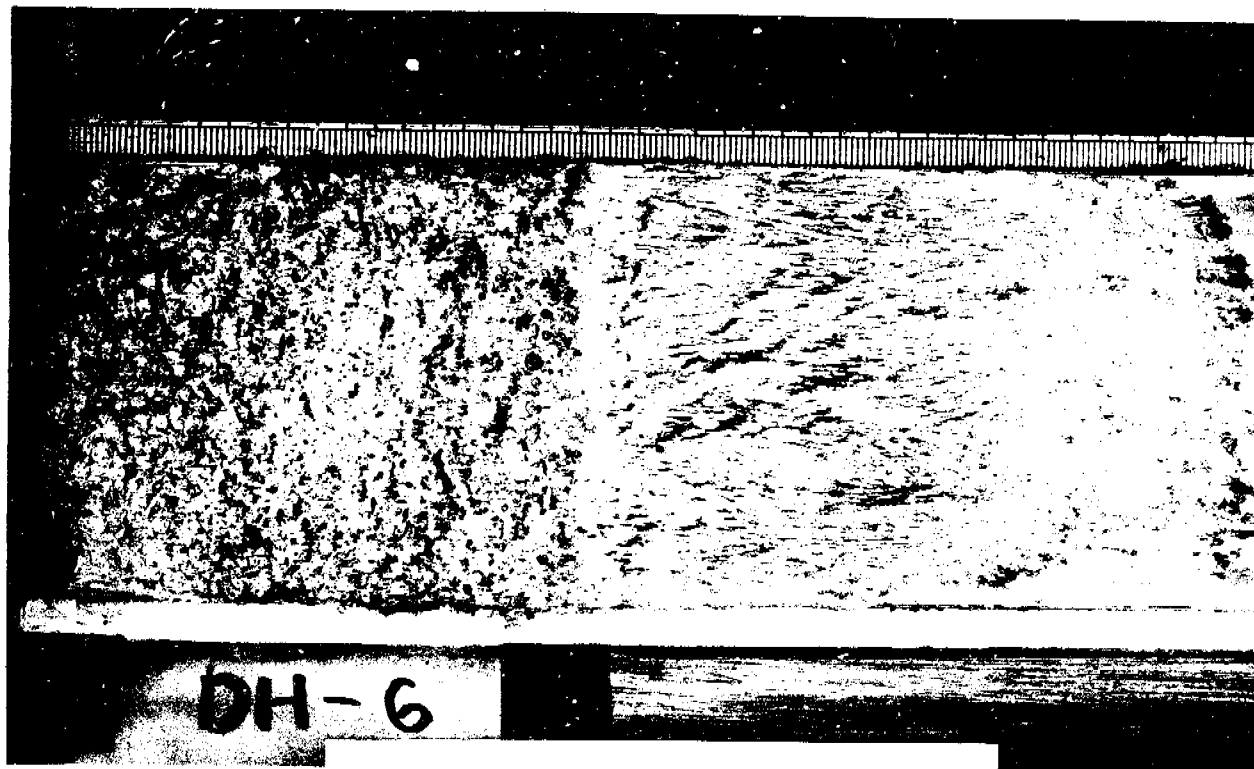


Figure 1

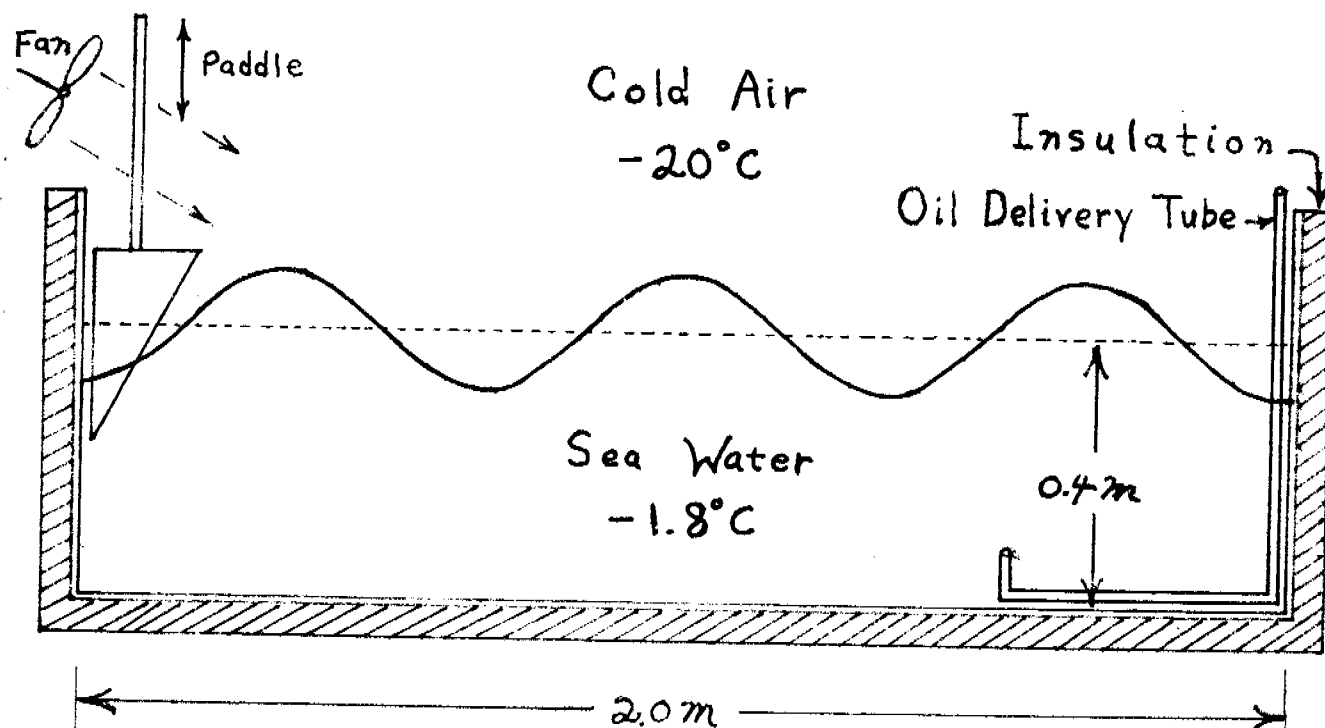


Figure 2

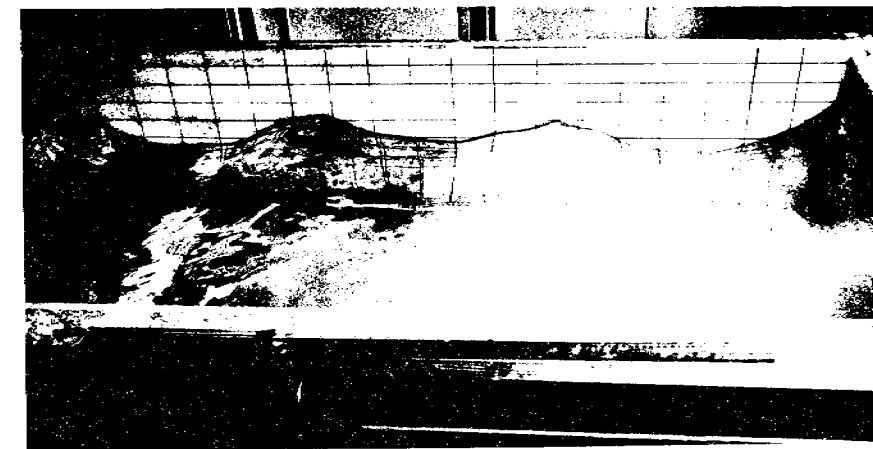
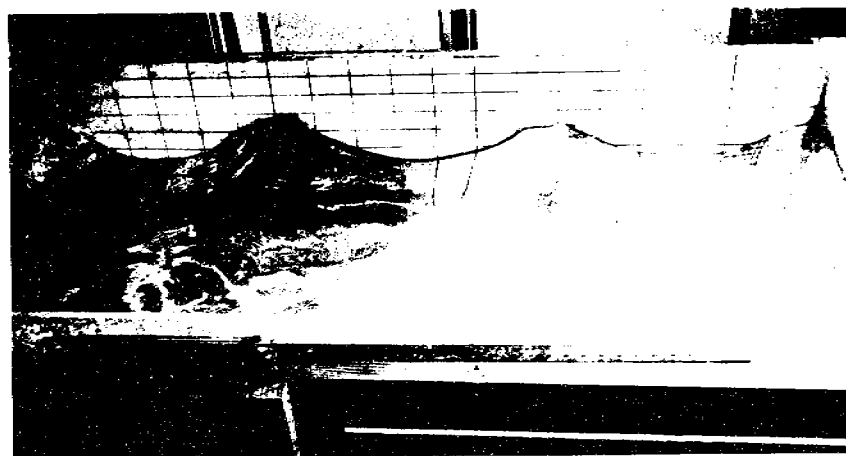


Figure 3

253



(4a)



Figure 4

(4b)

22

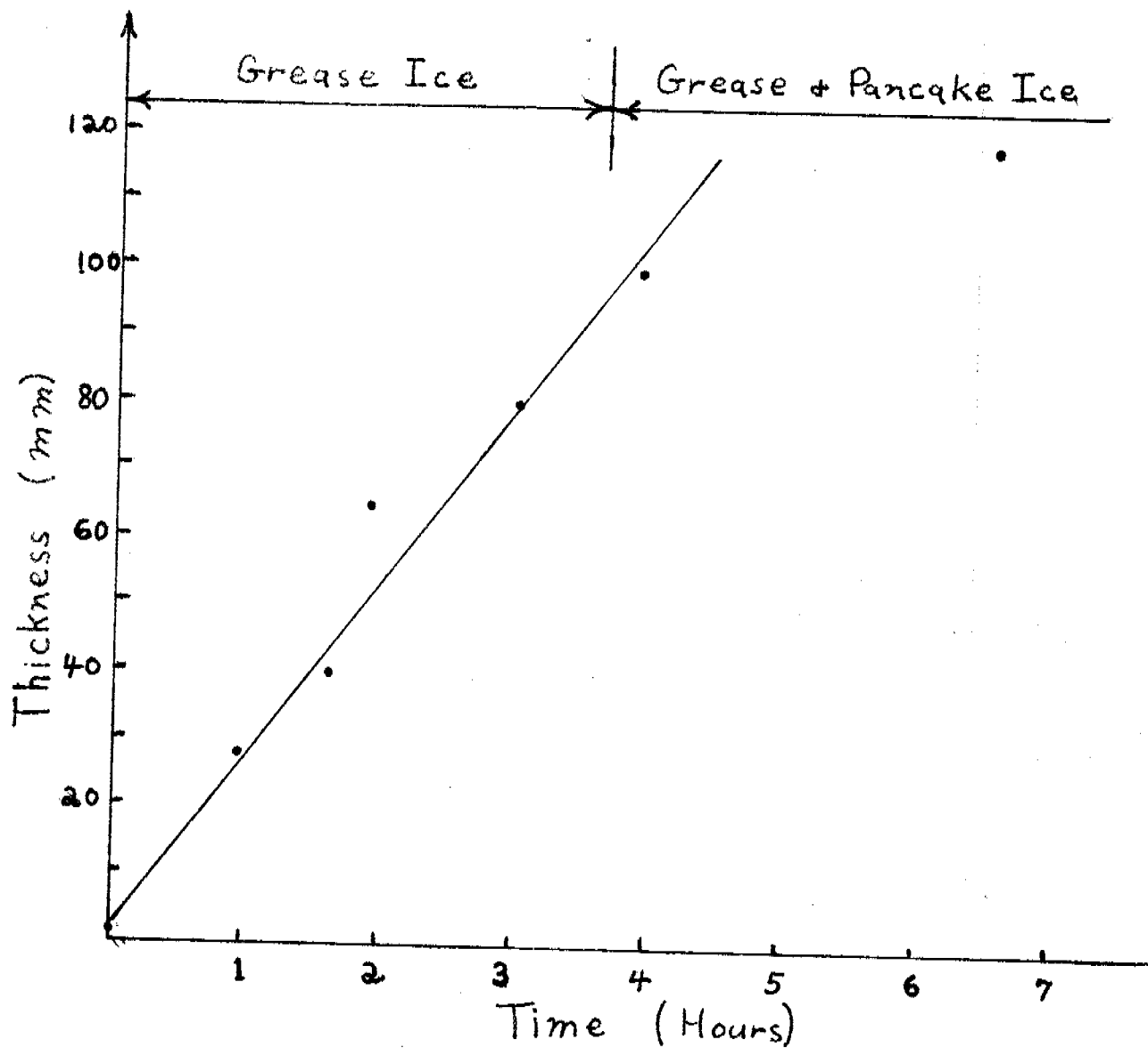
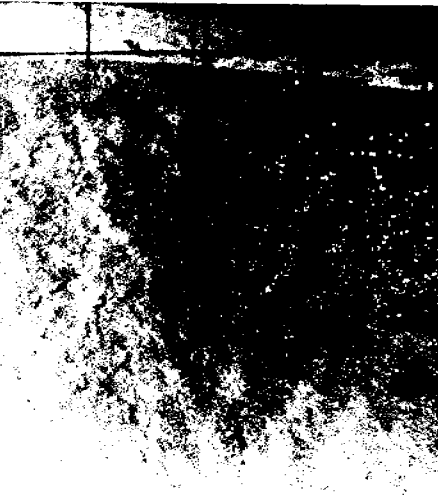
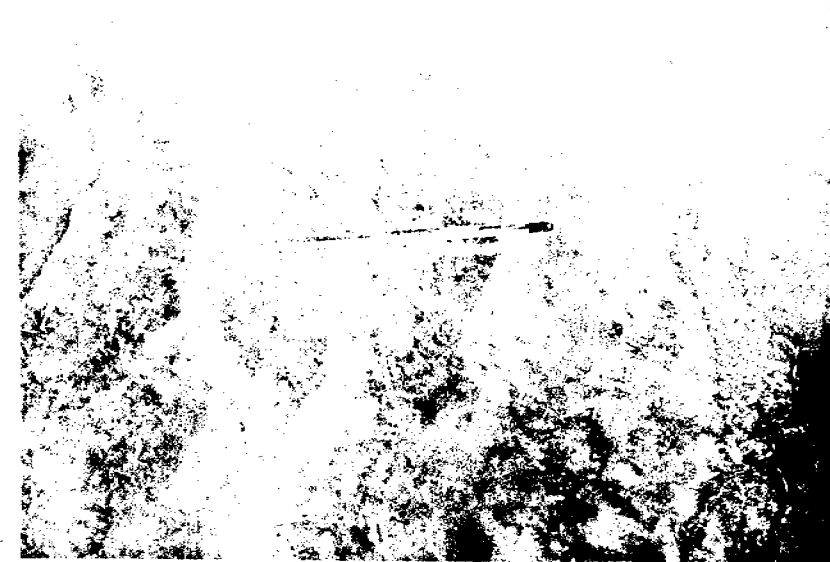


Figure 5



(6a)

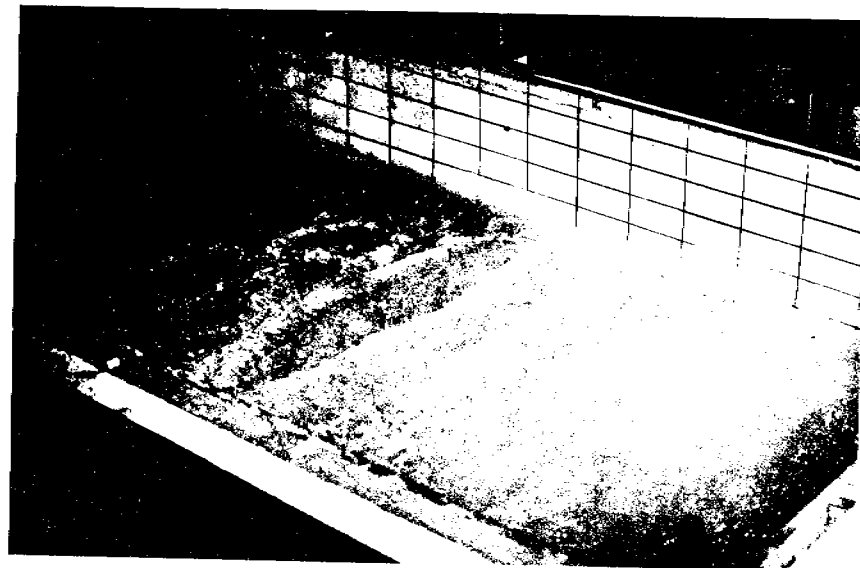


(6c)

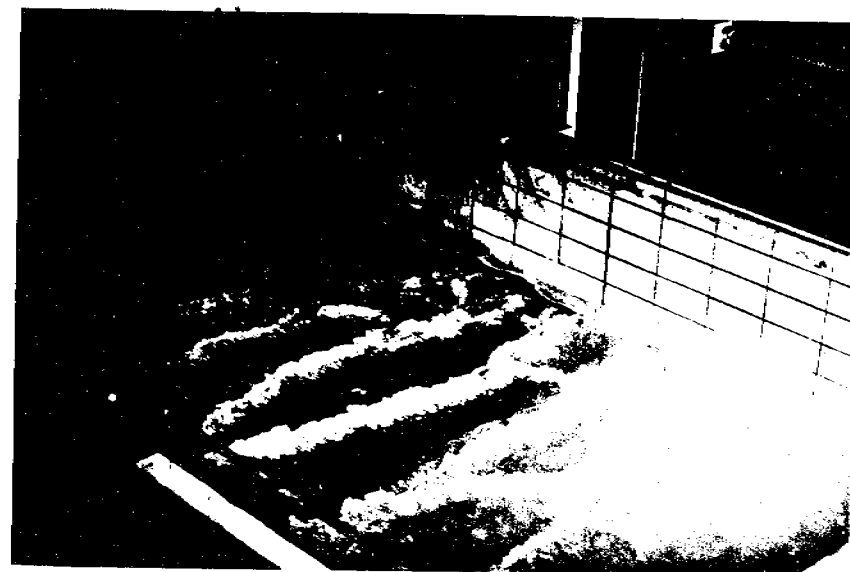
Figure 6

(6b)





(7a)



(7b)



(7c)



(7d)

Figure 7

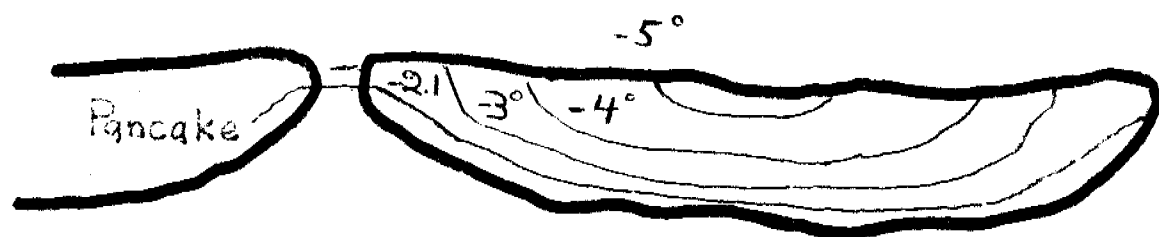


(8a)



(8b)

Figure 8



Grease Ice

Figure 9

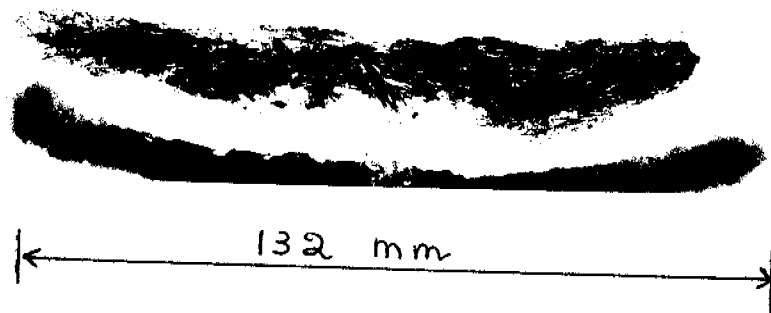


Figure 10

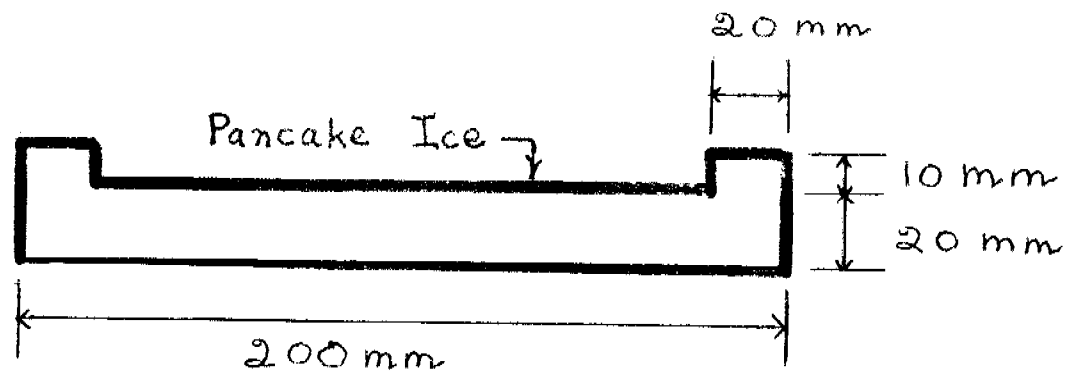


Figure 11



Figure 12

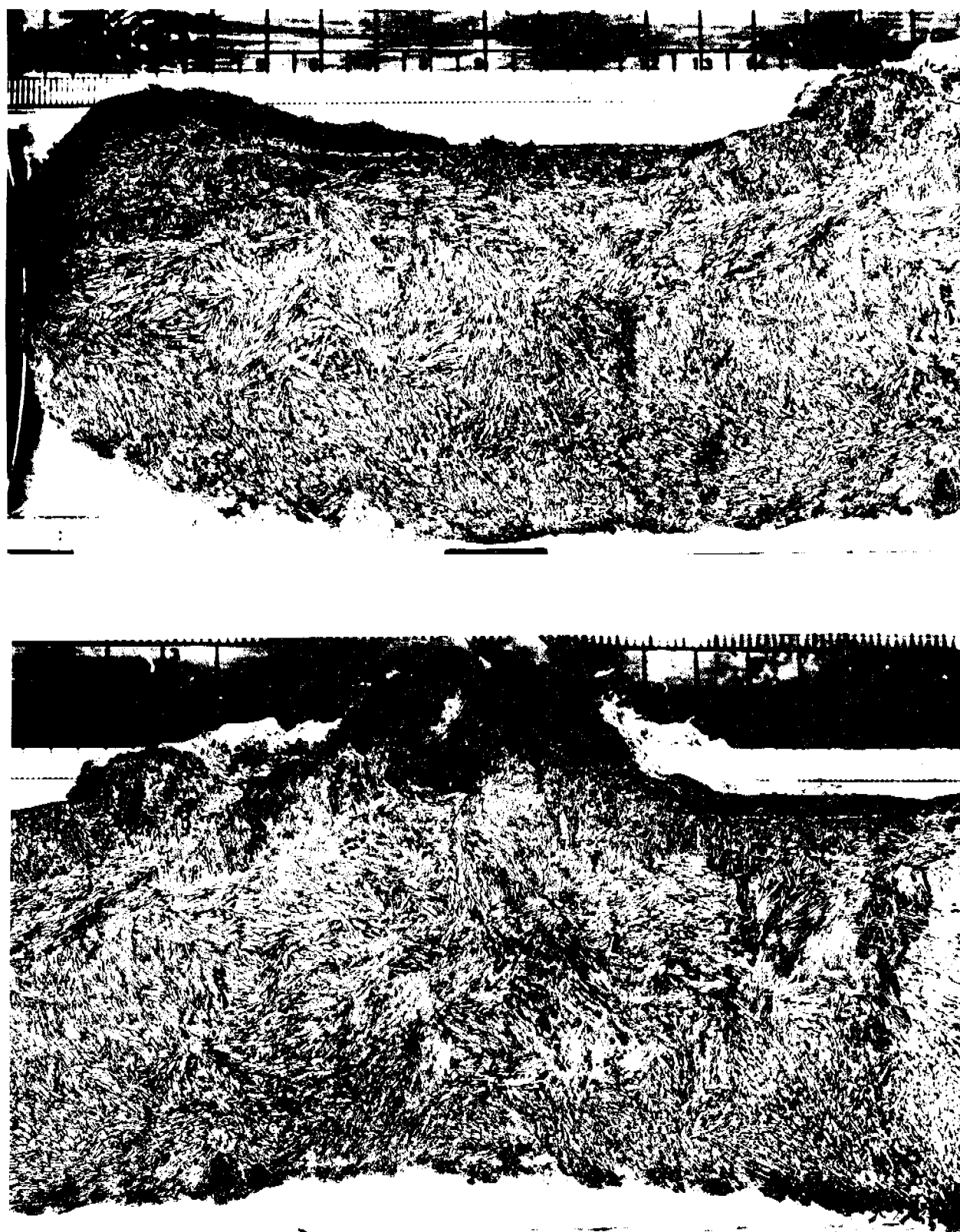


Figure 13

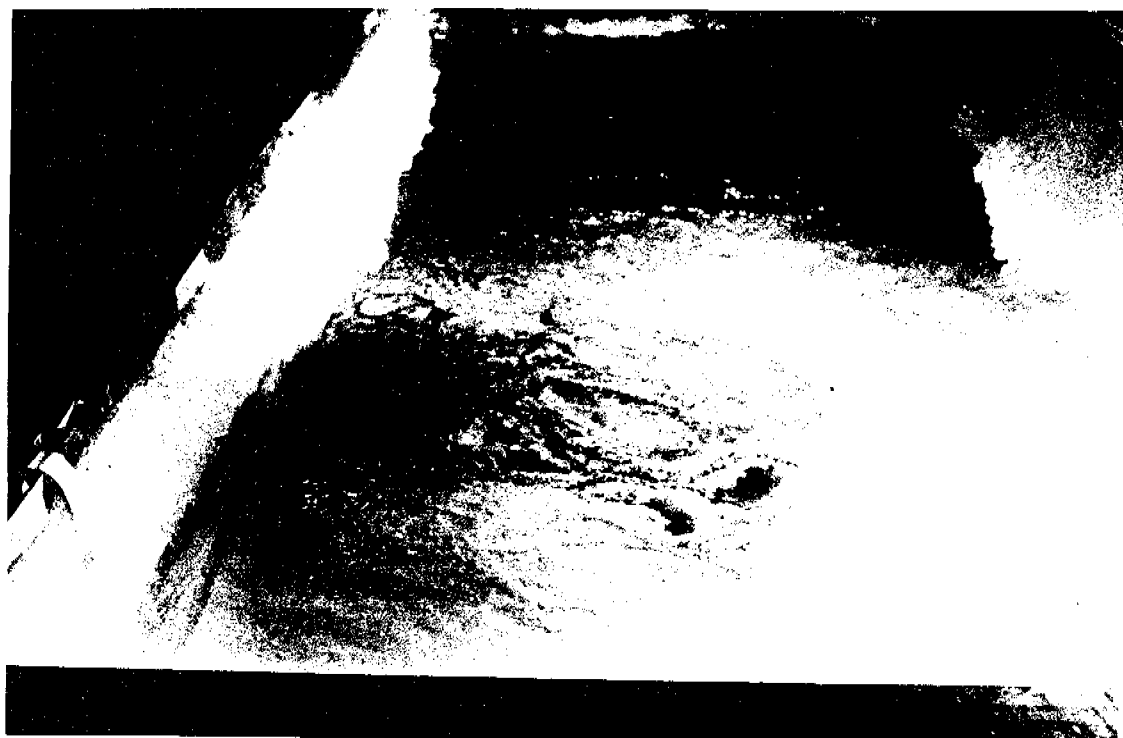


Figure 14

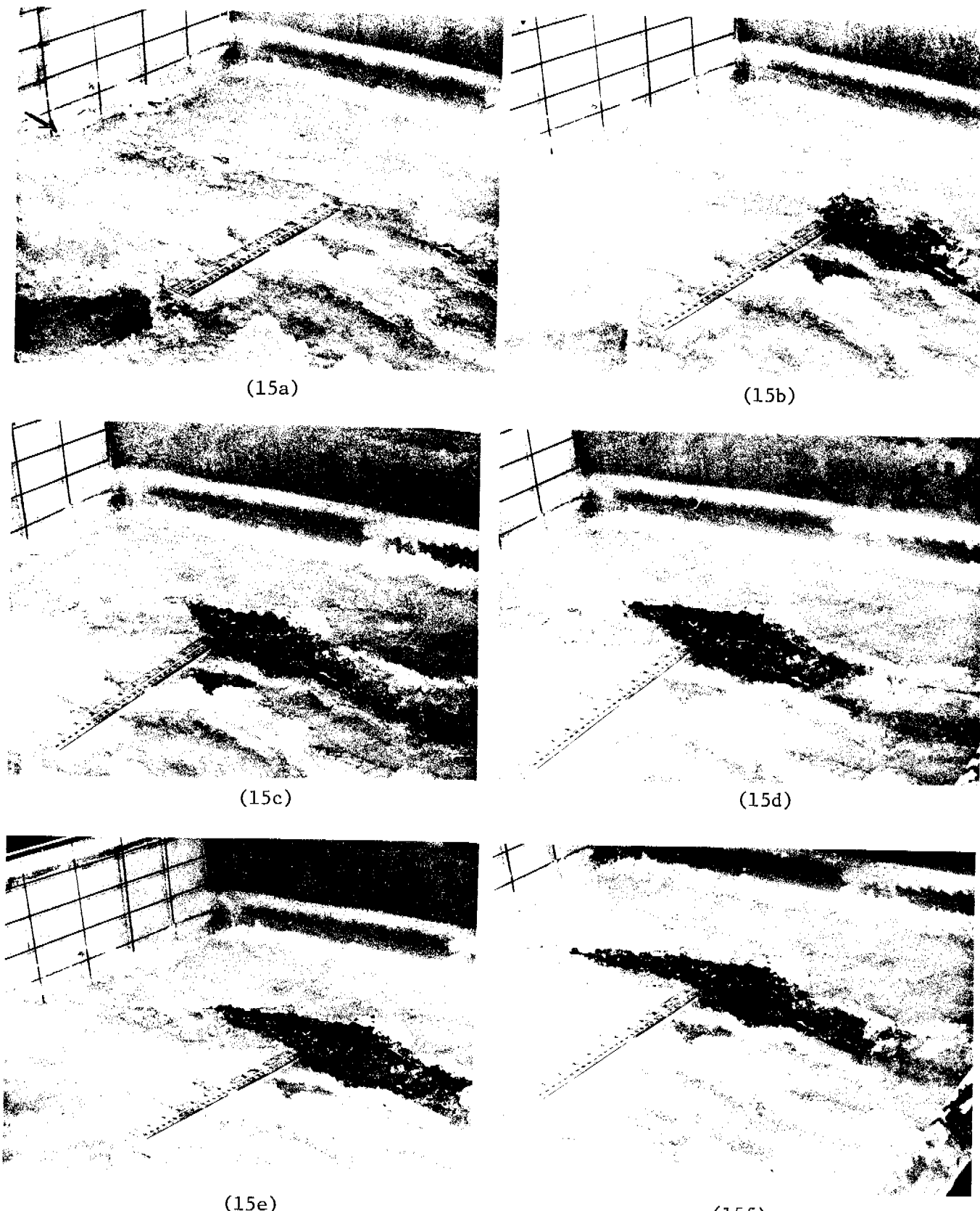


Figure 15

263



(16a)

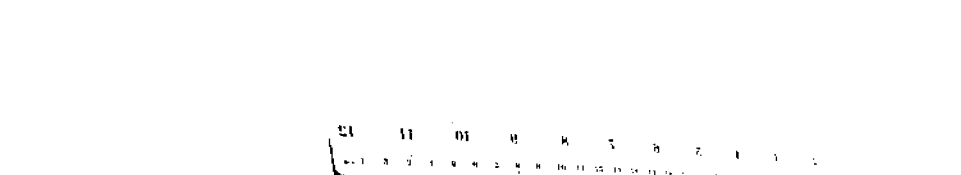
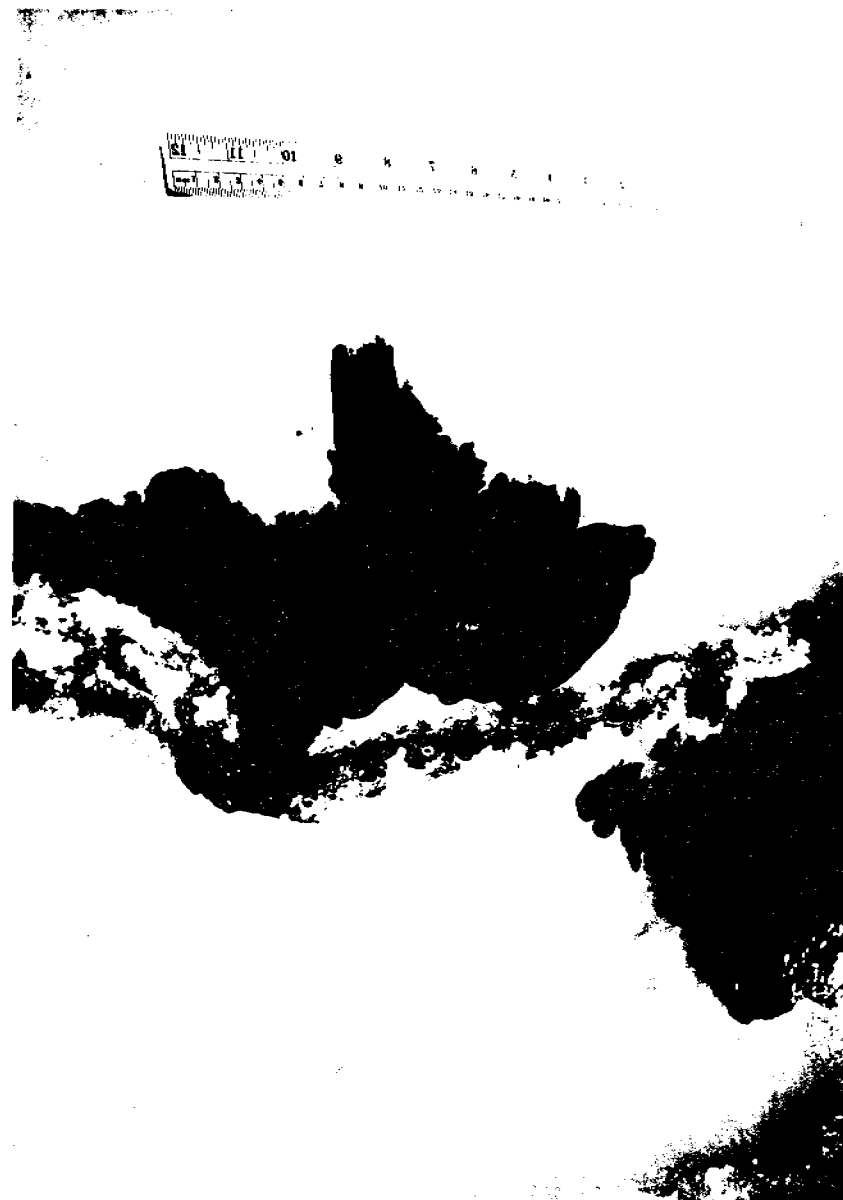
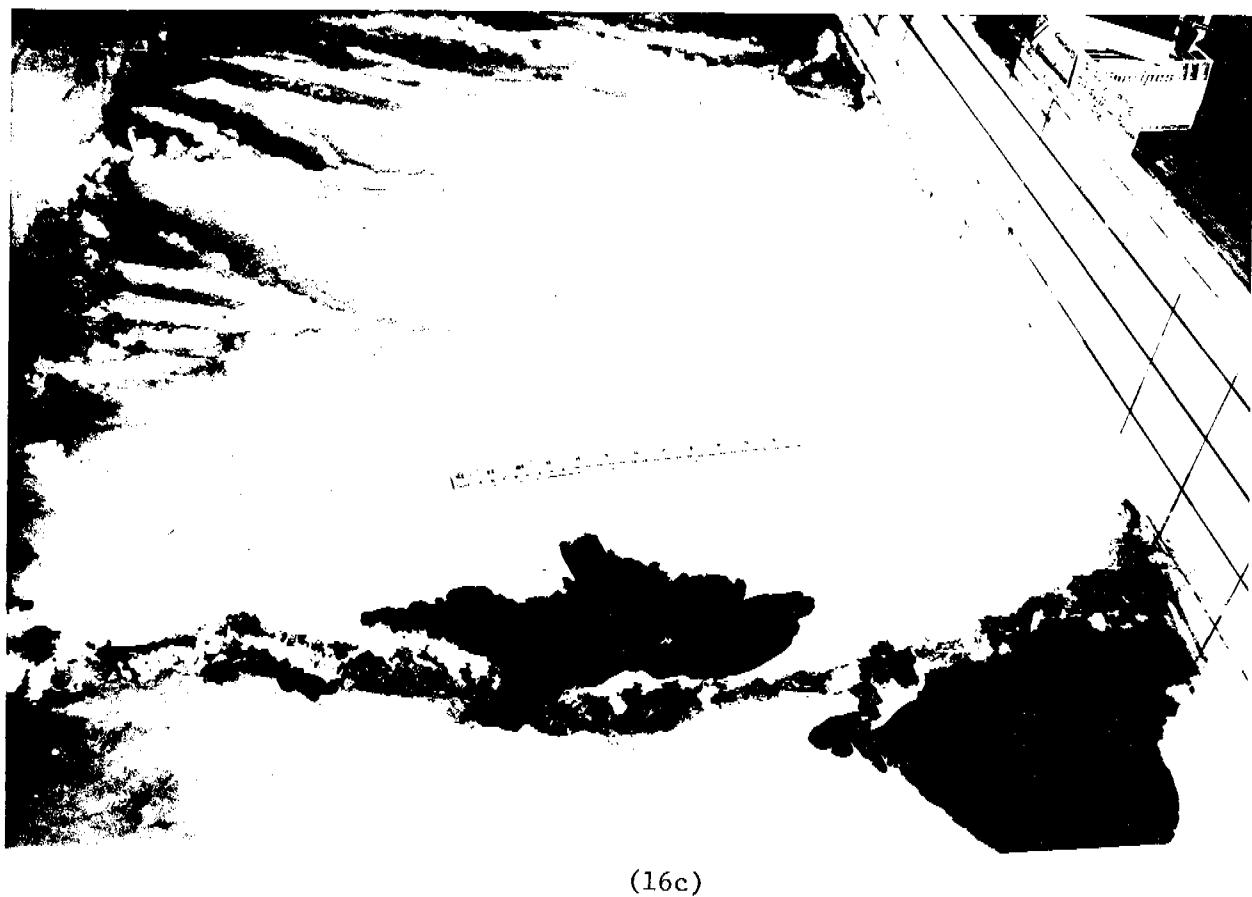


Figure 16



(16b)

32



(16c)

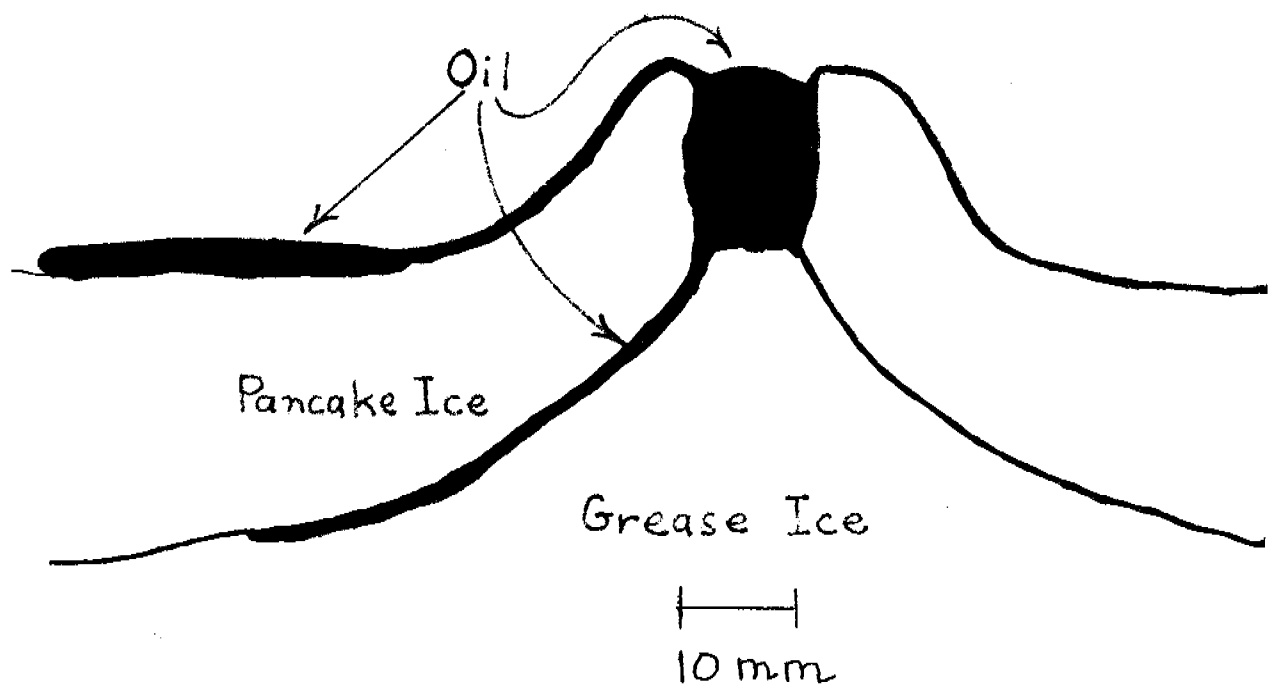


Figure 17

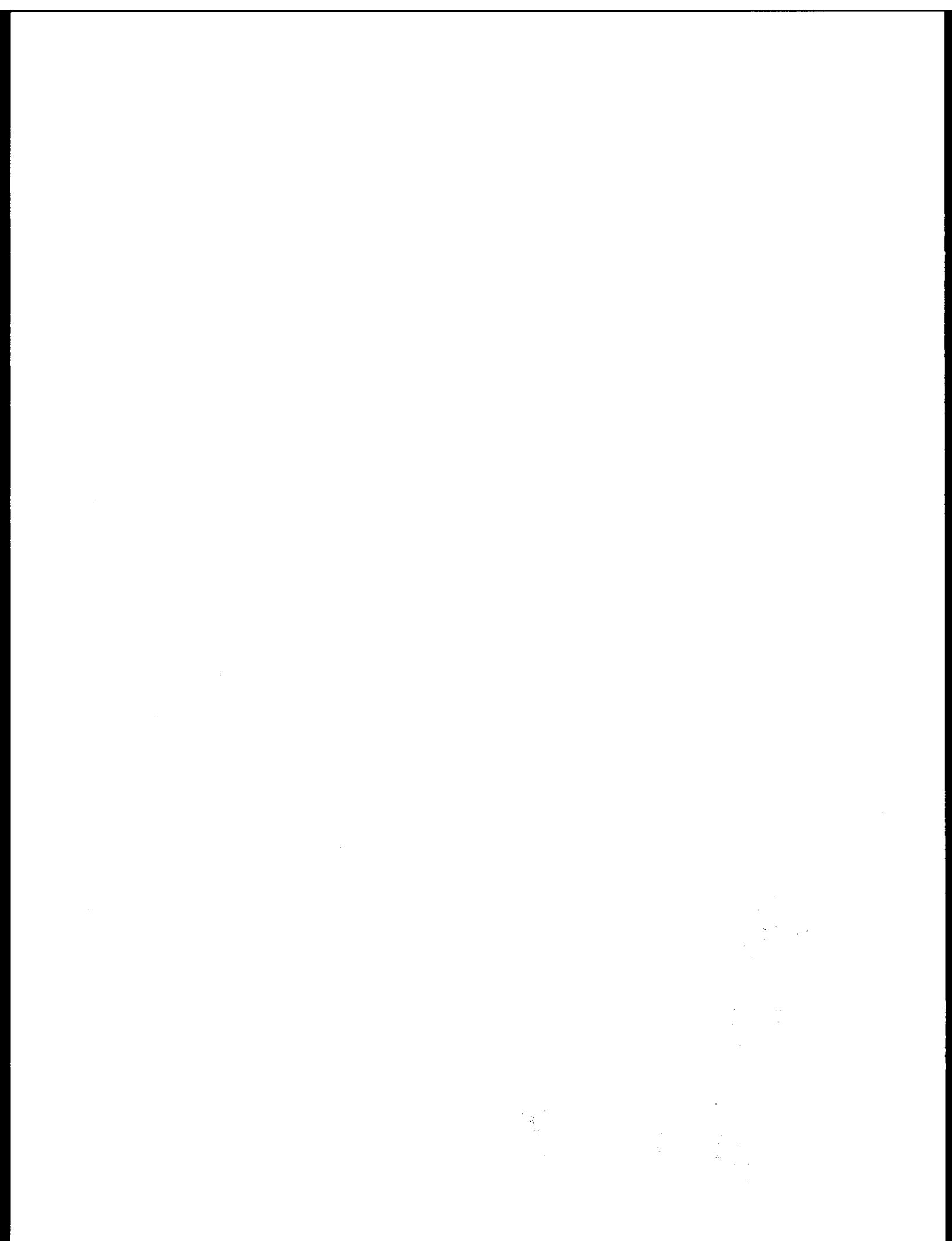


(18a)



(18b)

Figure 18



QUARTERLY REPORT

RU# 88: Dynamics of Near-shore Ice  
P.O.: 01-5-022-1651  
Reporting Period: July 1976-  
September 1976  
Number of Pages: 9

Dynamics of Near-Shore Ice

W. F. Weeks and A. Kovacs

Cold Regions Research and Engineering Laboratory  
Hanover, New Hampshire 03755

28 September 1976

## I. Task Objectives

### 1. Narwhal Island

- a. Collect quantitative information on the movements (velocities, directions, accelerations, and deformation rates) of the near-shore pack ice and the fast ice along the southern coast of the Beaufort Sea.
- b. Make observations on major ice deformation features that occur near the edge of the fast/pack ice boundary.
- c. Test the operation of an air-borne radar system for measuring the thickness of sea ice.
- d. Document the nature of the internal crystal structure of the fast ice in the vicinity of Narwhal Island.

### 2. Bering Strait

Complete arrangements leading to the installation of an ice monitoring radar system at the Bering Straits.

### 3. Remote Sensing

Obtain further laser profiles over the near-coastal sea ice.

## II. Field and/or Laboratory Activities

### 1. Narwhal Island

During the present reporting period no field observations were made and all the project personnel worked on data analysis and report writing. All data have now been reduced and are on-file in our computer. Transfer of the complete data set (ice movement observations via laser and radar and atmospheric pressure, wind speed and direction and air temperature) to the OSCEAP data bank will be completed as soon as a suitable format can be agreed upon.

Project personnel during the present period were A. Gow, A. Kovacs, S. J. Mock, W. B. Tucker and W. F. Weeks.

## 2. Bering Strait

Field inspection of the Tin City site was completed in July and discussions were initiated with the Director of Operations of the Alaskan Air Command relative to the installation of the sea ice surveillance radar unit on the top of Cape Mountain. Because of logistics problems it was decided to abandon the attempt to install an M-33 S and X-band unit and instead use a smaller 50 KW commercial X-band unit that can be installed within the existing raydome on Cape Mountain. Project personnel were M. Frank, D. S. Sodhi and W. F. Weeks.

## 3. Remote Sensing

- a. Schedule. The third series of laser flights was completed in the Chukchi and Beaufort Seas during late August using the NARL C-117.
- b. Scientific Party. M. Frank and W. B. Tucker
- c. Methods. A Spectra-Physics Geodolite Laser was used for the ice profiling. A Hasselblad 2 camera set with automatic feed magazines was also used to provide aerial photography of part of the ice included in the laser profiles.
- d. Aircraft Tracklines. 3 sampling lines were used: 1 in the Chukchi Sea starting from Barrow, and heading out to sea on a heading of  $315^{\circ}$  true and 2 in the Beaufort Sea starting from Lonely and Cross Island with a heading of  $025^{\circ}$  true. Each flight line proceeded out to sea for 200 km and back. The transects from Wainwright and Point Lay were not made because the edge of the pack was located quite far from shore at both locations. The Barter Island transect was cancelled because of low fog over the ice.

- e. Data collected. Roughness of the ice surface was measured over roughly 1000 km of total track. The majority of the data was collected with a full scale setting of 20 feet. Aerial photographs were made over representative portions of the sample tract.
- f. Data analysis. Analysis of the laser data is just starting. We currently are replaying the data tapes on an expanded ridge height and time scale so that we can conveniently make measurements of ridge heights and spacings. Analysis of the USGS SLAR imagery is also underway. Project personnel are M. Frank, W. B. Tucker, and W. F. Weeks.

### III. Results

#### 1. Narwhal Island

- a. A preliminary short paper based on the Narwhal Island data and entitled "Studies of the Movement of Coastal Sea Ice Near Prudhoe Bay, Alaska" by W. F. Weeks, A. Kovacs, S. J. Mock, W. B. Tucker, W. D. Hibler and A. J. Gow was presented at the "Symposium on Applied Glaciology" organized by the International Glaciological Society. The paper will be published in the Journal of Glaciology, Vol 19, No. 81 (1977). An expanded version of this paper is also in preparation and will be published as a CRREL report.
- b. The paper entitled "Grounded Ice in the Fast Ice Zone along the Beaufort Sea Coast of Alaska" by A. Kovacs has been completed and describes the observations made on major grounded

ice features. This paper will be published as a CRREL Report 76-32 in October, 1976.

- c. A report by A. Kovacs describing the results of the ice thickness profiling tests is currently in preparation. Preliminary results indicate that with minor modifications the unique dual antenna impulse radar system tested in April near Narwhal Island should be capable of profiling both first and multi-year sea ice thickness from the air. Data collected from the ice surface clearly reveals the undulating relief under both first and multi-year sea ice and initial data analyses have provided information on the quantity of oil which can be expected to be trapped within the depressions under both ice types. Follow up studies in 1977 verifying the preliminary results obtained in 1976 are necessary but uncertain because of funding limitations.
- d. A paper "Some Characteristics of Grounded Floebergs Near Prudhoe Bay, Alaska" by A. Kovacs and A. J. Gow will be published in the September issue of ARCTIC.
- e. A report by A. J. Gow and W. F. Weeks describing the results of the structural observations on the fast ice north of Narwhal Island is partially finished in that all the data analysis and figures have been completed. We are currently in the process of preparing the accompanying text.
- f. A report by A. Kovacs on a large pile of volcanic rocks found on an ice flow north of Narwhal Island is in preparation.

## 2. Bering Strait

- a. Final negotiations that will allow us to install our commercial X-band radar within the existing raydome on Cape Mountain have just been finalized with the Alaskan Air Command with formal approval being received on 13 September 1976.
- b. The competitive bids on supplying the 50KW marine radar system have also been received. The unit that we are selecting (Raytheon RM 1250/12XR) appears to be ideal for the task. We expect the system to be delivered to CRREL for final testing and camera mounting by the first week in October. We anticipate installing the equipment on Cape Mountain during either late October or early November 1976.
- c. A paper entitled "A Study of Ice Arching and Pack Ice Drift" has been completed by D. S. Sodhi and is currently being edited. This paper applies theoretical concepts developed for the flow of granular media through hoppers to the flow of sea ice through a narrow strait such as the Bering Strait. Predictions of the theory are compared to observations from satellite imagery.

## 3. General

A review paper entitled "Engineering Properties of Sea Ice" by J. Schwarz and W. F. Weeks is in the final stages of completion. This paper was presented at the Symposium on Applied Glaciology and will be published in the Journal of Glaciology Vol. 19, No. 81 (1977). Dr. Weeks' work on this paper was partially supported by OCSEAP.

#### IV. Preliminary Interpretation of Results

##### 1. Narwhal Island

- a. Laser observations of fast ice motion at sites close to Narwhal Island show long term changes in the distance to targets located on the ice that are believed to be primarily the result of the thermal expansion of the sea ice. The main ice motion was outward normal to the coast (in the least-constrained direction). The maximum movement was approximately 1 m with short term changes of 30 cm.
- b. Radar observations of fast ice sites further off-shore from the barrier islands do not permit the study of small motions (as do the laser records) because of insufficient measurement resolution. However, these records show many larger events with the standard deviation of the motion measured parallel to the coast increasing systematically with distance off-shore reaching a value of  $\pm 6.6$  m at 31 km. The ice motions show short term displacements of as much as 12 m at the sites furthest from the coast. The observations also show systematic changes in line length (up to 6 m over a distance of 30 km) that are believed to be the result of thermal expansion of the ice. Correlations between the wind and the ice movement are only appreciable for movements normal to the coast.
- c. Radar targets located within the pack ice showed large short term movements (up to 2.7 km) but negligible net motion along the coast. There was no significant correlation between the

motion of the pack and the local wind suggesting that models for predicting coastal ice movement in the Beaufort Sea during the March-June time period can only succeed if they are handled as part of a regional model which incorporates the lateral transfer of stress through the pack ice.

- d. Off-shore from Narwhal and Cross Islands the fast ice-pack ice boundary was usually located (during March-May 1976) in 30 to 35 m of water as opposed to 18 m of water where the boundary has been observed at sites further west along the Alaskan coast.
- e. The large grounded multiyear shear ridge formations that were studied along Beaufort Sea coast in the Harrison Bay/Prudhoe Bay area must be considered as formidable obstacles in the development of off-shore operations in this region. In the design of off-shore drilling structures significant considerations must be given to not only the forces which can develop when these formations are pushed against the structures, but also to the potential for ice piling up and over riding them. The inner edges of the multi-year shear ridge formations studied north of Cross Island were found to be as high as 12.5m and to be grounded along the ~15 m depth contour. This depth is significantly less than the ~19 m contour previously considered to be the water depth at which grounded shear ridges begin to form. The grounded ice formations studied formed in the fall of 1974 and have remained through the summer of 1976.

V. Estimate of Funds Expended (as of 30 September 1976)

	<u>Original</u>	<u>Expended</u>	<u>Remaining</u>
Narwhal Island	\$184,198	\$185,198	\$ 0
Bering Strait	\$ 98,579	\$ 98,579	\$ 0
Remote Sensing	\$ 42,000	\$ 42,000	\$ 0

QUARTERLY REPORT

Contract: 03-50-022-67, No. 5  
Research Unit: 98  
Reporting Period: 1 July - 30 Sept. 1976  
Number of pages: 4

DYNAMICS OF NEAR SHORE ICE  
(Data Buoys)

Norbert Untersteiner  
Professor of Atmospheric Sciences and Geophysics  
AIDJEX Project Director  
Division of Marine Resources  
University of Washington  
Seattle, Washington 98195

1 October 1976

## I. Task Objectives

The University of Washington, under Task Order No. 5 of NOAA Contract 03-5-022-67, as amended, agreed to deploy 20 ice buoys to gather data on ice movement and oceanographic and atmospheric conditions in the near-shore areas of the Beaufort and Chukchi Seas of the Arctic Ocean and assist with the development of six additional buoys for later deployment. The buoy developments were to be accomplished in conjunction with field work being conducted by the Arctic Ice Dynamics Joint Experiment (AIDJEX). Three types of buoys were developed and produced for the task under contracts from the NOAA Environmental Research Laboratory monitored by the NOAA Data Buoy Office (NDBO). Fourteen of the buoys are designed to be dropped by parachute from aircraft and report position through the Random Access Measuring System (RAMS) of the NIMBUS-6 satellite. Two additional buoys of this type have been modified to include a pressure sensor. All 16 of these buoys and the six future buoys are produced by Polar Research Laboratory, Inc., (PRL) of Santa Barbara, California. The other four buoys are of a more complex design and are instrumented with atmospheric pressure and temperature sensors, current meters at 3 and 30 meters under the ice, and a RAMS platform to provide position. Again, all data are transmitted through the NIMBUS-6 satellite. These buoys were developed and produced by the Applied Physics Laboratory, University of Washington. Data from the buoys are placed in the AIDJEX Data Bank after receipt from NASA.

## II. Field and Laboratory Activities

### A. Field trip schedule

None.

### B. Scientific party

None.

C. Methods

1. All the buoys mentioned in this report are sampled by the Random Access Measurement System on board Nimbus VI. Position is determined and barometric pressure and ocean current data are recovered several times each day.

D. Sample localities

No new deployments.

E. Data collected or analyzed

1. A total of 14 OCS buoys were tracked during the quarter, the movements of which correspond to the ice drift. Useful barometric measurements were obtained from two of these buoys, and ocean mixed-layer currents were measured from two other buoys.
2. The position data are being corrected, filtered, and smoothed to produce estimates of position at uniform times. The ocean current data are being decoded and uniform data files are being constructed.
3. The buoys which operated through the quarter drifted an average of 150 miles to the northwest (Figure 1).

III. Results

1. Two of the three Met-Ocean buoys operating at the beginning of the period continued to operate at the end. The failure mode of the third buoy, which was not providing good environmental data, is unknown, but it is unlikely that the power supply was depleted.
2. Five of the eight air-drop buoys deployed in December 1975 were operating at the beginning of the quarter. One of these buoys continues to operate at the end of the quarter, a total of nearly 10 months. The other buoys lasted 6-8 months, which was the design goal.

3. Three of six air-drop buoys deployed in March 1976 continue to operate at the end of the quarter, and can be expected to quit in October. One of three which quit did so after only four months of operation and may have been consumed by the ice in the active coastal shear zone in which it was deployed. Another failed after nearly six months of operations and having drifted on an ice floe away from the edge of the ice pack, as revealed by satellite imagery. The last of the three which failed did last six months, despite the extra power required to operate a barometric pressure sensor.

#### IV. Preliminary Interpretation of the Results

The ice movement in the summer was dramatically different than from the previous summer in that large westerly and offshore movement occurred. Buoys to the north and east moved to the east and shoreward in agreement with the long-term mean clockwise gyre characteristic of ice movement in the Beaufort Sea. In fact, ice drift this summer contrasts most sharply with that in the summer of 1975 in that stagnation and anti-clockwise drift, common in summer months and prevalent in 1975, was notably absent this year.

#### V. Problems Encountered and Recommended Changes

The small safety margin in power supply of the air-drop buoys and the disparity in performance between Met-Ocean buoys makes the recovery of buoys for engineering evaluation desirable.

#### VI. Estimate of Funds Expended

As of 30 September, actual expenditures under this contract totaled \$71,094.13. The estimated obligation under the contract which were not yet expended were about \$4,506.87.

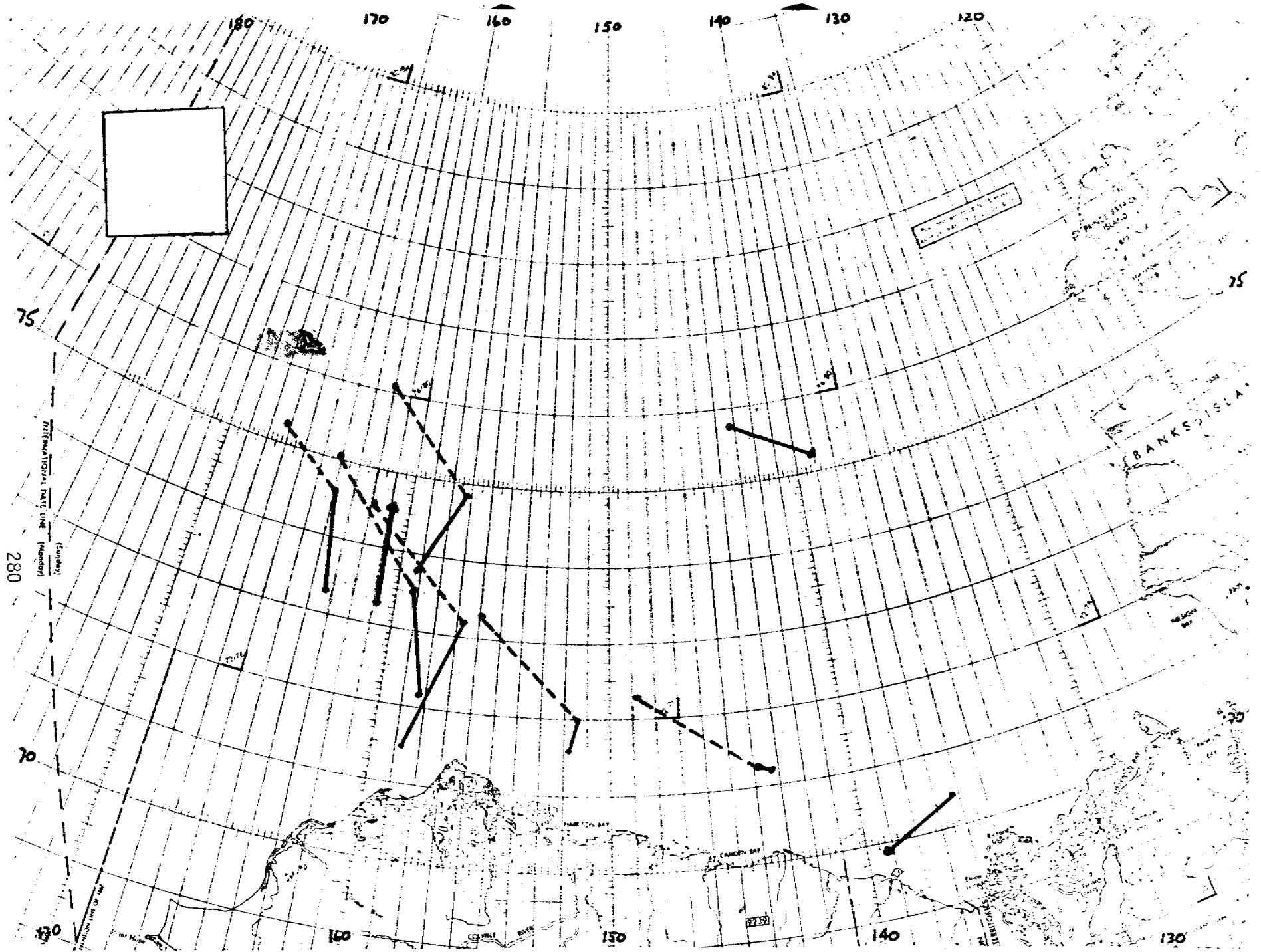
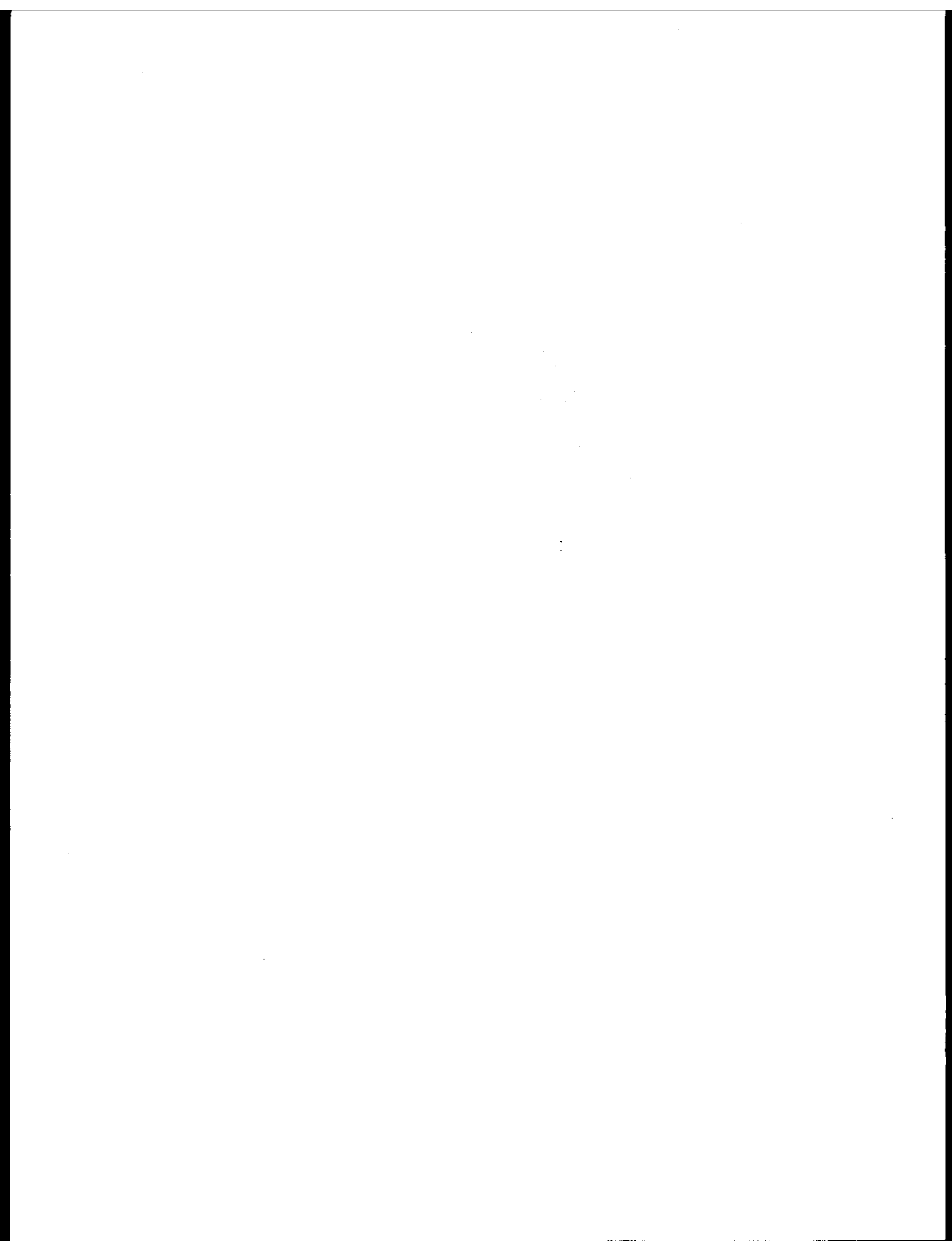


Figure 1. Ice Movement July 21 - August 26 —

August 26 - September 19 - - - - -

RU# 244

A LAR SYS printout is available from the Principal Investigator.



#### Appendix 1: LARSYS printout. (SAMPLE ONLY)

BATMED  
L.A.BARTOLUCCI

LABORATORY FOR APPLICATIONS OF REMOTE SENSING  
PURDUE UNIVERSITY

SEPT 8, 1976  
11 38 16 AM  
LARSYS VERS104

## OUTLINED FIELDS IN CLASSIFICATION OF FAST-ICE

CLASSIFICATION STUDY 612947013  
RUN NUMBER..... 74031601  
FLIGHT LINE... 170221093 ALASKA  
DATA TAPE/FILE NUMBER.. 2706/ 3  
REFORMATTING DATE, FEB 21,1976

CLASSIFIED MAY 7, 1976  
DATE DATA TAKEN... JUNE 25, 1974  
TIME DATA TAKEN.... 1009 HOURS  
PLATFORM ALTITUDE..3062000 FEET  
GROUND HEADING.... 180 DEGREES

CLASSIFICATION TAPE/FILE NUMBER: 673/

#### CHANNELS USED

CHANNEL 1 SPECTRAL BAND 0.50 TO 0.60 MICRORAMETERS CALIBRATION CODE = 1 CO = 0.0  
CHANNEL 2 SPECTRAL BAND 0.60 TO 0.70 MICRORAMETERS CALIBRATION CODE = 1 CO = 0.0  
CHANNEL 3 SPECTRAL BAND 0.70 TO 0.80 MICRORAMETERS CALIBRATION CODE = 1 CO = 0.0

## CLASSES

SYMBOL	CLASS
*	NULL 0.1
	2
-	3
=	4
#	5

SYMBOL	CLA
/	6
1	7
0	8
2	9
x	10

#### TEST EISLOS DILUTED WITH A

400  
401  
402  
403  
404  
405  
406  
407  
408  
409  
410  
411  
412  
413  
414  
415  
416  
417  
418  
419  
420  
421  
422  
423  
424

QUARTERLY REPORT

Contract #03-6-022-35179

Research Unit #244

Reporting Period: July 1 - Sept. 30, 1976

Number of Pages: 27

STUDY OF CLIMATIC EFFECTS ON FAST ICE EXTENT  
AND ITS SEASONAL DECAY IN THE CHUKCHI SEA AREA

Principal Investigator

R. G. Barry

Acting Director, Professor of Geography

Institute of Arctic and Alpine Research

University of Colorado

Boulder, Colorado 80309

September 30, 1976

## I. TASK OBJECTIVES

The primary objective of this study is to assess the role of climatic factors in determining the extent and seasonal decay of fast ice along the Chukchi Sea coast. Emphasis during this quarter has continued to be placed on analysis of meteorological data due to the delay in delivery of Landsat imagery ordered from EROS.

## II. 1. FIELD ACTIVITIES

None.

## II. 2. OFFICE ACTIVITIES

### A. Period

1 July - 30 September 1976.

### B. Personnel

R. G. Barry - Principal Investigator

J. Rogers - Research Associate

R. Keen - Research Assistant

G. Wohl - Research Assistant (from 15 July)

M. Eccles - Programming Consultant

### C. Methods

#### 1. Mapping Ice Surface Morphological Characteristics

Landsat imagery now acquired is being used to map ice surface characteristics of the shorefast ice during the decay seasons of 1973-75. The location of ice features is determined by overlay techniques as follows. An outline of the coastline and significant landmarks is traced onto clear acetate from the OCS 1:1,000,000 scale UTM map. Geographical coordinate grid

ticks are also traced for use as registration marks. The LANDSAT scene under consideration is then fixed to a light table beneath the overlay. On the image, the sections of coast and/or landmarks nearest to a given ice feature are aligned with the overlay and the outline of the ice feature is traced. After each image is mapped in this way, the ice feature outlines are transferred to our sector maps, also based on the OCS UTM projection, using the grid ticks for registration.

Identification and interpretation of significant LANDSAT ice information is divided into two stages. First, each decay season's set of sequential Landsat images is examined, sector by sector. Where available, Dr. Stringer's OCS maps will also be used as a reference. Areas of homogeneous-appearing grey tone and texture are then delimited and mapped on the overlays. Images of poor quality (e.g., underexposed and underdeveloped) are also analyzed on the Spatial Data Systems Datacolor machine (Model #703, SOS, Inc., Goleta, CA.), which divides the continuous photographic gray tones into discrete levels and displays these in color-coded form. This procedure facilitated the grouping or separating of ice areas based on gray-scale tone.

In the second stage, the imagery and maps are viewed again and the mapped gray tone and texture areas are interpreted. The interpretive keys used in this step are based on:

- (1) Field experience of the analyst(s) along the northern Chukchi Sea coast (see field reports in Quarterly Reports).

- (2) Detailed analysis of the spectral characteristics of melt-season ice types on LANDSAT data for a scene from the Beaufort Sea area (See Quarterly Report, September 30, 1976, Contract #03-5-022-91).
- (3) Available literature discussing ice-interpretation from LANDSAT data.
- (4) Inferences gleaned from the time-sequential behavior of the ice on LANDSAT data.

2. Meteorological Data

a.) Mean sea-level pressure patterns.

The synoptic typing scheme is similar to that used for the Beaufort Sea (Annual Report, March 1976, #03-5-022-91), with two changes: The Chukchi grid is a 5 x 7 point subset of the NMC grid, shown in Fig. 1; the clustering was done using the normalized pressure grids for a 1866-day sample selected by a random number program.

b.) Wind Indices

Seventeen wind indices have been computed on a daily basis for the Chukchi Sea area bounded by grid points 13, 14, 18, 19, 23, and 29 in fig. 1. Pressure differences between grid points are converted into wind speed (V, m/sec) using the geostrophic equation

$$V = \frac{RT}{pf} \frac{\Delta p}{\Delta x}$$

where: R = gas constant for dry air

T = the normal monthly temperature for the region,  
averaged between Barrow and Kotzebue

p = average pressure at the two points

f = Coriolis parameter

$\Delta p$  = pressure difference between the two points

$\Delta x$  = distance between the two grid points

The seventeen surface wind indices computed, and the grid point pairs used, are:

1. On Shore, 18-14
2. 2 On Shore, 23-14
3. Long Shore, 19-13
4. Southerlies 72N, 14-13
5. Southerlies 68N, 19-18
6. Southerlies 65N, 24-23
7. Westerlies 70N 170W, 18-13
8. Westerlies 70N 160W, 19-14
9. Westerlies 66N 170W, 23-18
10. Westerlies 66N 160W, 24/19
11. Average Southerlies: Mean of Indices 4,5,6
12. Average Southerlies: Mean of Indices 4,5
13. Average Westerlies 70N: Mean of Indices 7,8
14. Average Westerlies 66N: Mean of Indices 9,10
15. Average Westerlies 170W: Mean of Indices 7,9
16. Average Westerlies 160W: Mean of Indices 8,10
17. Average Westerlies All: Mean of Indices 7,8,9,10

D. Localities

Not applicable.

E. Date Collected/Analyzed

### 1. Landsat Imagery obtained

The Landsat images now obtained from EROS for analysis are listed in Table 1. The late delivery of this imagery has permitted only preliminary analyses to be carried out during this quarter.

### 2. Meteorological Data

- 1.) Daily NMC grid-point MSL pressure data have been analyzed using the methods summarized in Section II.C.2. for the area shown in Fig. 1 for the period 1946-73.
- 2.) Daily wind indices, as detailed above, together with their monthly means and standard deviations, have been calculated for 1966-73 and exist as a punched card file.
- 3.) Landsat images have been analyzed for a case study discussed in Section IV as follows:

(1) Landsat 1694-22071	6/17/74
(2) Landsat 1710-21551	7/3/74
(3) Landsat 1727-21485	7/20/74

Meteorological data for this study were wind directions (geostrophic) computed between grid points of the NMC pressure data for the northern Chukchi and western Beaufort Sea.

## III. RESULTS

### A. Synoptic type maps

The grid-point printouts of the MSL pressure patterns for 22 key days have been obtained. Figures 1A through D illustrate the first four types. Type 1 encompasses 31% of all the days in the catalog. Two

catalog file tapes have been made; one listing, for each day, the synoptic type classification, the score with that type, and the central pressure, mean pressure, and RMS pressure variation across the 5 x 7 grid point field; the other listing only the type classification by date. A tape file will be provided during the next quarter.

B. Index tables and graphs

Tables of monthly normals and standard deviations of the indices have been produced. They are:

Table 2. Mean values of the indices, by months, for the period 1946-73. N is the number of days for which each mean was computed. Two additional indices, resultant velocity and direction, were computed from indices 12 and 13, using the equations

$$V = \sqrt{I_{12}^2 + I_{13}^2}$$

$$\text{Dir} = \text{Arctan}(I_{13}/I_{12}) + 5.4^\circ$$

These two indices give the average winds in the box bounded by grid points 13,14,18, and 19 in polar coordinates. The direction is in degrees east of north.

Table 3. The standard deviation of the N days about the 28-month mean.

The resultant standard deviation ( $SD_r$ ) was computed from

$$SD_r = \sqrt{SD_{12}^2 + SD_{13}^2}$$

and is the radius of the 1 standard deviation circle about the vector point defined by the resultant velocity and direction.

Table 6. Standard deviation of the 28 individual monthly means about the aggregate mean. Resultant computed as in Table 3.

Table 5. Average of the 28 standard deviations computed for days within each of the 28 months. Resultant as in Table 3.

Table 6. Average of the 28 standard errors computed for each month. These values are those in Table 5 divided by  $\sqrt{N/28}$ .

Table 7. The ratio of Table 4 / Table 6.

Two graphs are:

Fig. 2. 12-month running means of Chukchi winds, computed from the monthly means and standard deviations for indices 12 and 13. These running means were converted into resultant directions, speeds, and standard deviations using the methods given for Tables 2 and 3.

Fig. 3. Yearly seasonal means have been computed for four seasons, defined as:

Summer: June-August

Winter: September-May

Spring: January-May

Annual: January-December

In Fig. 3, the yearly value of the summer resultant direction, and various running means, are plotted. The weights of the running means are shown on the figure.

#### IV. INTERPRETATION

##### A. Meteorological Indices

When considering monthly averages and standard deviations, many of the indices exhibit very similar seasonal and interannual variability. As a result some of the indices are not worth further consideration. In

future work only the composite indices, 11, 12, 14, and 17, which are considered to provide the most complete representation of the individual Westerly and Southerly indices, are used, together with the Onshore and Longshore indices 1, 2, and 3, and the resultant indices.

Table 2 shows the prevailing winds to be E to ENE in all months of the year, except July when they are light SE'ly.

The standard deviation of the individual monthly means (Table 6) is, in general, larger in winter than in summer for all indices.

The standard deviation of days within a month (Table 5) is also larger in winter, and therefore so is the average standard error (Table 6).

The ratio of the year-to-year variability of monthly means to the standard error of the estimate of individual monthly means (Table 7) is an index of the significance of the interannual variability of each index. This ratio is constant throughout the year at about 2.0 for all the southerly indices, while for the westerlies it is greater in winter ( $\approx 2.5$ ). The larger ratio for westerlies than for southerlies in all months of the year implies that the fluctuations of longer than a year are most pronounced in the strength of the E-W component of the flow, and that anomalous N-S components have a smaller amplitude of variability on these time scales.

The 12-month running means fail to show any true periodicities, although some quasi-periodicities lasting three cycles or so are apparent. There is an inverse relationship between the values of the standard deviation and speed, i.e., within a twelve month period, greater daily

variability leads to a lower mean speed.

The running means of the summer wind direction (Fig. 3) fail to show any consistent periodicity, but a trend is apparent in the longer running means. Winds were SE'ly in the early 1950's, backing to E'ly in the 1960's, and since 1970 returning to SE'ly.

B. Comparison of Chukchi and Beaufort Synoptic Types

To compare the selection of synoptic types for the Chukchi and Beaufort typing schemes, the Beaufort type classification and score was found for each of the 22 Chukchi type key dates. These data, including the percentage frequency for the Chukchi types are listed in Table 8. The reverse comparison (Chukchi classification of Beaufort key dates) has also been made, but is not listed.

All 22 of the Chukchi key dates are classified in the first 10 of the 21 Beaufort types, (i.e., the most frequently occurring) implying a general independence between the types. Seven of the Chukchi key dates are classified as Beaufort Type 3, and three as Beaufort Type 5. The primary feature in Beaufort Types 3 and 5 is a low over southeastern Chukchi and to influence its pressure gradients.

In only three cases does the comparison between Beaufort and Chukchi Types compare with the reverse comparison. The Chukchi and Beaufort Types for these cases are, respectively, 1 and 1, 7 and 10, and 12 and 2. Apparently, these three cases are the only ones where the dominant feature in both the Chukchi and Beaufort types is located in the region of overlap between the two grids. These results suggest that it may be necessary to work with the independent classifications rather than attempting to develop a common classification scheme for the larger

area as originally planned.

C. A Case Study of the Similarity of Break-up Patterns at Peard Bay and Pt. Barrow

In the Chukchi and Beaufort Seas several factors affect the extent and decay of the fast ice including meteorological parameters, ocean bottom depth, and the contour and direction of the shoreline. With regard to the latter factor, the Beaufort Sea coast has a relatively unchanging west-northwest to east-southeast orientation as compared with, on the one hand, the southwest to northeast orientation in the Chukchi between Cape Lisburne and Barrow and the northwest to southeast orientation between Pt. Hope and Kotzebue on the other. These differences in shoreline contour and direction will account for differences in the effect of some meteorological parameters, such as wind direction, on the break-up of fast ice between the two seas. However, this case study shows that in two different areas, one on the Chukchi Sea (Peard Bay), and one on the Beaufort Sea (Pt. Barrow to Cape Simpson), the timing and manner of break-up are approximately the same under conditions of similar shore line orientation and meteorology.

The data for this study are listed in Section II.E.3. Similar to the area of fast ice east of Pt. Barrow, the Peard Bay region is characterized by (1) a relatively large area of offshore fast ice, (compared to much of the Chukchi Sea), (2) a general west-east shoreline orientation, and (3) barrier islands.

The scene of 17 June 1974 (1694-22071), shows the large fast ice region in the Peard Bay area bounded by a large lead in the Chukchi.

The smaller and smoother appearing section of this fast ice, largely enclosed by barrier islands, is darkening and probably puddling. The 3 July 1974 image (1710-21551) shows little dissimilarity in degree of darkening of the fast ice in the Beaufort and Chukchi. The 20 July 1974 (1727-21485) Landsat image is the crucial one to this analysis, showing that the fast ice both in the area northeast of Pt. Barrow and northeast of Peard Bay is breaking up and clearing of ice. Fast ice areas along the Chukchi coast that are oriented more north-south are not breaking up. The break-up was possibly induced by a wind event, probably southerly and westerly winds, since in both areas the ice has cleared to the northeast of the barrier islands and not within the barrier islands except where they are not conterminous. The area of open water is about the same in both regions.

Wind direction data derived from the NMC grid point pressure data for the northern part of the Chukchi and western Beaufort seas shows that south-southwesterly winds prevailed on three days (July 14, 17, and 18) prior to these break-up events. Southwesterly winds had only previously occurred on July 1 and one day in mid-June. It is hypothesized that similar temperature conditions prevailed over these two areas, causing weakening and melting of the ice, and then the occurrence of the moderately southerly winds allowed for removal of the ice since other factors were also nearly the same (i.e. shoreline orientation and barrier islands). Break-up in the remainder of the Chukchi would be delayed until later that summer. These inferences will be examined more closely in future analyses.

The Peard Bay area appears to have two fast ice regimes, one of heavily ridged ice which characterizes the Chukchi as a whole and does not break-up until later in the summer, and a second area of fast ice which is well protected and thus similar to the Pt. Barrow region.

General differences in the relationship between pack and fast ice in the Beaufort and Chukchi Seas can also be seen in the Landsat imagery. In the Beaufort the fast ice generally melts and breaks up while the pack ice remains in the Sea up to the 20 meter isobath. In the Chukchi, however, pack ice is generally moving southward and the pack may clear leaving open water in the sea while the fast ice remains in place for a few more weeks. In the Beaufort Sea pack ice is always within one or two days from the Alaskan Coast if favorable storm winds were to occur and blow the ice in. Most of the Chukchi will not have ice within the vicinity of the Alaskan Coast during the summer.

#### V. PROBLEMS/RECOMMENDATIONS

The delay in delivery of Landsat imagery from EROS forced concentration on the meteorological phase of the study. About 60% of the imagery ordered is now on hand and interpretation and mapping will be emphasized in the next quarter. The parallel analysis for the Beaufort Sea coast has demonstrated the great importance of having SLAR coverage for more reliable interpretation of Landsat data. The provision of such imagery is strongly recommended. Future work under this project will be facilitated by the merging of the continued programs for the Beaufort and Chukchi Sea coasts.

#### VI. ESTIMATE OF FUNDS EXPENDED

\$13,500.00

SUMMARY OF OBJECTIVES AND FINDINGS  
WITH RESPECT TO OCS DEVELOPMENT PLANNING

The objective of this study is to assess the role of climatic factors in determining the extent and seasonal decay of fast ice along the Chukchi Sea coast. Analyses to date have concentrated on the climatic data due to slow delivery of satellite imagery. Preliminary results suggest that the timing and manner of fast ice break-up are closely comparable along shorelines of similar orientation and meteorology on the northern Chukchi Sea and western Beaufort Sea coasts. However, the atmospheric circulation patterns affecting the two coasts appear to be sufficiently different to require the use of independent classification schemes (already developed).

TABLE 1.

<u>Landsat Scenes for the Chukchi Sea Coast</u>			
Landsat Number	Bands	Landsat Number	Bands
101022145	4	129521590	4
100822034	4	131221531	4,7
104622145	4,7	131321585	4,7
104622143	4,7	131422043	4,7
106222035	4	133422155	4,6
101022142	4,7	130022271	4
101022135	4,7	131922324	7
104422024	4	131622153	4,7
122622162	4	130022265	4
122622153	4	131922322	4,7
124222034	4	134921571	4,7
124322093	5	135122095	4,7
126222151	7	133522210	4,7
124121591	4	131722205	4,7
126222160	4	131722203	4,7
126222154	4	133522204	4,7
122722214	4	133722321	4,7
125921591	4	133522201	4,7
127922092	4	138722092	5,7
129622033	4	138722083	4,7
129822161	4	140622145	5
133021525	4,7	140722200	5

Landsat Number	Bands	Landsat Number	Bands
140622133	5	162021574	5
143921565	7	163821572	5
144022023	4	163821583	5
142622252	7	162422210	5
144222131	7	162222093	5
145922063	4	162122032	5
146222240	4	162322154	5
140722194	5	163922032	5,6
140522075	5	165521522	4
138722090	5,7	165621580	4
156621595	4	165521510	5
156722053	6	165722025	4
158822220	4	166022200	4
158722160	4	165922144	4
160121533	4	167522031	5
160322034	4	167722141	4
160422093	5	167321515	5
160522154	4	167421561	4
158622110	6	167421573	4
161921531	5	169422082	4
158722162	4	169422080	4
158622095	4	169522073	4
160221580	4	169422071	5
160522160	4	169522134	4

Landsat Number	Bands
174421434	4
174822063	4
173022064	4
174922115	4
173022062	4
173122120	4
171021562	4,7
171021551	4,7
172721485	4,7
171322121	4,7
171422182	4,7
180222043	4
180322094	4
180222034	6
180322092	4
180322085	4
181721471	4
182122094	4
177921364	4
180222040	6
183521463	4
194521521	4
194722043	4
194621582	4
198121515	4
198322025	4

**TABLE 2**  
MONTHLY NORMALS OF CHURCHI SEA WIND INDICES; 28-YEAR AVERAGE

MONTH	N	ON SHORE	2 ON SHORE	LONG SHORE	SOUTHERLY 72N	WINDS 68N	70N 170W	WESTERLIES 160W	66N 170W	66N 160W	
1	855	-2.1	-3.8	-2.4	.0	-1.5	.5	-2.9	-3.5	-5.7	-4.7
2	783	-1.9	-4.5	-5.2	-1.6	-3.2	-2.3	-4.2	-5.8	-7.5	-6.6
3	863	-1.8	-3.7	-4.5	-1.0	-2.7	-2.4	-3.6	-5.3	-5.8	-5.4
4	836	-2.2	-3.4	-4.2	-1.5	-2.4	-2.2	-3.6	-5.4	-4.5	-4.3
5	866	-2.8	-3.5	-3.9	.1	-1.7	-1.8	-3.8	-5.6	-4.0	-4.0
6	837	-1.6	-1.6	-2.0	.5	-1.1	-1.2	-1.7	-3.3	-1.3	-1.3
7	865	-1.1	-1.6	.2	1.2	.6	1.0	-1.3	-1.0	.2	.6
8	867	-.9	-1.2	-1.4	-.1	-.6	.1	-1.4	-1.9	-1.4	-.7
9	839	-1.3	-2.3	-3.6	-1.2	-2.1	-1.8	-3.0	-3.9	-3.4	-3.0
10	857	-2.1	-3.2	-3.6	-.6	-1.5	-1.0	-3.6	-4.4	-4.2	-3.8
11	839	-2.9	-4.5	-4.2	-.8	-1.0	.1	-4.9	-5.1	-6.1	-4.9
12	866	-1.6	-3.6	-4.3	-1.5	-2.4	-1.4	-3.7	-4.6	-6.0	-5.0
-YEAR	19173	-1.8	-3.0	-3.2	-.5	-1.5	-1.0	-3.1	-4.1	-4.1	-3.6

**TABLE 3**

STANDARD DEVIATION OF ALL DAYS

MONTH	N	ON SHORE	2 ON SHORE	LONG SHORE	SOUTHERLY 72N	WINDS 68N	70N 170W	WESTERLIES 160W	66N 170W	66N 160W	
1	855	6.3	6.2	7.9	6.3	7.9	8.7	7.2	8.1	7.8	7.4
2	783	5.0	6.0	7.0	5.2	6.8	7.5	6.8	7.9	7.4	7.0
3	863	5.4	5.5	6.8	5.2	6.5	7.1	6.5	7.2	7.0	6.6
4	836	5.0	5.1	7.1	5.3	7.0	7.6	6.1	7.0	6.8	6.5
5	866	4.2	4.2	5.8	4.4	5.7	6.3	5.0	6.0	5.7	5.5
6	837	3.9	3.4	5.6	4.5	4.8	5.1	5.0	5.7	5.0	4.5
7	865	4.1	3.3	5.6	4.9	5.2	5.1	5.1	5.4	5.0	4.4
8	867	4.5	4.3	5.9	5.0	5.7	6.2	5.4	6.1	5.6	5.3
9	839	5.2	5.0	6.6	5.4	6.3	7.2	6.2	6.8	6.1	6.0
10	857	5.6	5.2	7.0	6.0	7.3	8.4	6.5	6.8	6.5	6.2
11	839	6.6	6.8	8.3	6.3	7.7	8.4	8.1	8.7	8.5	7.8
12	866	6.4	6.3	7.5	5.7	7.4	8.0	7.5	8.1	7.5	7.1

**TABLE 4**

STANDARD DEVIATION OF 28 MONTHLY MEANS

MONTH	N	ON SHORE	2 ON SHORE	LONG SHORE	SOUTHERLY 72N	WINDS 68N	70N 170W	WESTERLIES 160W	66N 170W	66N 160W	
1	855	2.1	2.8	4.0	2.3	3.1	3.5	3.4	4.2	3.8	3.7
2	783	2.8	2.6	3.4	1.9	2.8	3.0	3.4	3.8	3.3	2.7
3	863	1.8	2.1	2.8	1.7	2.2	2.5	2.6	2.8	2.8	2.6
4	836	1.5	2.1	3.2	1.9	2.4	2.4	2.6	3.1	3.0	2.9
5	866	1.5	1.9	2.4	1.5	1.9	1.8	2.1	2.6	2.6	2.2
6	837	1.5	1.5	2.1	1.3	1.8	1.9	2.1	2.3	1.6	1.4
7	865	1.6	1.6	1.8	1.4	1.2	1.5	2.1	2.0	1.7	1.5
8	867	1.5	1.5	2.5	1.9	2.2	2.5	2.1	2.6	1.7	1.9
9	839	1.9	1.9	2.5	1.7	2.2	2.4	2.4	2.8	2.1	1.9
10	857	1.8	1.6	2.4	1.5	2.2	2.7	2.5	2.5	1.7	1.9
11	839	2.4	2.9	4.5	2.3	3.0	3.0	4.2	4.6	3.9	3.9
12	866	2.5	2.6	3.4	1.9	2.8	3.0	3.5	3.8	2.9	2.7

TABLE 2 (cont.)

SOUTHERLIES	AVERAGE 70N	AVERAGE 66N	AVERAGE 170W	AVERAGE 160W	WESTERLY WINDS ALL	RESULTANT VEL	DIR
.0	-.2	-3.2	-5.2	-4.3	-4.1	-4.2	3.2
-2.4	-2.4	-5.0	-7.0	-5.8	-6.2	-6.0	5.5
-2.1	-1.9	-4.5	-5.6	-4.7	-5.4	-5.0	4.8
-1.7	-1.5	-4.5	-4.4	-4.1	-4.8	-4.5	4.8
-1.1	-.8	-4.7	-4.0	-3.9	-4.8	-4.3	4.7
-.6	-.3	-2.5	-1.3	-1.5	-2.3	-1.9	2.6
1.0	.9	-.6	-.4	-.1	-.2	-.1	1.1
-.2	-.3	-1.7	-1.0	-1.4	-1.3	-1.4	1.7
-1.7	-1.7	-3.5	-3.2	-3.2	-3.5	-3.3	3.9
-1.1	-1.1	-4.0	-4.0	-3.9	-4.1	-4.0	4.1
-.6	-.9	-5.0	-5.5	-5.5	-5.0	-5.2	5.1
-1.8	-2.0	-4.2	-5.5	-4.9	-4.8	-4.8	4.6
-1.0	-1.0	-3.6	-3.8	-3.6	-3.8	-3.7	3.7

TABLE 3 (cont.)

SOUTHERLIES	AVERAGE 70N	AVERAGE 66N	AVERAGE 170W	AVERAGE 160W	WESTERLY WINDS ALL	RESULTANT VEL	DIR
7.2	6.9	7.4	7.4	7.0	7.4	7.0	7.1
6.0	5.8	7.2	6.9	6.5	7.0	6.6	6.5
5.9	5.7	6.6	6.6	6.2	6.4	6.1	6.2
6.3	6.0	6.3	6.5	6.0	6.3	6.0	6.2
5.0	4.8	5.3	5.4	4.9	5.4	5.0	5.1
4.3	4.4	5.2	4.5	4.6	4.8	4.5	4.8
4.6	4.8	5.0	4.5	4.5	4.5	4.4	4.9
5.1	5.1	5.5	5.2	4.9	5.3	4.9	5.3
5.8	5.6	6.3	5.8	5.6	6.0	5.6	5.9
6.7	6.4	6.3	6.1	5.9	6.1	5.7	6.3
7.0	6.8	8.2	7.9	7.7	7.8	7.6	7.5
6.6	6.3	7.6	7.1	6.9	7.1	6.8	7.0

TABLE 4 (cont.)

SOUTHERLIES	AVERAGE 70N	AVERAGE 66N	AVERAGE 170W	AVERAGE 160W	WESTERLY WINDS ALL	RESULTANT VEL	DIR
2.8	2.6	3.7	3.7	3.6	3.9	3.7	3.2
2.4	2.3	3.5	2.9	3.2	3.1	3.1	3.0
2.0	1.9	2.7	2.6	2.5	2.5	2.5	2.3
2.1	2.1	2.8	2.9	2.7	2.9	2.8	2.5
1.6	1.6	2.3	2.4	2.3	2.4	2.3	2.0
1.6	1.5	2.1	1.5	1.7	1.8	1.7	1.8
1.2	1.2	2.0	1.6	1.8	1.7	1.7	1.7
2.1	2.0	2.3	1.7	1.8	2.2	1.9	2.1
1.9	1.9	2.6	1.9	2.2	2.2	2.1	2.2
2.0	1.8	2.4	1.7	1.9	2.1	1.9	2.1
2.6	2.6	4.3	3.8	4.0	4.1	4.0	3.6
2.5	2.3	3.6	2.7	3.1	3.1	3.1	3.0

TABLE 5

AVERAGE STANDARD DEVIATION OF DAYS WITHIN EACH MONTH

MONTH	N	ON	2 ON	LONG	SOUTHERLY WINDS			70N	WESTERLIES	66N
		SHORE	SHORE	SHORE	72N	68N	65N	170W	160W	170W
1	855	5.9	5.6	6.3	5.8	7.3	8.0	6.4	6.9	6.8
2	783	5.5	5.4	6.1	4.9	6.2	6.8	5.9	6.9	6.6
3	863	5.1	5.0	6.3	4.9	6.1	6.7	5.9	6.6	6.0
4	836	4.6	4.7	6.3	5.0	6.5	7.3	5.5	6.3	5.9
5	866	3.9	3.7	5.3	4.2	5.4	6.0	4.5	5.3	5.1
6	837	3.5	3.5	5.2	4.3	4.5	4.7	4.5	5.3	4.7
7	865	3.8	3.4	5.3	4.7	5.0	4.9	4.7	5.0	4.7
8	867	4.2	4.0	5.4	4.6	5.2	5.7	4.9	5.5	5.4
9	839	4.8	4.7	6.1	5.1	5.9	6.8	5.7	6.1	5.7
10	857	5.3	5.0	6.6	5.8	6.9	8.0	6.0	6.3	5.9
11	839	6.1	6.1	7.0	5.8	7.1	7.9	6.9	7.4	7.5
12	866	5.8	5.7	6.7	5.4	6.9	7.5	6.6	7.2	7.0

TABLE 6

AVERAGE STANDARD ERROR OF THE 28 MONTHLY MEANS

MONTH	N	ON	2 ON	LONG	SOUTHERLY WINDS			70N	WESTERLIES	66N
		SHORE	SHORE	SHORE	72N	68N	65N	170W	160W	170W
1	855	1.1	1.0	1.2	1.1	1.3	1.5	1.2	1.2	1.2
2	783	1.0	1.0	1.2	.9	1.2	1.3	1.1	1.3	1.2
3	863	.9	.9	1.1	.9	1.1	1.2	1.1	1.2	1.1
4	836	.9	.9	1.2	.9	1.2	1.3	1.0	1.2	1.1
5	866	.7	.7	1.0	.8	1.0	1.1	.8	1.0	.9
6	837	.7	.6	.9	.8	.8	.9	.8	1.0	.9
7	865	.7	.6	1.0	.9	.9	.9	.8	.9	.7
8	867	.8	.7	1.0	.8	.9	1.0	.9	1.0	.9
9	839	.9	.9	1.1	.9	1.1	1.2	1.0	1.1	1.0
10	857	1.0	.9	1.2	1.0	1.3	1.4	1.1	1.1	1.1
11	839	1.1	1.1	1.3	1.1	1.3	1.4	1.3	1.4	1.2
12	866	1.1	1.0	1.2	1.0	1.2	1.3	1.2	1.3	1.2

TABLE 7

RATIO OF ST. DEV. OF MONTHS TO AVERAGE ST. ERR. OF MONTHLY MEANS

MONTH	N	ON	2 ON	LONG	SOUTHERLY WINDS			70N	WESTERLIES	66N
		SHORE	SHORE	SHORE	72N	68N	65N	170W	160W	170W
1	855	2.0	2.7	3.3	2.2	2.4	2.4	3.0	3.4	3.1
2	783	2.4	2.6	2.9	2.1	2.4	2.3	3.0	2.9	2.6
3	863	1.9	2.3	2.5	1.9	2.0	2.1	2.5	2.4	2.4
4	836	1.7	2.4	2.7	2.0	2.0	1.8	2.6	2.7	2.7
5	866	2.1	2.8	2.5	2.0	1.9	1.6	2.6	2.7	2.5
6	837	2.3	2.3	2.2	1.7	2.2	2.2	2.6	2.4	1.9
7	865	2.3	2.6	1.8	1.6	1.3	1.7	2.5	2.2	2.1
8	867	2.1	2.1	2.6	2.3	2.3	2.4	2.4	2.6	2.1
9	839	2.2	2.3	2.3	1.8	2.0	1.9	2.3	2.5	2.0
10	857	1.9	1.7	2.0	1.5	1.7	1.9	2.3	2.2	1.5
11	839	2.2	2.6	3.5	2.2	2.3	2.0	3.3	3.4	2.9
12	866	2.4	2.5	2.9	2.0	2.3	2.2	2.9	2.9	2.3

TABLE 5 (cont.)

AVERAGE SOUTHERLIES	AVERAGE WESTERLY WINDS					RESULTANT	
	70N	66N	170W	160W	ALL	VEL	DIR
6.6	6.3	6.4	6.4	6.0	6.3	6.0	6.4
5.5	5.3	6.2	6.3	5.7	6.3	5.8	5.8
5.5	5.3	6.1	6.1	5.6	5.9	5.6	5.7
5.9	5.6	5.7	5.8	5.3	5.6	5.3	5.6
4.8	4.6	4.7	4.8	4.3	4.8	4.4	4.7
4.0	4.2	4.7	4.3	4.2	4.4	4.2	4.4
4.4	4.7	4.6	4.2	4.2	4.2	4.0	4.6
4.7	4.7	5.0	4.9	4.6	4.8	4.5	4.8
5.4	5.2	5.7	5.5	5.2	5.5	5.2	5.5
6.4	6.1	5.9	5.8	5.5	5.7	5.4	6.0
6.5	6.2	6.9	6.9	6.6	6.6	6.4	6.6
6.1	5.9	6.7	6.6	6.2	6.3	6.1	6.3

TABLE 6 (cont.)

AVERAGE SOUTHERLIES	AVERAGE WESTERLY WINDS					RESULTANT	
	70N	66N	170W	160W	ALL	VEL	DIR
1.2	1.1	1.2	1.2	1.1	1.1	1.1	1.2
1.0	1.0	1.2	1.2	1.1	1.2	1.1	1.1
1.0	1.0	1.1	1.1	1.0	1.1	1.0	1.0
1.1	1.0	1.0	1.1	1.0	1.0	1.0	1.0
.9	.8	.9	.9	.8	.9	.8	.8
.7	.8	.9	.8	.8	.8	.8	.8
.8	.8	.8	.8	.7	.8	.7	.8
.8	.8	.9	.9	.8	.9	.8	.9
1.0	1.0	1.0	1.0	.9	1.0	.9	1.0
1.2	1.1	1.1	1.1	1.0	1.0	1.0	1.1
1.2	1.1	1.3	1.3	1.2	1.2	1.2	1.2
1.1	1.1	1.2	1.2	1.1	1.1	1.1	1.1

TABLE 7 (cont.)

AVERAGE SOUTHERLIES	AVERAGE WESTERLY WINDS					RESULTANT	
	70N	66N	170W	160W	ALL	VEL	DIR
2.3	2.3	3.2	3.2	3.3	3.4	3.4	2.8
2.2	2.3	3.0	2.4	2.9	2.7	2.8	2.7
2.1	2.0	2.5	2.4	2.5	2.4	2.5	2.3
2.0	2.0	2.7	2.7	2.8	2.8	2.8	2.4
1.8	1.9	2.7	2.7	3.0	2.8	2.9	2.4
2.1	1.9	2.5	1.9	2.3	2.2	2.3	2.3
1.5	1.4	2.4	2.1	2.5	2.2	2.4	2.0
2.4	2.3	2.6	1.9	2.2	2.5	2.4	2.4
1.9	1.9	2.5	1.9	2.3	2.2	2.3	2.2
1.7	1.6	2.3	1.6	1.9	2.0	2.0	2.0
2.2	2.3	3.4	3.0	3.3	3.4	3.4	3.0
2.2	2.2	3.0	2.3	2.7	2.7	2.8	2.7

Table 8

Beaufort Synoptic Typings of Chukchi Type Key Dates

Chukchi		Beaufort	
Type	% Occurrence	Type	Score
1	30.7	1	2.8
2	10.4	4	23.5
3	5.1	5	18.7
4	9.4	3	15.6
5	3.6	1	5.2
6	2.8	5	19.3
7	1.8	10	13.0
8	2.6	9	18.1
9	3.7	3	11.8
10	2.9	5	27.2
11	3.7	3	18.9
12	3.0	2	4.0
13	3.5	4	19.8
14	2.2	9	20.4
15	2.1	3	13.6
16	1.6	3	5.5
17	2.4	1	20.4
18	.5	8	14.1
19	1.0	3	13.9
20	.5	10	18.0
21	1.0	7	28.7
22	.9	3	9.4

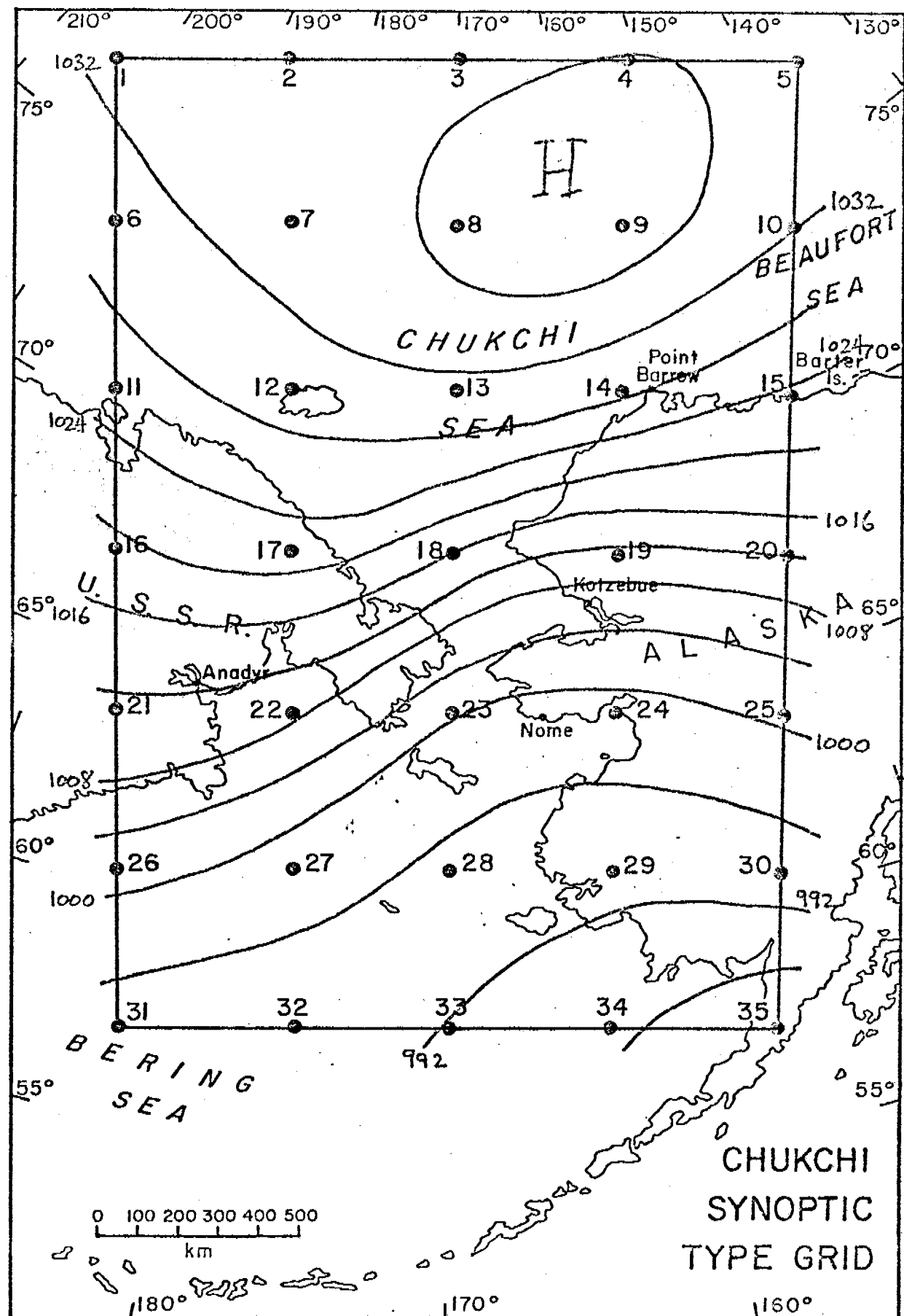


Fig. 1A

Type I. Key Date 3/14/70

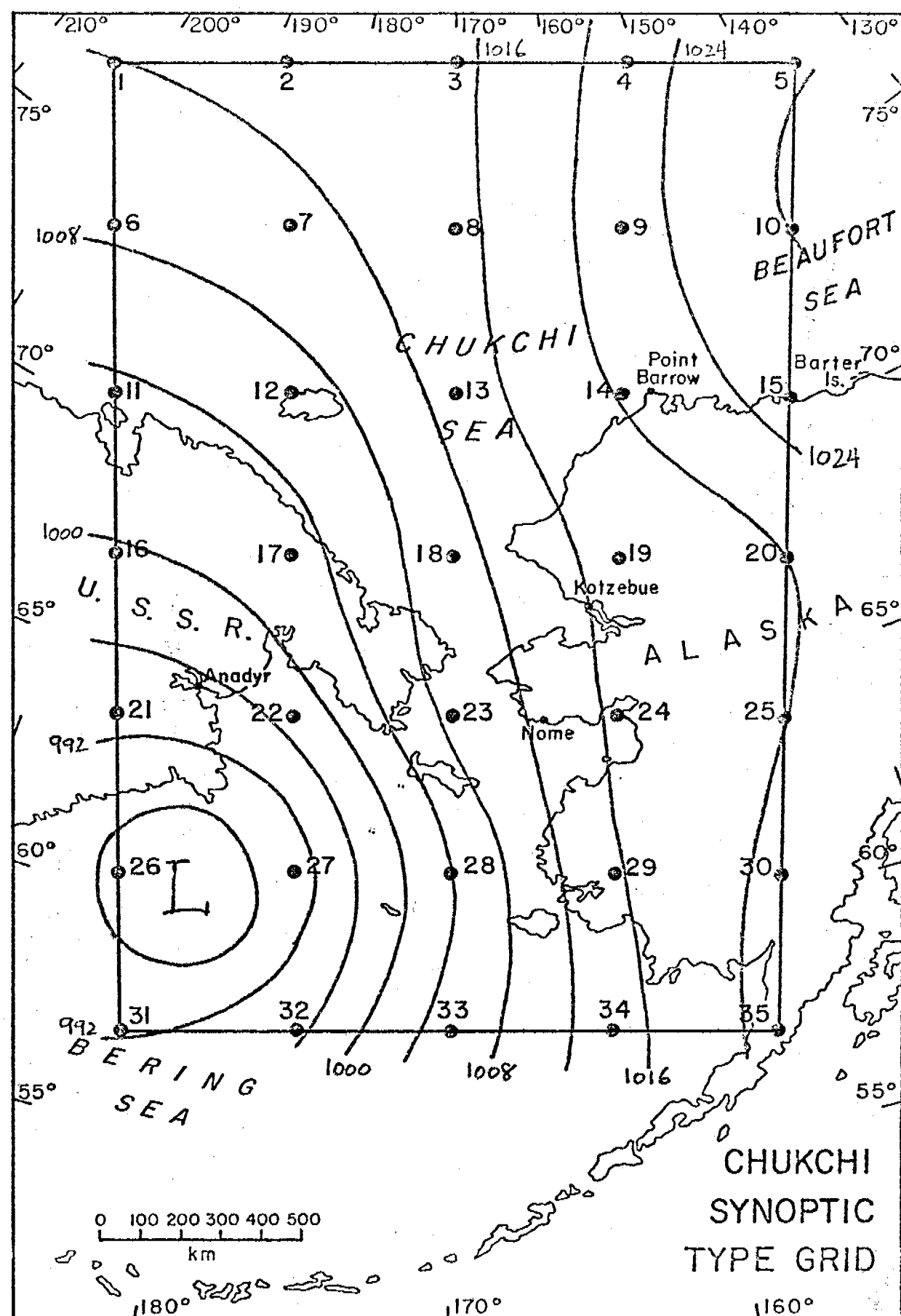


Fig. 1B

Type 2. Key Date 8/7/68

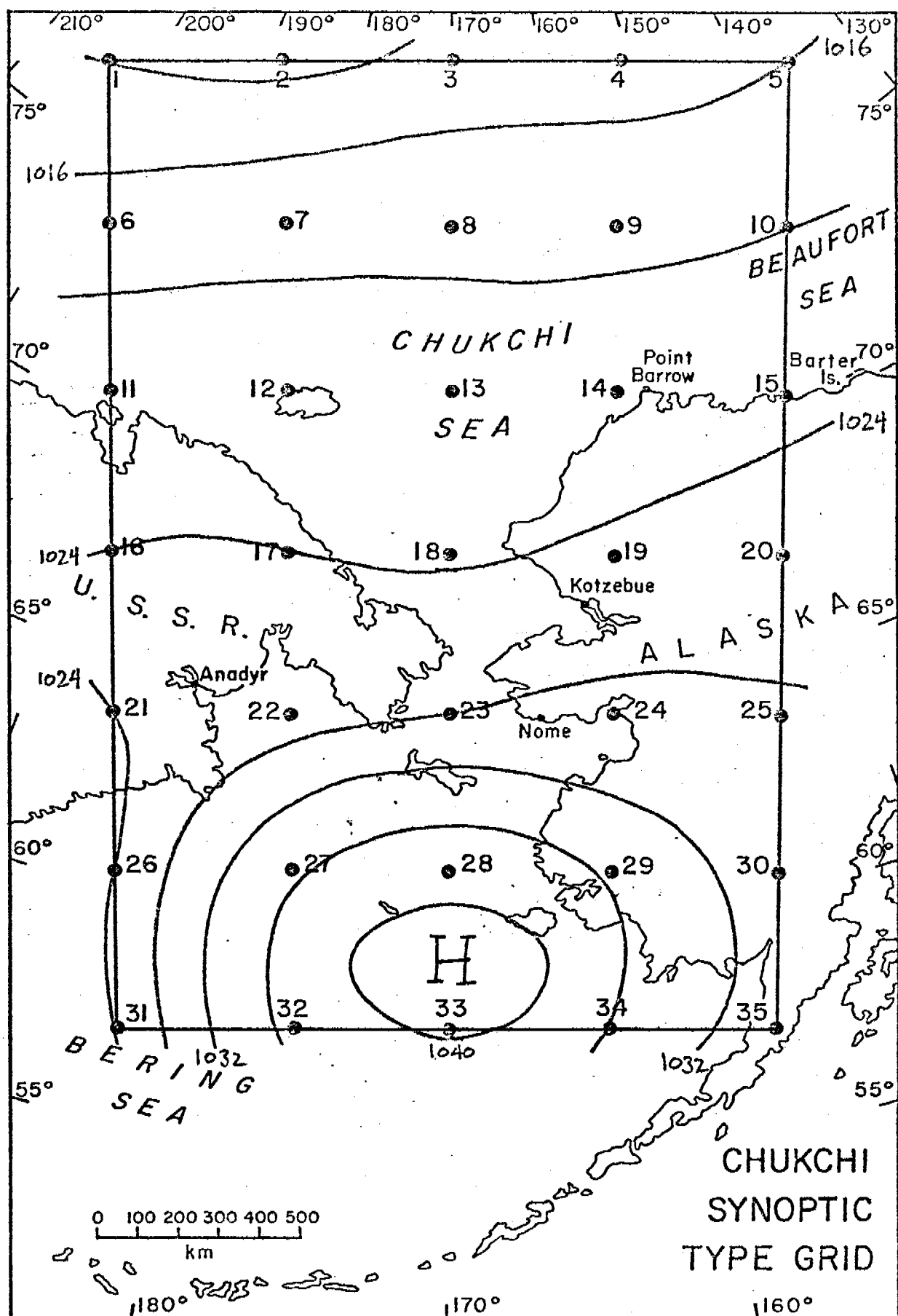


Fig. 1C.

Type 3. Key Date 3/20/67

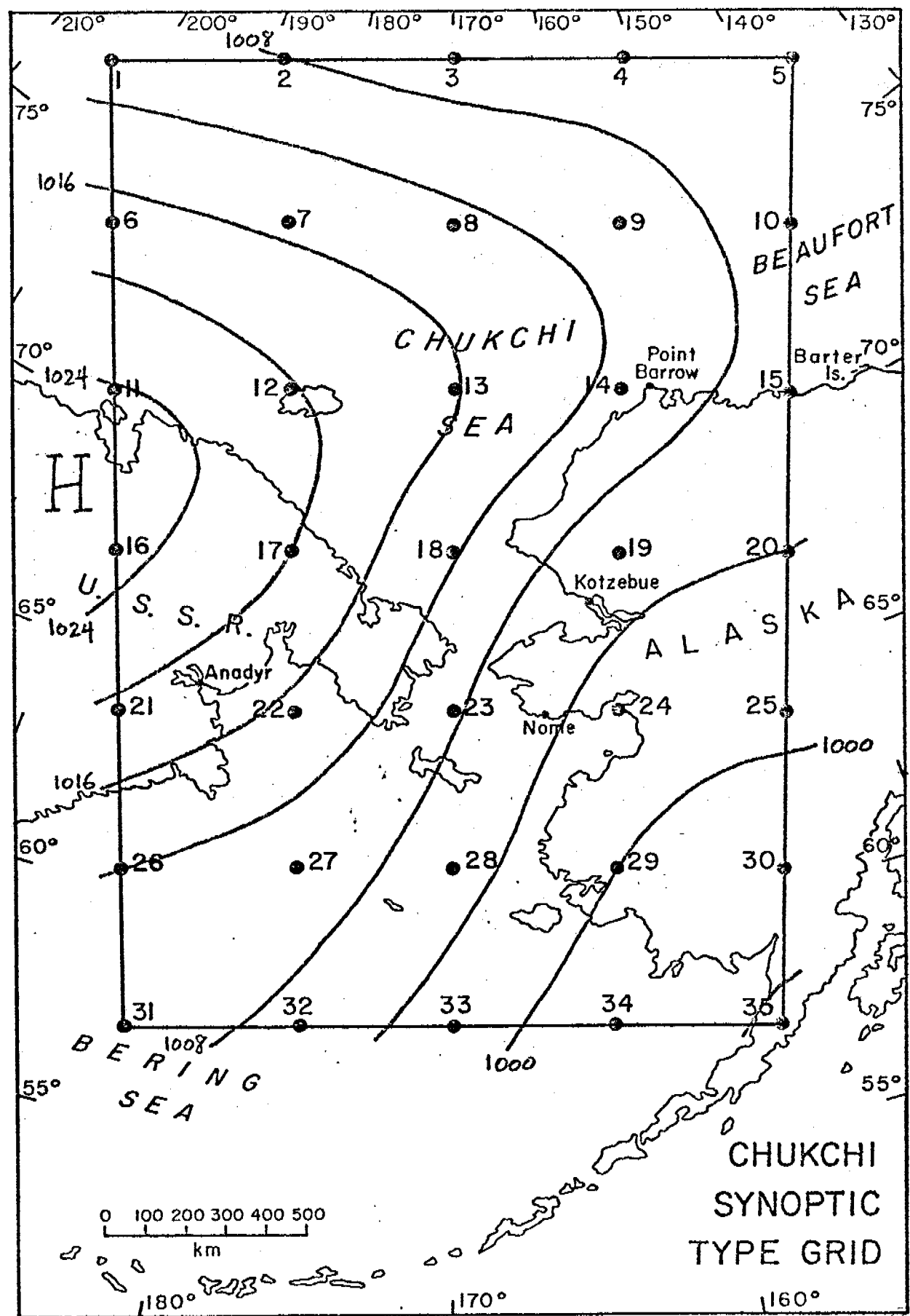


Fig. 1D

Type 4. Key Date 2/2/61

Fig. 2

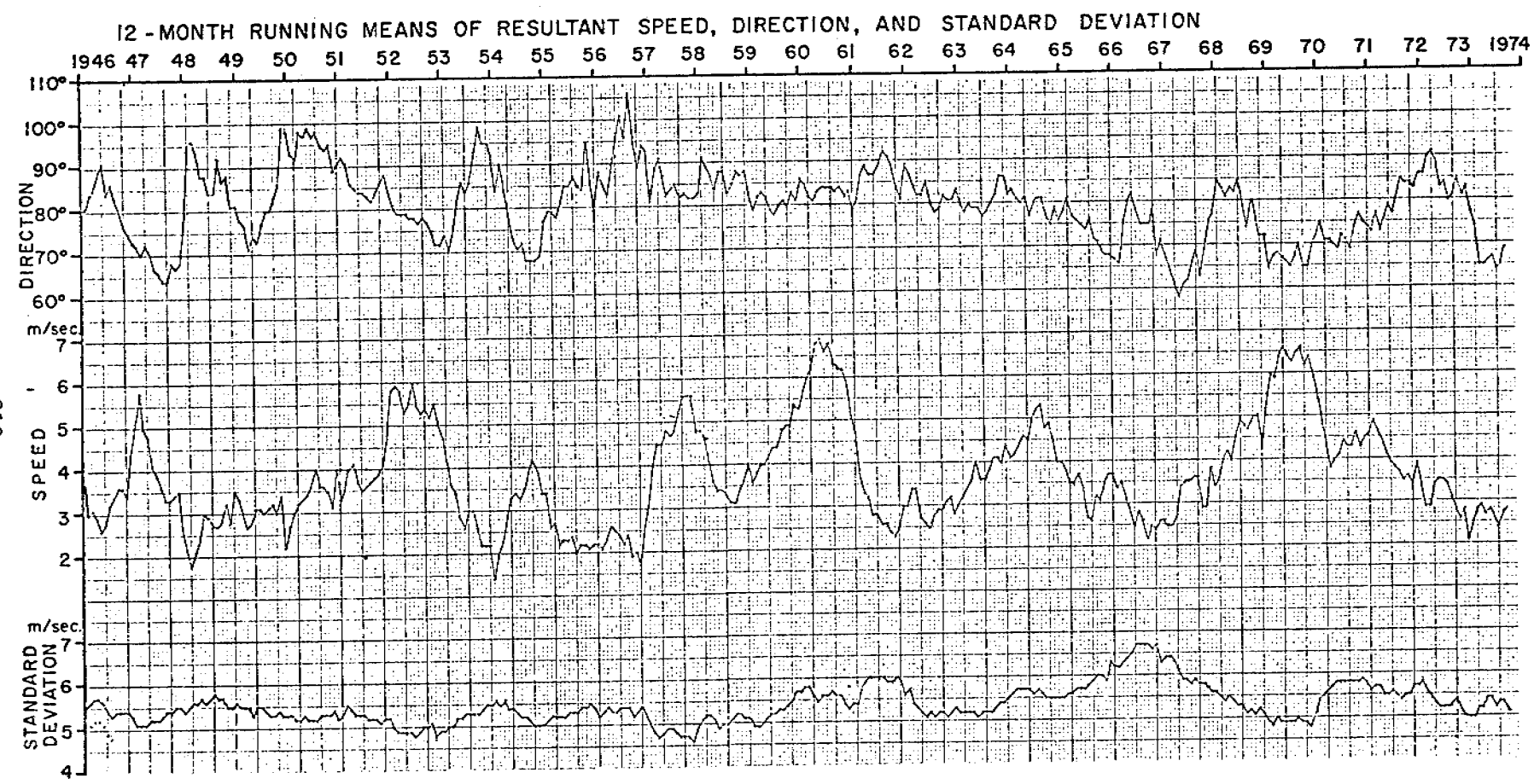
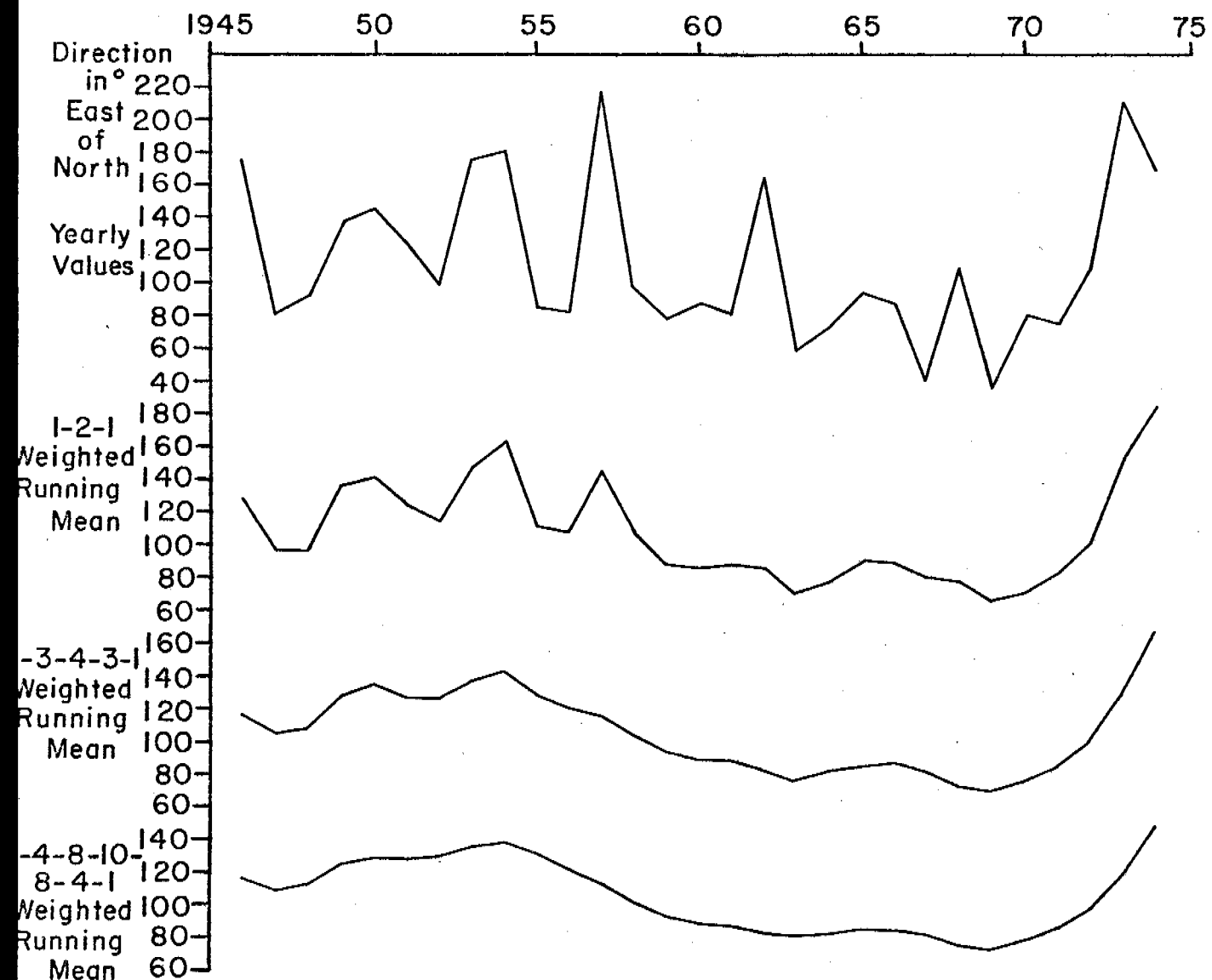
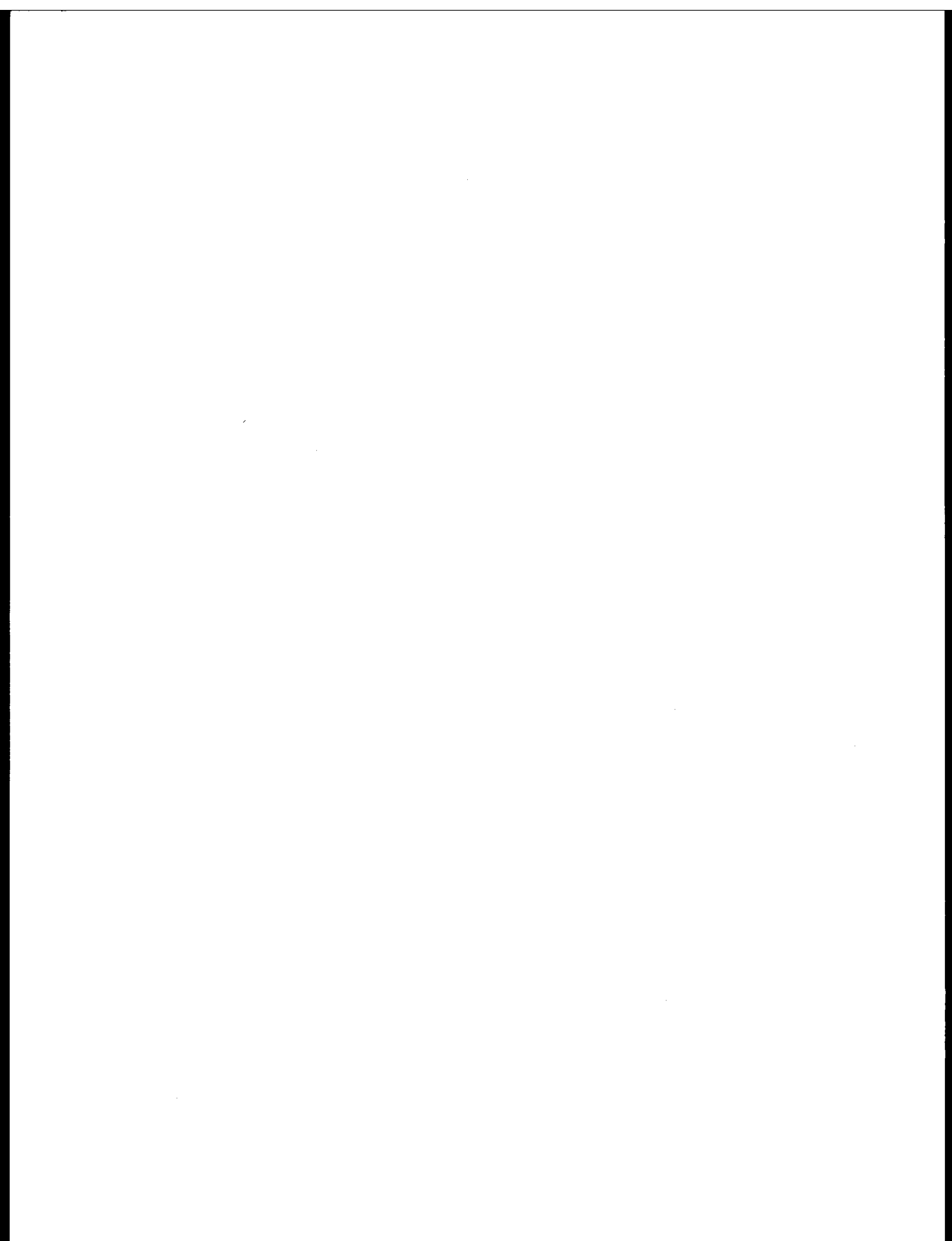


Fig. 3

CHUKCHI SEA WIND DIRECTION -  
SUMMER AVERAGES





QUARTERLY REPORT

Contract #03-5-022-91

Research Unit #244

Reporting Period: July 1-Sept. 30, 1976

Number of Pages: 98

STUDY OF CLIMATIC EFFECTS ON ICE EXTENT  
AND ITS SEASONAL DECAY ALONG THE BEAUFORT SEA COAST

Principal Investigator

R. G. Barry

Acting Director, Professor of Geography  
Institute of Arctic and Alpine Research  
University of Colorado  
Boulder, Colorado 80309  
September 30, 1976

## I. TASK OBJECTIVES

The primary objective of this study is to assess the role of climatic factors in determining the extent and seasonal decay of fast ice along the Beaufort Sea Coast. Emphasis during this quarter has been on the preparation of specific data products anticipated in the Work Plan.

## II. 1. FIELD ACTIVITIES

None.

## II. 2. OFFICE ACTIVITIES.

### A. Period

1 July - 30 September 1976.

### B. Personnel

R. G. Barry - Principal Investigator

J. Rogers - Research Associate

R. E. Moritz - Research Assistant

M. Eccles - Programming Consultant

W. Vaughn - Work Study Student

E. Yeoman - Hourly

### C. Methods

#### 1) Remote Sensing Data

##### a. LARSYS Analysis of LANDSAT Data for Mapping Shorefast Sea Ice.

The methods used for analysis of the automatic mapping and classification process as applied to shorefast sea ice fall into two categories:

- (1) Machine processing of LANDSAT Computer Compatible Tape (CCT) data, carried out at LARS, Purdue University, under subcontract.

(2) Interpretation and analysis of ice types and their correspondence to the LARSYS spectral classes, carried out at INSTAAR.

The machine processing methods are treated first.

The LANDSAT CCT's for scene 1702-21093 (25 June 1974) were received at LARS on 1 March 1976. A Black and White reproduction of Band 7 of this scene is shown in Figure 1. As shown in the figure,  $\frac{1}{4}$  of the scene was geometrically reformatted for compatibility with the LARSYS computer system. This sample for digital processing comprises 1,302,301 picture elements (pixels). The LARSYS clustering algorithm, described in Swain and Staff (1972), was then run on each of 7 fields taken from the  $\frac{1}{4}$  scene. These fields were selected as representative of the ice-types occurring on the scene. This sample comprised 12,000 pixels. Each of the 7 fields produced a set of spectral classes which are defined by their means and standard deviations of reflected radiance in each LANDSAT band. Similar classes from different fields were then merged with one another, to obtain the maximum number of spectrally separable classes. The separability of any two classes was assessed by computing the inter-class transformed divergence (ITD) (see Swain, 1973). This statistic is a measure of the ability of the classifying algorithm (LARSYS) to correctly classify pixels based on their reflected radiances in the LANDSAT bands (Figure 2).

A threshold value of 1750 was taken to be the minimum acceptable for spectrally distinct classes, based on the experience of the LARS investigators. The merging process was done by gradually increasing the threshold value of ITD to its final value of 1750, i.e., very similar classes were merged first ( $ITD < 500$ ), and the ITD's recomputed for the merged classes. Then less similar classes were merged, and so on, until no two classes had an ITD of less than 1750.

Following the identification of the spectrally separable classes, every pixel in the entire  $\frac{1}{4}$  scene was classified, based on a maximum likelihood criterion (see Swain and King, 1973). A 1:25,000 scale line-printer 'map' of the  $\frac{1}{4}$  scene was generated, displaying each pixel as a symbol corresponding to its spectral class, and color-coded slides of the  $\frac{1}{4}$  scene classification were made. These products were used as the data base for interpretation of the LARSSYS spectral classes. Finally, several fields identified by INSTAAR as 'homogeneous ice types' were processed at LARS to produce histograms of reflected radiance for each band and separability (ITD) statistics with the original LARSSYS spectral classes.

After receiving the line printer output from LARS, INSTAAR personnel proceeded with the "ice-truthing" and interpretation tasks. In order to identify the types of geophysical surface which comprise each of the LARSSYS spectral classes, several remote sensing data products

were assembled (see II. 2. E. 1. a.) and laid out on a drafting table. A set of control points was established on easily identifiable land and immobile ice features on all the images. Grid lines connecting these points were drawn on acetate overlays and the approximate positions of ice features on the various data products were measured from these. Positive identifications of ice features on the images were made by comparing shapes, spatial patterns and textures in the general area found by measurement from the grid. In this manner, then, 38 sample fields were found and delimited on each data product. These fields were chosen from homogeneous areas of one spectral class on the line printer output. Each of the classes generated by LARSYS was represented by two or more such fields. The fields were then described in terms of surface roughness (very low, low, medium, high), percent of surface water covered ( $\pm 10\%$ ), puddle depth (shallow, medium, deep), and any relevant special characteristics, including apparent changes in the time intervals between SLAR, U-2, and LANDSAT overpasses. These fields were used to identify the types of surface classified by LARSYS. Histograms of radiances in the four LANDSAT bands were studied as an aid also.

b. Mapping Ice Surface Morphological Characteristics.

In order to compare effectively the spatial and temporal characteristics of the shorefast sea ice among several seasons, maps of ice surface characteristics have been prepared from

LANDSAT imagery for the decay seasons, 1973-1975. The location of ice features was accomplished by overlay techniques as follows. An outline of the coastline and significant landmarks was traced onto clear acetate from the OCS 1:1,000,000 scale UTM map. Geographical coordinate grid ticks were also traced for use as registration marks. The LANDSAT scene under consideration is then fixed to a light table beneath the overlay. On the image, the sections of coast and/or landmarks nearest to a given ice feature are aligned with the overlay and the outline of the ice feature is traced. After each image is mapped in this way, the ice feature outlines are transferred to our sector maps, also based on the OCS UTM projection, using the grid ticks for registration.

Identification and interpretation of significant LANDSAT ice information is divided into two stages. First, each decay season's set of sequential LANDSAT images is examined, sector by sector. When available, Dr. Stringer's OCS maps are also used as a reference. Areas of homogeneous-appearing grey tone and texture are then delimited and mapped on the overlays. Images of poor quality (e.g., underexposed and underdeveloped) are also analyzed on the Spatial Data Systems Datacolor machine (Model #703, SOS, Inc., Goleta, CA.), which divides the continuous photographic gray tones into discrete levels and displays these in color-coded form. This procedure facilitated the grouping or separating of ice areas based on gray-scale tone.

In the second stage, the imagery and maps are viewed again and the mapped gray tone and texture areas are interpreted. The interpretive keys used in this step are based on:

- (1) Field experience of the analyst(s) on the Beaufort Sea ice (see field reports in Quarterly Reports).
- (2) Detailed analysis of the spectral characteristics of melt-season ice types on LANDSAT data for one particular scene (see secs. II. 2. C. 1. a. and III. A. 1.).
- (3) Available literature discussing ice-interpretation from LANDSAT data (see "Ice Interpretation" section under References).
- (4) Inferences gleaned from the time-sequential behavior of the ice on LANDSAT data.

c. Dating and Analysis of Significant Decay-Season Ice Events.

The assessment of climate-related interannual variation in shorefast sea ice behavior and characteristics is central to this project. As a first step towards quantifying some of this information, a set of 6 ice events is defined and an attempt to date the events for three years (1973-1975) is made (see Quarterly Report, 6/30/76, sec. II. 2. B. 1. b.) using LANDSAT images.

- (i) The first event is defined as the earliest noticeable spring darkening in river channels between the foot of the Brooks Range and the coast. The rivers considered are the Mead, Colville, Sagavanirkto, Canning, and Jago Rivers. Holmgren et al. (1974, p. 361) showed how the major north

slope river channels darken considerably between March and May on LANDSAT images, indicating the development of continuous open water channels in the streams. The date of such darkening is indicative of a particular stage in the river breakup, and may give some early indication of the advancement or retardation of coastal breakup. Additionally, river flooding onto the shorefast sea ice lowers its albedo during the period of ever-increasing solar energy input rates. Each year's sequence of late-winter LANDSAT images is examined, and the scene ID's and dates are compiled for the latest scene showing little or no change in the river channel and the earliest scene showing definite darkening.

(ii) The second event which is dated and tabulated is the flooding of near-shore ice by each of the respective rivers above. Again, the method is to find the latest LANDSAT image showing little or no change from winter conditions and the earliest image showing a distinct and often fan-shaped dark area at the river mouth.

(iii) Ice-surface darkening due to the initiation of in situ melting is the third event dated. Interpretive keys for identifying this event are primarily related to the gray-scale contrasts between various ice surfaces. For example, prior to the onset of melting, it has been observed that large ice deformation features (ridges and hummock fields) appear darker than surrounding areas, possibly due to roughness and shadow effects. With the onset of melting, however, the flat ice areas darken as the water

ponds on the surface, while rough, elevated ice features appear light, due to drainage of meltwater. This "signal-reversal" gives the analyst a tool for dating this particular event.

(iv) Dating the first openings in movements of the fast ice depends on delimiting its boundaries at some earlier date. Dr. Stringer's OCS maps are used for this purpose. Movements are detected by overlay techniques, using the coastline for positional control. Openings are subjectively identified by a dark, black tone on all LANDSAT bands.

(v) The fifth decay-season event occurs when the coastal segment under consideration becomes "ice-free." In practice, this is taken to be the date on which a continuous strip of open water or very rarefied pack ice exists between shore and the offshore pack. No extensive grounded fast ice features remain on this date.

(vi) The final event is the first appearance of new ice in the fall. Ordinarily, the interpretation is easy, because new ice usually conforms to embayment and lagoon boundaries and contrasts sharply with open water. However, the presence of pack ice in near-shore areas complicates this task.

2) Meteorological Data

a. Synoptic Pressure Pattern Climatology.

As directed by the Arctic Project Office, Juneau, the data used for the synoptic climatology are being validated

and checked for quality and accuracy. The methods used for this analysis are described in this section.

The basic data set for control (taken to be accurate) consists of the NOAA publication "Daily Series Synoptic Weather Maps, Part 1, Northern Hemisphere Sea Level and 500 mb Charts," from 1946 to 1967, and the NMC 1200Z Surface Analysis Charts (on microfilm at NCAR) from 1968 onward. Our lowest-order data set for the synoptic typing is a 7-track magnetic tape containing 36 MSL pressure values for each day since 1/1/1946. In order to check this tape, the 36-point grid (see Annual Report, March 1976) is accessed, printed, and contoured for the first day of every 10th tape record (approximately 100 sample days, evenly spaced from 1946 to 1974). This plot is then checked for pressure magnitude and pattern similarity accuracy by hand against the control data set. For this same sample, a short, simple FORTRAN program also calculates the mean and standard deviation for the grids, plots the normalized grid values (see Annual Report, March 1976), calculates the scores with each key day, and prints out this information with the number of good data points (usually 36). The data are checked against the original (punched card) synoptic-typing output to ensure that (1) minimum score corresponds to proper key day; (2) minimum score has the same magnitude as on the cards; (3) mean, standard deviation and number of points are correct; and (4) contoured normalized grid values correspond to normalized key day maps.

It is noted that the original synoptic typing program is quite lengthy, and involves various large-capacity storage devices, whereas the checking program is short and simple. Additionally, the programming of the checking routine was done independently by a separate programmer to avoid repeating any (possible) errors.

Further work during this quarter has involved plotting mean frequencies by month for the types and assessing interannual variations in type frequencies by season.

b. Statistical Analysis of Meteorological Elements.

The daily climatic elements (LCD) for Barrow and Barter Island (punched and verified) for 1969-1974 have been analyzed according to season and synoptic type.

Frequency histograms have been generated for daily temperature departures, resultant wind speeds, resultant wind directions, precipitation (solid and w.e.) and cloudiness. Inspection of the histograms facilitated preliminary hypotheses and formulation of appropriate statistical tests for assessing type-characteristics which are important for shorefast sea ice.

3) Climate-Ice Interaction Case Studies

Three case studies of climate-ice interactions have been carried out (section III. C.). The methods used to analyze data for these case studies are as follows:

(1) Wind data - Surface wind speed and direction data were analyzed for case studies 2 and 3. These data, collected for 6 Junes, 7 Julys, and 6 Augests (see II. E. 3.), were

analyzed to associate the synoptic types to specific wind directions and velocities. The months chosen for analysis were two each of the coldest and warmest for the period of record as well as those for which LANDSAT data are available. A cross-tabulation of types versus wind direction and wind speed was made. A frequency distribution of wind directions indicated which direction was most commonly associated with a particular synoptic type. Wind speed data were summarized by a mean and standard deviation.

- (2) Geostrophic winds - Geostrophic wind data, described in previous quarterly reports, were used in case study 2 to determine wind effect upon breakup of fast ice in the Pt. Barrow vicinity. The parameter of greatest importance, geostrophic wind direction, was divided into 8 categories of  $45^{\circ}$  each ( $0^{\circ}$  = North =  $360^{\circ}$ ). Categories 6, 7, and 8 ( $150^{\circ}$  to  $195^{\circ}$ ,  $195^{\circ}$  to  $240^{\circ}$ , and  $240^{\circ}$  to  $285^{\circ}$  respectively) are of greatest importance since they are the southerly and westerly flow types frequently referred to in section III. C. The categorization of the wind direction data was based on the sign (+ or -) of the I and J components of the wind and whether or not the magnitude of I was greater than or less than the magnitude of J.
- (3) Temperature data - Temperature data were converted into thawing degree days (TDDs) (case studies 1 and 2). Thawing degree days (TDDs) are the positive departure of average daily temperature from  $32^{\circ}\text{F}$ . Thus, a day with an average

temperature of 46° F accumulated 14 TDDs. Accumulated TDDs is a very useful indicator of the amount of atmospheric heating over the ice and the severity/mildness of a summer. The summation of TDDs begins on the first day after which a continuous daily sum remains above zero, and they end on the date of the maximum sum.

D. Sample Localities

Not applicable.

E. Data Collected/Analyzed

1) Remote Sensing Data

a. Data Set for LARSYS Analysis

The "ice truth" data used for interpretation and analysis of the LARSYS spectral classes consist of:

- (1) A photomosaic of 3 NASA U-2 color-infrared photographic prints at 1:131,500 scale (NASA-Ames roll 01819, frames 9658, 9660, 9662). Flight date - 6/21/74.
- (2) 1:32,750 scale enlargement of frame 9662, above.
- (3) 2 X-band ( $\lambda = 3\text{cm}$ ) SLAR-track images at approximately 1:250,000 scale, flown on coast-parallel transects. Flight date - 4/29/74 (courtesy of W. Weeks, CRREL; J. Wayenberg, U.S.G.S., Tacoma).
- (4) 1:250,000 scale paper print of Landsat scene 1702-21093, in "false-color" composite form.
- (5) 1:250,000 scale paper prints of Landsat scene 1702-21093 bands 4 and 7 in B & W.

The data set for digital processing consists of CCT 1702-21093.

Also used in the analysis was a 1:25,000 scale line-printer map depicting each pixel in the 1/4 scene as a symbol corres-

ponding to its spectral class.

b. Mapping Ice Surface Morphological Characteristics

Initial mapping efforts have been concentrated on the decay-season, 1974, because we have more information about the ice in that year (SLAR, CIR, LARSYS). The mapping procedure has been carried out for the following Landsat scenes:

<u>Scene ID</u>	<u>Date</u>
1702-21093	6/25/74
1703-21151	6/26/74
1721-21143	7/14/74
1722-21202	7/15/74
1723-21260	7/16/74
1740-21194	8/2/74
1773-21011	9/4/74
1775-21124	9/6/74
1777-21240	9/8/74

The data sets described in Section II.2.E.1.a. were also used to aid interpretation of the maps.

c. Dating and Analysis of Significant Ice Events

The Landsat scene ID numbers used to date significant ice events during the decay season (described under Section II.2.C.1.c) are listed in Tables 1A-F.

2) Meteorological Data

a. Validation of Synoptic Types

The data set analyzed for validation of synoptic type catalog consists of one 7-track BCD magnetic tape. This lists

the date, synoptic type, score with key day, central pressure, mean pressure, standard deviation of the pressures and number of good data points in date order.

The validation procedure also used the USWB historical daily weather map series for the northern hemisphere, NMC weather maps, and the 36-point MSL pressure grid derived from the NMC data tapes.

The sample dates used to check the synoptic typing are listed in Table 2.

b. Statistical Analysis of Meteorological Elements

Data on the Local Climatological Data sheets for Barrow and Barter Island, obtained from MCC, Asheville, were punched for the period 1/1/69 to 8/31/74. These cards were verified and listed, and the output checked for accuracy against the originals. They were then written onto magnetic tape along with the synoptic type category for each day. This tape is the basic data set from which histograms and statistical parameters are generated.

3) Climate-Ice Interaction Case Studies

Data were analyzed for the given case studies of section III. C. for the following periods:

- (a) Daily Geostrophic Winds - summer months 1972-1974 for case study #2.
- (b) LANDSAT Imagery - all available 1972-1975 frames for case studies 2 and 3.
- (c) Thawing degree days - computed for all summers for the period of record at Barrow and Barter Islands (1953-1975 and 1957-1975, respectively) and also computed at 5-day intervals for case studies 1 and 2.
- (d) Synoptic types for summers 1972-1974 and for other months listed below in (e) were used in case studies 2 and 3. Reference previous reports for the synoptic type catalogue.
- (e) Wind direction and speed data at Barrow were tabulated across synoptic types for the individual months of June 1964, 1965, 1966, 1971, 1973, 1974; July 1963, 1968, 1969, 1971, 1972, 1973, 1974; August 1962, 1968, 1969, 1971, 1973, 1974 for use in case studies 2 and 3. Summer averages presented in Table 2 and 4 (section III. C.) were based on these months.

### III. RESULTS

#### A. Remote Sensing Data

##### 1) Results of the LARSYS experiment

The results of the automatic classification and mapping analysis of Landsat CCT data for fast ice can be conveniently presented in 2 parts; results generated by machine processing at LARS (under subcontract) and results of INSTAAR's "ice truthing" and interpretation procedures.

A preliminary statistical analysis of the reflected radiances for scene 1702-21093 revealed high correlation between band 6 and 7 radiances for the 7 sample fields, indicating redundancy in the data set. Thus it was decided to apply the clustering algorithm to the data for bands 4, 5 and 6 alone to conserve computer time. The initial clustering run generated 45 spectral classes from the 7 selected fields. A 45 by 45 matrix of interclass transformed-divergence (ITD) statistics was printed for inspection, and the classes with low ITD's were merged as discussed previously. Repetition of this process with an increasing ITD threshold finally yielded a set of 9 spectral classes. With all four bands used for computation, the minimum ITD for this group is 1796.

In order to have a "square" line-printer map, a set of null-class pixels are printed for areas not within the boundaries of the scene (see Figure 1). These pixels are listed as class "Null 0.2" in statistical summaries, so the significant spectral classes are numbered 2 through 10. The line-printer output map, depicting each

pixel as a symbol corresponding to one of the 10 classes, is enclosed as Appendix 1 (scale: 1:38,750 ).

It was found that one of the 10 classes (#5) possesses a systematic spatial pattern, occurring on every 6th scan line along the spacecraft track whenever the reflected radiances for the given pixel are near saturation values. This problem derives from the introduction of electronic noise into the radiometer signal every sixth line. Because it is a sensor-package problem. it cannot be rectified. Fortunately, there is only one "real" class with mean radiances near saturation (#4), so the two classes have been grouped for analysis. The net result is that we have 8 classes containing spectral information.

It is noted that the basic pixel data are transformed by NASA from radiances (units:  $w \text{ cm}^{-2} \text{ sr}^{-1}$ ) to a normalized scale in the range 0 to 128 for bands 4-6 and 0 to 64 for band 7. All statistics cited below refer to these normalized values. Each of these normalized values is linearly proportional to the reflected radiance received at the satellite, although the constants of proportionality are different for the different bands.

Tables 3 A-E show the means and standard deviations of normalized reflected radiances for each band and each class. Also shown is the interband correlation matrix for each class. Figure 3 is a plot of these means against the band number. The ITD statistics for the best 4,3,2, and 1 band combinations are set out in Tables 4 A-D. The best combination for 3 or less bands is determined by a maximum

weighted average ITD. The significance of these figures can be assessed by reference to Figure 2 . The interpretation of these statistics is presented in Section IV.

"Ice truthing" operations carried out at INSTAAR involve 38 sample fields in the 1/4 scene. The fields, selected for homogeneity of spectral class, are outlined on the line printer map. Table 5 is a list of the field numbers, their coordinates on the Landsat CCT, their spectral classes, and the surface description and analysis categories. Histograms of normalized radiances and interband correlation coefficients for each of these fields were also used to aid interpretation. Discussion and interpretation of these results and their implications are presented in Section IV.

2) Maps of surface morphological characteristics

Working maps of the 1974 decay season Landsat sequence in the sector between Cape Halkett and the Canning River have been prepared using the techniques described in section II.2.C.1.b. The interpretation of these maps is largely based on the results of our multi-spectral analyses of remote sensing data, presented in section IV.B.1. The final data products are now being drafted onto the OCS Universal Transverse Mercator base maps, and will be forwarded to the project office upon completion. The results of the map analysis are pertinent to the overall conclusions and interpretation presented in section IV. Therefore, we present them below in descriptive prose format. It is noted here that the attempted quantitative gray-scale analysis discussed in the Annual Report was

dropped since the absolute gray-scale varies irregularly between scenes.

On 25 June (scene 1702-21093) the seaward limits of continuous ice are fairly well-defined. Band 7 shows several distinct but connected ice-boundaries extending across the entire scene from West to East. Examination of Band 4 shows that open water areas of various sizes occur at several points seaward of these boundaries, but nowhere to shoreward. Between Oliktok and Brownlow Point, the seaward extent of this continuous ice ranges between 15 and 32 km. On this date, the pack ice concentration (assessed on an areal scale of approx.  $10^3$  sq. km) is 9-10/10 all along the ice edge. This scene shows many elongate ice features, some of which are elevated, ice deformation zones (pressure and shear ridges, hummocked ice, etc.) as determined from the SLAR imagery. Most noteworthy is a tear-shaped ice mass, composed of highly-deformed and well-grounded ice, located at  $70^{\circ}44' N$ ,  $149^{\circ}30' W$ . Considerable spatial variability in the amount of ice-surface meltwater is obvious on this scene in all the bands. The most-puddled ice on the frame extends in an east-west belt of 0-15 km width, roughly centered on a line about 17 km seaward of the coast. Shoreward of this ice is a belt with very complex texture, containing many areas with light tones on the Landsat imagery, indicating a lesser amount of surface water. It is interesting to note that our analysis of the SLAR data showed that several of these areas with poorly-developed puddling were essentially smooth ice. The cause for such variations in puddling on apparently similar ice types is unknown at present. The ice between this intermediate

belt and the coast is essentially flat, extending from Oliktok to Brownlow point. West of the Kuparuk River, this smooth ice is mainly confined to the shoreward side of the Jones Islands. This ice extends up to 10km seaward of the coast to the east of the Sagavanirktox River. A number of light-toned linears extending seaward from the coast through this ice probably represent cracks which form drainage 'sinks' for the surrounding surface meltwater (cf. Jacobs et al. 1975). The only openings in the continuous ice sheet on this date are at the mouths of the major rivers.

In summary, we can delimit the continuous ice, which contains a number of deformation features, some of which are grounded. Surface meltwater amounts vary greatly over the image, and apparently within otherwise-similar ice categories. The darkest ice occupies a coast-parallel belt near the pack ice edge, and is possibly in a more-advanced stage of ablation than ice to shoreward.

On the following day, 26 June, we have a scene of the ice between mid-Harrison Bay and the Maguire Islands (scene 1203-21151). Again the continuous ice limits are fairly well-defined, and can be extended to a point in central Harrison Bay on the same basis as above. No change in the position of any major ice features within the continuous ice boundary of 25 June can be detected. The pack ice remained up against the seaward edge of continuous ice in 9-10/10 concentration. Pack ice motions between 6/25 and 6/26 were towards the West. Displacements along the continuous ice edge were very small, generally <0.25km, and directed to the west off Prudhoe Bay. The major velocity shear occurred between

10 and 20 km seaward of the continuous ice limits. Displacements shoreward of this zone were generally of the order of 1 km while the seaward floes were displaced ca. 10 km. It is noted that the pack ice floes shoreward of this zone of shear are generally smaller than those to seaward on this scene, indicating a possible connection between the shearing stress and floe-breakup. Indeed this two frame sequence shows pack ice pieces breaking apart in an area 50 km due N of the mouth of the Kuparuk River.

The section of continuous ice east of Oliktok remained much the same between 6/25 and 6/26, although the newly-imaged areas in Harrison Bay exhibit several interesting characteristics. Foremost is the presence of a second, larger grounded ice mass, located at  $70^{\circ}58' N$ ,  $150^{\circ}42' W$ . The edge of continuous ice makes a seaward bulge to a point 4 km north of this feature. The zone of maximum puddling noted on June 25 is seen to terminate at approximately  $149^{\circ}30' W$ , giving way to a lighter-toned area comprising central Harrison Bay. This area has a texture indicating a great number of large, light-toned individual ice pieces frozen into a matrix of slightly darker-toned ice. Shoreward of this ice, a 0-5 km wide crescent-shaped belt of very dark tone extends across the bay. The SLAR imagery shows this to be relatively flat, undeformed ice. Shoreward of this belt a strip of lighter ice of 1-2 km width extends along the same arcuate path. Fairly dark-toned ice occupies the rest of the bay up to the mouth of the Colville, where much of the ice has melted out completely.

On 26 June, then, we have at least two important grounded areas and a stable continuous ice edge. Great spatial variability in gray tones indicates a correspondingly wide variety of ice-types and puddling conditions. The pack ice appears to be shearing, but with little or no effect on the continuous ice sheet, because most of the shear takes place away from its seaward boundary. The only evidences of breakup progression are the dark, puddled ice surfaces and the open-water areas near river mouths.

The scene from 29 June (1706-21322) shows the area west of Oliktok point. A light cloud cover obscures much of NW Harrison Bay, but it is clear that the continuous ice boundary is unchanged from 26 June east of the larger grounded ice mass. Pack ice again appeared fairly compacted along the continuous ice edge, but displacements could not be determined due to clouds. Other features of interest include a highly-contrasting area NNE of C. Halkett with very light tone and homogeneous texture. SLAR and CIR data show this to be a very flat ice area, again contrasting sharply in puddle-development with neighboring areas of almost equally-smooth ice. Also evident is an increase in the open water area created at the outlet of the Colville river.

The next frame in the sequence is 12 July (1719-21031) covering the ice between a point seaward of Kuparuk River and Brownlow Point. The continuous ice edge has receded to a point about 5 km seaward of Brownlow Point. Openings are present in the ice which was in the darker toned belt on June 25. The continuous ice edge to

the west of Flaxman Island appears to be similar to that of 25 June, although some small displacements have occurred along this boundary. The pack ice is again very compact against the ice edge, and a 70 x 30 km area of advanced puddling seen in the pack ice off Prudhoe Bay. Motions could not be reliably determined using this frame. Within the continuous ice zone, several changes are evident. Some of the smooth ice between Tigvariak Island and Brownlow Point has undergone a lightening in tone, relative to other ice and the tundra. This phenomenon probably signals the drainage of formerly-puddled ice into the cracks and open areas. The Canning River mouth has melted out further. In the ice nearest shore from Tigvariak Island Westward, breakup has commenced with large openings and cracks evident in band 4. It appears that some of the near-shore smooth ice and the complex-textured intermediate belt mentioned above underwent considerable relative darkening since 25 June. Along this section of coast, then, the darkest ice on 25 June is still intact on 12 July, while lighter ice to shoreward is breaking up.

The next image in the sequence is 14 July (1721-21143) showing ice between Atigaru Pt. and the Maguire Islands. The continuous ice limits on this scene have undergone displacements since June. The ice which defined the seaward limit of continuous ice between the two grounded masses on 29 June is displaced up to 9 km to the SSW and openings in the ice cover are now evident in this area. East of the Kuparuk delta, the continuous ice edge

was displaced between 0 and 2 km shoreward since 26 June.

Pack ice on 14 July is compacted against the continuous ice along the entire coastal sector in 10/10 concentration. Motions during the interval 26 June-14 July included a 17 km westward displacement of pack ice immediately adjacent to the continuous ice edge.

Within the former continuous ice boundaries, openings have now formed. Notably, the ice shoreward of the large grounded ice mass in Harrison Bay has sheared away from the mass and moved southward, under compressive stress from the pack ice.

Cracks and openings of lesser size are evident at several other points to the east and also at distances between 15 and 30 km offshore. In near-shore areas, the major river mouth zones have melted out completely with open water areas of  $\sim 300 \text{ km}^2$ ,  $\sim 60 \text{ km}^2$  and  $\sim 80 \text{ km}^2$  at the mouths of the Colville, Kuparuk and Sagavanirktok rivers, respectively. Most of the near-shore ice on this scene is now deeply puddled and appears dark in all Landsat bands, although a great number of limited areas with light tones still exist. Breakup and movement of near-shore ice commenced on or before 12 July off the Sagavanirktok River, with giant floes cracking away from the main ice sheet on 14 July. This ice was displaced shoreward about 3 km after breaking off. In summary, then, this scene indicates three modes of ice decay:

- 1) Pack ice forces displacing the seaward edge of fast ice and causing opening and disaggregation of the once-continuous ice.

- 2) In situ melting in an advanced stage, particularly at river mouths.
- 3) Ice sheet breakup and movement in the shore polynyas created by the rivers.

July 15 (1722-21202) shows essentially the same ice phenomena as the previous scene, with an are coverage from Cape Halkett to the Sagavanirktoq River. The continuous ice limits, puddling distribution and pack ice characteristics are the same.

Motions in the pack were to the SSW near the coast and in the NE 1/4 scene, but were almost due south in the NW quarter-frame. One-day displacements ranged from 0 km along some parts of the continuous ice edge to 2 km in the pack ice 100 km off Prudhoe Bay.

On 16 July we have a scene centered on Harrison Bay (1723-21260). Noteworthy developments include the breakup of previously continuous ice in the area 10-30 km east of the smaller grounded ice mass. This ice had continually presented a relatively light tone on all images, yet the ice is sufficiently weak to fracture and move. The ice in this area is now displaced almost 2 km SW of its July 14 position.

Substantial openings in the ice were created by this movement.

Ice between the two grounded ice masses and in central Harrison Bay continued to move South, with a maximum displacement of 4 km. in two days.

At  $70^{\circ}42'N$ ,  $148^{\circ}45'W$  a mass of ice remained in place during the fracture and displacement of previously adjacent ice, causing

a small polynya. It appears that this mass may be a third major grounded feature.

Smoothen ice in the interior of Harrison Bay continued to melt, break apart and move, and generally presents the appearance of very advanced ablation.

Pack ice motions 100 km offshore of mid-Harrison Bay shifted towards the WSW between July 15 and 16, and were approximately 2 km magnitude. This general mode of displacement also occurred in pack ice off the Jones Islands. At the (now ill-defined) continuous ice edge, displacements were similarly about 1 to 2 km to WSW offshore of the tear-shaped grounded ice mass. No well-defined shear zone such as we saw on June 25-26 could be identified.

The final image in the 1974 summer sequence analyzed so far is on 2 August (1740-21194). On this scene, the fast ice sheet of 25 June is essentially broken up or melted, with the exception of the grounded masses identified previously. A fourth grounded ice feature was located 4 km seaward of Bodfish Island. Very rarefied pack ice extends a further 7 to 25 km seaward of the shore lead to the edge of pack ice. Motions during the previous two weeks were difficult to determine. However, displacements of isolated ice pieces were 17 km E and 10 km NE, measured at points 60 km north of Prudhoe Bay and 100km north of the Colville delta, respectively.

3) Dates of significant decay-season ice events

The compiled lists for dating each of the events described in section II.E.1.c. are presented in Tables 1A-F. The mean dates

of occurrence of the several events are:

- 1) First in situ puddling - June 11
- 2) First openings inside fast ice - June 29
- 3) First darkening in river channels - April 22
- 4) First flooding of near-shore ice by rivers - approximately May 25
- 5) Fast ice effectively broken and gone - July 28
- 6) New ice forming - October 4

It was found that the interannual variability in the date of these events was considerably less than the uncertainty in dating the event due to Landsat data gaps. Therefore, a climatological average is the only real result. Certain individual cases are being studied separately where good time continuity happens to be available.

B. Meteorological Data

1) Validation of Synoptic Catalog: Results

As described in section II.2.C.2.a., a sample of 100 days was checked for accuracy of classification and statistics. The results showed that the assigned types were 100% correct. All means, standard deviations and scores calculated from the raw data matched those on the 29-year file. All sample days were classified correctly with the proper key day also. It was found that a range of patterns (individual daily maps) can pass the threshold tests with any given key day, and thus some within-type variation in pressure patterns can be expected. Visual comparison did show, however, that the most salient characteristics (e.g. positions of major lows and highs, gradient directions, etc.) of the pressure patterns were similar within type groups. The basic daily catalog and related statistics are being read onto a 7 track BCD tape. This tape will be forwarded shortly to the Arctic Project Office along with hard-copy listing and full documentation in the near future.

2) Mean Monthly Frequencies of Synoptic Patterns, 9/1968-8/1974

The six years 9/1968 through 8/1974 comprise the main local climatological data set used for computer analysis of type weather characteristics. In this section, the mean monthly frequency of each type is presented (Figure 4). An obvious seasonal trend is evident on this graph. Type I dominates the circulation in late fall and late winter, but reaches a minimum in mid-summer. This

pattern is characterized by low pressure in the central Gulf of Alaska and a ridge over the Beaufort Sea, with easterly, cyclonically-curved isobars along the coast. Type 3 is also common in the cold season months, and has a low in the northeastern Gulf with a ridge extending right along the Beaufort Coast. It appears from inspection of the time series of types that this pattern preferentially follows type 1. This corresponds to an eastward displacement of the low pressure center and a southward displacement of the ridge over the Beaufort Coast. Contingency analysis of type-transition frequencies is in progress to assess the significance of this type of conclusion. Types 4 and 7 are also major contributors to the winter conditions. 4 is a high pressure cell centered in the Yukon and extending northwest into the Beaufort Sea, with decreasing pressure to the southwest. Type 7 shows lows to the southwest and northeast with a ridge along the Beaufort coast between them.

During the transition season from winter to summer, type 17 reaches a maximum in its monthly frequency. This pattern has a col in the pressure field over central Alaska. During the short summer, type 2 dominates, with a low to the northwest and southerly geostrophic flow across the state. Type 5 has relatively high frequency in this season, with a central Alaska ridge separating lows to the North and southeast. Types 6 and 8 both represent central Alaska troughs at the surface.

The weather characteristics of the types are being assessed, as discussed in section III.B.3. Once the relationships between weather and the types are established, the variability in seasonal frequency of the types can be examined to see whether or not they contribute to significant acceleration or retardation of various ice formation and decay processes.

3) Statistical Analysis of Weather Characteristics of Synoptic Types

Initial results of Analysis of Variance (ANOVA) tests on temperature anomaly data for Barter Island showed promise that some types had very distinct weather characteristics (see report). More recent analysis of LCD data in frequency tables has shown that the parametric ANOVA is probably not the appropriate test. For example, although it is believed that large differences do exist, the linear autocorrelation relationship explains less than 5% of the variance in the time series of daily temperature departures at Barter Island, 1969-73 at lags >5 days. If we assume, then, that a sample consisting of every fifth day is effectively uncorrelated in time, we may stratify it by synoptic type and calculate ANOVA parameters. However, Figs. 5A-D illustrate the problems encountered. These figures are frequency histograms for daily anomalies at Barter Island stratified by type and season for every fifth day, 1/1/69-8/31/74. The normal distribution function is also plotted, using the means standard deviations for each data set.

It is apparent that the data sets are not normally distributed. Furthermore, the variances of the different types are quite inhomogeneous and the samples are not very large, allowing little

relaxation in conformity with the assumed distribution. It seems more logical to examine the data set for each station by inspection first, and to formulate quantitative tests for important weather correspondences as they are found.

Figures 6 A-L show some of the more interesting type-characteristics analyzed thus far, again presented as frequency histograms. These are frequency histograms for Barrow daily temperature departures ( $\leq -15^{\circ}$  to  $\geq 15^{\circ}$ F) for every day, 1/1/1969-8/31/74. On these histograms, season 1 is January - April, Season 2 is May, Season 3 is June, Season 4 is July - August, season 5 is September. In winter, for example, type 2 (southerly flow) and type 3 (ridge over the Beaufort Sea coast) give rise to very different temperature departures which influences ice growth (Figures 6B & C). In the spring transition, however, type 1 (easterly cyclonic flow) is associated with nearly normal temperatures (Figure 6D). This analysis is currently being extended for all types, seasons, and other climatic parameters identified as being significant for ice decay (see "Word Model" in Section IV B).

C. Climate-Ice Interaction Case Studies

The results and products of the climate-ice interaction case studies are presented below. Some of the case studies are not entirely completed but significant results can be shown for three items:

- 1) Analysis and Probability of severe ice summers along the Pt. Barrow to Prudhoe Bay shipping route.
- 2) Fast ice breakup between Pt. Barrow and Cape Halkett - Associated synoptic types and meteorological conditions.
- 3) Wind velocities, synoptic types, and ice movement.

- 1) Case Study #1 - Analysis and probability of severe ice summers along the Pt. Barrow to Prudhoe Bay shipping route.

Barnett (1976) ranked the severity of summers in terms of ice since 1953 along the Pt. Barrow to Prudhoe Bay shipping route and his tabulation is reproduced in Table 6 with summers ranked from mildest = 1 to most severe = 23. Also included in Table 6 is a tabulation of summertime accumulated thawing degree days (TDDs) for Barrow and Barter Island, Alaska.

Since TDDs are an indicator of summertime mildness/severity in terms of air temperature, the summers are ranked in a similar fashion to the ice severity ranking in columns 4 and 6 of Table 6.

In terms of summer severity based on ice conditions along the shipping route (column 2) it was arbitrarily decided that

the first 11 ranked summers would be considered mild ice summers while the remaining 12 would be considered severe ice summers. From Barnett's data a severe ice summer would be one in which the ice edge retreats less than 15 km northward Pt. Barrow on either August 10 or September 15. Mild ice summers are those in which the ice retreats much further northward. Combining the data in Table 3, one finds that in terms of TDDs:

- (a) Mild Summers -Average TDD accumulation = 646 with a standard deviation = 165.
- (b) Severe Summers -Average TDD accumulation = 355 with a standard deviation = 61.

The difference between mild and severe ice summers in terms of temperature is apparent from the above statistics and is further emphasized by Column 4 of Table 6 which shows that during the period of record there are no summer TDD totals between 462 (1965) and 636 (1957). The distribution of Barrow summer temperatures is bimodal with the two segments of the distribution delimiting severe and mild ice summers in most cases. All 12 severe ice summers occur in the "cold" part of the distribution while 8 of the 11 mild ice summers form the "warm" side of the bimodal distribution. The remaining 3 mild summers, 1959, 1961, and 1963 had 441, 456, and 371 TDDs respectively and are therefore part of the "cold" side.

The analysis clearly indicates that over 475 TDDs are needed for mild ice summers and here it is further suggested that a transition range of between 400 and 475 TDDs also exists, wherein a summer could be mild or severe depending on the time

when the crucial number of TDDs is reached. With this criteria, 1959 and 1961 are joined by 1965 and 1971 in being transitional summers, the latter two being severe ice summers. Evidence supporting these categories of ice summers and temperature relationships comes from case study 2 below.

Since 1953 the percentage occurrence of obviously mild summers is 35% (8 of 23); 57% of the summers (12 of 23) have been transitional or mild (greater than 400 TDDs) with one missed case (1963 with 371 TDDs mentioned above). Two of the transitional cases ended up being severe summers by definition. Between 1959 and 1971 there were 2 mild, 4 transitional, and 7 severe summers. Since 1971, 3 of 4 winters along the Pt. Barrow to Prudhoe shipping route have been mild. The summer-time climate of the region is at a balance point over the 1953-1975 period. Future decrease in average summer temperature of 1°F over 100 days would result in 100 fewer TDDs from the current 23-year normal of 494 and the number of severe summers would increase. A similar 1°F amelioration of summer climate would prove very favorable along the shipping route. Whether or not this amelioration has taken place since 1971 is difficult to establish.

A similar analysis will be made later for the region centered on Barter Island, since in some summers the mildness/severity ranking does not follow that of Barrow.

- 2) Case Study #2 - Fast ice breakup between Pt. Barrow and Cape Halkett - associated synoptic types and meteorological conditions.

During the 4 summers for which LANDSAT imagery is available, breakup progresses as follows:

- (a) In 1972 National Weather Service breakup information for Barrow, Alaska (not included in the region of study) indicated first movement of ice by July 13 and boating permissible in the area by July 19. Based on LANDSAT imagery for the remaining 3 summers (1973-1975) and breakup data provided by Shapiro (pers. comm.), it appears that the fast ice between Pt. Barrow and Cape Halkett breaks up before the fast ice at Barrow. The only LANDSAT frame available (7/29/72) cannot be used to prove that the breakup in the Beaufort Sea Coast was before July 19, but the photo indicates that ice cleared for a considerable distance in both the Beaufort and Chukchi Seas, except for ice near the barrier islands. July 14 saw the first incidence of southerly geostrophic flow which persisted until 7/19/72.
- (b) There was incomplete LANDSAT coverage in 1973. By 7/7/73 ice still remains in the area of analysis, but this is the last frame of imagery available until October 4. In other regions, fast ice is clearing in the Barter Island area by 7/16/73 and is a considerable distance from shore in the 7/23/73 photo of Prudhoe Bay. Breakup of fast ice is a process which takes several days to complete and it appears that the process occurs more or less simultaneously along the Beaufort Coast. Thus, it is assumed that in the Pt. Barrow to Cape Halkett region breakup of fast ice may have occurred between July 10 and July 23.

By 10 July, 114 TDDs had accumulated, with 159 TDDs by July 20 and 221 by July 25. The first period of summer with consistently geostrophic flow begins on July 13 and ends by July 27. Radar observations by Sackinger and Rogers (1974) indicate breakup at Barrow between July 23 and July 31.

- (c) In 1974 there are LANDSAT images showing breakup in progress on July 20 and July 21. A July 16 photo shows breakup starting at the lonely DEW station and eastward. Only 59 TDDs had accumulated by July 15, with 107 by July 20. These are unusually low totals compared with those of previous summers. The first period of southerly geostrophic flow is between July 14 and July 18 and then between July 24 and July 31. Shapiro's (pers. comm.) radar work does not indicate breakup in the Barrow area until mid-August.
- (d) In 1975, a severe ice summer, meteorological conditions were favorable through July 20 to permit breakup of fast ice (but no northward retreat of the pack). The July 20 through July 23 LANDSAT images confirm this. The breakup at this time is more advanced than in 1974 and the only available data indicate 236 TDDs accumulated by July 20. The data suggest a good relationship between temperatures, an initial period of southerly geostrophic flow, and breakup of fast ice. The synoptic types which occurred during these known and assumed periods of breakup are as follows:

- (i) 7/10 - 7/21/72: type 2 (6 days); type 1 (2 days); types 4, 20, and 5 (once each).
- (ii) 7/10 - 7/23/73: type 2 (7 days); type 5 (4 days); type 14 (twice); type 11 (once).
- (iii) 7/15 - 7/22/74: type 2 (3 days); type 14 (2 days); types 7, 9, and 11 (once each).
- (iv) 7/18 - 7/23/75: No data.

It is worth mentioning here that these periods were the initial occurrences of type 2 (low to north, high to south) during 3 or more consecutive days in each of the summers. The data show a good relationship between the occurrence of types 2, 4 (high to southeast), 5 (low to north, ridge to south), and 15 (low to north, high to southeast) on days with southerly geostrophic flow.

At Barrow and vicinity of all days during the summers of 1972-1974 with southerly geostrophic flow, types 2, 4, 5, and 15 occurred on 8 of 11 June days, 34 of 38 July days and 29 of 36 August days.

During the periods of breakup just described, southerly surface winds occurred on many of the days but the relationship is not as clear as it is for geostrophic flow and synoptic types 2, 4, 5, and 15. Types 2 and 5 are the only types associated with southwest or west surface winds, all others preferring northerly and easterly directions (see Table 7).

Figure 7 shows the number of daily occurrences of types 2 and 5 on a monthly basis since 1946 and for comparison the two major types of easterly circulation, types 1 and 4, are given. This figure shows the diminution of easterly flow and increase of the westerlies in July and August. Whether breakup of fast ice and retreat of the pack would occur without the increase in these two types appears doubtful considering the available evidence.

A more precise scenario of fast ice breakup indicates that about 100 to 250 TDDs are needed for initial melting of ice and decreasing its thickness, after which synoptic patterns causing southerly geostrophic flow result in further advection of heat and winds favorable to the removal of the ice.

This case study is not completed in that more data and analysis are needed for the area of study, and the analysis must be expanded to cover the entire coast.

- 3) Case Study #3 - Wind velocities, synoptic types, and ice movement.

Cases of detectable movement of ice on LANDSAT imagery have been tabulated for areas north of Pt. Barrow and eastward as far as Cape Halkett, and for an area north of Brownlow Pt. to the Canadian border including Barter Island. (The study will be extended to cover the intervening areas later.) Data on wind direction, wind speed, and synoptic pattern type were collected for the days of the images and a few preceding days to examine how these factors are related. Table 8 shows

the tabulation of data. Table 3 shows the average wind speeds associated with the major synoptic types during the summer months.

The analysis of these data indicates:

- (a) The direction of ice movement is almost always the same as the direction of the wind from the two land National Weather Service stations, even though the moving ice may be hundreds of kilometers from those stations.
- (b) Type 1 is associated with the fastest wind speeds on a monthly average basis relative to the other types. It is also the most consistently northeasterly wind direction type (Table 7 ).
- (c) Tables 8 and 9 show that type 1, probably as a result of its characteristics described in (b) above, is associated with almost all cases of ice movement having a westward direction (i.e., ice drift to right of wind).
- (d) Ice movement north of Pt. Barrow is associated with lower wind speeds than ice movement north of Barter Island. At Barrow ice movement can occur during winds less than 5 m/s whereas at Barter Island breaking ice in the pack or shorefast area apparently requires persistent winds of 8-9 m/s.

IV. INTERPRETATION

A. Remote Sensing Data

1) LARSYS Analysis

The analysis of machine-processing on Landsat CCT 1702-21093 and related remote sensing data yielded several conclusions. The 8 spectral classes containing information included 6 ice classes, 1 water class and 1 tundra class. The classes were interpreted as follows:

<u>Class</u>	<u>Roughness</u>	<u>%Puddles</u>	<u>Depth</u>	<u>Other</u>
2	Flat to Ridged	25-50	S-D	
3	Flat to Hummocked	50-100	S-D	
4	Flat to Ridged	<40	S	
5	Noise Class	-	-	
6	Flat	60-80	S-D	
7	-	-	-	Water
8	Flat	70-90	S-M	
9	-	-	-	Tundra
10	Flat	Flooded	D	

The differences between ice classes were exclusively related to surface water characteristics. Such characteristics as ice age, relief and origin were not distinguished except as they related to surface water. For example, ridges occurred in these classes also. A unique relationship between spectral classes and percent surface area covered by puddles is not obtainable by this method. Individual puddled areas are usually sub-resolution size, so that their frac-

tional area in a pixel is represented in the reflected radiance level. However, the depth of each individual puddle element also determines the reflected pixel radiance, so we have an infinite variety of depth-area combinations for any given reflectance. It is possible, however, to assess the surface water characteristics based on both areal coverage of puddles and puddle depth.

A further significant result is the redundancy of the multispectral data. Figure 3 shows the mean reflected radiances for each class. All of the curves for ice classes drop off in band 6, and only two curves intersect (3 and 8). This indicates that any one band provides the great majority of information. This fact shows up in the high interband correlations (tables 3A-3E) and in the high ITD statistics for one- and two-band combinations (Tables 4C and 4D). Considerable expense might be saved by using only one or two bands for computer analysis rather than three or four.

In summary, the data indicate that the characteristics of early-summer fast ice are such that only surface water variations can be distinguished using spectral information exclusively. Spatial patterns, time sequential behaviour and supplementary data (such as SLAR) are necessary for obtaining more information.

2) 1974 Ice Decay Seasons: Harrison Bay to Brownlow Point

The Landsat sequence for the 1974 decay season indicates that 3 modes of ice-decay are operative. These are:

- 1) In situ ablation.
- 2) Breakup in shore polynyas caused by wind and water stress.
- 3) Breakup to seaward caused by impingement of pack ice.

The belt of maximum meltwater on the ice surface originated on the ice to seaward and progressed towards shore. The breakup was hastened by proximity of the pack ice and occurrence of wind-driven compressional forces at the fast ice edge. Four grounded ice features remained in place after the main sheet had melted and broken up. These features were stable during pack ice impingement and probably extended the period of continuous ice. The climatic/meteorological causes of the individual breakup processes are presently under investigation. The relationships between breakup date, ice behavior and climatic variables appear to be complex.

B. Climate - Ice Interactions

Until more case studies, similar to those presented in III.C. can be carried out for other summers, the formulation of statements regarding climatic effects on fast ice extent and decay must remain tentative. A preliminary interpretation has been developed, however, in the form of a simple conceptual "word model", presented in Table 10. This summarizes the primary variables for which data are readily available, the process involved in their effect on the ice and the nature of the interactions, according to season.

V. PROBLEMS/RECOMMENDATIONS

The value of SLAR coverage in interpreting the Landsat imagery has become increasingly apparent. We have concentrated on interpreting 1974 data owing to the availability of SLAR and strongly urge that provision be made for some periodic coverage during winter months.

VI. ESTIMATE OF FUNDS EXPENDED

\$46,000.

SUMMARY OF OBJECTIVES AND FINDINGS  
WITH RESPECT TO OCS DEVELOPMENT PLANNING

The objective of this study is to assess the role of climatic factors in determining the extent and seasonal decay of fast ice along the Beaufort Sea coast. The period of stable fast ice, which extends to about the 18 m contour, terminated approximately July 7 during 1973-74. Both were relatively mild years at Barrow with only average ice conditions by comparison with 1955, 1969, and 1975. Southerly air flows favor ice removal given antecedent melting. Temperature and wind conditions related to ice decay differ along the coast but can be specified and are ultimately, therefore, predictable. The first new fast ice formed about October 4 (in 1973-75).

Multispectral digital data from Landsat can be classified to generate maps of ice-surface melt characteristics during the decay season, given suitable ground truth, but other interpretation requires SLAR data.

A preliminary "word model" of climate-ice interaction has been developed.

REFERENCES

- Holmgren, B., Benson, C. and Weller, G. 1974. A Study of the Breakup on the Arctic Slope of Alaska by Ground, Air and Satellite Observations. In: Climate of the Arctic, 24th Alaska Science Conference, Fairbanks, 1973, 358-366.
- Jacobs, J. D., Barry, R. G. and Weaver, R. L. 1975. Fast ice characteristics with special reference to the eastern Canadian Arctic. Polar Record, V. 17, 521-536.
- Sackinger, W. M. and Rogers, J. C. 1974. Dynamics of break-up in Shore-fast ice. In: The Coast and Shelf of the Beaufort Sea, eds. J. C. Reed and J. E. Sater, 367-376.
- Swain, P. H. 1973. A Result from Studies of Transformed Divergence. LARS Tech. Mem. T-8-050173, LARS, Purdue Univ.
- Swain, P. H. and Staff. 1972. Data processing 1: Advancements in machine analysis of multispectral data. LARS Info. Note No. 012472, Purdue University.
- Swain, P. H. and King, R. C. 1973. Two Effective Feature-Selection Criteria for Multi-spectral Remote Sensing. LARS Info. Note, presented at International Joint Conference on Pattern Recognition. Washington, D. C. November, 1973. 5 pp.

REFERENCES: ICE INTERPRETATION

- Barnes, J. C. and Bowlex, C. J. 1974. The Application of ERTS Imagery to Monitoring Arctic Sea Ice. Environmental Research and Technology, Inc. ERT Document 0408-F, Lexington, Massachusetts. 90 pp.

Barnes, J. C., Bowley, C. J. and Smallwood, M. D. 1975. The Application  
of ERTS Imagery to Monitoring Arctic Sea Ice: Supplemental Report.

Env. Res. and Tech., Inc., Lexington, Mass. ERT Document 0408-S.

47 pp.

Bryan, M. L. 1975. A Comparison of ERTS-1 and SLAR Data for the Study  
of Surface Water Resources. Environmental Research Institute of  
Michigan. NASA ERIM 193300-59-F. 104 pp.

Campbell, W. J., Weeks, W. F., Ramserer, R. O. and Gloersen, P. 1975.  
Geophysical Studies of Floating Ice by Remote Sensing. J. of  
Glaciology, V. 15, No. 73, 305-327.

Table 1A

Landsat Dates for Initiation of Fast-ice Meltwater

1973

<u>Sector</u>	<u>No Meltwater</u>	<u>Meltwater Present</u>
1	5/14 (1295-21575)	5/30 (1311-21461)
2	4/5 (1256-21405)	5/30 (1311-21461)
3	5/6 (1287-21120)	6/14 (1326-21284)
4	5/24 (1305-21115)	
5	5/24 (1305-21115)	
6	4/14 (1265-20493)	

1974

<u>Sector</u>	<u>No Meltwater</u>	<u>Meltwater Present</u>
1	5/10 (1656-21562)	6/29 (1706-21322)
2	5/21 (1667-21162)	6/25 (1702-21093)
3	5/21 (1667-21162)	6/25 (1702-21093)
4	5/19 (1665-21045)	6/25 (1702-21093)
5	5/19 (1665-21045)	6/21 (1698-20470)
6	5/15 (1661-20423)	6/21 (1698-20470)

Table 1A (cont.)

1975

<u>Sector</u>	<u>No Meltwater</u>	<u>Meltwater Present</u>
1	5/15 (2113-21563)	6/18 (2147-21452)
2	4/20 (2088-21170)	
3	4/20 (2088-21170)	6/28 (2157-20595)
4	4/17 (2085-20595)	6/28 (2157-20595)
5	4/30 (2098-20313)	6/28 (2157-20595)
6	4/30 (2098-20313)	

Table 1B

Landsat Dates Showing First Large-Scale Movements in  
Fast Ice

1973

<u>Sector</u>	<u>No Openings and Movements</u>	<u>Movement</u>
1	6/17 (1329-21455)	7/2 (1344-21283)
2	6/17 (1329-21455)	7/2 (1344-21283)
3	6/14 (1326-21284)	7/2 (1344-21283)
4	5/24 (1305-21115)	8/2 (1375-20595)
5	5/24 (1305-21115)	7/14 (1356-20540)
6	5/02 (1283-20493)	7/14 (1356-20540)

1974

<u>Sector</u>	<u>No Openings and Movements</u>	<u>Movement</u>
1	5/28 (1674-21555)	6/29 (1706-21322)
2	5/21 (1667-21167)	6/26 (1703-21151)
3	5/19 (1665-21045)	6/25 (1702-21093)
4	5/19 (1665-21045)	6/25 (1702-21093)
5	5/19 (1665-21045)	6/21 (1698-20470)
6	5/15 (1661-20423)	6/21 (1698-20470)

Table 1B (cont.)

1975

<u>Sector</u>	<u>No Openings and Movements</u>	<u>Movement</u>
1	5/13 (2111-21450)	7/6 (2165-21452)
2	5/13 (2111-21450)	7/6 (2165-21452)
3	None	None
4	None	None
5	None	None
6	5/5 (1986-20361)	7/14 (2173-20481)

Table 1C

Landsat Dates for Spring Darkening in River Channels

1973

<u>River</u>	<u>No Darkening</u>	<u>Darkening</u>
Chipp	4/10 (1260-22032)	5/14 (1295-21575)
Colville	5/5 (1256-21405)	6/14 (1326-21284)
Sagavanirktok	5/3 (1254-21292)	6/14 (1326-21284)
Canning	5/6 (1287-21120)	5/24 (1305-21115)
Jago	None	None

1974

<u>River</u>	<u>No Darkening</u>	<u>Darkening</u>
Chipp	4/1 (1617-21403)	5/7 (1653-21394)
Colville	3/31 (1616-21345)	4/18 (1634-21342)
Sagavanirktok	3/11 (1596-21234)	5/2 (1648-21111)
Canning	None	None
Jago	4/11 (1627-20545)	4/28 (1644-20489)

1975

(Analysis Incomplete)

Table I.D.

Landsat dates showing over-ice flooding at river mouths

1973

<u>River</u>	<u>No Flooding</u>	<u>Flooding</u>
Chipp	5/30 (1311-21461)	6/17 (1329-21455)
Colville	5/4 (1650-21223)	6/14 (1326-21284)
Sagavariktok	5/4 (1650-21223)	6/14 (1326-21284)
Canning	5/6 (1287-21120)	5/24 (1305-21115)
Jago	None	None

1974

<u>River</u>	<u>No Flooding</u>	<u>Flooding</u>
Chipp	5/8 (1654-21452)	6/29 (1706-21322)
Colville	5/21 (1667-21162)	6/26 (1703-21151)
Sagavariktok	5/21 (1667-21162)	6/25 (1702-21093)
Canning	5/3 (1649-21165)	5/19 (1665-21045)
Jago	5/15 (1661-20423)	6/21 (1698-20470)

1975

(Analysis Incomplete)

Table 1 E.

Landsat dates showing post-breakup fast ice condition

1973

<u>Sector</u>	<u>Pre-Breakup</u>	<u>Post-Breakup</u>
1	7/7 (1349-21564)	10/4 (1438-21495)
2	7/2 (1344-21283)	8/23 (1397-21220)
3	7/2 (1344-21283)	8/23 (1397-21220)
4	5/24 (1305-21115)	8/23 (1397-21220)
5	5/14 (1295-21575)	7/16 (1358-21052)
6	5/14 (1295-21575)	7/16 (1358-21052)

1974

<u>Sector</u>	<u>Pre-Breakup</u>	<u>Post-Breakup</u>
1	7/21 (1728-21541)	8/22 (1760-21302)
2	7/16 (1723-21260)	8/2 (1740-21194)
3	7/16 (1723-21260)	8/2 (1740-21194)
4	7/14 (1721-21143)	9/4 (1773-21011)
5	7/12 (1719-21031)	9/4 (1773-21011)
6	None (1719-21031)	9/20 (1789-20493)

1975

(Analysis Incomplete)

Table I F.

Landsat dates showing first new ice in fall

1973

<u>Sector</u>	<u>No New Ice</u>	<u>New Ice</u>
1	10/4 (1438-21495)	10/19 (1453-21321)
2	9/28 (1432-21153)	10/19 (1453-21321)
3	9/28 (1432-21153)	10/19 (1453-21321)
4	9/28 (1432-21153)	10/15 (1449-21092)
5	9/5 (1409-20475)	10/15 (1449-21092)
6	9/5 (1409-20475)	10/14 (1448-21040)

1974

<u>Sector</u>	<u>No New Ice</u>	<u>New Ice</u>
1	8/22 (1760-21302)	10/18 (1817-21460)
2	9/6 (1775-21124)	10/13 (1812-21172)
3	9/6 (1775-21124)	10/13 (1812-21172)
4	9/6 (1775-21124)	10/13 (1812-21172)
5	9/20 (1789-20493)	10/6 (1805-20373)
6	9/20 (1789-20493)	10/6 (1805-20373)

Table 2.

Sample Dates Used to Validate the Synoptic Catalog

1/1/46	7/15/52	1/29/59
4/29/46	10/29/52	5/15/59
8/1/46	2/1/53	8/29/59
11/15/46	5/29/53	12/01/59
3/1/47	9/1/53	3/15/60
6/15/47	12/15/53	6/29/60
9/29/47	4/1/54	10/01/60
1/1/48	7/15/54	1/15/61
4/15/48	10/29/54	5/1/61
7/29/48	2/1/55	8/15/61
11/1/48	5/29/55	11/29/61
2/15/49	9/1/55	3/15/62
6/1/49	12/15/55	6/29/62
9/15/49	3/29/56	10/01/62
12/29/49	7/01/56	1/15/63
4/15/50	10/15/56	5/1/63
7/29/50	1/29/57	8/15/63
11/1/50	5/15/57	11/29/63
2/15/51	8/29/57	3/01/64
6/1/51	12/01/57	6/15/64
9/15/51	3/29/58	9/29/64
12/29/51	7/1/58	1/1/65
4/1/52	10/15/58	4/29/65

Table 2 (cont.)

8/01/65	12/15/72
11/15/65	4/1/73
3/01/66	7/15/73
6/15/66	10/29/73
9/29/66	2/01/74
1/01/67	5/29/74
4/29/67	
8/01/67	
11/15/67	
2/29/68	
6/01/68	
9/15/68	
12/29/68	
4/15/69	
7/29/69	
11/01/69	
2/15/70	
6/01/70	
9/15/70	
12/29/70	
4/15/71	
7/29/71	
11/01/71	
2/15/72	
5/29/72	
9/01/72	

Table 3 A. Radiance Statistics for Classes Null and 2

CLASS NULL 0.2

CHANNEL	1	2	3
SPECTRAL	0.50 -	0.60 -	0.70 -
BAND	0.60	0.70	0.80
MEAN	0.0	0.0	0.0
STD. DEV.	0.32	0.32	0.32

CORRELATION MATRIX

SPECTRAL	0.50 -	0.60 -	0.70 -
BAND	0.60	0.70	0.80
0.50 -			
0.60	1.00		
0.60 -			
0.70	0.0	1.00	
0.70 -			
0.80	0.0	0.0	1.00

CLASS 2

CHANNEL	1	2	3
SPECTRAL	0.50 -	0.60 -	0.70 -
BAND	0.60	0.70	0.80
MEAN	110.24	101.39	79.66
STD. DEV.	11.51	11.03	9.46

CORRELATION MATRIX

SPECTRAL	0.50 -	0.60 -	0.70 -
BAND	0.60	0.70	0.80
0.50 -			
0.60	1.00		
0.60 -			
0.70	0.88	1.00	
0.70 -			
0.80	0.69	0.89	1.00

Table 3.B. Radiance Statistics for Classes 3 and 4

CLASS 3

CHANNEL	1	2	3	
SPECTRAL BAND	0.50 - 0.60	0.60 - 0.70	0.70 - 0.80	
MEAN	53.46	45.02	34.51	
STD. DEV.	12.28	12.52	10.48	

CORRELATION MATRIX

SPECTRAL BAND	0.50 - 0.60	0.60 - 0.70	0.70 - 0.80
0.50 - 0.60	1.00		
0.60 - 0.70	0.95	1.00	
0.70 - 0.80	0.88	0.96	1.00

CLASS 4

CHANNEL	1	2	3
SPECTRAL BAND	0.50 - 0.60	0.60 - 0.70	0.70 - 0.80
MEAN	127.00	127.00	116.75
STD. DEV.	0.06	0.18	5.23

CORRELATION MATRIX

SPECTRAL BAND	0.50 - 0.60	0.60 - 0.70	0.70 - 0.80
0.50 - 0.60	1.00		
0.60 - 0.70	0.93	1.00	
0.70 - 0.80	0.03	0.04	1.00

Table 3 C. Radiance Statistics for Classes 5 and 6

CLASS 5

CHANNEL	1	2	3
SPECTRAL BAND	0.50 - 0.60	0.60 - 0.70	0.70 - 0.80
MEAN	126.99	126.59	101.71
STD. DEV.	0.15	1.18	3.95

CORRELATION MATRIX

SPECTRAL BAND	0.50 - 0.60	0.60 - 0.70	0.70 - 0.80
0.50 - 0.60	1.00		
0.60 - 0.70	0.17	1.00	
0.70 - 0.80	0.03	0.20	1.00

CLASS 6

CHANNEL	1	2	3
SPECTRAL BAND	0.50 - 0.60	0.60 - 0.70	0.70 - 0.80
MEAN	79.68	59.33	42.74
STD. DEV.	12.88	10.69	13.13

CORRELATION MATRIX

SPECTRAL BAND	0.50 - 0.60	0.60 - 0.70	0.70 - 0.80
0.50 - 0.60	1.00		
0.60 - 0.70	0.27	1.00	
0.70 - 0.80	-0.15	0.88	1.00

Table 3 D. Radiance Statistics for Classes 7 and 8

CLASS 7

CHANNEL	1	2	3
SPECTRAL BAND	0.50 - 0.60	0.60 - 0.70	0.70 - 0.80
MEAN	25.73	12.88	7.71
STD. DEV.	1.90	1.55	1.54

CORRELATION MATRIX

SPECTRAL BAND	0.50 - 0.60	0.60 - 0.70	0.70 - 0.80
0.50 - 0.60	1.00		
0.60 - 0.70	0.72	1.00	
0.70 - 0.80	0.59	0.63	1.00

CLASS 8

CHANNEL	1	2	3
SPECTRAL BAND	0.50 - 0.60	0.60 - 0.70	0.70 - 0.80
MEAN	72.20	52.01	22.15
STD. DEV.	7.26	6.38	6.03

CORRELATION MATRIX

SPECTRAL BAND	0.50 - 0.60	0.60 - 0.70	0.70 - 0.80
0.50 - 0.60	1.00		
0.60 - 0.70	0.72	1.00	
0.70 - 0.80	0.44	0.82	1.00

Table 3 E. Radiance Statistics for Classes 9 and 10

CLASS 9

CHANNEL	1	2	3
SPECTRAL BAND	0.50 - 0.60	0.60 - 0.70	0.70 - 0.80
MEAN	29.30	25.72	26.89
STD. DEV.	1.83	1.71	2.13

CORRELATION MATRIX

SPECTRAL BAND	0.50 - 0.60	0.60 - 0.70	0.70 - 0.80
0.50 - 0.60	1.00		
0.60 - 0.70	0.61	1.00	
0.70 - 0.80	0.19	0.45	1.00

CLASS 10

CHANNEL	1	2	3
SPECTRAL BAND	0.50 - 0.60	0.60 - 0.70	0.70 - 0.80
MEAN	32.83	25.74	15.93
STD. DEV.	3.46	3.12	2.13

CORRELATION MATRIX

SPECTRAL BAND	0.50 - 0.60	0.60 - 0.70	0.70 - 0.80
0.50 - 0.60	1.00		
0.60 - 0.70	0.87	1.00	
0.70 - 0.80	0.14	0.31	1.00

TABLE 4A

ITD of all 4-band combinations

CHANNELS	DIJ(MIN)	D(AVE)	WEIGHTED INTERCLASS DIVERGENCE (DIJ)												
			12 (10)	13 (10)	14 (10)	15 (10)	16 (10)	17 (10)	18 (10)	19 (10)	23 (10)	24 (10)	25 (10)	26 (10)	
1. 1 2 3 4	1796.	1986.	1922	2000	2000	1847	2000	2000	2000	2000	2000	2000	2000	1796	2000

375

CONTINUED...

WEIGHTED INTERCLASS DIVERGENCE (DIJ)																	
27 (10)	28 (10)	29 (10)	34 (10)	35 (10)	36 (10)	37 (10)	38 (10)	39 (10)	45 (10)	46 (10)	47 (10)	48 (10)	49 (10)	56 (10)	57 (10)	58 (10)	59 (10)
1. 1978	2000	2000	2000	2000	2000	2000	2000	2000	2000	2000	2000	2000	2000	1947	2000	2000	

CONTINUED...

WEIGHTED INTERCLASS DIVERGENCE (DIJ)															
67 (10)	68 (10)	69 (10)	78 (10)	79 (10)	89 (10)										
1. 2000	2000	1999	2000	2000	1999										

Note: Channels 1-4 correspond to Landsat bands 4-7

TABLE 4B  
ITD of all 3-band combinations

CHANNELS	DIJ(MIN)	D(AVE)	WEIGHTED INTERCLASS DIVERGENCE (DIJ)													
			12 (10)	13 (10)	14 (10)	15 (10)	16 (10)	17 (10)	18 (10)	19 (10)	23 (10)	24 (10)	25 (10)	26 (10)	27 (10)	
1.	1 2 3	1719.	1982.	1916	2000	2000	1833	2000	2000	2000	2000	2000	1719	2000	1973	
2.	1 2 4	1667.	1972.	1917	2000	2000	1826	2000	1999	2000	2000	2000	1731	2000	1854	
3.	1 3 4	1539.	1960.	1919	2000	2000	1792	2000	2000	2000	2000	2000	1697	2000	1942	
4.	2 3 4	961.	1953.	1898	2000	2000	1781	2000	2000	2000	2000	2000	961	2000	1972	

CONTINUED...

WEIGHTED INTERCLASS DIVERGENCE (DIJ)

	28 (10)	29 (10)	34 (10)	35 (10)	36 (10)	37 (10)	38 (10)	39 (10)	45 (10)	46 (10)	47 (10)	48 (10)	49 (10)	56 (10)	57 (10)	58 (10)	59 (10)	67 (10)
ω	1.	2000	2000	2000	2000	2000	2000	2000	2000	2000	2000	2000	2000	2000	1942	2000	2000	2000
76	2.	2000	2000	2000	2000	2000	2000	2000	2000	2000	2000	2000	2000	2000	1667	2000	2000	2000
	3.	2000	2000	1706	2000	2000	2000	2000	2000	2000	2000	2000	2000	2000	1539	2000	2000	2000
	4.	2000	2000	1978	2000	2000	2000	2000	2000	2000	2000	2000	2000	2000	1707	2000	2000	2000

CONTINUED...

WEIGHTED INTERCLASS DIVERGENCE (DIJ)

	68 (10)	69 (10)	78 (10)	79 (10)	89 (10)
1.	2000	1999	2000	2000	1973
2.	2000	1999	2000	2000	1998
3.	2000	1949	2000	2000	1998
4.	2000	1998	2000	2000	1999

Note: Channels 1-4 correspond to Landsat bands 4-7

TABLE 4C  
ITD of all 2-band combinations

CHANNELS	DIJ(MIN)	D(AVE)	WEIGHTED INTERCLASS DIVERGENCE (DIJ)													
			12 (10)	13 (10)	14 (10)	15 (10)	16 (10)	17 (10)	18 (10)	19 (10)	23 (10)	24 (10)	25 (10)	26 (10)	27 (10)	
1.	1 3	1500.	1952.	1913	2000	2000	1782	2000	1999	2000	2000	2000	2000	1607	2000	1923
2.	2 3	904.	1948.	1895	2000	2000	1772	2000	2000	2000	2000	2000	2000	904	2000	1970
3.	2 4	757.	1929.	1892	2000	2000	1753	2000	1999	2000	2000	2000	2000	757	2000	1815
4.	1 4	841.	1911.	1914	2000	2000	1736	2000	1999	2000	2000	2000	2000	1320	2000	1811
5.	1 2	839.	1910.	1908	2000	2000	1821	2000	1989	2000	2000	2000	2000	1700	2000	1475
6.	3 4	367.	1855.	1854	1972	1891	1559	2000	1999	2000	2000	2000	2000	367	2000	1001

CONTINUED...

WEIGHTED INTERCLASS DIVERGENCE (DIJ)

	28 (10)	29 (10)	34 (10)	35 (10)	36 (10)	37 (10)	38 (10)	39 (10)	45 (10)	46 (10)	47 (10)	48 (10)	49 (10)	56 (10)	57 (10)	58 (10)	59 (10)	67 (10)
1.	2000	1999	1658	2000	2000	2000	2000	2000	2000	2000	2000	2000	2000	2000	1500	2000	2000	2000
2.	2000	1999	1974	2000	2000	2000	2000	2000	2000	2000	2000	2000	2000	2000	1669	2000	2000	2000
3.	2000	2000	1911	2000	2000	2000	2000	2000	2000	2000	2000	2000	2000	2000	1335	2000	2000	2000
4.	2000	2000	841	2000	2000	2000	2000	2000	2000	2000	2000	2000	2000	2000	1379	2000	2000	2000
5.	2000	1952	2000	2000	2000	2000	2000	2000	2000	2000	2000	2000	2000	2000	839	2000	2000	2000
6.	1984	1997	1593	2000	2000	2000	2000	2000	2000	2000	2000	2000	2000	2000	1371	2000	2000	1999

CONTINUED...

WEIGHTED INTERCLASS DIVERGENCE (DIJ)

	68 (10)	69 (10)	78 (10)	79 (10)	89 (10)
1.	2000	1913	2000	2000	1969
2.	2000	1996	2000	1998	1965
3.	2000	1997	2000	1999	1998
4.	2000	1814	2000	2000	1998
5.	2000	1998	2000	2000	1085
6.	2000	1910	1989	1302	1997

Note: Channels 1-4 correspond to Landsat bands 4-7

TABLE 4D  
ITD of all 1-band combinations

CHANNELS	DIJ(MIN)	D(AVE)	WEIGHTED INTERCLASS DIVERGENCE (DIJ)														
			12 (10)	13 (10)	14 (10)	15 (10)	16 (10)	17 (10)	18 (10)	19 (10)	23 (10)	24 (10)	25 (10)	26 (10)	27 (10)	28 (10)	
1.	3	147.	1799.	1849	1970	1841	1542	2000	1999	2000	2000	2000	2000	147	2000	704	1785
2.	2	195.	1797.	1890	2000	2000	1694	2000	1988	2000	2000	2000	2000	362	2000	406	2000
3.	1	328.	1728.	1885	2000	2000	1097	2000	1829	2000	2000	2000	2000	840	2000	943	2000
4.	4	81.	1647.	1719	1730	1220	1439	2000	1998	1964	2000	2000	1997	81	2000	905	728

CONTINUED...

WEIGHTED INTERCLASS DIVERGENCE (DIJ)

	29 (10)	34 (10)	35 (10)	36 (10)	37 (10)	38 (10)	39 (10)	45 (10)	46 (10)	47 (10)	48 (10)	49 (10)	56 (10)	57 (10)	58 (10)	59 (10)	67 (10)	68 (10)
1.	1996	1527	2000	2000	2000	2000	2000	2000	2000	2000	2000	2000	2000	1312	1994	2000	1997	2000
2.	1935	1891	2000	2000	2000	2000	2000	2000	2000	2000	2000	2000	2000	337	2000	2000	2000	1999
3.	1906	554	2000	2000	2000	2000	2000	2000	2000	2000	2000	2000	2000	328	2000	2000	2000	738
4.	1839	397	1998	2000	2000	2000	2000	1984	2000	2000	2000	2000	2000	1211	868	1955	1819	2000

378

-166-

CONTINUED...

WEIGHTED INTERCLASS DIVERGENCE (DIJ)

	69 (10)	78 (10)	79 (10)	89 (10)
1.	1869	1039	1250	1927
2.	1992	2000	1993	195
3.	1421	2000	2000	678
4.	1271	1867	321	1995

Note: Channels 1-4 correspond to Landsat bands 4-7

Table 5.

Field Numbers and Their Characteristics Used in the LARSH Analysis

<u>Field</u>	<u><math>\lambda</math>-Class</u>	<u>Rows</u>	<u>Columns</u>	<u>*Roughness</u>	<u>%Puddling</u>	<u>**Depth</u>	<u>Other</u>
1	2	1123-1140	889-934	L	40	S	
2	2	1056-1064	636-652	L	30	S	
3	2	873-878	425-442	L	25	S-D	
4	2	909-919	554-562	L	50	S	
5	2	1013-1016	870-884	H	0-100	D	
6	3	1059-1068	488-502	L	70	S-D	
7	3	893-903	557-569	M	50	D	
8	3	1005-1013	595-605	L	50	M-D	
9	3	1155-1161	743-752	L	70	S-D	
10	3	1044-1052	800-812	L	60	M	
11	3	1053-1060	1017-1028	L+M	0-100	S-M	
12	3	1047-1050	400-406	L	50	M-D	
13	4	910-919	443-468	L	40	S	
14	4	1004-1009	400-416	L	25	S	
15	4	1091-1098	400-412	L	0	-	
16	4	921-932	689-695	L-H	0-70	S	Hummocky
17	4	943-951	785-793	L-M	15	S	
18	4	1006-1017	906-910	L	40	S	
19	4	1104-1120	710-723	L	20	S	
20	4	917-921	747-755	H	0-100	S	

-67-

(cont.)

\* L = Low

\*\* S = Shallow

M = Medium

M = Medium

H = High

D = Deep

Table 5 (cont.)

Field Numbers and Their Characteristics Used in the LARsys Analysis

<u>Field</u>	<u>λ-Class</u>	<u>Rows</u>	<u>Columns</u>	<u>*Roughness</u>	<u>%Puddling</u>	<u>**Depth</u>	<u>Other</u>
21	6	1025-1028	497-512	L	50	S-M	Ridged
22	6	970-975	834-838	L	80	M	
23	6	1092-1097	864-871	L-M	50	M	
24	6	1154-1159	759-763	L	60	M	
25	6	1237-1240	1002-1012	L	60	S-M	
26	7	1144-1149	809-818	L	100	D	
27	7	466-486	1372-1398	-	-	OW	
28	8	1067-1074	434-436	L	80	S	Lake Ice
29	8	1112-1115	595-599	L	70	S	Lake Ice
30	8	1323-1333	939-945	L	90	S-M	Lake Ice
31	8	1032-1034	490-500	L	50	S-M	
32	9	1086-1083	431-441	-	-	-	
33	9	983-986	455-462	-	-	-	
34	9	1120-1130	595-599	-	-	-	
35	9	1116-1121	658-666	-	-	-	Wet Ground
36	10	1123-1130	471-476	L	-	-	Delta
37	10	1180-1185	800-810	L	-	-	
38	10	783-788	439-443	L	80-100	D	

\*, \*\* (see previous page)

Table 6. Mildness/Severity of Summers Since 1953 in Terms of Ice and Temperature at Barrow and Barter Island.

Summer	Ice severity Rank, Barrow to Prudhoe Bay (1 = mildest)	Summer TDD accumulation at Barrow (°F)	Rank Summer TDDs at Barrow (1 = mildest)	Summer TDD accum- ulation at Barter Is.	Rank Summer TDDs at Barter Is. (1 = mildest)
1953	15	366	17		
1954	9	925	1		
1955	22	303	22		
1956	20	321	20		
1957	11	636	8	844	2
1958	1	737	4	1118	1
1959	7	441	11	384	18
1960	17	351	18	439	13
1961	4	456	10	616	8
1962	3	721	5	669	5
1963	6	371	16	594	9
1964	18	311	21	406	16
1965	14	462	9	363	19
1966	13	389	13	571	10
1967	12	379	14	520	11
1968	2	760	3	737	3
1969	21	227	23	386	17
1970	19	375	15	430*	14
1971	16	426	12	618	7
1972	8	765	2	639	6
1973	5	645	7	717	4
1974	10	655	6	429	15
1975	23	346	19	461	12
<hr/>					
Mean values		494		576	

\* Estimate due to some missing data.

Table 7. Prevailing Wind Directions Associated with the Major Synoptic Types.

Type	Total Days	Determined Prevailing Direction (tens of degrees)	# of Days with Prevailing Direction	Prevailing Direction Alphabetic
Type 1	94	05 to 10	72	NE
Type 2	102	20 to 28	50	SW
Type 4	52	08 to 13	30	E-ESE
Type 5	47	23 to 31	36	W
Type 6	24	02 to 13	18	NE
Type 8	57	35 to 07	26	NNE
Type 9	5	08 to 13	4	ESE
Type 11	11	08 to 10	7	E
Type 14	23	08 to 10, 26 to 28	6 & 5	Mixed
Type 16	13	08 to 10	9	E
Type 15	28	08 to 13, 23 to 28	20	Mixed

Table 8. Ice Movement and Associated Wind Directions, Speeds, and Synoptic Types.

LANDSAT Date	Direction Ice Movement	Wind Direction & Dates	Wind Speed (m.p.h.) & Dates	Synoptic Types & Dates	Ice Type Moving
B A R R O W      A R E A					
3/18 to 3/23/73	ENE to WSW	06(all)	11.5,18.7,16.8, 11.7,17.4,14.8	3,1,1,1,1,1 (18th-23)	Pack
4/9 to 4/10/73		05(both)	12.2 & 6.9	1,1	
5/14/73	SW-NE	15,16,16,23 (11th-14th)	6.8,8.2,8.3, 11.5(11th-14)	12,12,10,4	Pack
10/21/73	S to N	16,16 (20th-21)	10.8,11.4 (20th-21)	3,3	Fast Ice
5/7 to 5/10/74	E - W	8,6,7,7 (7th-10)	10.1,13.7,15.5, 13.8	1,1,1,1	
7/20 to 7/21/74	to SW	34,01	6.9 & 6.8	14,14	Fast Ice
6/18/75	S to N	18,26,9 (16th-18)	8.8,12.4,11.4 16th-18th)	No Data	Attached Ice
4/25 to 4/27/75		5,3,5	12.7,10.8,7.9	No Data	Pack
B A R T E R      I S L A N D      A R E A					
3/8/73	W to E	15,27,27 (6th-8th)	5.3,19.7,17.7	13,1,1	Pack
4/13/73	SW - NE	34,26,25 32,9 (9th-13th)	11.2,7.2,4.8 6.8,7.3	17,4,1, 1,1	Pack
3/30/73	SE to NW	8,9 (29th-30)	21.4,21.6	1,1	
5/6/73		9,9,9 (4th-6)	21.4,22.4, 23.6	1,1,1	

Table 8. Continued.

5/24/73		09	25.7	1	
6/21/74	SE - NW	9,9,9 (18th-20)	23.6,21.3, 16.1	21,21,1,16 (18th-31)	Pack
10/6/74		10,8,9	25.0,31.6,12.2 (4th-6th)	No Data	Shorefast
3/16/75	SW - NE	27,27,8	23.4,22.1,21.0 (14th-16th)	No Data	
before 4/3/75		10,10,10 9,11,1 (26th-31)	25.0,24.4,31.8 47.7,15.8 (26th-30)	No Data	Pack
4/4/75	to WSW	09	15.1	No Data	Pack

Table 9. Wind Speeds Associated with Major Synoptic Types. (m.p.h.)

	June	July	August
TYPE 1	$\bar{v} = 14.75$	15.34	12.69
	SD = 4.26	5.09	5.09
	N = 47	22	25
TYPE 2	$\bar{v} = 9.07$	11.90	10.70
	SD = 2.34	3.13	3.59
	N = 15	51	31
TYPE 4	$\bar{v} = 10.38$	11.96	11.58
	SD = 4.00	5.61	3.01
	N = 13	10	25
TYPE 5	$\bar{v} = 11.32$	10.79	9.63
	SD = 2.84	3.14	3.26
	N = 13	23	15
TYPE 6	$\bar{v} = 11.86$	10.56	10.54
	SD = 2.98	3.13	3.25
	N = 5	10	12
TYPE 8	$\bar{v} = 9.57$	10.75	11.05
	SD = 2.63	2.25	4.97
	N = 23	20	20

Table 10

SUMMARY OF CLIMATE-ICE INTERACTION

## A. Winter Season

<u>Variable</u>	<u>State</u>	<u>Process</u>	<u>Ice Response</u>	<u>Links</u>
1) $\Delta T$	$>0 (<0)$	Heat Conduction	Slow (rapid) accretion	2,3,7,8:
2) C	High (low)	Net Radiation	Slow (rapid) accretion	7,8:1,10
3) V	High (low)	Heat Transfer	Enhances (retards) (1)	:1
4) V	High (low)	Ice Dynamics	Enhanced (decreased) activity	-
5) DIR	$270^{\circ}$ - $360^{\circ}$ , $0^{\circ}$ - $30^{\circ}$	Ice Deformation	Ridging, fast ice extension see 7,8	
6) DIR	$30^{\circ}$ - $270^{\circ}$	Ice Deformation	Lead formation, less ridging	
7) DIR	$120^{\circ}$ - $250^{\circ}$	Temp. Advection	Rapid accretion	:1,2
8) DIR	$290^{\circ}$ - $080^{\circ}$	Temp. Advection	Slow accretion	:1,2
9) SG	High (low)	Insulation	Decreased (increased) accretion	10:
10) S	High (low)	Link #13		:9

TABLE 10

\*Key:

<u>Variables</u>	$\Delta T$ -	Mean Daily Temperature Departure from Normal
	C -	Mean Daily Cloud amount
	V -	Magnitude of daily resultant surface winds
	DIR -	Direction of daily resultant surface winds
	SF -	Depth of Snow on the Ground
	S -	Solid Precipitation
	R -	Liquid precipitation
	Rn -	Net Radiation

Links:  $x$  denotes the variable in Col. 1,  $y$  is a variable under Col. 5. If  
 $y$  occurs before the colon the link is  $y \rightarrow x$ ; if after, the link is  $x \rightarrow y$ .

TABLE

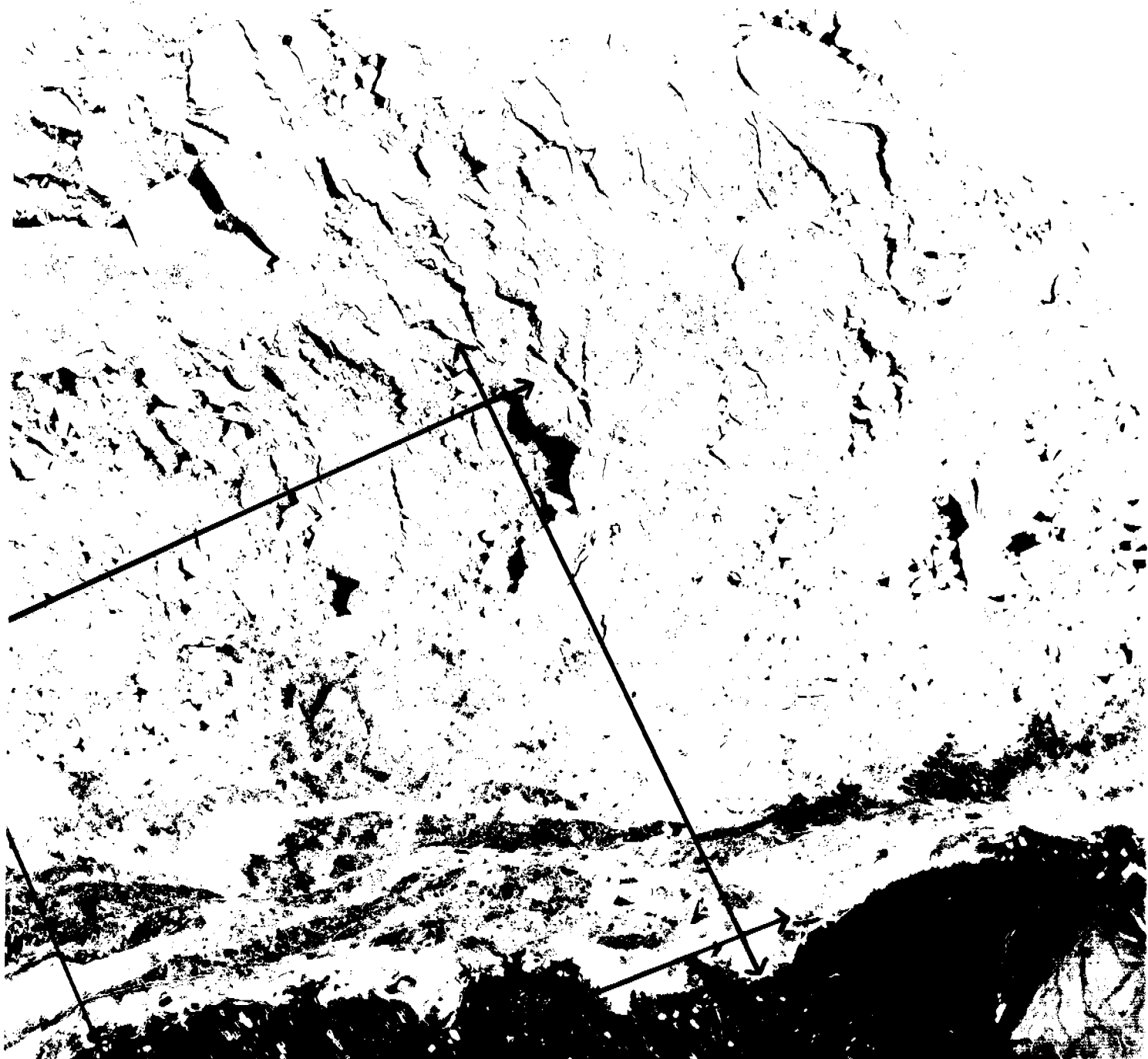
## B. Spring Transition

<u>Variable</u>	<u>State</u>	<u>Process</u>	<u>Ice Response</u>	<u>Links</u>
1) $\Delta T$	$>0 (<0)$	Heat Conduction	Enhanced (retarded) ice and snowpack warming	2,3,7,8: 9,11
2) C	High (low)	Net Radiation	Complex, f (albedo)	7,8: 1,10
3) V	High (low)	Heat Transfer	Advances (retards) (1)	: 1,2
4) V	High (low)	Ice Dynamics	Enhanced (decreased) activity	-
5) DIR	$270^\circ$ - $360^\circ$ , $0^\circ$ - $30^\circ$	Ice Deformation	Ridging, fast ice extension	see 7,8
6) DIR	30 - $270^\circ$	Ice Deformation	Lead formation, Decay of attached ice	see 7,8
7) DIR		Temperature Advection	Increases (1)	: 1,2
8) DIR		Temperature Advection	Increases (2)	: 1,2
9) SG	High (low)	Heat Sink	Later (earlier) puddling, date	10,11:
10) S	High (low)	Albedo	Later (earlier) puddling	:9
11) R	High (low)	Heat input	Advances (retards) snow melt	:9

TABLE 10

## C. Summer Season

<u>Variable</u>	<u>State</u>	<u>Process</u>	<u>Ice Response</u>	<u>Links</u>
1) $\Delta T$	>0 (<0)	Ice Melt	Rapid (slow) ablation	2,7,8,11: 9,10,11
2) C	High	Net Radiation	Slow (rapid) ablation	7,8: 2,11
3) V	High (low)	Heat Transfer	Enhances (retards) (1)	: 1
4) V	High (low)	Ice dynamics	Enhances (retards) breakup	-
5) DIR	$270^{\circ}$ - $360^{\circ}$ , $0^{\circ}$ - $30^{\circ}$	Breakup	Compressive displacements, with onshore pack	see 7,8
6) DIR	$30^{\circ}$ - $270^{\circ}$	Breakup	Expansive displacements, pack offshore	see 7,8
7) DIR		Temperature Advection	Enhances ablation	: 1,2
8) DIR		Temperature Advection	Retards ablation	: 1,2
9) S	High (low)	Albedo	Retards (advances) ablation	: 11
10) R	High (low)	Heat input	Advances (retards) ablation	1:
11) Rn	High (low)	Heat radiation	Advances (retards) ablation	1,2,9: 1



25 JUN 78 W 150° 00' N 70° 53' W 146° 58' N N 70° 49' W 146° 37' MSS

W 148° 00' N 70° 00' W 147° 00'  
7 D SUN EL 42 AZ 167 207-9791 A-L-N D-IL NASA ERTS E-1702-21093-7 02

FIGURE 1

LANDSAT Scene 1702-21093. LARsys Classification Area

Outlined in Black.

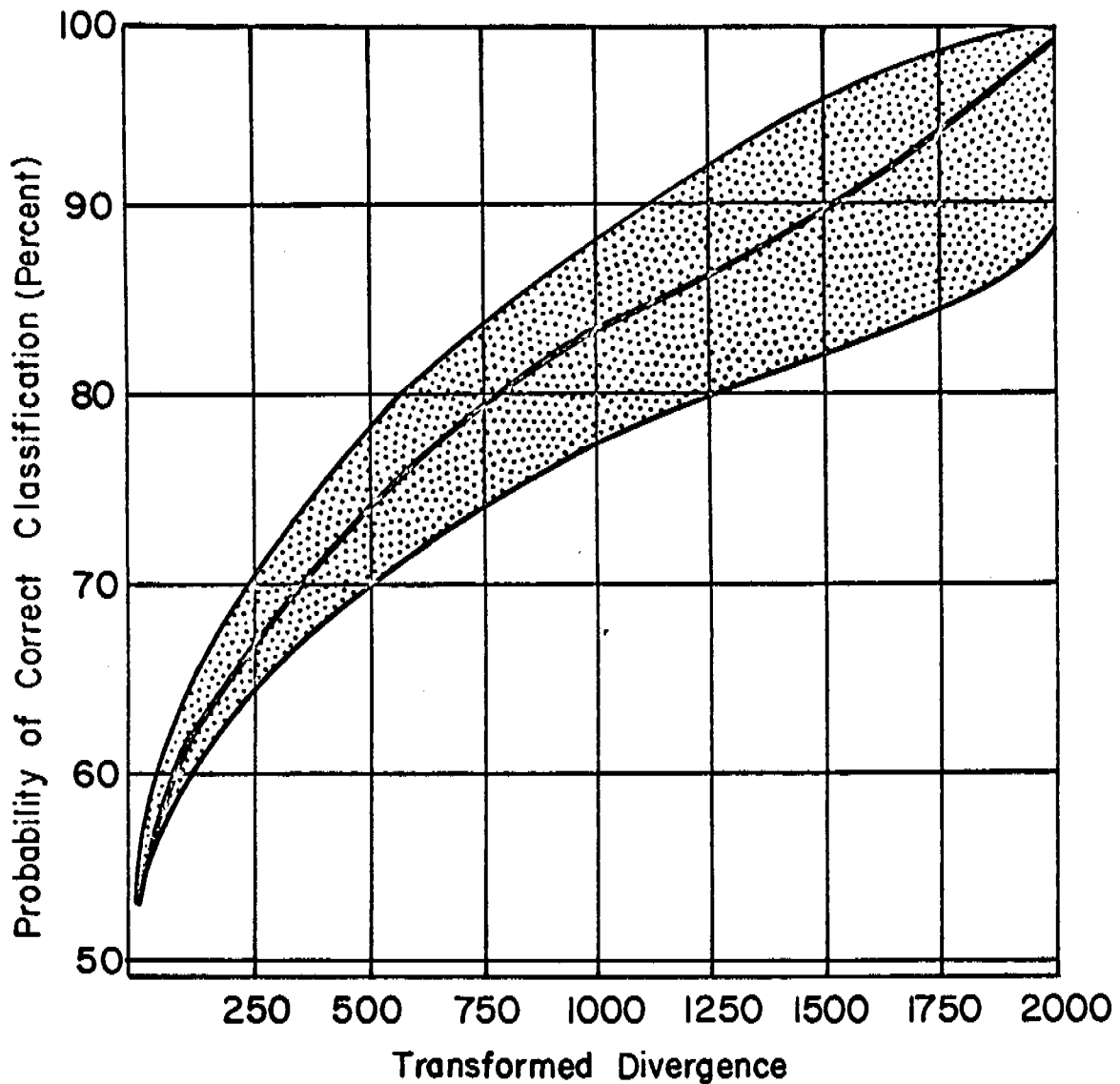


**Figure 2** Empirical relation between transformed divergence and correct recognition (1-6 features). [Swain, 1973]

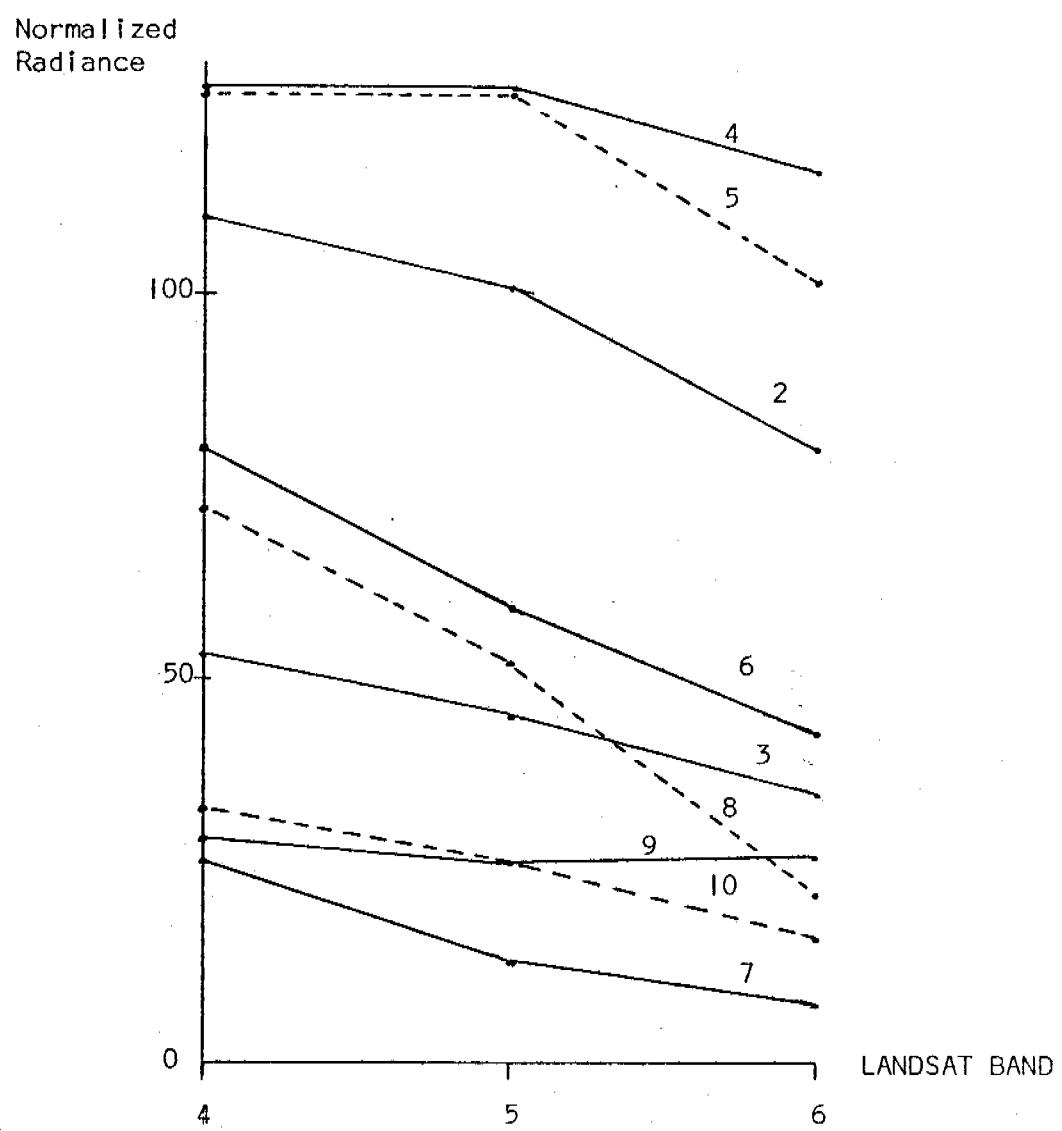


Figure 3: Mean normalized radiances of spectral classes versus band number generated by LARSYS clustering algorithn.

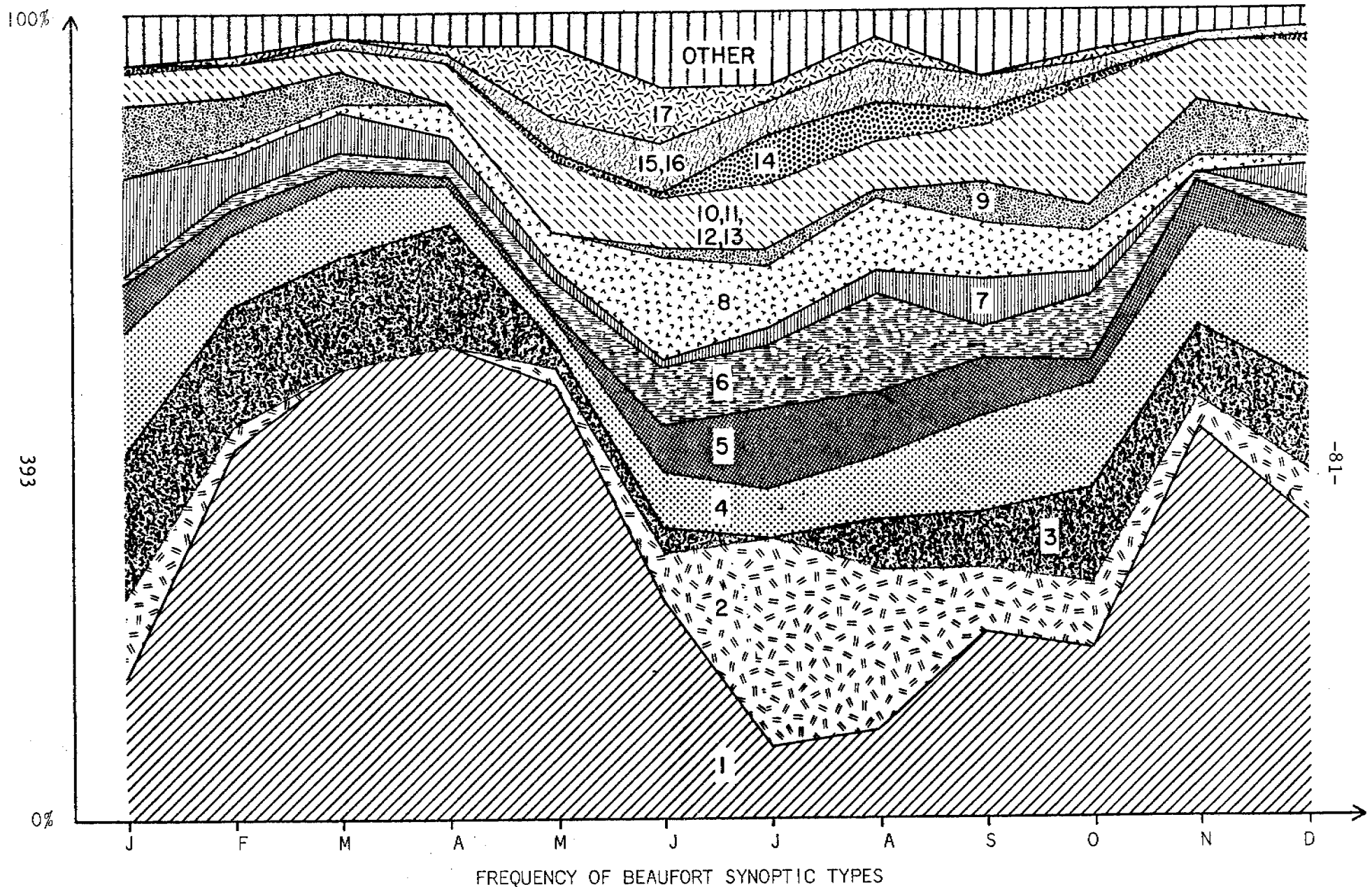
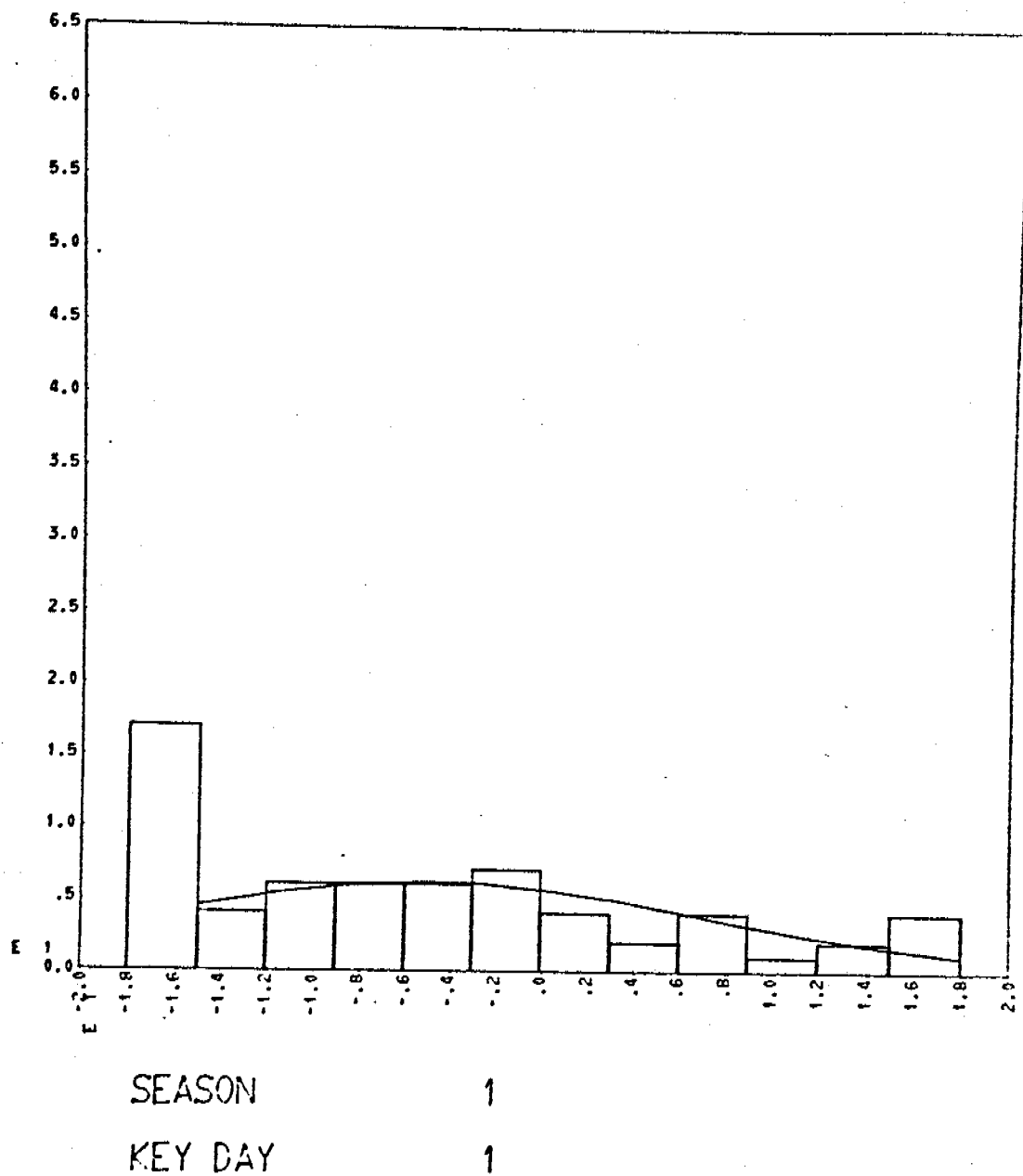


Fig. 4

September, 1968 to August, 1974

Fig. 5A



\*\*Figs. 5 A-D - Histogram ( $E=\text{power of ten}$ ) of daily temperature from normal ( $E=10^1$ ) and normal distribution curve with synoptic types at Barter Island, every 5th day, 1969-74. (Type and season defined in text.)

Figure 5 B

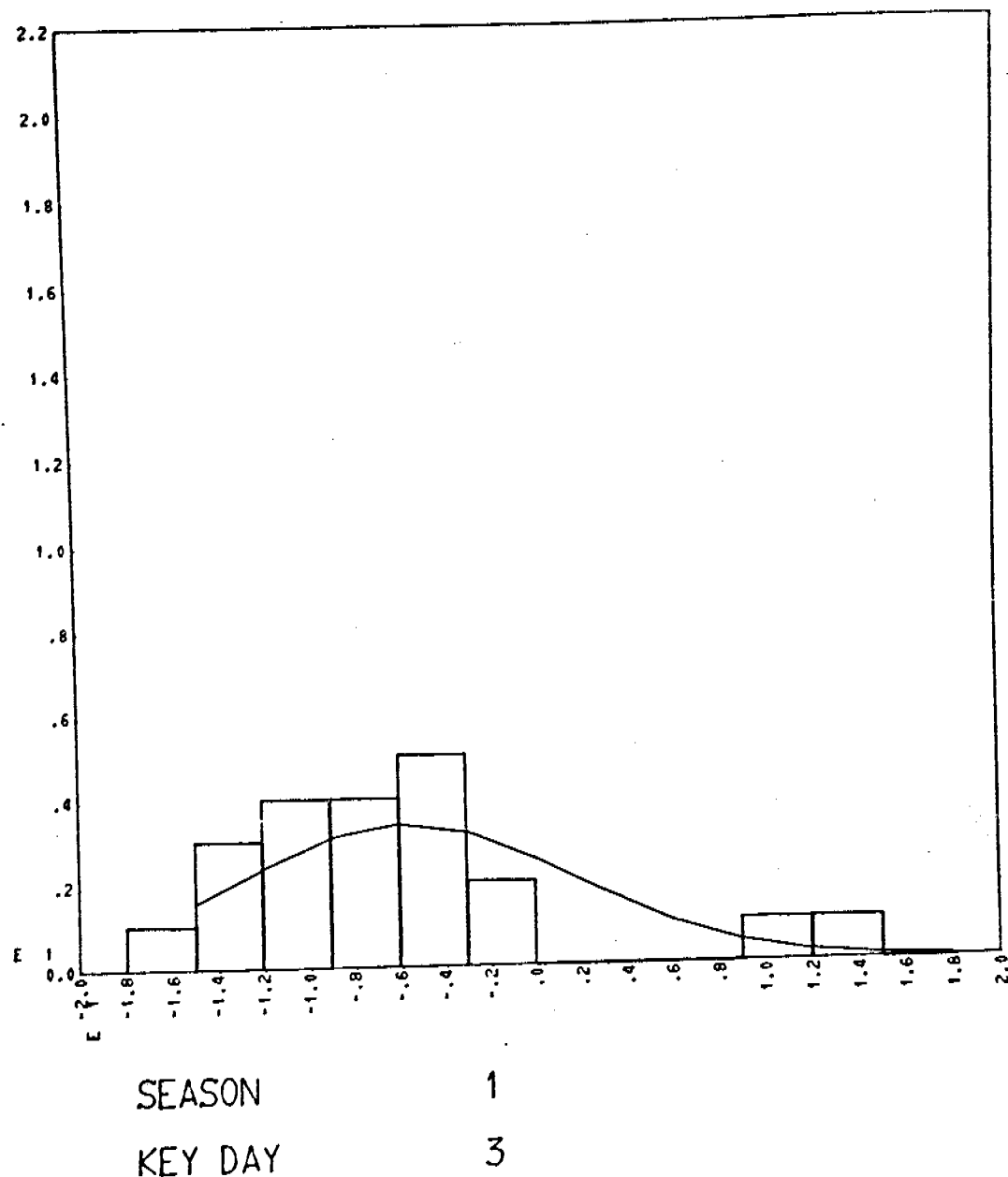


Figure 5C

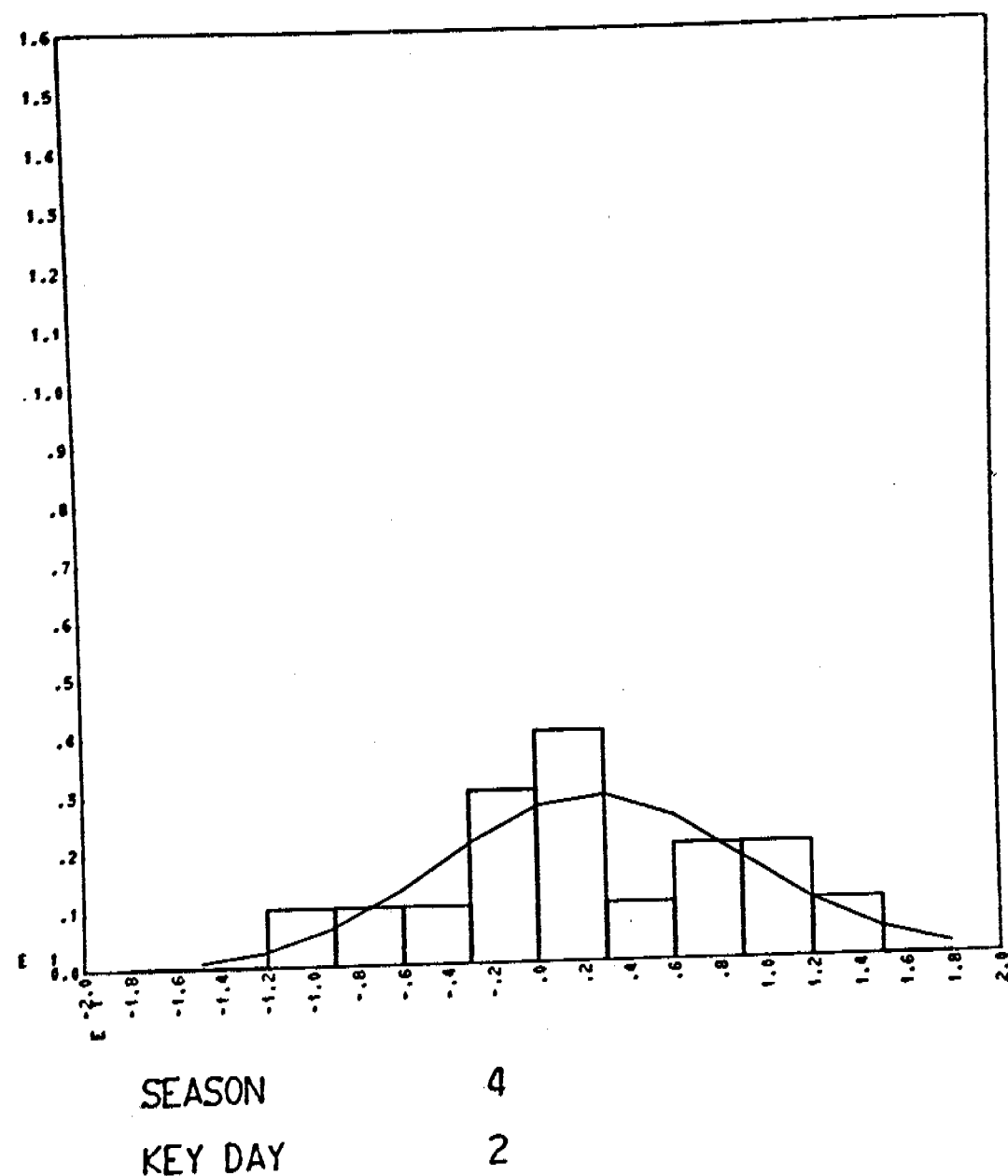


Figure 5D

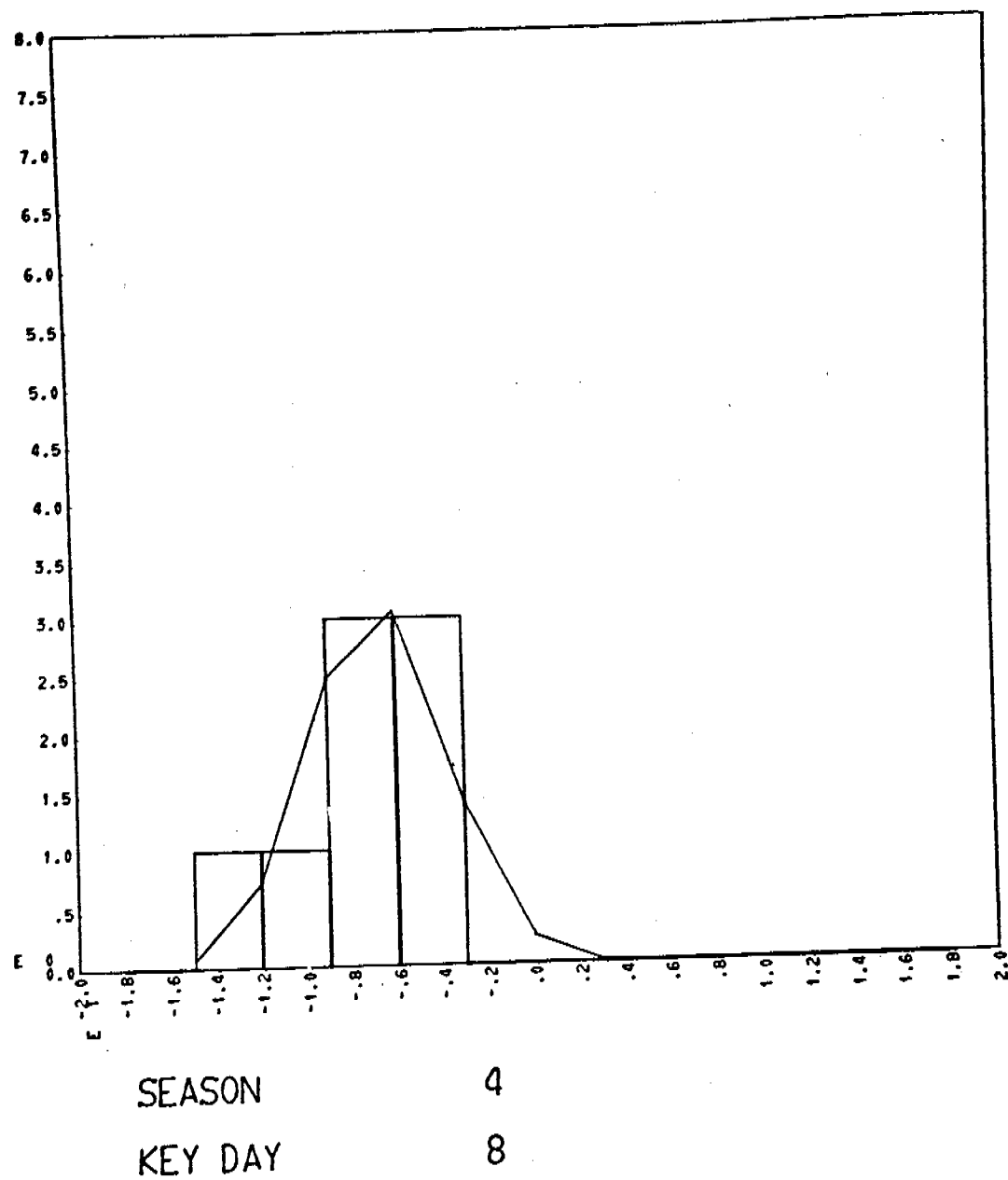
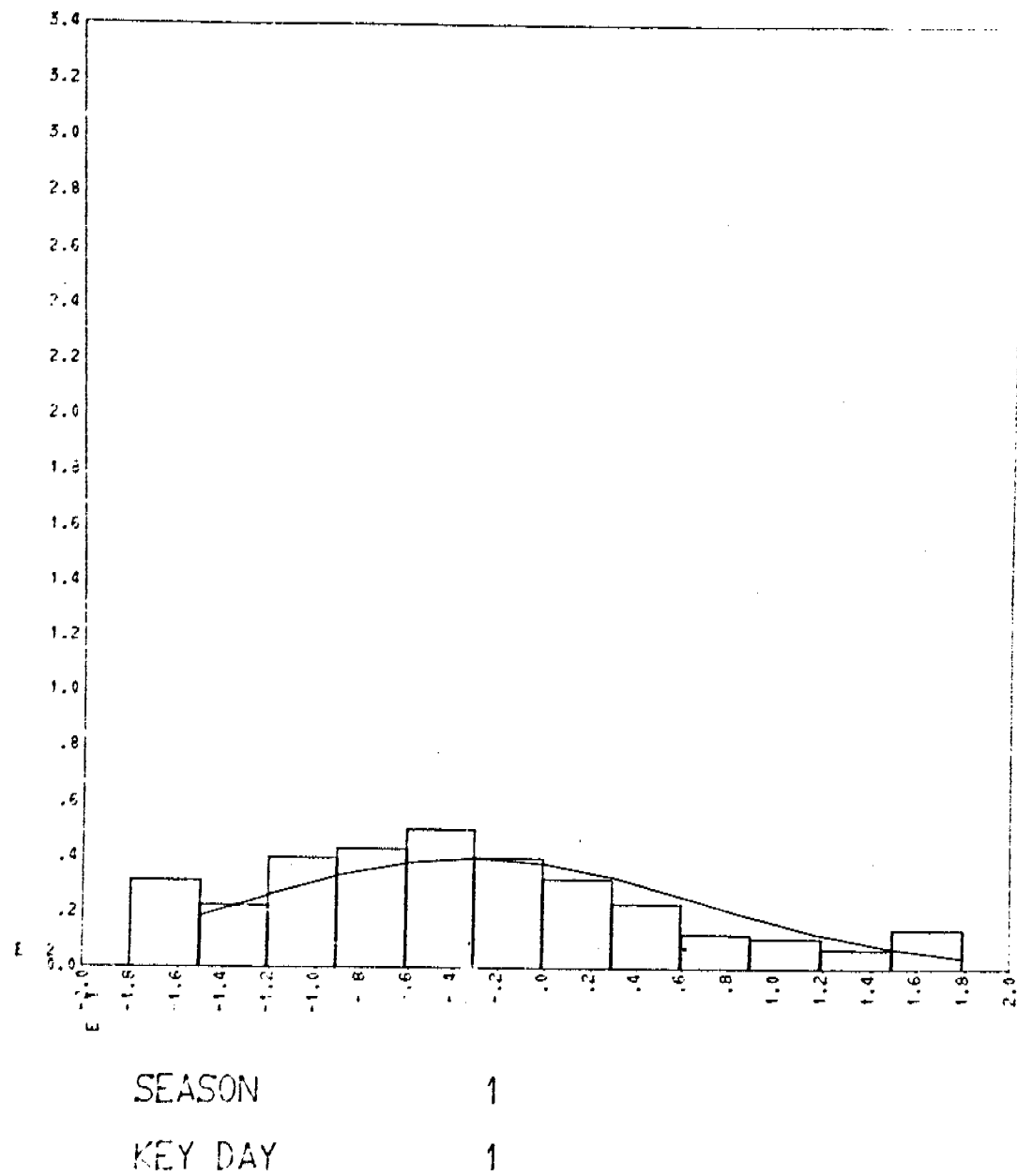


Figure 6A



\*\*Figs. 6 A-L - Frequency histograms ( $E = \text{power of ten}$ ) of daily temperature departure from normal ( $E=10^1$ ) and normal distribution curve at Barrow, every day, 1969-74. (Type and season defined in text.)

Figure 6 B

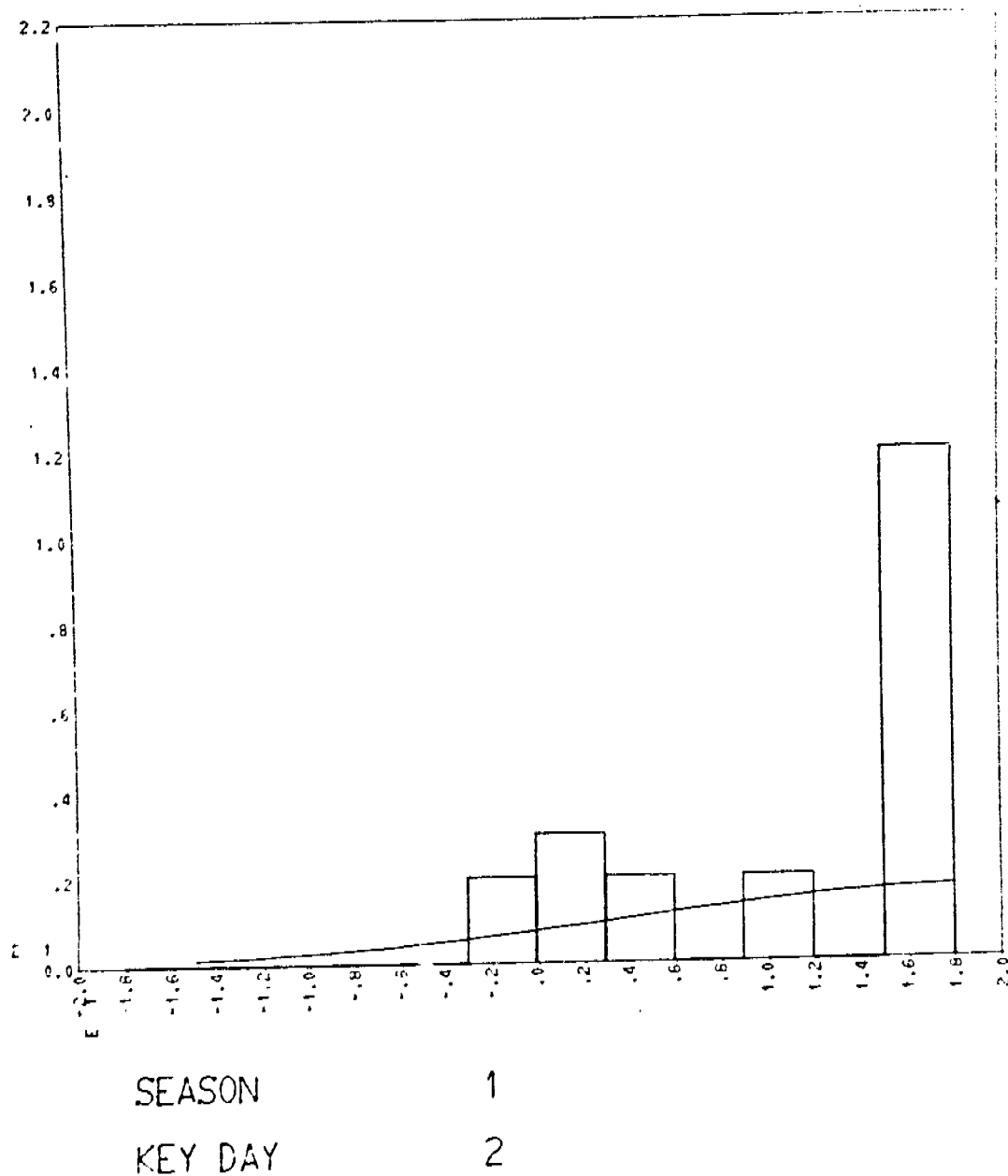


Figure 6 C

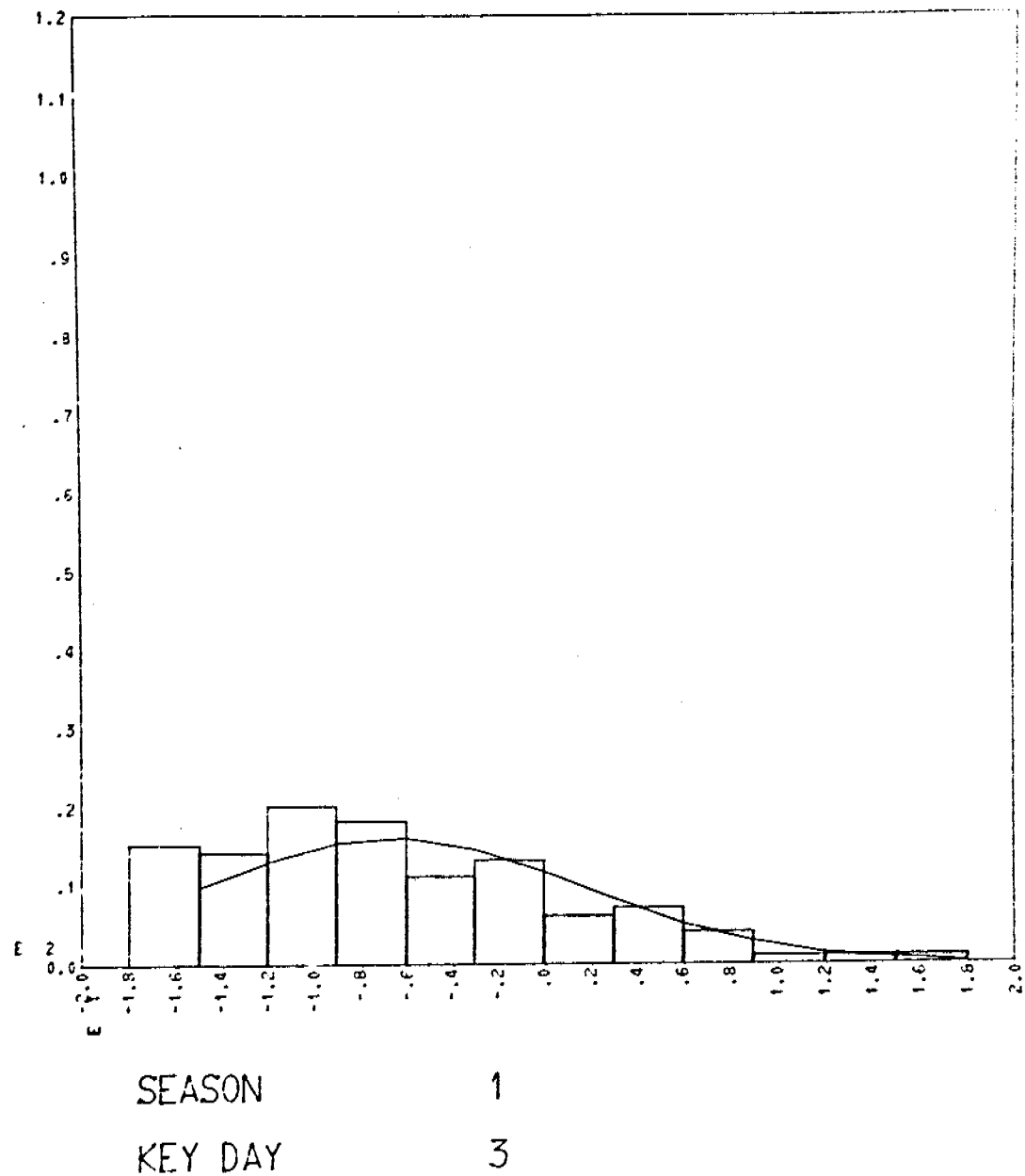


Figure 6 D

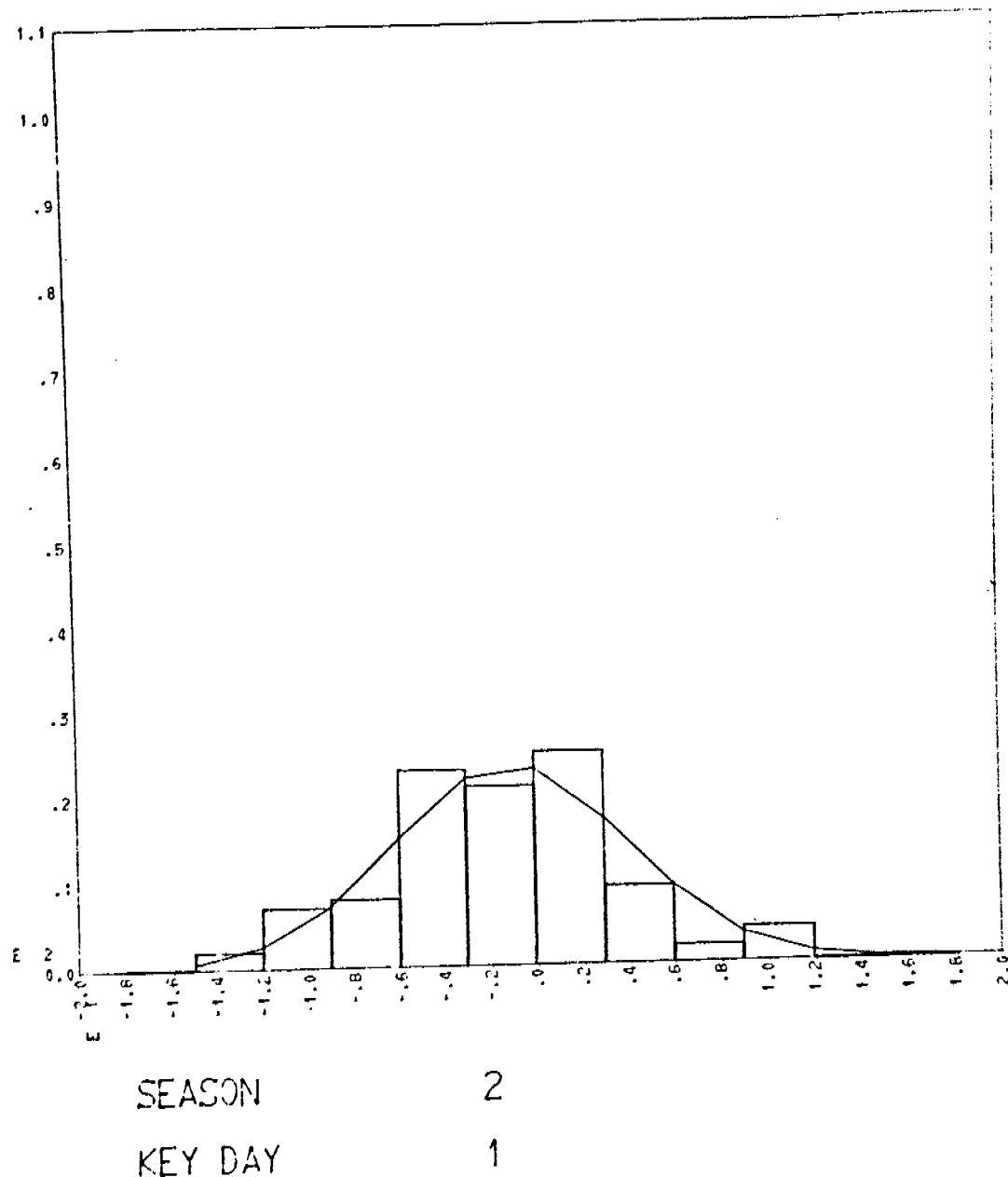
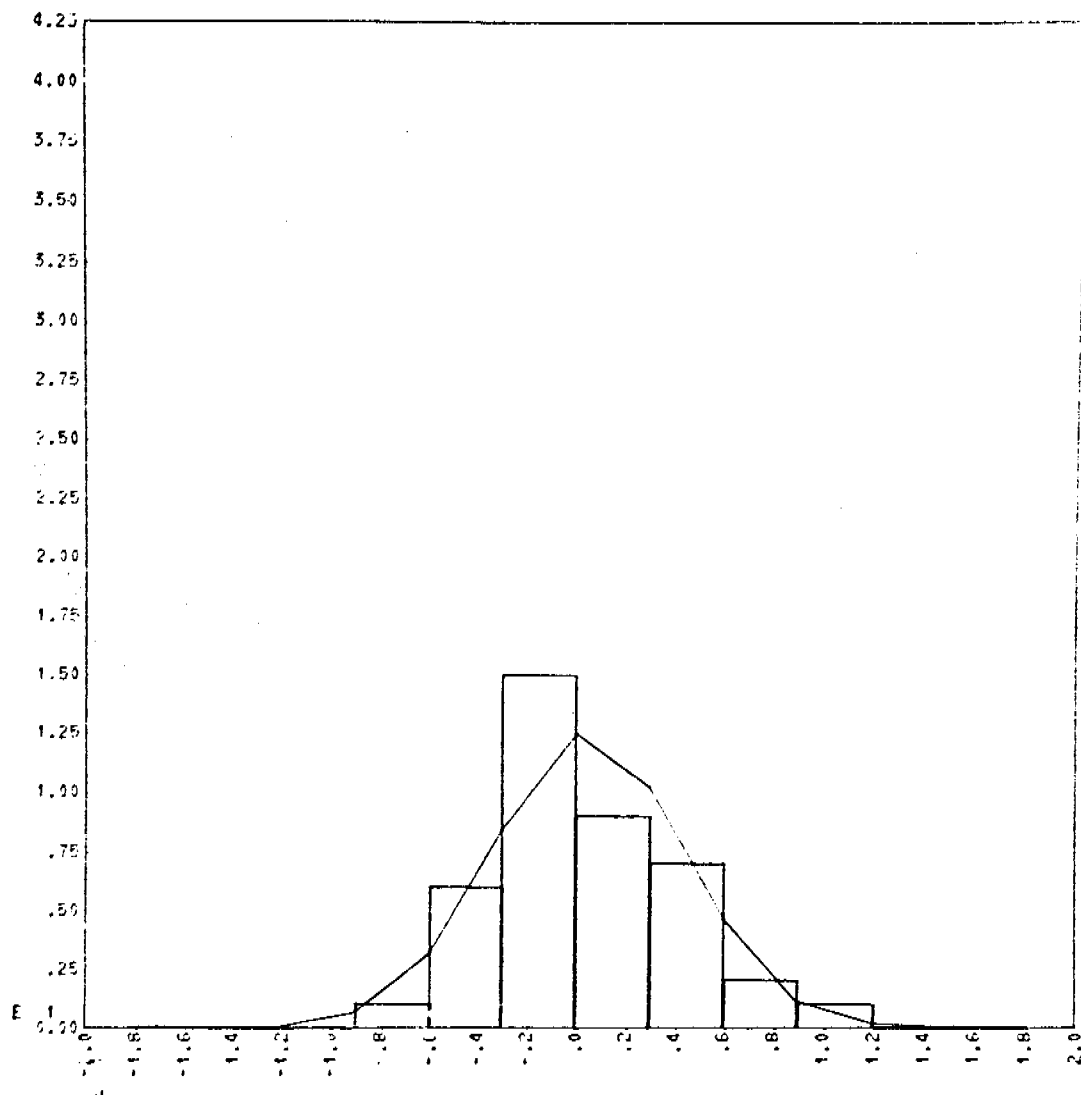


Figure 6 E



SEASON

3

KEY DAY

1

Figure 6 F

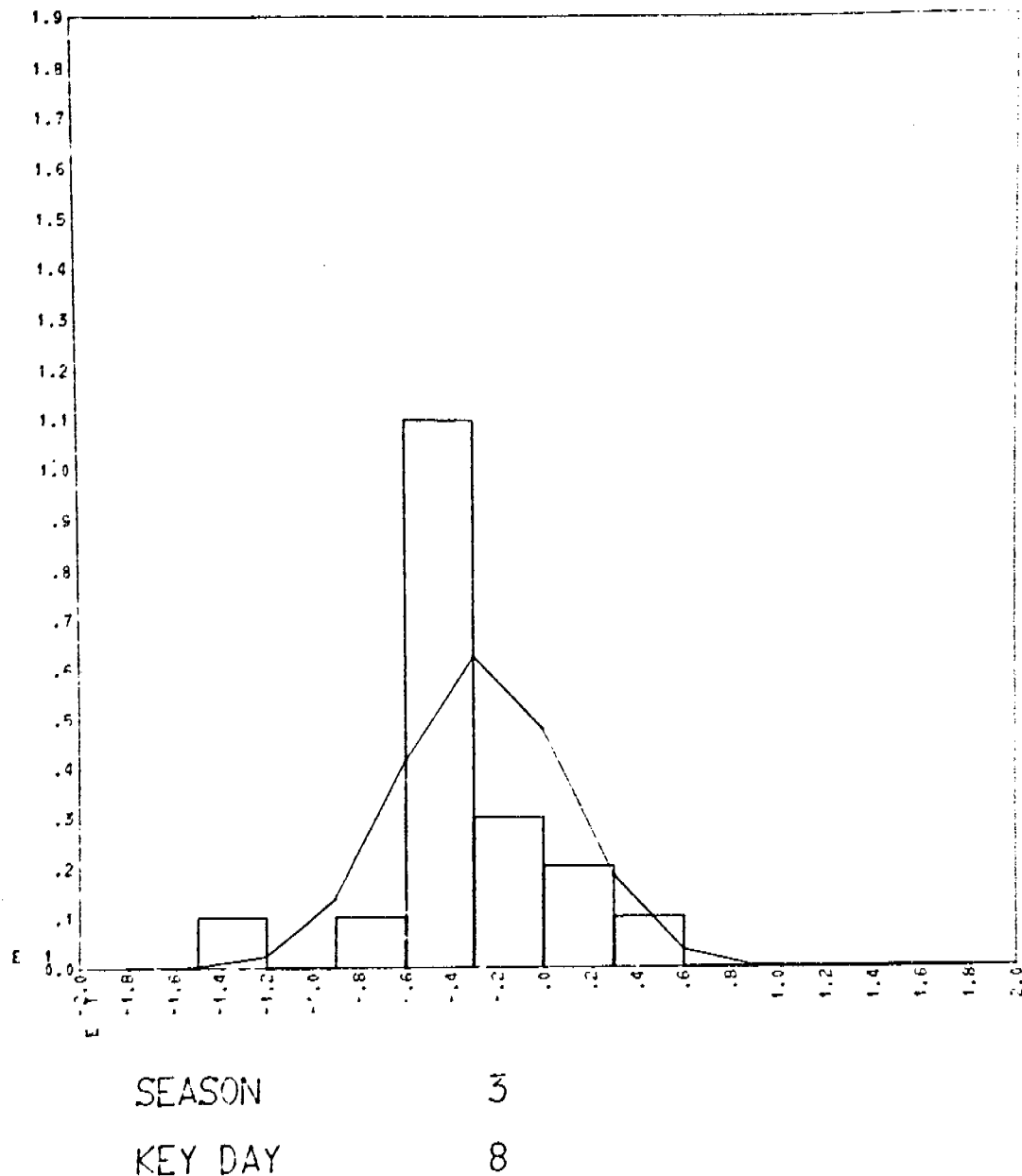


Figure 6 G

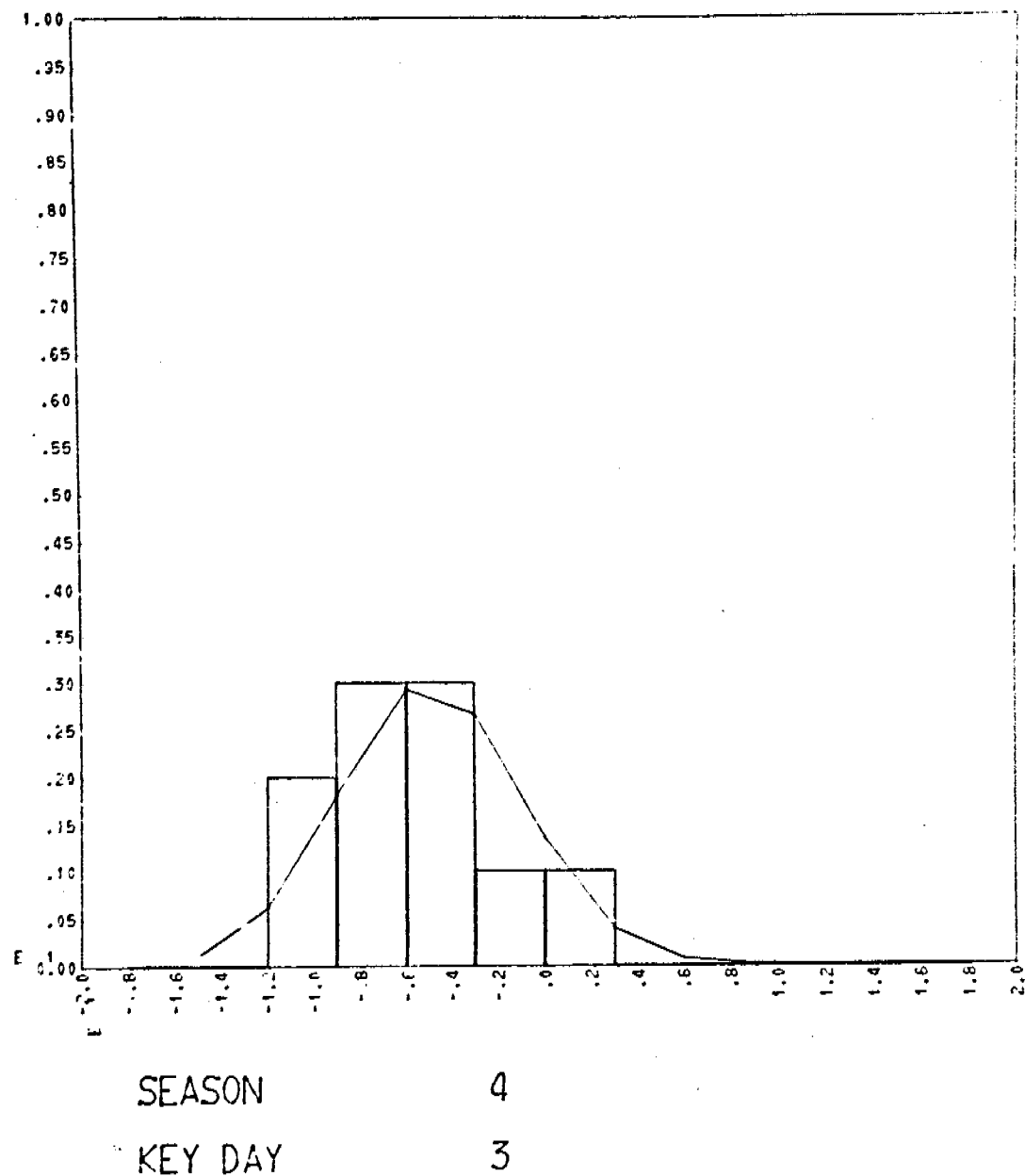


Figure 6 H

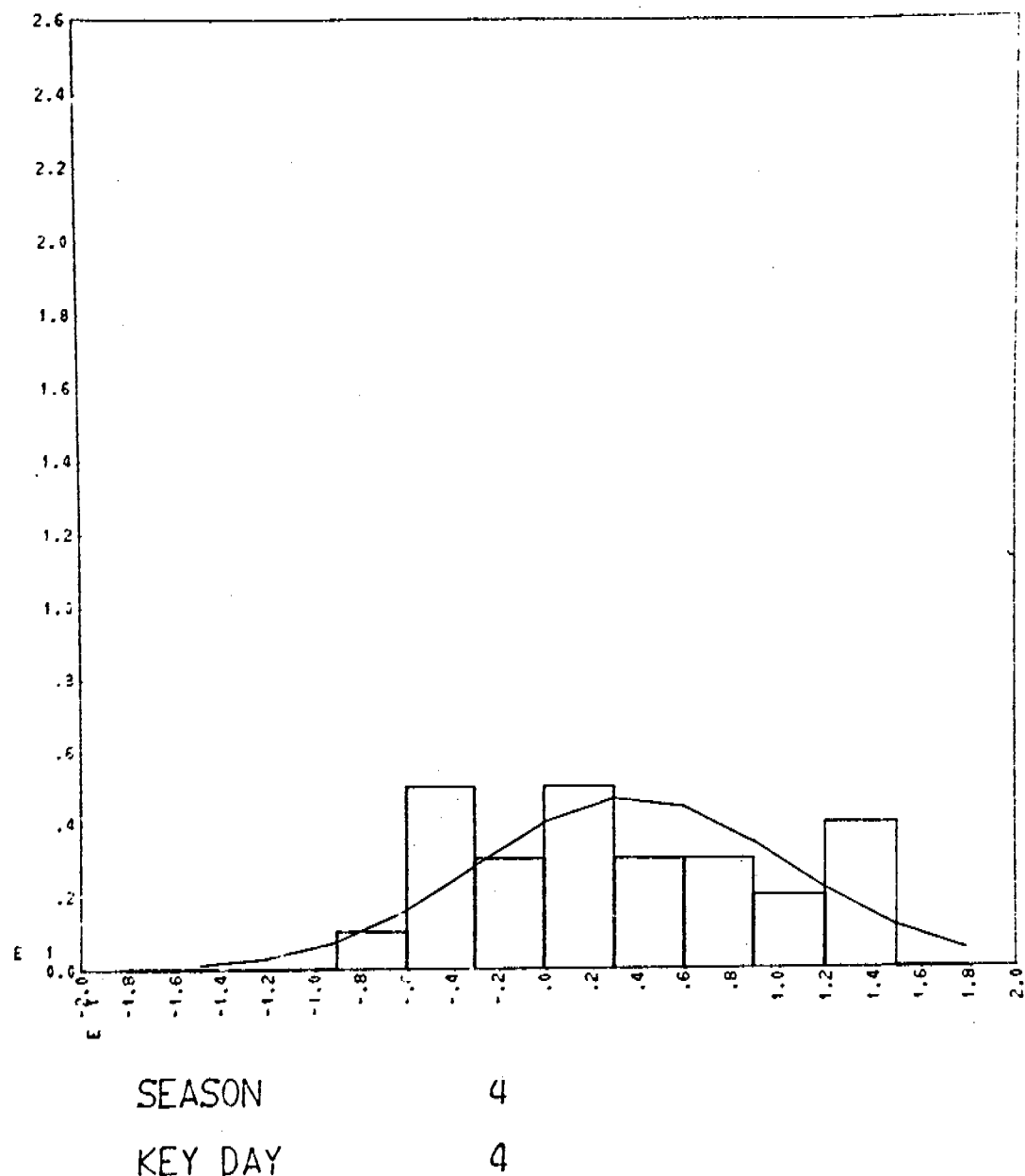
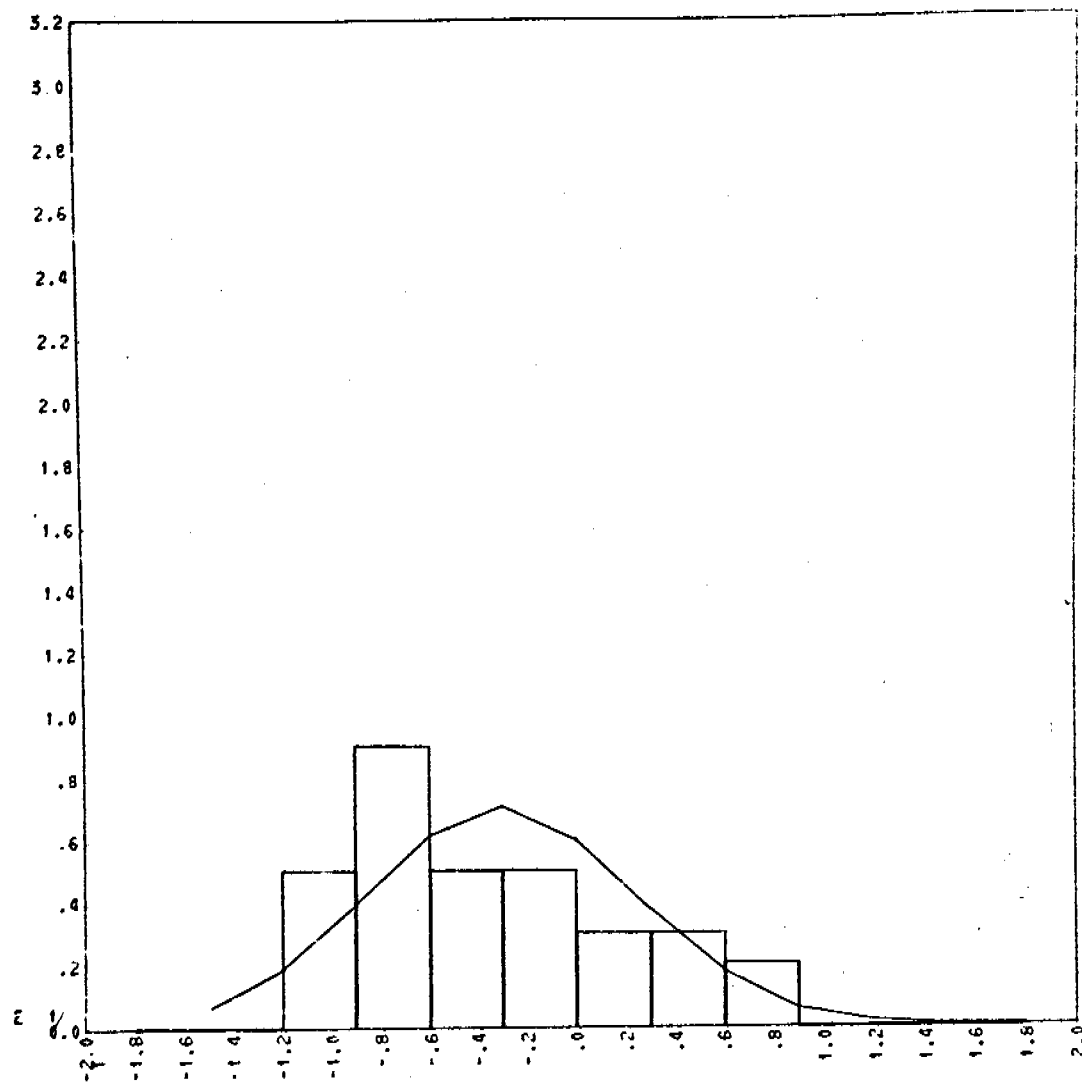


Figure 6 I



SEASON

4

KEY DAY

5

Figure 6 J

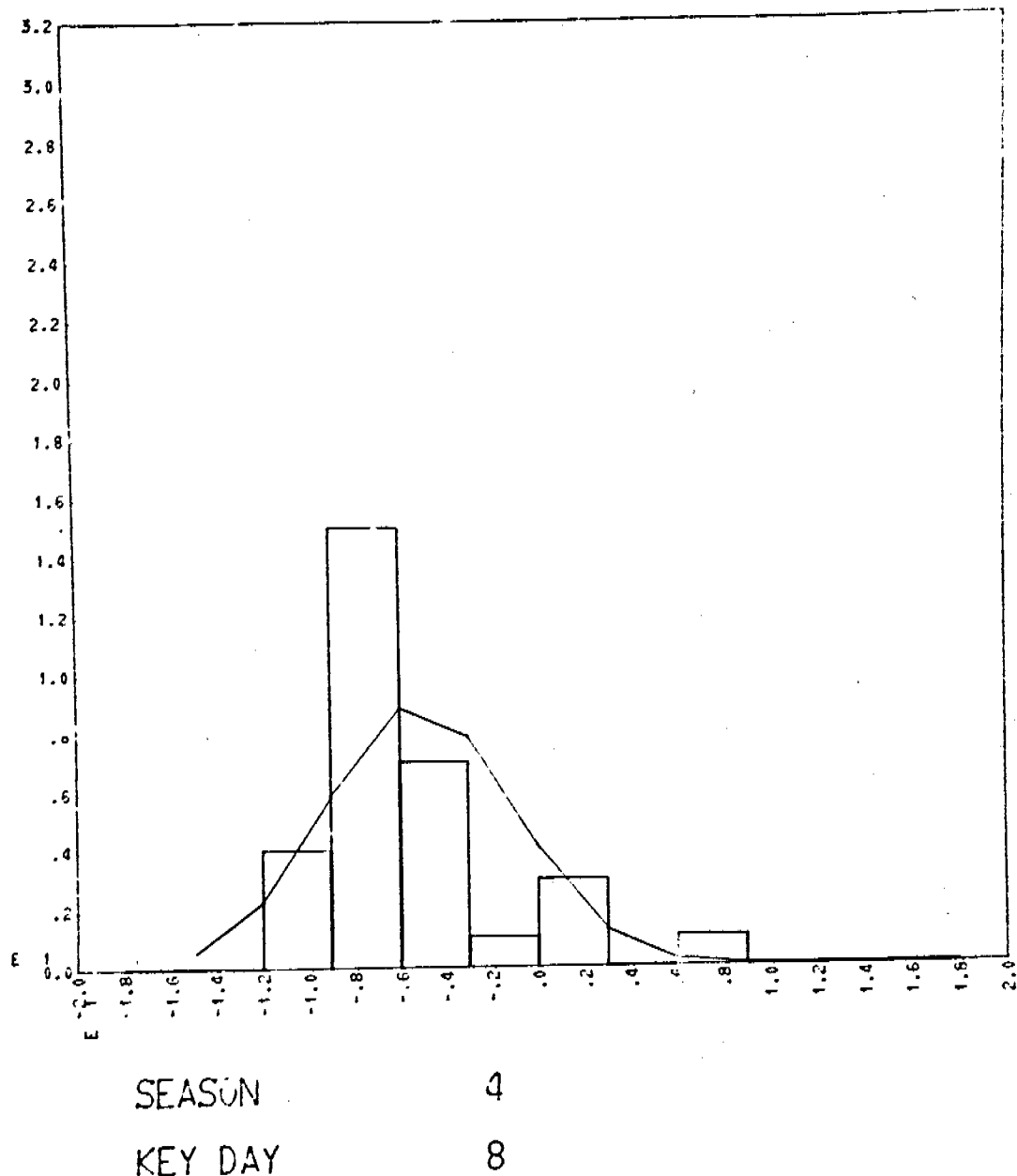


Figure 6 K

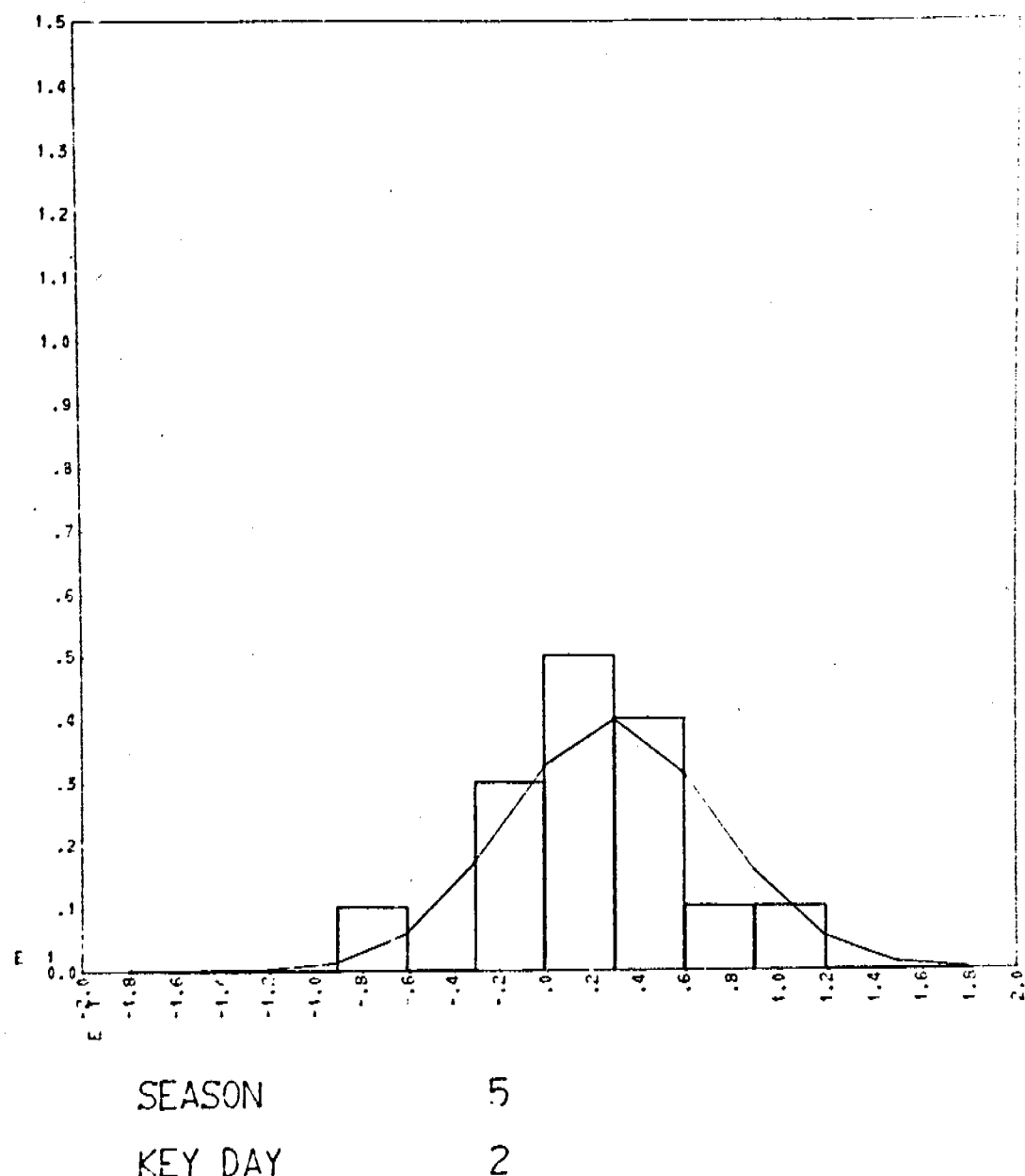
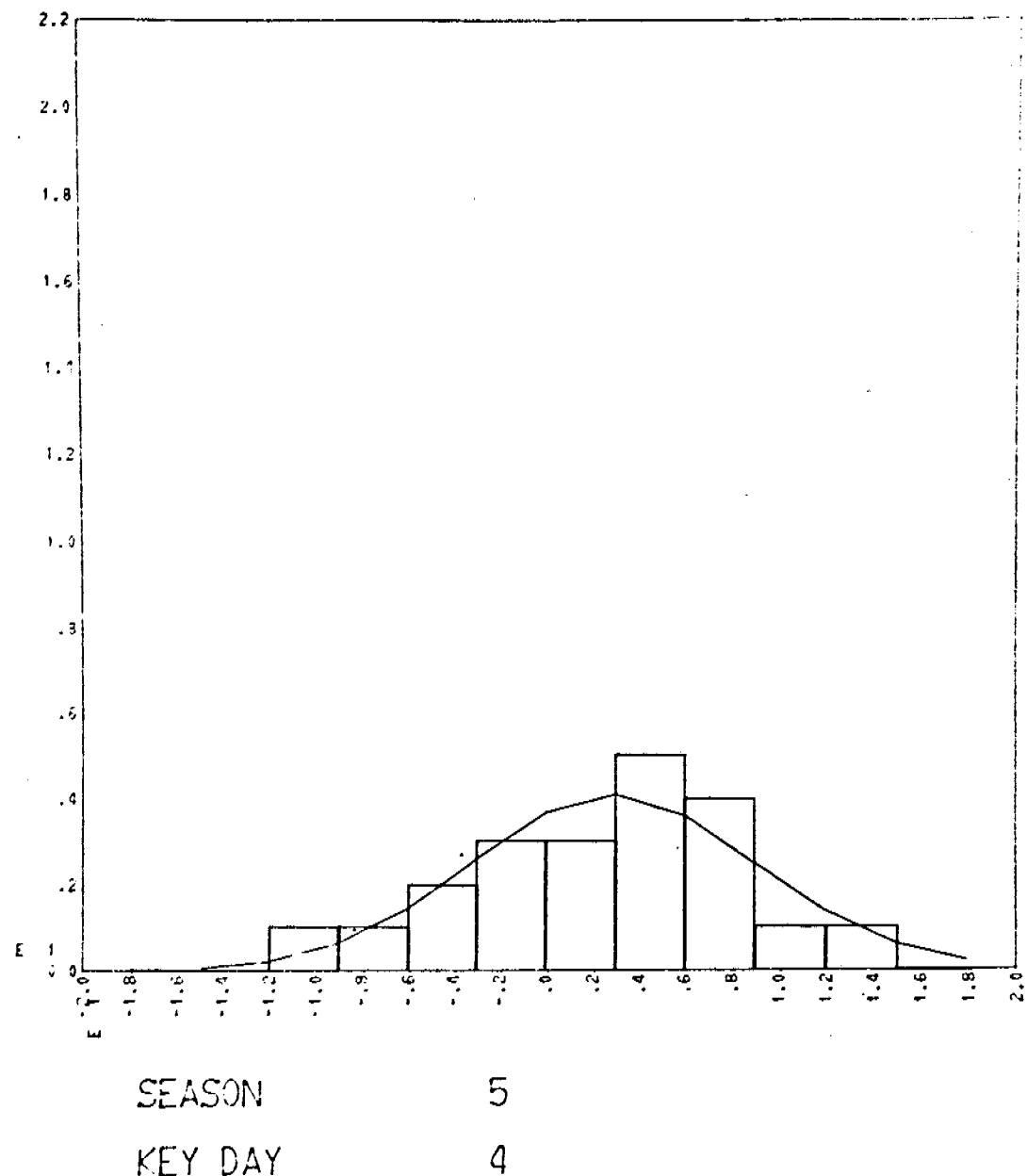


Figure 6 L



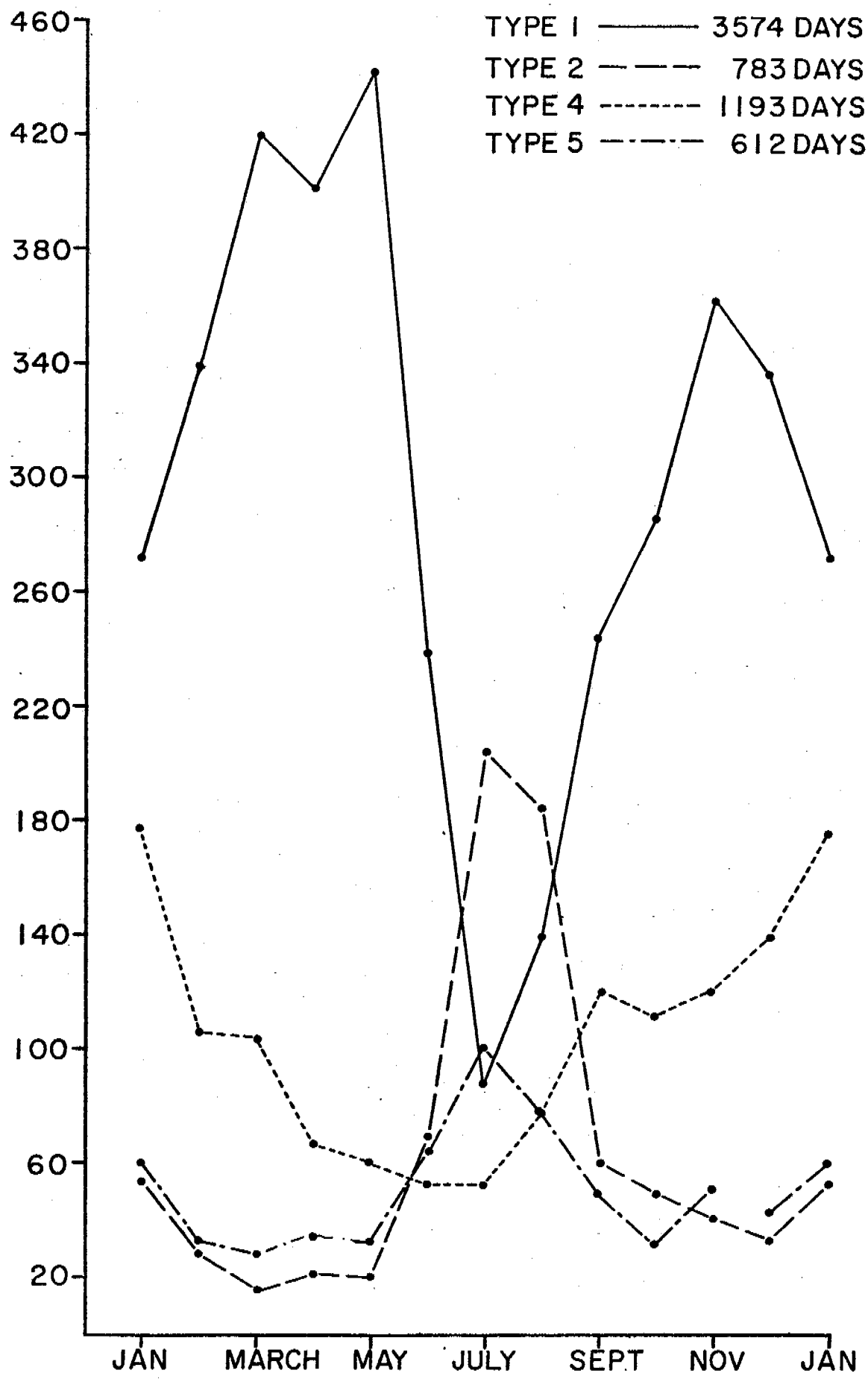


FIGURE 7 - Number of days of occurrence of four major synoptic types  
by month since 1946

## APPENDIX A

MAPS OF NEAR-SHORE ICE CONDITIONS FOR THE PRUDHOE BAY SECTOR PREPARED FROM 1974 DECAY-SEASON LANDSAT IMAGERY.

### Introduction

The maps presented in the following section represent highly-interpreted data products. In addition to the shape, tonal, textural and time-sequential information contained in the LANDSAT data, SLAR imagery, color-infrared photography, and meteorological data were consulted. The "key" at the left margin is intended only as a rough guide to aid analysis of the larger areas of "homogeneous" ice. The explanatory description of each scene must be consulted for a proper interpretation. Additionally, the large areas of "homogeneous" ice (e.g. smooth ice, puddling 4) are labeled so as to describe the essential characteristics of large ice fields. It should not be taken to mean that no ice deformation features exist within such boundaries. Only those features which appear important to the decay process and/or its interpretation are mapped individually.

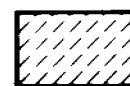
25 JUNE, 1974: SCENE 1702-21093.

A WELL DEFINED CONTINUOUS ICE LIMIT (A) EXTENDS ACROSS THE SCENE, VARYING FROM 15 TO 32 KM OFFSHORE. PACK ICE (B) IS PRESENT IN 9/10 TO 10/10 CONCENTRATION ALONG THIS LIMIT. A NUMBER OF AREAS CONTAINING ICE DEFORMATION FEATURES ARE EVIDENT ON SLAR IMAGERY OF THIS SECTOR, FLOWN 29 APRIL, 1974. TWO OF THE MORE PROMINENT FEATURES WITH HIGH REFLECTANCE ON THE SLAR WERE DETERMINED TO BE GROUNDED (FROM LATER LANDSAT DATA), AND ARE SHOWN AS SUCH ON THE MAP (LOCATIONS: N70°44', W149°30'; N70°42', W148°45'). THE LATTER MASS OF ICE COINCIDES WITH THE EDGE OF CONTINUOUS ICE. GREAT SPATIAL VARIABILITY IN AMOUNTS OF ICE SURFACE MELTWATER IS EVIDENCED BY WIDE VARIATION IN GREY TONES ON ALL FOUR LANDSAT BANDS. THE DARKEST (MOST PUDDLED) ICE EXTENDS IN A ROUGHLY COAST-PARALLEL BELT, CENTERED APPROXIMATELY 17KM FROM SHORE (DESIGNATED "PUDDLING 3" ON MAP). ICE WITHIN THE CONTINUOUS ICE LIMIT BUT UNDESIGNATED ON THE MAP HAS COMPLEX TONE AND TEXTURE ON THE LANDSAT IMAGES. SEVERAL QUASI-LINEAR FEATURES CAN BE IDENTIFIED WITHIN THIS ZONE, POSSIBLY REPRESENTING THE PREVIOUS POSITIONS OF THE CONTINUOUS ICE LIMIT AT VARIOUS TIME DURING WINTER. SLAR IMAGERY SHOWS SEVERAL RIDGED AND HUMMOCKED AREAS IN THIS ICE, ALTHOUGH ONLY ONE APPEARED TO BE GROUNDED WELL ENOUGH TO REMAIN IN PLACE UNTIL AUGUST. THIS MASS CONSISTED OF RIDGES LOCATED AT N70°33', W149°10' (DESIGNATED AS "C" ON MAP). THE SLAR IMAGERY ALSO REVEALED SEVERAL AREAS OF ESSENTIALLY FLAT ICE WHICH, FOR SOME REASON, REMAINED VERY REFLECTIVE IN ALL LANDSAT BANDS ON THIS DATE, INDICATING POORLY-DEVELOPED PUDDLING. THE MOST PROMINENT OF THESE IS DESIGNATED "PUDDLING 1" ON MAP. VERY SMOOTH ICE WITH INTERMEDIATE PUDDLE DEVELOPMENT EXTENDS ALONG THE COAST FROM OLIKTOK POINT TO FLAXMAN ISLAND (DESIGNATED "PUDDLING 2" ON MAP). A NUMBER OF LIGHT-TONED LINEAR FEATURES ARE VISIBLE ON THIS ICE, PROBABLY REPRESENTING DRAINAGE CRACKS (DRAWN IN BLACK ON MAP). THE MAJOR RIVER MOUTH AREAS HAVE MELTED OUT AND ARE DESIGNATED AS "OPEN WATER".

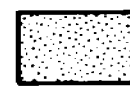
**KEY:**

SMOOTH ICE

Puddling 1



Puddling 2



Puddling 3



Puddling 4

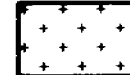


413 ROUGH ICE

Ridging and Hummocking



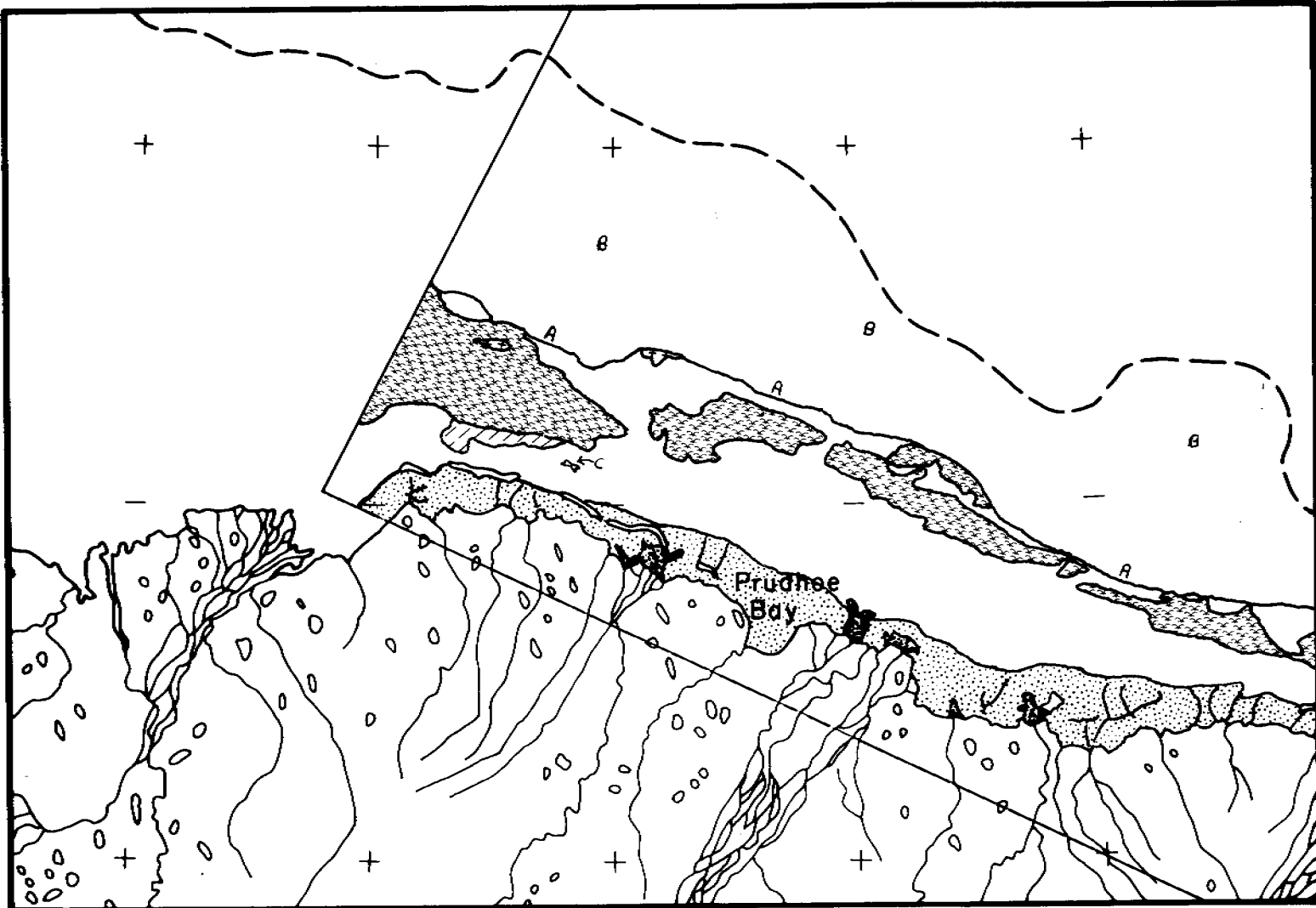
Grounding



Pack Ice



Open Water



SHOREFAST SEA ICE

SURFACE MORPHOLOGICAL CHARACTERISTICS

BEAUFORT SEA COAST: PRUDHOE SECTOR

25 JUNE, 1974

26 JUNE, 1974: SCENE 1703-21151

THE CONTINUOUS ICE LIMIT (A) HAS BEEN EXTENDED WEST INTO OUTER HARRISON BAY. NO MOTIONS COULD BE DETECTED WITHIN THE 25 JUNE CONTINUOUS ICE LIMIT. PACK ICE (B) REMAINED COMPACTED AGAINST THE CONTINUOUS ICE EDGE. PACK ICE DISPLACEMENTS IN THE TIME INTERVAL 25-26 JUNE ARE SHOWN ON THE MAP AS SOLID ARROWS. THE "≠" SYMBOL DENOTES A "NO MOTION" CONDITION AT A PARTICULAR POINT. THE SHEAR ZONE IS CLEARLY NOT LOCATED AT THE EDGE OF CONTINUOUS ICE BUT RATHER SOME 15-20 KM SEAWARD OF IT. THE PREVAILING WIND DIRECTIONS FOR 25 JUNE AT BARTER ISLAND AND OLIKTOK ARE SHOWN AS DOUBLE ARROWS (BTI AND OLI, RESPECTIVELY). THEIR RESPECTIVE MAGNITUDES WERE 5.7 and 6.2 M/SEC. THE ICE DRIFT BEYOND THE SHEAR ZONE AGREED VERY WELL WITH EXPECTATIONS BASED ON ZUBOV'S RULE (ICE DRIFTS AT 1/30TH TO 1/50TH THE WIND SPEED AND AT AN ANGLE OF ABOUT 30° TO THE RIGHT OF THE WIND). THE PLOTTED VECTORS BEYOND THE SHEAR ZONE ARE BETWEEN 1/35TH AND 1/50TH OF THE WIND SPEED AND 30 TO 40° TO THE RIGHT. NEAR-SHORE ICE BETWEEN OLIKTOK AND THE EASTERN EDGE OF THE MAP REMAINED SIMILAR TO THE PREVIOUS DAY EXCEPT THAT THE ICE BETWEEN PRUDHOE BAY AND THE KUPARUK RIVER DELTA APPEARS TO HAVE DRAINED. THIS IS INDICATED ON THE LANDSAT DATA BY THE DISAPPEARANCE OF THE DRAINAGE CRACKS AS WELL AS BY A RELATIVE LIGHTENING IN TONE. THE NEWLY-IMAGED AREAS IN HARRISON BAY EXHIBIT SEVERAL INTERESTING CHARACTERISTICS. FOREMOST IS THE PRESENCE OF A LARGE GROUNDED ICE MASS AT N70°58', W150°42'. THE SEAWARD "PUDDLING 3" BELT OF 25 JUNE TERMINATES IN EASTERN HARRISON BAY AT A BOUNDARY WITH MUCH LIGHTER ICE, SSE OF THE LARGE GROUNDED MASS. THE LIGHTER ICE HERE HAS A TEXTURE ON LANDSAT INDICATING A GREAT NUMBER OF LIGHT-TONED FLOE-LIKE ICE PIECES EMBEDDED IN A SLIGHTLY DARKER MATRIX OF ICE. ANALYSIS OF THE COLOR INFRARED PHOTOGRAPHY FROM 21 JUNE AND APRIL SLAR IMAGERY IN THIS REGION LEADS US TO CONCLUDE THAT THE EASTERN PORTION OF THIS ICE ("C") CONSISTS OF 2ND- AND/OR MULTI-YEAR ICE FLOES, VARYING FROM SMALL TO VAST FLOE SIZE, AND EMBEDDED IN A 1ST-YEAR ICE MATRIX. SHOREWARD OF THIS ICE, A CRESCENT-SHAPED BELT OF VERY DARK TONE EXTENDS ACROSS THE BAY (DESIGNATED "PUDDLING 4" ON MAP). THE SLAR IMAGERY SHOWS THIS TO BE RELATIVELY FLAT, UNDEFORMED ICE. SHOREWARD OF THIS BELT IS A SECOND ARCUATE ICE AREA OF LIGHTER TONE ("D"), WHICH HAS MODERATELY DEFORMED ICE WITH POORER PUDDLING DEVELOPMENT ON 26 JUNE. THE BOUNDARY AREA ("E") TO THE EAST OF THESE BELTS CONTAINS SEVERAL PROMINENT RIDGES AND A NUMBER OF HEAVILY-HUMMOCKED AREAS. MODERATE TO HEAVY PUDDLING CONDITIONS EXIST ON THE REMAINING HARRISON BAY ICE, UP TO THE COLVILLE MOUTH AREA, WHERE OPEN WATER HAS EXTENDED OUT FROM THE DELTA.

**KEY:**

SMOOTH ICE

Puddling 1



Puddling 2



Puddling 3



Puddling 4



ROUGH ICE

Ridging and Hummocking



Grounding



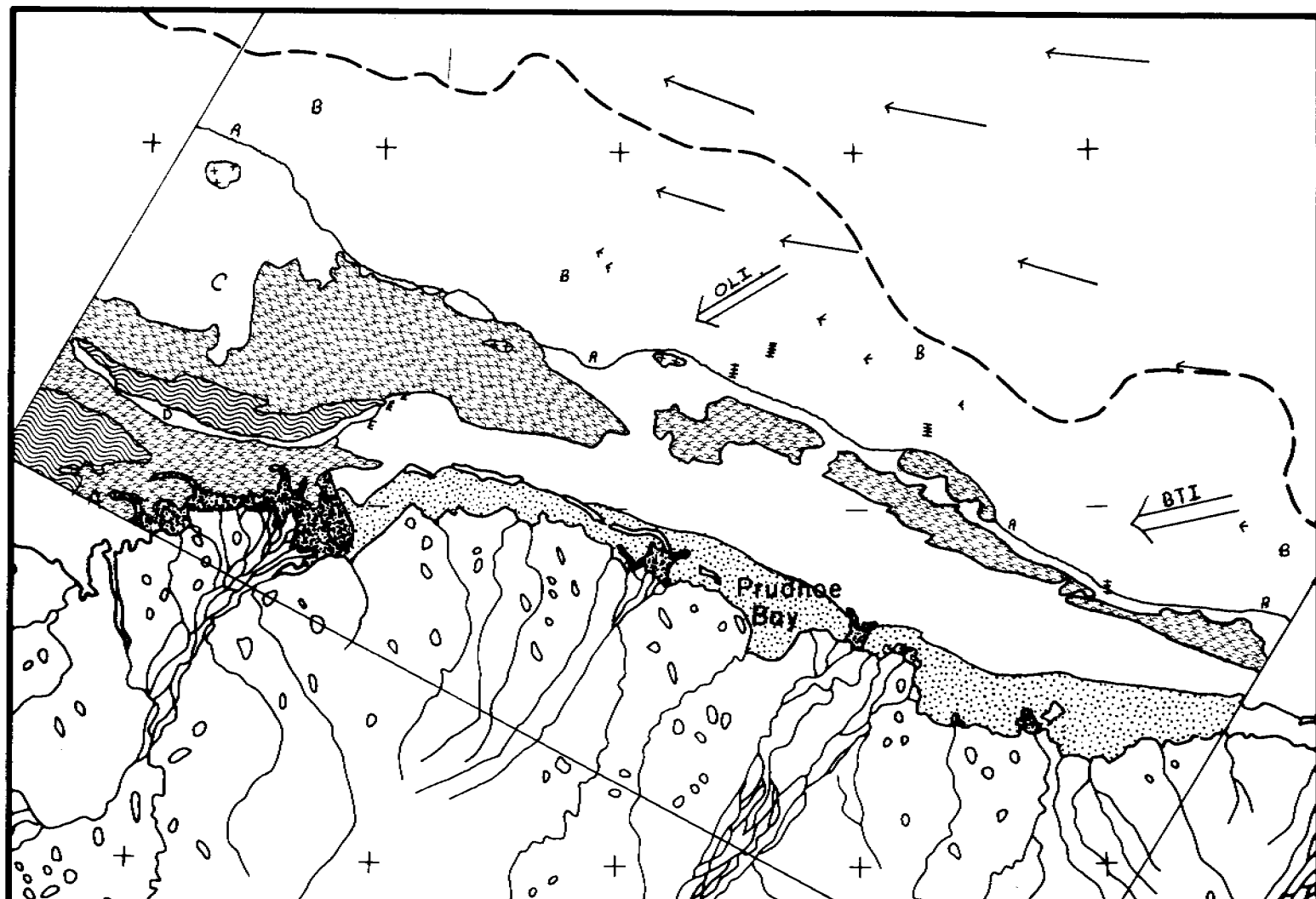
Pack Ice



Open Water



40m Isobath ——



SHOREFAST SEA ICE  
SURFACE MORPHOLOGICAL CHARACTERISTICS  
BEAUFORT SEA COAST: PRUDHOE SECTOR

26 JUNE, 1974

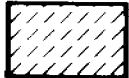
29 JUNE, 1974: SCENE 1706-21322

THIS SCENE SHOWS THE ICE IN HARRISON BAY. ALTHOUGH CLOUD OBSCURES MUCH OF NW HARRISON BAY FROM VIEW, IT WAS DETERMINED THAT THE CONTINUOUS ICE LIMIT EAST OF THE LARGE GROUNDED MASS WAS STATIONARY SINCE 26 JUNE. FEATURES OF NOTE ON THIS SCENE INCLUDE A TONAL-TEXTURAL BOUNDARY IN CENTRAL HARRISON BAY, SEPARATING THE 2ND- AND/OR MULTI- YEAR ICE (A) FROM AREA "B", WHICH IS PRIMARILY COMPOSED OF MANY FIRST-YEAR ICE PANS BORDERED BY NUMEROUS SMALL RAFTS AND RIDGES. AREA "C", NEAR SHORE, IS FLAT ICE WHICH HAS APPARENTLY DRAINED IN MANY PLACES. A SMALL INCREASE IN THE AREA OF OPEN WATER OFF THE COLVILLE RIVER IS ALSO NOTED.

**KEY:**

**SMOOTH ICE**

Puddling 1



Puddling 2



Puddling 3



Puddling 4



**ROUGH ICE**

Ridging and Hummocking



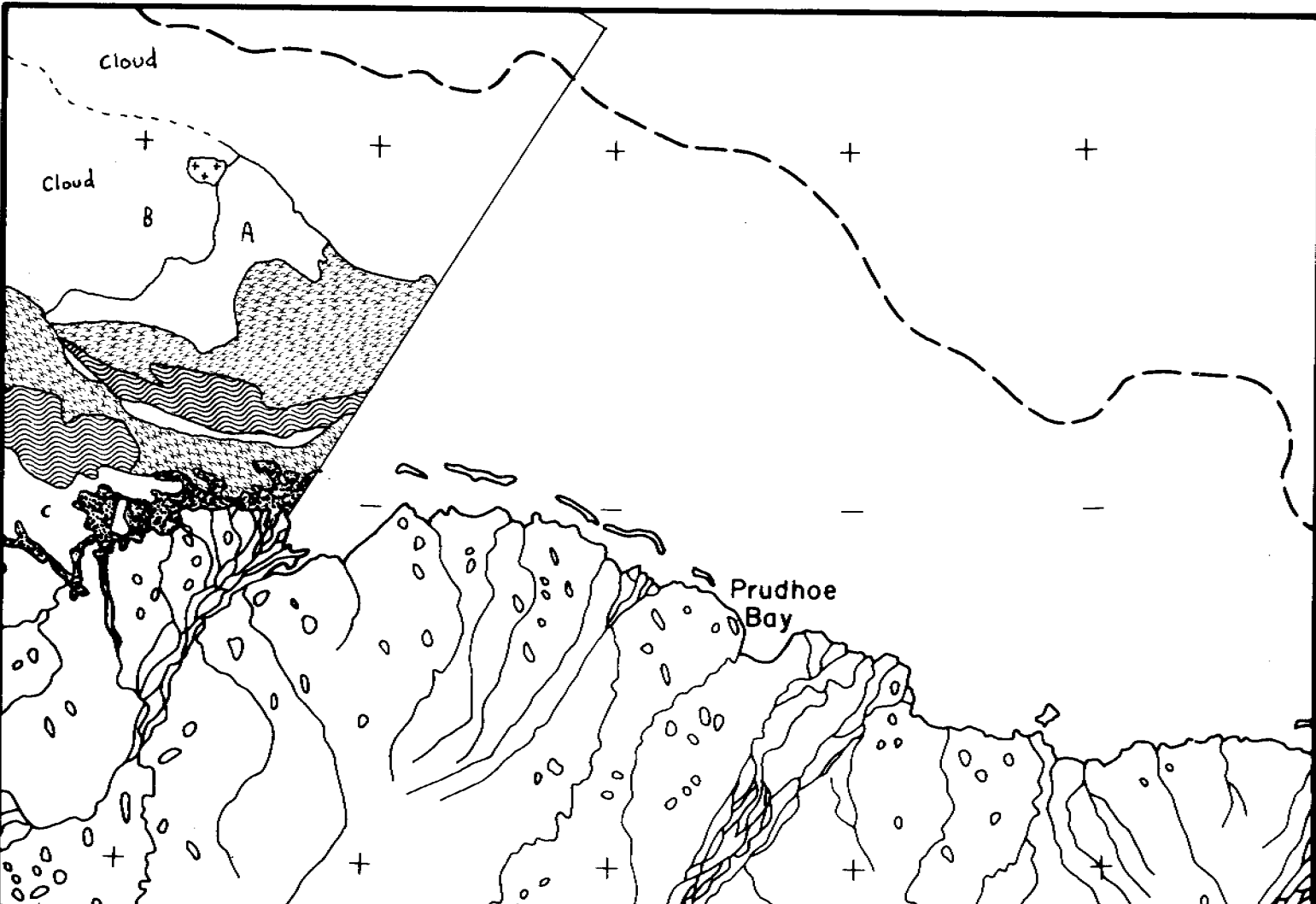
Grounding



Pack Ice



Open Water



**SHOREFAST SEA ICE**

**SURFACE MORPHOLOGICAL CHARACTERISTICS**

**BEAUFORT SEA COAST: PRUDHOE SECTOR**

**29 JUNE, 1974**

12 JULY, 1974: SCENE 1719-2103I

THE SEAWARD EXTENT OF CONTINUOUS ICE JUST EAST OF THE EASTERN MAP EDGE HAD DECREASED TO ABOUT 5 KM ON THIS DATE, DUE TO THE BREAKUP OF PART OF THE SEAWARD BELT OF HEAVY PUDDLING (NOTED ON 25 JUNE SCENE). ON THE MAP, THE CONTINUOUS ICE LIMIT (C) IS APPROXIMATE WHERE DOTTED, DUE TO CLOUDS. ONE SMALL DISPLACEMENT WAS MEASURED (SOLID ARROW ON MAP) IN THE INTERVAL 25 JUNE-12 JULY ALONG THIS EDGE. PACK ICE MOTIONS COULD NOT BE DETERMINED FROM THIS SCENE. PACK ICE REMAINED COMPACTED AGAINST THE EDGE OF CONTINUOUS ICE AND A 70X30KM AREA (A) OF PACK ICE SHOWED MUCH HEAVIER PUDDLING THAN THE REST OF THE PACK. SEVERAL CHANGES WITHIN THE CONTINUOUS ICE LIMITS TOOK PLACE BETWEEN 25 JUNE AND 12 JULY. NOTABLY, SOME OF THE SMOOTH NEAR-SHORE ICE BETWEEN TIGVARIAK AND FLAX-MAN ISLANDS (B) UNDERWENT A RELATIVE TONAL LIGHTENING, COMPARED TO THE TUNDRA AND OTHER ICE. THIS PROBABLY SIGNALS THE DRAINAGE OF FORMERLY PUDDLED ICE INTO THE CRACKS AND OPENINGS IN THE CANOPY. THE SAGAVANIRKTOK RIVER HAD CONSIDERABLY EXTENDED ITS INFLUENCE, AS EVIDENCED BY AN INCREASE IN OPEN WATER OFFSHORE FROM ITS MOUTH. MUCH OF THE ICE IN THE "INTERMEDIATE BELT" OF 25-26 JUNE HAD DARKENED, AND IS DESIGNATED AS "PUDDLING 3" AND "PUDDLING 4" ON THE MAP. BREAKUP HAD COMMENCED IN THE SHORE POLYNYA FORMED NEAR THE RIVER MOUTHS, WITH OPEN WATER AREAS BETWEEN THE BROKEN ICE FLOES NW OF TIGVARIAK ISLAND. SOMETIME PRIOR TO THIS DATE, THEN, THE NEAR-SHORE ICE WEAKENED ENOUGH TO BEGIN BREAKING, AND THE DARK, PUDDLED ICE BELT TO SEAWARD BECAME SUSCEPTIBLE TO BREAKUP BY PACK ICE FORCES. ANALYSIS OF COLOR INFRARED PHOTOGRAPHY FLOWN 21 JUNE SHOWS THAT THE ICE OFF BROWNLOW POINT WHICH BROKE UP BEFORE 12 JULY LACKED THE PRONOUNCED DEFORMATION FEATURES OF ICE TO THE EAST AND WEST.

## KEY:

### SMOOTH ICE

Puddling 1

Puddling 2

Puddling 3

Puddling 4

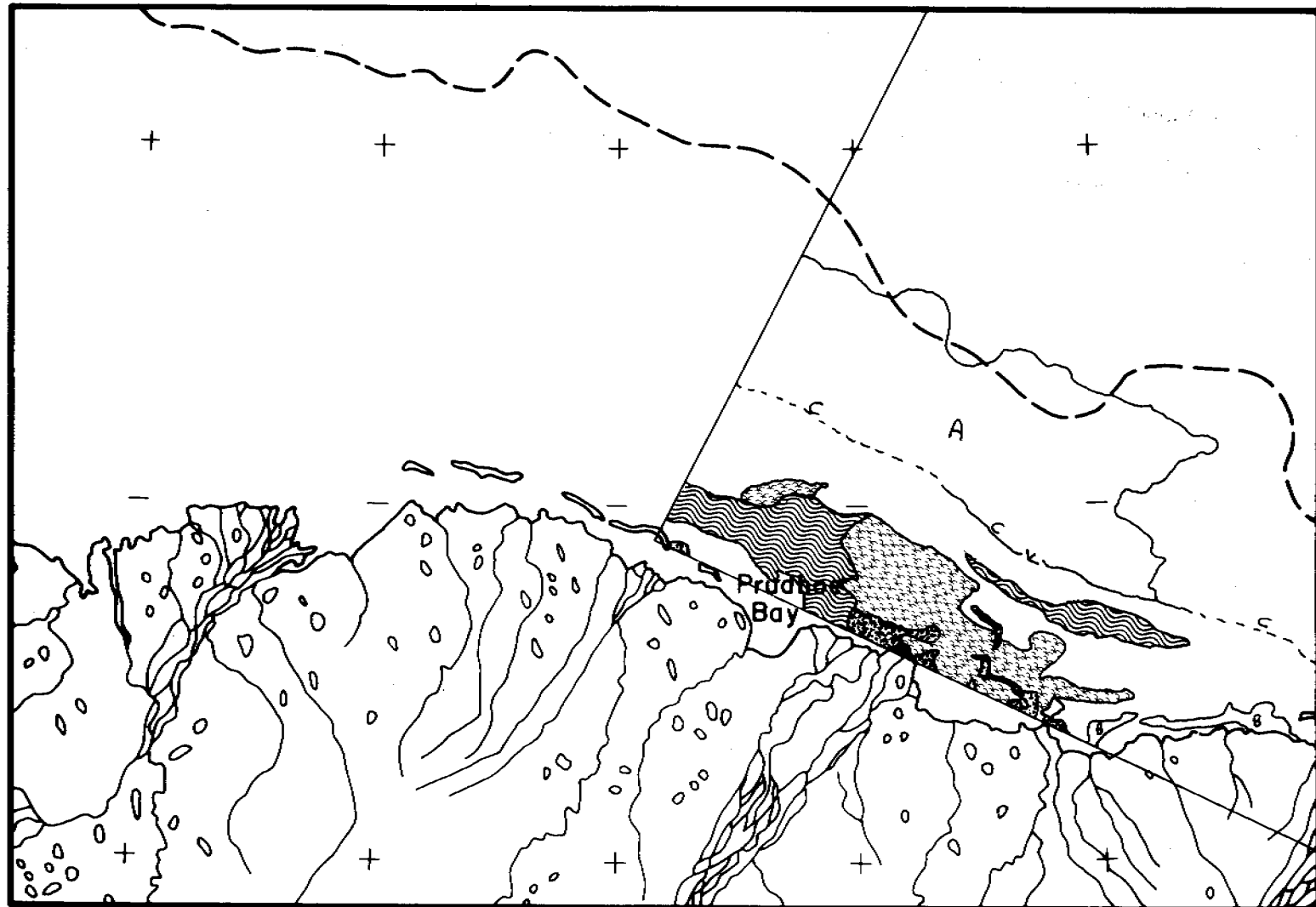
### ROUGH ICE

Ridging and Hummocking

Grounding

Pack Ice

Open Water



SHOREFAST SEA ICE  
SURFACE MORPHOLOGICAL CHARACTERISTICS

BEAUFORT SEA COAST: PRUDHOE SECTOR

12 JULY, 1974

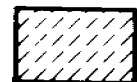
14 JULY, 1974: SCENE 1721-21143

THE CONTINUOUS ICE EDGE OF 26 JUNE HAS EXPERIENCED DISPLACEMENTS ALL ALONG ITS EXTENT SHOWN ON THIS SCENE. 26 JUNE-14 JULY CONTINUOUS ICE DISPLACEMENTS ARE SHOWN AS SOLID ARROWS. PACK ICE DISPLACEMENTS DURING THE SAME INTERVAL ARE DEPICTED AS DOTTED ARROWS ON THE MAP. THE WELL-GROUNDED NATURE OF THE THREE ICE MASSES SO DEPICTED ON THE MAP WAS DETERMINED FROM THIS SCENE AND THE TWO FOLLOWING SCENES. IN THE MIDST OF SHEARING AND/OR PRESSURED ICE FIELDS, ALL THREE MASSES REMAINED ESSENTIALLY STATIONARY. THE SHEARING ICE AROUND THE TWO WESTERNMOST GROUNDED MASSES CREATED CRACKS (BLACK LINES) AND OPENINGS (SHOWN AS OPEN WATER) IN THEIR VICINITY. THE DISPLACEMENTS OF PREVIOUSLY-CONTINUOUS ICE APPEAR TO BE LARGER IN EASTERN HARRISON BAY THAN FURTHER EAST. PACK ICE IS COMPACTED ALL ALONG THE PREVIOUSLY-CONTINUOUS ICE AND WAS DISPLACED SOUTHWEST, THE SAME DIRECTION AS THE CONTINUOUS ICE. THE MECHANISM OF BREAKUP, THEN, APPEARS TO BE THE SHOREWARD PRESSURING OF CONTINUOUS ICE BY THE PACK. FAILURE HAS OCCURRED AT A GREAT MANY POINTS IN THE ICE FIELD, LEAVING ONLY THE WELL-GROUNDED ICE IN PLACE. ALTHOUGH LIMITED AREAS OF LIGHTER TONE REMAIN ON THIS SCENE, MOST OF THE NEAR SHORE ICE IS NOW DEEPLY-PUDDLED (PUDDLING 4) OR MELTED COMPLETELY. THE OPEN WATER AREAS OFF ALL THE MAJOR RIVERS HAVE INCREASED, MOST NOTABLY THOSE OF THE COLVILLE, KUPARUK AND SAGAVANIRKTOK RIVERS. THE SHORE-POLNYA BREAKUP NW OF TIGVARIAK ISLAND (NOTED PREVIOUSLY) HAS DEVELOPED FURTHER SINCE 12 JULY, WITH WIDER CRACKS AND OPEN WATER AREAS IN EVIDENCE.

## KEY:

### SMOOTH ICE

Puddling 1



Puddling 2



Puddling 3



Puddling 4



### ROUGH ICE

Ridging and Hummocking



Grounding



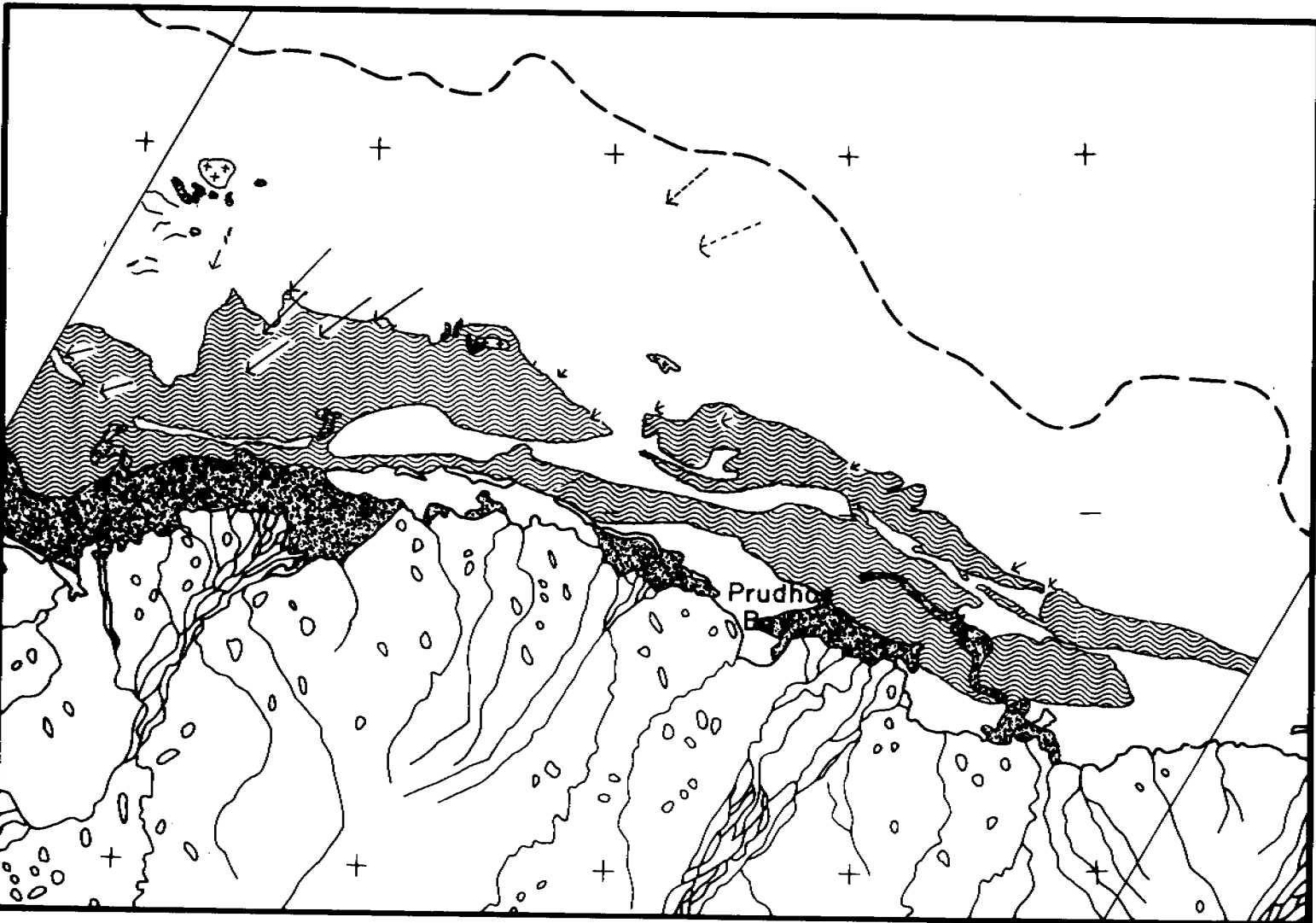
Pack Ice



Open Water



40m Isobath



SHOREFAST SEA ICE  
SURFACE MORPHOLOGICAL CHARACTERISTICS  
BEAUFORT SEA COAST: PRUDHOE SECTOR

14 JULY, 1974

15 JULY, 1974: SCENE 1722-21202

PUDDLING CHARACTERISTICS, ICE BOUNDARIES, PACK ICE CONCENTRATION AND OPEN WATER AREAS ARE SIMILAR TO 14 JULY AND ARE NOT MAPPED. THE THREE MAJOR GROUNDED MASSES REMAINED IN PLACE. DISPLACEMENTS IN THE INTERVAL 14-15 JULY WERE GENERALLY SO SMALL THAT THEIR MAGNITUDES COULD NOT BE ACCURATELY DEPICTED ON THE MAP. THEREFORE, THE SOLID ARROWS DESIGNATE THE DIRECTION OF THE DISPLACEMENTS ONLY. AS SHOWN, THESE VARIED FROM ABOUT 0.3 KM IN HARRISON BAY TO 1.5 KM IN THE PACK ICE SEAWARD OF TIGVARIAK ISLAND. 14 JULY WIND DIRECTIONS AT OLIKTOK AND BARTER ISLAND ARE SHOWN AS DOUBLE ARROWS, WITH RESPECTIVE MAGNITUDES OF 5.3 AND 6.2 M/SEC. THE ICE DID NOT CONFORM TO ZUBOV'S DRIFT RULE HERE. THE WINDS SHIFTED FROM NW ON 12 AND 13 JULY TO ENE ON 14 JULY. POSSIBLY MUCH OF THE WIND STRESS BETWEEN 14 AND 15 JULY WAS EXPENDED IN ARRESTING THE MOMENTUM INDUCED IN THE MOBILE ICE ON THE PREVIOUS TWO DAYS. THIS MIGHT MANIFEST ITSELF IN VERY SMALL NET DISPLACEMENTS, WHICH ARE IN FACT OBSERVED. THE DOTTED ARROW EXTENDING SOUTHWEST FROM THETIS ISLAND INDICATES THE TRUE-SCALE DISPLACEMENT OF A PREVIOUSLY-IMMOBILE ICE PIECE IN THE NEAR SHORE AREA. THIS FLOE BROKE AWAY FROM THETIS ISLAND UNDER THE INFLUENCE OF THE NE WINDS. IT IS ALSO NOTED THAT THE WINDS HAVE A SMALL ONSHORE COMPONENT, WHICH, IN THE ABSENCE OF ICE MOTION, INDICATES A COMPONENT OF STRESS PRESSURING THE SEAWARD LIMIT OF CONTINUOUS ICE TOWARD SHORE.

## KEY:

### SMOOTH ICE

Puddling 1

Puddling 2

Puddling 3

Puddling 4

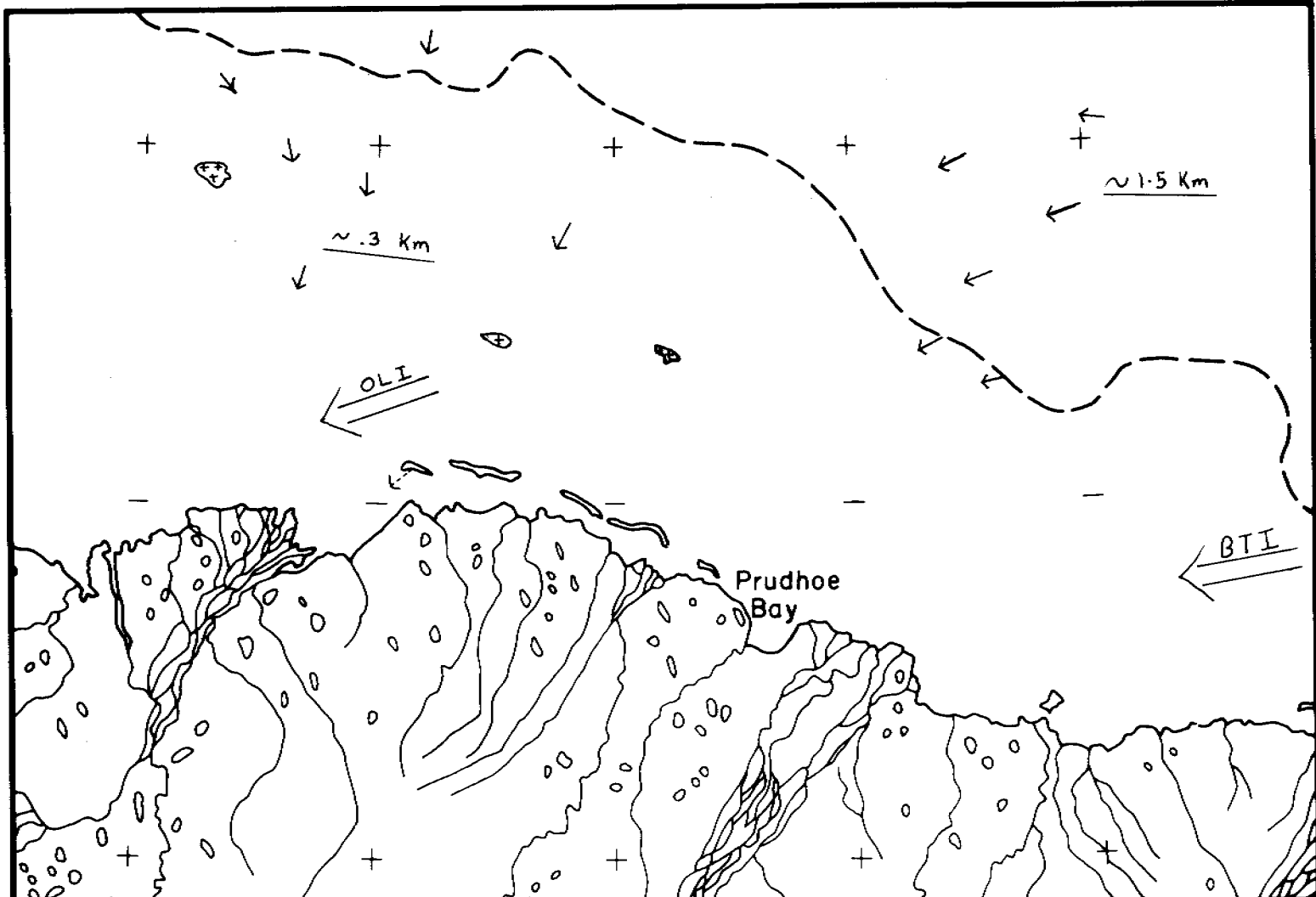
### ROUGH ICE

Ridging and Hummocking

Grounding

Pack Ice

Open Water



SHOREFAST SEA ICE  
SURFACE MORPHOLOGICAL CHARACTERISTICS  
BEAUFORT SEA COAST: PRUDHOE SECTOR

15 JULY, 1974

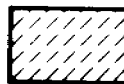
16 JULY, 1974: SCENE 1723-21260

WINDS FOR 15 JULY WERE SIMILAR TO THOSE OF 14 JULY AT OLIKTOK AND BARTER ISLAND, WITH MAGNITUDES OF 4.8 AND 5.7 M/SEC, RESPECTIVELY. 15-16 JULY ICE DISPLACEMENTS ARE DEPICTED IN TRUE SCALE ON THIS AMP, AND IT IS EVIDENT THAT MOTIONS WERE LARGER IN THIS TIME INTERVAL THAN IN THE PREVIOUS ONE. DIRECTIONAL AGREEMENT WITH ZUBOV'S RULE WAS MUCH BETTER THAN FOR 14-15 JULY, BUT THE PACK ICE N OF HARRISON BAY MOVED MORE SLOWLY THAN WOULD BE EXPECTED. THIS WOULD DECREASE THE CORIOLIS EFFECT AND BRING ICE DRIFT MORE CLOSELY IN LINE WITH WIND DIRECTION. THE SLOWING OF THIS ICE MAY BE DUE TO COMPACTION FURTHER WEST. A RIDGE SYSTEM WHICH PREVIOUSLY DEFINED THE LIMIT OF CONTINUOUS ICE N AND NE OF THE EASTERNMOST GROUNDED MASS (A) WAS DISPLACED WESTWARD BY PACK ICE PRESSURES. HOWEVER, ALL OF THE GROUNDED MASSES HELD THEIR POSITIONS. MAXIMUM DISPLACEMENTS OCCURRED IN CENTRAL HARRISON BAY, WHERE THE VERY DARK TONE OF THE ICE INDICATES AN ADVANCED ABLATION CONDITION ("ROTTEN ICE"), OFFERING LITTLE RESISTANCE TO MOTION. AT "B", INSIDE PINGOK ISLAND, MUCH OF THE FLAT, DRAINED ICE VISIBLE ON 15 JULY BROKE UP AND DISAPPEARED, LEAVING SOME FLOE FRAGMENTS AND OPEN WATER BEHIND. THIS IS TAKEN TO INDICATE THAT DRAINED ICE CAN AND DOES BECOME WEAK AND BREAKS UP, EVEN THOUGH IT REMAINS LIGHT-TONED IN ALL LANDSAT BANDS RIGHT UP TO BREAKUP TIME.

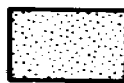
KEY:

SMOOTH ICE

Puddling 1



Puddling 2



Puddling 3



Puddling 4

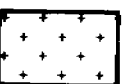


ROUGH ICE

Ridging and  
Hummocking



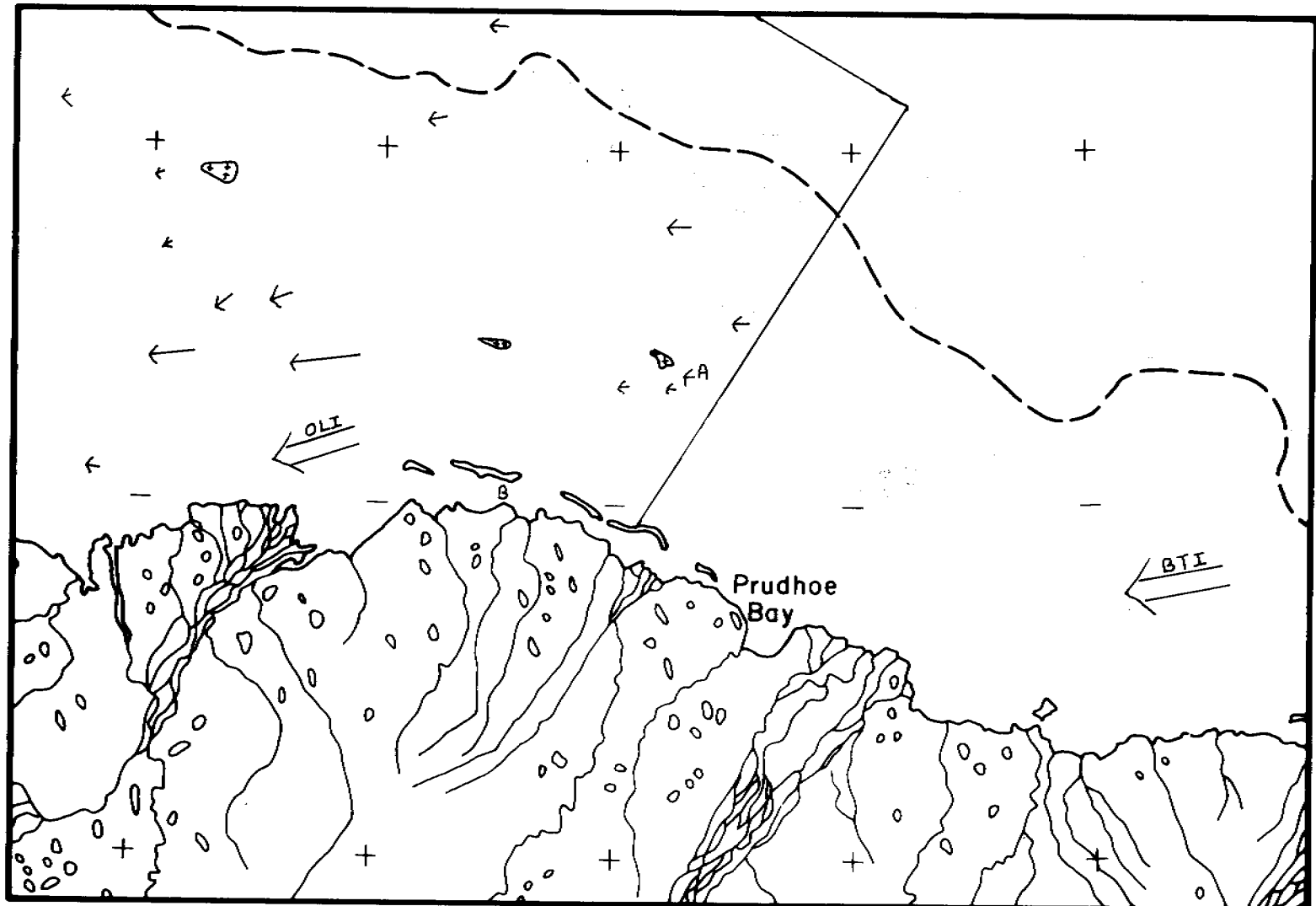
Grounding



Pack Ice



Open Water



SHOREFAST SEA ICE

SURFACE MORPHOLOGICAL CHARACTERISTICS

BEAUFORT SEA COAST: PRUDHOE SECTOR

16 JULY, 1974

2 AUGUST, 1974: SCENE 1740-21194

ON THIS SCENE THE CONTINUOUS ICE SHEET OF 25-26 JUNE IS ESSENTIALLY GONE. THE THREE LARGE GROUNDED MASSES NEAR THE FORMER CONTINUOUS ICE EDGE REMAIN IDENTIFIABLE AND UNMOVED, ALTHOUGH THEY HAVE DECREASED IN AREA. THE FOURTH GROUNDED MASS NEAR BODFISH ISLAND IS DEPICTED AS "C". TRULY "SHOREFAST" ICE EXISTED BETWEEN THE SEWARD GROUNDED MASSES AND THE COAST EARLIER IN THE YEAR. OPEN WATER NOW COVERS MOST OF THE FAST ICE ZONE, WITH LOOSE PACK ICE (A) SEPARATING IT FROM COMPACT PACK ICE (B). ALL PACK ICE PRESENTS THE APPEARANCE OF ADVANCED SURFACE MELTING ON THIS SCENE. SEVERAL LIGHT-TONED AREAS APPEARED ON THE LANDSAT DATA FOR THIS DATE IN ZONE "B", WHICH, FROM THEIR SHAPE, APPEAR TO BE BROKEN UP FRAGMENTS OF RIDGES WHICH FORMERLY COMPSED PART OF THE CONTINUOUS ICE.

KEY:

SMOOTH ICE

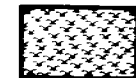
Puddling 1



Puddling 2



Puddling 3



Puddling 4



ROUGH ICE

Ridging and

Hummocking



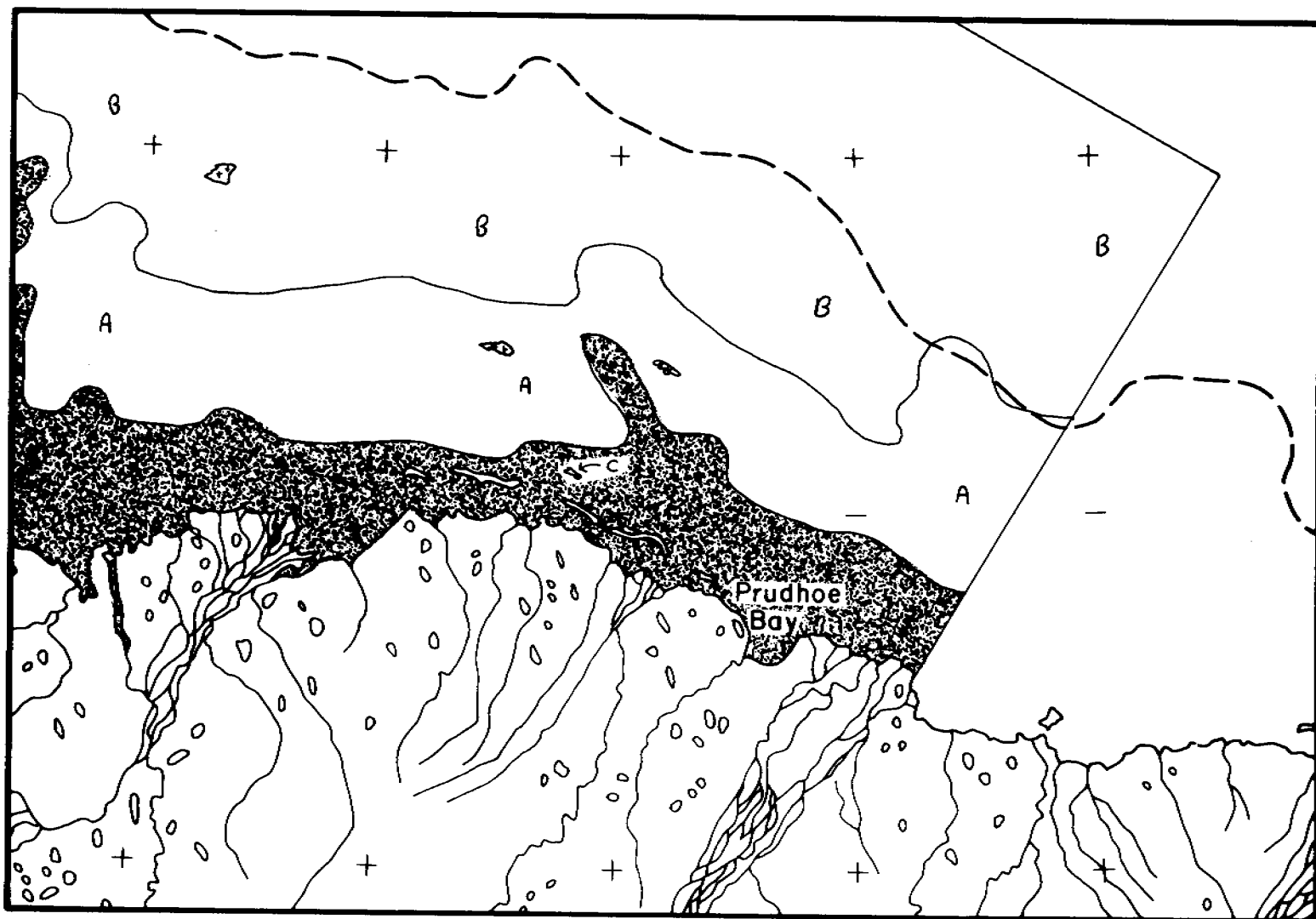
Grounding



Pack Ice



Open Water



SHOREFAST SEA ICE  
SURFACE MORPHOLOGICAL CHARACTERISTICS

BEAUFORT SEA COAST: PRUDHOE SECTOR

2 AUGUST, 1974

40m Isobath ——

## SIXTH QUARTERLY REPORT

TITLE: Mechanics of Origin of Pressure Ridges, Shear Ridges and Hummock Fields in Landfast Ice

PERIOD: July 1, 1976 - September 30, 1976

PRINCIPAL INVESTIGATORS: Lewis H. Shapiro and William D. Harrison  
Geophysical Institute, University of Alaska

I. TASK OBJECTIVES: To determine the mechanics of origin of pressure ridges, shear ridges and hummock fields in landfast ice.

II. FIELD AND LABORATORY SCHEDULE: Evaluation of results and continuation of preliminary theoretical work.

III. RESULTS: The results of the field work on newly formed ridges along the beach at Barrow, which was noted in the last quarterly report, were combined with other results of similar work from the summer of 1975. A preliminary report of this work was presented at the AAAS meeting in Fairbanks in August. A more comprehensive summary will appear in the next annual report of this project.

During September, a bathymetric survey was conducted of the area within the field-of-view of the University of Alaska radar system at Barrow. A continuous recording fathometer was installed for this purpose on the R. V. Natchick, operated by NARL. The ship's course during the survey was monitored and recorded by the radar. The data are presently being plotted, and will be utilized for interpretation of ridging patterns in the area.

IV. PRELIMINARY INTERPRETATION: None.

V. PROBLEMS ENCOUNTERED/RECOMMENDED CHANGES: None.

VI. ESTIMATED FUNDS EXPENDED: \$10,000.

## OCS COORDINATION OFFICE

University of Alaska

## Quarterly Report for Quarter Ending September 30, 1976

Project Title: Morphology of Beaufort Near Shore Ice Conditions by Means of Satellite and Aerial Remote Sensing

Contract Number: 03-5-022-55

Task Order Number: 8

Principal Investigator: W. J. Stringer

**I. Task Objectives:**

The objective of this study is to develop a comprehensive morphology of near shore ice conditions in the Beaufort Sea, including a synoptic picture of the development and decay of fast ice and related features along the Beaufort Sea coast, and in the absence of fast ice, the nature of other ice (pack ice, ice islands, hummock fields, etc.) which may occasion the near shore areas in other seasons. Special emphasis will be given to consideration of potential hazards to offshore facilities and operations created by ice dynamics. A historical perspective of near shore ice dynamics will be developed to aid in determining the statistical rate of occurrence of ice hazards.

**II. Field and Laboratory Schedule:**

This project has no field schedule. All remote sensing aircraft data is to be provided by project management. The work to be done does not involve laboratory activities.

**III. Results:**

Using LANDSAT band 7 hard copy produced at 1:500,000 scale, preliminary Beaufort Sea near shore ice maps have been compiled for late spring and early summer ice seasons of 1973, 1974 and 1976. These maps have been reproduced here at half scale for reporting convenience. Particular care, described in earlier reports, has been taken to locate ice features relative to geographic coordinates and the bathymetric 10-fathom contour. The half-scale reproductions of these maps have been reproduced here as Appendix A with annotation for each map discussing the significance of the features delineated.

**IV. Preliminary Interpretations:**

The paper "Ice Hazards to Offshore Oil Operations in Arctic Alaskan Waters" presented September 21, 1976 at the 31st Annual Petroleum Mechanical Engineering Conference in Mexico City, contains many preliminary interpretations of this project and has been attached as Appendix B.

V. Plans for Next Reporting Period:

During this next reporting period the preparation of retroactive maps will continue. However, a special emphasis will be placed on final work on "special event" maps to present some of these results at the American Geophysical Union Meeting in San Francisco during December.

VI. Problems Encountered/Recommended Changes:

None.

VII. APPENDICES:

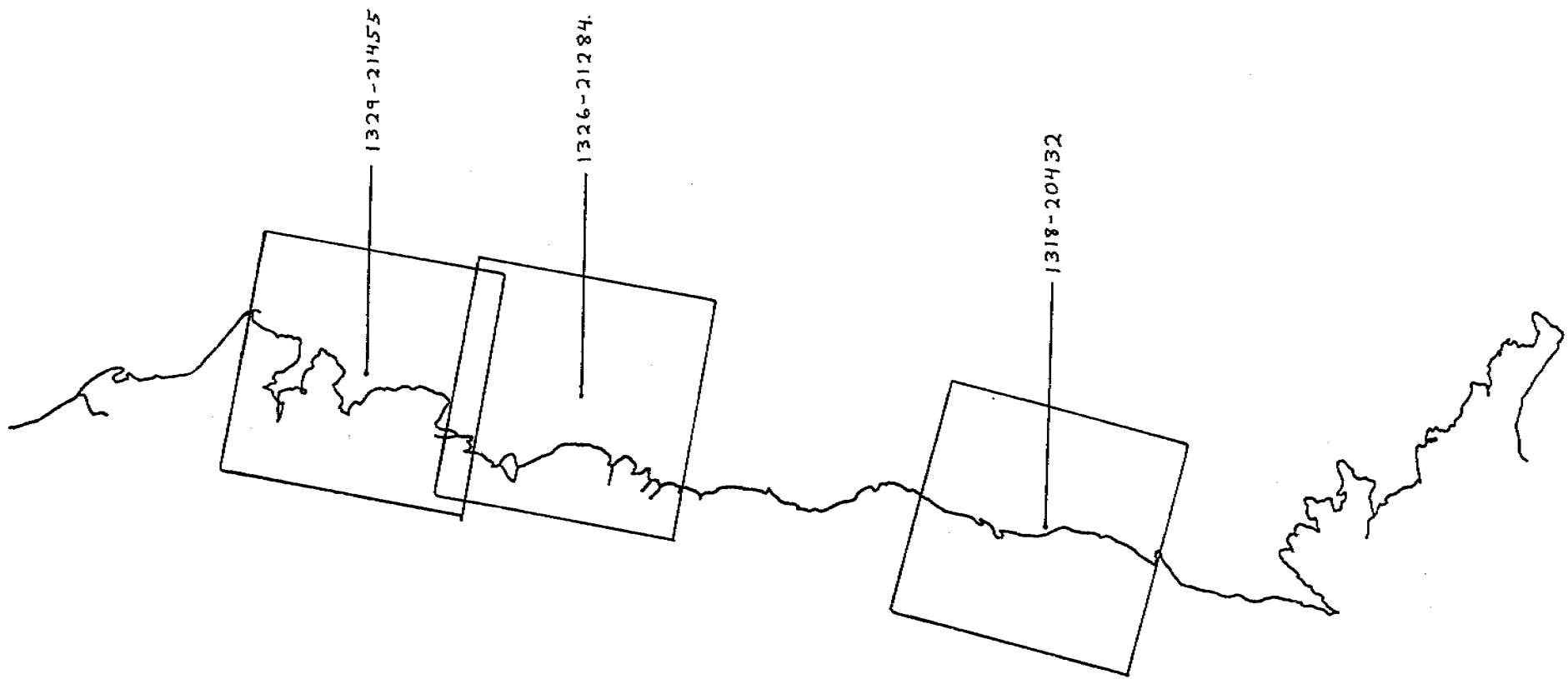
(Attached).

SYMBOLS AND DEFINITIONS

- A River overflow (aufeis)
- B Boundary between apparently different ice types.
- BN Broken sheet of new ice.
- BPN Pans in broken matrix of new ice.
- BPY Pans in broken matrix of young ice.
- BY Broken sheet of young ice.
- C Stationary ice - ice which is contiguous with the shore.
- CF Fragmented or broken contiguous ice.
- D Rotting or decaying ice, characterized by a dark, mottled color indicating holes and puddling.
- F Ice floe.
- FW Open water with numerous floes of various sizes.
- FY(B) First year ice (broken or fragmented).
- G Grounded ice floe or stranded ice.
- H Hummocked ice - sea ice piled haphazardly one piece over another to form an uneven surface.
- I Young ice.
- L A lead, usually open, but may be too narrow to determine if it is open or not.
- M New ice, characterized by dark color, and smooth texture.
- N Newly refrozen lead of polyna - a lead or polyna composed of dark ice, not yet fractured and milky or covered with snow, thin enough to allow light to pass through to the water.
- O Old refrozen lead - a lead old enough to have either turned milky with cracks or been covered by snow; thick enough to reflect most of the incident sunlight and thus appear gray or white.

- P Partially refrozen lead, usually some dark ice with open water.
- PN Pans in matrix of new ice.
- PY Pans in matrix of young ice.
- R Ridge system, may be either pressure ridge or shear ridge system.
- S Smooth ice of uncertain age.
- T Tidal or tension cracks - cracks due to tidal action in shallow waters, may be indicated by piled ice and/or snow drifts.
- UP Unconsolidated pack ice consisting of flows and broken ice of varying sizes. More dense than FW
- W Open water.
- Y Polynya.
- Z Zone of shear.

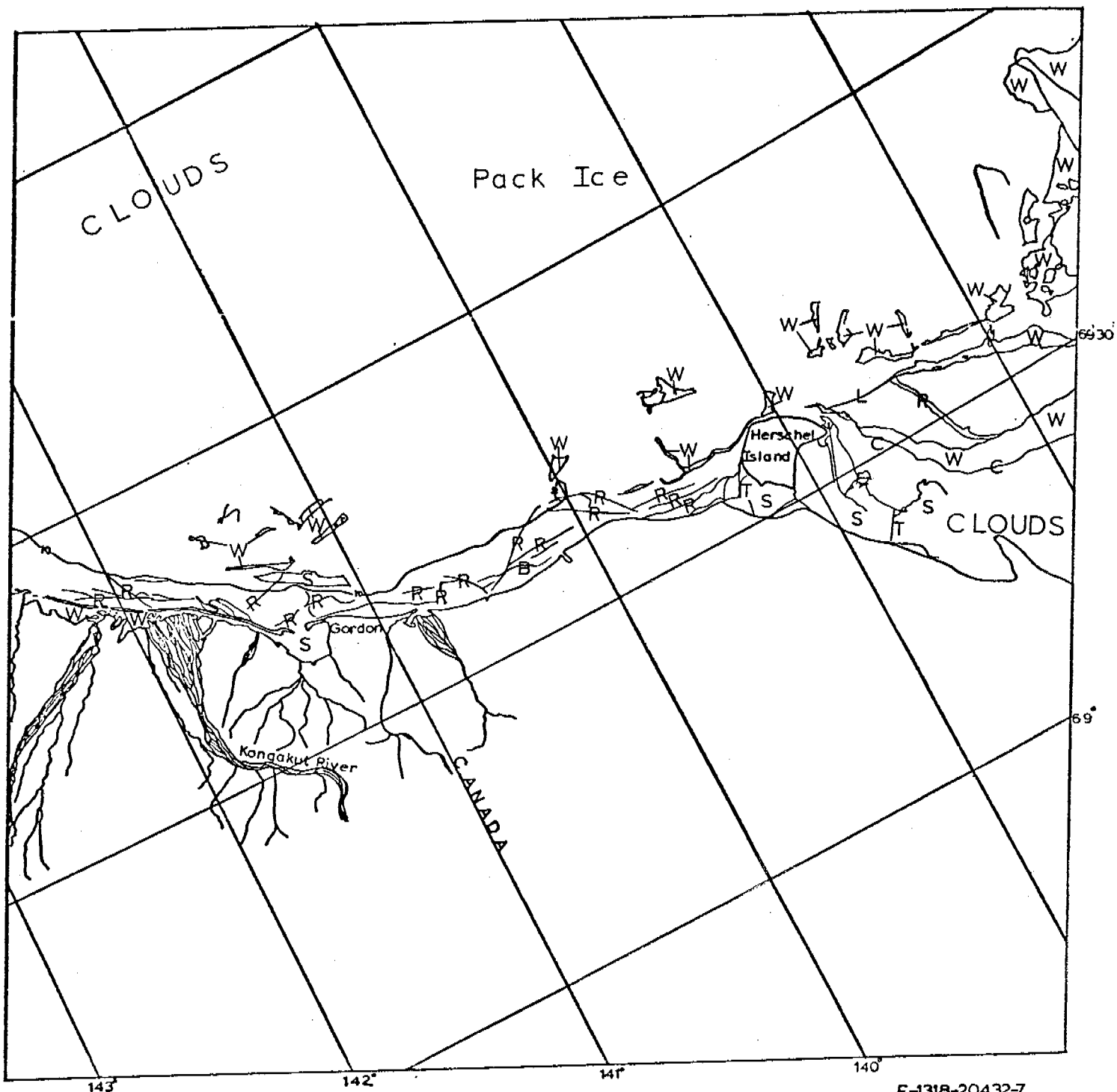
433



BEAUFORT SEA  
31 MAY - 17 JUNE 1973  
Images: 1312 - 1329

Scene E-1318-20432

This scene shows late spring (6 June) 1973 ice conditions along the Beaufort coast from Herschel Island eastward to the mouth of the Kongakut River. The boundary between the pack ice and fast ice is not clearly defined. However, only at a considerable distance from shore are there large patches of open water presumably caused by shifting of pack ice. In the near shore area there are to be found many 1 - 3 acre melt ponds on the ice and large expanses of flooded ice. This area is crossed by many ridges and apparent fossil tension cracks located shoreward of the 10-fathom contour while the large patches of open water are located seaward of this bathymetric contour. Large leads have opened east and west of Herschel Island perhaps defining the boundary of fast ice in those locations. In the very near shore areas large expanses of open water and flooded ice can be found.



KILOMETERS

0    10    20    30    40    50

[ ] [ ] [ ] [ ] [ ]

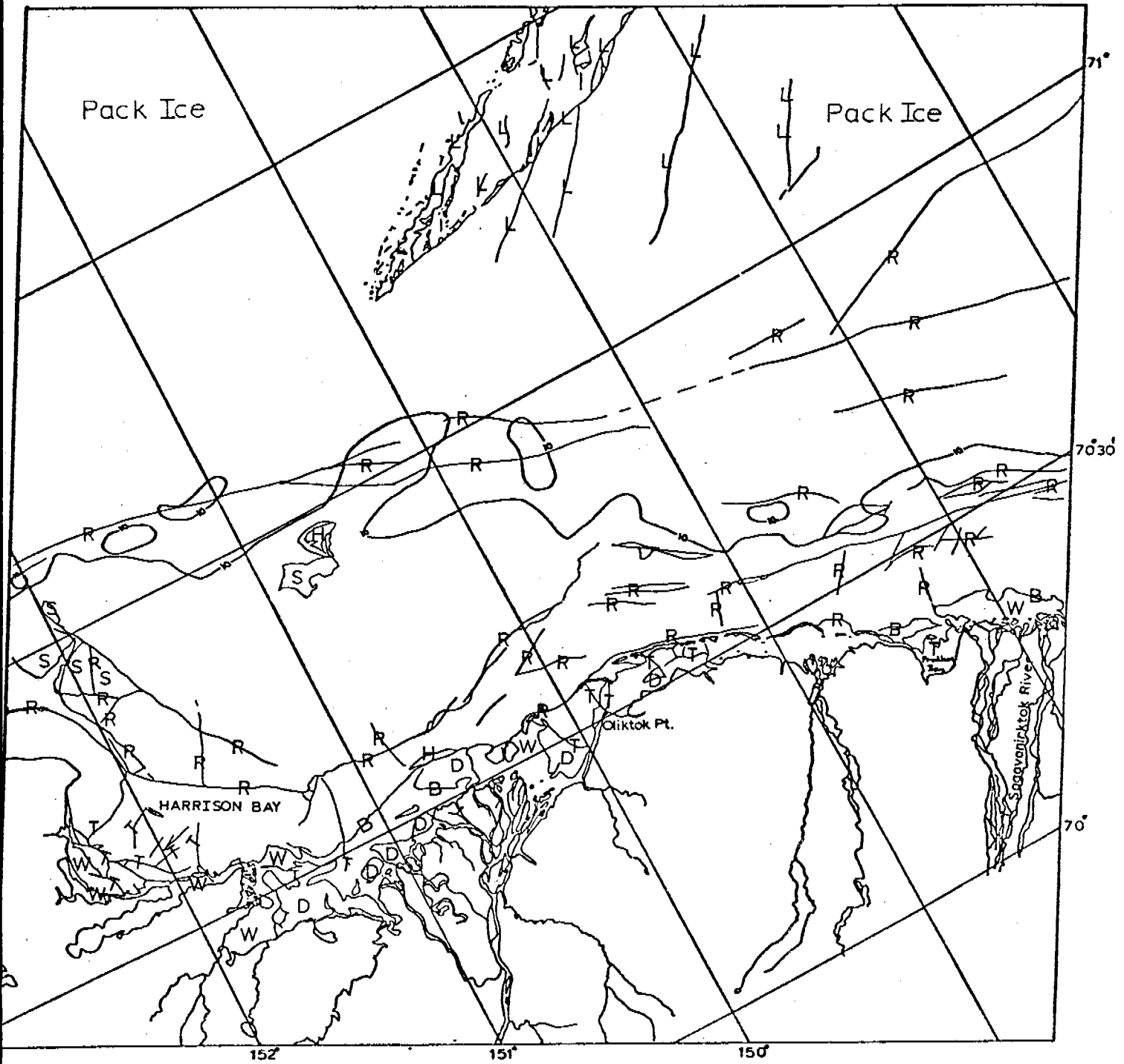
SCALE APPROX 1:1,000,000

## BEAUFORT SEA

E-1318-20432-7  
6 JUNE 1973

Scene E-1326-21284

This scene shows the portion of Beaufort coast from Harrison Bay eastward to the mouth of the Sagavanirkto River for late spring (14 June) 1973. The boundary between pack ice and fast ice is not well defined. The leads noted in the northern portion of this scene are obviously located in deep water well beyond the pack ice boundary. Two major ridge systems running roughly parallel to the coastline could be found. The first of these coincides with the 10-fathom contour across western Harrison Bay and then continues eastward in the same direction although the 10-fathom contour indents toward the coastline. The second set of ridges runs just inshore of the 10-fathom contour eastward from a point midway between Prudhoe Bay and Oliktok Point. Throughout this scene there is evidence of pressured ice, the major exception being interior Harrison Bay. In the very inshore areas the ice has either been flooded with melt water or has melted entirely.



KILOMETERS

0 10 20 30 40 50

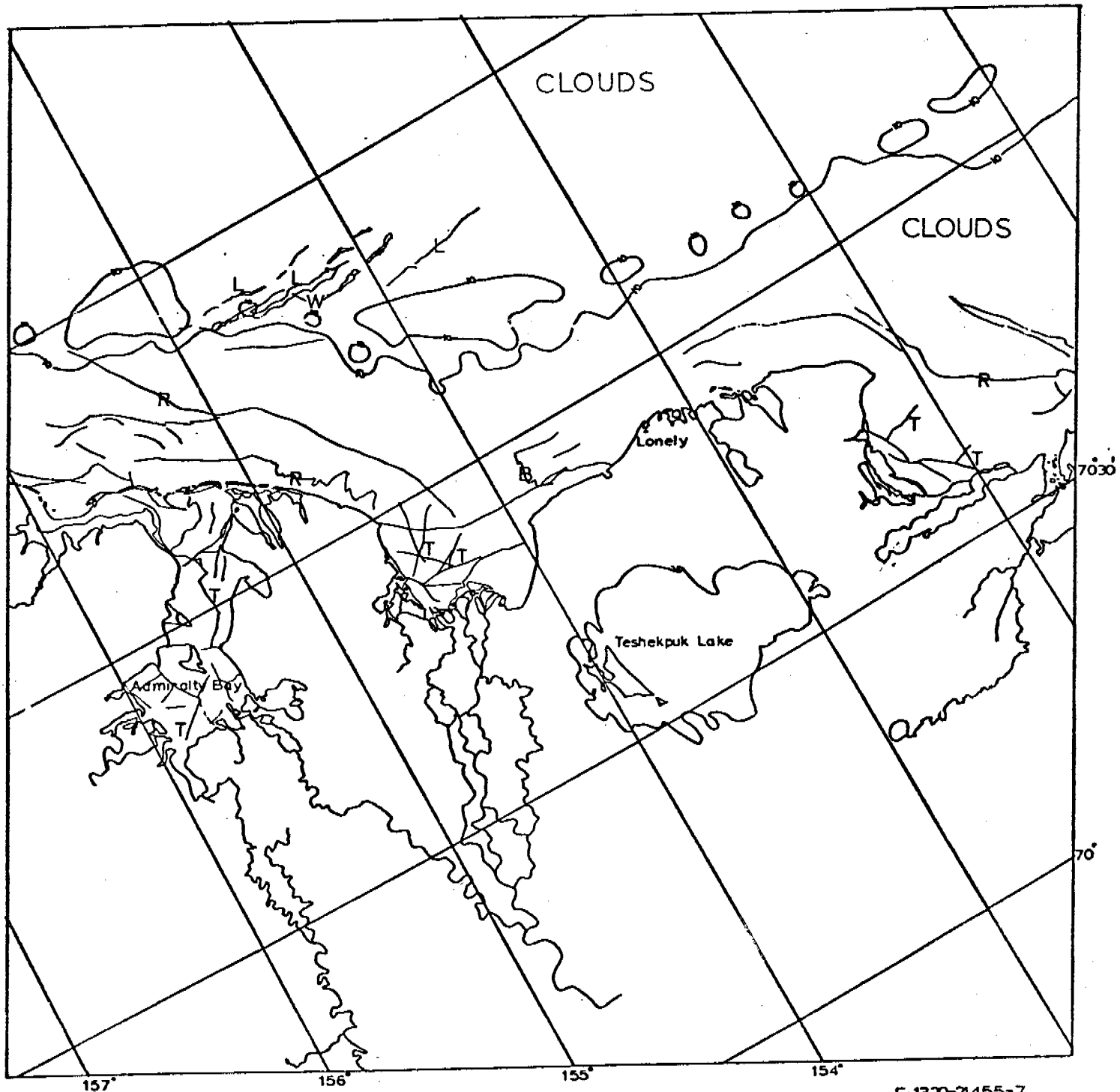
SCALE APPROX 1:1,000,000

## BEAUFORT SEA

E-1326-212847  
14 JUNE 1973

Scene E-1329-21455

This late spring (17 June) 1973 scene shows the portion of Beaufort coast eastward from Harrison Bay past Admiralty bay. Although partly obscured by clouds, sufficient detail can be seen on this Landsat scene to map significant ice features. Although considerable ponding is evident, the only open water resulting from shifting ice lies beyond the 10-fathom contour. There is no strong evidence of major shear ridging westward of Lonely; further, there is considerable evidence of only minor pressuring during the past winter, particularly between Smith and Admiralty Bays. In the very near shore areas considerable flooding and melting has taken place: inside Admiralty Bay, only the ridges raised as a result of refreezing of tension cracks remain drained of melt water. The only clear evidence of a boundary between pack ice and fast ice is the open water resulting from shifting of broken-up and freely-floating ice located just beyond the 10-fathom contour.

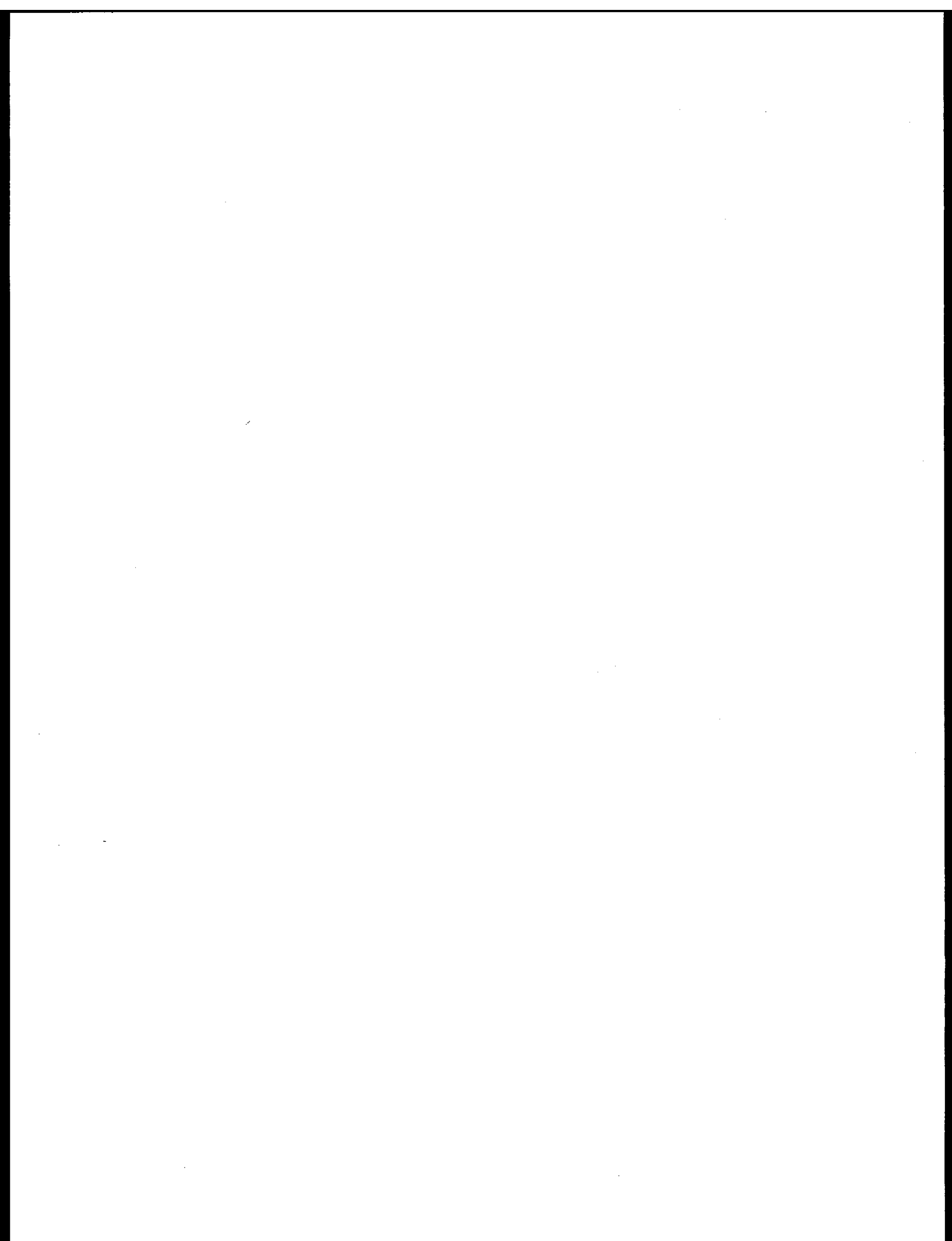


KILOMETERS

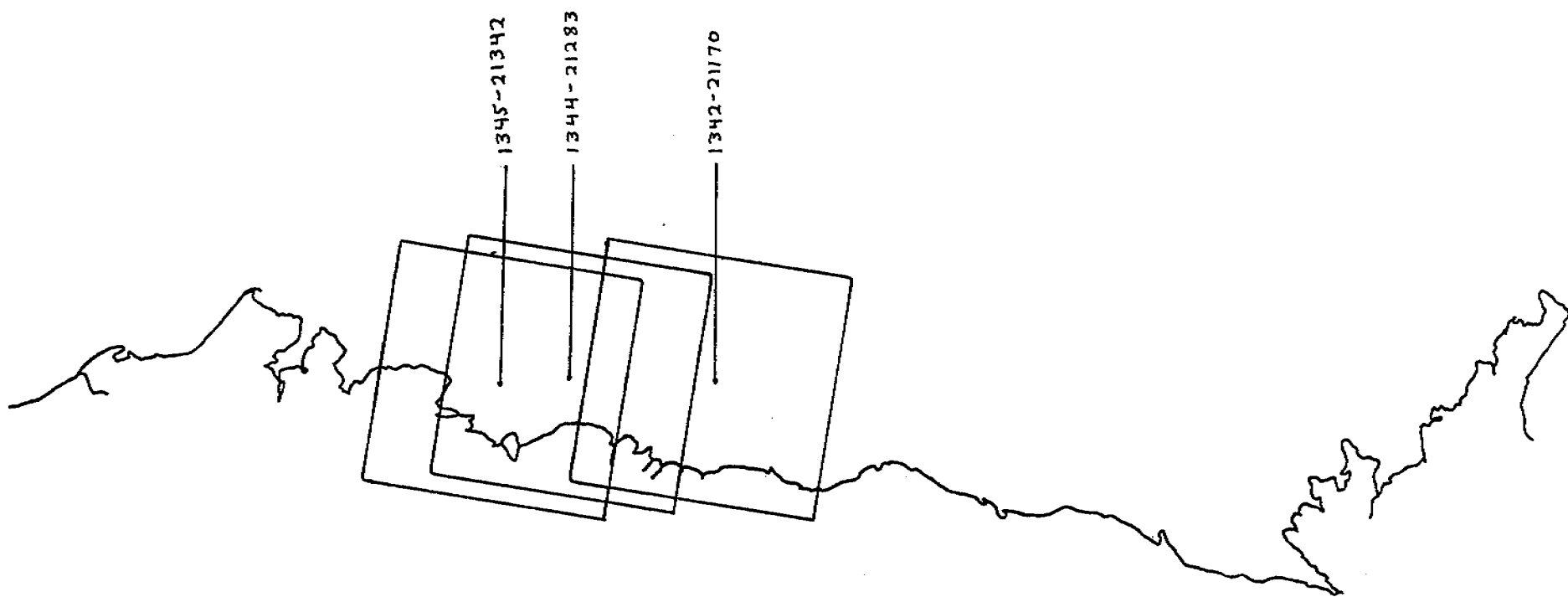
**SCALE APPROX 1:1,000,000**

## BEAUFORT SEA

E-1329-21455-7  
17 JUNE 1973



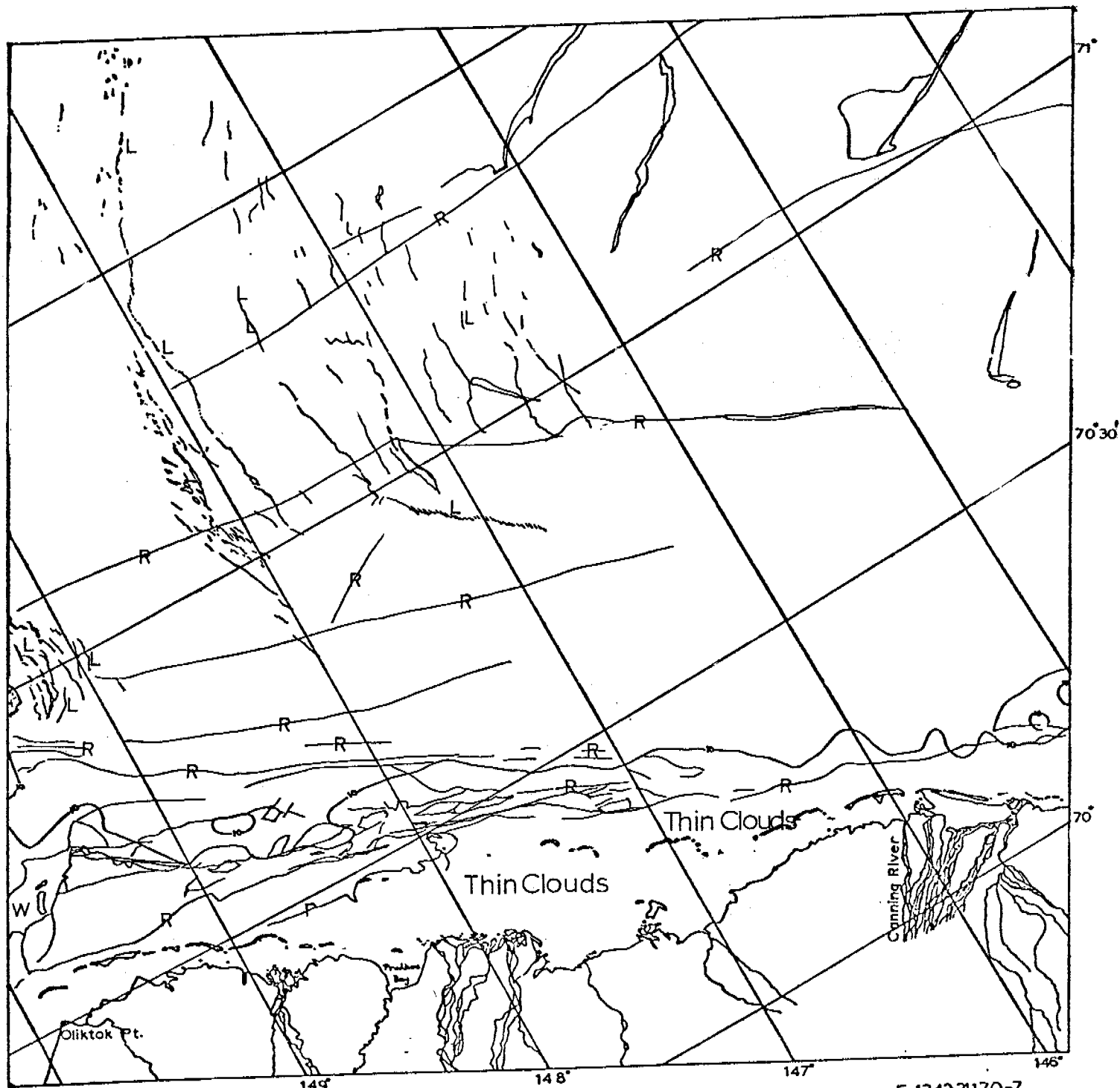
174



BEAUFORT SEA  
18 JUNE-5 JULY 1973  
1330 - 1347

Scene E-1342-21170

This end of spring (30 June) 1973 Landsat scene shows the portion of Beaufort coast between Oliktok Point and the mouth of the Canning River. This scene shows considerable evidence of past shear ridging extending from the near shore areas far seaward. The most extensive ridging has taken place in the vicinity of the 10-fathom contour between Oliktok Point and the mouth of the Sagavanirkto River, and is found between the offshore islands and the 10-fathom contour. Shoreward of the most shoreward ridge mapped there is evidence of minimal pressuring of ice during the previous winter. In the very recent past two series of concentric lead systems have developed in the pack ice. However, the pack ice is no longer a continuous sheet with the result that shifting pans are quickly making the leads into irregularly-connected patches of open water.



KILOMETERS  
0 10 20 30 40 50  
SCALE APPROX 1:1,000,000

BEAUFORT SEA

E-1342-2170-7  
30 JUNE 1973

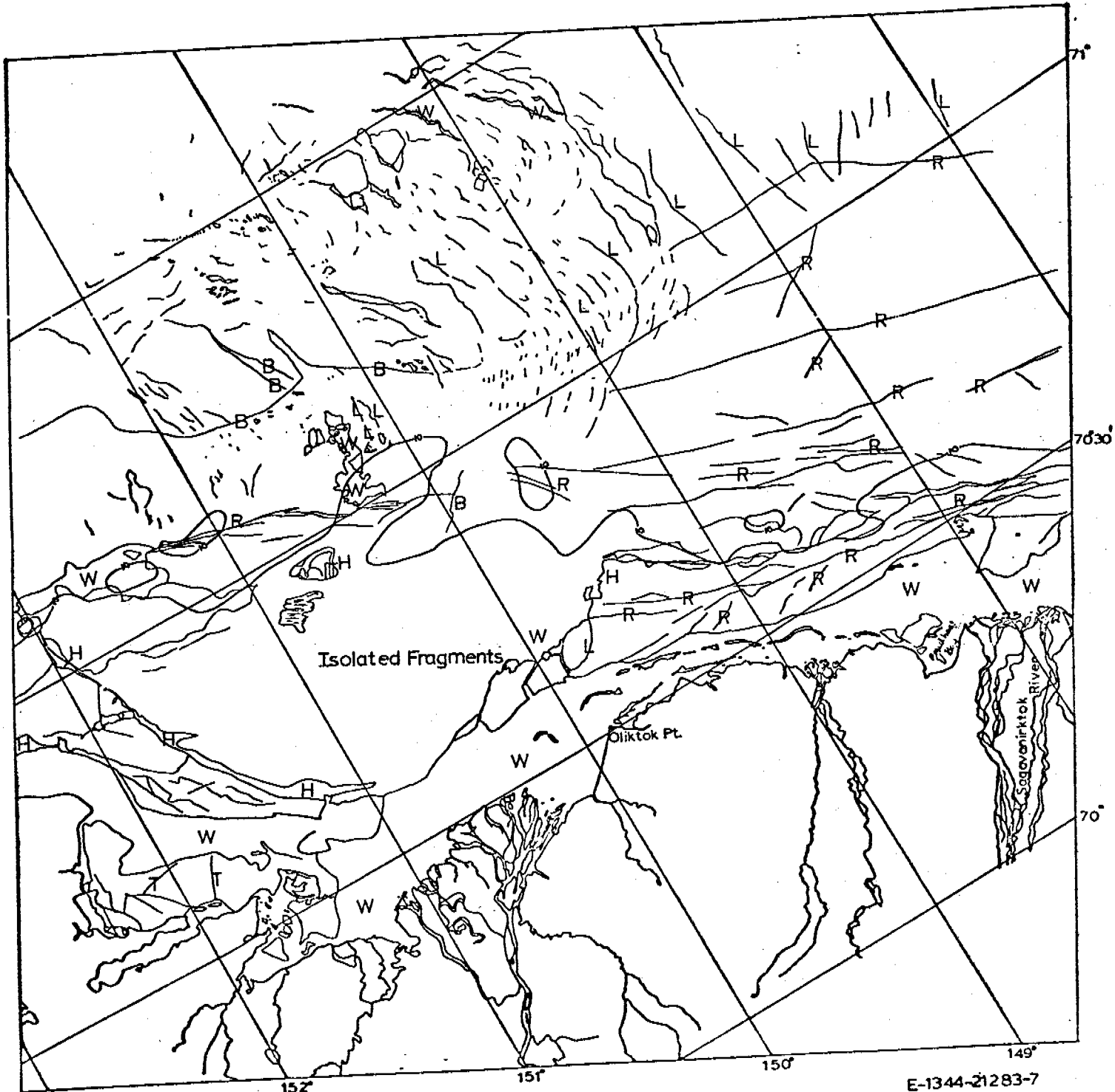
Scene E-1344-21283

This Landsat scene shows the portion of Beaufort coast between Harrison Bay and the mouth of the Sagavanirktok River for early summer (2 July) 1973. This scene allows some distinction between pack ice and grounded features. To the west from the top center of this image pack ice is fracturing in concentric rings and drifting westward. To the east of top center the polar ice sheet remains generally continuous. In this zone many large shear ridges have been mapped in ice quite seaward from the 10-fathom contour.

Nearer shore, many shear ridges can be found running roughly parallel to the shore line across the image. Some of these give evidence of being grounded: to the west of center, one group of ridges run across a raised portion of ocean floor eastward to a protruding finger of the 10-fathom contour. Seaward of these ridges is moving pack ice. However, just westward of the western terminus of these ridges is an open body of water located over another raised portion of sea floor. Presumably in this location the extensions of these same ridges have been rafted away.

On the eastern side of the image the absence of moving pack ice does not allow determination of the polar ice-grounded ice boundary. However, it is interesting to note that there are generally two systems of ridges: one considerably seaward bridging a landward indentation of the 10-fathom contour and another series roughly parallel with the indented portion of the 10-fathom contour.

In the near shore areas, there is considerable open water resulting from spring time flooding of near shore ice by river water.



E-1344-21283-7  
2 JULY 1973

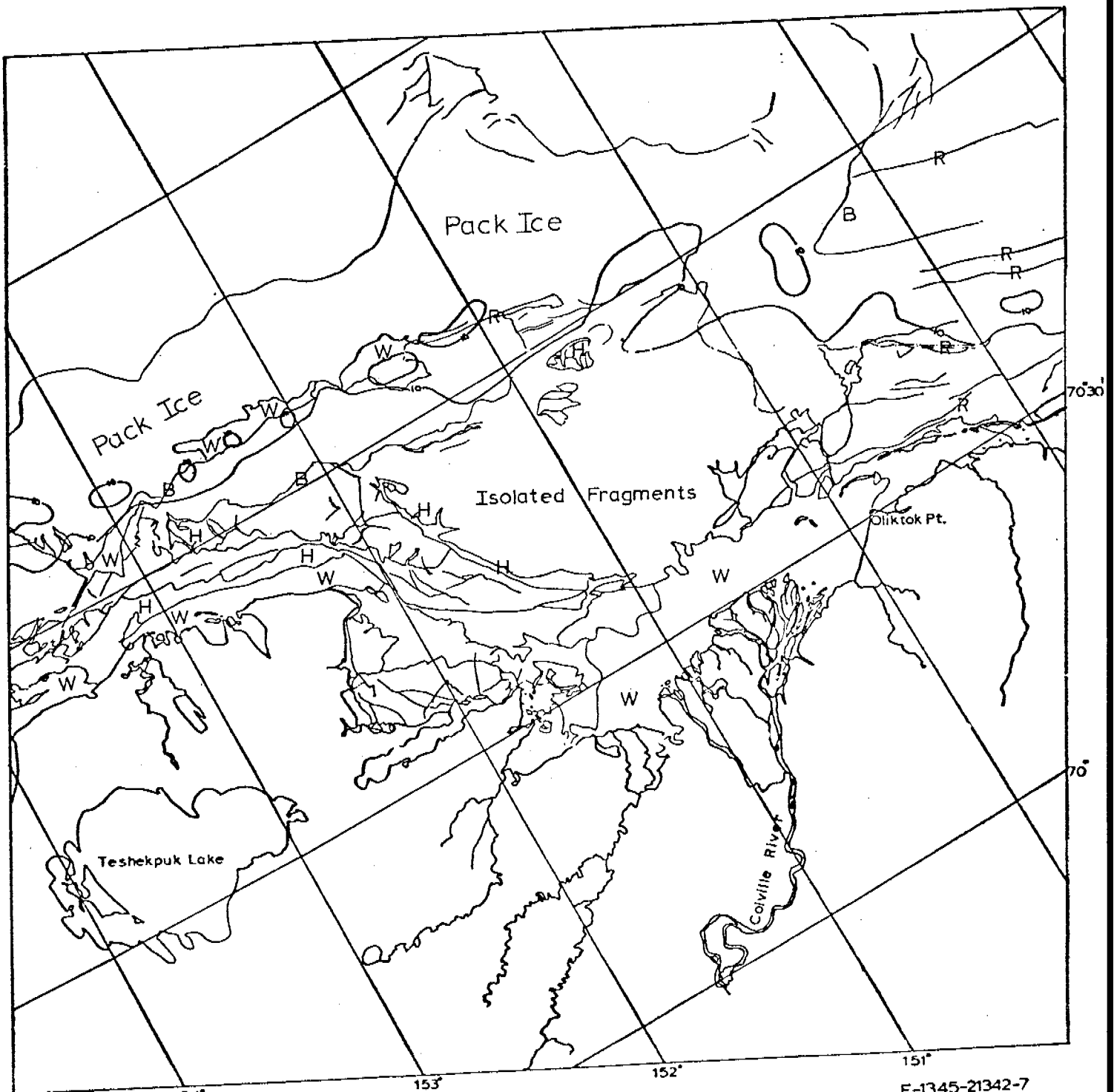
KILOMETERS  
0 10 20 30 40 50  
SCALE APPROX 1:1,000,000

## BEAUFORT SEA

Scene E-1345-21342

This scene shows the portion of Beaufort coast from east of Oliktok Point westward to Lonely for early summer (3 July) 1973. Because of the considerable overlap with scene E-1344-21283 obtained the previous day, this discussion will concentrate on that (western) portion not described for that image. Detailed analysis shows that during the 24-hour period between the two images, the pack ice has moved several kilometers westward.

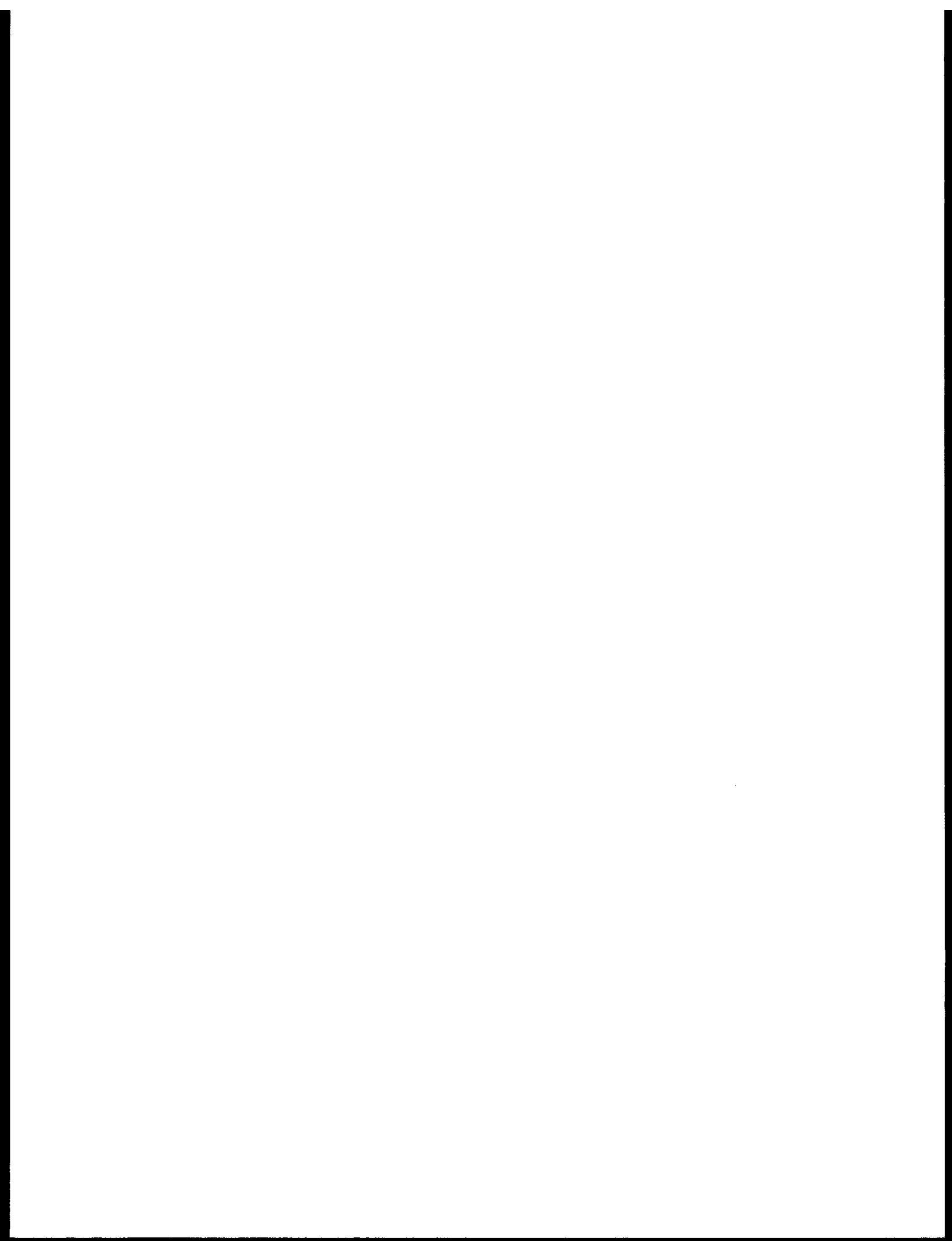
On the western portion of this image the boundary between open water and ice presumably grounded is irregular although it generally follows the 10-fathom contour. The extensions of the shear ridges mapped just to the east have apparently continued westward. On the western side of the image can be seen a noteable exception to the general rule of grounded ice following the 10-fathom contour: there is a large shoreward extension of open water. No shear ridges are evident in this area.



E-1345-21342-7  
3 JULY 1973

KILOMETERS  
0 10 20 30 40 50  
SCALE APPROX 1:1,000,000

### BEAUFORT SEA



674



BEAUFORT SEA  
13 JUNE - 30 JUNE 1974  
Images: 1690-1707

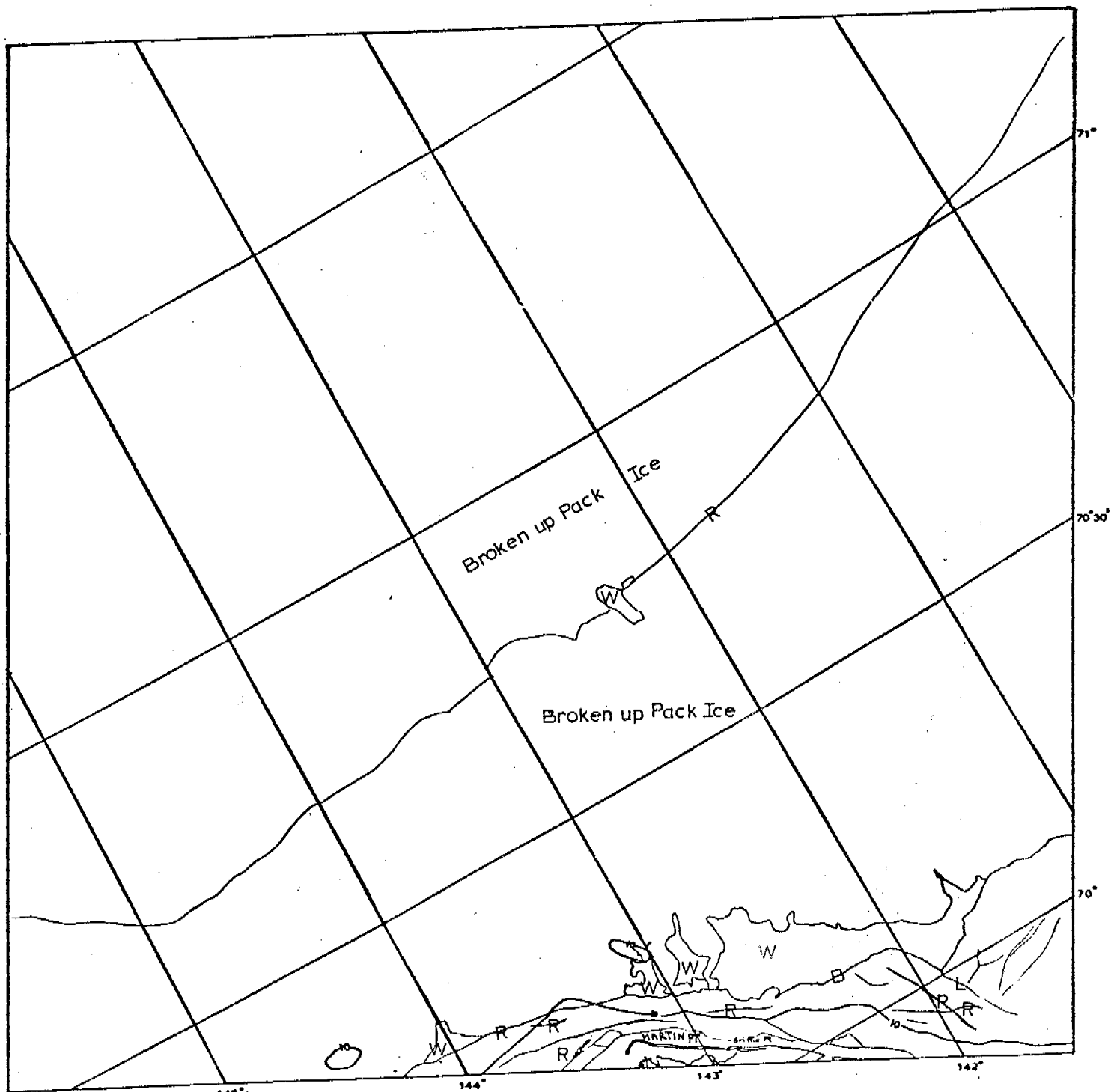
Scene E-1699-20522

This scene shows the portion of Beaufort Sea coast in the vicinity of Martin Point for late spring (22 June) 1974.

To the west of Martin Point it has been possible to identify a well-defined boundary between pack ice and stable ice. This boundary gives strong indications of being a shear ridge. To the east of Griffin Point the boundary between pack ice and stationary ice can not be identified. A boundary which is an extension of the shear ridge to the west has been mapped. However, this boundary achieves its distinction by being the boundary between shore-bound ice and open water. It is very likely that this boundary is not determined by grounded ice.

Martin Point is the most prominent feature on the eastern Beaufort coast and as a result one would anticipate that shear ridges might be constructed in its vicinity. Although one ridge coincides with the 10-fathom contour, the most prominent shear ridge is located well shoreward of the seaward bulge of this contour.

Well seaward the remains of a very large extended ridge system can be seen.



KILOMETERS  
 0 10 20 30 40 50  
 SCALE APPROX 1:1,000,000

## BEAUFORT SEA

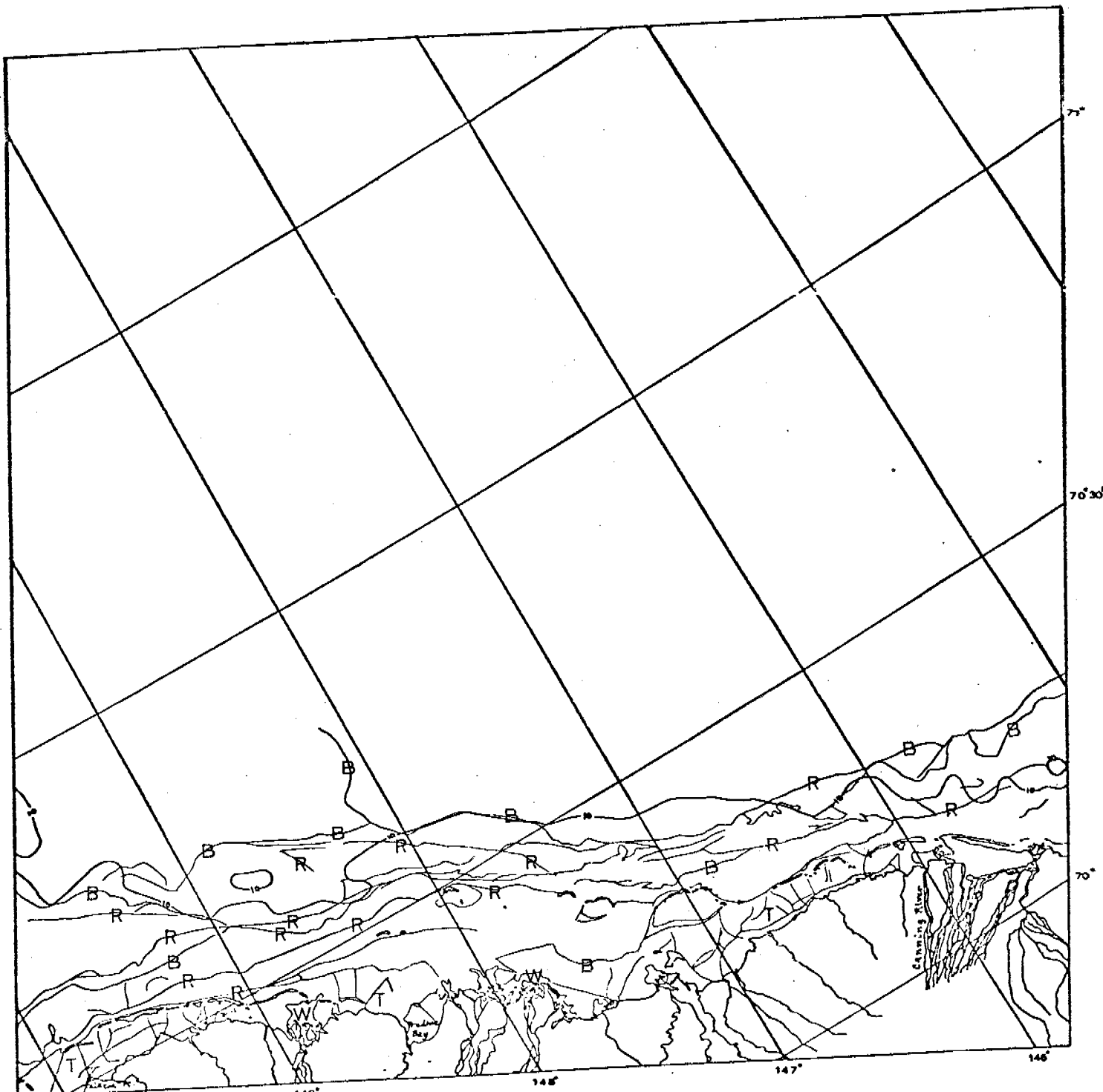
E-1699-20522-7  
 22 JUNE 1974

Scene E-1702-21093

This scene shows the portion of Beaufort Sea coast between Oliktok Point on the west and the mouth of the Canning River on the east for late spring (25 June) 1974. A boundary has been drawn roughly coinciding with the 10-fathom contour separating the broken-up ice pack from apparently more stable ice shoreward. Portions of this boundary are smooth and appear to have been determined by the locations of ridges while other portions of the boundary are irregular, suggesting this relationship does not hold in these locations.

Between this boundary and the shore, there are many long, curving features suggesting shear ridges. In some cases the ice piles associated with these features are sufficiently broad to have been resolved by the Landsat imaging system.

In the very near shore areas at the mouths of rivers, flooding has resulted in the creation of open water.



E-1702-21093-7

25 JUNE 1974

KILOMETERS

0 10 20 30 40 50

SCALE APPROX 1:1,000,000

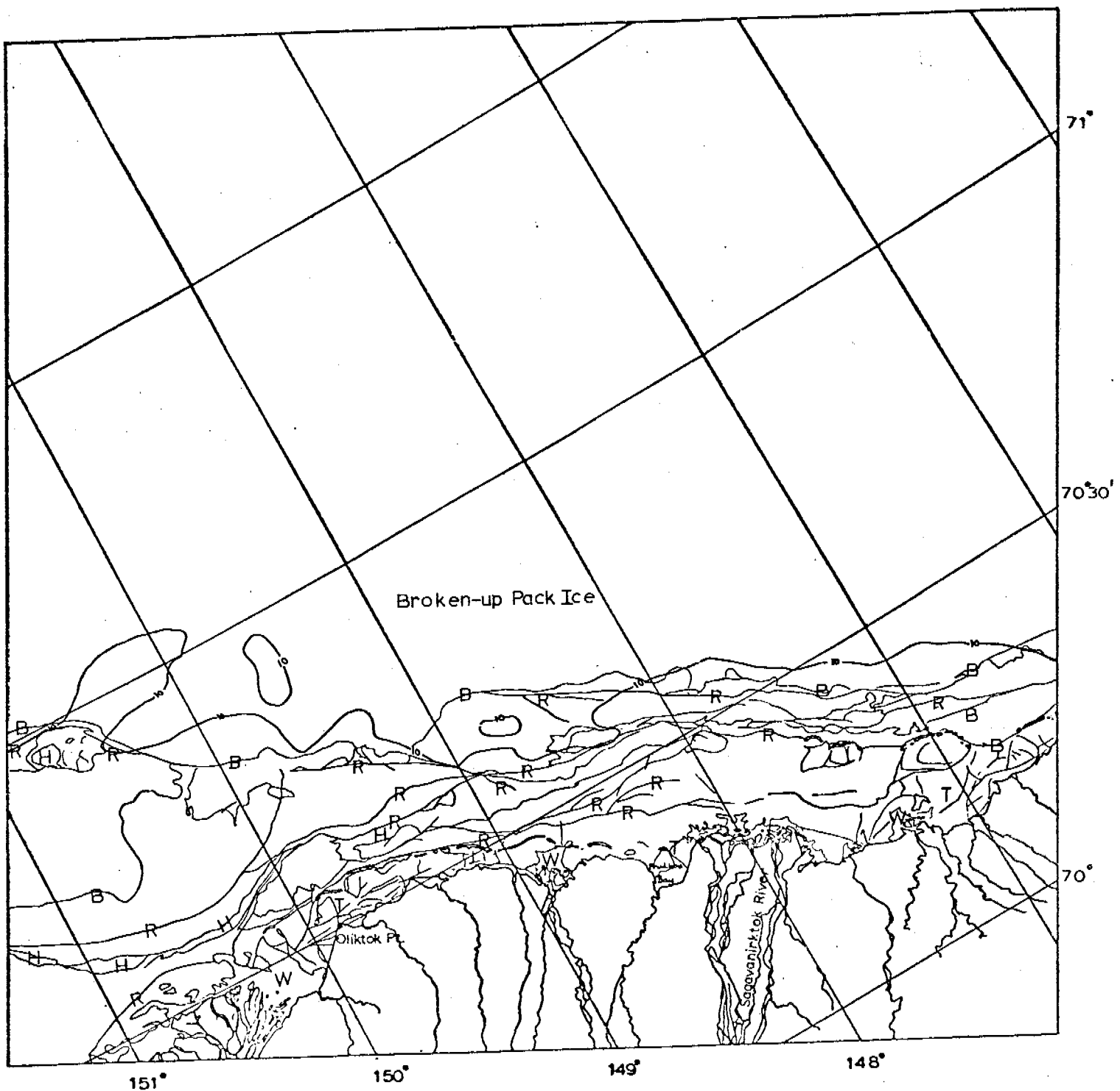
BEAUFORT SEA

Scene E-1703-21151

This Landsat image shows the portion of the Beaufort Sea coast between the mouth of the Colville River on the west to beyond the Sagavanirktok River delta on the east. The image was obtained on 26 June 1974 and shows late spring ice conditions. A boundary has been drawn roughly coinciding with the 10-fathom contour separating the broken-up pack ice seaward from apparently more stable ice shoreward. Portions of this boundary are smooth and their positions appear to have been governed by locations of ridges while other portions of the boundary are irregular, suggesting that this is not the case in these locations.

Between the boundary noted above and the shore, there are many long, slightly curving features suggesting shear ridges. In some cases the ice piles associated with these features are sufficiently broad to have been resolved by the Landsat imaging system.

In the very near shore areas at the mouths of rivers, flooding has resulted in the creation of open water.



KILOMETERS  
 0 10 20 30 40 50

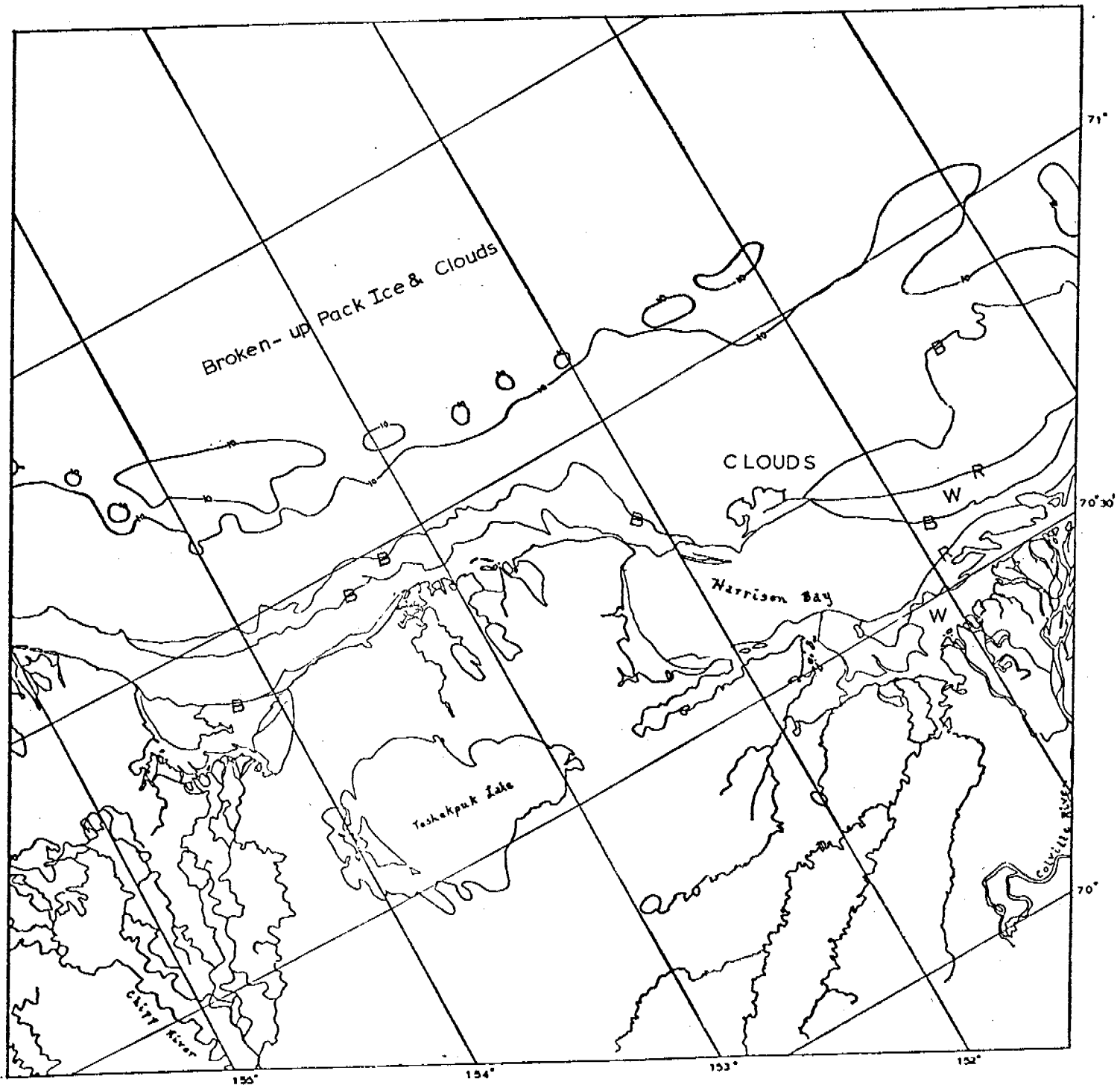
SCALE APPROX 1:1,000,000

## BEAUFORT SEA

E-1703-21151-7  
 26 June 1974

**Scene E-1706-21322**

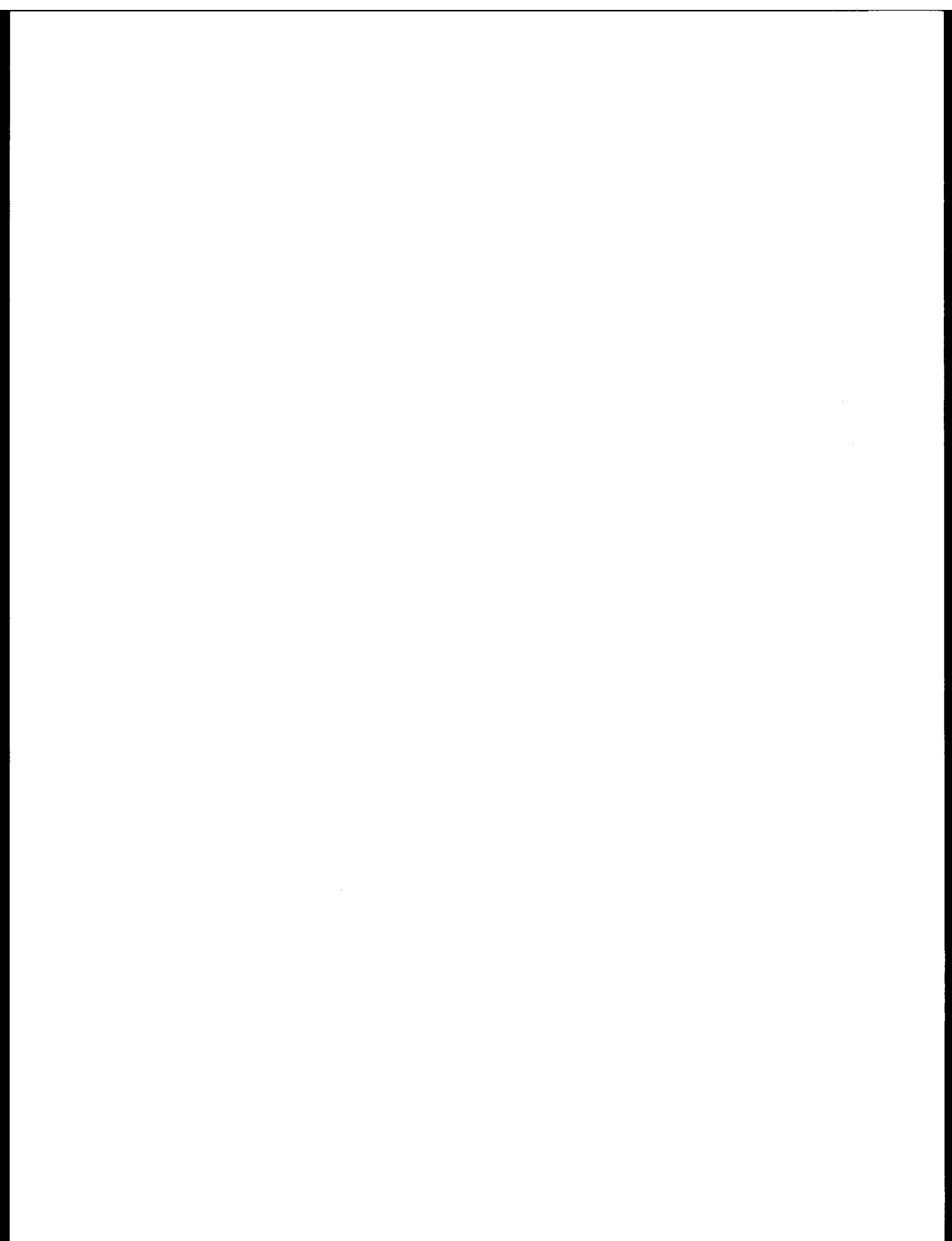
This scene shows the portion of Beaufort Sea coast from Smith Bay to the mouth of the Colville River for late spring (29 June) 1974. Clouds obscure most far offshore ice features except for the area in the vicinity of Smith Bay. In this area, the apparent boundary between stationary and pack ice is well-within the 10-fathom contour.



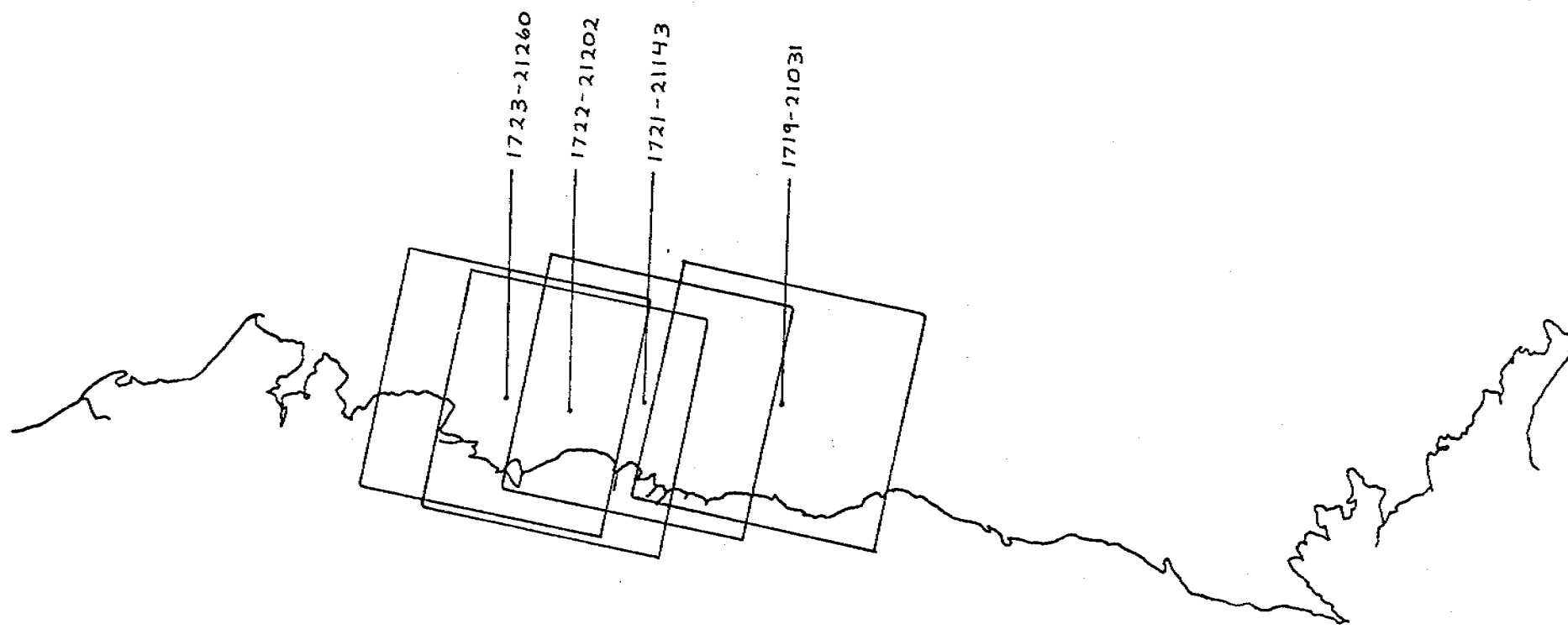
KILOMETERS  
 0 10 20 30 40 50  
 SCALE APPROX 1:1,000,000

### BEAUFORT SEA

E-1706-21322-7  
 29 JUNE 1974



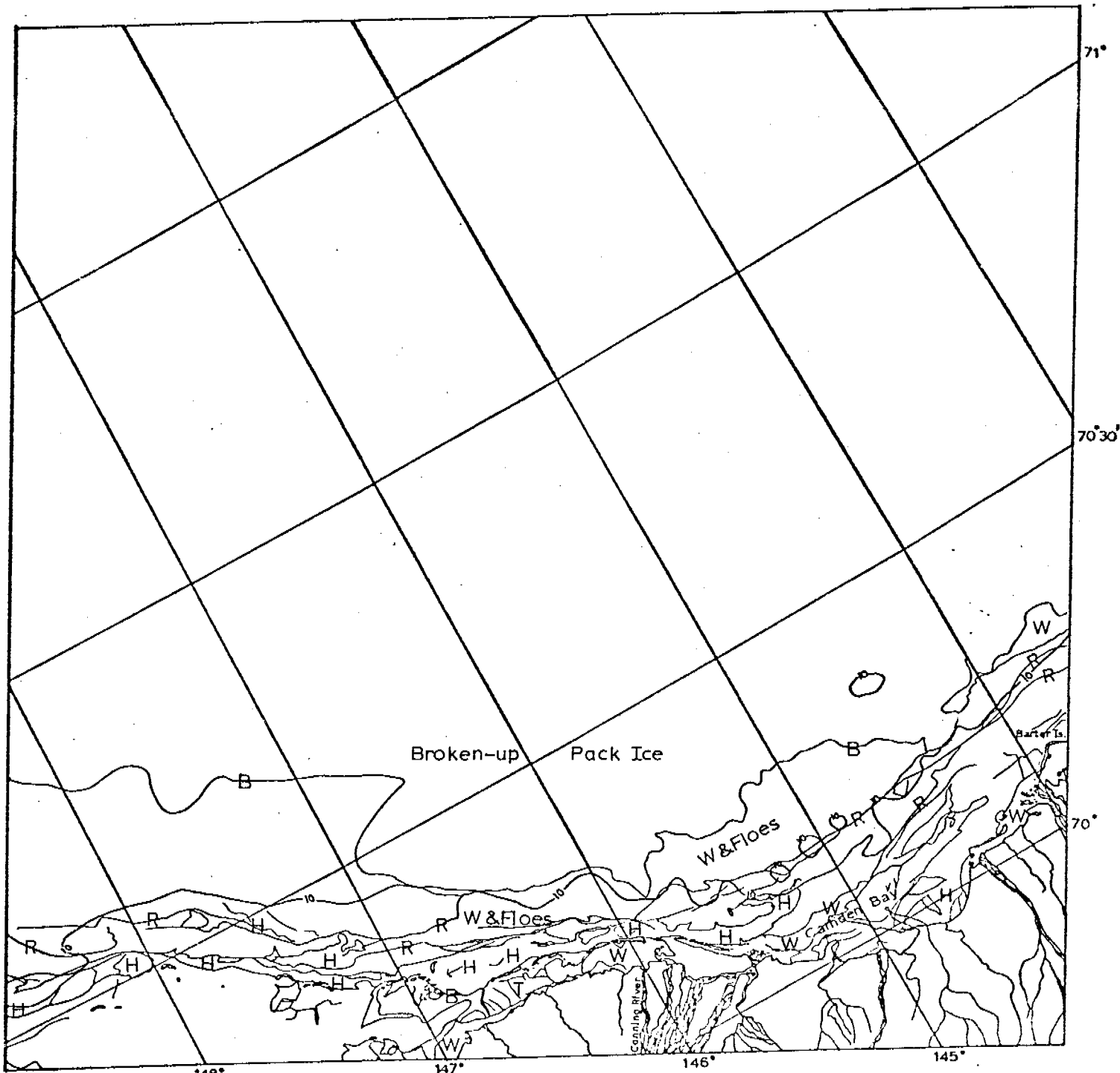
654



BEAUFORT SEA  
1 JULY - 18 JULY 1974  
1708-1725

Scene E-1719-21031

This Landsat image shows the portion of Beaufort coast from Barter Island on the east to Cross Island on the west for early summer (12 July) 1974. In this area there is a fairly good distinction between free-floating pack ice and ice stationary with respect to the shore. Along most of this edge a ridge can be identified which roughly coincides with the 10-fathom contour. The most severe ridging seems to have occurred northeast of Barter Island and west of Cross Island.



KILOMETERS  
 0 10 20 30 40 50  
  
 SCALE APPROX 1:1,000,000

## BEAUFORT SEA

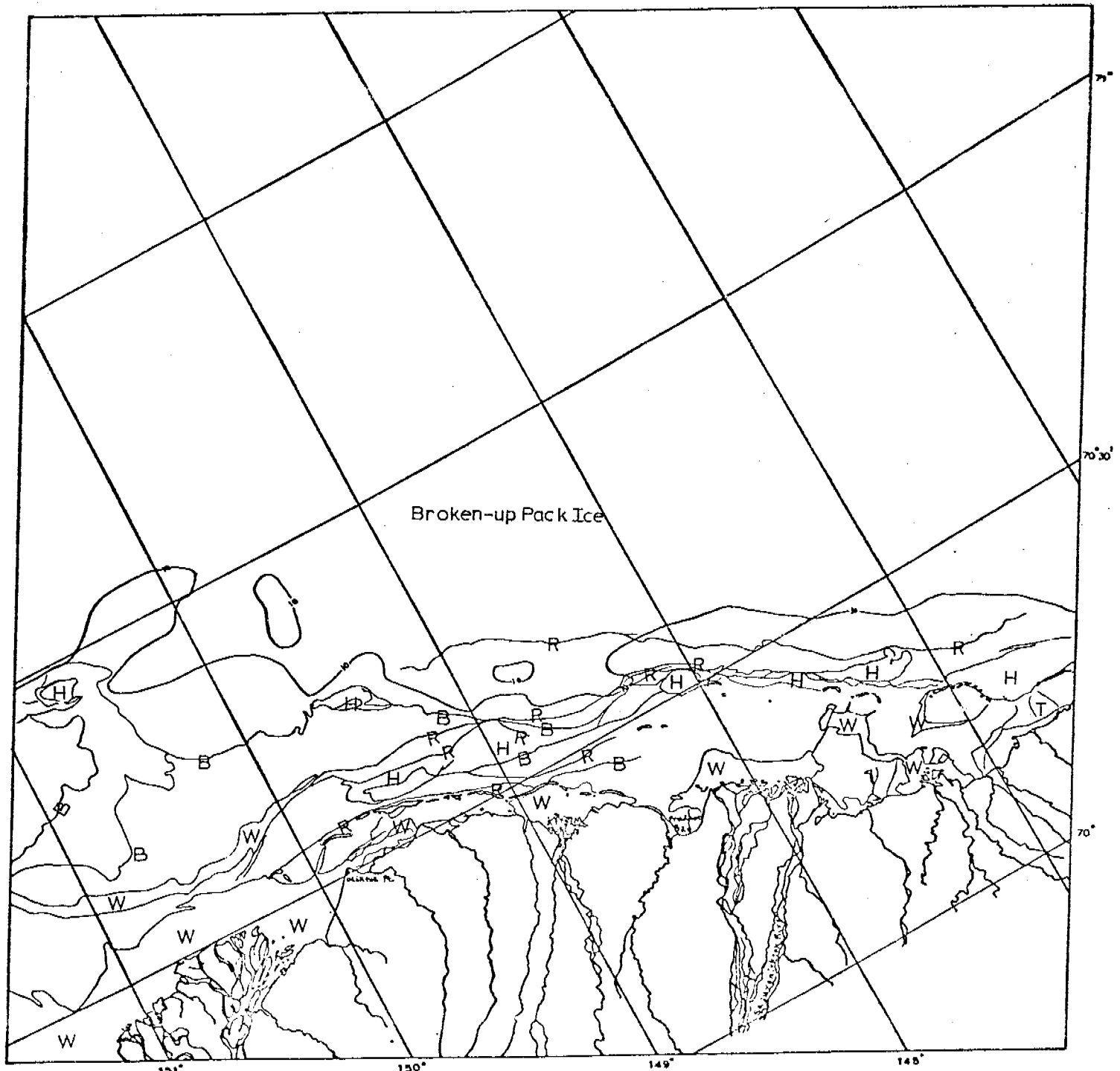
461

Scene E-1721-21143

This scene shows early summer (14 July) 1974 ice conditions for the Beaufort Sea coast between the mouth of the Colville River and Flaxman Island. It is not possible to distinguish everywhere between free-floating pack ice and ice grounded and stationary with respect to the shore. Generally speaking, east of  $149^{\circ}30'$  hummock fields or ridges can be identified which appear to serve as this boundary while west of this line only one hummock field can be seen which is apparently gounded. Between this hummock field and the one at  $149^{\circ}30'$  the boundary drawn is the dividing line between nearly melted ice and ice with a drained surface. No ridges can be identified along this boundary and the ice appears to consist of many individual pans of various sizes.

East of this line the boundary is characterized by many extensive ridge systems. A very large system of massive ridges can be seen just seaward of the hummock field mapped at  $148^{\circ}W$ ,  $70^{\circ}30'N$ , adjacent to Cross Island. Shoreward of these ridge systems there are a few other ridges, some hummock fields, and a considerable quantity of well-melted ice.

Several ice features in this scene were photographed during an aerial reconnaissance of the Beaufort Sea just a few days later than this image date. Comparison of these photographs with corresponding portions of the Landsat image will constitute a special report.



KILOMETERS  
0 10 20 30 40 50  
SCALE APPROX 1:1,000,000

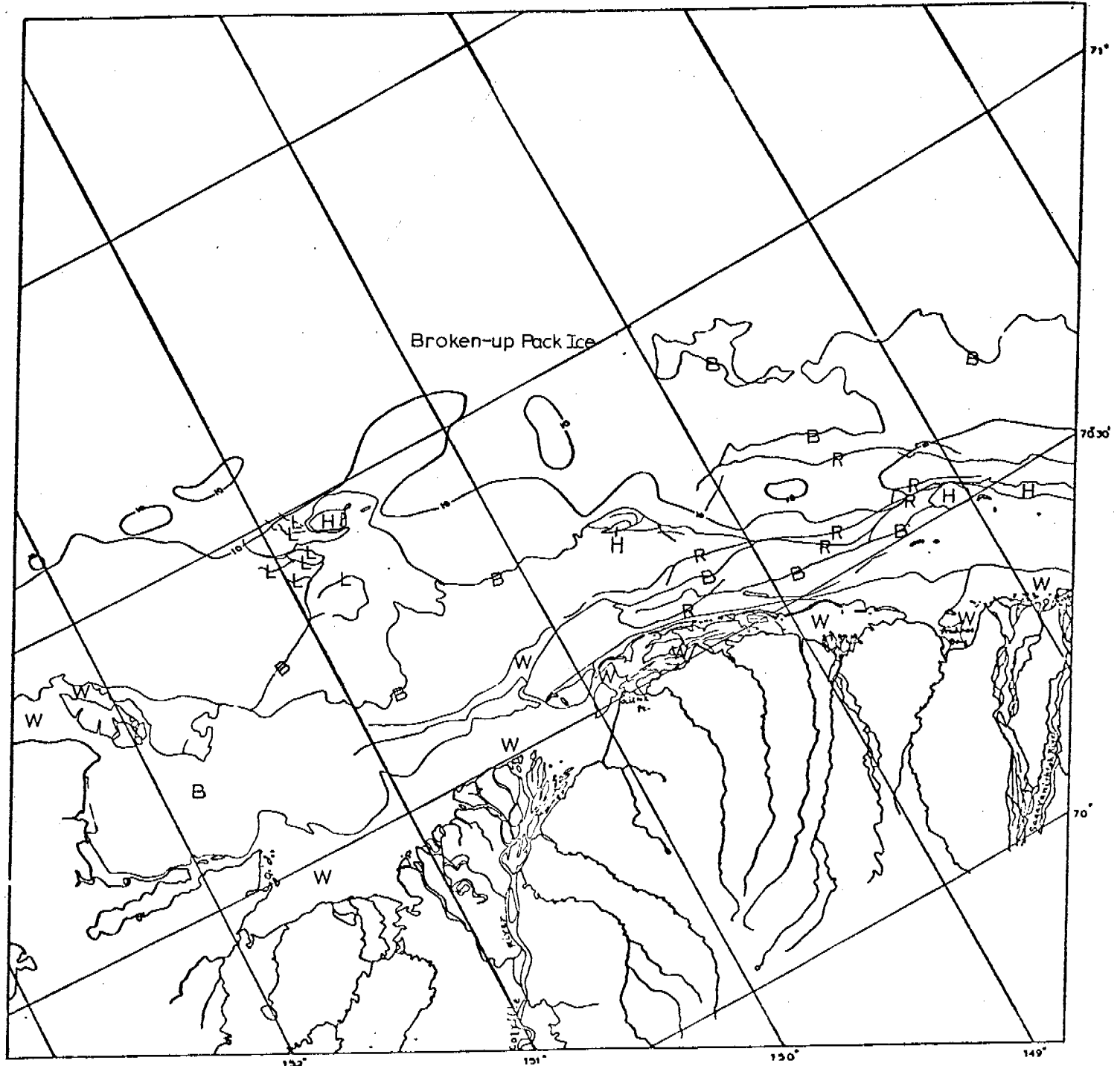
### BEAUFORT SEA

E-1721-21143-7  
14 JULY 1974

Scene E-1722-21202

This Landsat scene shows early summer (15 July) 1974 ice conditions for the Beaufort Sea coast between Cape Halkett and the mouth of the Sagavanirktoq River. It is not possible to distinguish everywhere between free-floating pack ice and ice grounded and therefore stationary. Generally, east of  $149^{\circ}30'$  hummock fields or ridges can be identified which appear to represent this boundary while west of this line only the hummock field located at  $150^{\circ}45'W$ ,  $70^{\circ}55'N$  appears to be grounded (note the leads formed in the pack ice in motion past this feature). Between these two hummock fields and on to the western side of the image, no ridge systems or hummock fields are mapped. However, on Scene E-1703-22151 this sort of feature was mapped in this area. Apparently these features were only poorly anchored (if at all) and have now been broken up and displaced.

Refer to Scene E-1721-21143 for a discussion of ice features on the eastern side of this image.



KILOMETERS

0 10 20 30 40 50

SCALE APPROX 1:1,000,000

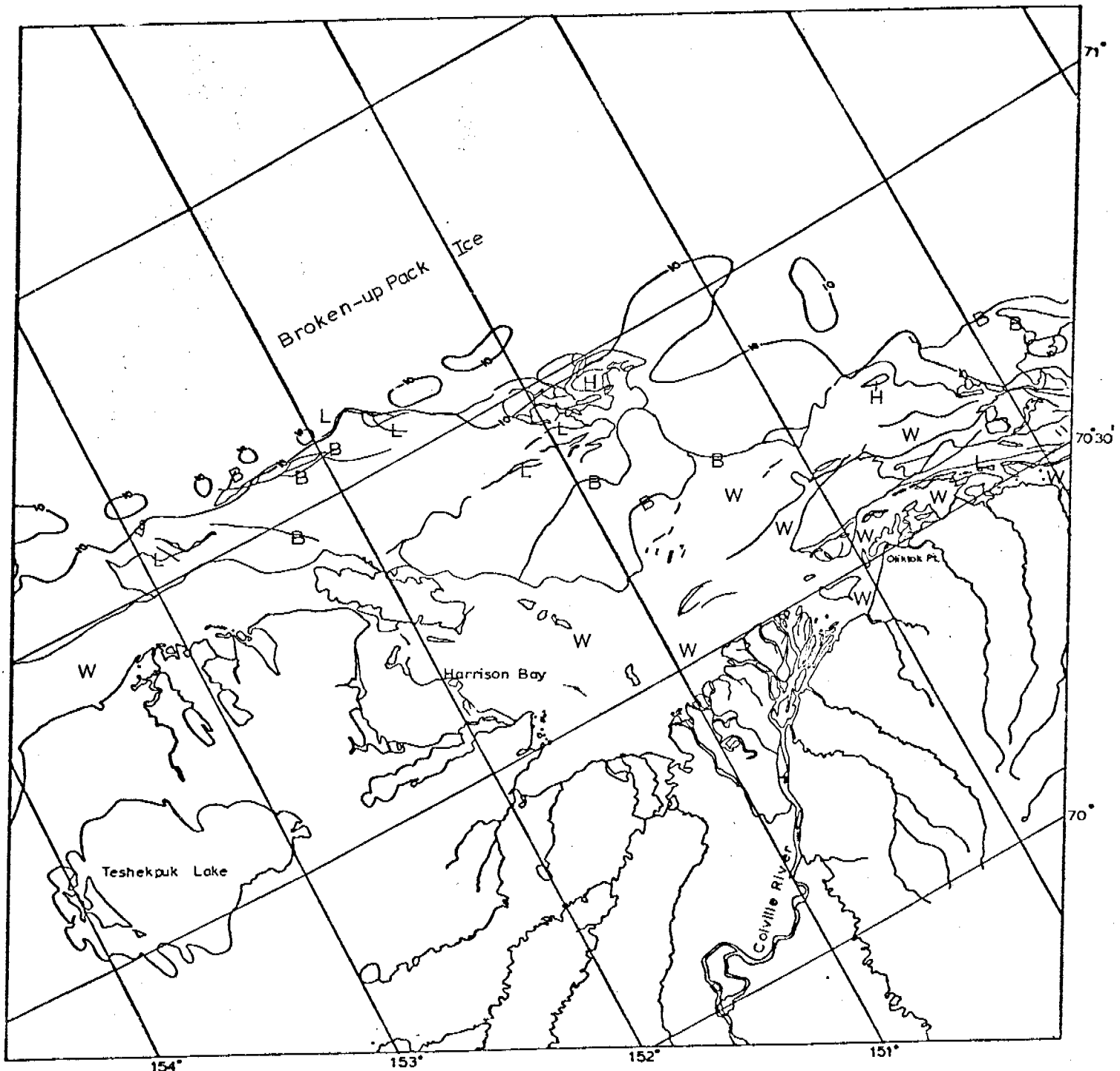
### BEAUFORT SEA

E-1722-21202-7  
15 JULY 1974

Scene E-1723-21260

This Landsat image shows early summer (16 July) 1974 conditions between Smith Bay in the far west and the barrier islands east of Oliktok Point. Most of this scene has been described in the texts for scenes E-1722-21202 and E-1721-21143. This scene shows an area west of Cape Halkett not seen on the previous days' image but there is little change in the description for this new area from the description for the adjacent area to the east: it is difficult to identify features indicating grounded ice, except for one group of linear features along the 10-fathom line at 152°W.

One striking feature of this image is the degree of melting which has taken place since the previous days' image.



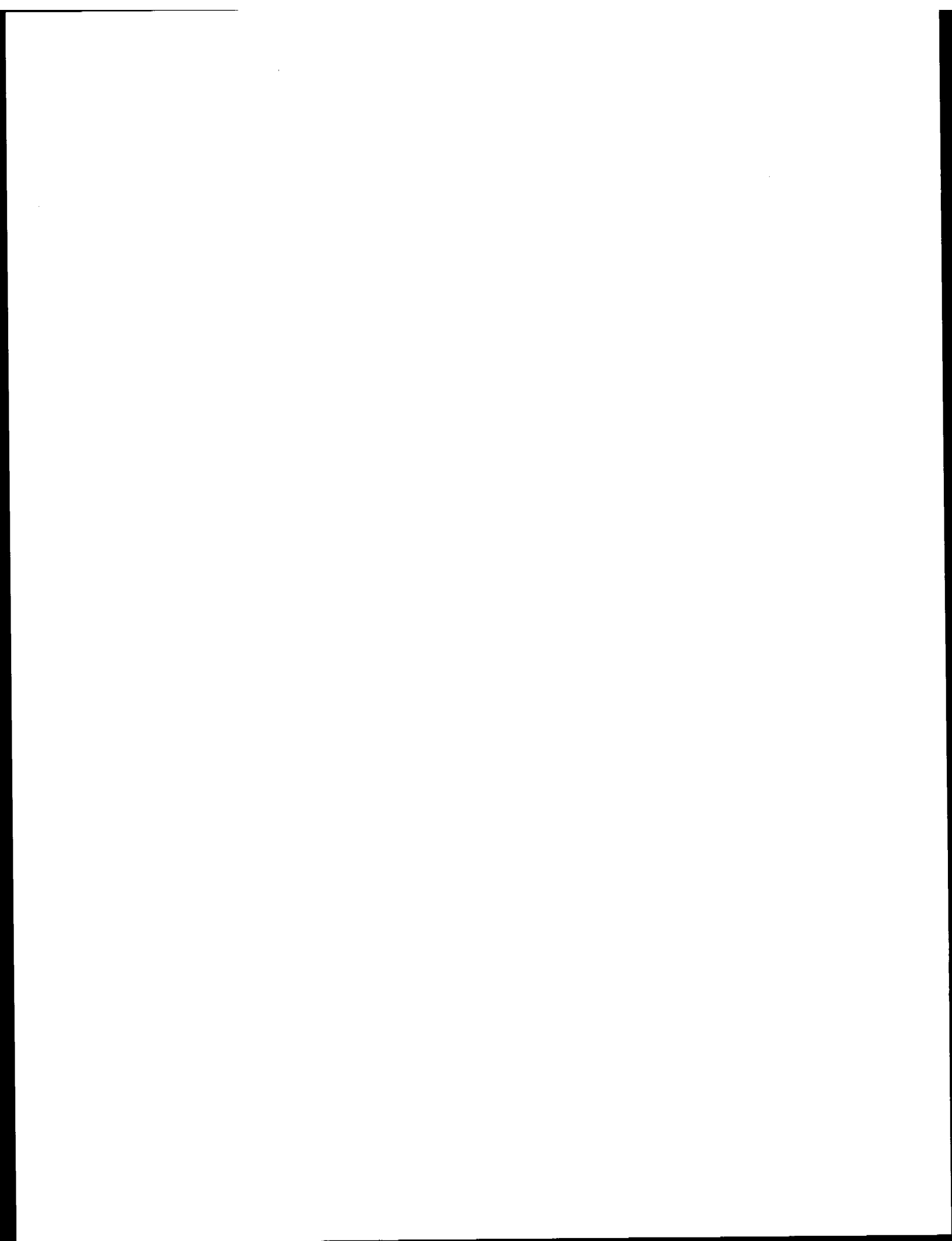
E-1723-21260-7  
16 JULY 1974

KILOMETERS

0 10 20 30 40 50

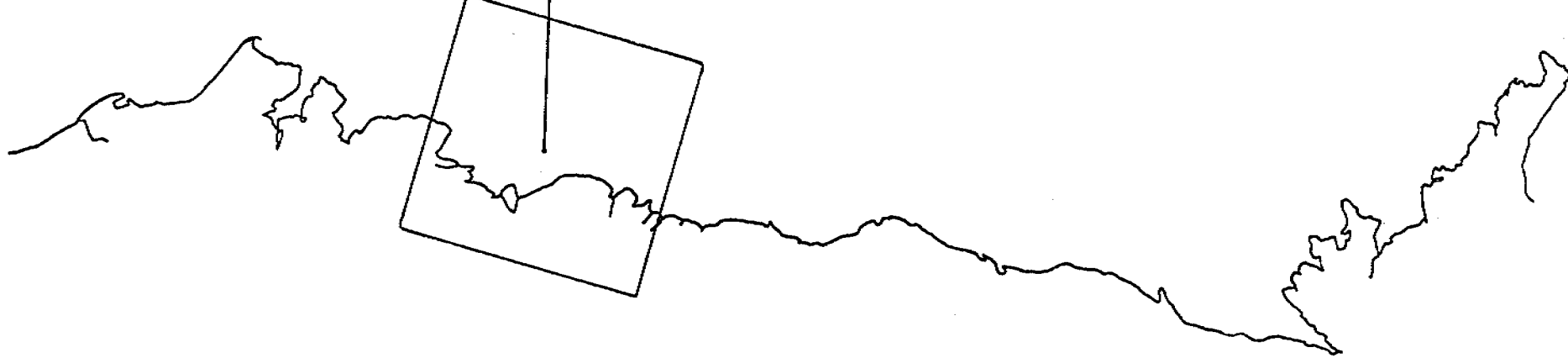
SCALE APPROX 1:1,000,000

BEAUFORT SEA



69

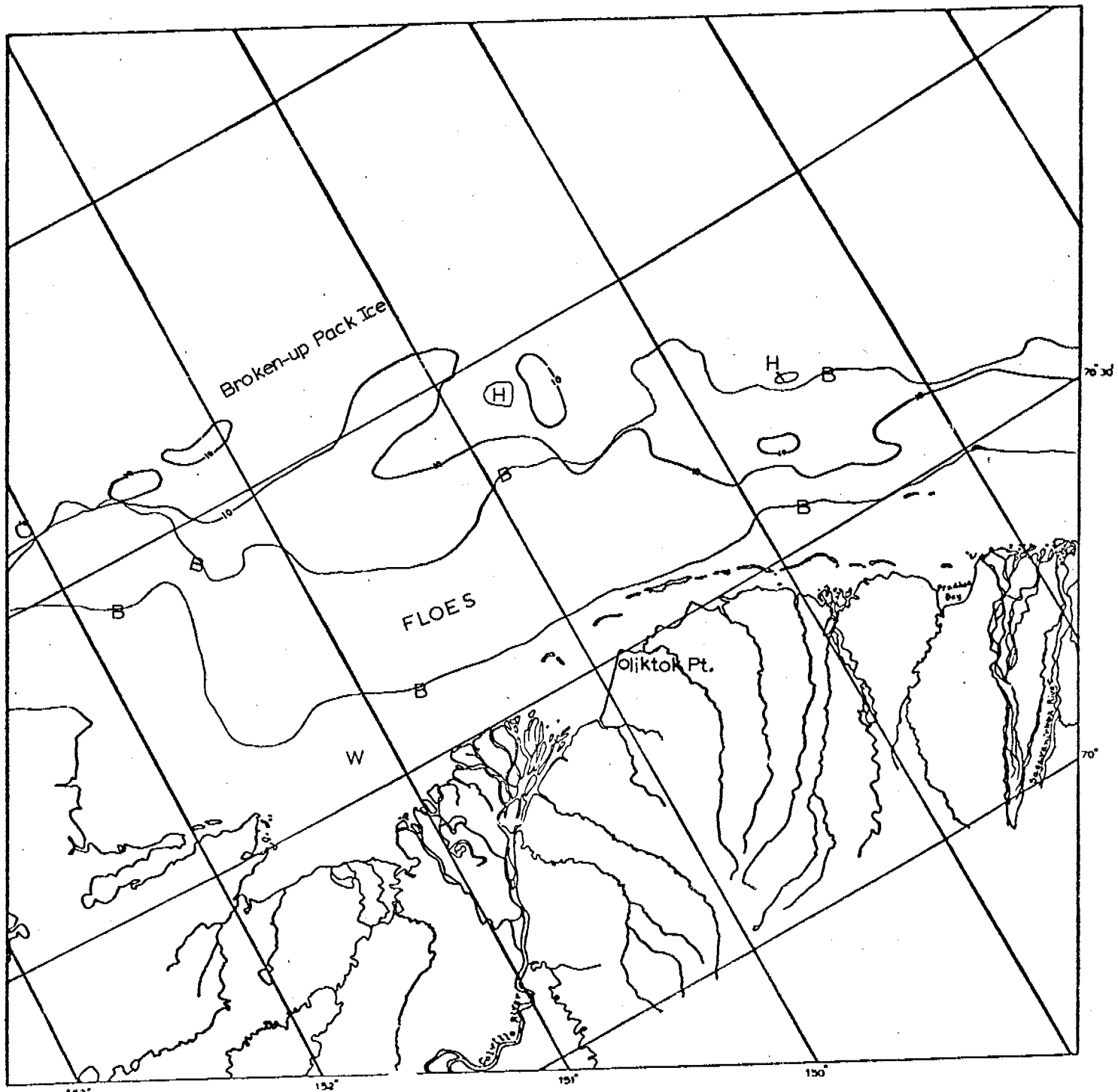
1740 - 21194



BEAUFORT SEA  
19 JULY - 5 AUGUST 1974  
Images: 1726 - 1743

Scene E-1740-21194

This scene shows the Beaufort coast from Cape Halkett to the mouth of the Sagavanirktoq River for mid-summer (2 August) 1974. Three major zones have been delineated: "broken-up pack ice" consisting of closely packed individual pans, an area of "occasional floes" consisting of individual floes surrounded by water, and a region of "open water". At least two hummock fields remain grounded in outer Harrison Bay.



E-1740-21194-7

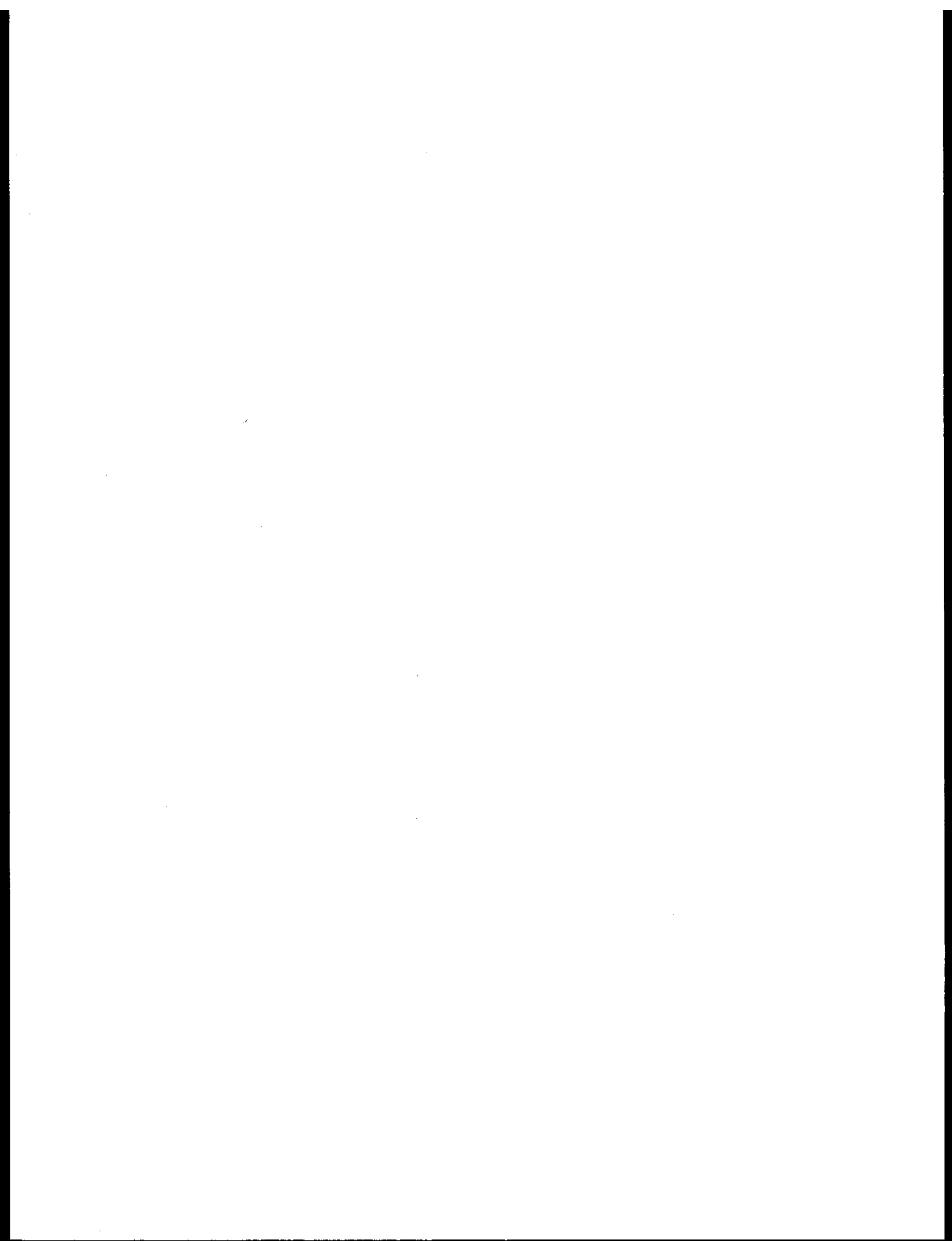
2 AUGUST 1974

KILOMETERS

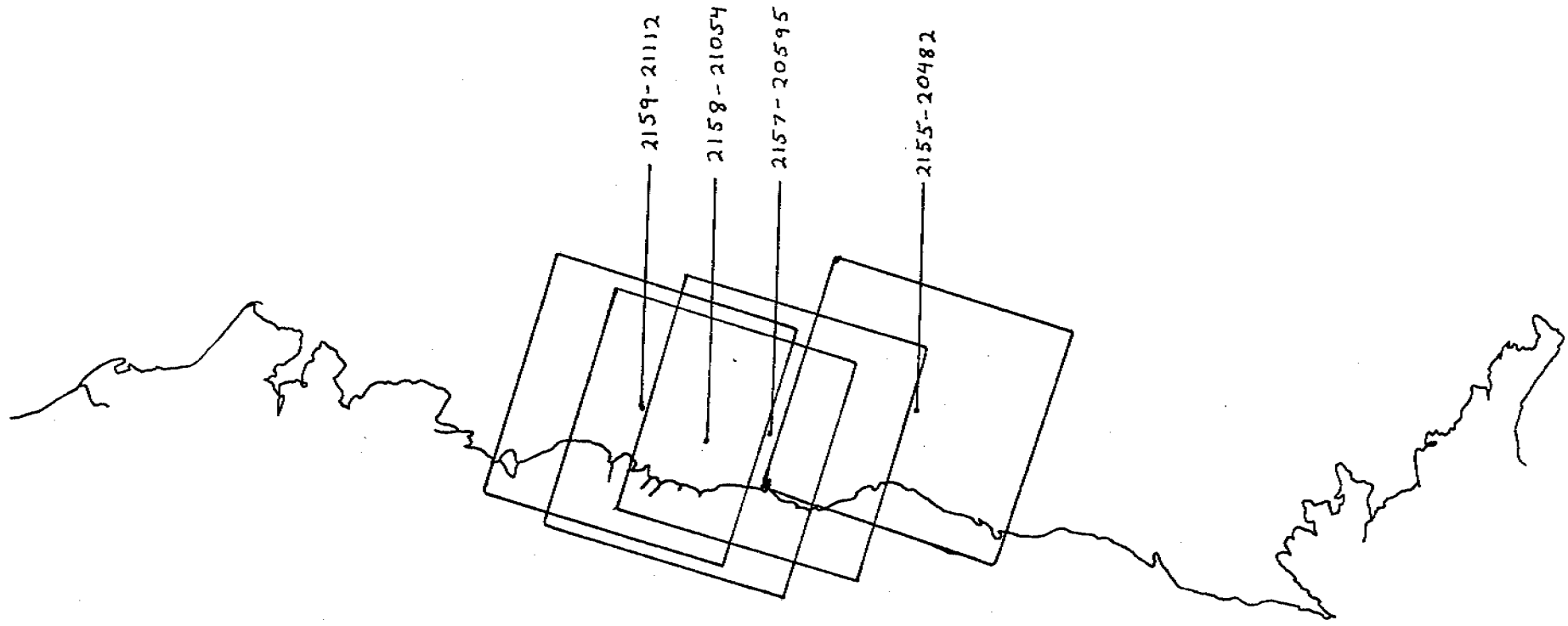
0 10 20 30 40 50

SCALE APPROX 1:1,000,000

## BEAUFORT SEA



473

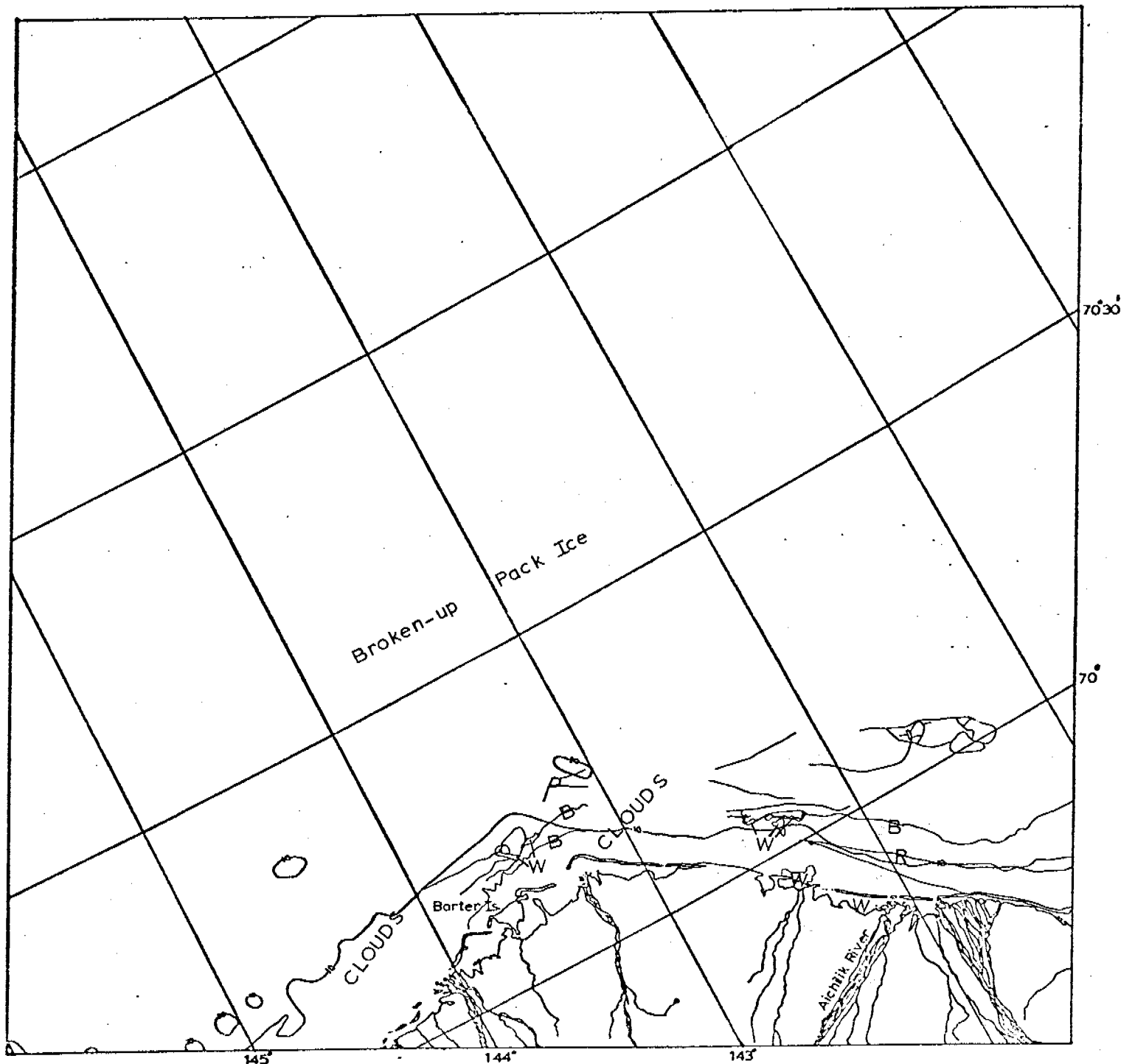


BEAUFORT SEA  
18 JUNE - 5 JULY 1975  
Images: 2147-2164

Scene E-2155-20482

This Landsat scene shows ice conditions in the Martin Point region of the Beaufort coast for late spring (26 June) 1975. This image contains considerable cloudiness and normally wouldn't be mapped except that in this instance the small amount of data to be gained was considered quite valuable.

To the west of Martin Point is a lead well within the 10-fathom contour. This lead can also be seen in scene E-2157-20595 (next in this sequence). The significance of this lead is discussed in the annotation for that scene. The area of interest here is to the east of Martin Point where, although there is no evidence of massive ridging, the boundary of stationary ice is well beyond the 10-fathom contour.



E-2155-20482-7  
26 JUNE 1975

KILOMETERS

0 10 20 30 40 50

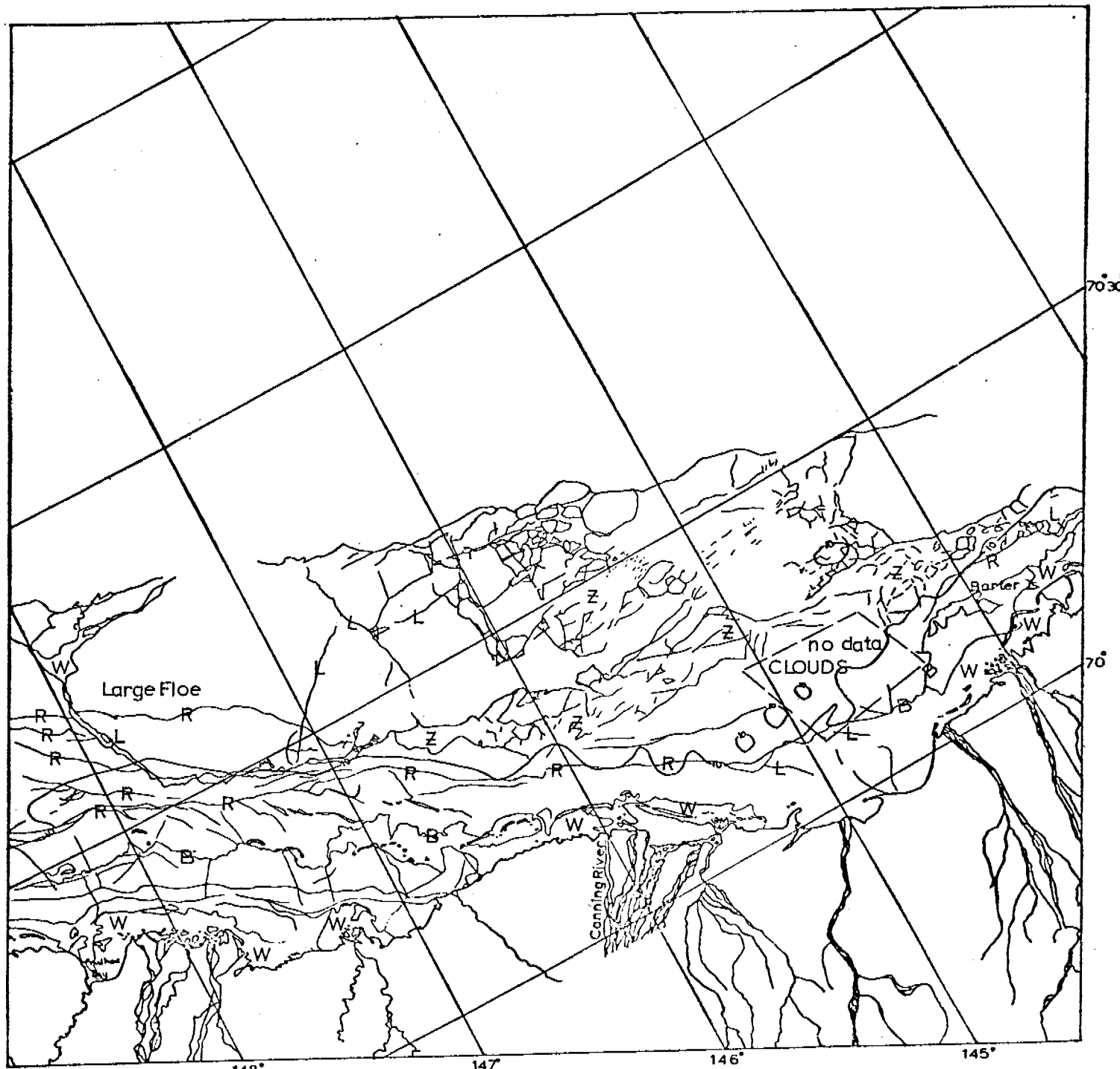
SCALE APPROX 1:1,000,000

BEAUFORT SEA

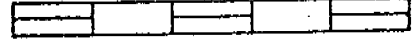
Scene E-2157-20595

This scene shows the portion of Beaufort coast between Barter Island and Prudhoe Bay for late spring (28 June) 1975. The west side of this image is overlaped by imagery obtained on succeeding days. Details of this area are discussed for that imagery. The area of interest provided by this image is from off the mouth of the Sagavanirktox to Barter Island. Over much of this distance there are ridges which appear to be grounded roughly following the 10-fathom contour. One small area of cloudiness obscures a very interesting portion of this coastal region: the somewhat sheltered Camden Bay. There is some evidence that the coastal ridge systems are not well-constructed in this area and at the time of this image are cut by fresh leads.

Note the large lead just off Martin Point at the extreme eastern side of this image. This lead is well within the 10-fathom contour. It would appear that the ice here is not nearly as stable as Harrison Bay ice which will be seen on later images in this Landsat cycle.



E-2157-20595-7  
28 JUNE 1975

KILOMETERS  
0 10 20 30 40 50  
  
SCALE APPROX 1:1,000,000

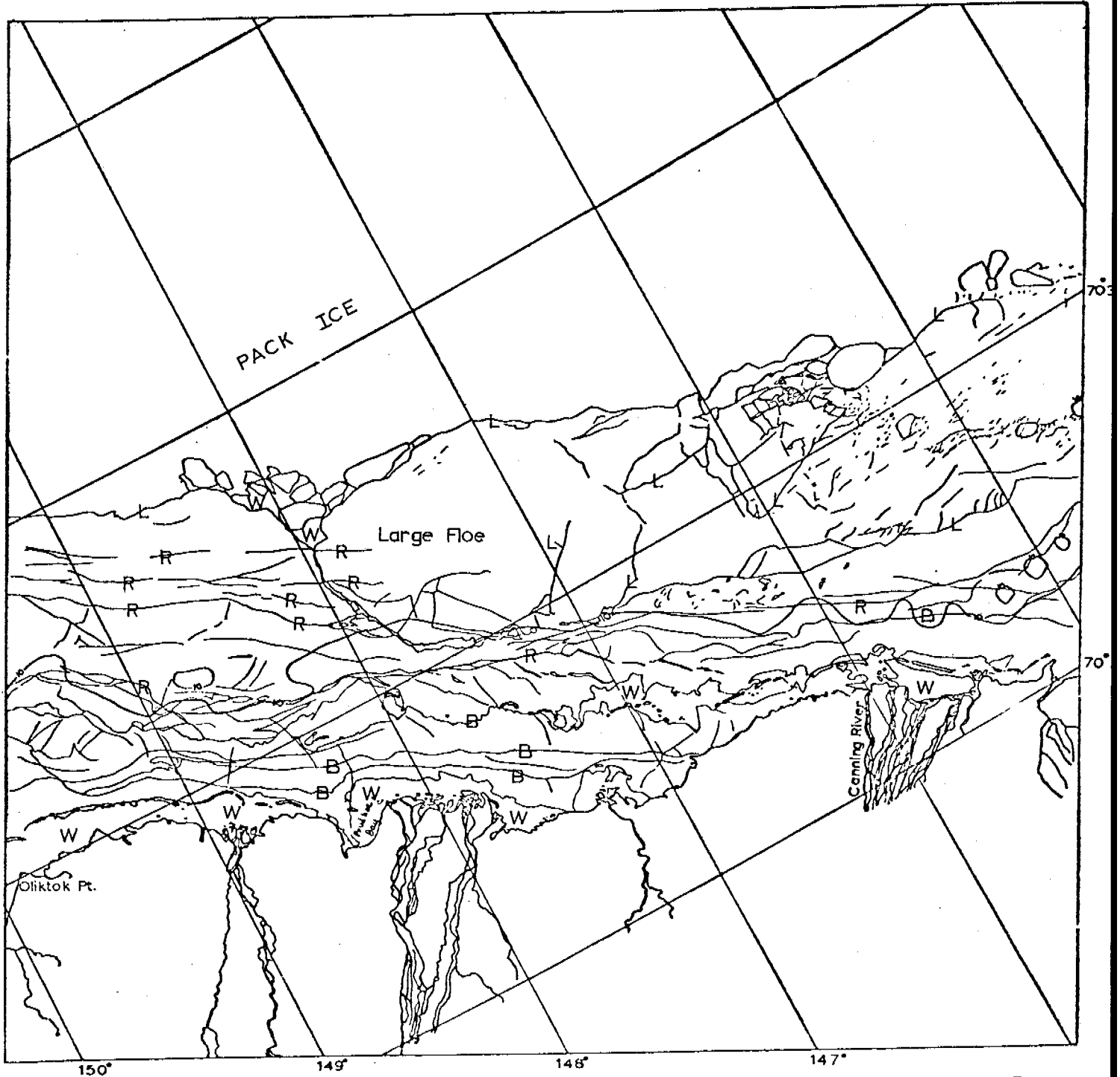
## BEAUFORT SEA

Scene E-2158-21 054

This scene shows the portion of Beaufort coast between Oliktok Point and the mouth of the Canning River for late spring (29 June) 1975.

An unusual amount of ice remains contiguous for this time of year. Perhaps part of the reason is the many well-developed ridge systems running parallel to the coast. Very recently a large piece of this contiguous ice sheet has broken off and moved slightly eastward, the motion in that direction being permitted by the shattered pack ice to the east.

From Prudhoe Bay eastward, the boundary of stationary ice appears to coincide with the 10-fathom contour. To the west of Prudhoe Bay contiguous ice extends considerably seaward of the line.



E-2158-21054-7  
29 JUNE 1975

## KILOMETERS

SCALE APPROX 1:1,000,000

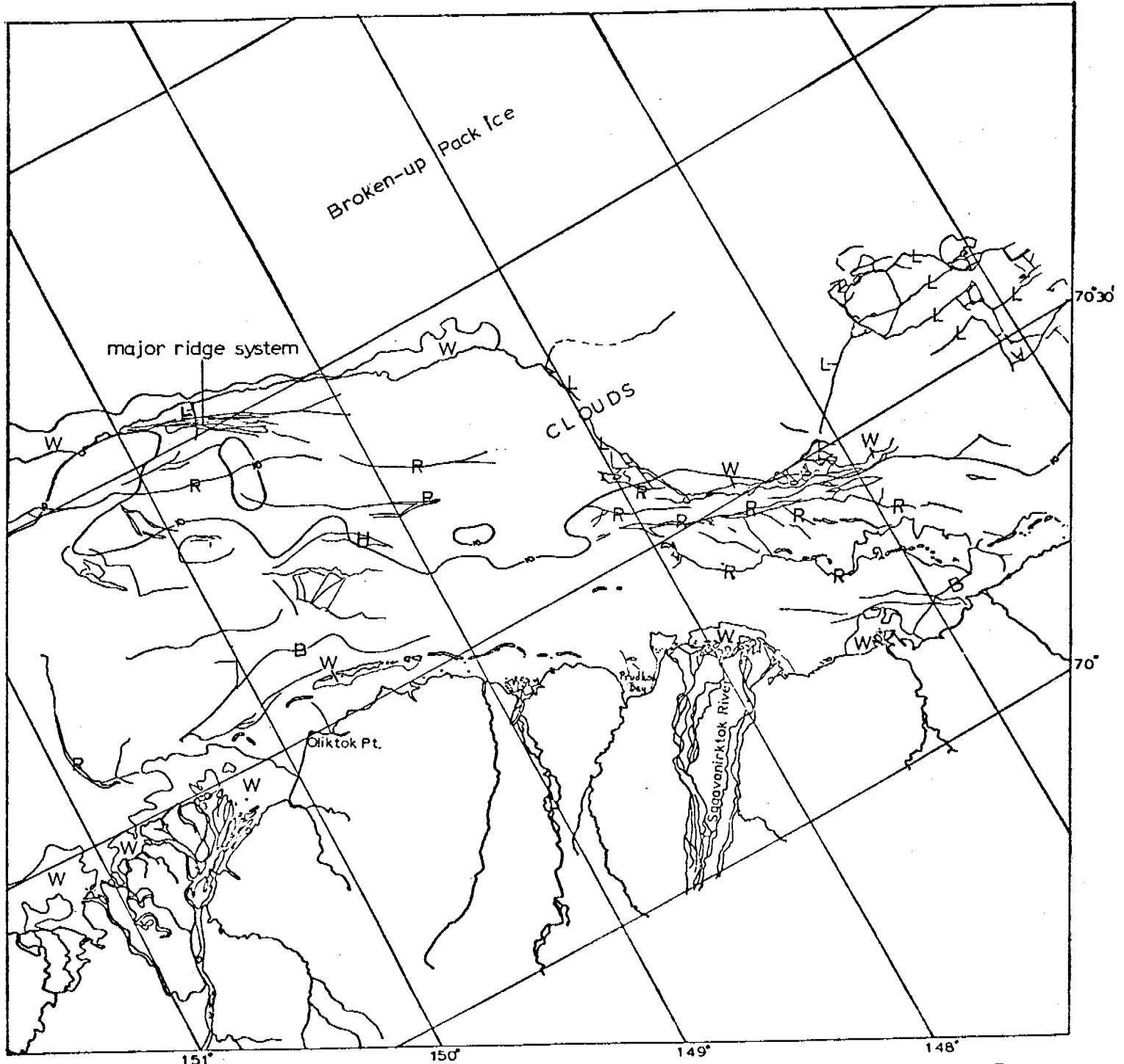
## BEAUFORT SEA

Scene E-2159-21112

This scene shows the portion of Beaufort coast from the mouth of the Colville River eastward to Maguire Island for late spring (30 June) 1975. There are several interesting features mapped from this image: the chief of which is the "major ridge system" indicated on the western side of the map. This ridge system will be seen to survive the 1975 melt season and remain in place through the winter of 1975-1976. It was not entirely stable however, and as shown here, was cut by a major lead.

Clouds obscure details in the central portion of the image making features there difficult to map. However, the boundary between pack ice and stationary ice can be mapped. It is interesting to note that this boundary is located at this time well beyond the 10-fathom contour to the west of Cross Island.

There are several areas of open water just offshore from the mouths of major rivers.



E-2159-21112-7

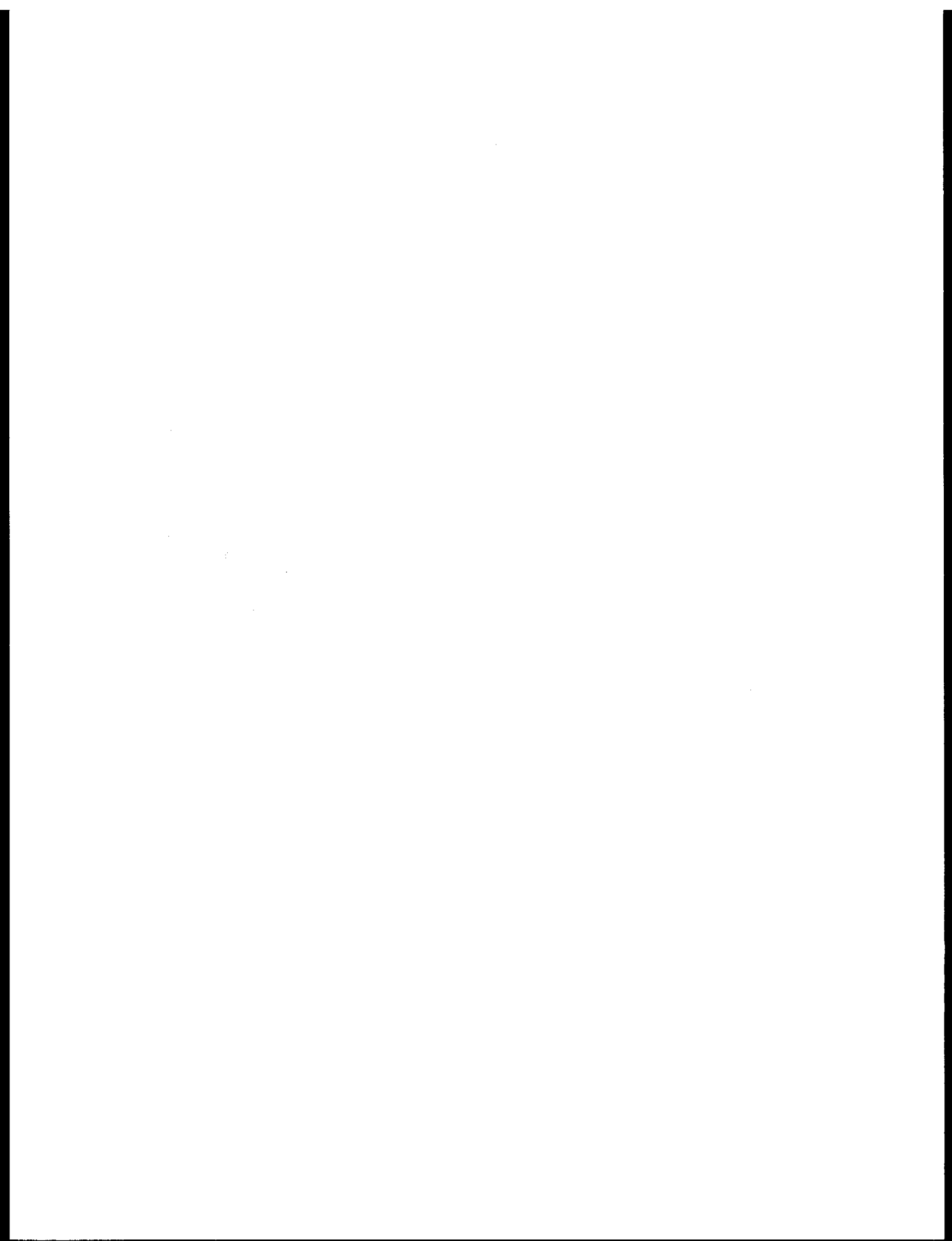
30 JUNE 1975

KILOMETERS

0 10 20 30 40 50

SCALE APPROX 1:1,000,000

BEAUFORT SEA



ICE HAZARDS TO OFFSHORE OIL OPERATIONS  
IN ARCTIC ALASKAN WATERS\*

W. J. Stringer  
W. M. Sackinger

Geophysical Institute  
University of Alaska  
Fairbanks, Alaska 99701

I. Introduction

Sea ice presents a hazard to offshore drilling structures and associated support activities which can exceed the normal hazards of winds and waves by a considerable margin (Hudson, 1973). Fortunately, along much of the Arctic coastline the ice is grounded during the last half of the winter, exerting only nominal internal stresses (Nelson et al., 1976). However, under breakup circumstances, this nominally shorefast ice can acquire velocities of 2 m/sec or more (Sackinger et al., 1974), and under such circumstances is likely to produce stresses which may be as great as those experienced in the moving ice pack.

Locations with more extreme ice hazards are found beyond the boundary of the shorefast ice, on the prevailing sides of coasts and islands, and in relatively deep ( $> 20$  m) unsheltered water where the ice moves virtually continuously. The proposed Outer Continental Shelf lease sale areas in the Bering, Chukchi and part of the Beaufort Sea are largely in this latter category. It is obviously important to document the regions of relatively safe, shorefast ice, and a study of LANDSAT (Land Imaging Satellite) imagery is currently in progress to do so. The dynamics of the shorefast breakup events are also being studied using time-lapse photography of the screen of the University of Alaska sea ice radar at Barrow, Alaska.

\*Presented at 31st Annual Petroleum Mechanical Engineering Conference, Mexico City, September 21, 1976.

In this paper, we describe the annual cycle of Beaufort Sea near shore ice events and discuss the possible hazards related to these various ice conditions.

## II. Beaufort Sea Near Shore Ice Conditions

Usually the Beaufort Sea coast is ice-free during August and September. Ice formation begins in October and generally does not form a dependably stable surface until late December or early January. The stable surface, when formed, is usually referred to as "shorefast ice". Although several slightly differing definitions of "shorefast ice" are in common usage, the term generally refers to ice stationary with respect to the shore and bounded by grounded ice features [shear and pressure ridges, floebergs, stamukhi, etc., (see Kovacs and Mellor, 1974)].

The processes at work during the formation of shorefast ice are not well-documented, largely because they have not been at the focus of attention. These processes occur during the dark winter months, when satellites with high resolution visible spectrum sensors are not operative.

However, it is known that the formation of the fast ice usually takes place in stages, often punctuated with episodes of wind-driven ice being piled and compacted into successive bands parallel to the coast. Many of these features are grounded and serve to anchor the surrounding ice in place. Along the Alaskan Beaufort coast this anchoring effect seems to function to a water depth of approximately 20 m. Hence, the 20 m bathymetric contour is usually taken to be the nominal seaward limit of Beaufort Sea shorefast ice.

Dynamic ice events can and do occur within the "shorefast" zone before the ice becomes sufficiently anchored to be reliably stable. Although these events are presently unobservable by means of high resolution imaging satellites, other techniques exist, which although limited in comprehensive geographic coverage, give detailed information. One of these techniques is imaging radar.

Radar has proven to be a valuable tool for the study of the dynamics of shorefast ice during formation and breakup. The University of Alaska sea ice radar facility was established at Point Barrow in March 1973, supported jointly by the Alaska Oil and Gas Association and the Alaska Sea Grant Program. Using time-lapse photography of a conventional cathode ray tube display, it has recorded the motion of sea ice for over three years.

A particularly severe and unusual breakup event has been analyzed by Shapiro (1975). Until 26 December 1973, the ice was landfast out to beyond the 20 meter water depth contour. An offshore wind in the range 13-24 km/hr prevailed for 15 hours when, at 0545 U.T. on 26 December, the ice broke free and drifted away from the coast at 0.7 km/hr. The windspeed reached 30 km/hr at that time. The time-lapse film shows subsequent ice motion parallel to the shoreline at 3.7 km/hr.

Subsequently, on 31 December the wind velocity increased to 90 km/hr (with gusts to approximately 150 km/hr) parallel to the shoreline. The ice drift velocity increased to 8.3 km/hr, parallel to the shore, and impact of this drifting ice was sufficient to drive out other ice floes which had grounded on shoals earlier. This sequence represents the most severe condition of drifting ice in the shorefast zone which has yet been analyzed.

In order to illustrate the optically observable portion of the annual cycle of near shore ice dynamics, a sequence of LANDSAT scenes showing the vicinity of Prudhoe Bay, Alaska, 1974 will be used. Near shore ice forms during the dark months when there is insufficient light for LANDSAT imagery to be obtained. Typically, the earliest LANDSAT scenes of the Prudhoe Bay area are available in late February or early March. Figure 1, obtained on March 10, shows the already formed "shore-fast" ice and evidence of shearing motions in the pack ice beyond. Because no imagery is available from the period of fast ice formation, knowledge of that period must be gleaned from this earliest scene, and as it will turn out, late season imagery.

Close examination of this LANDSAT scene shows several discontinuous bands of similarly textured or shaded ice more or less parallel to the coast. These bands represent various stages in the "freeze-up" of the near shore ice. The stages represented include freezing in place, compaction, piling and rafting of ice frozen in place, and piling and rafting of newly-formed or multi-year pack ice driven into the near shore area. The boundaries of each of these bands were each once the seaward edge of the ice, fixed with respect to the shore, and could have been the site of formation of shear or pressure ridges for some period of time.

Each boundary is located in successively deeper water and hence could be subject to more severe ridging conditions. Just seaward of the most pronounced bands a series of large, massive shear ridges can be identified on the imagery. These too, formed during "freeze-up".

However, as will be seen, these ridges are well shoreward of the location of shearing conditions by the date of this image.

The most visible indications of shear are the newly-formed and refrozen lead systems running somewhat parallel to the coast. Examining first the older, now refrozen, lead it can be seen that its formation involved displacement of the pack ice to the east a distance of several kilometers. Further, the pattern exhibited by the other refrozen leads is that of stress relief, showing that the release was not limited to the slippage along this lead. The appearance of the outermost of the refrozen leads indicates that after their formation, there may have been some westward slippage of the polar ice beyond this lead, thereby opening it up.

Now, on March 10, after this lead system has frozen over, a new lead system is forming. Examination of this new lead system indicates westward displacement along two lines: The outermost new lead coincides with the outermost lead of the former lead system and the inner lead runs for some distance within the boundaries of the refrozen leads, but then strikes off slightly seaward of the former lead.

This image then illustrates the concepts of "shorefast" ice and the active "shear zone".

The next LANDSAT image available for this area was obtained on March 28 (Figure 2) during the succeeding LANDSAT cycle. Where formerly the ice exhibited a displacement gradient with westward displacements increasing with distance from shore, it appears that sometime during this 18 day interval, the ice seaward of the most shoreward of the old lead system has moved several kilometers westward as a block, largely

obliterating the old refrozen lead. Presumably during this time pressure and shear ridges of considerable magnitude were created. Examination of imagery from the summer melt season will show that the ridges formed during this event persisted into that period.

The next LANDSAT data would have been obtained in mid-April, but this image is not available - probably due to excessive cloud cover. The May 3 image (Figure 3), obtained on the second LANDSAT cycle after the late March scene, shows that little, if any, change has taken place other than perhaps further compression of the refrozen leads. Hence, during this period of over one month, Beaufort Sea ice off Prudhoe Bay was not subject to conspicuous shear or breakage for at least 50 miles offshore. Apparently this is a somewhat common occurrence, having been observed the previous year also (see Stringer, 1974).

On the west side of this image is an oblong ice feature which, while extant on the earlier images, can be examined for detail for the first time this season on the LANDSAT image under discussion. This grounded hummock field appears to be a recurring feature and has been reported earlier (Stringer, 1974), based on 1973 observations. An aerial reconnaissance of this feature was performed in July 1974, which confirmed the nature of its structure. There is reason to believe that this feature and the large grounded feature west of Barrow (Stringer and Barrett, 1975) are the result of similar processes and represent essentially the same general type of ice feature. Note that lead systems are strongly deflected around this feature, indicating the major role played by its presence. On subsequent scenes it will be seen that the boundary of shorefast ice was seaward of this feature.

The next available LANDSAT image was obtained on May 21 (Figure 4). Here, the ice exhibits a marked change over the previous image. Whereas before this date the polar ice off Prudhoe Bay formed mainly a sheet continuous with the shorefast ice, now the polar ice is breaking up. This general behavior has been observed on imagery from other years at this date. However, it may be unusual for the pack ice to be broken up with such large voids between individual pans. Obviously, at this time the "shear zone" begins at the boundary of the ice continuous with the shore and the open water. On the west side of the image, the shear boundary nearly coincides with the boundary defined by much earlier ice activity but it is still actually somewhat seaward of this location. The grounded hummock field mentioned earlier is located at this point and it is worthwhile to note that this feature remained within the shear boundary. Our contention is that this feature was a factor in determining the shear boundary.

The shear boundary runs nearly eastward across the image, increasing its distance from shore and the edge of the shorefast ice toward the east. It is not uncommon for the shear boundary to coincide with the edge of shorefast ice at this time, however (see Stringer, 1974).

The next LANDSAT imagery of Beaufort Sea ice off Prudhoe Bay is available for June 25 and 26 (Figures 5 and 6). By this time, the Beaufort Sea pack ice is well broken up and moving. Examination of the LANDSAT images for these dates shows that there is a definite boundary between moving and non-moving ice. Further, this boundary coincides with the shear and pressure ridges observed under construction in late March. The late June images are especially useful for examination of

the make-up of the ice within the boundary mentioned. Many authors consider this ice "shorefast ice" but this definition is not held universally. Melting conditions have removed most of the snow cover from the ice, showing for the first time the detailed structure of the ice which was obscured on previous imagery. Here, the successive bands of ice within the shorefast zone can be examined for clues about their origin and alterations. It can be seen that some bands appear to consist of uniform sheets of ice which probably formed in situ, while others consist of compacted blocks of ice which were formed elsewhere and driven into their present location. Hence, the "freeze-up" of the shorefast zone was a dynamic event bringing highly variable ice conditions. We have seen that radar observations of shorefast ice formation at Barrow generally corroborate this behavior.

By July 14, when the next LANDSAT image is available (Figure 7), considerable deterioration of the shorefast ice has taken place. Near shore - particularly near river mouths - it has melted completely, while seaward particular pans and areas of pans have melted. Hummock field, shear and pressure ridges become more distinct due to their persistence.

The last LANDSAT image for the Prudhoe Bay area in this year was obtained on September 6 (Figure 8). It shows the near shore areas free of ice and the polar ice pack far beyond. Between the coast and the pack ice are several groups of floes which appear to be stranded at locations far offshore. Evidence supporting the contention that these groups of floes are stranded can be found in that other floes are passing around them toward the west exhibiting typical slip-stream patterns. This is not an uncommon occurrence (Reimnitz, 1976) and results when a

few pieces of ice of deep draft become grounded (or remain from the previous ice season). Currents and winds cause other ice floes to pile up against them. Brooks (1974) studied one occurrence of this phenomena and remarked on the relatively small number of grounded obstructions required to produce this effect. Presumably, ice of this nature can persist into the next year's ice season. However, this is not always the case, as demonstrated by the October 4, 1972 image.

The October 1972 image (Figure 9), although not related to the sequence described above, demonstrated early freeze-up conditions. From this image it can be seen how the near shore ice forms in successive bands. Although young ice may be formed over quite an extensive area, only the most protected ice remains fixed in location. Portions of new ice are broken off and drift under the influence of wind and currents. This mechanism repeats successively during the freeze-up period, accounting for the many bands of differently textured ice in the near shore areas.

### III. Discussion

It can be seen that throughout the year there is a series of ice conditions representing hazards to operations related to offshore petroleum exploration and extraction activities. These will be discussed in terms of each season.

Freeze-up (October-January): During this time there is not a clear distinction between a shorefast zone and pack ice. Hummock fields, shear and pressure ridges form in all near shore areas, providing load-bearing surfaces with large cross-sectional areas. Consequently, large

forces may be impressed on obstructions to ice motion regardless of their location. It would be extremely difficult, for example, to maintain a barge or drill ship in a desired location during this time. Modes of travel to offshore locations would be restricted to airborne methods. Bottom-fast structures may be subjected to rather large lateral forces.

Post Freeze-up (February-April): The most stable ice conditions are found during this time. Once the grounded features which define the shorefast zone are established, that area becomes suitable for surface travel. Further, bottom-fast structures within this area could be protected from large forces even if they did develop in that zone by means of a number of artificial strain-release mechanisms. (For instance, explosives could be used to eliminate physical continuity of the ice.) During this period there is also the greatest likelihood of stability of ice beyond the shorefast ice ... perhaps affording a temporary platform for seismic exploration.

Spring (April-May): Shear becomes active along the edge of the shorefast ice. There is some danger of transmission of forces to points within the shorefast ice and consequent strain release within this zone (Stringer, 1974). Beyond the shorefast ice great lateral forces can be exerted by moving pack ice.

Melt Season (June-July): Shear continues beyond the shorefast ice. Within the shorefast zone ice movement takes place by non-grounded ice. Such occurrences have been observed on the satellite data (Stringer, 1974) and by radar (Sackinger et al., 1974). Severe ice conditions may develop within the shorefast zone resulting from summer storms.

Ice-Free Season (August-September): This period is generally the span of time that the coastal area is ice free. However, this condition is not entirely dependable as was demonstrated by the September 6, 1974 image (Figure 8). During this time the entire coastal area is prone to severe ice conditions resulting from storms. The well-known Beaufort Sea storm surge beach ridges offer testimony that these events do occur.

It is interesting to speculate on the effect of a number of man-made structures placed in the near shore areas. If placed within the present shorefast zone, the effect could be that of increased hummocking in their vicinity and greatly increased stability of the ice sheet within the perimeter defined by the structures. In the extreme case there might be a tendency for the ice within this perimeter to become permanent. If placed beyond the present boundary of shorefast ice, man-made structures could very likely move the edge of shorefast ice out to that location. In either case, in the ice-free season the structures would serve the same purpose as the grounded ice fragments during that period and result in large groups of ice floes forming a barrier to seaward.

#### IV. Implications: Effects of Ice on Offshore Operations

If petroleum exploration is initiated from floating drillships, as is planned for the Canadian Beaufort Sea, drilling can proceed only during the ice-free (less than 10% ice cover) periods. Based upon the limited number of years of satellite and aircraft observation data available, this can range from approximately eight months in the St. George Basin of the Bering Sea to a mean of 28 days in the Prudhoe Bay area of the Beaufort Sea. Anomalous weather conditions can shorten or

segment these ice-free periods, as occurred in the summer of 1975 in the Beaufort Sea. Ice-reinforced drilling and resupply vessels would permit an extension of the drilling time and should be seriously considered. Exploration from gravity structures which could resist ice pressure would result in longer working periods, but platform service and resupply access would be primarily by helicopter, hovercraft, or in the case of shorefast ice, by wheeled vehicles over the ice after mid-winter. The shorefast ice zone is the safest region for winter drilling operations. On the prevailing side of coasts and islands, or indeed beyond the shorefast ice in water deeper than 20 meters, ice pressures are more severe and virtually continuous.

Eventual production would require the development of subsea production equipment which can withstand occasional ice scour. Continuous petroleum production throughout the year from the western coast of Alaska will be likely to require a fleet of ice-reinforced tankers, as well as an ice-resistant deepwater loading terminal offshore. For the annual ice encountered in the Bering Sea, this appears to be within the capabilities of present technology, although the existence of sufficient reserves, together with the economics of the situation, remain to be determined. The relationship between ice motion and meteorological variables would be operationally important, so that accurate ice forecasts could be made.

#### ACKNOWLEDGMENTS

The research reported here was supported in part by NASA Grant NAS5-20959 and OCSEAP 03-5-022-55.

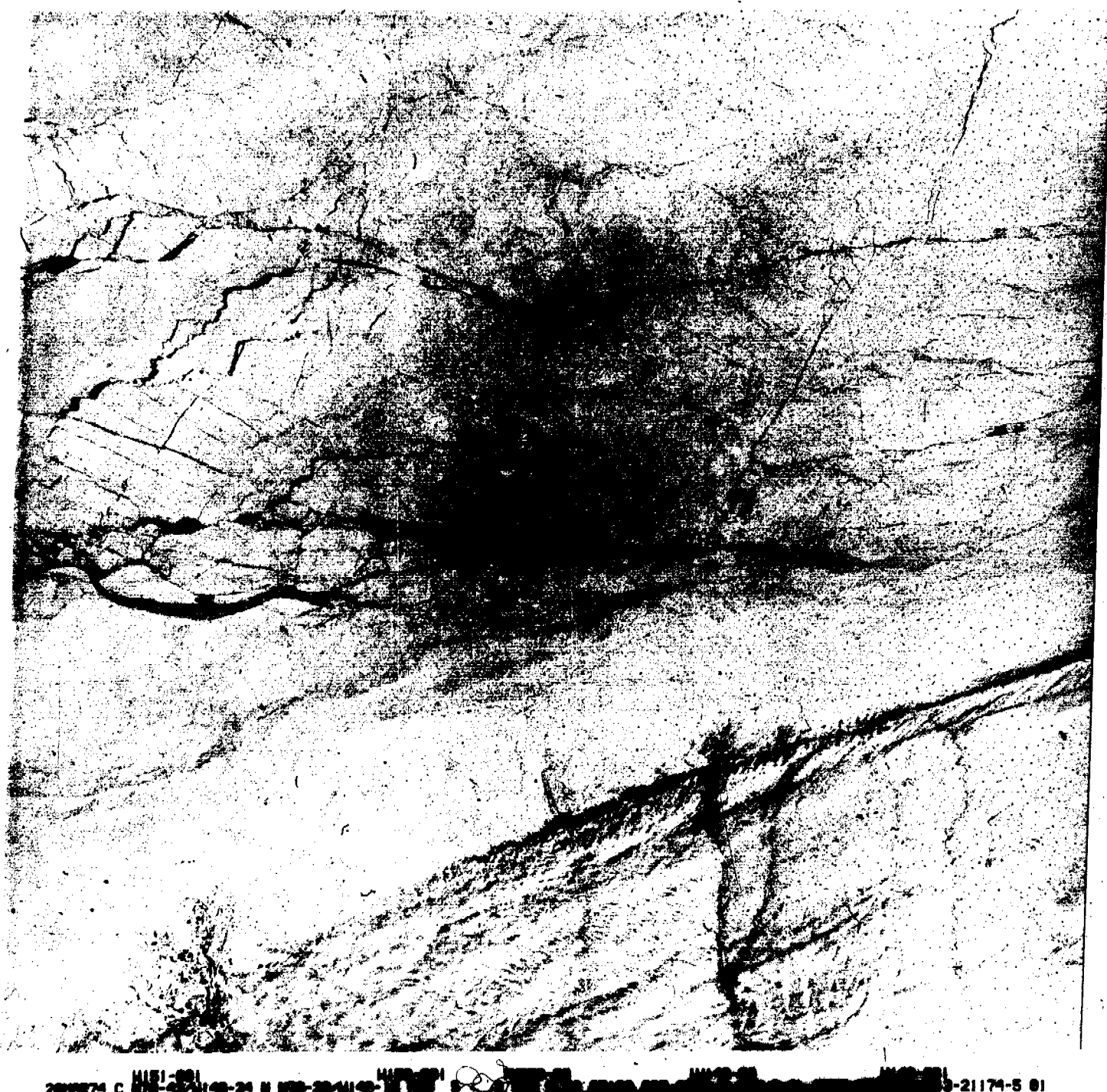
## REFERENCES

- Brooks, L. D., Ice Scour on Northern Continental Shelf of Alaska, Proceedings of the Symposium of Beaufort Sea Coast and Shelf Research, Arctic Institute of North America, 355-366, 1974.
- Hudson, T. A., Arctic Offshore Data Gaps and How to Fill Them, Offshore Technology Conference, Houston, Texas, May 1973.
- Kovacs, A. and M. Mellor, Sea Ice Morphology and Ice as a Geologic Agent in the Southern Beaufort Sea, Proceedings of the Symposium on Beaufort Sea Coast and Shelf Research, Arctic Institute of North America, 113-162, 1974.
- Nelson, R. G. and W. M. Sackinger, Stresses in Sea Ice, 31st Petroleum ASME Conference, Mexico City, September 1976.
- Reimnitz, E., L. Toimil and P. Barnes, Development of the Stanukhi Zone and Its Relationship to Arctic Shelf Processes and Morphology, Beaufort Sea, Alaska (preprint), 1976.
- Sackinger, W. M., J. C. Rogers and R. D. Nelson, Arctic Coastal Sea Ice Dynamics, Offshore Technology Conference, Houston, Texas, May 1974.
- Shapiro, L. H., A Preliminary Study of the Formations of LANDSAT Ice at Barrow, Alaska, Winter 1973-1974, Geophysical Institute Report UAG R-235, Sea Grant Report No. 75-7, June 1975.
- Stringer, W. J., Shorefast Ice in the Vicinity of Harrison Bay, The Northern Engineer, Vol. 5, No. 4, Winter 1973/1974.
- Stringer, W. J. and S. A. Barrett, Ice Motion in the Vicinity of a Grounded Floeberg, Proceedings of the Third Conference on Port and Ocean Engineering under Arctic Conditions, University of Alaska (in press), 1976.
- Stringer, W. J., The Morphology of Beaufort Sea Shorefast Ice, Proceedings of the Symposium on Beaufort Sea Coast and Shelf Research, Arctic Institute of North America, 165-172, 1974.



10MAR74 C W151-00 W150-00 W149-00 IN070-00 IW148-00  
N70-50/W148-05 N N70-47/W147-59 MSS 7 D SUN EL14 AZ168 207-8299-A-1-N-D-IL NASA ERTS E-1595-21180-7 01

Figure 1: Landsat image 1595-21180 obtained 10 March, 1974 showing near-shore ice from the Colville River eastward to the vicinity of Flaxman Island.



281174 C 1613-21174-24 N 160-281174-25 E 1613-21174-5 01

Figure 2: Landsat image 1613-21174 obtained 28 March, 1974 showing near-shore ice from the Colville River eastward to the vicinity of Flaxman Island.



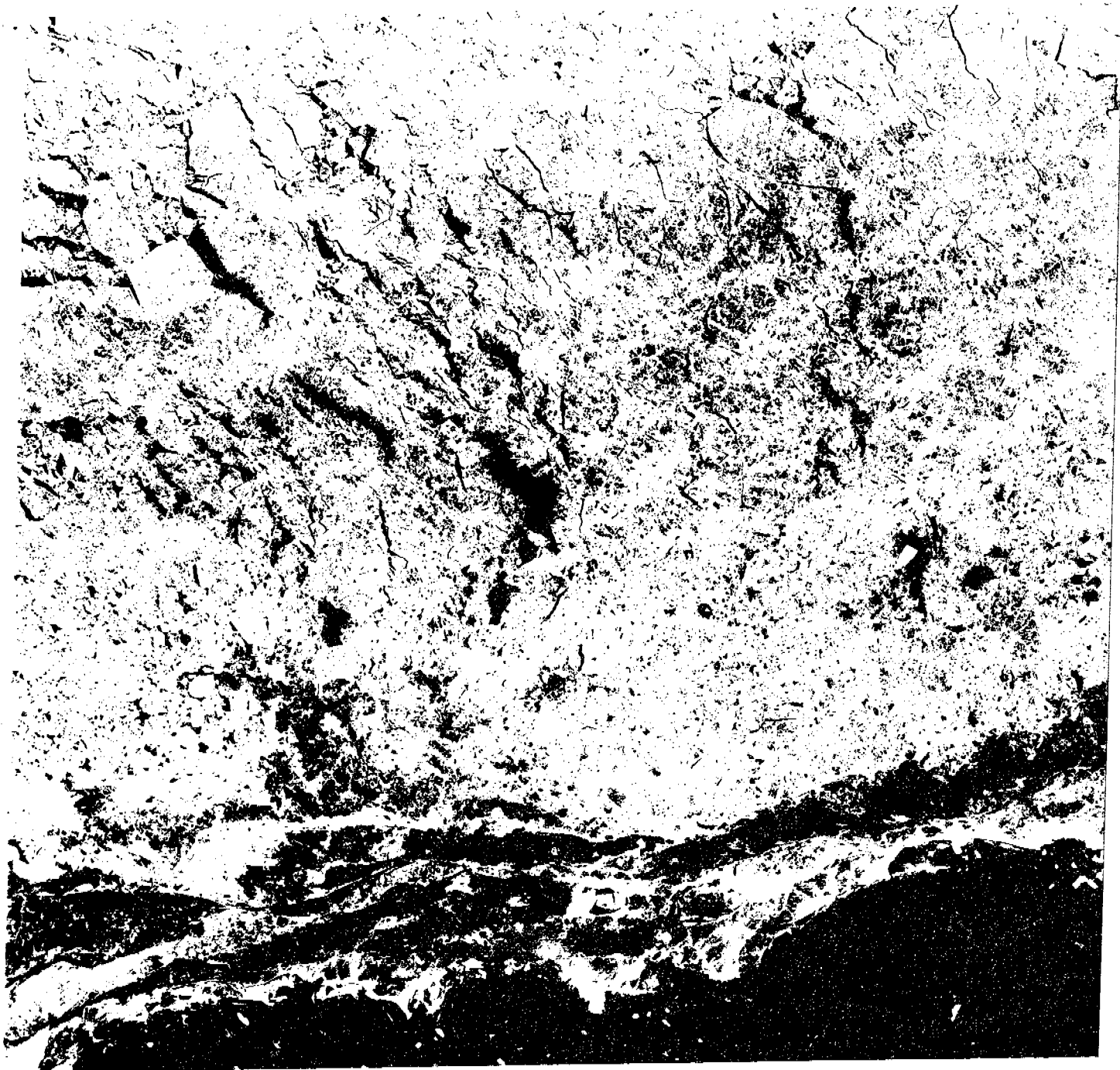
H151-001 H152-001 H153-001 H149-001  
03 MAY 74 C N78-41/H149-00 N N78-37/H149-22 H156 7 D 80N EL34 AZ170 297-302-R-1-N-D-II, N164-001 H149-001  
H149-001

Figure 3: Landsat image 1649-21165 obtained 3 May, 1974 showing near-shore ice from the Colville River eastward to the vicinity of Flaxman Island.



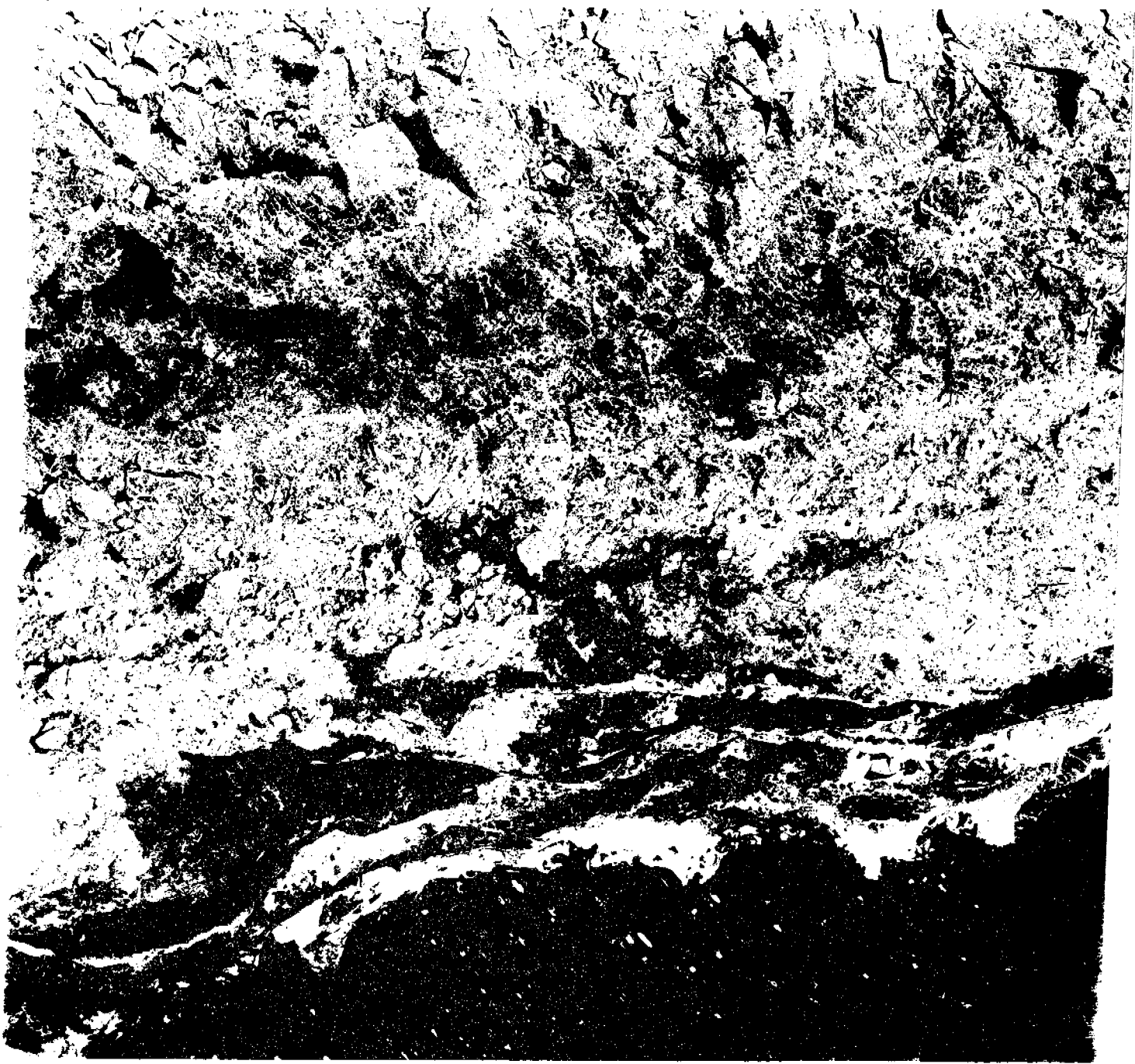
21 MAY 74 C H151-001 H152-001 H153-001 H154-001 H155-001  
H156-001 H157-001 H158-001 H159-001 H160-001 H161-001 H162-001  
211667-211668-20 H 167-001 168-001 169-001 170-001 171-001 172-001 173-001

Figure 4: Landsat image 1667-21162 obtained 21 May, 1974 showing near-shore ice from the Colville River eastward to the vicinity of Flaxman Island.



IW150-00      IW149-001      IW148-001      N070-001      IW147-00  
25JUN74 C N70-53/W146-58 N N70-49/W146-37 MSS      7 D SUN EL42 RZ167 207-9791-A-1-N-D-IL NASA ERTS E-1702-21093-7 02

Figure 5: Landsat image 1702-21093 obtained 25 June, 1974 showing near-shore ice from the Colville River eastward to the vicinity of Flaxman Island.



26JUN74 C N70-54/W148-17 N N70-50/W148-01 MSS      W150-001  
W149-001      7 D SUN EL42 AZ167 207-9805-A-1-N-D-1L NASA ERTS E-1703-21151-7 01

Figure 6: Landsat image 1703-21151 obtained 26 June, 1974 showing near-shore ice from the Colville River eastward to the vicinity of Flaxman Island.



4151-001 W150-001  
14JUL74 C N70-50/W148-27 N N70-46/W148-07 MSS 7 D SUN EL40 AZ166 207-0058 H-I-N-D 12 NASA ERTS E-1721 21143 102

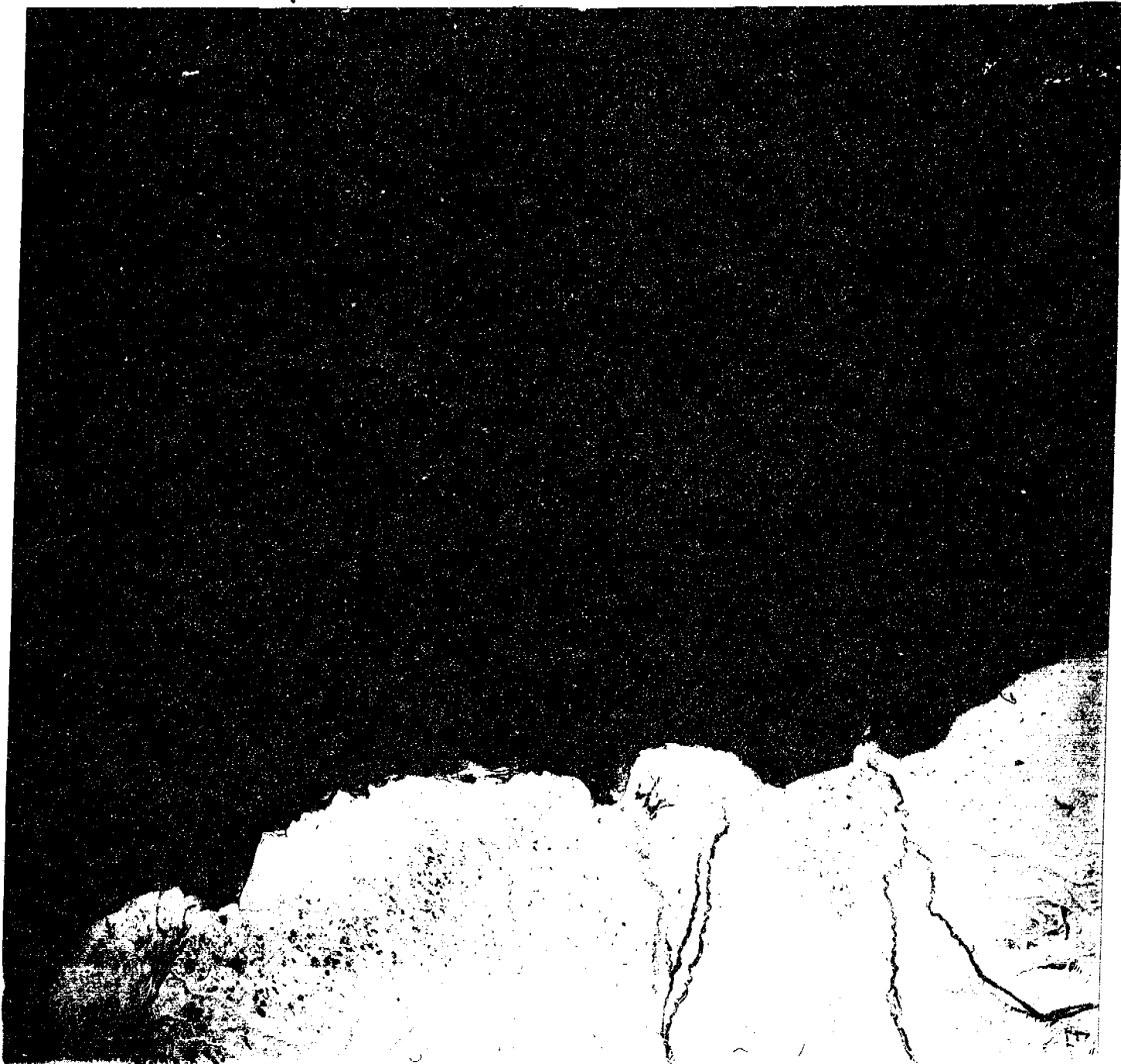
Figure 7: Landsat image 1721-21143 obtained 14 July, 1974 showing near-shore ice from the Colville River eastward to the vicinity of Flaxman Island.



06SEP74 N70°36'41" W158°13'48" NB/10-28

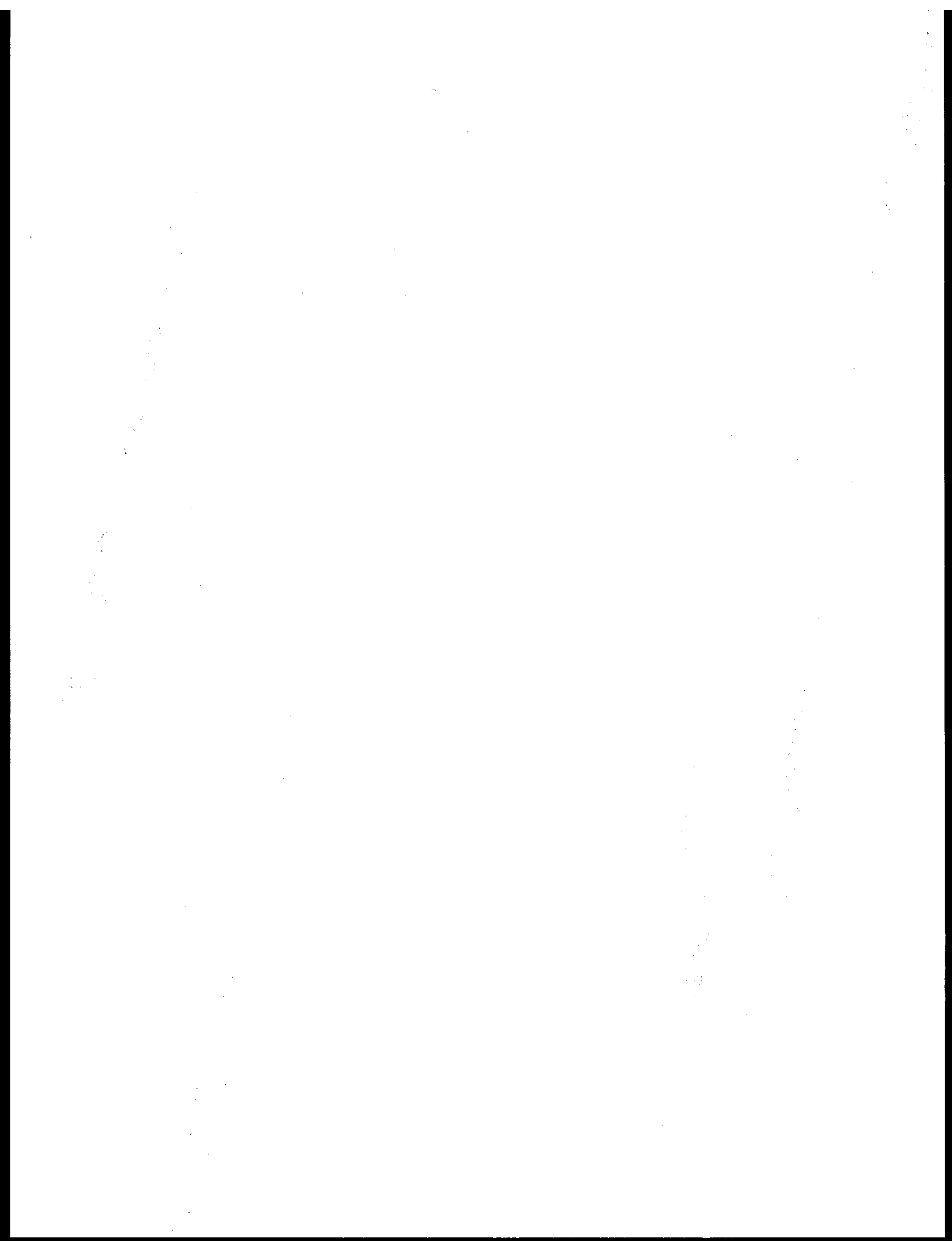
SUN 1125 12.65 201 0809-F N-4 12 NASA ERTS E-1 1775-21124

Figure 8: Landsat image 1775-21124 obtained 6 September, 1974 showing near-shore ice from the Colville River eastward to the vicinity of Flaxman Island.



W151-001 W150-001 W149-001 IN070-00 W148-001  
04OCT72 C N70-46/W147-55 N N70-42/W147-49 MSS 7 D SUN EL14 AZ175 207-1020-A-1-N-D-1L NASA ERTS E-1073-21223-7 01

Figure 9: Landsat image 1073-21223 obtained 4 October, 1972 showing near-shore ice from the Colville River eastward to the vicinity of Flaxman Island.



## OCS COORDINATION OFFICE

University of Alaska

## Quarterly Report for Quarter Ending September 30, 1976

Project Title: Morphology of Bering Near Shore Ice Conditions  
by Means of Satellite and Aerial Remote Sensing

Contract Number: 03-5-022-55

Task Order Number: 5

Principal Investigator: W. J. Stringer

I. Task Objectives:

The objective of this study is to develop a comprehensive morphology of near shore ice conditions in the Bering Sea, including a synoptic picture of the development and decay of fast ice and related features along the Bering Sea coast, and in the absence of fast ice, the nature of older ice (pack ice, hummock fields, etc.) which may occasion the near shore areas in other seasons. Special emphasis would be given to consideration of potential hazards to offshore facilities and operations created by near shore ice dynamics. A historical perspective of near shore ice dynamics will be developed to aid in determining the statistical rate of occurrence of ice hazards.

II. Field and Laboratory Schedule:

This project has no field schedule. However, attempts will be made through project management to obtain reconnaissance flights for photographic documentation and verification of ice conditions mapped

III. Results:

Using LANDSAT band 7 hard copy produced at 1:500,000 scale, preliminary Bering Sea near shore ice maps have been compiled for late spring and early summer 1973, 1974 and 1975. These maps have been reproduced here at half scale for reporting convenience. Particular care, described in our previous report, has been taken to locate ice features relative to geographic coordinates and bathymetric 10-fathom contour. The half-scale reproductions of these maps have been reproduced here with annotation discussing the features delineated as Appendix A.

IV. Preliminary Interpretations:

Interpretations are given in detail in the annotation of each map in Appendix A.

V. Plans for Next Reporting Period:

During this reporting period the preparation of comprehensive regional maps of sea ice conditions in the Bering Sea will be initiated. "Special event" descriptions and maps will be made.

VI. Problems Encountered/Recommended Changes:

We will require aerial reconnaissance/verification flights in the Bering Sea during March, April 1977 to document conditions described in these reports.

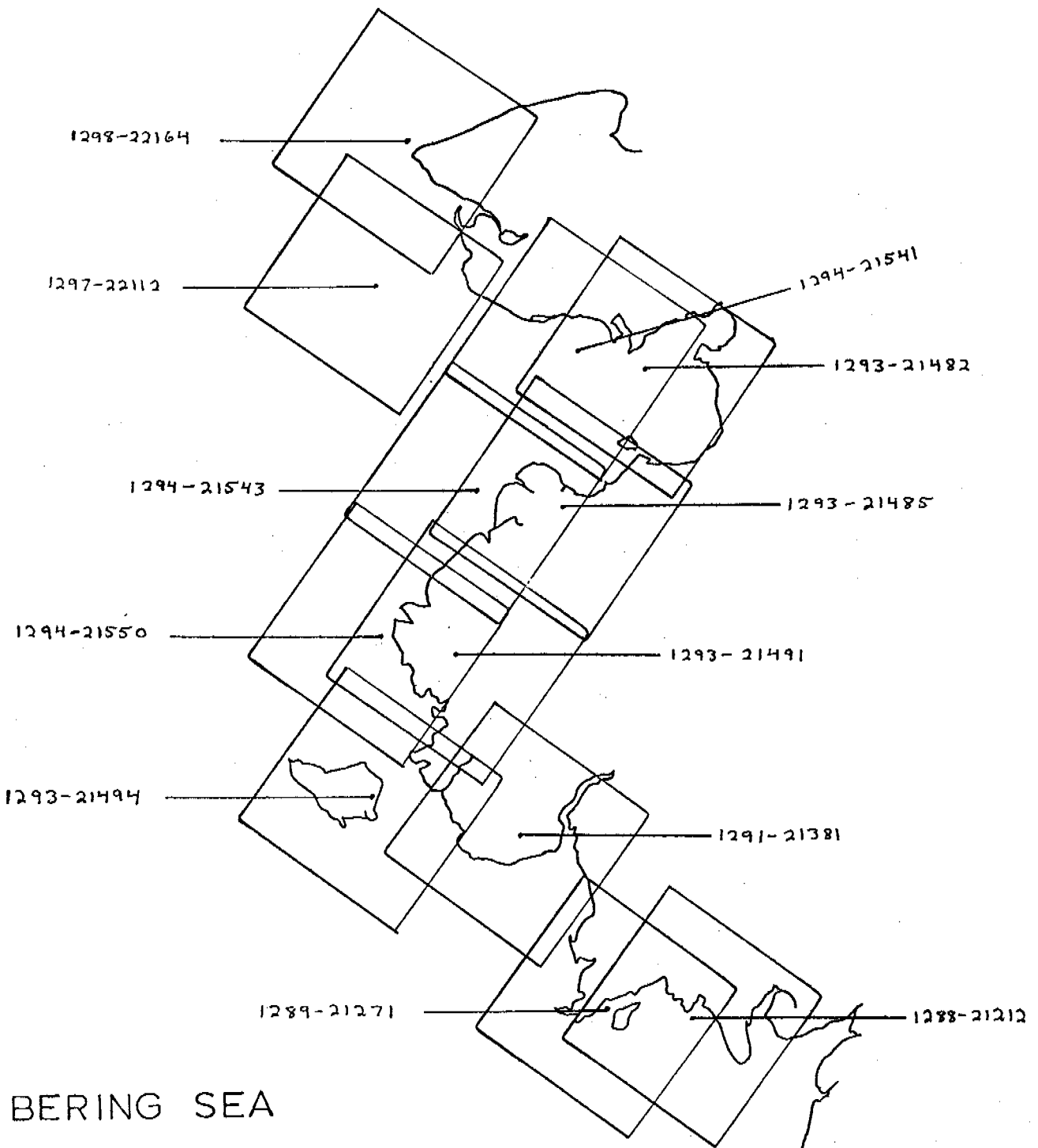
VII. Appendices:

(Attached).

SYMBOLS AND DEFINITIONS

- A River overflow (aufeis)
- B Boundary between apparently different ice types.
- BN Broken sheet of new ice.
- BPN Pans in broken matrix of new ice.
- BPY Pans in broken matrix of young ice.
- BY Broken sheet of young ice.
- C Stationary ice - ice which is contiguous with the shore.
- CF Fragmented or broken contiguous ice.
- D Rotting or decaying ice, characterized by a dark, mottled color indicating holes and puddling.
- F Ice floe.
- FW Open water with numerous floes of various sizes.
- FY(B) First year ice (broken or fragmented).
- G Grounded ice floe or stranded ice.
- H Hummocked ice - sea ice piled haphazardly one piece over another to form an uneven surface.
- I Young ice.
- L A lead, usually open, but may be too narrow to determine if it is open or not.
- M New ice, characterized by dark color, and smooth texture.
- N Newly refrozen lead of polyna - a lead or polyna composed of dark ice, not yet fractured and milky or covered with snow, thin enough to allow light to pass through to the water.
- O Old refrozen lead - a lead old enough to have either turned milky with cracks or been covered by snow; thick enough to reflect most of the incident sunlight and thus appear gray or white.

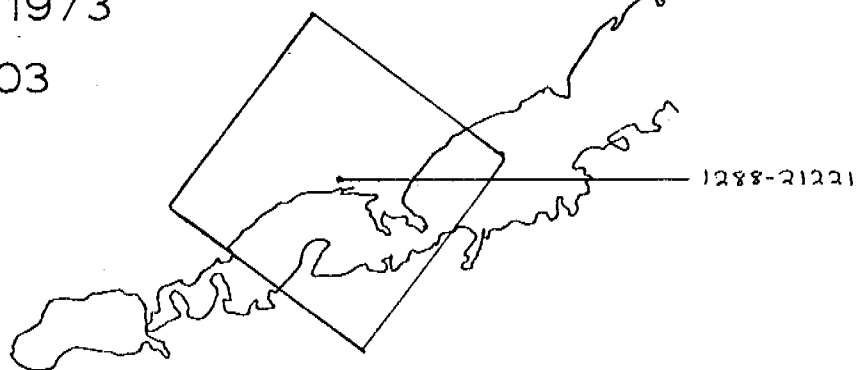
- P Partially refrozen lead, usually some dark ice with open water.
- PN Pans in matrix of new ice.
- PY Pans in matrix of young ice.
- R Ridge system, may be either pressure ridge or shear ridge system.
- S Smooth ice of uncertain age.
- T Tidal or tension cracks - cracks due to tidal action in shallow waters, may be indicated by piled ice and/or snow drifts.
- UP Unconsolidated pack ice consisting of flows and broken ice of varying sizes. More dense than FW
- W Open water.
- Y Polynya.
- Z Zone of shear.



BERING SEA

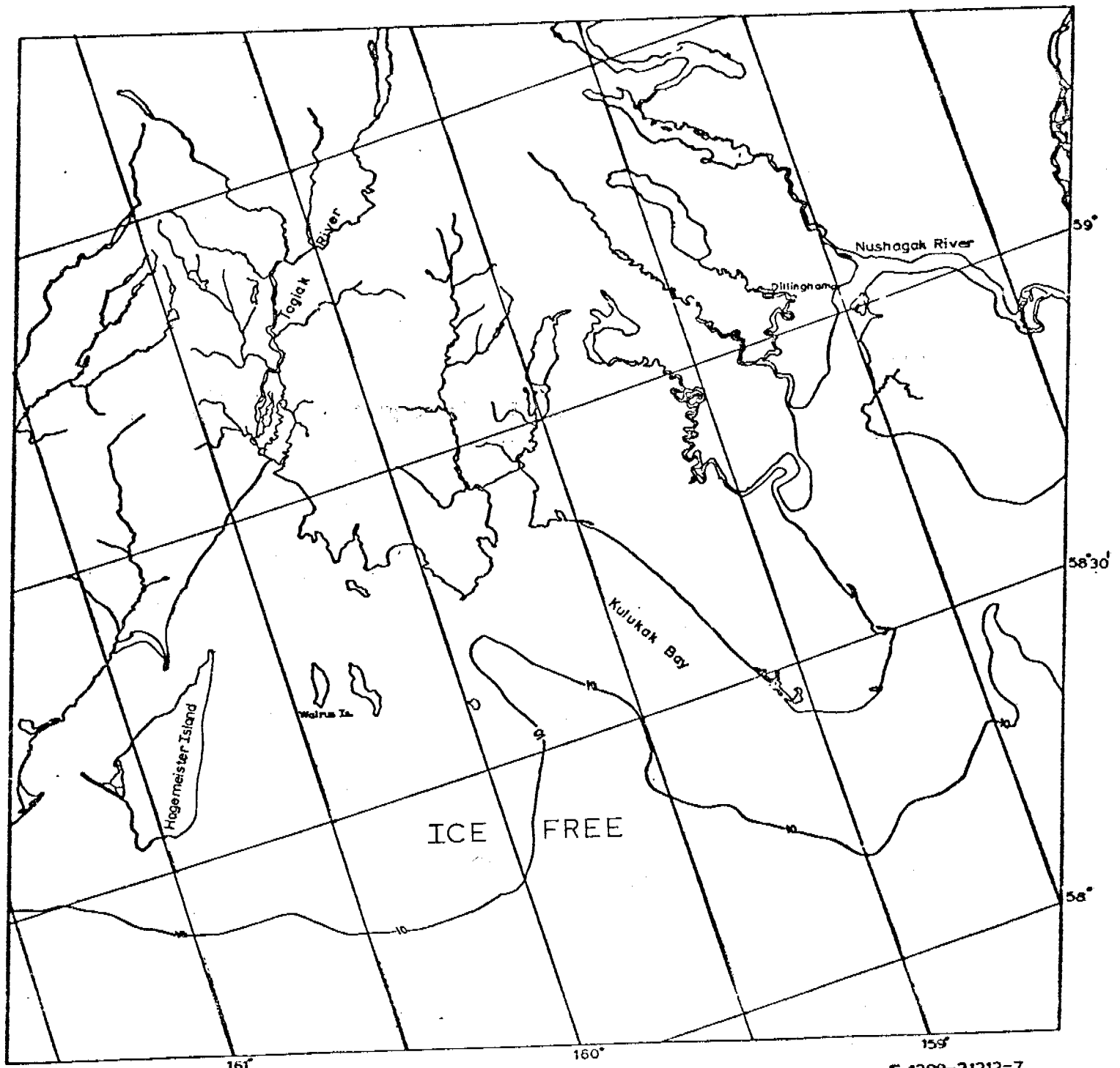
5 MAY - 22 MAY 1973

Images 1286-1303



Scene 1288-21212

This scene of northern Bristol Bay is completely free of sea ice,  
except for very well protected shallow areas.

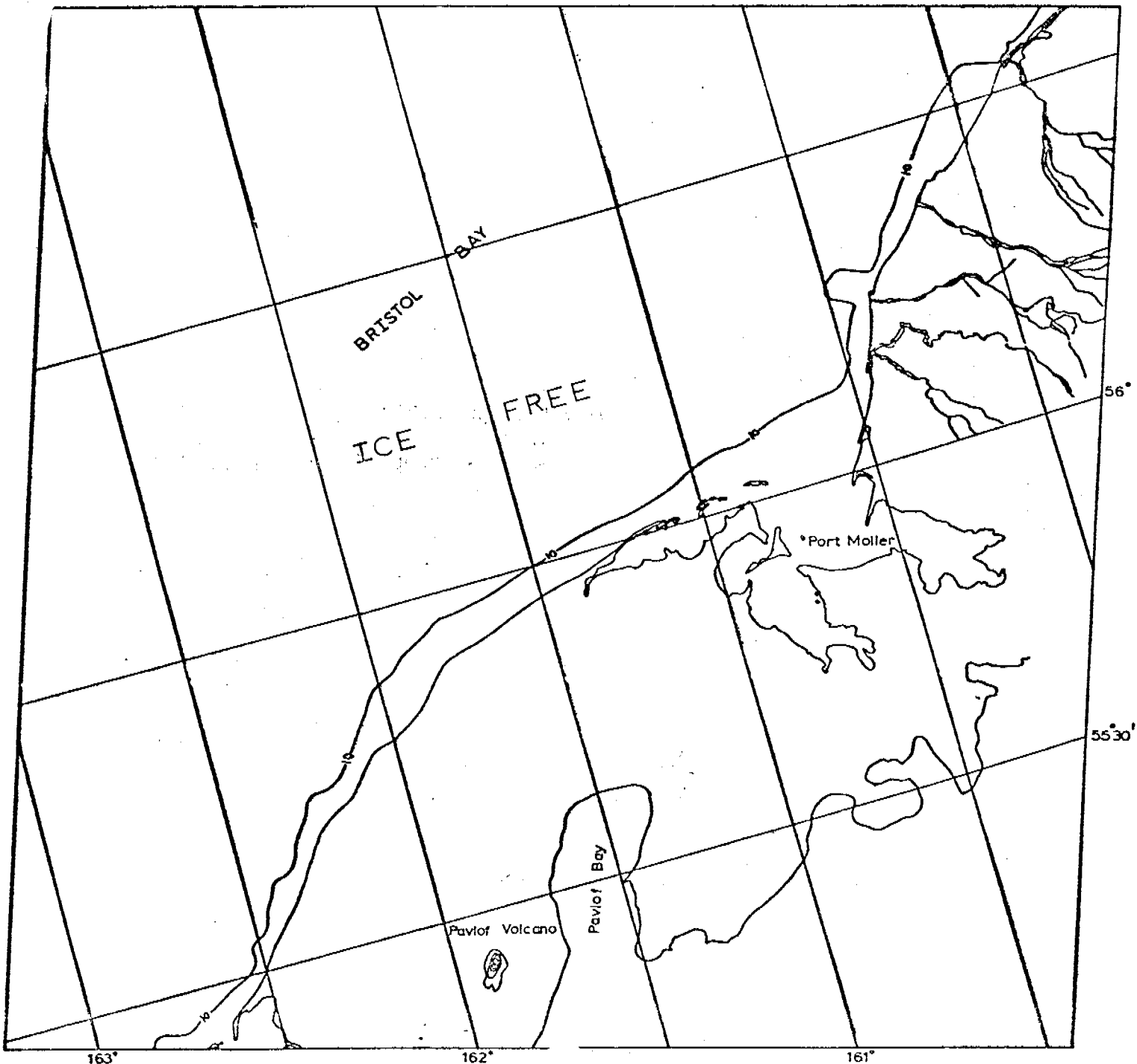


KILOMETERS  
0 10 20 30 40 50  
SCALE APPROX 1:1,000,000

BERING SEA

Scene 1288-21221

This scene of southern Bristol Bay is completely free of sea ice.



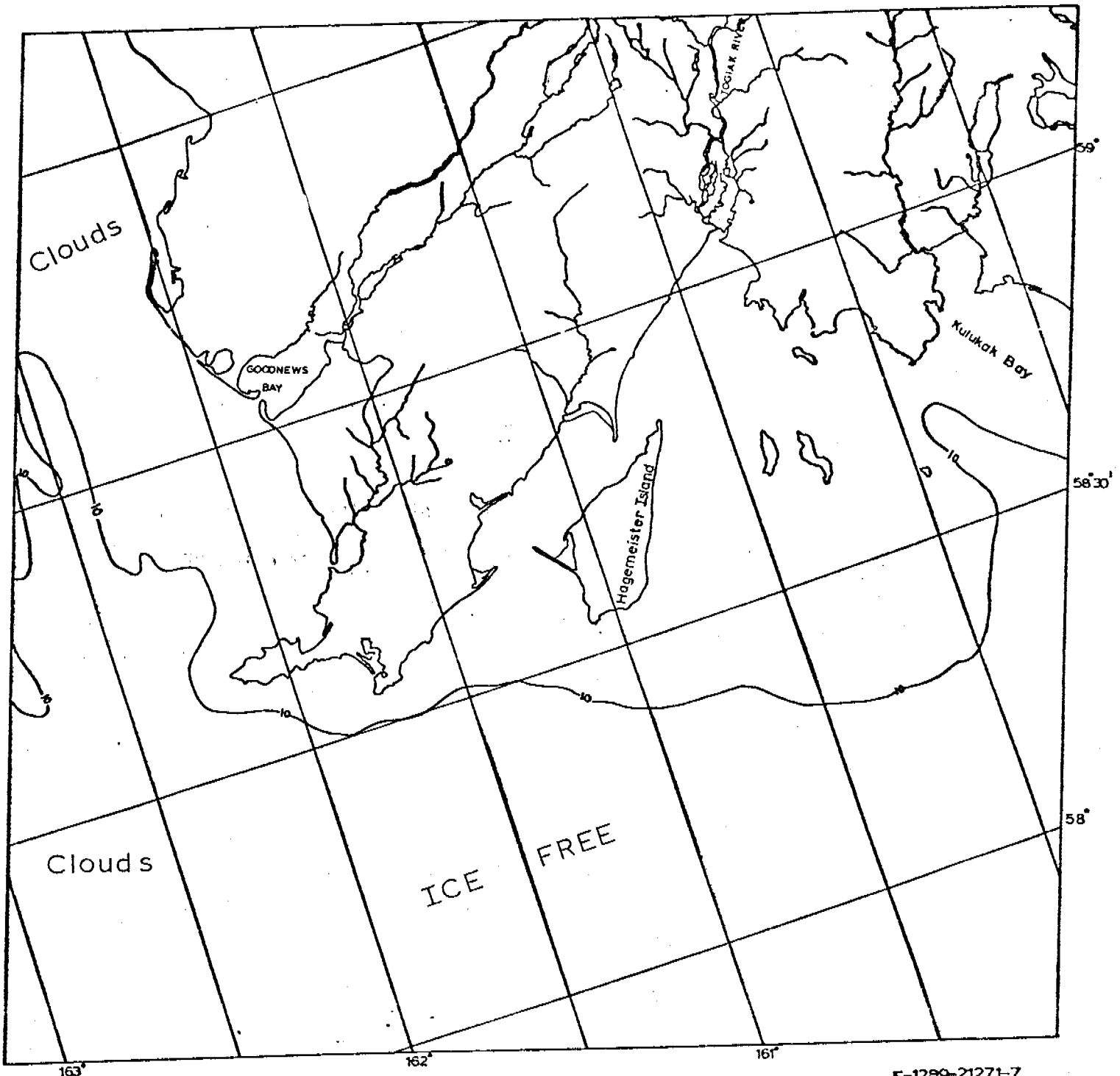
KILOMETERS  
0 10 20 30 40 50  
SCALE APPROX 1:1,000,000

BERING SEA

E-1289-21221-7  
7 MAY 1973

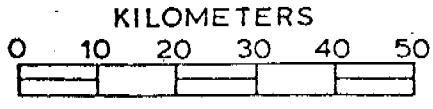
Scene 1289-21271

This scene of western Bristol Bay is partially obscured by clouds but appears to be completely free of sea ice except for very protected shallow areas.



E-1289-21271-7

© MAY 1973

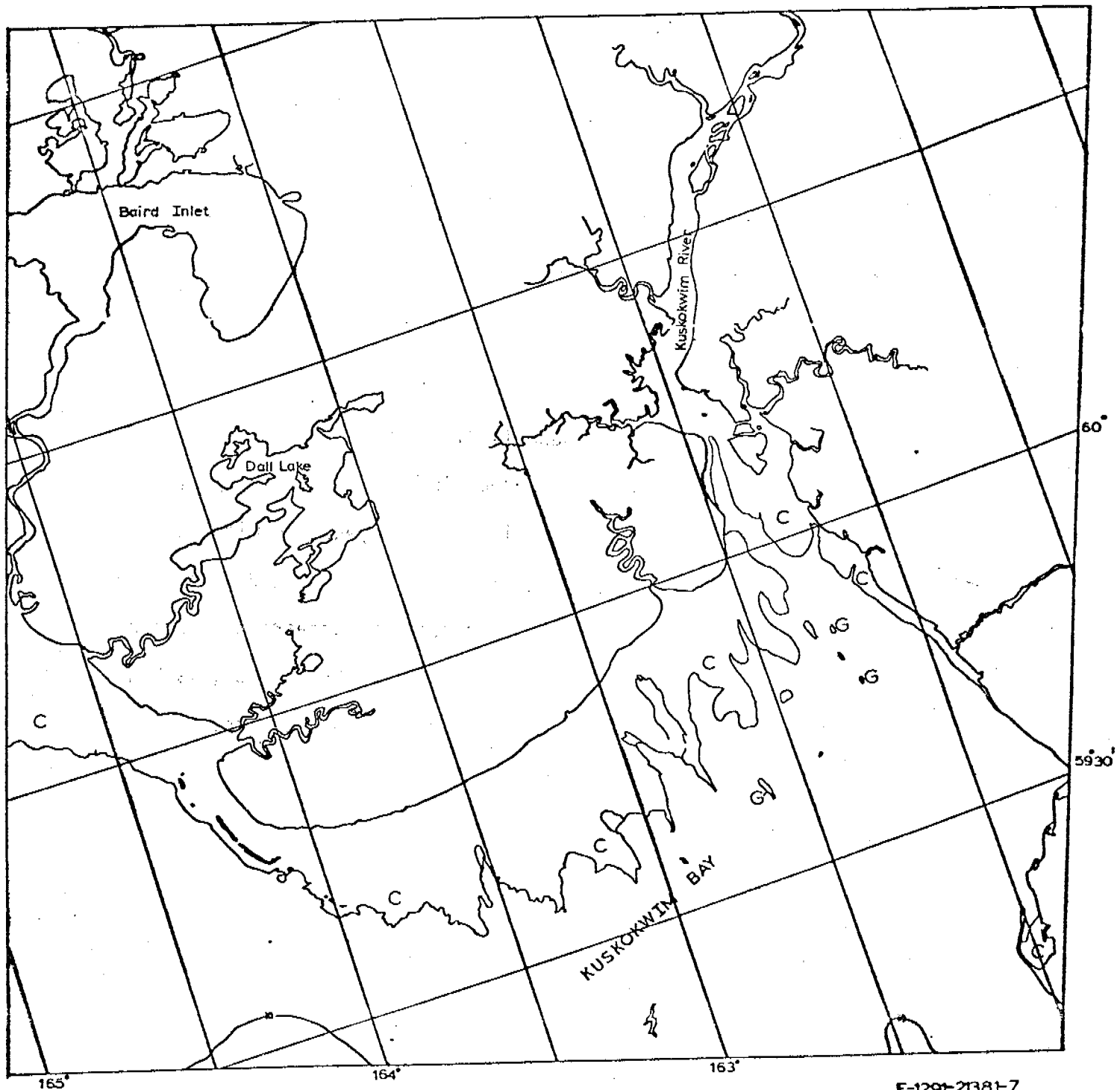


SCALE APPROX 1:1,000,000

## BERING SEA

Scene 1291-21381

This scene of Kuskokwim Bay is too high of contrast to see much detail but shows the extent of contiguous ice. There are a few grounded ice floes in the mouth of the Kuskokwim River.

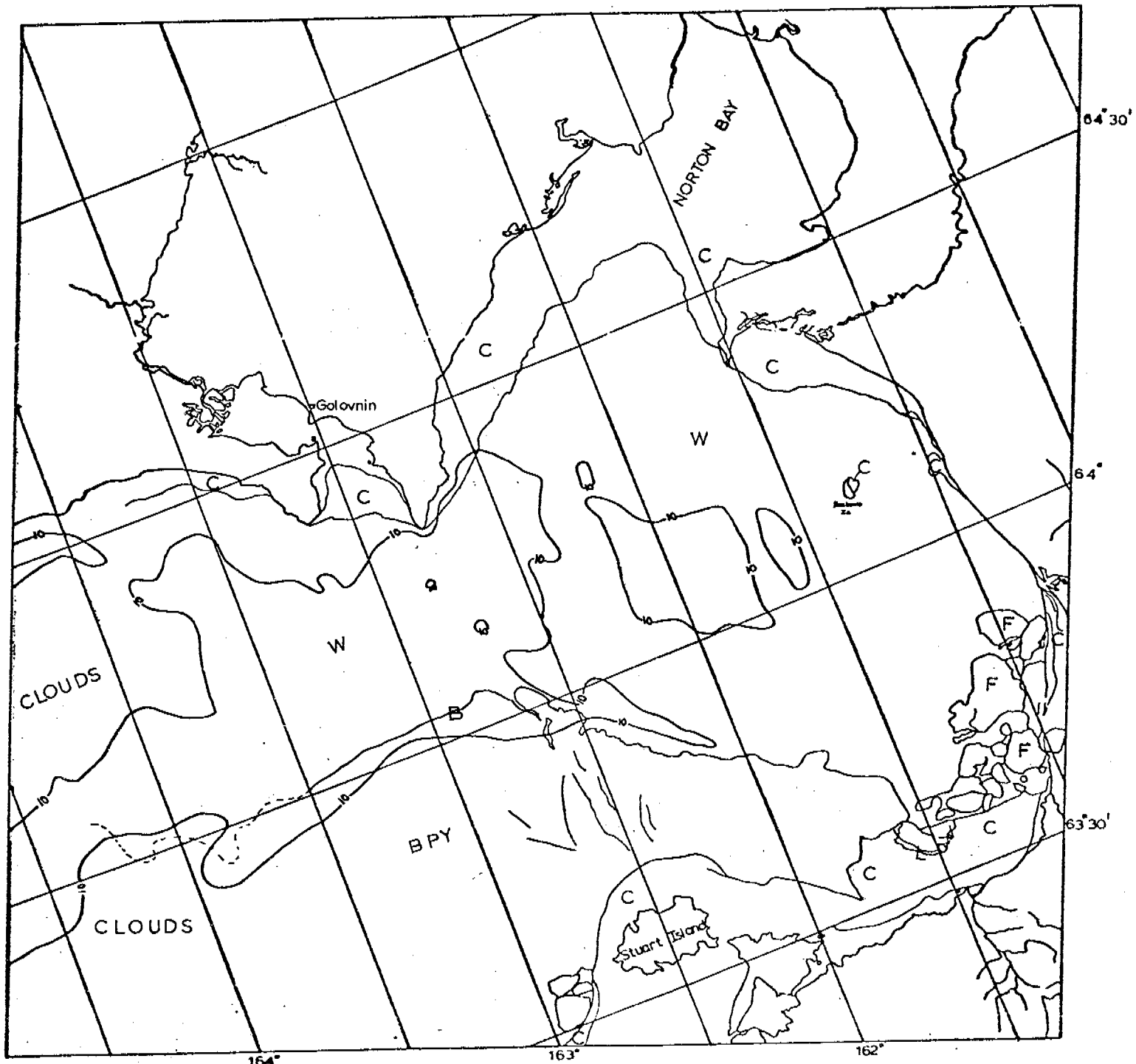


KILOMETERS  
0 10 20 30 40 50  
SCALE APPROX 1:1,000,000

BERING SEA

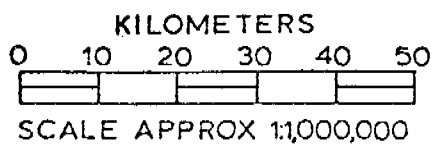
Scene 1293-21482

The central part of Norton Sound is almost totally ice-free. Norton Bay is still filled with contiguous ice. The southern part of the sound is filled with a broken matrix of first year ice with pans. Ice is still contiguous to the Yukon Delta and Stuart Island. The western part of the image is obscured by clouds but appears to contain some ice floes. Note the sharp boundary between water and ice, marked "B", that follows the 10-fathom contour north of Stuart Island.



E-1293-21482-7

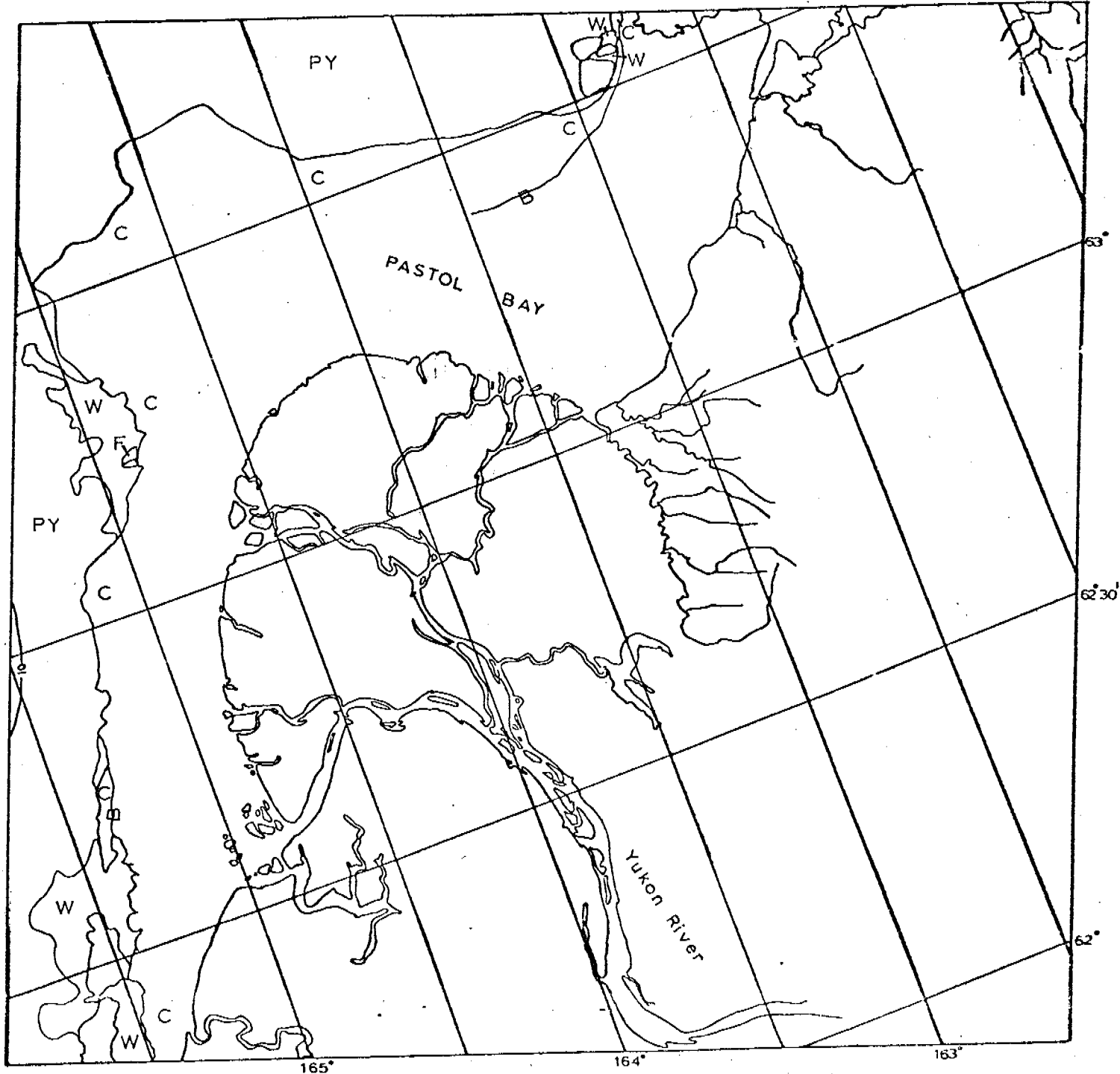
12 MAY 1973



## BERING SEA

Scene 1293-21485

The contiguous ice extends several kilometers from shore. Adjacent to the contiguous ice are pans and floes on a matrix of first year ice. In some places, open water separates the contiguous ice from the matrix.



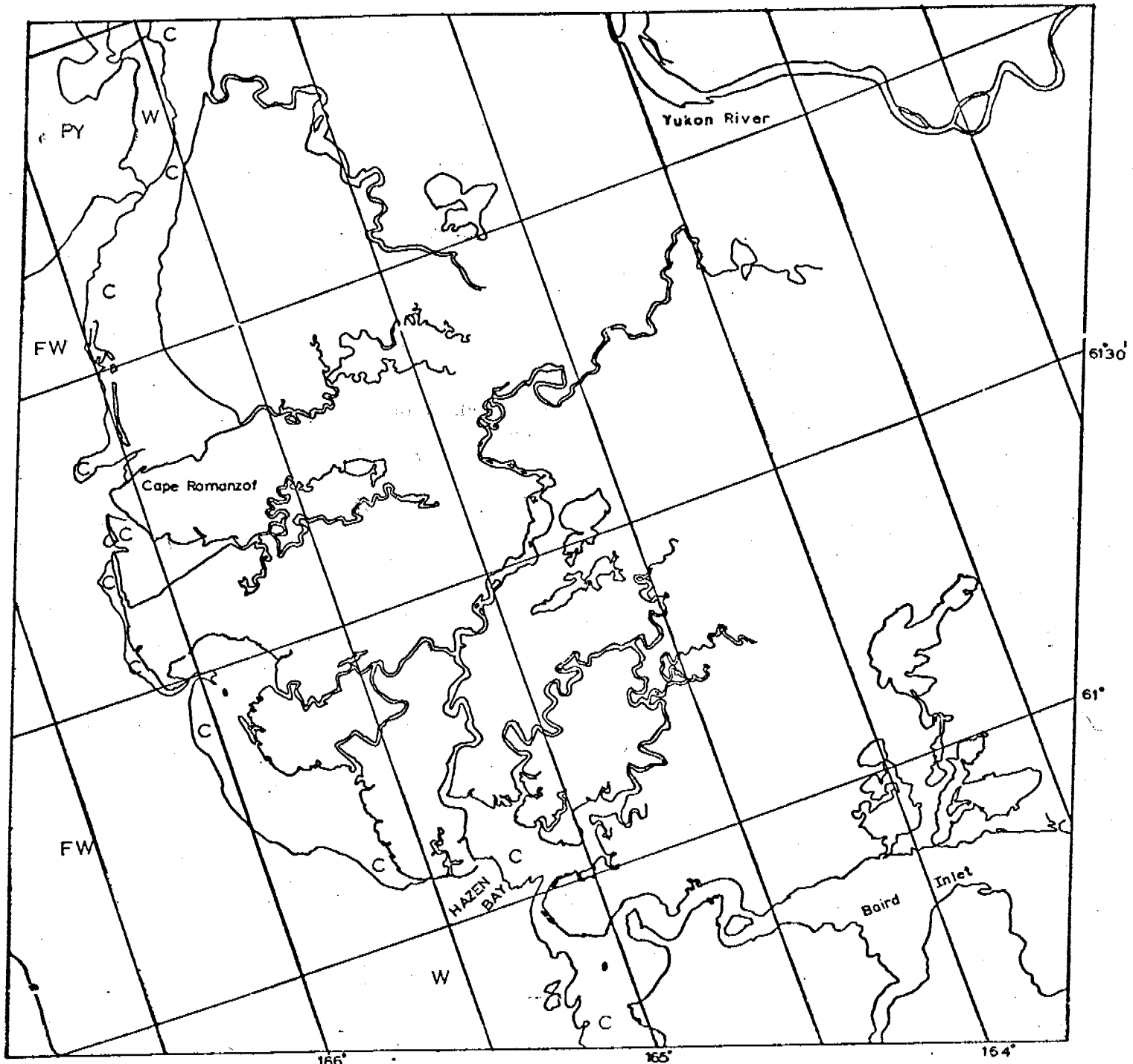
KILOMETERS  
0 10 20 30 40 50  
SCALE APPROX 1:1,000,000

BERING SEA

E-1293-21485-7  
12 MAY 1973

Scene 1293-21491

The contiguous ice forms a relatively thin shelf along the shore well shoreward of the 10-fathom contour in this scene. Some ice floes are evident in the westernmost part of the image and some pack ice is present to the north, consisting of pans and floes in a matrix of first year ice. No new ice is evident.



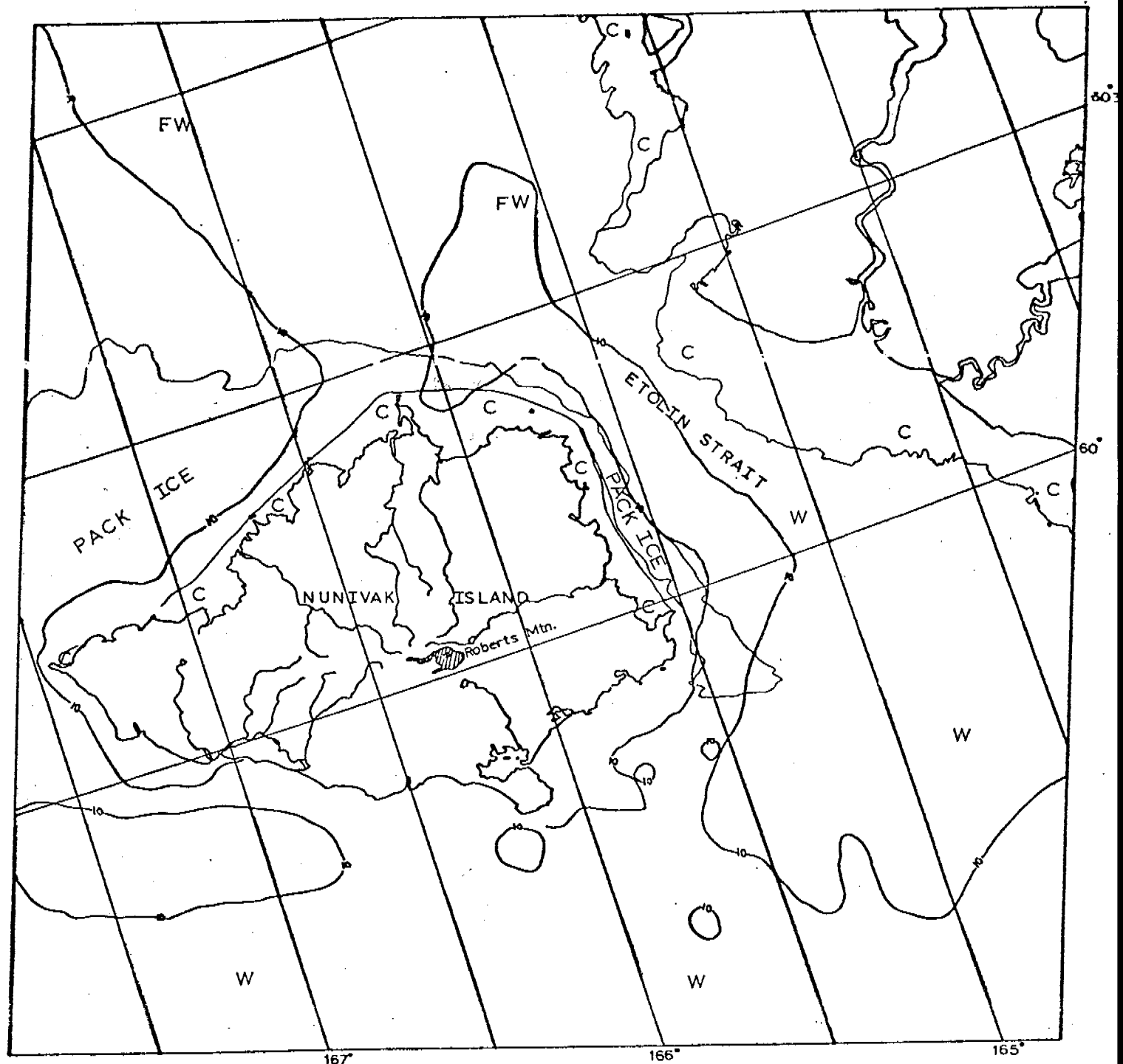
E-1293-21491-7  
12 MAY 1973

KILOMETERS  
0 10 20 30 40 50  
SCALE APPROX 1:1,000,000

## BERING SEA

Scene 1293-21494

A thin shelf of contiguous ice extends around the north and east sides of Nunivak Island and a somewhat thicker shelf is present along the eastern side of Etolin Strait. To the north of Nunivak Island are numerous floes in open water. Open water exists south of Nunivak Island. Pack ice is piled up on the north side of Nunivak Island.



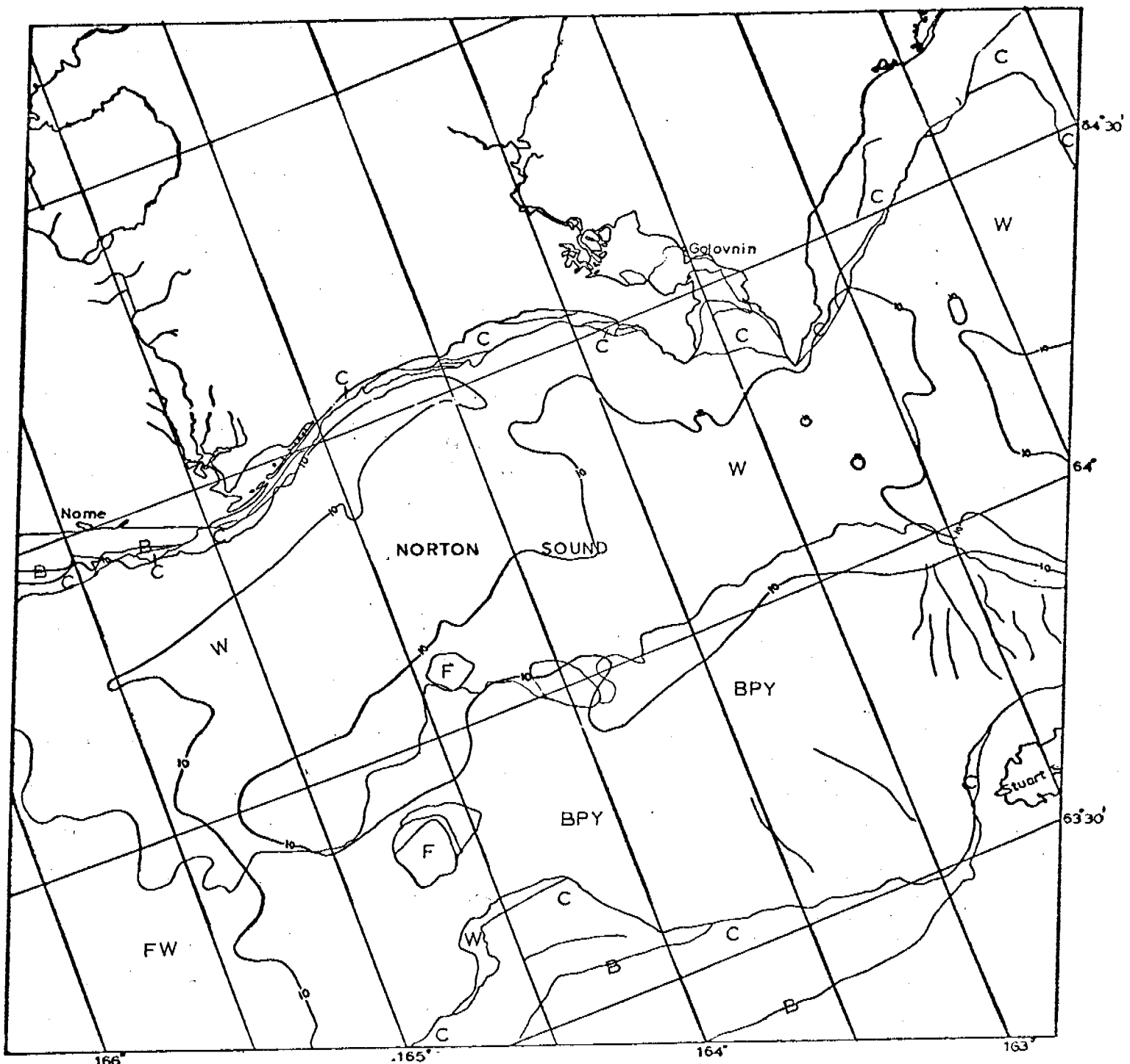
E-1293-21494-7  
12 MAY 1973

KILOMETERS  
 0 10 20 30 40 50  
  
 SCALE APPROX 1:1,000,000

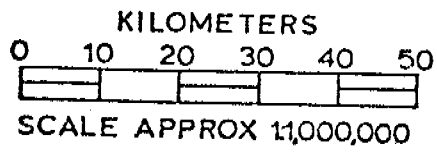
## BERING SEA

Scene 1294-21541

A narrow shelf of contiguous ice exists along the shore of the north side of Norton Sound, widening somewhat near Nome. At Nome, a boundary, "B", separates what appears to be shorefast ice from a matrix of pans, all of which is "contiguous". A thick shelf of contiguous ice is attached to the Yukon Delta. Adjacent and to the north of this is a matrix of young ice containing numerous small pans, grading westward into numerous floes in open water.



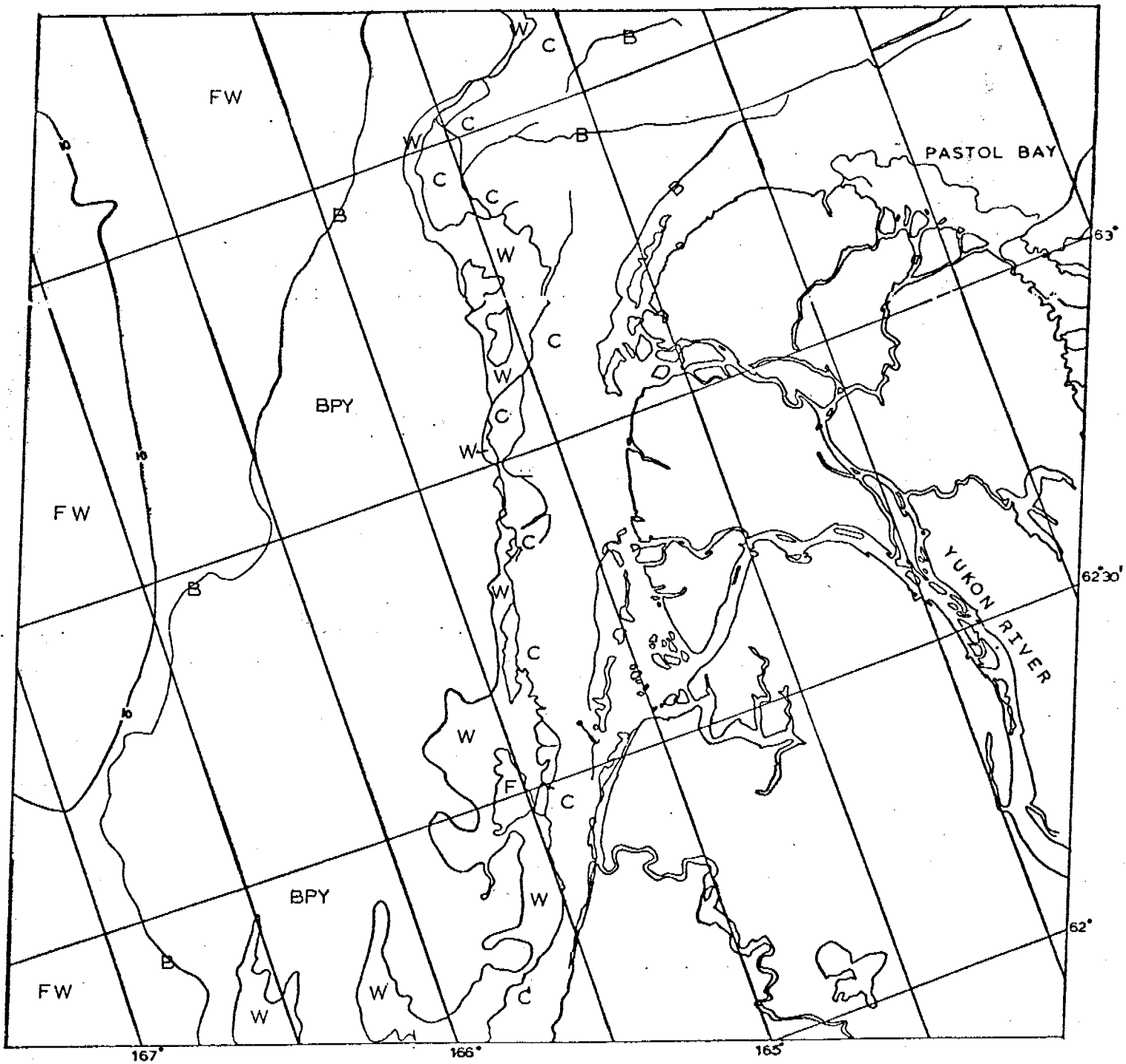
E-1294-21541-7  
13 MAY 1973



## BERING SEA

Scene 1294-21543

A large shelf of contiguous ice several tens of kilometers wide can be seen off the north side of the Yukon River Delta, narrowing to a few kilometers westward. Separated from this by a narrow lead of open water is the pack ice consisting of a matrix of new ice with numerous pans close to shore and a jumble of numerous flows surrounded by open leads further seaward.



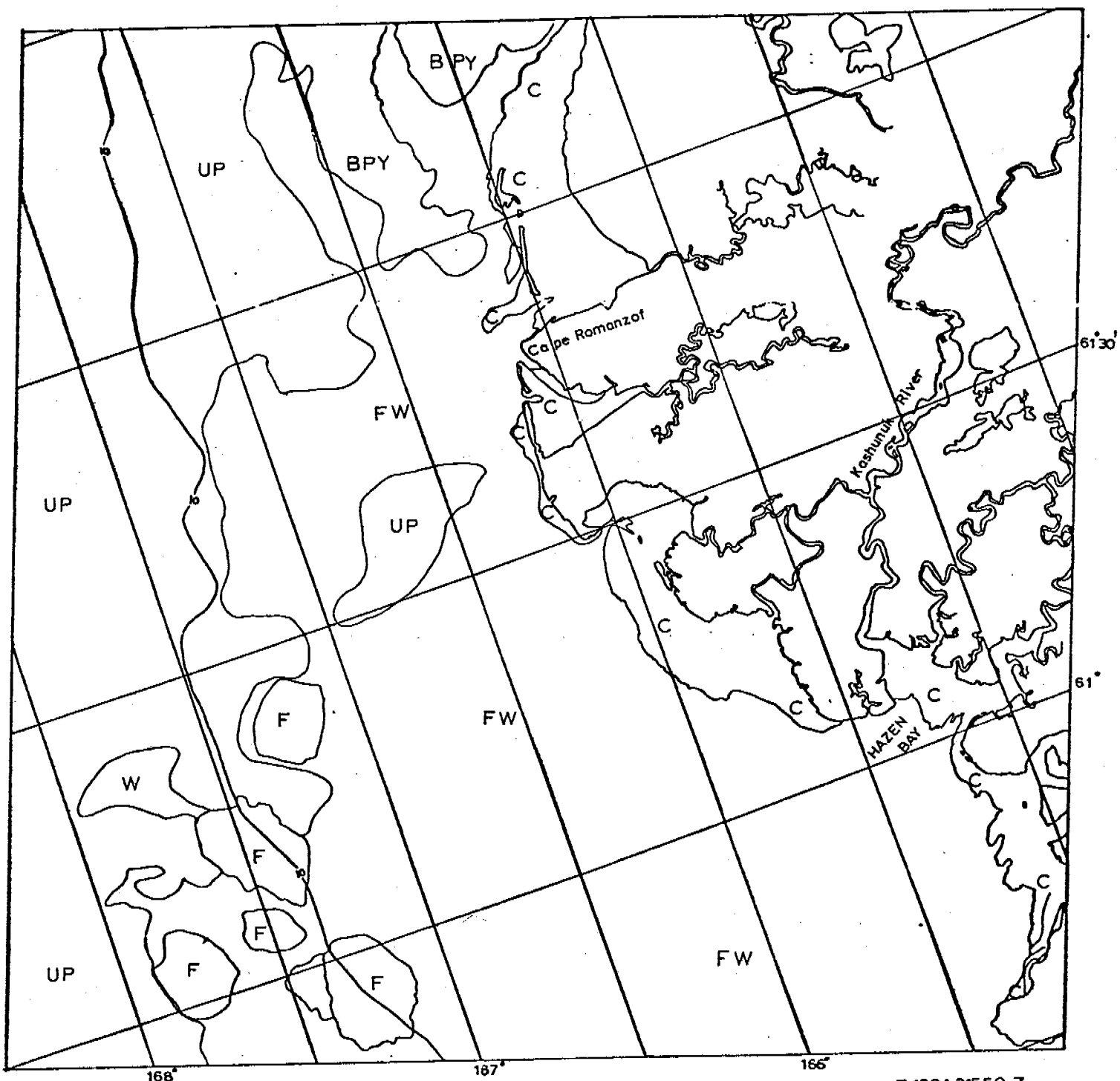
KILOMETERS  
0 10 20 30 40 50  
SCALE APPROX 1:1,000,000

BERING SEA

E-1294-21543-7  
13 MAY 1973

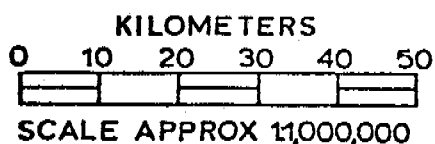
Scene 1294-21550

Most of the contiguous ice is concentrated between promontories which seem to protect it from tidal breakage, such as between Dall Point and Hazen Bay, and between Cape Romanzof and the islands north of the cape. The shelf of contiguous ice is thin or non-existent on the promontories themselves. The pack ice consists of unconsolidated flows of varying sizes, grading into a thicker matrix of young ice and floes northward. Between the shore and the contiguous ice and the pack ice is mostly open water with a few floes.



E-1294-21550-7

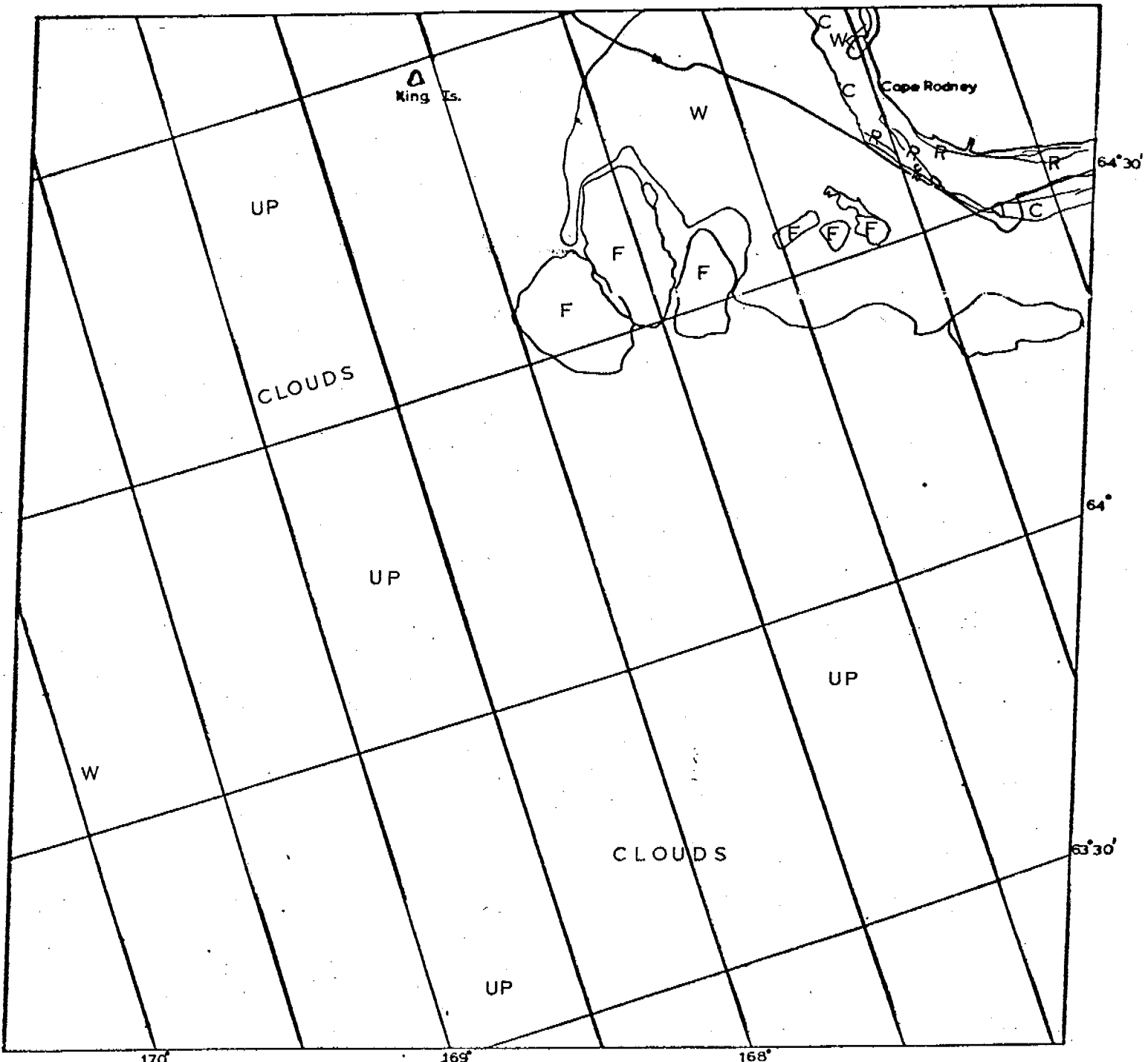
13 MAY 1973



## BERING SEA

Scene 1297-22112

A thin shelf of contiguous ice exists off Cape Rodney. What appears to be ridges can be seen running parallel to shore. A stretch of open water exists between shore and the pack ice, which is composed of mostly unconsolidated floes. Most of the pack ice is obscured to varying degrees by clouds.



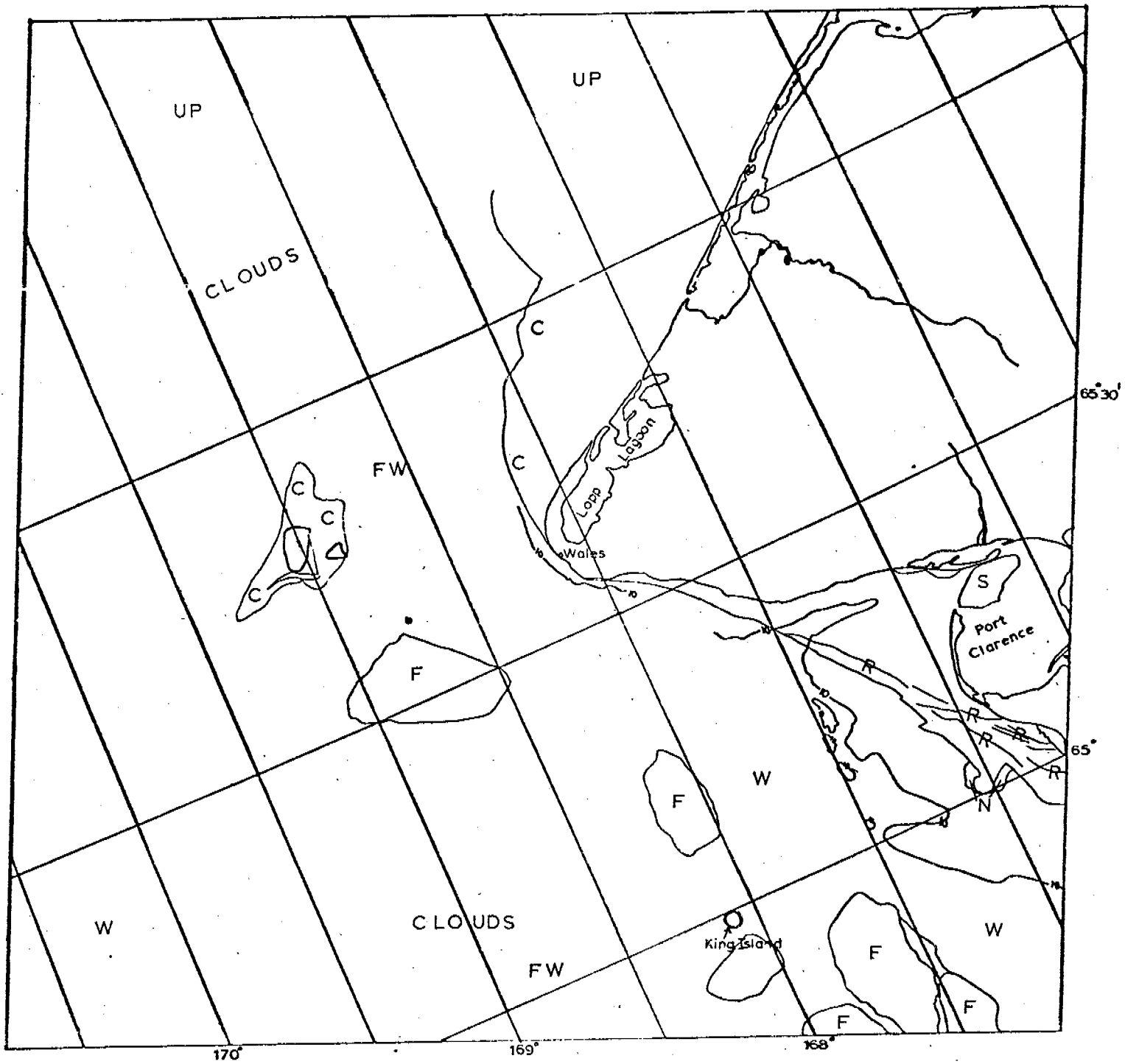
E-1297-22112-7  
16 MAY 1973

KILOMETERS  
0 10 20 30 40 50  
SCALE APPROX 1:1,000,000

## BERING SEA

Scene 1298-22164

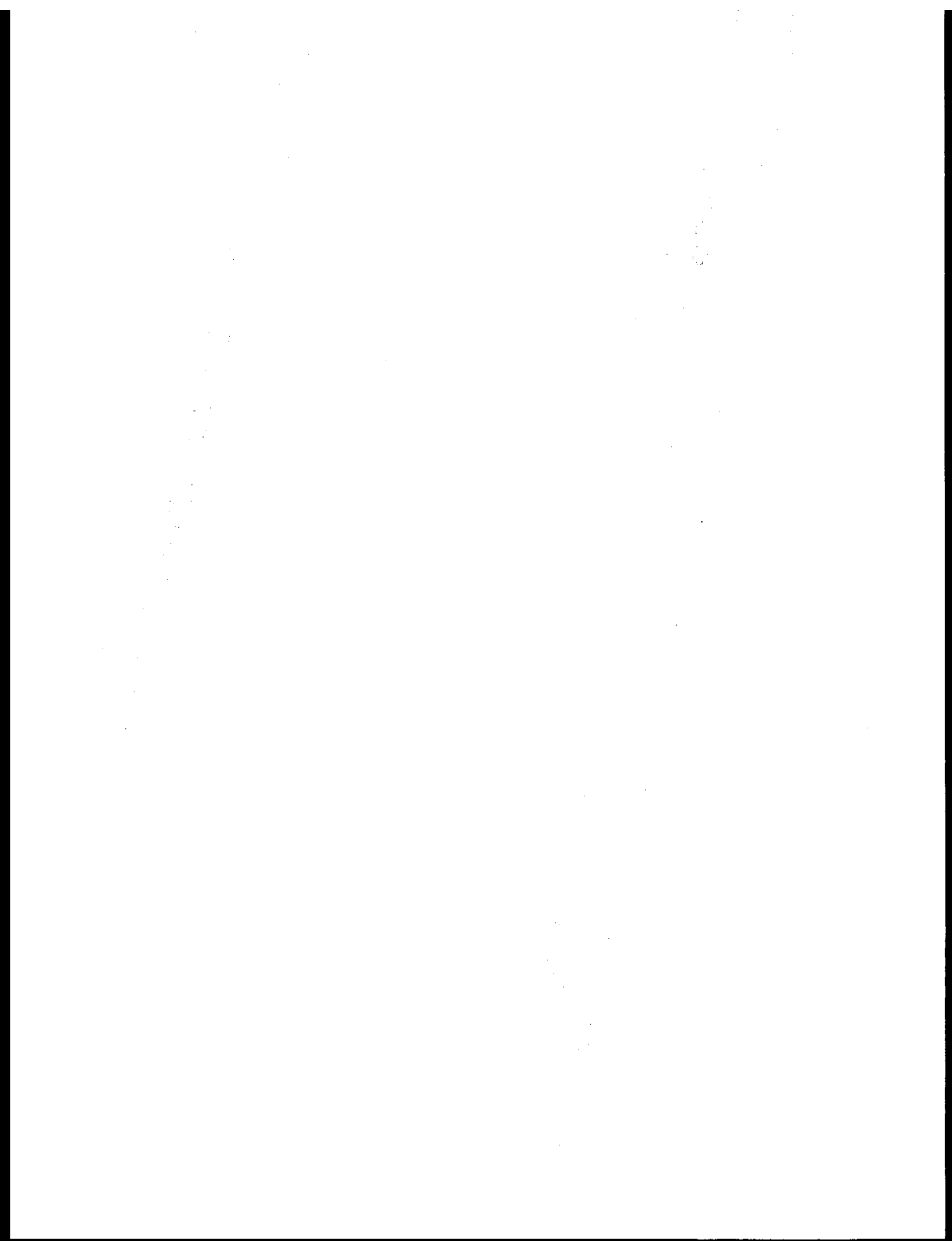
The seaward edge of the contiguous ice is well shoreward of the 10-fathom contour. The contiguous ice in the vicinity of Port Clarence appears to be made up of pans with ridging around their edges. There are several linear features running parallel to shore that appear to be old pressure/shear ridges. A small shelf of new ice, marked "N", has formed south of Port Clarence. The pack ice is mostly obscured by clouds, but that portion south of the Diomedes is mostly loose floes while that to the north appears to be a dense pack of unconsolidated floes. There is also a fairly large shelf of contiguous ice around the Diomede Islands.

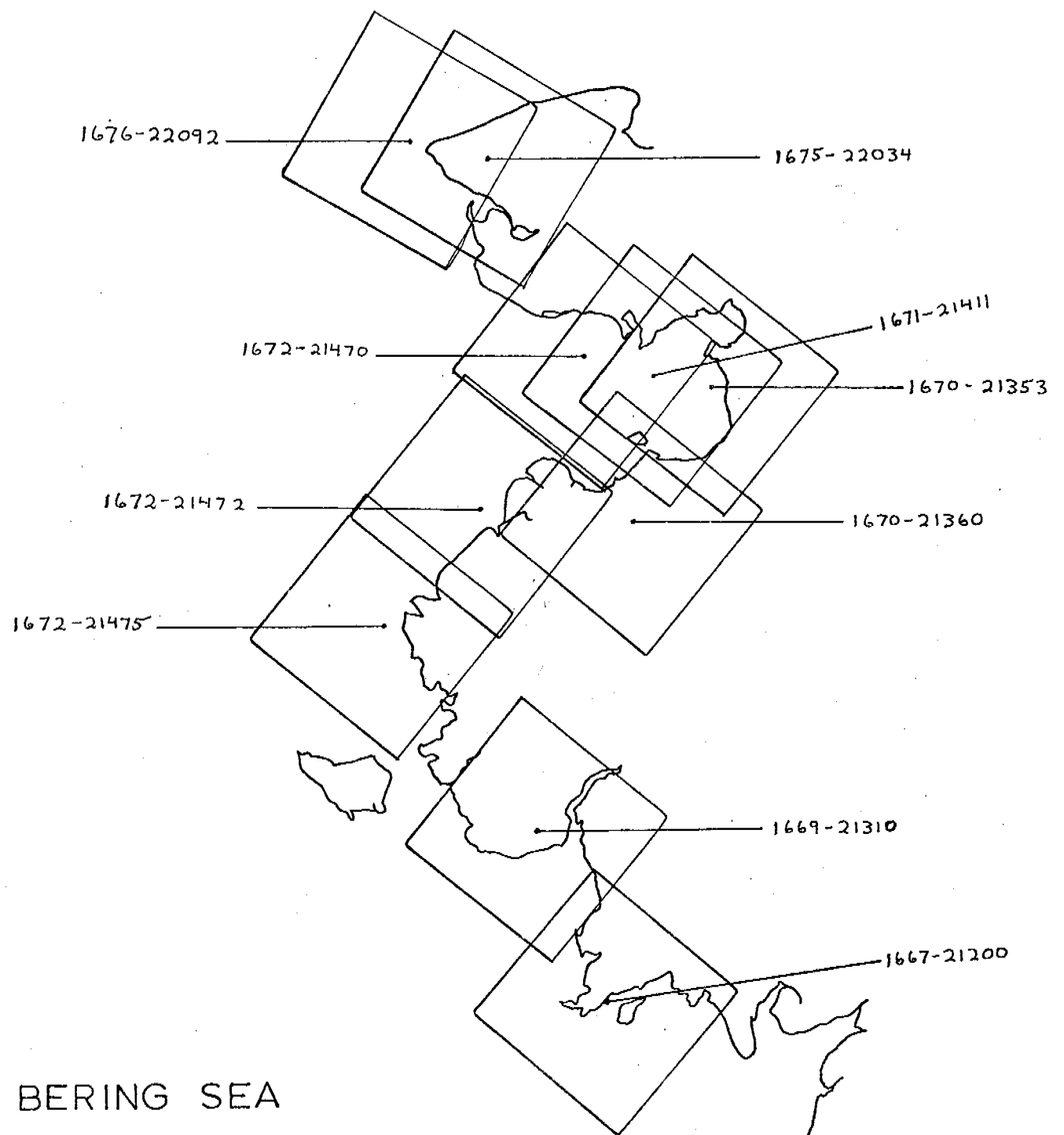


E-1298-22164-7  
17 MAY 1973

KILOMETERS  
0 10 20 30 40 50  
SCALE APPROX 1,000,000

## BERING SEA





BERING SEA

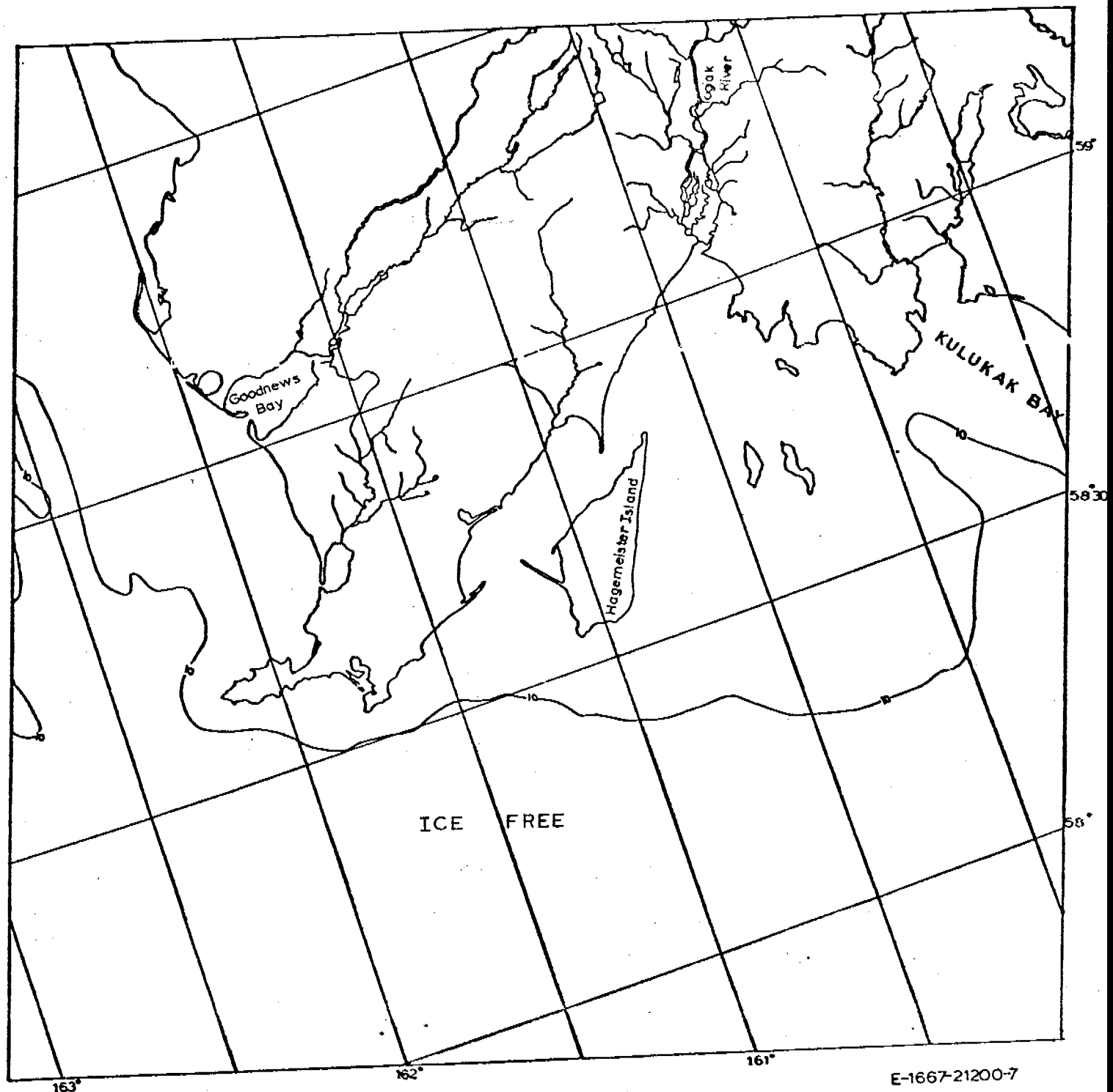
18 MAY - 4 JUNE 1974

Images 1664-1681



Scene 1667-21200

This area is completely ice-free, not even any shorefast ice.



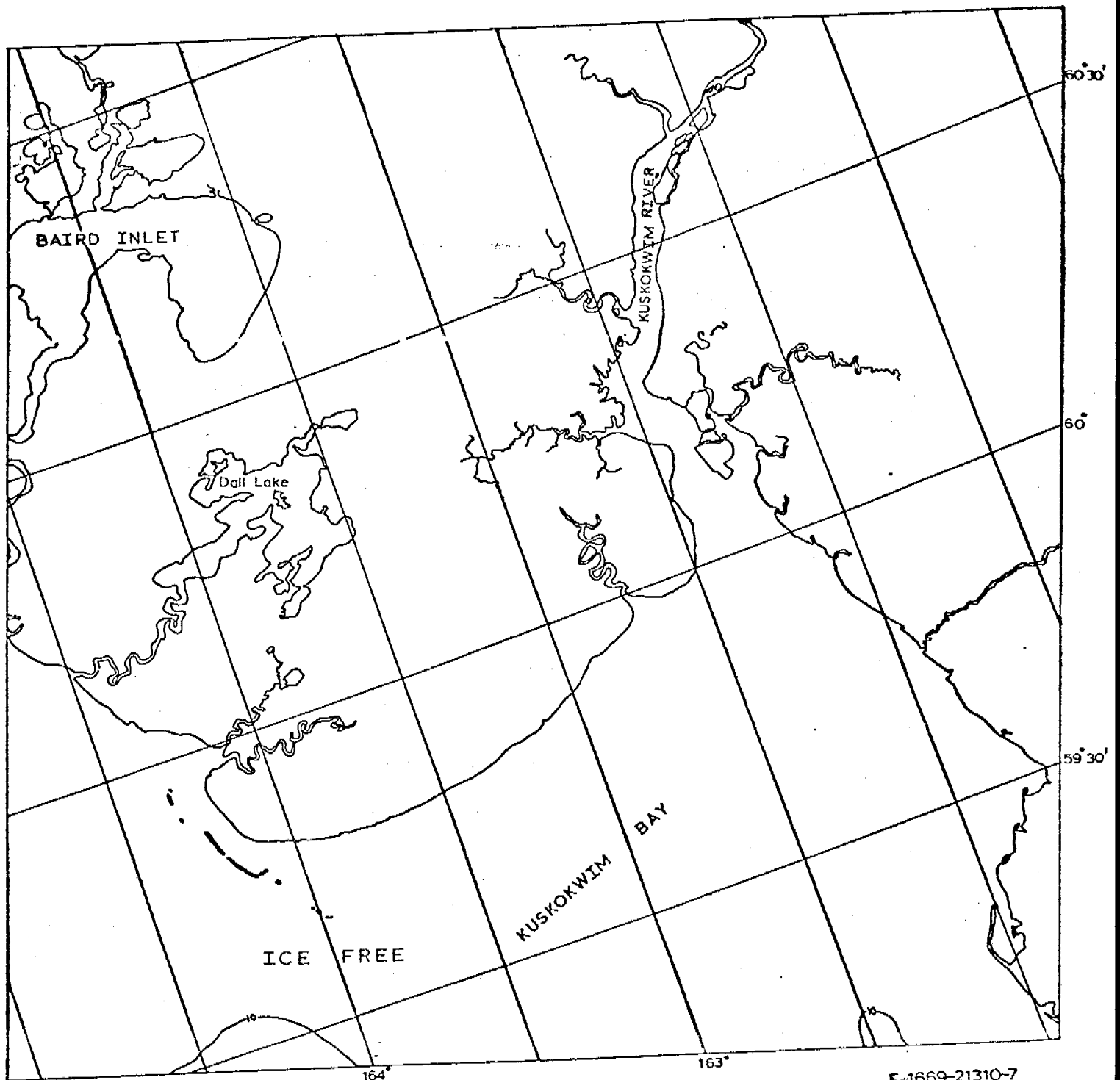
BERING SEA

541

E-1667-21200-7  
21 MAY 1974

Scene 1669-21310

There is no sea ice in this scene. A few of the lakes are still partially ice-covered.

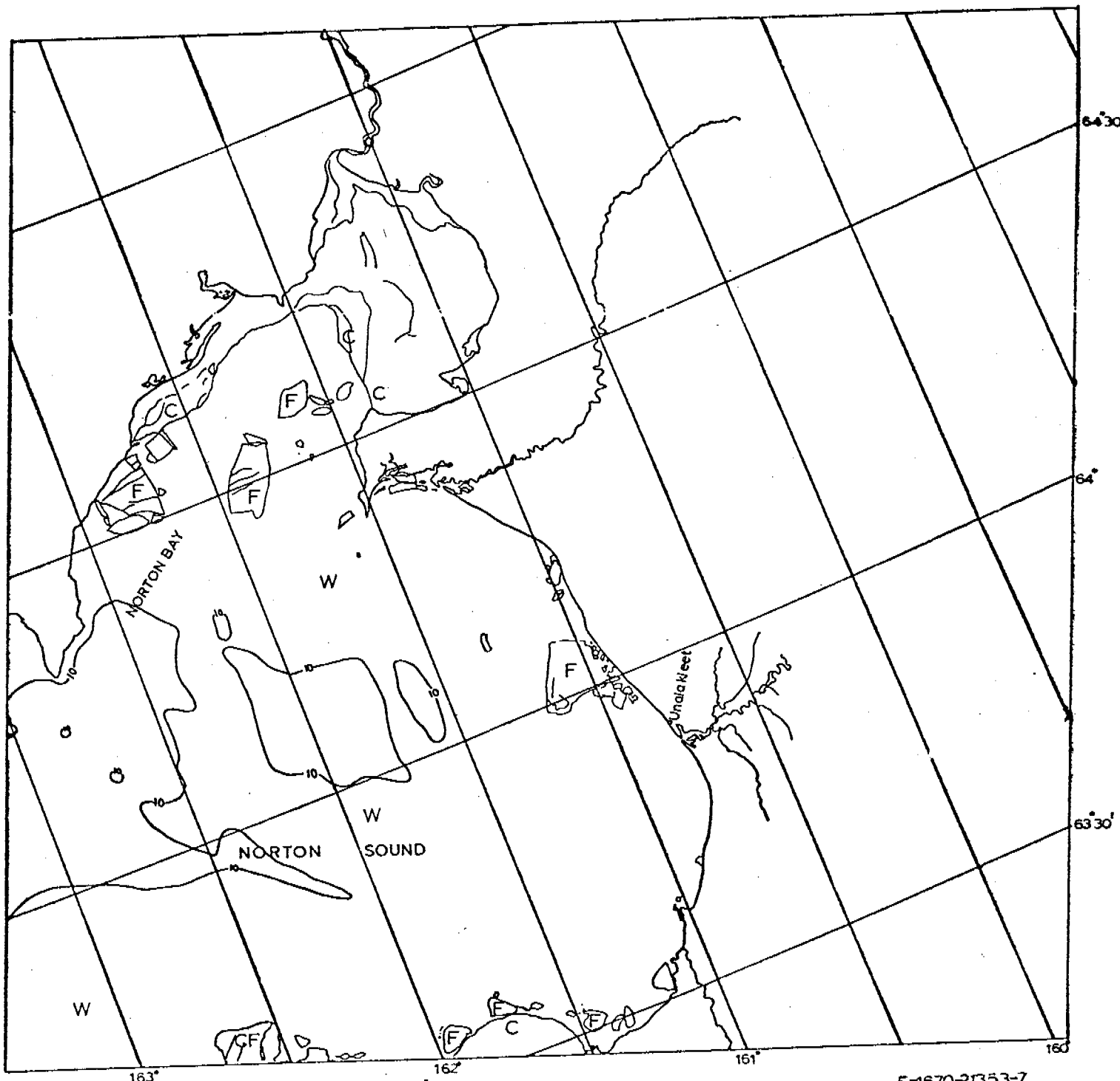


KILOMETERS  
0 10 20 30 40 50  
SCALE APPROX 1:1,000,000

BERING SEA

**Scene 1670-21353**

Norton Sound in this scene is almost completely ice-free, with the exception of Norton Bay, which is still filled with contiguous ice and a few floes; and other floes can be seen around the shore edges of the Sound.



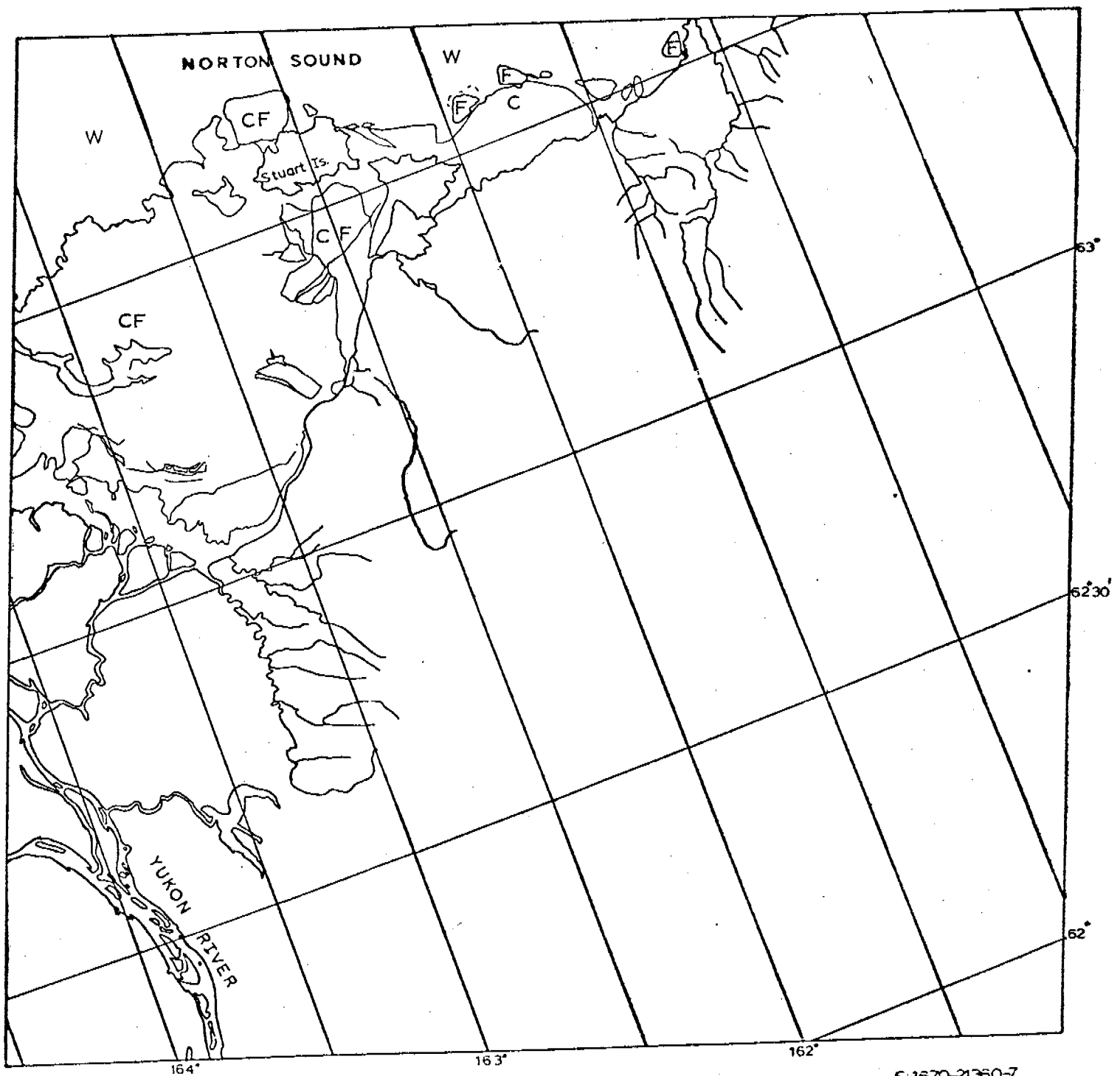
E-1670-21353-7  
 24 MAY 1974

KILOMETERS  
 0 10 20 30 40 50  
 SCALE APPROX 1:1,000,000

## BERING SEA

Scene 1670-21360

This scene shows the area just north of the Yukon River. The only ice that is left by this time is some cracked and fragmented contiguous ice.



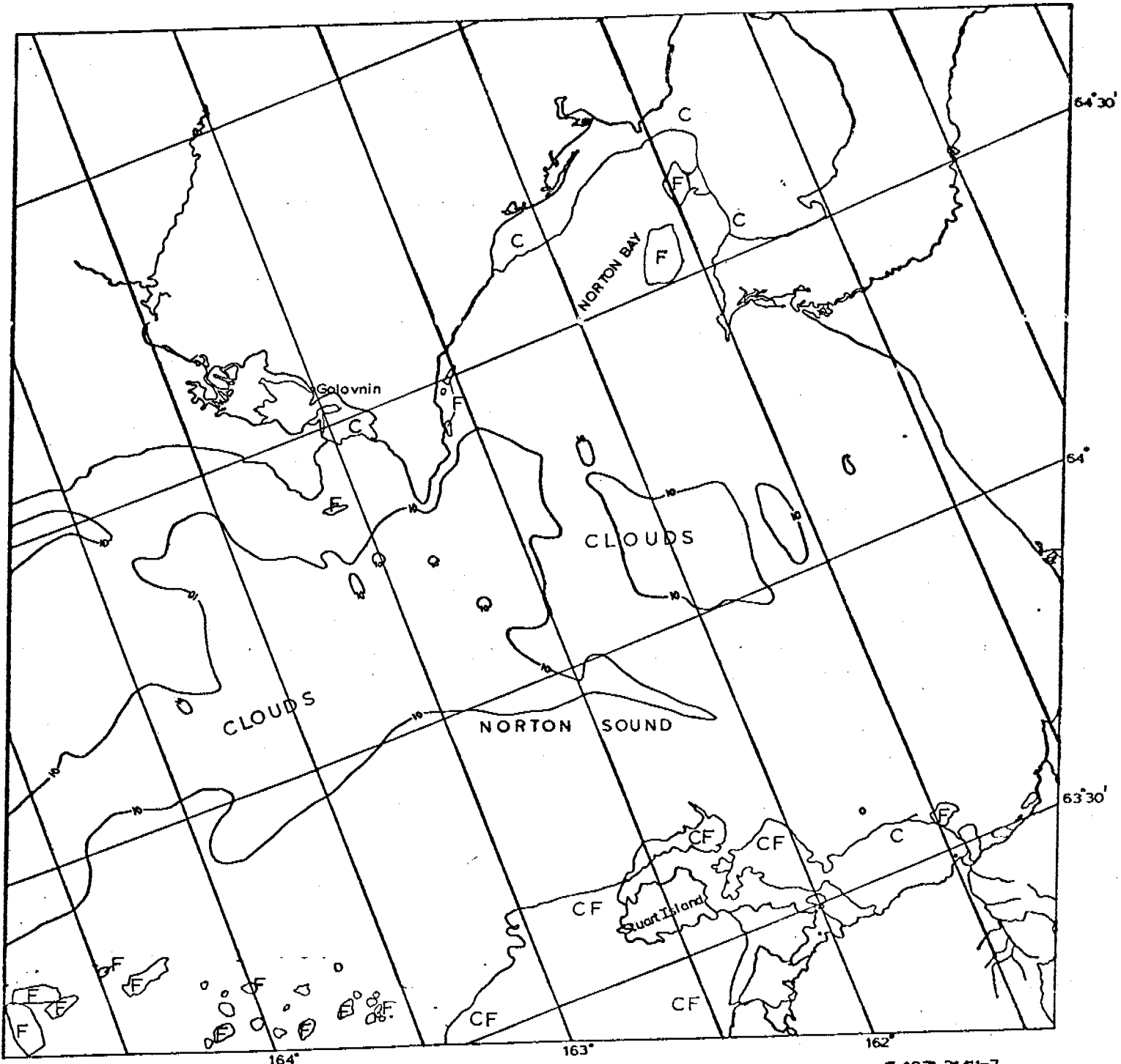
E-4670-21360-7  
24 MAY 1974

KILOMETERS  
0 10 20 30 40 50  
SCALE APPROX 1:1,000,000

BERING SEA

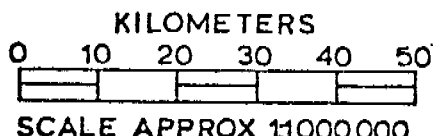
Scene 1671-21411

This scene of Norton Sound is dominated by the low pressure cloud system which obscures most of the image. However, as on the previous day, contiguous ice with a few floes can be seen in Norton Bay. North of the Yukon River the contiguous ice is fragmented and broken. There are numerous floes extending northwestward from this fragmented ice, apparently breaking loose from it.



E-167-21411-7

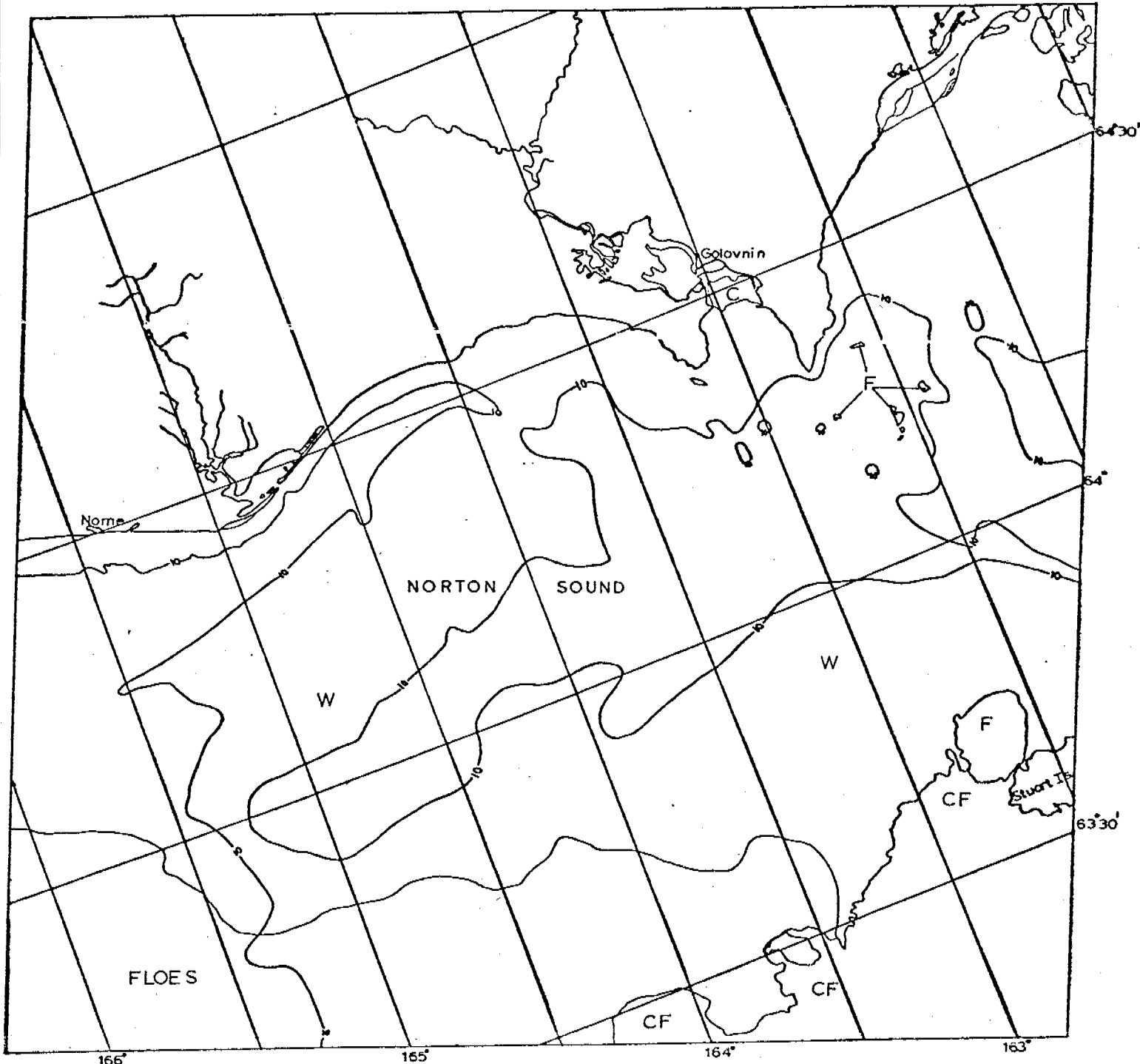
25 MAY 1974



## BERING SEA

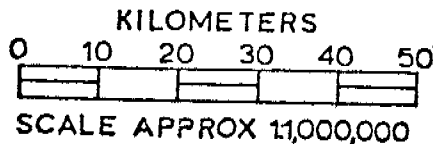
Scene 1672-21470

This scene of western Norton Sound is nearly ice-free with some broken and fragmented contiguous ice between Stuart Island and the Yukon Delta. There are numerous floes ranging from 10 km to less than 100 meters in diameter extending northwestward from this contiguous ice. There is still contiguous ice in Norton Bay and Galovnin Bay.



E-1672-21470-7

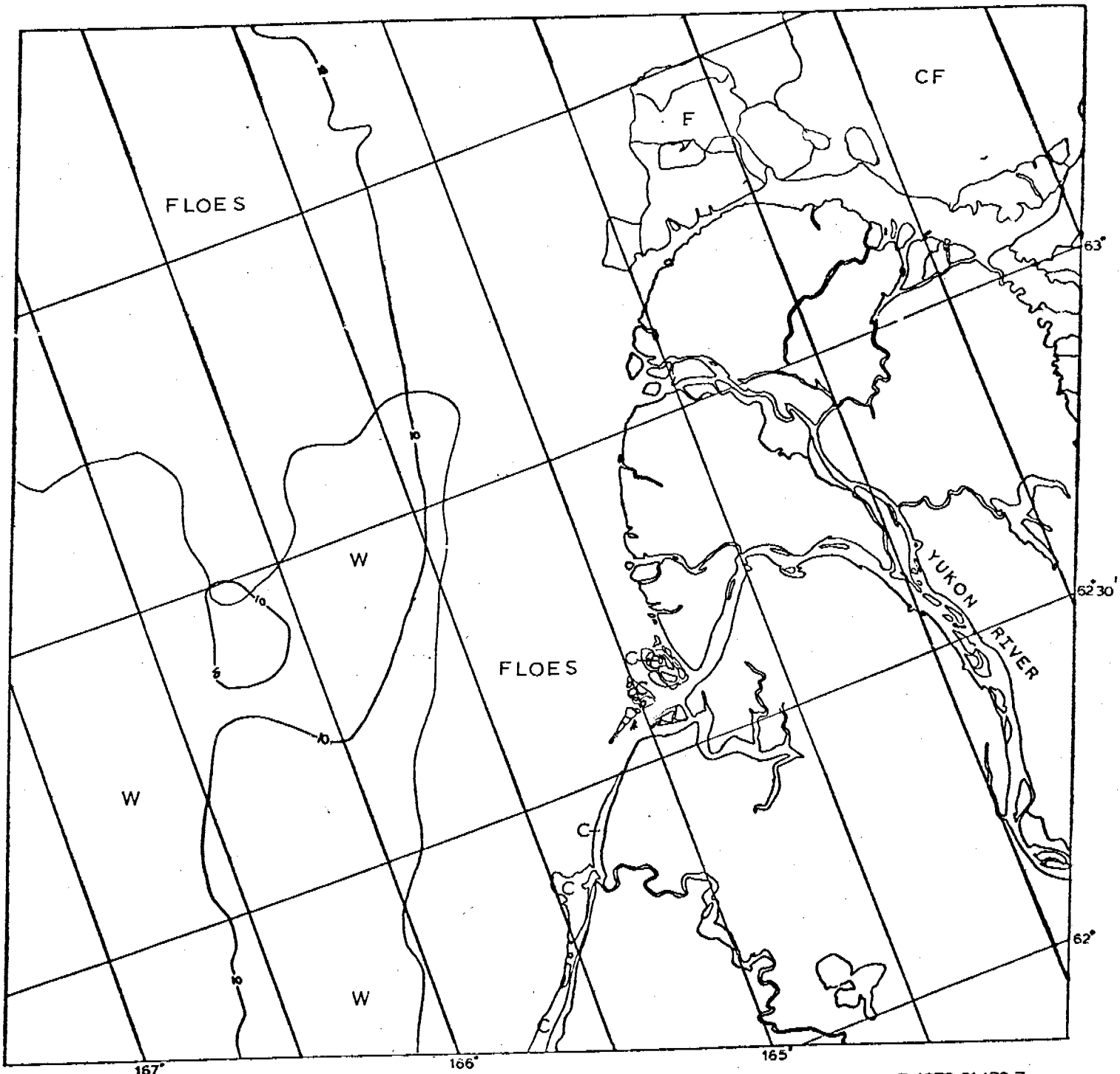
26 MAY 1974



## BERING SEA

Scene 1672-21472

This scene west of the Yukon Delta contains numerous ice floes and shows the fragmenting and breaking off of the floes from the contiguous ice north of the delta. There is a thin shelf of contiguous ice along the shore south of the delta.



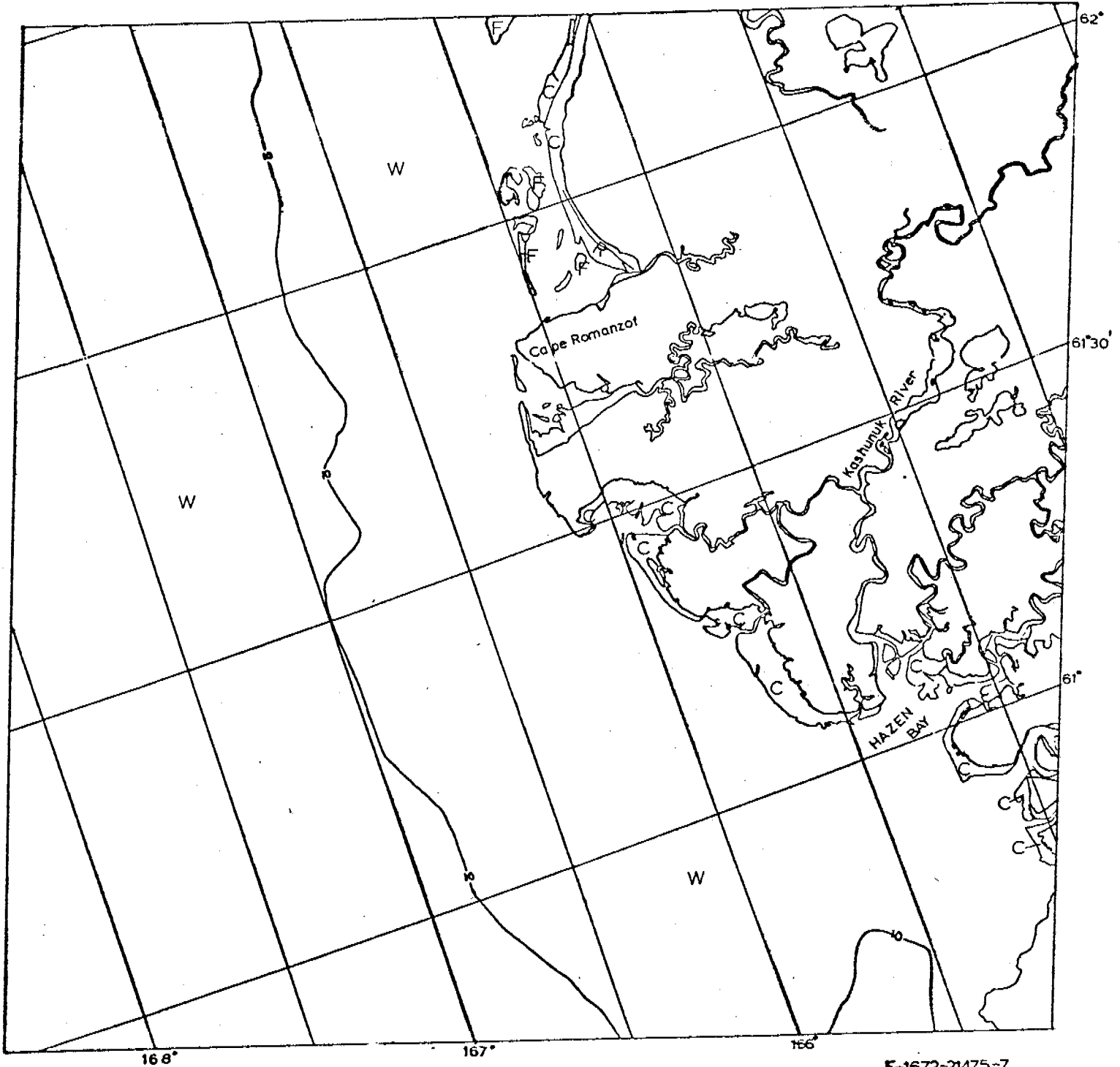
E-1672-21472-7  
26 MAY 1974

KILOMETERS  
0 10 20 30 40 50  
SCALE APPROX 1:1,000,000

## BERING SEA

Scene 1672-21475

Only a thin shelf of fast ice along the shore is left in this scene  
with the exception of a few floes near the top of the image.



E-1672-21475-7

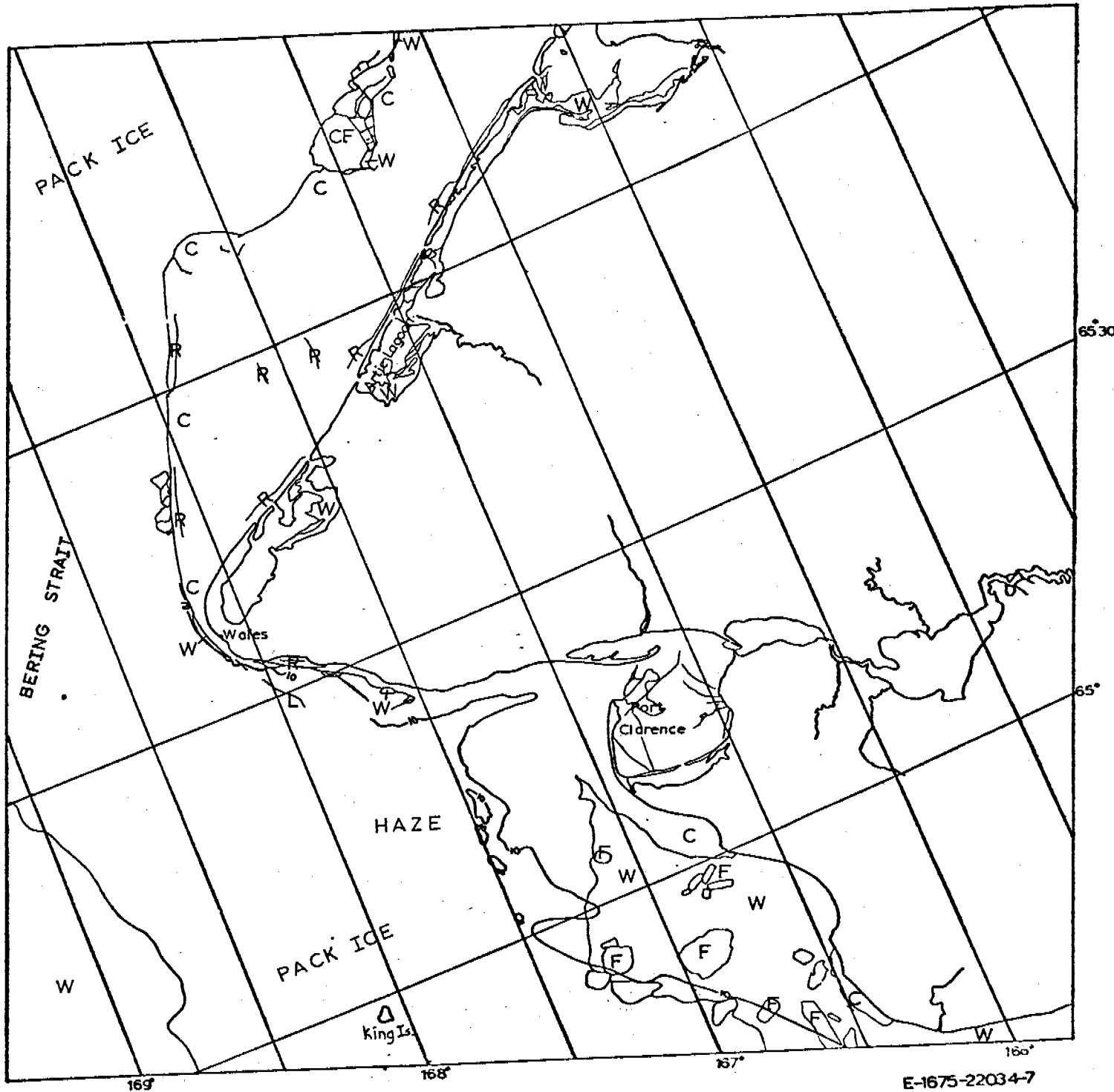
26 MAY 1974

KILOMETERS  
0 10 20 30 40 50  
SCALE APPROX 1:1,000,000

## BERING SEA

Scene 1675-22034

This scene is of the western tip of the Seward Peninsula and the eastern Bering Strait. There is a large piece of contiguous ice on the northern side of the Seward Peninsula, and some contiguous ice filling the approach to Port Clarence, which is ice-covered. There are a few ridges at the edge of the contiguous ice and near shore. Most of the rest of the water in this scene is filled with pack ice, with open water to the west. There is also open water to the south of the Seward Peninsula, with some ice floes in it. The lower part of the image is obscured by a light haze, making it difficult to see details.



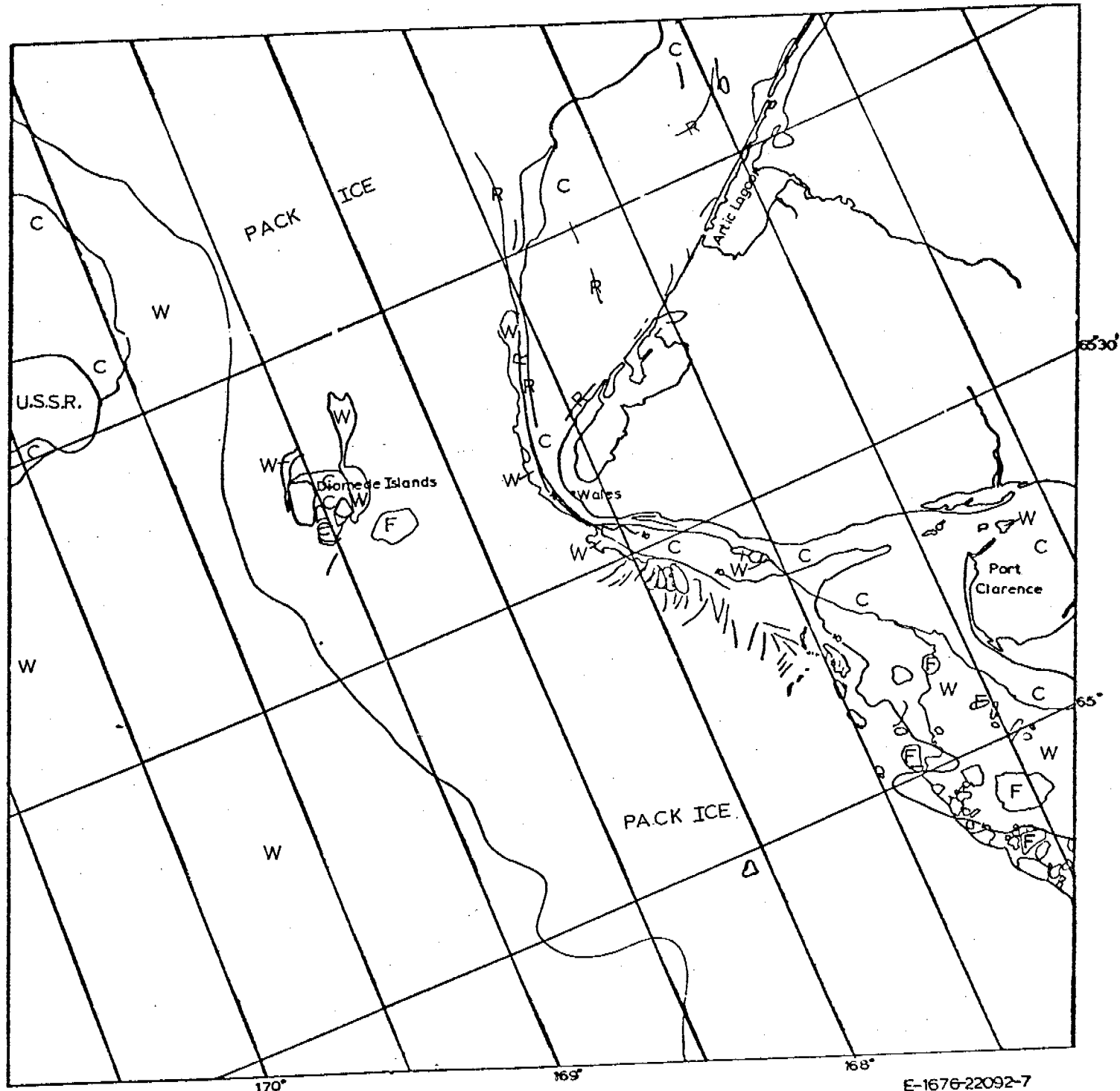
KILOMETERS  
0 10 20 30 40 50  
SCALE APPROX 1:1,000,000

## BERING SEA

557

Scene 1676-22092

This scene is just west of the previous one and includes the western tip of the Chukotsk Peninsula in Siberia. The eastern half of the Bering Strait is choked with a matrix of pack ice containing various sized ice floes. This matrix extends southward past Port Clarence. The sky has cleared up and the extent of the contiguous ice can now be seen. An arcuate pattern of lines can be seen in the pack ice next to the contiguous ice west of Port Clarence, indicating a shearing motion against the contiguous ice. This indicates that the pack ice is moving south. There is some contiguous ice between the Diomede Islands. Numerous ridges can be seen in the contiguous ice north of the Seward Peninsula and the outermost ones appear to follow the 10-fathom contour.

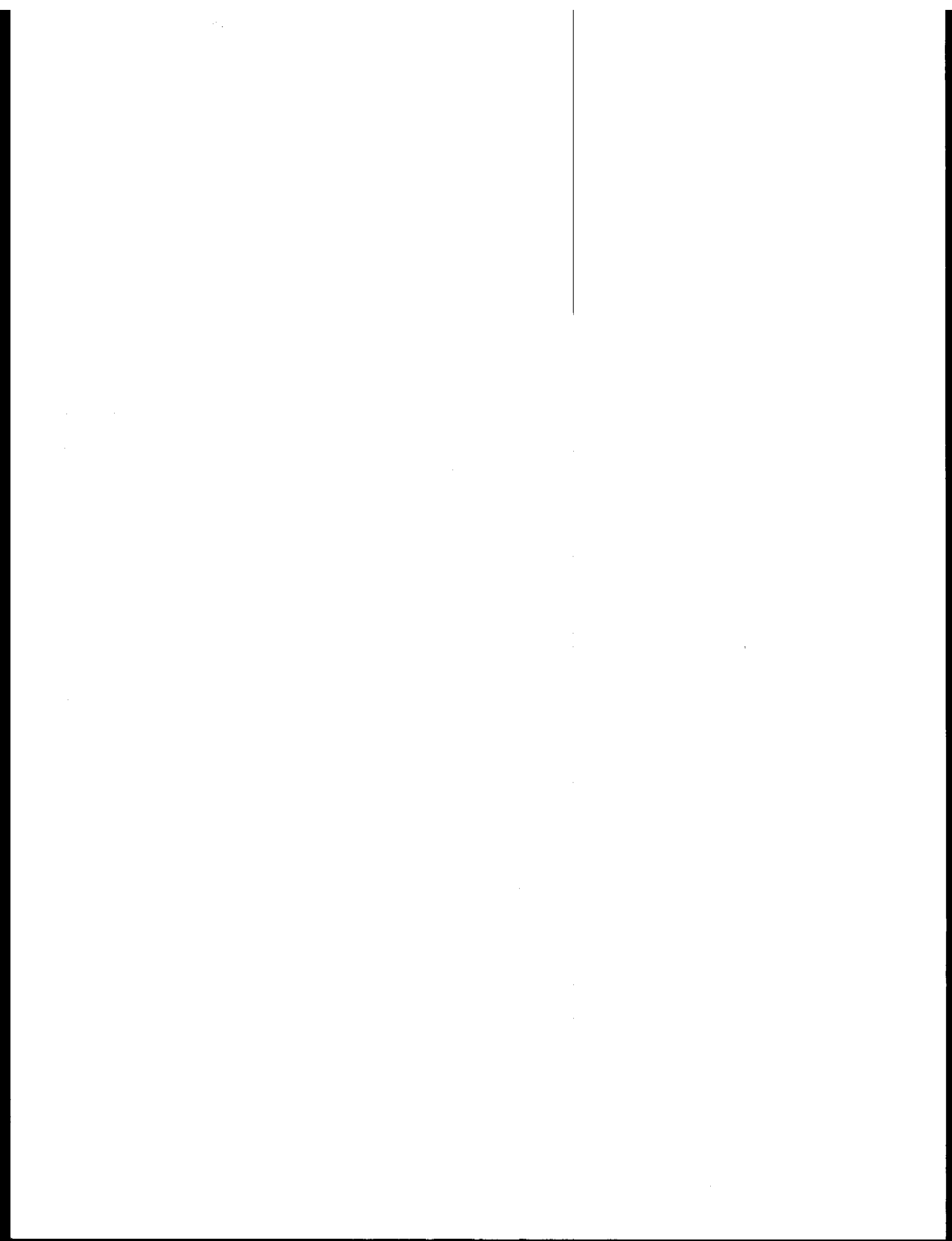


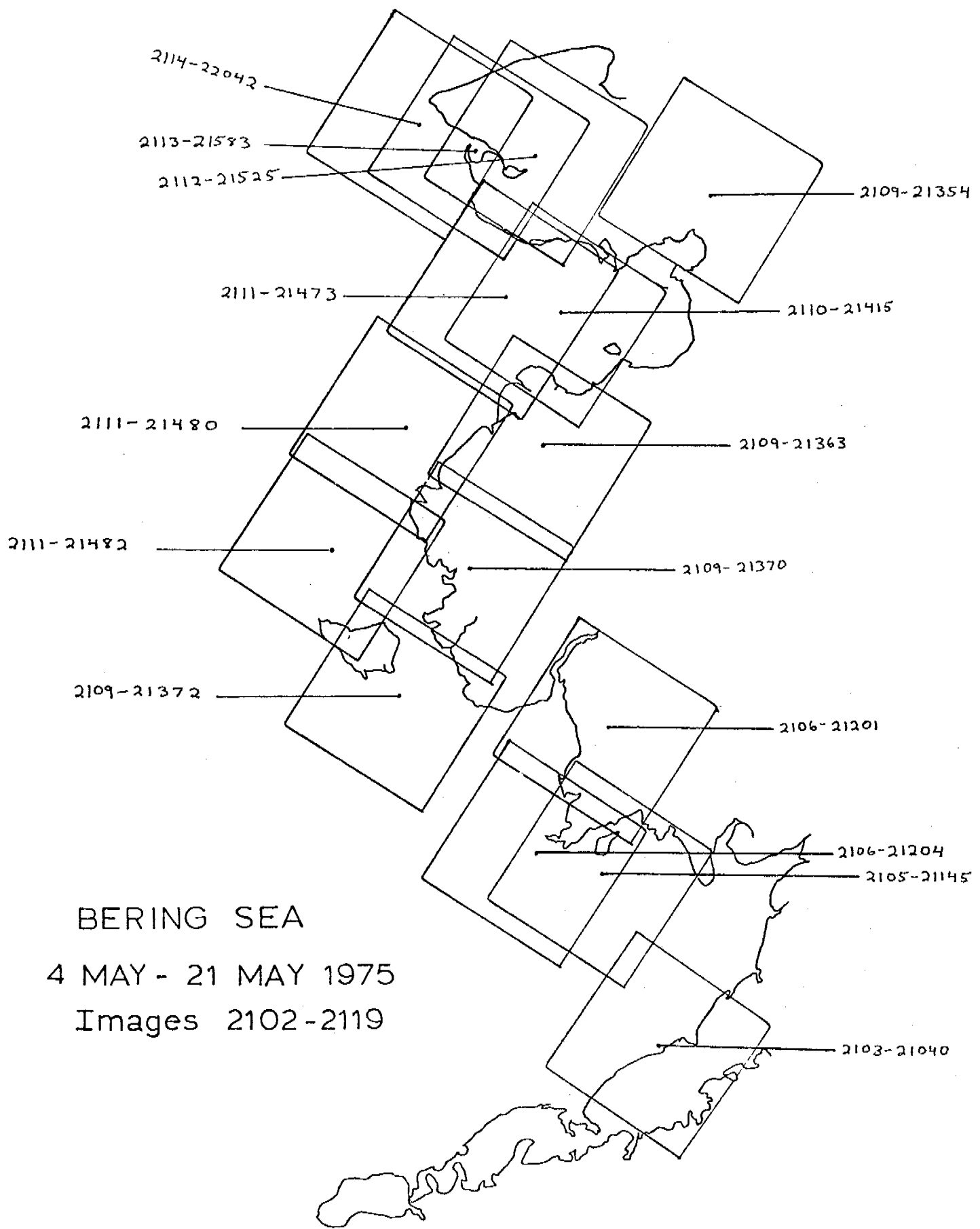
E-1676-22092-7

30 MAY 1974

KILOMETERS  
 0 10 20 30 40 50  
 SCALE APPROX 1,000,000

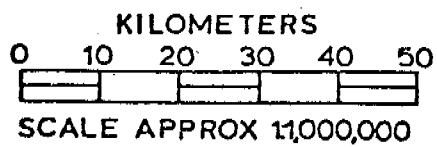
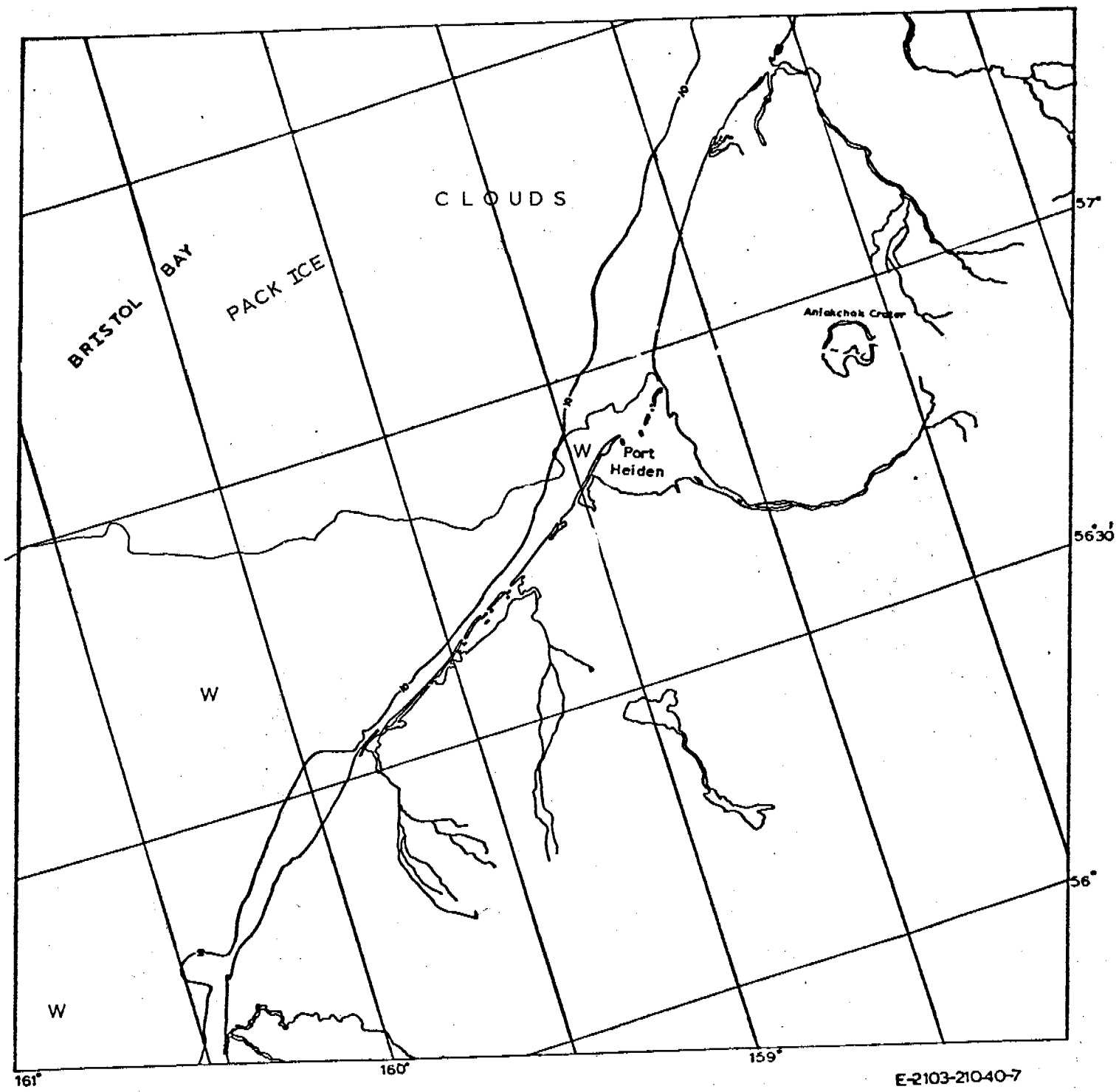
## BERING SEA





Scene 2103-21040

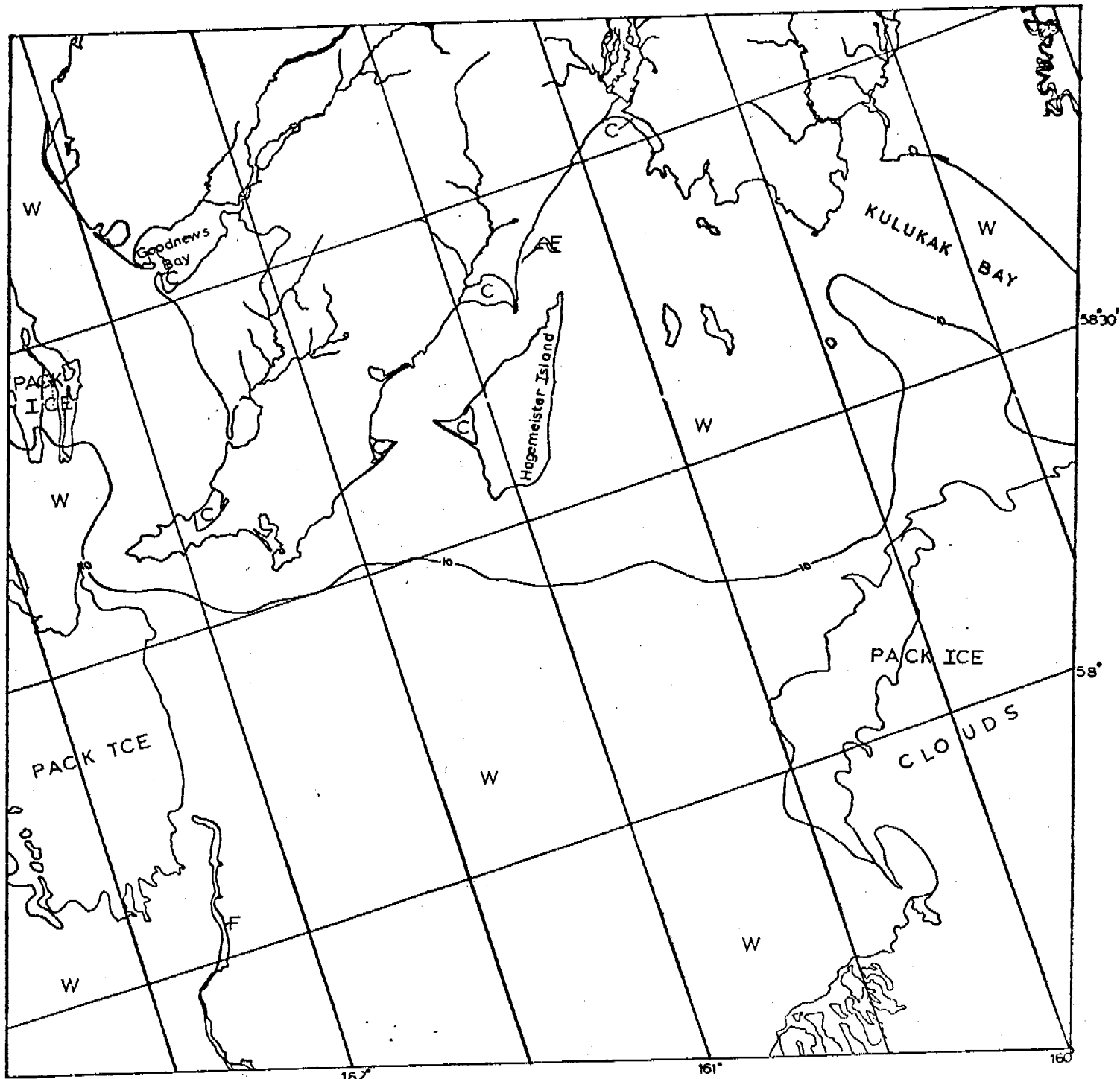
Clouds obscure most of the shoreline, but what can be seen appears to be free of shorefast ice. The pack ice appears to be limited to the north half of the scene with open water to the south.



BERING SEA

Scene 2105-21145

What contiguous ice remains is confined to small coves and inlets such as at Goodnews Bay and on Hagemeister Island. There is some pack ice present, although it appears to be melting rapidly and is not too extensive. The pack ice on the eastern side of the scene is mostly just ribbon-like remnants, although it is partially obscured by clouds.

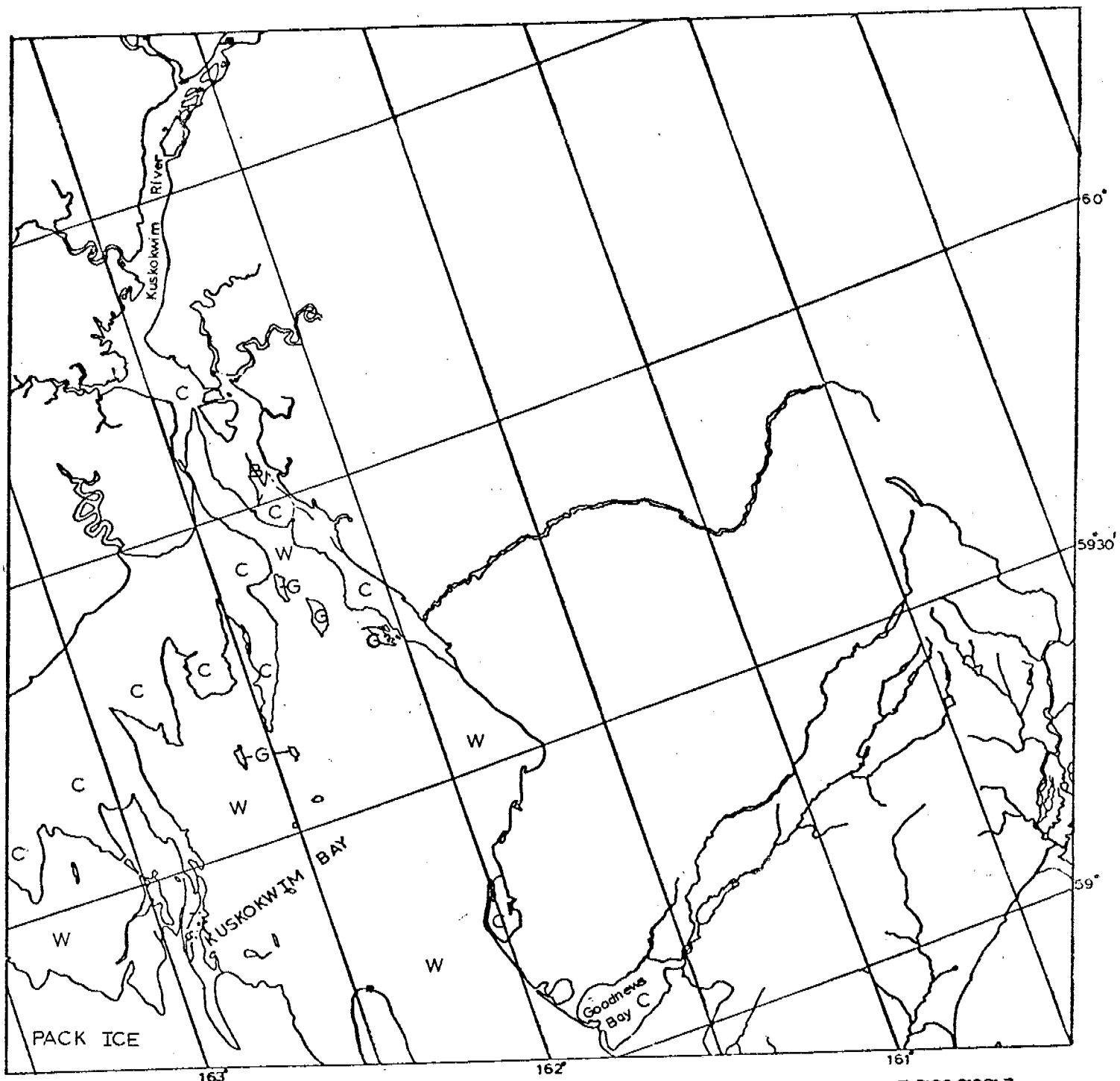


KILOMETERS  
0 10 20 30 40 50  
SCALE APPROX 11,000,000

## BERING SEA

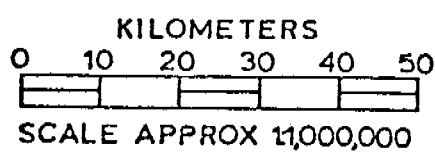
Scene 2106-21201

The contiguous ice remaining on the north side of Kuskokwim Bay is grounded in very shallow water. The water in this region, according to USC&GS nautical charts is less than a fathom deep. The floes marked "G" are grounded on shoals.



E-2106-21201-7

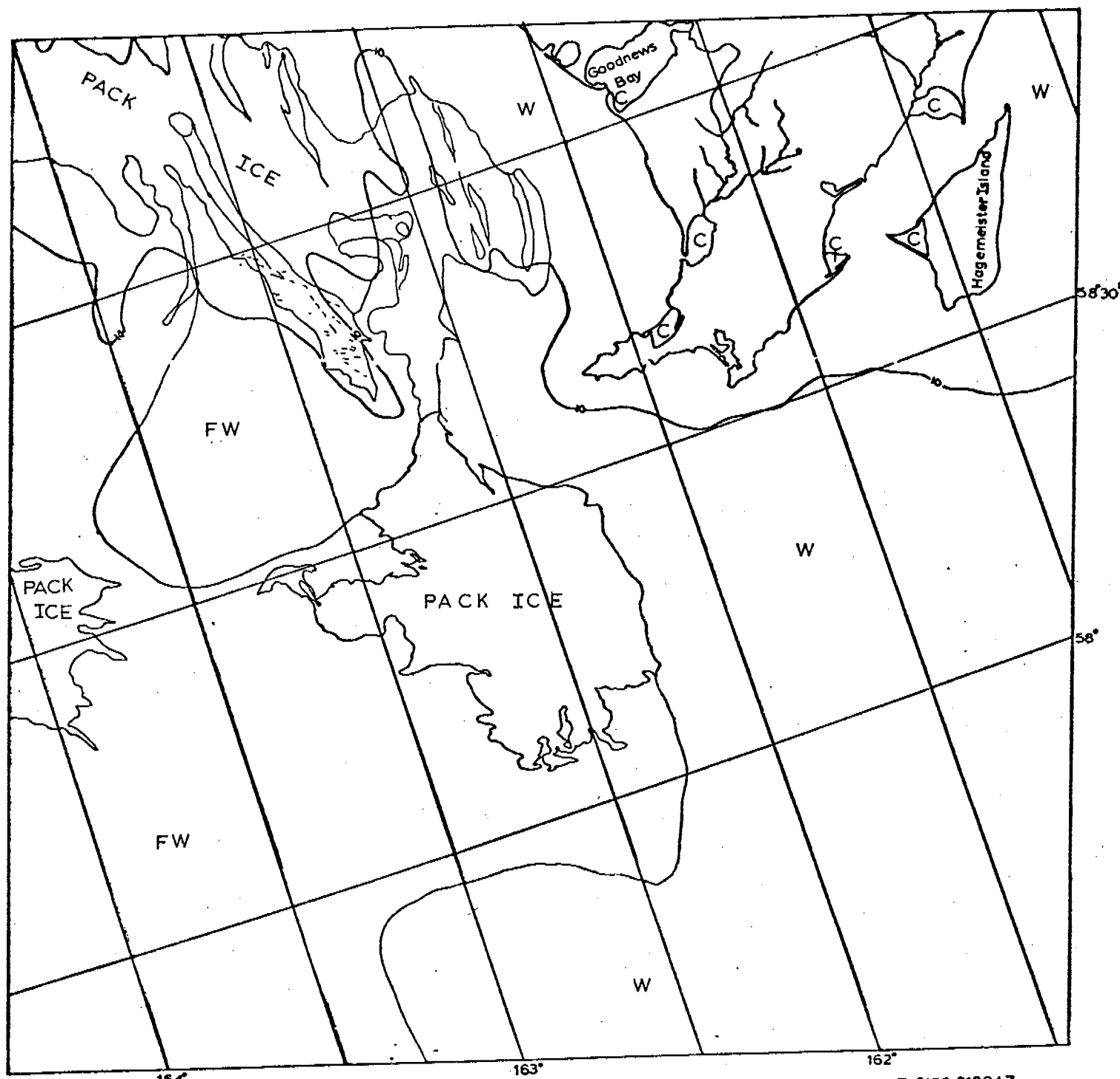
8 MAY 1975



## BERING SEA

**Scene 2106-21204**

The only contiguous ice remaining in this scene is in small bays and inlets. The pack ice is almost gone, with two small areas of consolidated ice and a large area of water containing loose, ribbon-like floes. Details are obscured by high clouds.



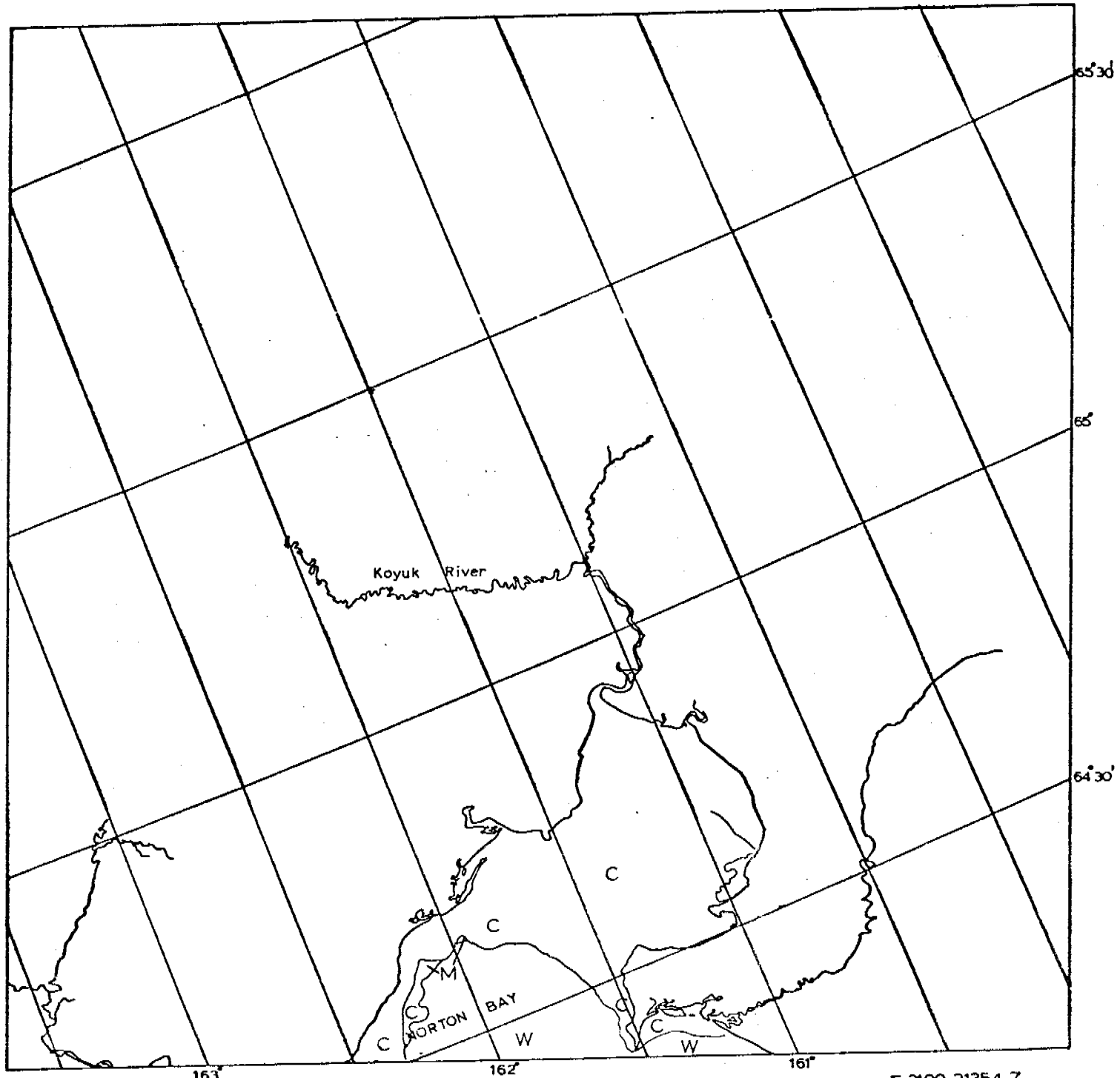
E-2106-212047  
8 MAY 1975

KILOMETERS  
0 10 20 30 40 50  
SCALE APPROX 1:1,000,000

## BERING SEA

Scene 2109-21354

The northern part of Norton Bay is filled with solid contiguous ice. A small shelf of new ice has formed on the western side. To the south is open water.



E-2109-21354-7

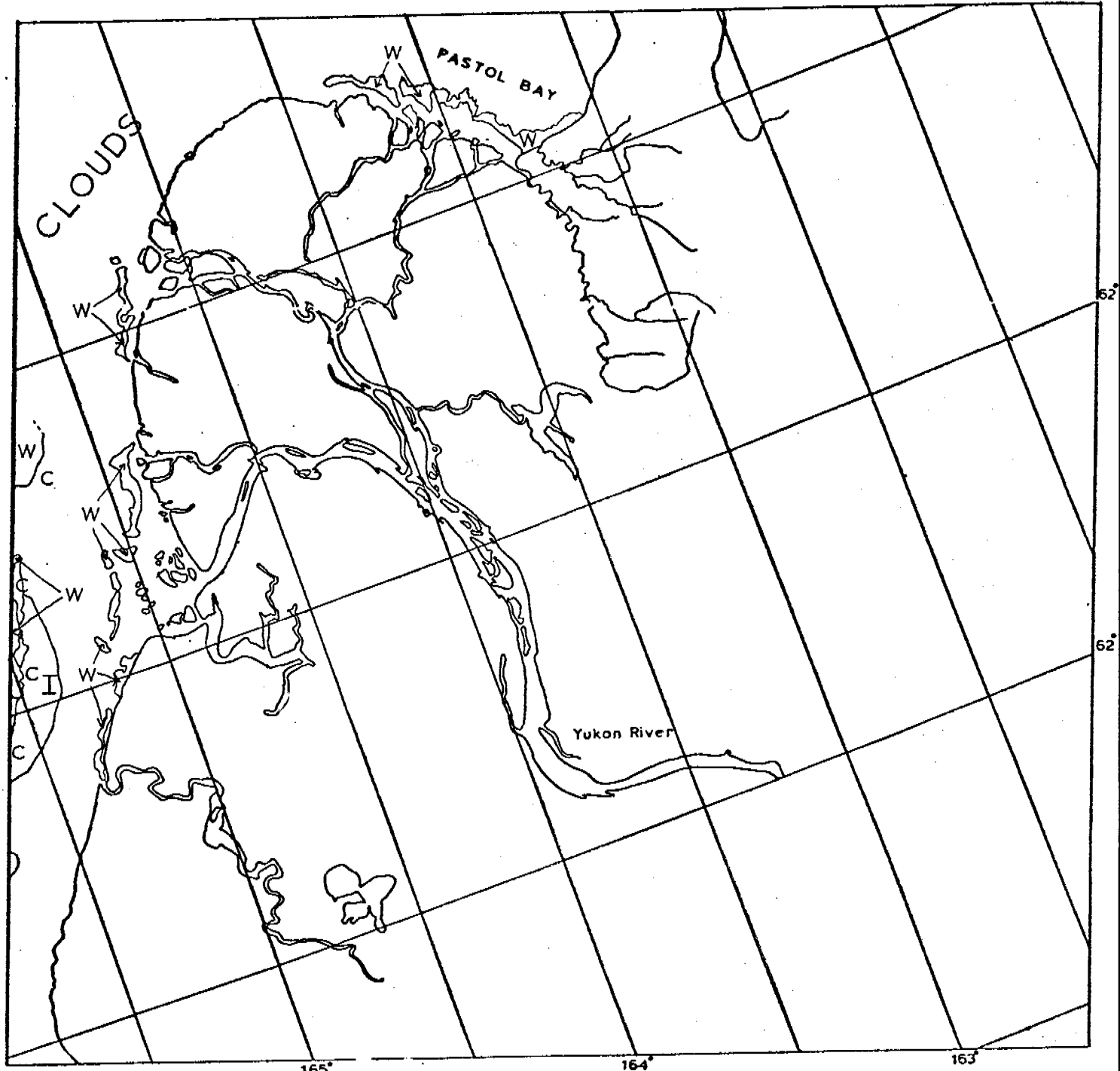
11 MAY 1975

KILOMETERS  
0 10 20 30 40 50  
SCALE APPROX 1:1,000,000

BERING SEA

Scene 2109-21363

Clouds obscure the northwestern part of this scene. The areas marked "W" close to shore are either patches of open water melted through by river water or else water on top of the ice. The shelf of contiguous ice is approximately 10-20 km wide here with a small extension of younger ice seen to the west.



KILOMETERS  
0 10 20 30 40 50  
SCALE APPROX 1:1,000,000

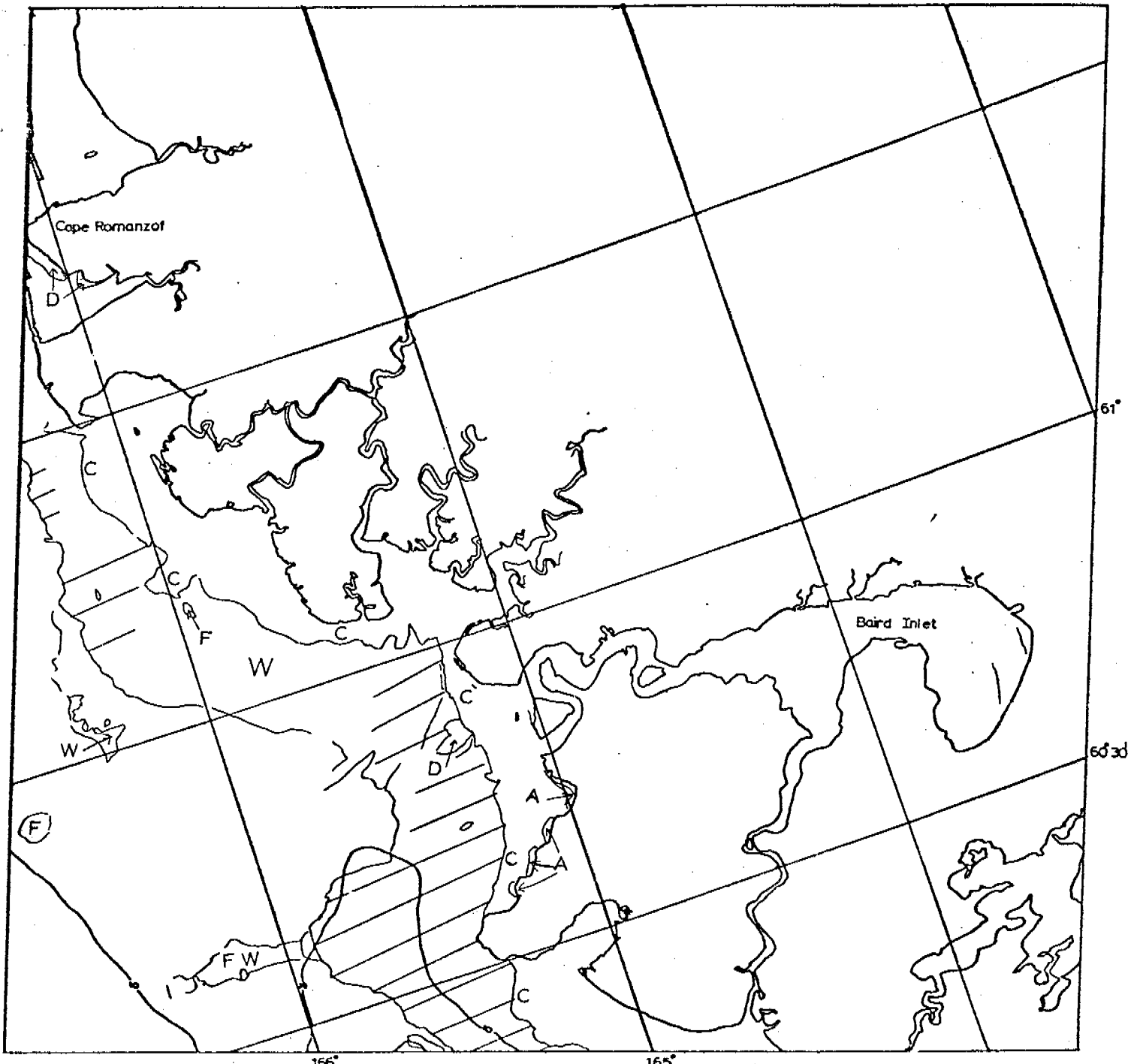
BERING SEA

E-2109-21363-7  
11 MAY 1975

Scene 2109-21370

The pack ice in this scene south of Cape Romanzof is separated from shore by an expanse of open water varying from 10 to 20 kilometers in width. The pack ice itself varies from a mixture of small pans and floes in a fine matrix of ground-up and subsequently frozen ice in the southern part of the image to more broken up ice with large floes to the north.

Not too much detail can be gleaned from the image about the shorefast ice, except that it does exist. The shelf of shorefast ice is up to 10 kilometers in width along the more sheltered sections of coast and is nonexistent along the most exposed sections. At the mouth of Baird Inlet, a small protrusion of decayed pack ice has attached itself to the shorefast ice. At the boundary of beach/shorefast ice in some locales, fresh water runoff has overflowed onto the the ice in areas up to a kilometer wide. These can be seen south of the mouth of Baird Inlet.



denotes Open Water

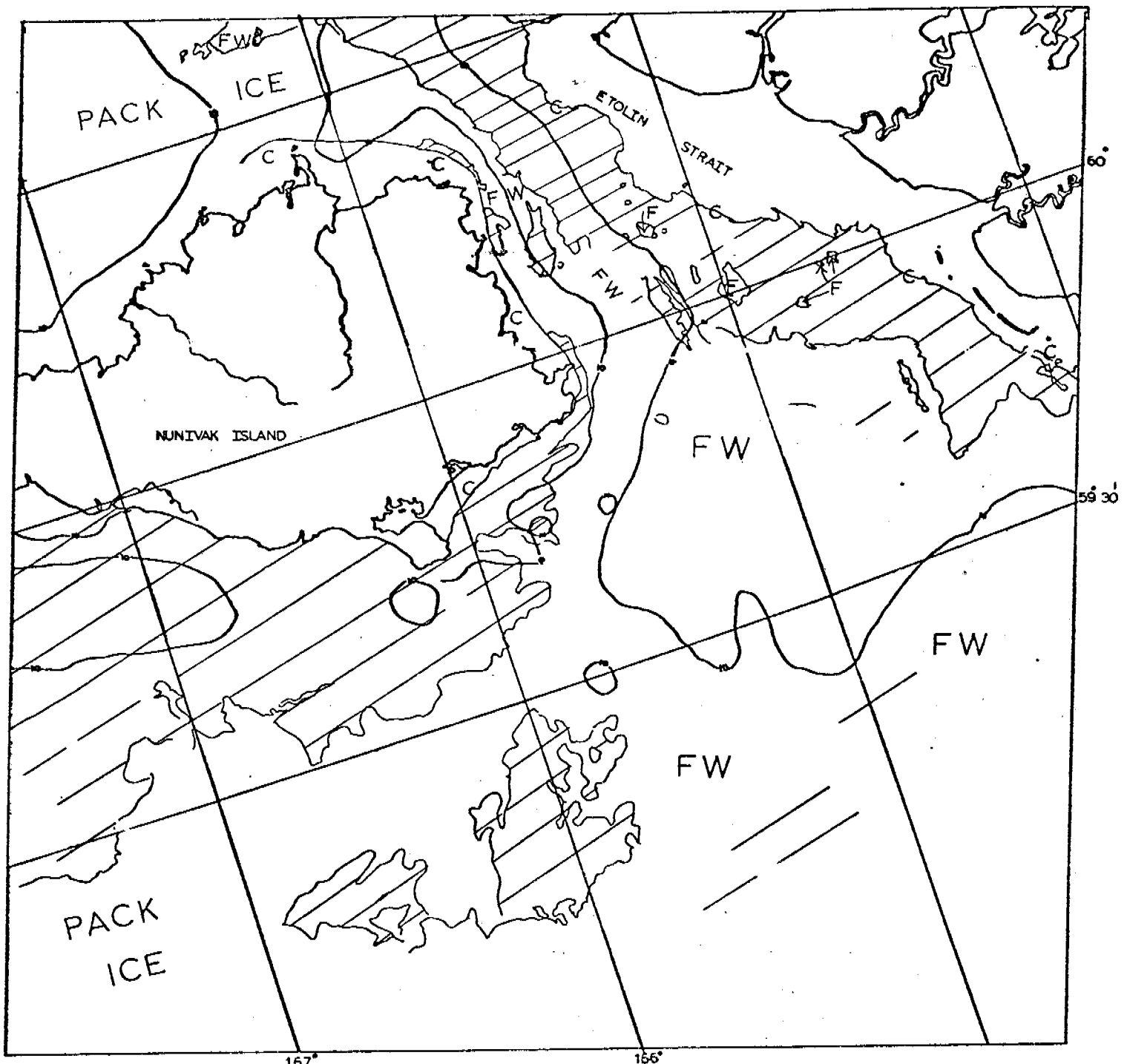
E-2109-21370-6  
11 MAY 1975

KILOMETERS  
 0 10 20 30 40 50  
  
SCALE APPROX 1:1,000,000

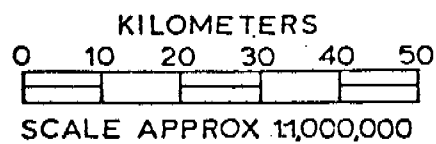
## BERING SEA

Scene 2109-21372

This LANDSAT scene, including Nunivak Island, shows the pack ice very dispersed. It consists of swirl patterns of very small floes and broken up ice, with some scattered, more densely packed areas. There are a few larger floes scattered about. On the north side of Nunivak Island the pack ice is more densely packed and is up against the contiguous ice, making the boundary difficult to ascertain. The shelf of contiguous ice on Nunivak Island is up to 8 kilometers wide in the sheltered areas. Inside Etolin Strait on the mainland side, the contiguous ice extends out up to 15 kilometers from shore. No details can be seen. The edge of the shelf of contiguous ice is rather irregular, indicating the pack ice pulled away from it rather than sheared off.



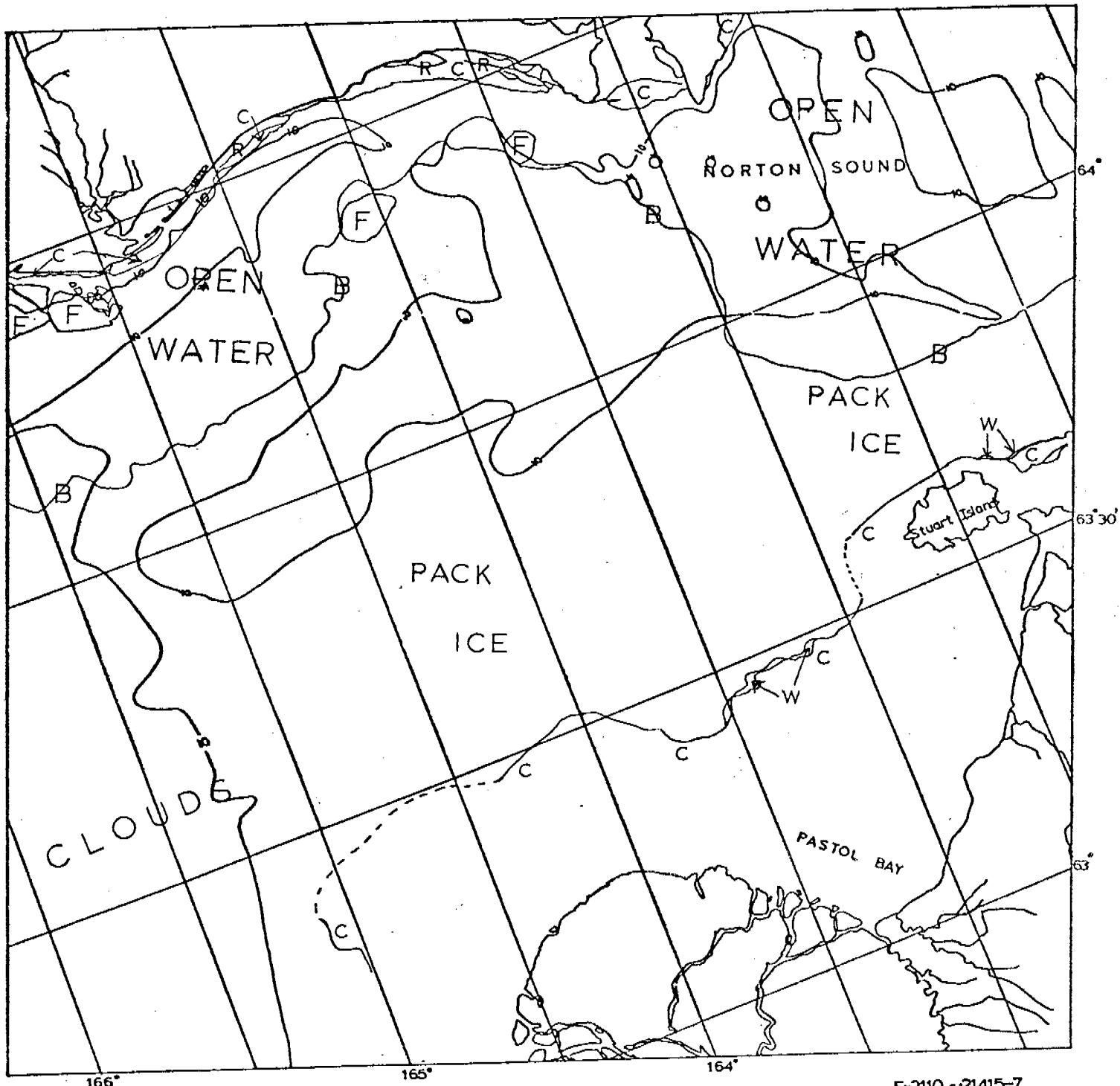
E-2109-21372-6  
11 MAY 1975



BERING SEA

Scene 2110-21415

A thin shelf of contiguous ice exists on the northern side of Norton Sound. In places the edge of the ice corresponds to the 10-fathom contour, while in other places there is no correspondence at all. A much thicker shelf appears to exist off the Yukon Delta; however, clouds obscure the area so that details cannot be seen. The pack ice, consisting of a broken matrix of floes in first year ice is adjacent to this shelf, while there is a wide stretch of open water between the pack and the northern shore. "B" indicates the boundary between the pack ice and the open water.



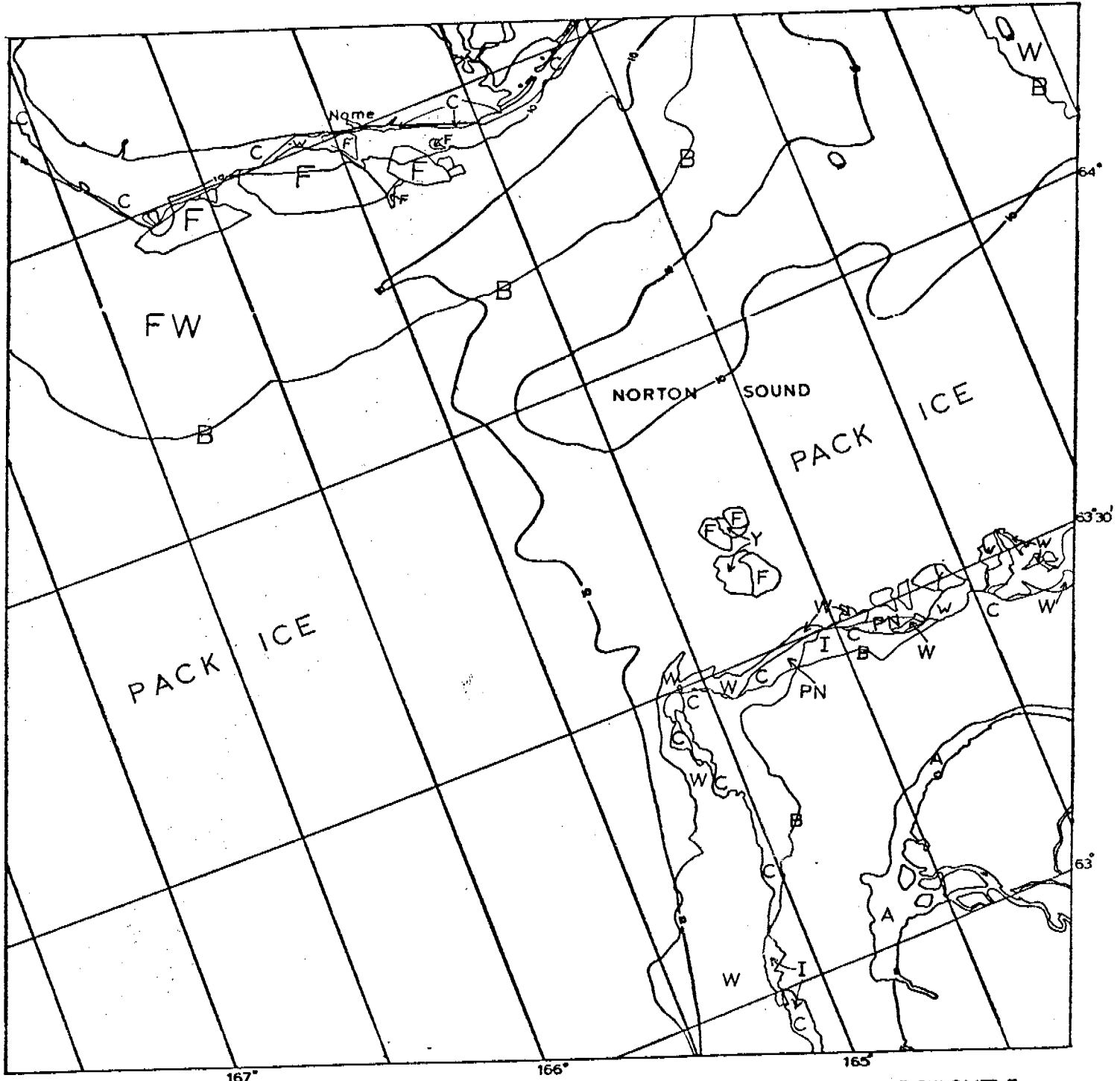
E-2110 -21415-7  
 12 MAY 1975

KILOMETERS  
 0 10 20 30 40 50  
 SCALE APPROX 11,000,000

BERING SEA

Scene 2111-21473

Several large chunks of contiguous ice off Nome have broken off and are drifting westward, leaving only a narrow apron of fast ice. The edge of the contiguous ice shelf approximated the location of the 10-fathom contour before breaking off. A rather thick shelf of contiguous ice still exists off the Yukon River Delta at this time. Several different ages of ice can be seen, with some river water overflow at the mouths of the river, marked "A". The pack ice, consisting of a broken matrix of pans and first year ice grading westward into unconsolidated floes is separated from the attached ice by open water.



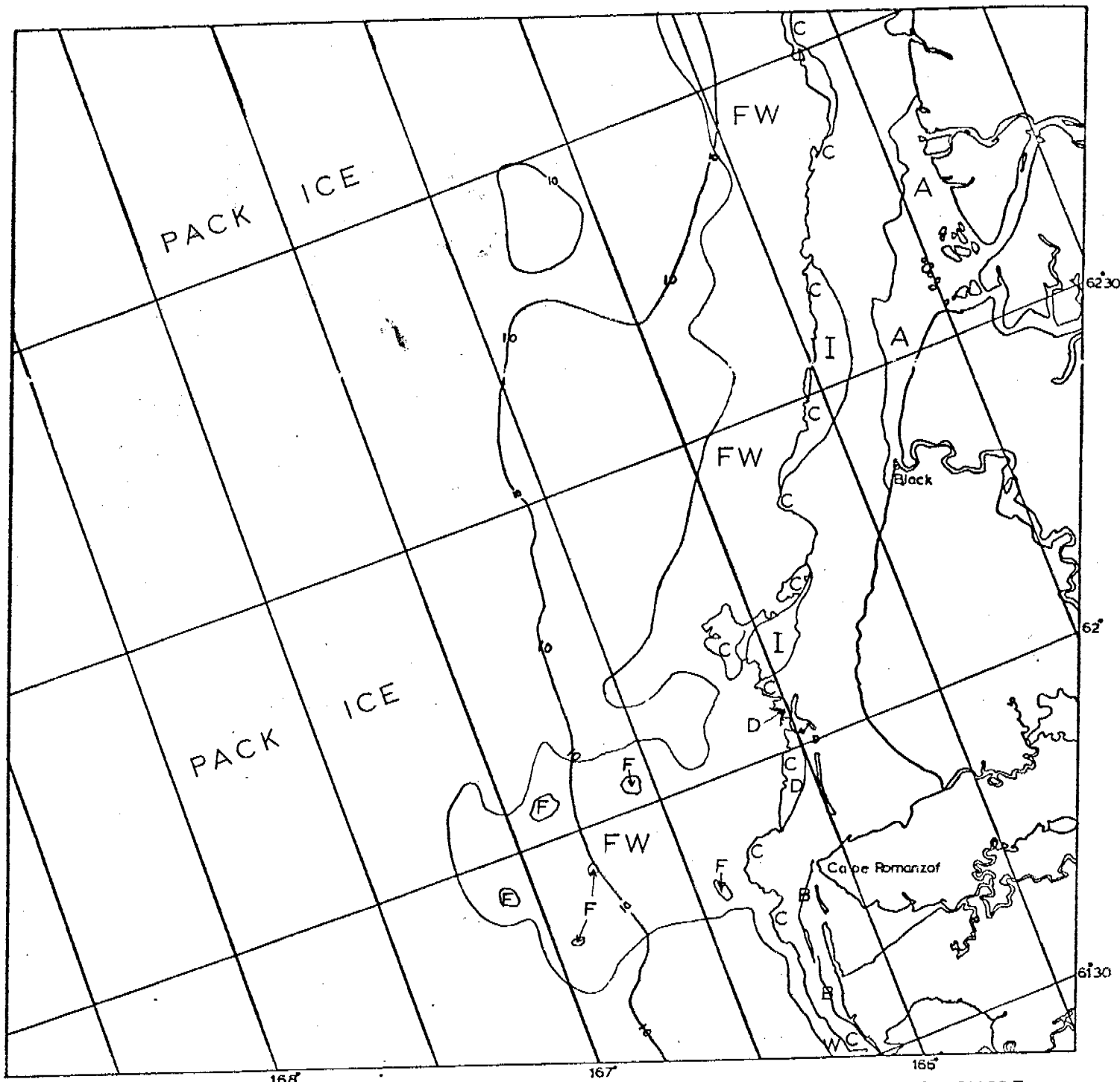
E-211-21473-7  
13 MAY 1975

KILOMETERS  
0 10 20 30 40 50  
SCALE APPROX 1:1,000,000

BERING SEA

Scene 2111-21480

The contiguous ice is approximately 15 kilometers wide at its widest, narrowing down to a few kilometers off Dall Point. On the seaward edge, areas of younger ice can be seen. A crescent-shaped section of what appears to be old, decayed ice with large ponds of standing water is located along the edge of the contiguous ice just north of Cape Romanzof. Open water is 15 to 20 kilometers wide, containing some loose floes, separates the pack ice from the contiguous ice. The pack ice grades from relatively consolidated floes in a matrix of first year ice in the east to less consolidated, larger floes in the west.

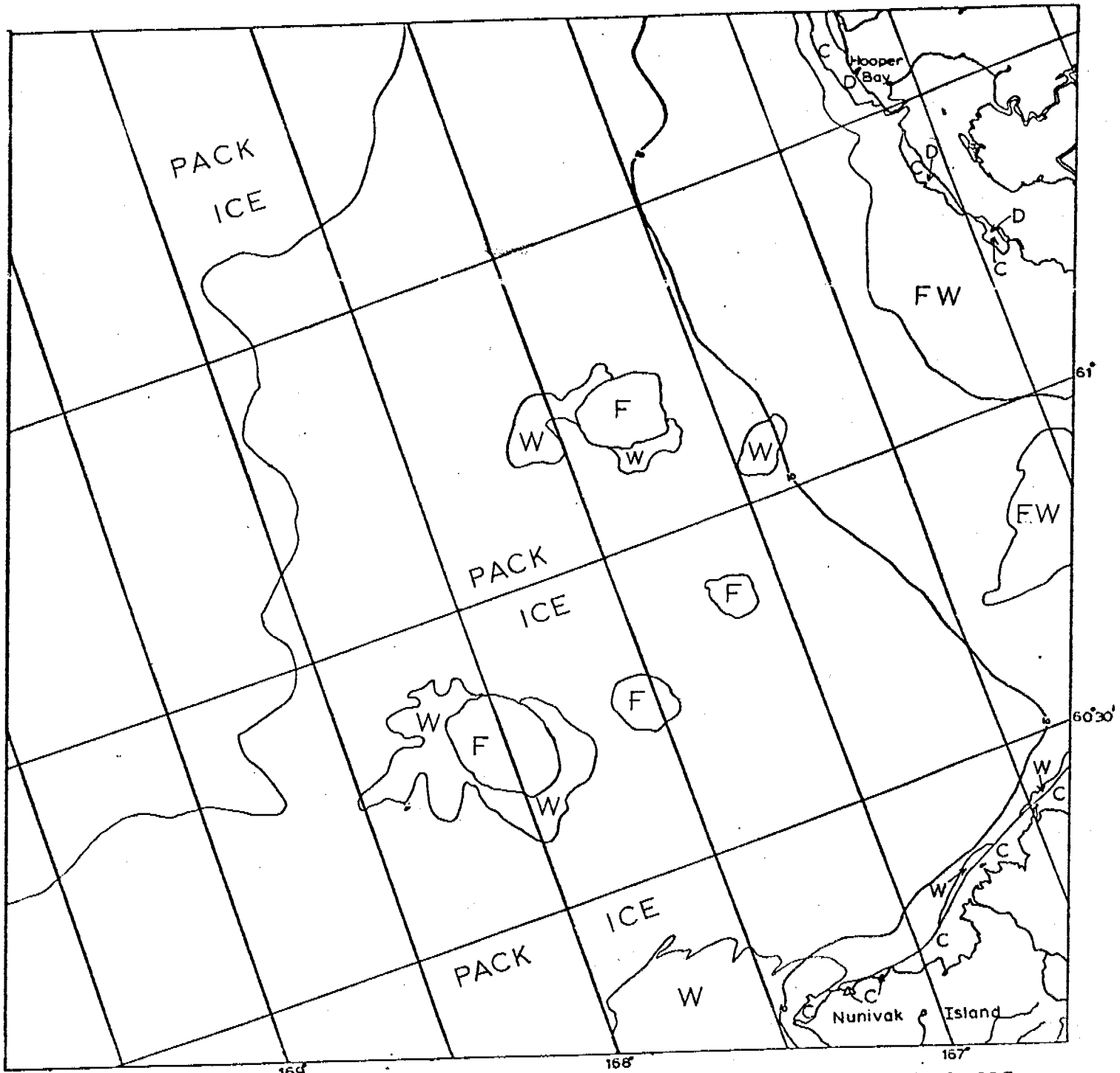


KILOMETERS  
 0 10 20 30 40 50  
 SCALE APPROX 1:1,000,000

BERING SEA

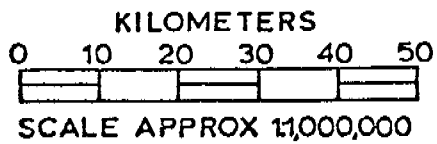
**Scene 2111-21482**

Some decayed ice remains attached to the rest of the contiguous ice in the vicinity of Hooper Bay. The pack ice grades east to west from a close-packed matrix of small floes and first year ice to unconsolidated floes of somewhat larger average size.



E-2111-21482-7

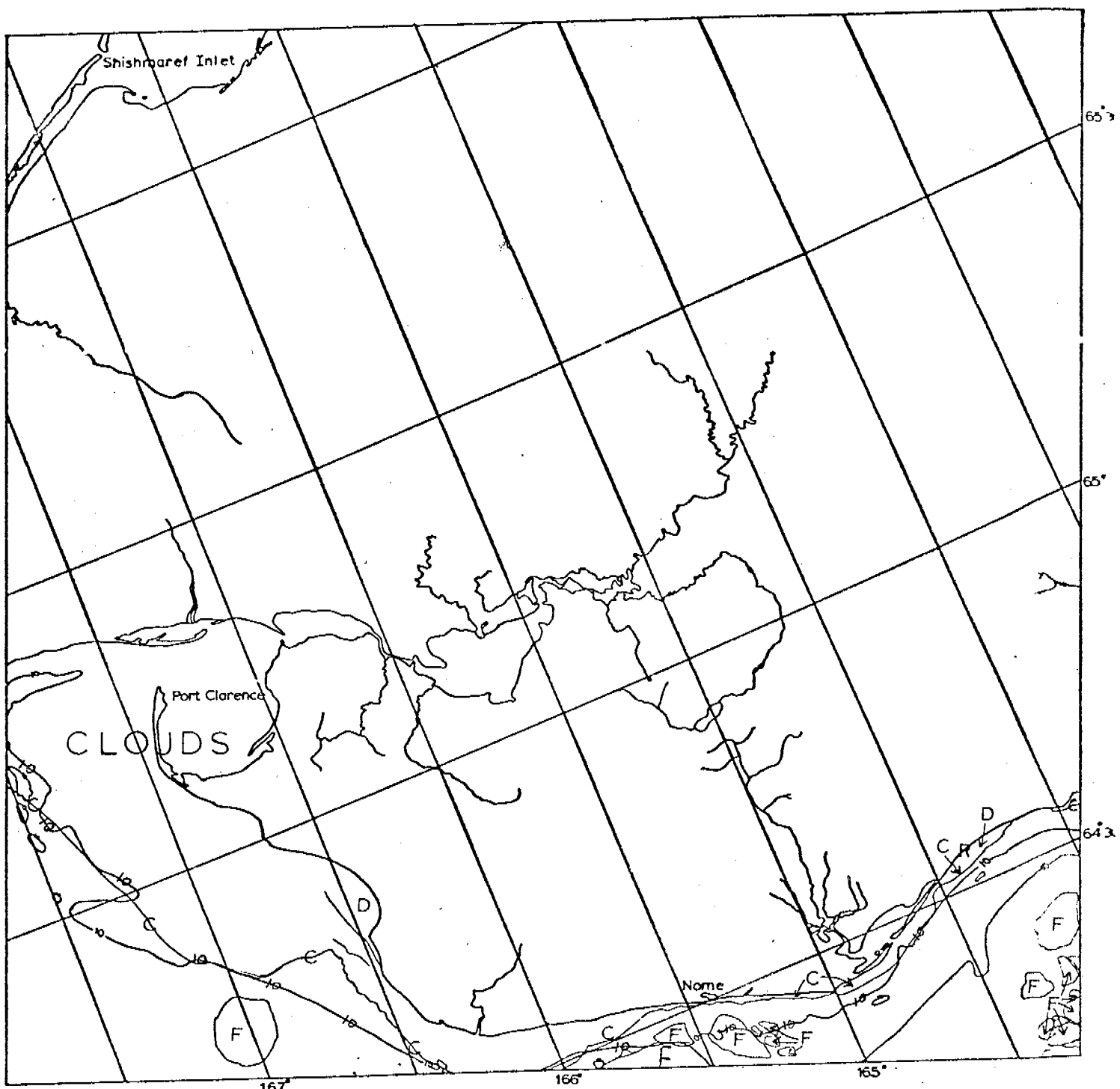
13 MAY 1975



BERING SEA

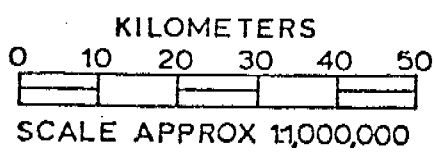
Scene 2112-21525

East of Nome the fast ice narrows and disappears. At the eastern-most extremity, it consists of what appears to be decayed ice. A ridge appears to be almost adjacent to shore here, with a very narrow lead of nearly open water between it and the barrier islands. A wide shelf of contiguous ice still exists around Port Clarence due to the very shallow water. Details are obscured by clouds.



E-2112-21525-7

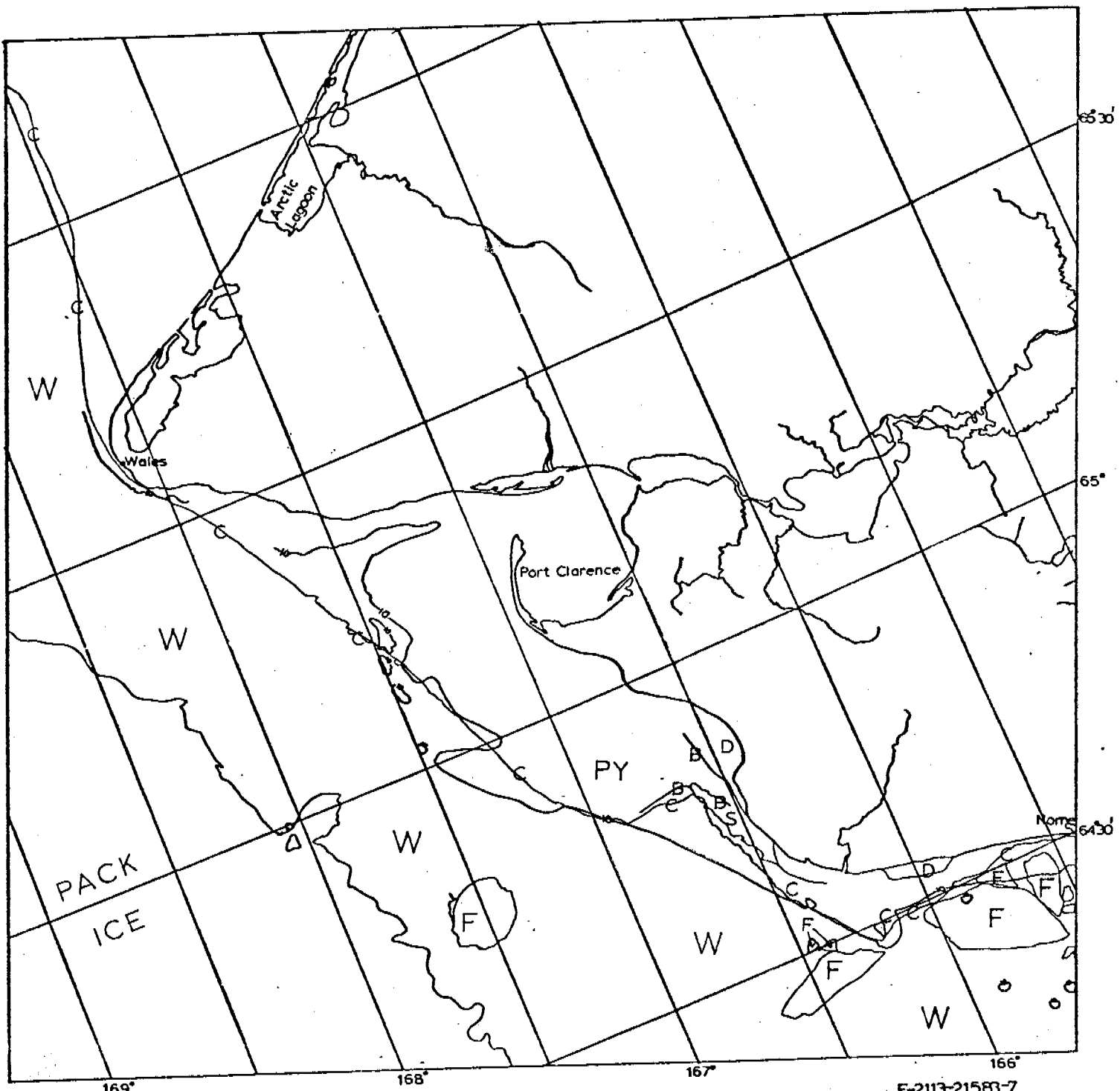
14 MAY 1975



## BERING SEA

Scene 2113-21583

The edge of the contiguous ice closely approximates the 10-fathom contour from Nome to Wales, with the exception of a few irregularities. South of Port Clarence, details of the fast ice character can be seen. It consists of a matrix of pans in younger year ice. A small region of smooth ice, marked "S", is noted. Just north of the smooth ice, the ice is decaying, apparently due to river water interaction. Just west of Nome, several large floes that were noted previously (Scene 2111-21473) to have broken off the contiguous ice shelf, have drifted several kilometers westward. The pack ice is separated from shore by at least 30 km of open water.



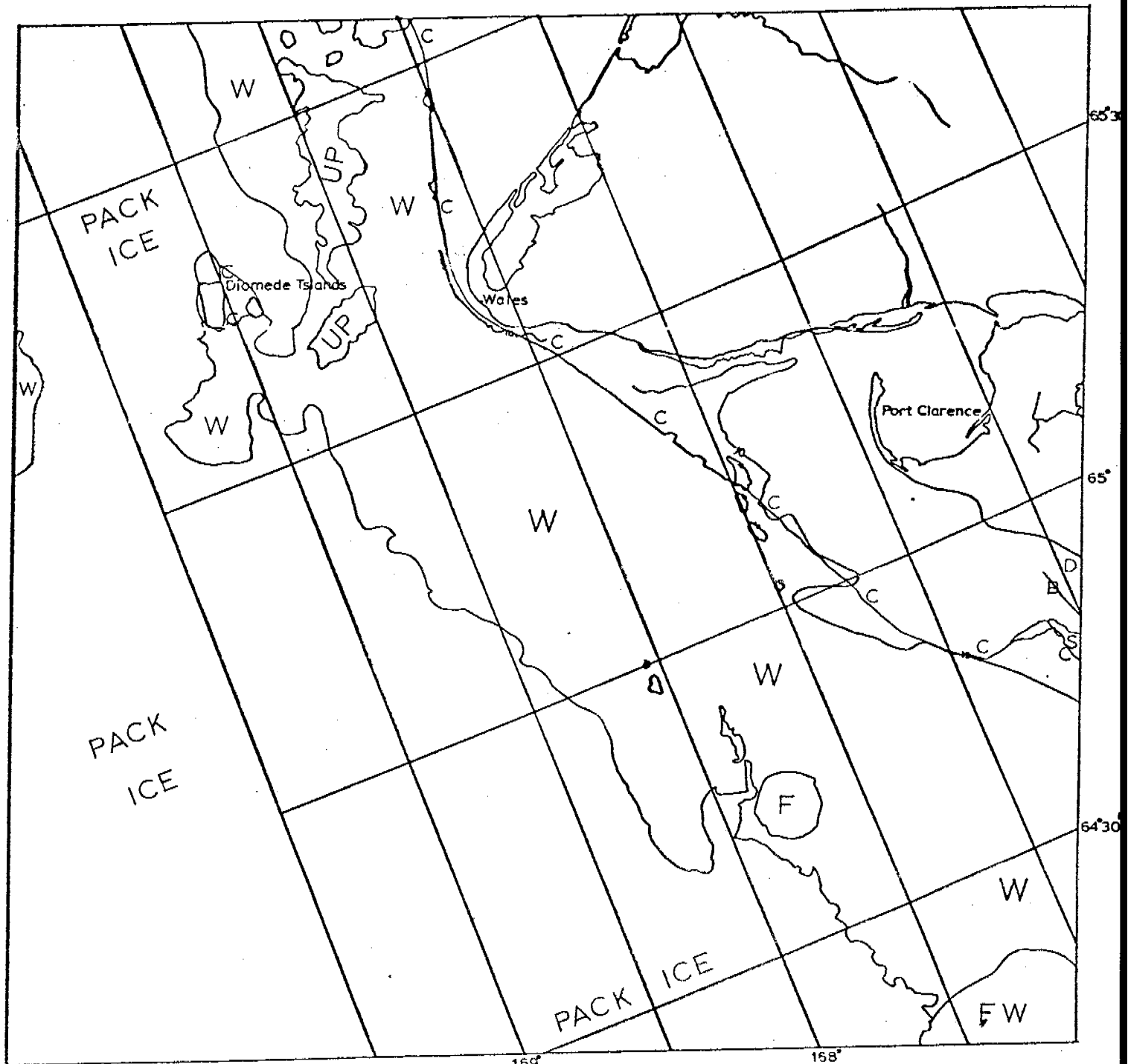
KILOMETERS  
 0 10 20 30 40 50  
  
 SCALE APPROX 11,000,000

## BERING SEA

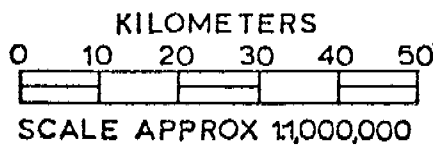
E-2113-21583-7  
15 MAY 1975

Scene 2114-22042

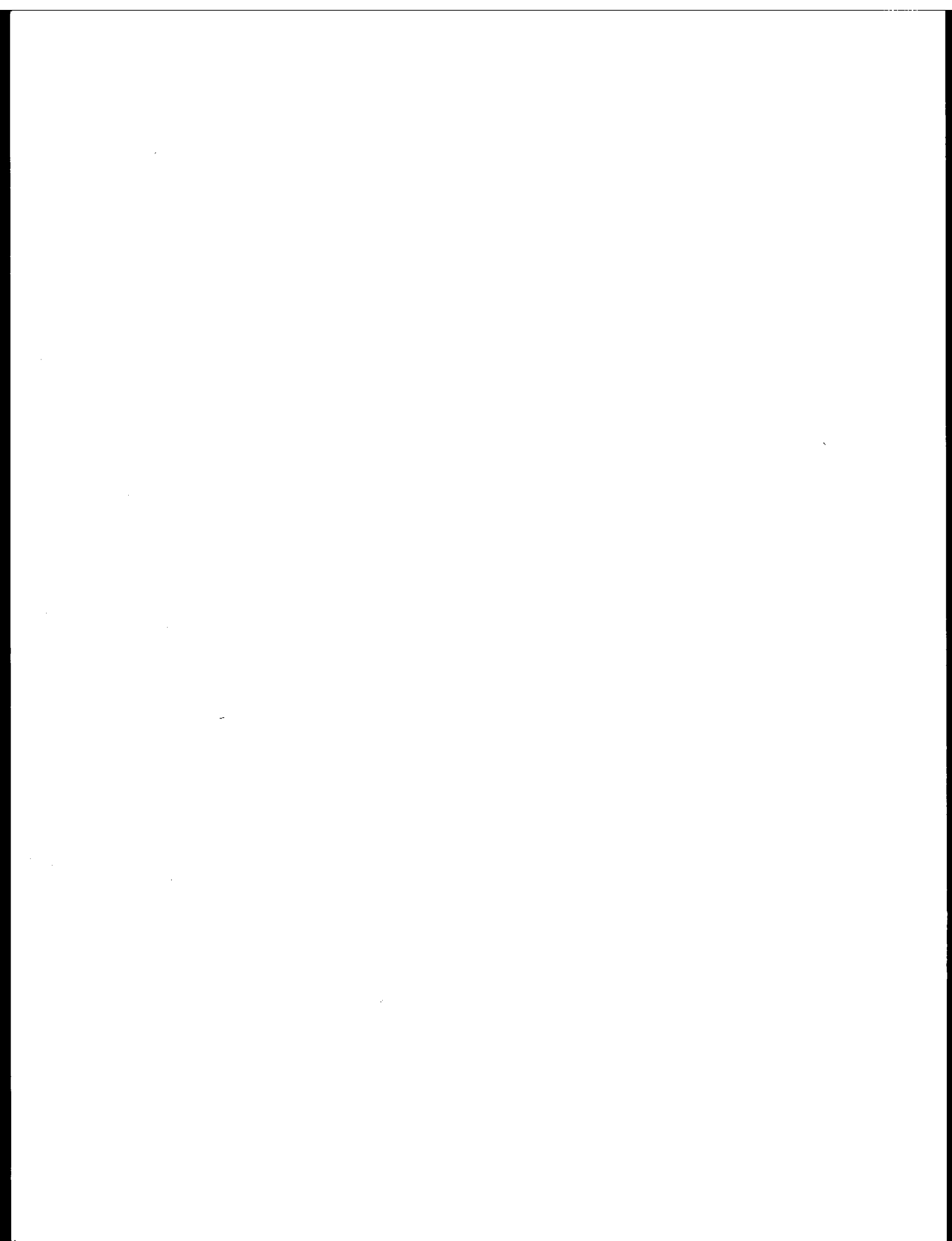
This scene, west of the previous one, is essentially the same except that the pack ice has moved further offshore. Also, some contiguous ice can be seen between the Diomede Islands.



E-2114-22042-7  
16 MAY 1975



## BERING SEA



**Quarterly Report**

Contract #03-5-022-55  
Research Unit #259  
Reporting Period 7/1 - 9/30/76  
Number of Pages 1

**EXPERIMENTAL MEASUREMENTS OF SEA ICE FAILURE STRESSES  
NEAR GROUND STRUCTURES**

R. D. Nelson  
Associate Professor of Mechanical Engineering

W. M. Sackinger  
Associate Professor of Electrical Engineering  
University of Alaska  
Fairbanks, Alaska 99701

October 1, 1976

## Quarterly Report

### I. Task Objectives

The objectives of this study are to measure, in-situ, the stresses generated in a sea ice sheet as it fails in the vicinity of a static obstacle, and the rate of approach of the ice sheet during this process.

### II. Field or Laboratory Activities

No field activities took place during the summer quarter. Progress was made on the computer software necessary for reduction and plotting of field data from the previous winter's experiments.

### III. Results

At the end of the quarter, a preliminary printout of data, containing the recorded ice stresses expressed as a function of time, with very fine time increments, was produced. Comparison of this highly-detailed record with the simultaneously recorded paper charts has begun.

### IV. Preliminary Interpretation of Results

It appears that an abruptly-increasing compressive stress event was recorded near the end of the recorded telemetry experiment. Since this occurred near the end of the time frame of the experiment, when storage batteries were nearly depleted, additional comparison of the two records must be made to ensure that the digitally-recorded variations are not equipment-related.

### V. Problems Encountered/Recommended Changes

The recommended changes in the program have been expressed in the proposal for continuation for an additional year. They include a sequence of measurements in ice striking grounded ridges near Barrow, and simultaneous detection of ice movement on the sea ice radar there. Ease of logistic deployment will permit installation of longer-lasting telemetry batteries, as well as continuous operation of digital recording at a shoreline site.

### VI. Estimate of Funds Expended.

\$64,200.

QUARTERLY REPORT

Contract No. 03-5-022-55  
or 261/262

Research Unit No.

Reporting Period:

July 1-Sept. 30, 1976

BEAUFORT SEA, CHUKCHI SEA, AND BERING STRAIT

BASELINE ICE STUDY PROPOSAL

William R. Hunt

and

Claus-M. Naske

Sept. 30, 1976

## QUARTERLY REPORT

### I. Task Objectives:

The investigators have recorded historic ice positions from 1870 to 1970 on twenty-six charts. These charts reflect the seasonal navigational conditions as recorded in ship logs--primarily those of the whaling vessels and U.S. Coast Guard ships. Compilation of data on unusual ice observations to be reported from these and other sources is continuing and this data will be presented in narrative form.

### II. Field Activities:

The researchers will continue to gather data from source materials as such material is discovered in source inventories and bibliographies. Two more trips to Washington, D.C. to the National Archives are planned.

### III. Results:

Data has been plotted on 26 charts. Ships usually entered Bering Strait at the beginning of June and left, at the latest, in October.

Chart 1, for example, records data for the month of July for the years 1873, 1876, 1878 and 1879. So far, no materials were found for the intervening years. Data, so far, covers the years 1876 - 1970, with gaps in between. The investigators are extracting information about unusual ice conditions and are working on the narrative accompanying the charts.

SIXTH QUARTERLY REPORT

TITLE: Development of Hardware and Procedures for *In-Situ* Measurement of Creep in Sea Ice

PERIOD: July 1, 1976 - September 30, 1976

PRINCIPAL INVESTIGATORS: Lewis H. Shapiro, William M. Sackinger and Richard D. Nelson, Geophysical Institute, University of Alaska

I. TASK OBJECTIVE: To develop hardware and procedures for *in-situ* measurement of creep sea ice.

II. SCHEDULE: Evaluation of results.

III. RESULTS: During the past quarter work was continued in three areas:

1. Several important improvements for our strain recording equipment have been designed and constructed. These will improve the accuracy of the timing system and provide better control of data acquisition and recording than was originally designed into the system as purchased.

2. Progress has been made in evaluating the creep test results presented by Peyton (1966). The results from approximately 200 tests have been plotted and organized to determine the range of conditions for which parameters for various stress-strain laws can be calculated from the data. Preliminary results indicate that, as expected, it may not be possible to fit these with a linear viscoelastic stress-strain law. However, the equations for a non-linear law, based upon a four-parameter viscoelastic model, were derived during this quarter. The first attempts to fit this law to the data are presently in progress.

3. A program of cold room calibration and testing of stress transducers at high loads has been planned and is being initiated.

IV. PRELIMINARY INTERPRETATION: None

V. PROBLEMS ENCOUNTERED/RECOMMENDED CHANGES: None

VI. ESTIMATED FUNDS EXPENDED: \$15,000.

QUARTERLY REPORT

Contract # 03-5-022-55, task 10  
Research Unit # 267  
Reporting Period, July 1 to  
September 30, 1976  
Number of Pages - 7

OPERATION OF AN ALASKAN FACILITY  
FOR APPLICATIONS OF REMOTE-SENSING DATA TO OCS STUDIES

Albert E. Belon  
Geophysical Institute  
University of Alaska

September 30, 1976

OPERATION OF AN ALASKAN FACILITY  
FOR APPLICATIONS OF REMOTE-SENSING DATA TO OCS STUDIES

Principal Investigator: Albert E. Belon  
Affiliation: Geophysical Institute, University of Alaska  
Contract: NOAA # 03-5-022-55  
Research Unit: # 267  
Reporting Period: July 1 to September 30, 1976

#### I. TASK OBJECTIVES

The primary objective of the project is to assemble available remote-sensing data of the Alaskan outer continental shelf and to assist other OCS investigators in the analysis and interpretation of these data to provide a comprehensive assessment of the development and decay of fast ice, sediment plumes and offshore suspended sediment patterns along the Alaskan coast from Yakutat to Demarcation Bay.

#### II. LABORATORY ACTIVITIES

##### A. Operation of the Remote-Sensing Data Library

We continued to search periodically for new Landsat imagery of the Alaskan coastal zone entered in the EROS Data Center (EDC) data base. As a result 398 cloud-free Landsat scenes were selected and ordered from EDC at a cost of \$1,365. These data products, which are gradually received from EDC, complete our files of Landsat data from the launch of the first satellite, July 26, 1972, with at least the following data products.

- 70mm positive transparencies of multispectral scanner (MSS) spectral bands 4, 5 and 7
- 70mm negative transparency of MSS, spectral band 5
- 9½ inch print of MSS, spectral band 6

We continued to receive and catalog daily copies of NOAA satellite imagery of Alaska in both the visible and infrared spectral bands under a standing order with the NOAA/NESS Fairbanks Satellite Data Acquisition Station. 239 NOAA scenes at a total cost of \$2169 were acquired in 10" positive transparency format during the reporting period.

We received and catalogued 25 runs (57 ft.) of side-looking radar (SLAR) imagery acquired by a U. S. Army Mohawk aircraft on August 5 to 10, 1976 under contract with NOAA/OCSEAP. The data

provide complete coverage of the Beaufort and Chukchi Sea shelves during the open water period. In addition, detailed SLAR coverage of the entire Kotzebue Sound and northern Seward Peninsula coast was obtained for the first time. These data are generally of very good quality. A catalog of these data will be distributed to OCS investigators through the next Arctic Project Bulletin and is reproduced here as an appendix.

#### B. Operation and Maintenance of Data Processing Facilities

Most of the data processing equipment was kept operational, in spite of several minor break-downs, during the reporting period and was utilized by several OCS investigators.

The CDU-200 Digital Color Display System was only partially operational (one channel out of 3), owing to extraordinary delays in the delivery of the necessary parts, but this did not cause problems for the OCS investigators because they used the system primarily for intensity-slicing and reflectivity profiles which require only one operating channel.

The digital image recorder, purchased with state funds, was received from the manufacturer in early May. Preliminary testing of the system indicated that the supplied software over-filled the 16 k memory of the NOVA 1620 minicomputer. This problem has been corrected, and all optical and electronic adjustments and tests were successfully completed early in the reporting period. The system is now fully operational and producing high quality color and black + white digital images.

The Variscan 9½" film projector, acquired from federal surplus is partially operational, but activation of the film transport mechanism awaits the delivery of necessary electrical components.

Other data processing equipment (color-additive viewer, zoom transfer scope, multi-format stereo light table, photographic equipment) remained operational and utilized throughout the reporting period.

#### C. Development of Data Analysis and Interpretation Techniques

Much of the project's activity in this area during the reporting period was devoted to the conversion of existing computer programs from the IBM 360/40 University of Alaska computer which is being phased out to the recently acquired Honeywell 66/20 timesharing computer. Programs for reading Landsat tapes and computing reflectivity profiles and multispectral histograms developed at the request of Dr. Lewis Shapiro (RU #248,249) were used frequently during the reporting period.

An "Isoclass" spectral clustering program for classification of sea-ice and land ecosystem was acquired from NASA/Johnson Space Center and is being converted to our computing facilities. Work on programming a "maximum likelihood classification" algorithm for use with the "isoclass" program will be started during the next reporting period.

Techniques for classifying and reproducing SLAR data have been developed in cooperation with Dr. Jan Cannon (RU #99).

#### D. Assistance to OCS investigators

Thirty-one OCS investigators requested substantial and often repeated assistance during the period, ranging from data searches and orders to operation of data processing equipment and digital analysis of Landsat data.

Data purchases by OCS investigators totalled \$2237 from the EROS Data Center and several hundred dollars in work orders to our photographic laboratory for urgent or custom reproduction of selected data, principally SLAR data. In addition many OCS investigators performed analysis of library copies of data in our facility.

The project participated in the formulation and supervision of the SLAR data acquisition program of a U.S. Army Mohawk data on August 5-10, 1976. Twenty-five data runs (several hundred flight line miles) were acquired with swath width of 25, 50 and 100 km. Most of the data is of very good quality (see appendix) and is already being used by OCS investigators.

The National Ocean Survey (NOS) Buffalo aircraft acquired natural color and color-infrared photographic data of the Bering Sea coast in response to an arrangement negotiated between NOS and OCSEAP. These data will be received and catalogued during the next reporting period. The aircraft also acquired detailed data of Shelikof strait (its primary NOS mission). Index maps of NOS aerial photography were ordered and received.

A Coast Guard C-130 aircraft equipped with a sophisticated side-looking radar (SLAR) and a technical crew from the NASA/Lewis Research Center flew repeated missions over the Beaufort Sea and northern Chukchi sea coasts in late August and early September. This mission was a test of an operational system for real time evaluation of sea-ice conditions for ship navigation purposes. The SLAR data are transmitted in real time via satellite to NASA/LRC where they are interpreted and the resulting sea-ice maps are transmitted back to the base of operation at Barrow within two hours. The OCSEAP Arctic Project Office arranged with NASA/LRC to provide the acquired SLAR data and sea-ice maps to our project (RU267) for the use of OCS investigators. They are expected to be received at the end of October.

Negotiations continued with the NASA/Ames Research Center for the acquisition of U-2 aerial photography of the entire Alaskan coastline during June 1976. The program was approved, but in late May problems with the aircraft and stratospheric sampling sensors caused the postponement of the Alaskan mission to late September. The U-2 aircraft arrived at Eielson AFB on September 28, 1976 and photographic missions in support of the OCS program are scheduled for the first two weeks of October, weather permitting.

While the OCSEAP/Arctic Project Office and our project have been fairly successful in negotiating remote-sensing data acquisition by other agencies on an irregular basis, such arrangements are not really satisfactory on a long-term basis because the type and format of the data vary from one mission to the next and the frequency of data acquisition is insufficient to provide good statistical information on sea-ice conditions and processes. For this reason we have worked with the Arctic Project Office on a plan which would utilize an available Naval Arctic Research Laboratory (NARL) aircraft, OCSEAP-purchased remote-sensing equipment, and local processing of the data to provide more frequent and more relevant data on a consistent format. This plan was proposed in a memo from G. Weller (Arctic Project Office) to R. Engelman (OCSEAP), dated September 28, 1976. We hope that it will receive serious consideration.

### III. RESULTS

None to be reported at this time, except for the distribution of remote-sensing catalogs through the Arctic Project Bulletins and the results discussed as part of the previous section.

### IV. PRELIMINARY INTERPRETATION OF RESULTS

This project provides a support function to the other OCS projects. Therefore disciplinary data interpretation will be reported by the individual user projects.

### V. PROBLEMS ENCOUNTERED/RECOMMENDED CHANGES

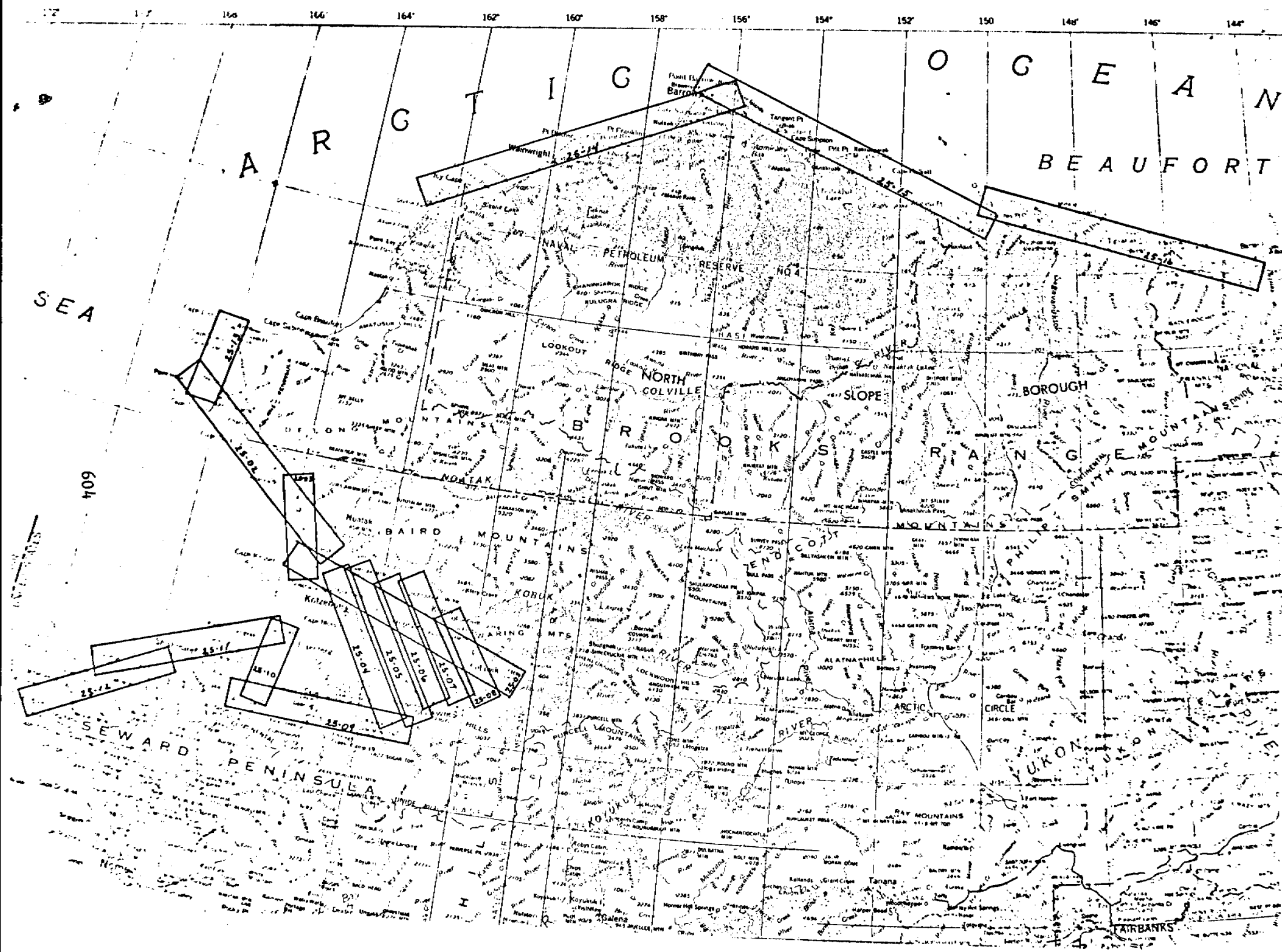
None of substance or unusual character.

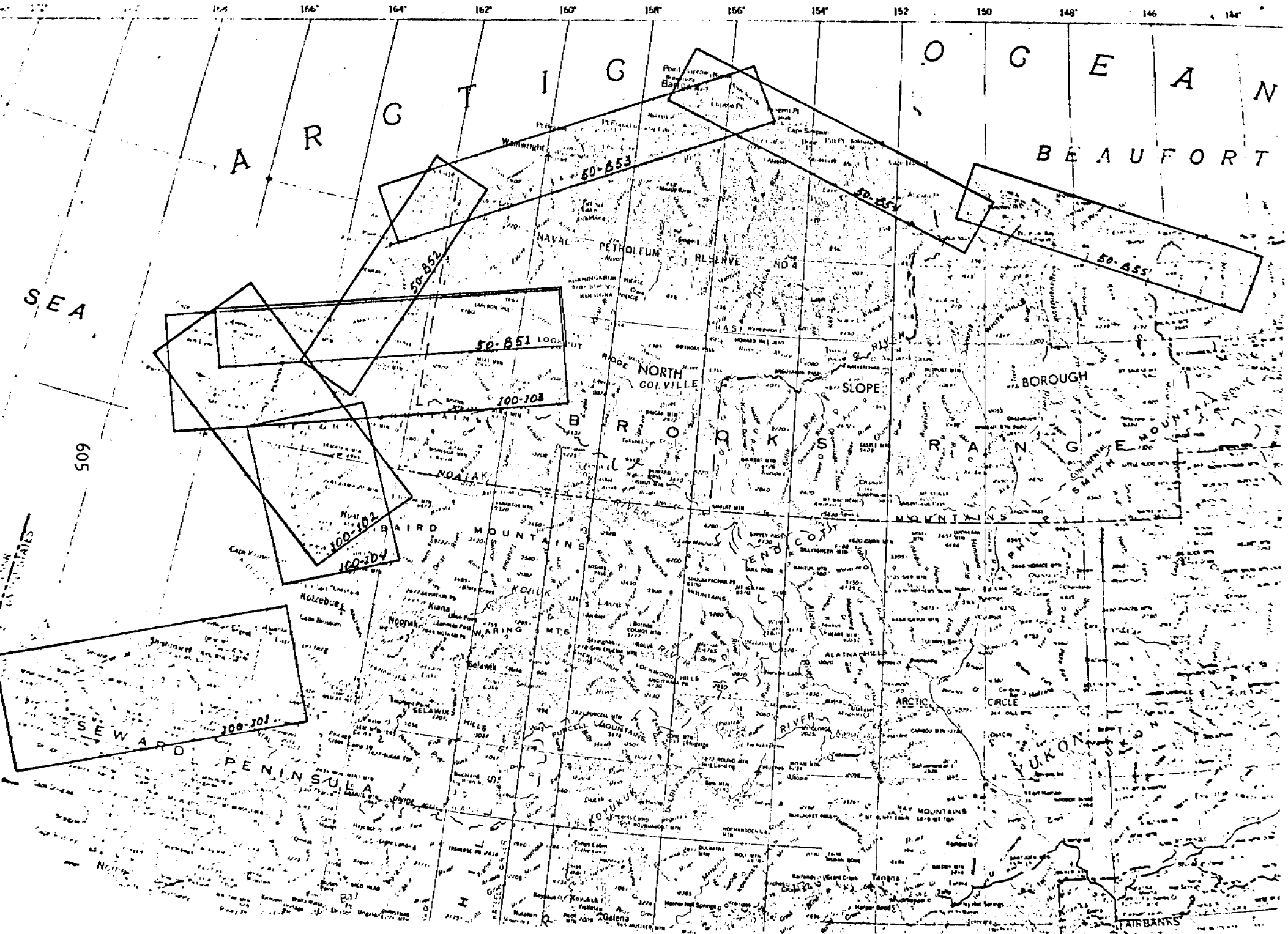
### VI. ESTIMATES OF FUNDS EXPENDED

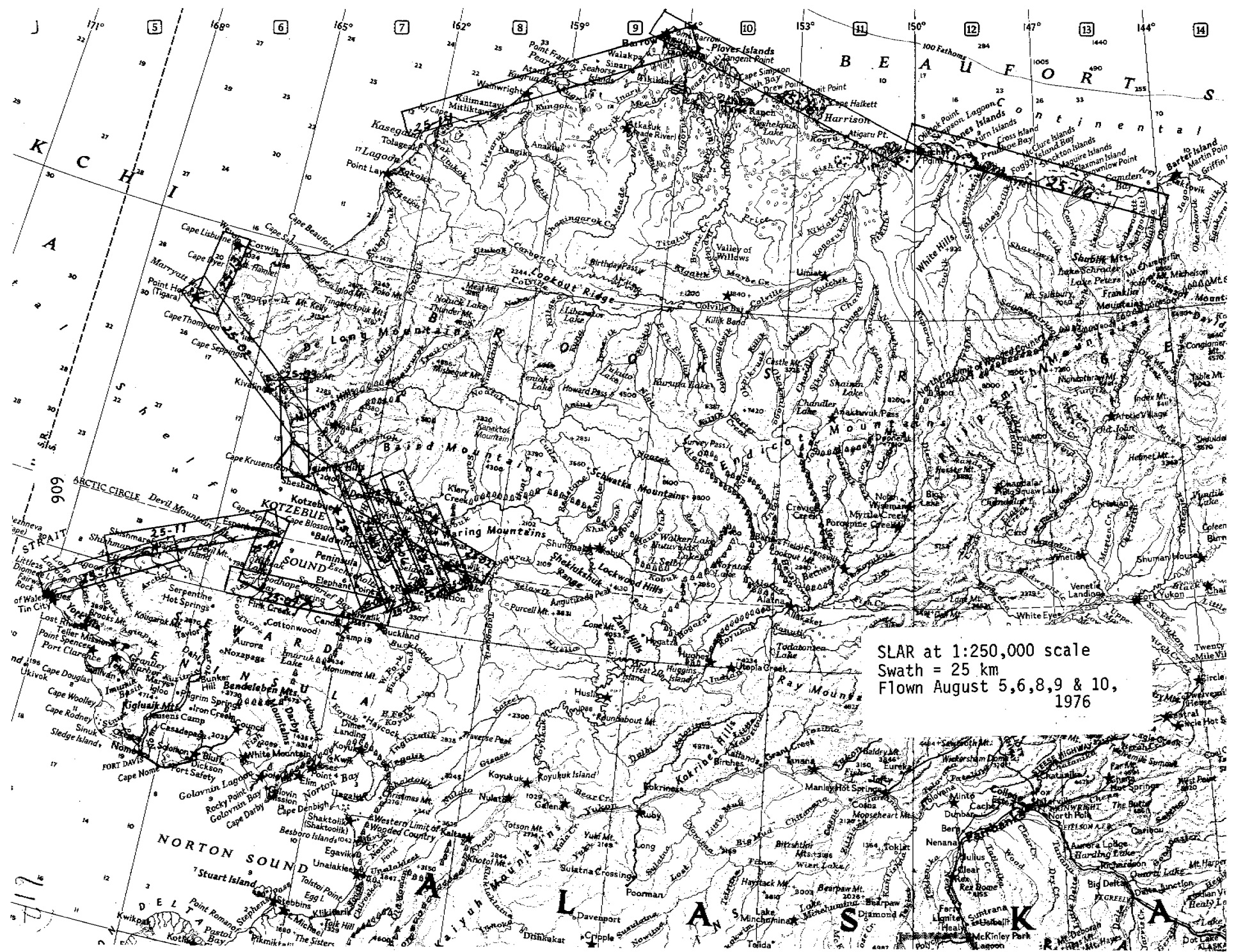
On July 30, 1976 (the last available fiscal report) the unexpended balance of the project was \$32,142.57. Estimated expenses and outstanding obligations incurred in August and September totalled approximately \$20,000 leaving an estimated unexpended balance of \$12,142 as of September 30, 1976, the end of the current reporting period.

Project: Outer Continental Shelf Energy Program  
 Location: Beaufort and Chukchi Seas  
 Aircraft: Mohawk OV-1  
 Flight Line: Between points indicated (see map)  
 Instrument: Motorola Side Looking Radar  
 X-Band (3.5 cm) Real Aperture  
 Dual Antenna Mode

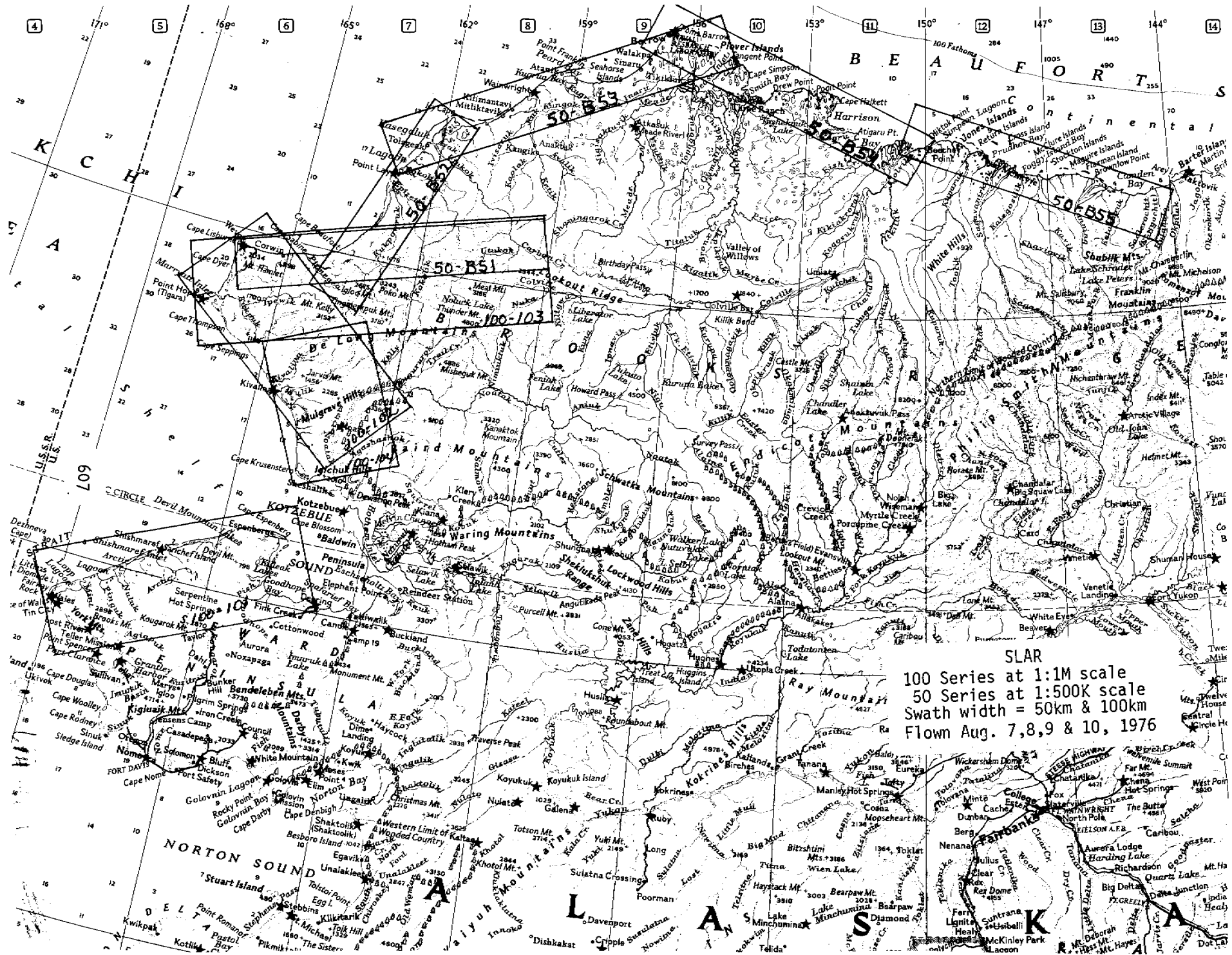
Date	Run	Flight Line	Range Swath	Lineal Ft of Film	Processing Quality	Film Quality
	25-					
8-05-76	01	Selawik - Cape Krusenstern	25	4'	very good	very good
8-08-76	02	Point Hope - Nauyoaruk	25	3'	very good	very good
8-05-76	03	Cape Krusenstern - Imikruk Lagoon	25	1'	very good	very good
8-06-76	04	Baldwin Peninsula	25	2'	very good	very good
8-06-76	05	Baldwin Peninsula	25	2'	very good	very good
8-06-76	06	Selawik Lake	25	2'	very good	very good
8-06-76	07	Noorvik	25	2'	very good	very good
8-06-76	08	Selawik	25	1'	very good	very good
8-06-76	09	Buckland - Goodhope River	25	2'	very good	very good
8-06-76	10	Espenberg - Goodhope Bay	25	1'	very good	very good
8-06-76	11	Espenberg - Sinrazat	25	3'	very good	very good
8-06-76	12	Wales - Cape Lowenstern	25	2'	very good	very good
8-08-76	13	Aiautak Lagoon - Cape Lisburne	25	1'	very good	very good
8-09-76	14	Icy Cape - Christie Point (Loss of Video on right CRT)	25	5'	very good	very good
8-10-76	15	Point Barrow - Nooiksut (Loss of Video on right CRT)	25	5'	very good	very good
8-10-76	16	Oliktok Point - Hulahula River (Loss of Video on right CRT)	25	5'	very good	very good
	50-					
8-08-76	B51	Cape Lisburne - Ketik River	50	2'	very good	very good
8-08-76	B52	Windy Lake - Icy Cape	50	2'	very good	very good
8-09-76	B53	Kasegaluk Lagoon - Christie Point	50	3'	very good	very good
8-10-76	B54	Point Barrow - Nooiksut	50	3'	very good	very good
8-10-76	B55	Oliktok Point - Hulahula River (Loss of Video on right CRT)	50	2'	very good	very good
	100-					
8-07-76	101	Wales - Espenberg	100	1'	good	good
8-07-76	102	Kotlik Lagoon, Pt. Hope, C. Lisburne	100	1'	good	good
8-07-76	103	Point Hope - Ketlik River	100	1½'	fair	good
8-08-76	104	Nameluk Mtn. - Kivalina River	100	1'	very good	very good

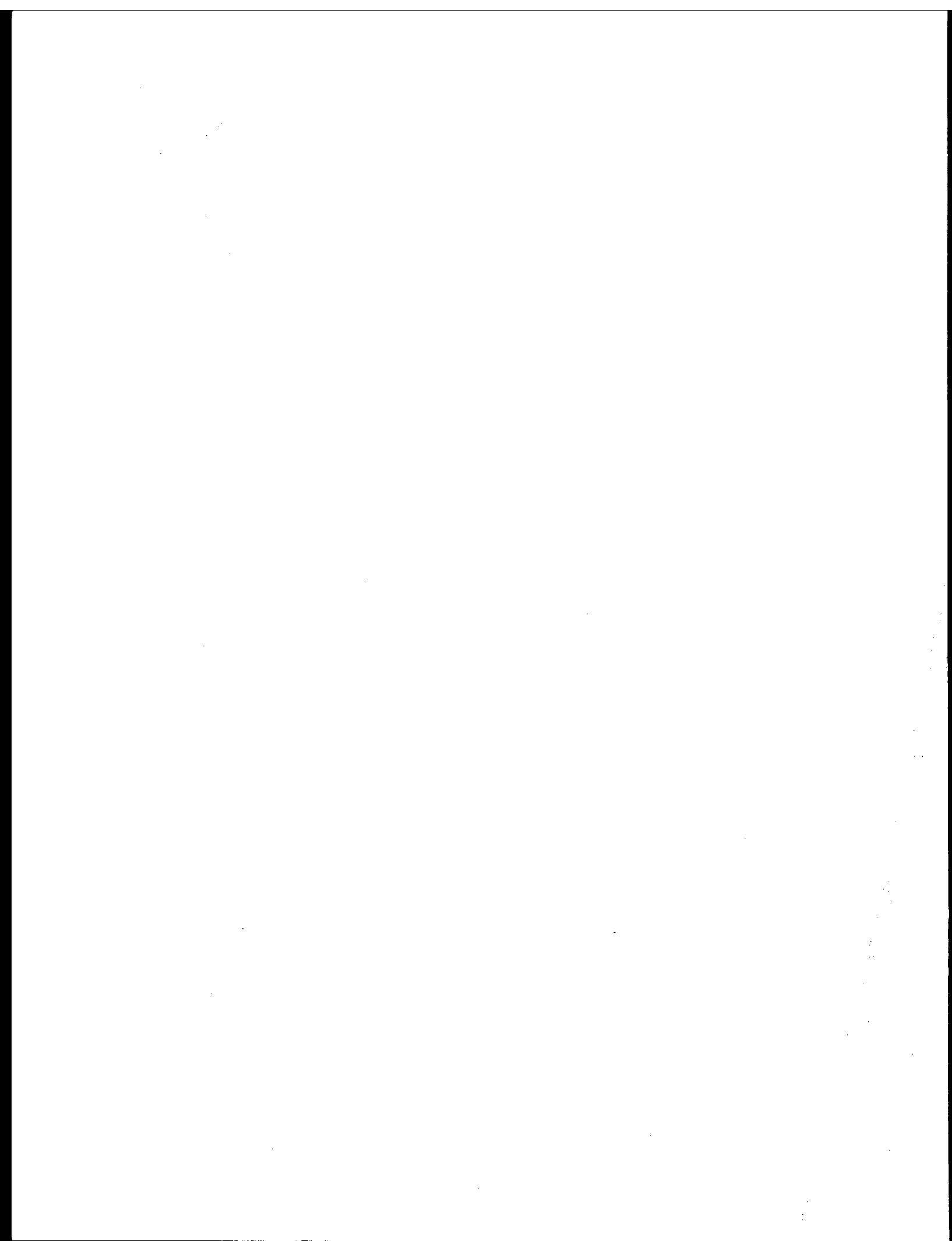




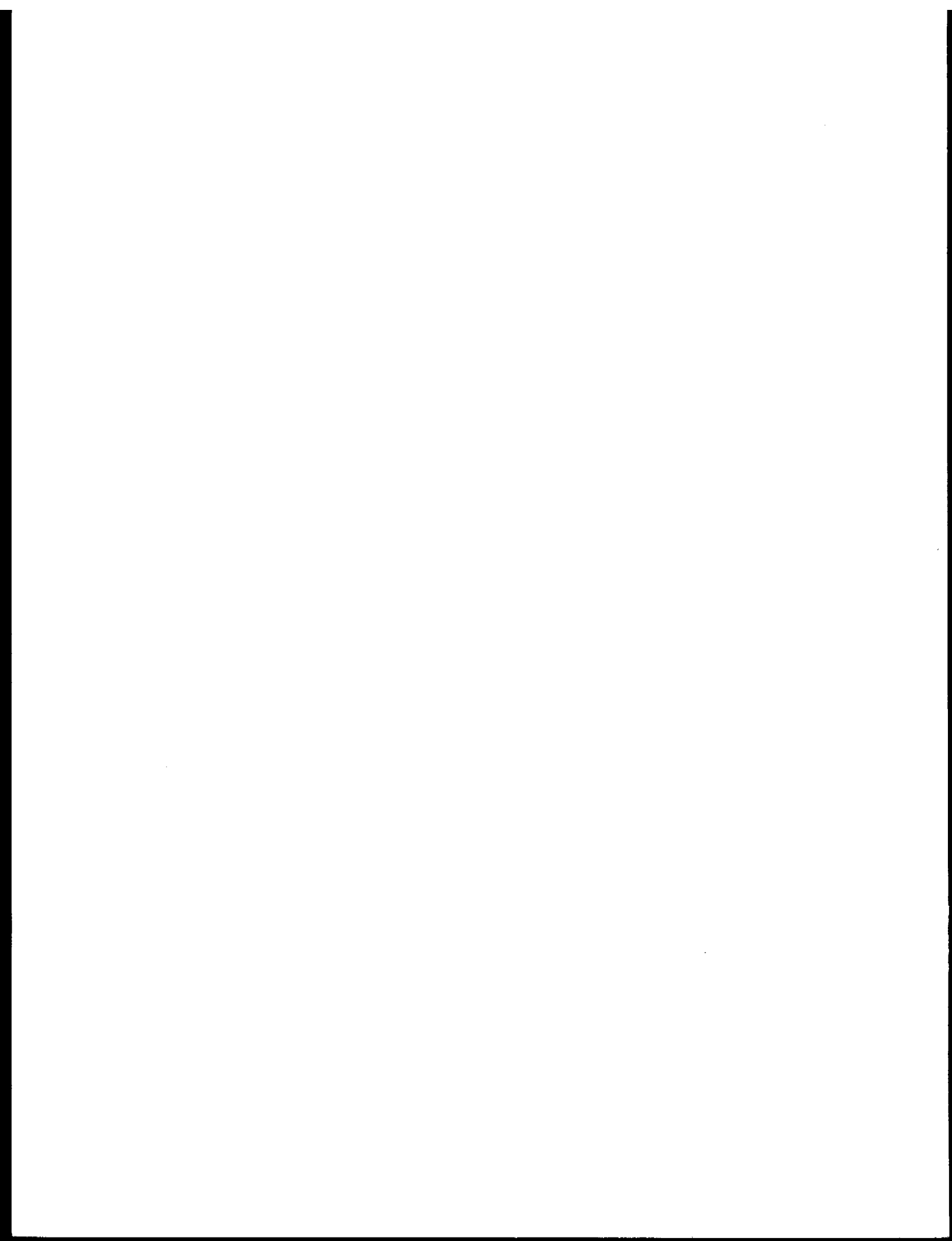


SLAR at 1:250,000 scale  
Swath = 25 km  
Flown August 5,6,8,9 & 10,  
1976



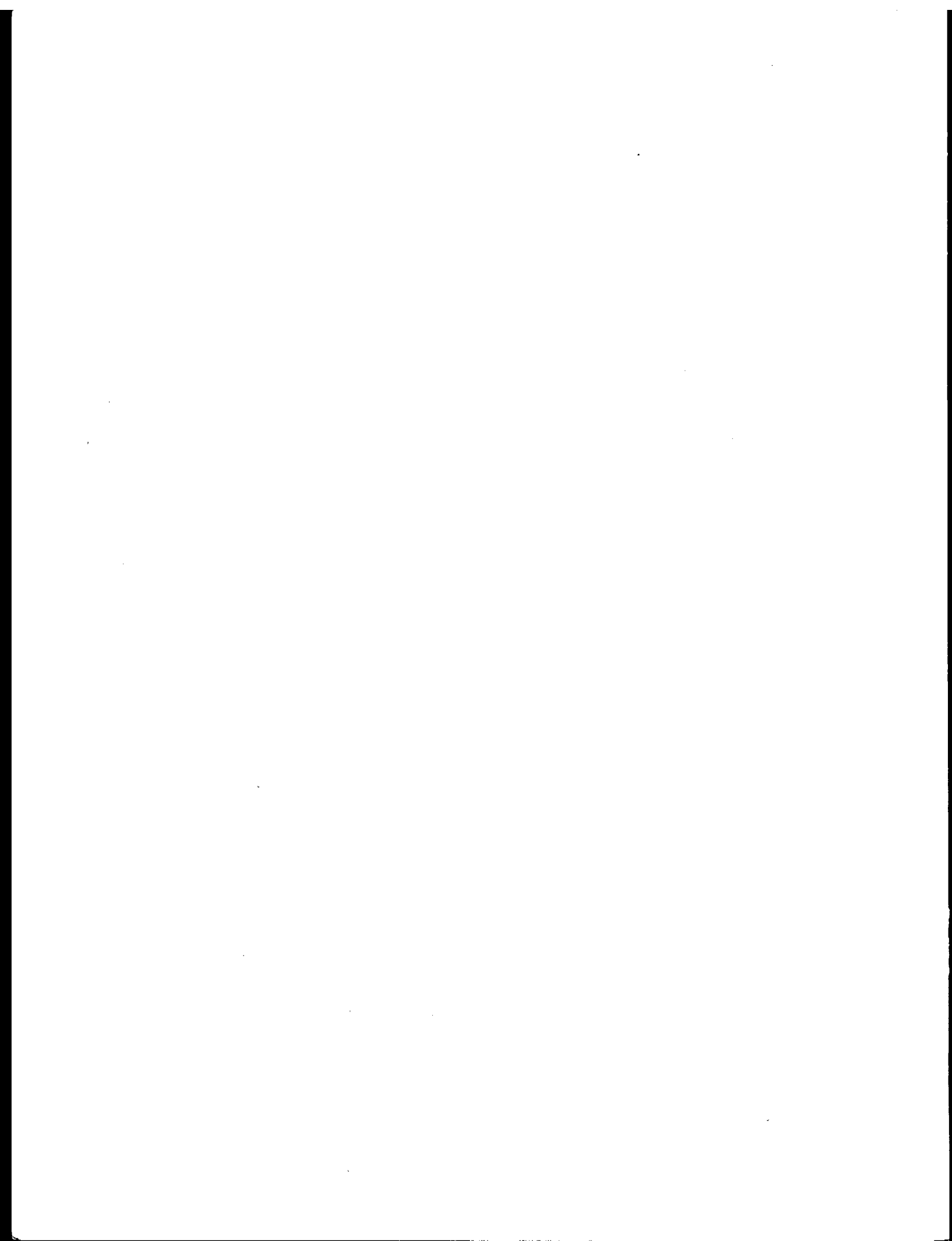


## DATA MANAGEMENT



## DATA MANAGEMENT

<u>Research Unit</u>	<u>Proposer</u>	<u>Title</u>	<u>Page</u>
350	Donald H. Rosenberg U. of Alaska	Alaska O.C.S. Program Coordination	613



**Quarterly Report**

**Contract #03-5-022-56  
Research Unit #350  
Reporting Period 7/1 - 9/30/76  
Number of Pages 4**

**ALASKA O.C.S. PROGRAM COORDINATION**

**Mr. Donald H. Rosenberg  
O.C.S. Coordination Office  
University of Alaska  
Fairbanks, Alaska 99701**

**October 1, 1976**

## Quarterly Report

### I. Task Objectives

This project provides for coordination of all NOAA/OCS Task Orders within the University of Alaska. It provides for a coordinator and related support services necessary for the accomplishment of the scientific program. These services include Data Management, Fiscal Management, and Logistic Coordination.

### II. Field and Laboratory Activities

Not applicable.

### III. Results

#### A. Data Management

##### 1. Data Management Plans

Data Management Plans have been approved and made contractual for the following Task Orders: #1, 2, 4, 5, 7, 9, 10, 11, and 13 - 26.

We await contractual approval of the Data Management Plans for Task Orders #3, submitted November 20, 1975; #6 submitted October 9, 1975; #8, submitted November 24, 1975; #12, submitted November 24, 1975, and #29 submitted August 16, 1976.

As yet, no Data Management Plans have been submitted for Task Orders #27 and 28.

##### 2. Data submitted this quarter

Task Order #1, Primary Productivity Data for *Discoverer 808*, *810*, and *Miller Freeman 815* on 9/7/76.

Task Order #13, Zooplankton Data for *Discoverer 810* on 8/10/76; *Surveyor 001*, *Miller Freeman 815*, and *Discoverer 808* on 8/31/76.

Task Order #14, CTD Data, for *Acona 197* on 8/20/76.

Task Order #15, Benthic Organism Data for *Discoverer 808* on 8/10/76.

Task Order #19 CTD Data, for *Oceanographer 805* and *Acona 212* on 7/29/76.

Task Order #20, Benthic Organism Data, for *Moana Wave 002* on 8/23/76.

Special Lower Cook Inlet Data report for Task Orders #5,  
12, 20, on 8/16/76.

Dr. Peter Connors data, keypunched the previous quarter, was submitted on 8/10/76.

### 3. Keypunch Service

We are currently keypunching data for G. Divoky, ADF&G, Fairbanks, as requested by the Project Office.

## B. Contract Monitoring

Last minute negotiations are now underway to prevent the necessary closing down of a majority of the Task Orders under both contracts. This has resulted from a failure of NOAA to notify the University of continuing funding on projects.

### C. Proposal and Work Statement Modification

During the last quarter extensive effort has been directed toward the coordination and official submission of work statement modifications and modified renewal proposals. Our records indicate that all requested proposals have now been submitted.

#### D. Logistics Coordination

Coordination of logistics for OCS cruises was rendered by this office. This coordination consisted of reviewing and correcting Project Instructions, and acting as a conduit between principal investigators and OCSEAP concerning any problems with ship suitability.

Cruises this quarter in which our personnel were involved are:

Miller Freeman Trawl Survey

## *Surveyor*      Geophysics

\* Chief Scientists' Report and ROSCOP form submitted through this office.

#### IV. Problems Encountered

A. Communication between the NOAA program office and this office still remain the largest problem. Copies of letters requesting proposals from principal investigators were not received by this office until after the due date.

- B. Copies of cruise reports for cruises where University personnel were not chief scientists are never received. These are necessary for data management purposes.
- C. Failure of NOAA or BLM to provide timely review of University proposals has caused a delay in notification of funding. This will, as of 5:00 o'clock P.M., 30 September, 1976, cause the University to stop all work on unfunded Task Orders and start preparing final reports.

OCS COORDINATION OFFICE

University of Alaska

ENVIRONMENTAL DATA SUBMISSION SCHEDULE

DATE: September 30, 1976

CONTRACT NUMBER: 03-5-022-56      T/O NUMBER: 2

PRINCIPAL INVESTIGATOR: Mr. Donald H. Rosenberg

No environmental data are to be taken by this task order as indicated in the Data Management Plan.<sup>1</sup> A schedule of submission is therefore not applicable

NOTE: <sup>1</sup> Data Management Plan has been approved and made contractual.

